



Pharmaceuticals in the Environment: Photolysis, Identification  
of Transformation Products - Environmental Risk Assessment  
for X-ray Contrast Media and Demonstrating the Feasibility of  
Designing Environmentally Biodegradable Derivatives Using  
the Example of  $\beta$ -Blockers

Kumulative Dissertationsschrift zur Erlangung des akademischen Grades

Doktor der Naturwissenschaften

(Dr. rer. nat.)

Angefertigt am Institut für Nachhaltige Chemie und Umweltchemie,

Fakultät Nachhaltigkeit, Leuphana Universität Lüneburg

vorgelegte Dissertation von

Tushar Rastogi

geb. 19 September 1985 in Lucknow, Indien

Lüneburg, Juni 2015

Eingereicht am: 23.10.2014

Betreuer und Erstgutachter: Prof. Dr. Klaus Kümmerer

Zweitgutachter: Prof. Dr. Martin Scheringer

Drittgutachter: Prof. Dr. Ralf Ebinghaus

Tag der Disputation: 20.05.2015

Die einzelnen Beiträge des kumulativen Dissertationsvorhabens sind oder werden wie folgt in Zeitschriften veröffentlicht:

1. **Tushar Rastogi**, Christoph Leder, Klaus Kümmerer (2014) Qualitative Environmental Risk Assessment of Photolytic Transformation Products of Iodinated X-ray Contrast Agent Diatrizoic acid. *Science of The Total Environment* 482–483: 378–388. DOI: 10.1016/j.scitotenv.2014.02.139
2. **Tushar Rastogi**, Christoph Leder, Klaus Kümmerer (2014) Designing green derivatives of  $\beta$ -blocker Metoprolol: A tiered approach for green and sustainable pharmacy and chemistry. *Chemosphere* 111: 493–499. DOI: 10.1016/j.chemosphere.2014.03.119
3. **Tushar Rastogi**, Christoph Leder, Klaus Kümmerer (2015) A sustainable chemistry solution to the presence of pharmaceuticals and chemicals in the aquatic environment – the example of re-designing  $\beta$ -blocker Atenolol. *RSC Advances* 5: 27-32. DOI: 10.1039/c4ra10294k
4. **Tushar Rastogi**, Christoph Leder, Klaus Kümmerer (2015) Addressing the Challenge of Micro-Pollutants in the Aquatic Cycle: Targeted Re-Designing the  $\beta$ -Blocker Propranolol for Environmental Biodegradability. *Environmental Science & Technology* (submitted)

Nachdruck mit freundlicher Genehmigung des Chemosphere (Elsevier), Science of the Total Environment (Elsevier), RSC Advances (RSC) and Environmental Science & Technology (ACS).



Pharmaceuticals in the Environment: Photolysis, Identification  
of Transformation Products - Environmental Risk Assessment  
for X-ray Contrast Media and Demonstrating the Feasibility of  
Designing Environmentally Biodegradable Derivatives Using  
the Example of  $\beta$ -Blockers

Cumulative Dissertation to Earn the Academic Degree  
Doctor of Natural Sciences  
(Dr. rer. nat.)

Carried out at the Institute of Sustainable and Environmental Chemistry,  
Faculty of Sustainability, Leuphana University of Lüneburg

Dissertation submitted by

Tushar Rastogi

Born on September 19, 1985 in Lucknow, India

Lüneburg, June 2015

Submitted on: 23.10.2014

Doctoral Supervisor and first reviewer: Prof. Dr. Klaus Kümmerer

Second reviewer: Prof. Dr. Martin Scheringer

Third reviewer: Prof. Dr. Ralf Ebinghaus

Date of disputation: 20.05.2015

The individual articles constituting this cumulative doctoral dissertation meet the formal requirements for a cumulative dissertation. The PhD thesis consists of the following publications:

1. **Tushar Rastogi**, Christoph Leder, Klaus Kümmerer (2014) Qualitative Environmental Risk Assessment of Photolytic Transformation Products of Iodinated X-ray Contrast Agent Diatrizoic acid. *Science of The Total Environment* 482–483: 378–388. DOI: 10.1016/j.scitotenv.2014.02.139
2. **Tushar Rastogi**, Christoph Leder, Klaus Kümmerer (2014) Designing green derivatives of  $\beta$ -blocker Metoprolol: A tiered approach for green and sustainable pharmacy and chemistry. *Chemosphere* 111: 493–499. DOI: 10.1016/j.chemosphere.2014.03.119
3. **Tushar Rastogi**, Christoph Leder, Klaus Kümmerer (2015) A sustainable chemistry solution to the presence of pharmaceuticals and chemicals in the aquatic environment – the example of re-designing  $\beta$ -blocker Atenolol. *RSC Advances* 5: 27-32. DOI: 10.1039/c4ra10294k
4. **Tushar Rastogi**, Christoph Leder, Klaus Kümmerer (2015) Addressing the Challenge of Micro-Pollutants in the Aquatic Cycle: Targeted Re-Designing the  $\beta$ -Blocker Propranolol for Environmental Biodegradability. *Environmental Science & Technology* (submitted)

Reprinted with the permission of *Chemosphere* (Elsevier), *Science of the Total Environment* (Elsevier) *RSC Advances* (RSC) and *Environmental Science & Technology* (ACS).

## Acknowledgement

I would like to express my special appreciation and thanks to my supervisor Professor Dr. Klaus Kümmerer, you have been a tremendous mentor for me. I would like to thank you for encouraging my research and for allowing me to grow as a research scientist. A person with an amicable and positive disposition, he has always made himself available to clarify my doubts despite his busy schedules and I consider it as a great opportunity to do my doctoral thesis under his guidance and to learn from his research expertise. Thank you Sir, for your help and support.

I would also like to express my special gratitude to Dr. Christoph Leder for introducing and assisting me with the *in silico* and *in vitro* analysis during this PhD work. I like to thank him for his help, support and his valuable suggestions and concise comments on the research articles of the thesis. Many thanks go to Dr. Mandy Schneider for her help to manage the project, advice, and answers to my questions.

A major research project like this is never the work of anyone alone. The contributions of many different people, in their different ways, have made this possible. I would like to extend my appreciation to my colleagues (in alphabetical order), Anju, Annette, Carlos, Christoph, Evgenia, Ewelina, Franziska, Jakob, Janin, Dieu, Karen, Lukasz, Mandy, Manuel, Marco, Marcelo, Matthias, Natalie, Nareman, Richard, Oliver, Philipp, Stefanie, Tarek, Tiba and Waleed. They have all extended their support in a very special way, and I gained a lot from them, through their personal and scholarly interactions, their suggestions at various points of my research program. I would also like to convey thanks to the German Ministry of Education and Research (NanoPharm, Project No. 03X0094C) for the financial support.

I must express my sincere gratitude to my parents for their unconditional support, encouragement and help at every stage of my personal and academic life. In particular, the

patience and understanding shown by my mum, dad, sister and fiancée during the year is greatly appreciated.

Last but not least, I thank to God for the wisdom, health and perseverance that he has been bestowed upon me during this research project, and indeed, throughout my life.

## **Dedication**

I dedicate this dissertation to my family, especially...

- to Dad and Mom for their love, endless support and instilling the importance of hard work and higher education;
- to grandma and late grandpa for their blessing;
- to Kopal for her love, patience and understanding.

## Table of content

Acknowledgement.....	a
Dedication .....	c
Table of content.....	d
List of symbols and abbreviations.....	i
Summary .....	ii
Zusammenfassung .....	iv
1. Introduction .....	1
2. Specific aim and objectives.....	5
3. Research approach.....	6
4. Results and discussion.....	12
5. Conclusion.....	19
5. Future perspectives.....	21
Reference.....	23
Curriculum Vitae.....	28
Declaration .....	31
Appendix – Declarations to the individual articles.....	32
<b>Article #1:</b> Qualitative Environmental Risk Assessment of Photolytic Transformation Products of Iodinated X-ray Contrast Agent Diatrizoic acid, <i>Science of The Total Environment</i> , <b>2014</b> , 482–483, 378–388. <a href="http://dx.doi.org/10.1016/j.scitotenv.2014.02.139">http://dx.doi.org/10.1016/j.scitotenv.2014.02.139</a>	
<b>Article #2:</b> Designing green derivatives of b-blocker Metoprolol: A tiered approach for green and sustainable pharmacy and chemistry, <i>Chemosphere</i> , <b>2014</b> , 111, 493–499. <a href="http://dx.doi.org/10.1016/j.chemosphere.2014.03.119">http://dx.doi.org/10.1016/j.chemosphere.2014.03.119</a>	
<b>Article #3:</b> A sustainable chemistry solution to the presence of pharmaceuticals and chemicals in the aquatic environment – the example of re-designing $\beta$ -blocker Atenolol. RSC Advances 5: 27-32. DOI: 10.1039/c4ra10294k	
<b>Article #4:</b> Addressing the Challenge of Micro-Pollutants in the Aquatic Cycle: Targeted Re-Designing the $\beta$ -Blocker Propranolol for Environmental Biodegradability. Environmental Science & Technology (submitted)	



## List of symbols and abbreviations

<b>4-OH PPL</b>	4-Hydroxypropranolol
<b>5-OH PPL</b>	5-Hydroxypropranolol
<b>7-OH PPL</b>	7-Hydroxypropranolol
<b>ADME</b>	Absorption, Distribution, Metabolism and Excretion
<b>API</b>	Active Pharmaceutical Ingredient
<b>ATL</b>	Atenolol
<b>CBT</b>	Closed Bottle Test
<b>DIAT</b>	Diatrizoic acid
<b>DOC</b>	Dissolved Organic Carbon
<b>EIC</b>	Extracted ion chromatogram
<b>EMA</b>	European Medicines Agency
<b>ESI-IT-MS<sup>n</sup></b>	Mass spectrometry with electrospray ionization and ion trap detector in tandem
<b>HO<sup>•</sup></b>	Hydroxyl radical
<b>HPLC (LC)</b>	High Performance Liquid Chromatography
<b>LC-MS/MS (LC-MS<sup>n</sup>)</b>	Liquid Chromatography Tandem Mass Spectrometry
<b>MTL</b>	Metoprolol
<b>min</b>	Minute
<b>MRT</b>	Manometric Respirometry test
<b>MS</b>	Mass spectrometry
<b>n</b>	The number of samples
<b>OECD</b>	Organization for Economic Co-operation and Development
<b>PBT</b>	Persistence, Bioaccumulation and Toxicity
<b>PPL</b>	Propranolol
<b>Photo-TP</b>	Photo-transformation product
<b>QSAR</b>	Quantitative structure-activity relationship
<b>REACH</b>	Registration, Evaluation, Authorization and Restriction of Chemicals
<b>STP</b>	Sewage treatment plant
<b>ThOD</b>	Theoretical oxygen demand
<b>TP</b>	Transformation product
<b>UV</b>	Ultraviolet

## Summary

Recent studies have confirmed that the aquatic ecosystem is being polluted with an unknown cocktail of pharmaceuticals, their metabolites and/or their transformation products (TPs). Although individual pharmaceuticals are typically present at low concentrations, their continuous input into the aquatic ecosystem and their toxic and persistent presence are the major environmental concerns. Therefore, it is necessary to assess the environmental risk caused by these aquatic pollutants. Data on exposure are required for quantitative risk assessment of parent compounds and their transformation products (TPs) and/or metabolites. Such data are mostly missing, especially for TPs, because of the non-availability of TPs and very often metabolites for experimental testing. Therefore, the application of different *in silico* tools for qualitative risk assessment can be used.

Also, the presence of these micro-pollutants (active pharmaceutical ingredients, APIs) in the aquatic cycle are increasingly seen as a challenge to the sustainable management of water resources worldwide due to ineffective effluent treatment and other measures for their input prevention. Given the poor prognosis for effluent treatment ('end of the pipe' approach) for input prevention of APIs in the environment, it is necessary to focus on the 'beginning of the pipe' strategy. The very beginning of the pipe is the molecules themselves. Therefore, novel approaches are needed like designing greener pharmaceuticals, i.e. better biodegradable ones in the aquatic environment after their release.

Therefore, the present research work focused on two important topics **a)** assessment of the environmental risk associated with the presence of highly prescribed drugs and their TPs; **b)** demonstrating the feasibility of the 'benign by design' concept for designing biodegradable drug derivatives, which will have the better biodegradability in the environment after their release. The present thesis includes four research articles (1-4) which address these approaches.

The **first article** is about the qualitative environmental risk assessment using the example of transformation products formed during photolysis (photo-TPs) of Diatrizoic acid (DIAT). Photolysis is the chemical reaction in which the compound is broken down by photons and often in combination with hydroxyl radicals. Photolysis is the most common abatement process of micro-pollutants in the environment. The qualitative risk assessment of DIAT and selected photo-TPs was performed by the PBT approach (i.e. Persistence, Bioaccumulation and Toxicity), using chemical analysis, experimental biodegradation test assays, QSAR models with several different toxicological endpoints and *in silico* read-across approaches.

The **second article** addresses a tiered approach of implementing green and sustainable chemistry principles for theoretically designing better biodegradable and pharmacologically potent pharmaceuticals derivatives. Photodegradation process coupled with LC-MS<sup>n</sup> analysis, biodegradability testing and *in silico* tools such as quantitative structure–activity relationships (QSAR) analysis and molecular docking proved to be a very significant approach for the preliminary stages of designing chemical structures that would fit into the “benign by design” concept in the direction of green and sustainable pharmacy. Metoprolol (MTL) was used as an example.

The **third article** was also the conceptual framework to get new drug derivatives that are biodegradable in order to tackle the global challenge of micro-pollutants in the aquatic cycle. This study increased the knowledge about the role of the attachment of certain functionalities to the parent drug molecule for its biodegradability whilst conserving drug-likeness. This approach was in the past a totally neglected issue within drug development. Atenolol (ATL), a selective  $\beta_1$  blocker, was selected as an example to incorporate the additional attribute such as biodegradability into its molecular structure while conserving its substructures responsible for  $\beta$  adrenergic receptor blocker activity.

In **fourth article**, the concept of designing green biodegradable pharmaceuticals has been proven through expanded experimental analysis setting out from the experiences collected as described in article two and three. This study could be considered as a more extensive feasibility study of rational design of green drug derivatives. The non-selective  $\beta$ -blocker Propranolol (PPL) was used as an example.

The risk assessment study (Article #1) contributes in enhancing the existing knowledge about the life cycle and behavior (fate) of pharmaceuticals with a special focus on photo-TPs which are generally formed during advanced effluent treatment and enter as such into the environment. Based on the obtained results, the application of the *in silico* tools for qualitative risk assessment analysis increased knowledge space about the environmental fate of TP in case of their non-availability for experimental testing.

The benign by design studies (Article #2-4) were based on the knowledge and experience collected during the work on DIAT. It demonstrated the feasibility of a novel approach of designing comparatively better degradable and pharmacological potent derivatives through the implementation of “green chemistry” principles. However, the present approach is in the juvenile stage and further knowledge has to be collected beforehand for the full implementation of this approach into drug development.

## Zusammenfassung

Neuere Studien haben bestätigt, dass das aquatische Ökosystem mit einem unbekanntem Cocktail von Medikamenten, deren Metaboliten und/oder deren Transformationsprodukte (TPs) belastet wird. Obwohl einzelne Arzneimittel in der Regel nur in geringen Konzentrationen in der Umwelt vorhanden sind, sind ihr ständiger Eintrag in das aquatische Ökosystem, sowie ihre giftigen Eigenschaften und anhaltende Präsenz ein großes Umweltproblem. Daher ist es notwendig, das durch diese Wasserschadstoffe verursachte Umweltrisiko zu bewerten. Daten über die Exposition sind für die quantitative Risikobewertung von Ausgangssubstanzen und deren Transformationsprodukte (TPs) und /oder Metabolite erforderlich. Solche Daten fehlen meistens, insbesondere für TPs, aufgrund der Nichtverfügbarkeit von TPs und häufig der Metaboliten für experimentelle Tests. Deshalb kann die Anwendung verschiedener *in silico* Methoden für die qualitative Risikobewertung herangezogen werden. Die Anwesenheit dieser Mikroschadstoffe (pharmazeutische Wirkstoffe, APIs) im aquatischen Kreislauf wird zunehmend weltweit als Herausforderung für die nachhaltige Bewirtschaftung der Wasserressourcen aufgrund ineffektiver Abwasserbehandlung und anderer Maßnahmen zur Eingabe-Prävention gesehen. Angesichts der schlechten Prognose für die Abwasserbehandlung („Ende der Leitung“-Ansatz) für die Eingabe-Prävention von APIs in die Umwelt ist es notwendig, sich auf die „Anfang des Rohres“-Strategie zu konzentrieren, z.B durch die Fokussierung auf Verbesserung der untersuchten Moleküle. Daher sind neue Ansätze wie die Gestaltung „grüner“ Arzneimittel erforderlich, d. h. Moleküle, die nach ihrer Freisetzung in die Umwelt besser biologisch abbaubar sind.

Daher konzentriert sich die vorliegende Forschungsarbeit auf zwei wichtige Themen **a)** Beurteilung der Umweltrisiken durch häufig verordnete Medikamente und durch ihre Abbauprodukte; **b)** Vorführung der Machbarkeit des „Benign by Design“ Konzeptes für die Gestaltung von biologisch abbaubaren Pharmazeutika-Derivaten, die eine verbesserte biologische Abbaubarkeit in der Umwelt nach ihrer Freisetzung haben. Die vorliegende Arbeit umfasst vier Forschungspublikationen (1-4), die diese Ansätze adressieren.

Im **ersten Artikel** geht es um die qualitative Bewertung der Umweltrisiken am Beispiel der Transformationsprodukte durch Photolyse (Photo-TP) von Diatrizoessäure (DIAT). Photolyse ist die chemische Reaktion, bei der die Verbindung mithilfe von Photonen und oft in Kombination mit Hydroxyl-Radikalen abgebaut wird. Photolyse ist der häufigste Eliminationsprozess von Mikroverunreinigungen in der Umwelt.

Die qualitative Risikobewertung von DIAT und ausgewählter photo-TP wurde mit dem PBT Ansatz (d. h. Persistenz, Bioakkumulation und Toxizität) in Kombination mit chemischer Analyse, experimentellen Tests der biologischen Abbaubarkeit, der Verwendung unterschiedlicher QSAR-Modelle mit verschiedenen toxikologischen Endpunkten und *in silico* „read-across“ Ansätzen durchgeführt.

Der **zweite Artikel** beschäftigt sich mit einer abgestuften Vorgehensweise der Umsetzung der Grundsätze der „grünen“ und nachhaltigen Chemie für die Gestaltung besser biologisch abbaubarer und gleichzeitig pharmakologisch wirksamer Arzneimittel. Photoabbauprozesse gekoppelt mit LC-MS<sup>n</sup> Analyse, Bioabbaubarkeitstests und *in silico* Methoden wie „quantitative structure–activity relationships“ (QSAR) Analyse und molekulares „Docking“ haben sich als ein sehr wichtiger Ansatz für die Gestaltung des „Benign by Design“ Konzeptes erwiesen. Metoprolol (MTL) wurde als Beispiel verwendet.

Der **dritte Artikel** ist auch eine konzeptionelle Arbeit, um neue Medikamenten-Derivate, die biologisch abbaubarer sind, zu bekommen, um die globale Herausforderung von Mikroverunreinigungen im aquatischen Kreislauf zu bewältigen. Diese Studie hat das Wissen über die Rolle bestimmter Funktionalitäten für die biologische Abbaubarkeit am Ausgangsmolekül erhöht, während gleichzeitig die Erhaltung gewünschter pharmakologischer/pharmazeutischer Eigenschaften untersucht wurde. Dieser Ansatz war in der Vergangenheit ein völlig vernachlässigtes Thema in der Medikamentenentwicklung. Atenolol (ATL), ein selektiver  $\beta_1$ -Blocker, wurde als Beispiel ausgewählt, um das zusätzliche Attribut „biologische Abbaubarkeit“ in die Struktur zu integrieren, während gleichzeitig die Erhaltung der Elemente für die  $\beta$ -adrenerge Rezeptor-Blocker-Aktivität angestrebt wurde.

Im **vierten Artikel** wurde das Konzept der Gestaltung biologisch abbaubarer Pharmazeutika durch eine erweiterte experimentelle Analyse zur Festigung der Erfahrungen aus den Manuskripten zwei und drei demonstriert. Diese Studie könnte als weitergehende Machbarkeitsstudie für das rationale „Design“ von grünen Medikamentenderivaten berücksichtigt werden. Der nichtselektive  $\beta$ -Blocker Propranolol (PPL) wurde als Beispiel verwendet.

Die Studie zur Risikobewertung (Artikel # 1) trägt zur Verbesserung der vorhandenen Kenntnisse über den Lebenszyklus und das Verhalten (Schicksal) von Arzneimitteln bei. Die Arbeiten haben den speziellen Fokus auf Photo-TP, die in der Regel während fortschrittlicher Abwasserbehandlung entstehen und als solche in die Umwelt gegeben werden. Basierend auf den erhaltenen Ergebnissen hat die Anwendung der *In silico*-Methoden für die qualitative

Risikobewertung das Wissen über das Umweltverhalten von TP im Falle ihrer Nichtverfügbarkeit für experimentelle Tests erhöht.

Die Studien zur gezielten Entwicklung umweltfreundlicher Medikamente (Artikel # 2-4) wurden auf dem Wissen und der Erfahrung aus der Arbeit an DIAT aufgebaut. Sie demonstrierten die Machbarkeit und Chancen eines neuartigen Ansatzes der Gestaltung vergleichsweise besser abbaubarer und pharmakologisch aktiver Derivate durch die Umsetzung der Prinzipien der „grünen Chemie“. Allerdings ist der vorliegende Ansatz im Anfangsstadium und das Wissen für die vollständige Umsetzung dieses Ansatzes in der Medikamentenentwicklung muss weiterhin vergrößert werden.

# 1. Introduction

Over the past decades, the presence of active pharmaceutical ingredients (APIs) residues, their metabolites and their transformation products (TPs) (often referred as micro-pollutants) in the aquatic environment are considered as a major environmental problem due to their continuous input into the aquatic ecosystem including sewage flows, surface and groundwater and persistent presence even at low concentrations ( $\text{ng L}^{-1}$  to  $\mu\text{g L}^{-1}$ ) (Daughton and Ternes, 1999; Halling-Sørensen et al., 1998; Heberer, 2002; Khetan and Collins, 2007; Kümmerer, 2008; Santos et al., 2010).

Generally, APIs enter the aquatic environment as unaltered or partially metabolized active chemicals through human excretion. The other sources of these micro-pollutants to enter the aquatic environment are from hospitals, pharmaceutical industry or from domestic waters, through disposal of unused drugs (Kümmerer, 2008; Santos et al., 2010).

The most extensively discussed strategies for the prevention of these micro-pollutants to enter into the aquatic environment are (advanced) treatment processes. These technical treatment processes like UV irradiation, ozonation and chlorination can also be responsible for the formation of stable TPs (Arnold and McNeill, 2007; Boxall, 2009; Joss et al., 2005; Kanda et al., 2003). These TPs can contribute significantly to the risk posed by the parent compound if (a) they are formed with a high yield and (b) they are persistent and/or have high a toxic potential (Fatta-Kassinos et al., 2011; Santiago-Morales et al., 2013; Trovó et al., 2009).

Furthermore, these advanced treatment procedures should not be considered as a general solution to the problem, but as a part of the solution and as well the problem as some of these treatment processes result in the generation of largely unknown TPs. Often, these treatment processes are not compatible with sustainable development because they focus on the end of pipe solutions. This means that they (treatment process) are normally implemented as a last stage of a process before the discharge of micro-pollutants to the aquatic environment.

However, these treatments have been reported to have their own specific limitations and drawbacks (Jones et al., 2007; Kümmerer, 2008; Wenzel et al., 2008). Also when these micro-pollutants enter into the environment, they are subjected to various abiotic and biotic processes but which may or may not end up in complete transformation or full mineralization. Several national and international studies published in the recent years have confirmed the occurrence of an aggregation of APIs and their persistent and sometime toxic TPs in surface waters (Chang et al., 2008; Han et al., 2006; Kormos et al., 2011; Michael et al., 2013; Miège

et al., 2009; Ternes et al., 2004). Therefore, it is necessary to perform risk assessment studies of these micro-pollutants in order to gain knowledge about their behavior (fate) in the aquatic environment.

Due to the given limited success of end of pipe technologies and the fact that pharmaceuticals even after properly and monitorially consumed finally end up in waste water, it is advantageous to shift the focus to the other strategies i.e. ‘beginning of the pipe’.

One of the principles of green chemistry is that chemical products should be designed in such a way that their efficacy is preserved while with reduced toxicity and improved biodegradability (Anastas and Warner, 1998). The latter means that to design APIs that can mineralize at a reasonable rate and more or less completely in normal effluent treatment and in the aquatic environment. One building block thereof is the benign by design concept (Kümmerer, 2007, 2012). It is most promising in terms of sustainability and an important building block within green and sustainable pharmacy and chemistry (Kümmerer, 2010). According to this concept, small alterations in the chemical structure of an API may have a significant impact on its activity, solubility and polarity on one hand and on biodegradability on the other hand. Therefore it is reasonable to assume that a set of functionalities exists that can foster both. Designing such biodegradable drugs is a challenge that is addressed in the research presented here.

The later approach of designing biodegradable pharmaceutical derivatives is a long-term approach for the sustainable management of the environment. But developments of such novel designing approaches require time and huge financial support before their full implementation. Therefore, it is quite important to identify the environmental impacts of the already existed APIs, after their release in the environment. Thus, the presented PhD work focusses on two important approaches **a)** assessment of the environmental risk associated with the presence of highly prescribed drugs and their TPs; **b)** demonstrating the feasibility of the benign by design concept for designing biodegradable drug derivatives, which are better biodegradable in the environment after their release. Both approaches are described below in detail.

#### **a) Environmental risk assessment approach**

Due to the ambiguous presence of APIs in environment, risk assessment studies will assist to identify such micro-pollutants that could have harmful impact to the environment. The research about the environmental impact of these micro-pollutants is a huge and difficult task



due to the lack of knowledge about their long-term effects like persistence, bioaccumulation, toxicity which certainly cannot be excluded (La Farré et al., 2008).

When carrying out an environmental risk assessment, the exposure of these micro-pollutants to the different environmental compartments needs to be estimated. Such exposure-driven assessments are carried out on the basis of available monitoring data and/or modeling. The environmental presence of transformation products further adds complexity to exposure driven risk assessment strategies. The transformation products of pharmaceuticals are usually formed in low concentrations within complex matrices. This makes their isolation and purification a difficult task (Trautwein and Kümmerer, 2012). Further these compounds are often not commercially available and targeted synthesis or isolation can be expensive and time consuming, making their experimental testing rather difficult. These shortcomings make it necessary to employ other tools for the environmental risk assessment of transformation products. One possibility is the usage of *in silico* tools which are based e.g. on quantitative structure–activity relationship (QSAR) calculations.

The technical guidance documents on risk assessment for chemicals within REACH, the European chemicals regulation (European Commission, 2003a, 2003b) recommends to apply *in silico* tools to perform the risk assessments for chemicals in case of a lack of information on their environmental fate and effects. The European Medicine Agency (2005) guidelines for environmental risk assessment do not explicitly mention the use of *in silico* tools. However, it refers to the EU technical guidelines.

Accordingly, the PBT (Persistence, Bioaccumulation and Toxicity) approach can also be used. Substances fulfilling the PBT criteria are of priority for risk management consideration. QSAR models should be used for a wide range of endpoints which are required for a risk assessment, including several toxicological and ecotoxicological endpoints and physico-chemical/fate parameters (including biodegradability) (European Commission, 2003b).

Thus, the combination of experiments, *in silico* tools and *in silico* read-across (i.e. predicting the required values for the target compound on the basis of the known values for similar structurally related substances) approaches can increase the understanding and assessment of the fate and risk imposed by the transformation products even when insubstantial data of their exposure to environment is available.

## **b) Demonstrating the feasibility of the benign by design concept for designing biodegradable drug derivatives**

The 'benign by design' concept is most promising in terms of sustainability and an important building block within green and sustainable pharmacy and chemistry (Kümmerer, 2010). Such approaches of designing better biodegradable chemicals and pharmaceuticals will not only implement chemistry and pharmacy towards the sustainability but will transform the chemistry and pharmacy itself to be more sustainable.

The first step to design such biodegradable chemicals and pharmaceuticals would be to identify the pharmacophore (i.e. the substructure responsible for a specific activity) and other substructures. Designing biodegradable APIs can be achieved by the attachment or removal of certain functional groups without disturbing the pharmacophore of the known drug molecule.

This PhD work was focused on  $\beta$ -blocker class of pharmaceuticals because of their high consumption in Europe especially in Germany (Schwabe and Paffrath, 2013) and their non-biodegradable and highly persistent nature (Santos et al., 2010). The additional attribute such as biodegradability was incorporated in the structures of  $\beta$ -blocker while conserving their substructures responsible for  $\beta$  adrenergic receptor blocker activity.

It is known that an aromatic ring and a  $\beta$ -ethanolamine moiety are considered essential (Gorre and Vandekerckhove, 2010; Gringauz, 1997) for their specific activity. The very first step to design biodegradable  $\beta$ -blocker APIs is thereof to generate new molecules that possess both the above mentioned substructures responsible for the specific action as a  $\beta$ -blocker i.e. aromatic ring and  $\beta$ -ethanolamine. These new drug-like derivatives (photo-transformation products, photo-TPs) were generated through UV photolysis in this PhD work. During photolysis the small molecular changes in the structure of  $\beta$ -blocker occur either by the attachment to or removal of certain functional groups from the parent structure.

In the present PhD work, three different  $\beta$ -blockers were selected, namely Atenolol [ATL], Metoprolol [MTL] and Propranolol [PPL]. ATL and MTL were used to collect the first knowledge on the feasibility of the approach designing green biodegradable derivatives. The knowledge collected and modification built on the experience from above mentioned two studies were applied for PPL study to proceed further to the proof of concept for such designing a new biodegradable drug molecule. Such studies demonstrated the feasibility and opportunities of a novel approach of designing comparatively better degradable and pharmacological potent new drug derivatives through the implementation of green chemistry principles.

## 2. Specific aim and objectives

The specific objectives of the PhD project were as follows:

1. Assessing the environmental risk associated with the photo-transformation products (photo-TPs) of a commonly used X-ray contrast agent Diatrizoic acid (DIAT). (**Article #1**)
  - ❖ Generation of photo-TPs under controlled conditions
  - ❖ Development of analytical methods for the identification of DIAT and its photo-TPs and elucidation of photodegradation pathways.
  - ❖ Aerobic biodegradation testing of the mixture of photo-TPs.
  - ❖ Application of various computer-aided QSAR models to predict the environmental fate and preliminary toxicity for the photo-TPs of DIAT.
  
2. Feasibility study for designing biodegradable  $\beta$ -blocker derivatives. (**Article #2-3**)
  - ❖ Generation of derivatives through photolysis process and their identification and pathways elucidation.
  - ❖ Screening these generated derivatives for biodegradability and identifying the comparatively better biodegradable derivatives (photo-TPs). Identification of structural changes in these biodegradable derivatives.
  - ❖ Investigation of pharmacological potency (Article #2) or drug-likeness (Article #3) of the selected biodegradable derivatives through *in silico* molecular docking analysis and ADME (Absorption, Distribution, Metabolism and Excretion) properties prediction, respectively.
  
3. Advanced feasibility study of designing green  $\beta$ -blocker derivatives. (**Article #4**)
  - ❖ Generation, identification and pathways elucidation of photo-TPs (derivatives).
  - ❖ Screening photo-TPs for biodegradability and pharmacological potency.
  - ❖ *In vitro* analysis of pharmacological potency of selected lead candidates.
  - ❖ ADME-Tox properties prediction of the lead candidate ( $\beta_1$  receptor binding).

### 3. Research approach

In order to fulfill the above mentioned objectives, the following work tasks were addressed in the four research articles.

**Objective 1: Assessing the environmental risk associated with the photo-transformation products (photo-TPs) of a commonly used X-ray contrast agent Diatrizoic acid (DIAT).**

**Title:** Qualitative environmental risk assessment of photolytic transformation products of iodinated X-ray contrast agent Diatrizoic acid. (**Article #1**)

This study focuses on the environmental risk assessment of one of the commonly used iodinated X-ray contrast agents Diatrizoic acid (DIAT) and its transformation products formed during photolysis (“photo-TPs”). Generally, iodinated contrast agents are designed to be persistent and very polar so that they are not metabolized in the human body and are excreted unchanged through urine within short period of time (half-life just a few hours) (Putschew and Jekel, 2006). DIAT undergoes incomplete elimination in sewage treatment plants (STPs) and is reported to be present in various environmental media (Howard and Muir, 2011; Putschew et al., 2000; Ternes and Hirsch, 2000).

DIAT itself is not biodegradable. It was however photolysed (150 W medium-pressure Hg-lamp) in order to check its photo-mineralization potential. The pathway of the formation of photo-TPs of DIAT was elucidated in this article. Then, the mixture of DIAT and photo-TPs formed during photolysis was tested in two aerobic biodegradation test assays of different bacterial density in order to investigate their biodegradability. Aerobic biodegradation test such as Closed Bottle Test [CBT, OECD 301 D] (OECD, 1992b) and Manometric Respirometry Test [MRT, OECD 301 F] (OECD, 1992a) were applied according to OECD 301 guidelines. CBT was employed because it is the most stringent biodegradation test with low bacterial density and diversity in order to avoid any false positive results.

The fate, physico-chemical and toxicological properties of photo-TPs of DIAT were assessed via a combination of advanced chemical analysis such as LC-MS analysis with experimental aerobic biological degradation assays, PBT profiler, and *in silico* read-across approaches. In order to keep the workload manageable, the photo-TPs with relative abundance  $\geq 2\%$  were selected as of main interest for *in silico* fate and toxicological properties predictions. Table 1 summarized different *in silico tools* (QSAR software) with various physico-chemical and toxicological endpoints’ models which were used for the assessment of the fate of photo-TPs

Table 1: List of all the *in silico* models and software used for the fate and toxicity predictions in all four articles (Article #1-4).

Activity	QSAR Software	Models	End points	References
Photodegradation products	METAPC v 1.8.1	Photodegradation	Photoproducts of chemicals under natural like conditions	(Sedykh et al., 2001)
Physico-chemical properties	Catalogic v 5.11.6 TB (OASIS)	BCF base-line model v.02.05	log BCF	(Dimitrov et al., 2005)
		BCF base-line model D/P v.01.01	log BCF with consideration of distribution coefficients (log D) and partitioning coefficients (log P)	(Dimitrov et al., 2012)
	PBT Profiler	PBT Profiler	Persistence, bioaccumulation and toxicity	(U.S Environmental Protection Agency)
Biodegradation	CASE Ultra v.1.4.5.1	MITI-I test (OECD 301C, module AU6)	Ready biodegradability according to MITI-I test	(Chakravarti et al., 2012)
	EPI Suite (EPIWEB 4.1)	BIOWIN 6	Nonlinear regression models predicting the Ready biodegradability according to MITI-I test	(EPA, 2013)
	Catalogic v 5.11.6 TB (OASIS)	CATABOL 301C model CATALOGIC 301C models	Ready biodegradability according to MITI-I test Ready biodegradability according to MITI-I test	(Laboratory of Mathematical Chemistry Bulgaria, 2012)

Toxicity	CASE Ultra v.1.4.5.1 (MultiCASE Inc.)	Human carcinogenicity (A0J)	Carcinogenicity	(Chakravarti et al., 2012; Saiakhov et al., 2013)
		Micronucleus formation in vivo composite (A7S)	Genotoxicity	
		Chromosome aberration in vitro composite (A7U)	Mutagenicity	
		Mutagenicity Ames (A2H)	Mutagenicity against <i>Salmonella Typhimurium</i>	
	Leadscope V. 3.0.11-1	Microtox toxicity environmental bacteria (AUA).	Bacterial toxicity	
		Bacterial mutagenesis (BM) model	Mutagenicity as a result of interaction with DNA of <i>Salmonella Typhimurium</i> or <i>Escherichia coli</i>	SAR Genotox Database 2012 (Roberts et al., 2000)
		Mammalian mutagenesis (MM)	Mutagenicity	
		In vitro chromosome aberration (IVCA)	Mutagenicity	
		In vivo micronucleus (IVMN)	Genotoxicity	
Catalogic v 5.11.6 TB (OASIS)	<i>Vibrio fischeri</i> pT5 v.01	Acute toxicity against <i>V. fischeri</i> after 5 min, IC50 [mg/L]	(Laboratory of Mathematical Chemistry Bulgaria, 2012)	
	<i>Vibrio fischeri</i> pT15 v.01	Acute toxicity against <i>V. fischeri</i> after 15 min, IC50 [mg/L]		
	<i>Vibrio fischeri</i> pT30 v.01	Acute toxicity against <i>V. fischeri</i> after 30 min, IC50 [mg/L]		
	<i>in vitro</i> Ames model	Mutagenicity against <i>Salmonella Typhimurium</i>		

in all the studies. The more detailed description of the experimental procedure can be found in Article #1 (see appendix).

### **Objective 2: Feasibility study for designing biodegradable $\beta$ -blocker derivatives.**

The second and third articles address the feasibility study for designing green, biodegradable pharmacologically potent drug derivatives.

**Title:** Designing green derivatives of  $\beta$ -blocker Metoprolol: A tiered approach for green and sustainable pharmacy and chemistry. (**Article #2**)

In the **second article**, Metoprolol (MTL) one of the highly prescribed  $\beta$ -blockers in Europe, which undergoes incomplete elimination in sewage treatment plants (STPs) (Maurer et al., 2007), was selected. A large number of derivatives (photo-TPs) were generated through photolysis. On the basis of the results and literature finding, a scheme of the photodegradation pathway of MTL was developed. The biodegradability of MTL and its derivatives (photo-TPs) were assessed by two aerobic biological degradation assays of different bacterial density i.e. CBT and MRT (similar like Article #1). Thereby, the derivatives (photo-TPs) that had improved biodegradability compared to the parent compound MTL were identified by the analysis of the samples from the start and end of each biodegradation tests by LC–MS.

The identified biodegradable derivatives were then *in silico* analyzed by QSAR models (summarized in Table 1) for ready biodegradability to get a further insight of the structural alterations. Software package Case Ultra (Multicase Inc.) identifies the structural changes in the derivatives (photo-TPs) molecule that would modulate their biodegradability. This knowledge contributes to a better understanding that would be the basis of a rational design of better biodegradable compounds in the future according to the benign by design approach.

The pharmacological activity was investigated for the identified biodegradable derivatives (photo-TPs) which were observed to undergo biodegradation  $\geq 10\%$  in the test assays and their docking scores were compared with MTL itself. Comparable docking scores provide evidence for non-inferior or improved pharmacological activity of the derivatives compared to MTL.

Evaluation of the pharmacological properties of MTL and its biodegradable derivatives (photo-TPs) was performed by molecular docking analysis (*in silico*) with software Schrodinger Maestro Version 2012 (v.9.3). Generally, MTL is known to be a selective but not specific  $\beta_1$  adrenergic receptor antagonist (Abrahamsson et al., 1988). Thus, it can be assumed that MTL has considerable affinity towards the  $\beta_2$  adrenergic receptor, too. Therefore, the

docking experiments were performed on the  $\beta_2$  adrenergic receptor instead of  $\beta_1$  receptor as x-ray structure of human  $\beta_1$  receptor grid is not publically available.

The output from *in silico* molecular docking analysis is called as docking score which indicates the binding interaction of the molecule to the protein or enzyme of interest. The lower the docking scores, the better the molecule is supposed to bind to the proteins. In present study, the docking score of ICI-118,551 (-8.7) was set as a reference score to identify pharmacologically active biodegradable derivatives. ICI-118,551, a selective  $\beta_2$  adrenergic receptor antagonist (Summerhill et al., 2008), binds to the  $\beta_2$  subtype receptor with at least 100 times greater affinity than to the two other  $\beta$  adrenergic receptors ( $\beta_1$  or  $\beta_3$ ) (Emorine et al., 1989; Mauriège et al., 1988). ICI-118,551 is not therapeutically used in humans although it has been used widely in research to understand the action of the  $\beta_2$  adrenergic receptor

A further important prerequisite for drug identities and APIs is that they should not be toxic. First of all mutagenicity, genotoxicity and carcinogenicity have to be absent. Therefore, *in silico* predictions for these toxicity endpoints for the lead candidates (biodegradable and pharmacologically comparable to MTL) were performed by employing the QSAR toxicity models summarized above in Table 1. The more detailed description of the experimental procedure can be found in Article #2 (see appendix).

**Title:** A sustainable chemistry solution to the presence of pharmaceuticals and chemicals in the aquatic environment – the example of re-designing  $\beta$ -blocker Atenolol. (**Article #3**)

In the **third article**, Atenolol (ATL) a selective  $\beta_1$  blocker was selected as an example to refine the above described approach by incorporating the additional attribute such as biodegradability in ATL molecule while conserving its substructures responsible for  $\beta$  adrenergic receptor blocker activity. ATL is not biodegradable in the aquatic environment and has frequently been detected in the aquatic environment including drinking water at concentrations up to  $120 \mu\text{g L}^{-1}$  (Santos et al., 2010).

The very first step was to generate new molecules that possess the pharmacophore (i.e. aromatic ring and a  $\beta$ -ethanolamine moiety) through photolysis. Photolysis of ATL resulted in numerous derivatives. Their supposed molecular structure and reaction pathways were elucidated by ion-trap LC-MS/MS. In the next step, aerobic biodegradation tests (CBT and MRT) for the assessment of chemicals' biodegradability in the environment were performed for the resulting mixture of photolytic treatment (same procedure as articles #1-2). Thereby, the derivatives (photo-TPs) that were found of improved biodegradability compared to the parent compound and still possessed the aromatic ring and a  $\beta$ -ethanolamine moiety were



identified through LC-MS analysis (similar like articles #2). They were then further assessed with the help of ready biodegradability model of software package Case Ultra (Multicase Inc.) in order to identify the structural alteration during photolysis which modulated the biodegradability of the derivatives' molecule (similar like article #2).

An indispensable prerequisite for new molecules that could serve as new lead structures for new drug candidates is that they can act as an API. Assessment of drug likeliness is a very first step within this context. Therefore the detainment of the drug-like properties (absorption, distribution, metabolism and excretion; ADME) of the biodegradable derivatives (photo-TPs) that still contained the aromatic ring and a  $\beta$ -ethanolamine moiety were investigated through *in silico* QikProp software. The derivatives which lack either of the essential substructures or are less drug-like and less orally available were omitted in respect of biodegradable ATL derivatives. The final step was an *in silico* toxicity assessment of those biodegradable and drug-like candidates. Therefore, *in silico* predictions for mutagenicity, genotoxicity and carcinogenicity endpoints for the lead candidates (biodegradable drug-like derivatives) of ATL were performed by employing the QSAR toxicity models summarized above in Table 1. The more detailed description of the experimental procedure can be found in Article #3 (see appendix).

### **Objective 3: Advanced feasibility study of designing green $\beta$ -blocker derivatives**

**Title:** Addressing the Challenge of Micro-Pollutants in the Aquatic Cycle: Targeted Re-Designing the  $\beta$ -Blocker Propranolol for Environmental Biodegradability. (**Article #4**)

The **fourth article** was a step forward for designing biodegradable  $\beta$ -blocker derivatives. In that article Propranolol (PPL), a non-selective  $\beta$ -blocker (Black et al., 1964) which has the affinity towards both  $\beta_1$  and  $\beta_2$  adrenergic receptor (Lechat, 2006) was selected for the investigations. It had been reported as a non-biodegradable and highly persistent (Benz et al., 2005) API and accordingly detected in sewage treatment plant effluent at a concentration range from 30 to 373 ng L<sup>-1</sup> (Santos et al., 2010).

The derivatives (photo-TPs) were generated by photolysis under UV light. The mixture of derivatives was screened for biodegradability through experimental aerobic biodegradation assays (similar like articles #1-3). The better biodegradable ones were shortlisted (procedure as describes in articles #2-3) for the further investigations. The pharmacological potency of the biodegradable derivatives was compared with PPL by *in silico* molecular docking analysis (same procedure as described in article #2). This combination of biodegradability and *in silico*

pharmacological activity analysis provided a few lead structures of better biodegradable and possibly pharmacologically potent derivative.

To confirm of the properties of shortlisted lead derivatives, it was necessary to test them in a single molecule set up in the respective test assays. It turned out that the three biodegradable derivatives of PPL (i.e. 4-OH PPL, 5-OH PPL and 7-OH PPL) were commercially available as racemic mixture. Therefore, they were individually tested in CBT to investigate their extent of aerobic biodegradation. The derivative with highest degree of biodegradation was then selected and tested with an *in vitro* pharmacological assay to confirm its predicted pharmacological potency.

*In vitro* pharmacological analysis was performed through the PathHunter® eXpress  $\beta$ -Arrestin Human and Ortholog GPCR kits (DiscoverX Corporation, USA). The kit contains a genetically modified CHO-K1 cell line expressing the human  $\beta_1$  adrenergic receptor (DiscoverX, 2013). Isoprenaline hydrochloride, an agonist for the  $\beta_1$  adrenergic receptor, was used as a positive control in the test assay. PPL and other selected biodegradable derivative were tested in the assay for their antagonist activity. The starting concentration of the agonist (Isoprenaline) was  $22 \times EC_{80}$  value while the starting concentrations of the antagonists (PPL and biodegradable derivatives) were  $1100 \times IC_{50}$  value. Three independent test runs were performed and the average activity from those experiments was plotted against the concentration of the test chemicals. One of the tested derivative was found to have the similar pharmacological potency as a  $\beta_1$  adrenergic receptor blocker as PPL. However, it was much more biodegradable than PPL.

Again, the ADME-Tox properties were assessed for that derivative through *in silico* QikProp software (as described in article #3) and were also compared with PPL and other selective  $\beta_1$  pharmaceuticals ATL and PPL. The more detailed description of the experimental procedure can be found in Article #4 (see appendix).

## 4. Results and discussion

### Article #1: Qualitative environmental risk assessment of photolytic transformation products of iodinated X-ray contrast agent Diatrizoic acid.

The photolytic degradation of DIAT follows first-order kinetics, which resulted in a complete primary elimination of parent compound without complete mineralization after 256 min of UV exposure. This partial mineralization indicates the formation of photo-TPs. Based on analytical results and chemical knowledge on reactivity, a scheme of the photolytic

degradation pathway was developed. The preferential pathway of the photodegradation of DIAT observed was the *ipso*- attack of hydroxyl radical ( $\cdot\text{OH}$ ) to the carbon atom that have either iodine atom or the carboxylic acid moiety (methanoate moiety). This *ipso*- attack of hydroxyl radical resulted in the formation of the phenolic photo-TPs.

DIAT was confirmed to be not readily biodegradable. This is in accordance with the earlier published studies (Haiß and Kümmerer, 2006; Joss et al., 2006; Kalsch, 1999). The PBT profiler predicted DIAT as a very persistent and non-bioaccumulative chemical, which might possess a moderate chronic toxicity towards fish. The predictions of  $\log k_{ow}$  indicated DIAT as a polar compound and therefore high mobility of DIAT should be expected in the aquatic environment. The water and air partitioning coefficient (Henry constant, H) prediction of DIAT indicates that its elimination through evaporation into the atmosphere is most likely insignificant.

QSAR software Case Ultra predicted DIAT as a nontoxic chemical against environmental bacteria. It also predicted DIAT as non-mutagenic chemical which is in accordance with the published literature (Wheeler et al., 1980). The human carcinogenicity model and genotoxicity model of Case Ultra predicted DIAT as non-carcinogenic and non-genotoxic chemical (see Table 2).

During the LC-MS analysis of biodegradation test samples 15 photo-TPs were found to be better biodegradable than DIAT itself in both biodegradation test assays. However, an inhibitory effect was observed within the first couples of days in the toxicity control of photodegraded samples (i.e. 32min, 128 min and 256 min samples) in both investigated aerobic biodegradation test assays. There was no such inhibitory effect observed in the toxicity control when the parent compound DIAT (i.e. 0 min sample) was subjected to test assays. This means that there might be a few photo-TPs present which had the toxicity against inoculum's bacteria. Thus, it can be concluded that a few photo-TPs had more toxic potency than the parent compound

The PBT profiler predicted that selected photo-TPs (relative abundance  $\geq 2\%$ ) of DIAT might be less persistent than DIAT and also do not possess any bioaccumulation threat to aquatic organism in the environment. But they might have a moderate chronic toxicity towards fish similar to DIAT. Predictions of  $\log k_{ow}$  indicated the selected photo-TPs might be more polar than DIAT and high mobility of those photo-TPs should be expected in the aquatic environment. Henry constant (H) prediction of photo-TPs indicates that their elimination through evaporation into the atmosphere will also be unlikely.

**Table 2:** *In silico* toxicity prediction by various models of Case Ultra, Catalogic and Leadscope software for DIAT and its selected photo-TPs (relative abundance  $\geq 2\%$ )

Photo-TPs	CASE Ultra					Leadscope	OASIS Catalogic V.5.11.6
	A	B	C	D	E	E	E
DIAT	-	-	-	-	-	-	-
TP <sub>1</sub> 351	-	+	+	-	-	+	-
TP <sub>2</sub> 351	-	+	+	-	-	+	-
TP 395	-	+	-	-	-	-	-
TP <sub>1</sub> 505	-	+	-	-	-	-	-
TP <sub>2</sub> 505	-	-	-	§*	-	-	-
TP <sub>3</sub> 505	-	+	-	-	-	-	-
TP <sub>4</sub> 505	-	-	-	§	-	-	-
TP <sub>1</sub> 522	-	+	-	OD	-	-	-
TP <sub>2</sub> 522	-	+	-	OD	-	-	-
TP <sub>3</sub> 522	-	+	-	OD	-	-	-

A- Human carcinogenicity; B- Micronucleus in vivo composite; C- Chromosome aberration; D- Microtox against environmental bacteria; E- Salmonella Mutagenicity; OD: Out of Domain means that the test chemical is not included in the applicability domain of the applied model; §\*: Inconclusive with asterisk symbol (\*) means both positive and deactivating alerts were found in the same molecule and therefore a clear result cannot be provided; §: Inconclusive means that the molecule contained too many unknown fragments; + : a positive alert for corresponding activity; - : a negative alert for corresponding activity.

Case Ultra provided ambiguous predictions for the shortlisted photo-TPs which are summarized in Table 2. The shortlisted photo-TPs were predicted to be non-mutagenic except TP<sub>1&2</sub> 351. This photo-TP TP<sub>1&2</sub> 351 had a positive alert for mutagenicity and requires further experimental testing to confirm this prediction. The human carcinogenicity model of Case Ultra predicted photo-TPs as non-carcinogens. The genotoxicity model adumbrated most of the selected photo-TPs (TP<sub>1-2</sub> 351, TP 395, TP<sub>1&3</sub> 505 and TP<sub>1-3</sub> 522) to be active, i.e. might be genotoxic.

Furthermore, Grönwäller (1998) reported the formation of cytotoxic mixture of TPs during the XeCl excimer laser irradiation of DIAT. However, the same TPs were formed in the

present study during UV photolysis. Therefore, it could be assumed that the mixture photo-TPs formed in the study might also have the cytotoxic properties and may cause threat to humans and the environment. Moreover, DIAT has also been classified as nephrotoxic (Andreucci et al., 2006; Harmon et al., 2009; Messana et al., 1988) and neurotoxic (Bryan et al., 1982) chemical. The photo-TPs formed during photolysis are structurally related to DIAT, therefore on the basis of read-across approaches it might be reasonable to assume that a few of the photo-TPs may possess similar properties and could have nephrotoxic and neurotoxic properties.

The results concluded from the *in silico* toxicological predictions significantly indicate the need of assessing photo-TPs toxicity through various experimental testing. The results of this part of the work demonstrate how *in silico* methods could be used to guide for further investigations (e.g. by priority setting) and risk assessment of parent compounds and TPs

## **Article #2: Designing green derivatives of $\beta$ -blocker Metoprolol: A tiered approach for green and sustainable pharmacy and chemistry.**

The UV exposure of MTL resulted in complete primary elimination of the parent compound with incomplete mineralization indicating the formation of derivatives (photo-TPs). Several derivatives (photo-TPs) were identified during photolysis. Various identified derivatives had the same respective nominal mass but eluted at different time during chromatographic analysis. They also exhibited the same MS<sup>2</sup> fragmentation pattern, indicating being the constitutional isomers.

The mixture of derivatives (photo-TPs) was tested for biodegradability through CBT and MRT. Both tests confirmed MTL as not readily biodegradable API. The LC–MS/MS analysis of start and end of each biodegradation test indicated that a few of the formed derivatives were better biodegradable than MTL itself. Most of the derivatives which were observed to biodegrade in the aerobic biodegradation test such as TP 252, TP<sub>1-2</sub> 284, TP 300, TP 302, TP 316, TP 318 and TP 332, were the hydroxylated derivatives of MTL. This is in accordance, as attachments of electron donating functionalities like oxygen atoms (as hydroxyl, aldehyde, carboxylic acid groups etc.) or amines to the aromatic ring of the molecule can improve its aerobic biodegradability (Howard, 2000).

QSAR Software package CaseUltra identified methoxybenzene moiety of MTL as the moiety responsible for reducing biodegradability of MTL. The methoxybenzene moiety of MTL was modified by the number and position of hydroxyl groups added to it. This biodegradability lowering moiety was transformed into a biodegradability favoring moiety (i.e. alcohol or

aldehyde moiety) under either of the two conditions: (a) addition of OH groups with subsequent opening of the aromatic ring as in case of TP 302 and TP 318 and (b) when all 4 hydrogen atoms of the aromatic ring of MTL were substituted with the hydroxyl groups as in case of TP 332.

It was also observed that the alteration in the basic structure of MTL caused by cleavage of certain moieties of side chains during photolysis can lead to the formation of better biodegradable derivatives like TP 134, TP 226, TP 238, TP 240, TP 252 and TP 254.

The pharmacological potency of the biodegradable derivatives was analyzed through *in silico* molecular docking analysis on  $\beta_2$  adrenergic receptor. As expected, MTL showed weak docking with the  $\beta_2$  receptor grid (docking score of  $-5.3$ ) due to its selective nature towards the  $\beta_1$  subtype receptor. The three derivatives which had the lowest docking score compared to MTL were di-hydroxylated MTL TP<sub>2</sub> 300 ( $-7.6$ ), tri-hydroxylated MTL TP<sub>3</sub> 316 ( $-7.8$ ) and non-hydroxylated derivate TP 238 ( $-6.9$ ). Thus, these three derivatives can be considered as promising candidates (green derivatives) who have improved biodegradability and might possess non-inferior or even improved pharmacological potency compared to MTL.

Further, *in silico* predictions for the toxicity of these promising candidates were performed. The toxicity models provided ambiguous predictions for the promising derivatives. They predicted that a few of the candidates might be genotoxic or mutagenic. These predictions strongly recommend experimental testing of the selected derivatives of MTL for genotoxicity, mutagenicity and ecotoxicity to confirm the predictions of QSAR models through experimental data.

### **Article #3: A sustainable chemistry solution to the presence of pharmaceuticals and chemicals in the aquatic environment – the example of re-designing $\beta$ -blocker Atenolol.**

New molecules that possess both substructures responsible for the specific action as a  $\beta$ -blocker i.e. an aromatic ring and a  $\beta$ -ethanolamine moiety were generated through photolysis of ATL. Based on the elucidated and proposed structures, kinetics of formation of derivatives and literature findings, six possible pathways were found to be involved in the formation of these derivatives (photo-TPs). The derivatives' mixture was tested for aerobic biodegradability in CBT and MRT. Both biodegradation test assays confirmed ATL as not readily biodegradable API. LC-UV-MS/MS analysis of the samples of both biodegradation tests indicated that a few of the formed derivatives (e.g. TP 207; TP 225; TP<sub>1&2</sub> 238; TP 265; TP 281; TP 283; TP<sub>2</sub> 295, etc.) were better biodegradable than ATL.

Generally, it is difficult to quantify the effect of one certain structural alteration on biodegradability in total. Biodegradable derivatives were *in silico* analyzed by QSAR models (Software package Case Ultra, Multicase Inc.) for ready biodegradability, too, to identify structural changes in the derivatives (photo-TPs) that would modulate their biodegradability. This knowledge contributes to a better understanding that would be the basis of a rational design of better biodegradable compounds in the future according to the benign by design approach. Experimental results and QSAR predictions on the one hand and available knowledge on the other were in good accordance. Therefore, the results presented can serve as a good starting point for the rational design of biodegradable drug derivatives.

The software package Schrödinger QikProp 3.8 (Schrödinger, LLC) predicts the drug-likeness of the derivatives according to their ADME properties. The software predicted a lot of derivatives either less orally available and/or less drug-likely. Also a few of the derivatives lacks either of the essential substructures (aromatic ring and  $\beta$ - ethanolamine). Therefore, derivatives which were either less orally available and/or less drug-likely or lack essential substructures were omitted from further development of new ATL derivatives.

A few biodegradable derivatives such as TP 207, TP 210, TP 223, TP 238 and TP<sub>2</sub> 295 were predicted to be drug-like and orally available and also possessed the essential substructures for  $\beta$ -blocker activity. Thus, these derivatives (TP 207, TP 210, TP 223, TP 238 and TP<sub>2</sub> 295) might be considered as the lead candidates i.e. biodegradable and drug-like molecules.

The predictions of mutagenicity, genotoxicity and carcinogenicity indicate that some of the biodegradable lead candidates such as TP 207, TP 210, TP 223 and TP 238 are neither carcinogenic, genotoxic nor mutagenic in mammals, while TP<sub>2</sub> 295 was predicted to be carcinogen. Therefore, TP<sub>2</sub> 295 will not be further considered as a lead candidate for development of new biodegradable ATL derived entities. However, chromosome aberration model of Leadscape software provided a positive alert for TP 207, TP 210, TP 223 and TP 238 lead candidates. The next step is to synthesize these shortlisted biodegradable drug-like candidates and test them through various experimental testing for their pharmacological potency and toxicity to confirm their predicted properties.

Thus, studies like this will increase the knowledge about the role of the attachment of certain functionalities to the parent drug for its biodegradability whilst conserving pharmacological properties which was in the past a totally neglected issue within drug development.

**Article #4: Addressing the Challenge of Micro-Pollutants in the Aquatic Cycle: Targeted Re-Designing the  $\beta$ -Blocker Propranolol for Environmental Biodegradability.**

16 new derivatives of PPL were generated through the UV photolysis and their structures were derived. Out of these, 13 derivatives were identified as hydroxylated derivatives of PPL. As observed during MTL and ATL study, the major mechanism responsible for the generation of derivatives of PPL was the attachment of hydroxyl radical (HO<sup>•</sup>) on the aromatic naphthalene ring of PPL. It often results in the opening of the naphthalene ring. The other mechanisms which were observed were the dealkylation and the loss of the ethanolamine side chain from the aromatic ring. Several identified photo-TPs (derivatives) had the same respective nominal mass but eluted at different times during chromatographic analysis. They also exhibited the same MS<sup>2</sup> fragmentation pattern thus indicating being the constitutional isomers. The same phenomenon of the formation of constitutional isomers during photolysis was also observed for MTL study in the present thesis.

Results of applied aerobic biodegradation tests confirmed PPL as non-readily biodegradable API. The LC-MS/MS analysis of samples of CBT and MRT indicated that a few of the formed derivatives were better biodegradable than PPL itself. All these observed better biodegradable photo-TPs were hydroxylated derivatives of PPL with or without the opening of naphthalene ring.

All the better biodegradable derivatives including all their possible constitutional isomers were *in silico* docked on the turkey  $\beta_1$  and human  $\beta_2$  adrenergic receptors to investigate their pharmacological potency. The docking results indicated that the hydroxylation on the naphthalene ring of PPL (as in TP<sub>1-7</sub> 276) and opening of the ring (as in TP 266) during photolysis lead to derivatives which might have non-inferior or even improved pharmacological potency as compared to PPL.

In order to confirm the biodegradability and pharmacological potency predictions of the derivatives, it was necessary to test them individually in CBT and *in vitro* pharmacological assay. Three hydroxyl derivatives of PPL (i.e. 4-OH PPL, 5-OH PPL and 7-OH PPL) were commercially available as racemic mixture. These three were tested in CBT to confirm their biodegradability. The highest degree of biodegradation and complete primary elimination was observed for 4-OH PPL, while the other derivatives showed no biodegradation or elimination. The DOC results also support the results of biodegradation as highest mineralization (48%) was observed for the 4-OH PPL. These analyses confirmed that 4-OH PPL is of improved biodegradability. Therefore, the focus of the subsequent work was on 4-OH PPL. As this derivative was available, an *in vitro* pharmacological analysis of its ability to bind to the  $\beta_1$  adrenergic receptor was performed. 4-OH PPL showed a similar dose response for the



reduction of agonist activity of receptor as PPL, which confirms that it is also an antagonistic API for  $\beta_1$  adrenergic receptor similar to PPL.

The ADME properties of 4-OH PPL were predicted and compared with the non-selective  $\beta$ -blocker PPL and known selective  $\beta_1$  blockers ATL and MTL. All the predicted ADME properties were within the recommended range or values and are satisfactorily comparable with PPL, ATL and MTL. The predictions of toxicological end-points for PPL and 4-OH PPL indicated that the 4-OH PPL could be non-carcinogenic and also neither genotoxic nor mutagenic.

This study confirms that 4-OH PPL can be considered a lead structure of an environmentally friendly (biodegradable)  $\beta_1$  adrenergic receptor blocking API. In this case the photo-TPs (derivatives) were commercially available for experimental testing. Combined results of this study also suggest that further analysis such as bio-distribution, pharmacokinetic and later on in case of positive outcome clinical trials should be carried out for 4-OH PPL. After successful trials at later stages it can be labelled and used as  $\beta_1$  adrenergic receptor blocker drug with the additional advantage of being biodegradable in the environment after its release.

## 5. Conclusion

The presented strategy of combining experimental methods and *in silico* analysis can add information for risk assessment of pharmaceuticals and other chemicals in the environment by filling data gaps in general. It can also contribute to improve the reliability of elucidation of a structural chemical formula of transformation products formed from parent compounds through photolysis and other technical and environmental processes. However, it is of even more importance for TPs especially the ones that are not commercially available as they often are new chemical structures. Chemical synthesis of TPs is expensive and time consuming as would their isolation from test mixtures. Especially in the case of photo-treatment and oxidative treatment often numerous TPs are formed because these treatment processes are radical driven reactions of low selectivity. This makes it even more difficult to test each of them experimentally. As a first step at least, elucidation of the structural formula of TPs is sufficient to collect appropriate data as a basis for a preliminary environmental risk analysis. These tools can be used for the environmental fate assessment of new compounds beforehand too, as they allow very early and comparatively cheap evaluation of properties of new compounds which in turn may contribute to a shorter time to market.

Generally, the application of QSAR analysis within the risk assessment process may save time and financial resources. It also increases the knowledge about the fate and effects of TPs if they are released into the environment. *In silico* predictions can also be used as supporting tools for deciding the further tests and/or to optimize testing strategies. This has been successfully demonstrated in this thesis. The wise combination of the experimental testing and results thereof (e.g. of biodegradation tests and/or toxicity tests) with *in silico* predictions will increase the robustness and reliability of the results in total and may lead to new insights.

In the present study (Article #1), the results obtained from the *in silico* biodegradability predictions gave further information about the relative important photo-TPs as biodegradable photo-TPs can be neglected for risk assessment. However, *in silico* toxicity predictions of photo-TPs can also indicate needs of further experimental testing e.g. in order to characterize the photo-TPs which were predicted to be mutagenic and genotoxic.

The other approach presented in this study (Article #2-4), i.e. photolytic generation of photo-TPs (i.e. derivatives) in combination with LC-MS/MS, biodegradability testing and *in silico* tools such as QSAR analysis and *in vitro* analysis proved to be a very powerful tool for the preliminary study for the rational design of green drug-like derivatives. This approach of designing greener derivatives would fit into the 'benign by design' concept as an important building block in the direction of green and sustainable pharmacy and chemistry. These studies provide evidence for a route of design of novel  $\beta$ -blocker derivatives. These novel  $\beta$ -blocker derivatives have functional groups in the molecules that have properties required for a successful pharmaceutical application and at the same time for ready or complete biodegradability of a molecule after its use and subsequent introduction into the aquatic environment.

From the work presented here, it can be further concluded that small molecular alterations even on the moieties responsible for the activity of pharmaceuticals are possible with comparable pharmacological potency of the resulting derivatives. The only condition which should be followed is that such small molecular changes should not disturb or rupture the pharmacophore of the drug molecule. The advantage of such a tiered approach is that it is not necessary to synthesize all the molecules that may be of interest beforehand. Only a few standard experiments and structure elucidation of promising candidates are enough for such screening purposes also with respect to pharmacological activity as well as some core endpoints of toxicity and off-target effects. Thus, it allows very early and comparatively

cheap evaluation of properties of a new compound and may contribute to a shorter time to market.

There are also some limitations in this tiered approach despite the fact that it opens direction in designing pharmaceuticals that are biodegradable after they are introduced into the aquatic environment. Therefore, these limitations should be addressed and overcome in the future for a better implementation of the present approach of designing pharmaceuticals in the context of green and sustainable pharmacy.

## 5. Future perspective

This cumulative thesis is a summary of research undertaken to further develop the concept for the rational design of green drug-like derivatives that would fit into the ‘benign by design’ concept. Some good progress was made. However, there still remain many parts of research in this area that require investigation in order to gain a stronger knowledge base of creating a refined medicinal chemistry in order to integrate environmental aspects into drug design and development. Some suggestions on the basis work presented here for future research are listed below:

1. **Refining the concept:** In the present work, derivatives were generated through the photolysis process. A future task could be to enlarge this toolbox using other techniques such as chlorination, (electro) oxidation, and enzymatic reactions etc. for the generation of derivatives. These different processes will yield a variety of new derivatives in some case or may be not in others. This has to be investigated.

One of the limitations faced during the work was the commercial availability of the screened biodegradable and pharmacological potent candidates. The synthesis of these candidates is a very expensive and time consuming process. Therefore, in future a technique is needed to be developed for the isolation and enrichment of the promising candidates. This could be performed by the application of preparative HPLC. With such isolation and enrichment techniques a proper experimental testing of the derivatives would be possible and improved and reliable structure elucidation through NMR analysis would also be possible too.

2. **Strengthening the concept:** During the study, it was observed that there were a few more interesting and promising candidates of  $\beta$ -blockers which were better biodegradable and predicted to be pharmacologically potent. But due to time constraint, their unavailability and limited resource they were not tested further. Therefore, it is required that these candidates should be tested individually in biodegradation tests and also *in*

*vitro* assays to strengthen the presented concept of designing biodegradable and pharmacologically potent drug derivatives.

- 3. Expanding and transferring the concept:** The presented tiered approach of rational designing environmentally biodegradable drug derivatives should also be implemented for different classes of drugs such as antibiotics, anticancer drugs etc. This might lead to innovative follow-up studies and would expand the knowledge and experience for an improved implementation of the concept of ‘benign by design’. A future goal to perform such studies is also to gain more information about the different functional groups which could alter the biodegradability of the molecule and to create a kind of combinatorial library for the drug designing software. Such an approach would provide a new paradigm for the rational design of biodegradable pharmaceuticals.

## Reference

- Abrahamsson T, Ek B, Nerme V. The  $\beta$ 1- and  $\beta$ 2-adrenoceptor affinity of atenolol and metoprolol: A receptor-binding study performed with different radioligands in tissues from the rat, the guinea pig and man. *Biochem. Pharmacol.* 1988;37:203–8.
- Anastas PT, Warner JC. *Green chemistry: Theory and practice*. New York: Oxford Univ. Press; 1998.
- Andreucci M, Fuiano G, Presta P, Esposito P, Faga T, Bisesti V et al. Radiocontrast media cause dephosphorylation of Akt and downstream signaling targets in human renal proximal tubular cells. *Biochem. Pharmacol.* 2006;72:1334–42.
- Arnold WA, McNeill K. Chapter 3.2 Transformation of pharmaceuticals in the environment: Photolysis and other abiotic processes. In: M. Petrović and D. Barceló, editor. *Comprehensive Analytical Chemistry Analysis, Fate and Removal of Pharmaceuticals in the Water Cycle*: Elsevier; 2007. p. 361–385.
- Benz D, Paxéus NA, Ginn TR, Loge FJ. Occurrence and fate of pharmaceutically active compounds in the environment, a case study: Höje River in Sweden. *J. Hazard. Mat.* 2005;122:195–204.
- Black JW, Crowther AF, Shanks RG, Smith LH, Dornhorst AC. A new adrenergic: Beta-receptor antagonist. *The Lancet* 1964;283:1080–1.
- Boxall ABA, editor. *Transformation Products of Synthetic Chemicals in the Environment*. Berlin, Heidelberg: Springer; 2009.
- Bryan RN, Centeno RS, Hershkowitz N, Poelstra RJ, Osato MS. Neurotoxicity of iohexol: a new nonionic contrast medium. *Radiology* 1982;145:379–82.
- Chakravarti SK, Saiakhov RD, Klopman G. Optimizing predictive performance of CASE Ultra expert system models using the applicability domains of individual toxicity alerts. *J. Chem. Inf. Model.* 2012;52:2609–18.
- Chang H, Hu J, Wang L, Shao B. Occurrence of sulfonamide antibiotics in sewage treatment plants. *Chinese Sci. Bull.* 2008;53:514–20.
- Daughton CG, Ternes TA. Pharmaceuticals and personal care products in the environment: agents of subtle change? *Environ. Health Perspect.* 1999;107:907–38.
- Dimitrov S, Dimitrova N, Georgieva D, Vasilev K, Hatfield T, Straka J et al. Simulation of chemical metabolism for fate and hazard assessment. III. New developments of the bioconcentration factor base-line model. *SAR QSAR Environ. Res.* 2012;23:17–36.
- Dimitrov S, Dimitrova N, Parkerton T, Comber M, Bonnell M, Mekenyan O. Base-line model for identifying the bioaccumulation potential of chemicals. *SAR QSAR Environ. Res.* 2005;16:531–54.

- DiscoverX. PathHunter® CHO-K1 ADRB1  $\beta$ -Arrestin Cell Line, 2013.  
<http://www.discoverx.com/product-data-sheets-3-tab/93-0488c2> (accessed April 24, 2014).
- ECHA. Guidance on Information Requirements and Chemical Safety Assessment - ECHA.  
<http://echa.europa.eu/web/guest/guidance-documents/guidance-on-information-requirements-and-chemical-safety-assessment> (accessed November 18, 2013).
- Emorine L, Marullo S, Briend-Sutren M, Patey G, Tate K, Delavier-Klutchko C et al.  
Molecular characterization of the human beta 3-adrenergic receptor. *Science* 1989;245:1118–21.
- EPA. OPPT/Exposure Assessment Tools and Models/Estimation Program Interface (EPI) Suite Version 3.12 (August 17, 2004), 2013.  
<http://www.epa.gov/oppt/exposure/pubs/episuite.htm> (accessed July 10, 2013).
- European Commission. Technical guidance document on risk assessment part II., 2003a.  
[http://ec.europa.eu/environment/chemicals/exist\\_subst/pdf/tgdpart2\\_2ed.pdf](http://ec.europa.eu/environment/chemicals/exist_subst/pdf/tgdpart2_2ed.pdf).
- European Commission. Technical guidance document on risk assessment part III., 2003b.  
[http://echa.europa.eu/documents/10162/16960216/tgdpart3\\_2ed\\_en.pdf](http://echa.europa.eu/documents/10162/16960216/tgdpart3_2ed_en.pdf).
- European Medicines Agency. GUIDELINE ON THE ENVIRONMENTAL RISK ASSESSMENT OF MEDICINAL PRODUCTS FOR HUMAN USE, 2005.  
<http://www.iss.it/binary/farm2/cont/guideline%20environmental%20risk%20assessment%20medicinal%20products.1109243627.pdf>.
- Fatta-Kassinou D, Meric S, Nikolaou A. Pharmaceutical residues in environmental waters and wastewater: current state of knowledge and future research. *Anal. Bioanal. Chem.* 2011;399:251–75.
- Gorre F, Vandekerckhove H. Beta-blockers: focus on mechanism of action. Which beta-blocker, when and why? *Acta Cardiol.* 2010;65:565–70.
- Gringauz A. Introduction to medicinal chemistry: How drugs act and why. New York: Wiley-VCH; 1997.
- Grönwäller EF, Wahl HG, Kehlbach R, Rodemann HP, Claussen CD, Duda SH. Stabilität jodhaltiger Röntgenkontrastmittel unter UV-Laser-Bestrahlung und Toxizität der Photoprodukte. *Rofo* 1998;169:537–41.
- Haiß A, Kümmerer K. Biodegradability of the X-ray contrast compound diatrizoic acid, identification of aerobic degradation products and effects against sewage sludge micro-organisms. *Chemosphere* 2006;62:294–302.
- Halling-Sørensen B, Nors Nielsen S, Lanzky PF, Ingerslev F, Holten Lützhøft HC, Jørgensen SE. Occurrence, fate and effects of pharmaceutical substances in the environment- A review. *Chemosphere* 1998;36:357–93.

- Han GH, Hur HG, Kim SD. Ecotoxicological risk of pharmaceuticals from wastewater treatment plants in Korea: Occurrence and toxicity to *Daphnia magna*. *Environ. Tox. Chem.* 2006;25:265–71.
- Harmon RC, Duffy SP, Terneus MV, Ball JG, Valentovic MA. Characterization of a novel model for investigation of radiocontrast nephrotoxicity. *Nephrol. Dial. Transplant.* 2009;24:763–8.
- Heberer T. Occurrence, fate, and removal of pharmaceutical residues in the aquatic environment: a review of recent research data. *Toxicology Letters* 2002;131:5–17.
- Howard PH. Biodegradation. In: Mackay D, Boethling RS, editors. *Handbook of property estimation methods for environmental chemicals: Environmental and health sciences*. Boca Raton: Lewis Publishers; 2000. p. 281–310.
- Howard PH, Muir DCG. Identifying New Persistent and Bioaccumulative Organics Among Chemicals in Commerce II: Pharmaceuticals. *Environ. Sci. Technol.* 2011;45:6938–46.
- Jones OAH, Green PG, Voulvoulis N, Lester JN. Questioning the excessive use of advanced treatment to remove organic micropollutants from wastewater. *Environ. Sci. Technol.* 2007;41:5085–9.
- Joss A, Keller E, Alder AC, Göbel A, McArdell CS, Ternes T et al. Removal of pharmaceuticals and fragrances in biological wastewater treatment. *Water Research* 2005;39:3139–52.
- Joss A, Zabczynski S, Göbel A, Hoffmann B, Löffler D, McArdell CS et al. Biological degradation of pharmaceuticals in municipal wastewater treatment: Proposing a classification scheme. *Water Research* 2006;40:1686–96.
- Kalsch W. Biodegradation of the iodinated X-ray contrast media diatrizoate and iopromide. *Sci. Total Environ.* 1999;225:143–53.
- Kanda R, Griffin P, James HA, Fothergill J. Pharmaceutical and personal care products in sewage treatment works. *J. Environ. Monit* 2003;5:823–30.
- Khetan SK, Collins TJ. Human Pharmaceuticals in the Aquatic Environment: A Challenge to Green Chemistry. *Chem. Rev.* 2007;107:2319–64.
- Kormos JL, Schulz M, Ternes TA. Occurrence of Iodinated X-ray Contrast Media and Their Biotransformation Products in the Urban Water Cycle. *Environ. Sci. Technol* 2011;45:8723–32.
- Kümmerer K. Sustainable from the very beginning: rational design of molecules by life cycle engineering as an important approach for green pharmacy and green chemistry. *Green Chem.* 2007;9:899–907.
- Kümmerer K. *Pharmaceuticals in the Environment: Sources, Fate, Effects and Risks*. 3rd ed. Berlin, Heidelberg: Springer-Verlag; 2008.

- Kümmerer K. Rational design of molecules by life cycle engineering. In: Kümmerer K, Hempel M, editors. *Green and sustainable pharmacy*. Berlin, Heidelberg: Springer; 2010. p. 135–146.
- Kümmerer K. Drugs. In: Anastas PT, Boethling R, Votchkova A, editors. *Handbook of Green Chemistry, Green Processes, Designing Safer Chemicals*. Weinheim: Wiley-VCH; 2012. p. 215–280.
- La Farré M, Pérez S, Kantiani L, Barceló D. Fate and toxicity of emerging pollutants, their metabolites and transformation products in the aquatic environment. *TrAC Trends in Anal. Chem.* 2008;27:991–1007.
- Laboratory of Mathematical Chemistry Bulgaria. OASIS Catalogic software V.5.11.6TB; 2012.
- Lechat P. Clinical pharmacology of beta-blockers in cardiology: trial results and clinical applications. *Hot Topics in Cardiology* 2006:7–44.
- Maurer M, Escher BI, Richle P, Schaffner C, Alder AC. Elimination of  $\beta$ -blockers in sewage treatment plants. *Water Research* 2007;41:1614–22.
- Mauriège P, Pergola G de, Berlan M, Lafontan M. Human fat cell beta-adrenergic receptors: beta-agonist-dependent lipolytic responses and characterization of beta-adrenergic binding sites on human fat cell membranes with highly selective beta 1-antagonists. *J. Lipid Res.* 1988;29:587–601.
- Messana JM, Cieslinski DA, Nguyen VD, Humes HD. Comparison of the toxicity of the radiocontrast agents, iopamidol and diatrizoate, to rabbit renal proximal tubule cells in vitro. *J. Pharmacol. Exp. Ther.* 1988;244:1139–44.
- Michael I, Rizzo L, McArdell CS, Manaia CM, Merlin C, Schwartz T et al. Urban wastewater treatment plants as hotspots for the release of antibiotics in the environment: A review. *Water Research* 2013;47:957–95.
- Miège C, Choubert JM, Ribeiro L, Eusèbe M, Coquery M. Fate of pharmaceuticals and personal care products in wastewater treatment plants – Conception of a database and first results. *Environ. Pollut.* 2009;157:1721–6.
- OECD. OECD Guidelines for the Testing of Chemicals: Ready Biodegradability 301F: Manometric Respiratory Test: OECD Pub; 1992a.
- OECD. OECD Guidelines for the Testing of Chemicals: Ready Biodegradability 301D: Closed Bottle Test: OECD Pub; 1992b.
- Putschew A, Jekel M. Iodinated X-ray Contrast Media. In: Reemtsma T, Jekel M, editors. *Organic pollutants in the water cycle: Properties, occurrence, analysis and environmental relevance of polar compounds*. Weinheim, Chichester: Wiley-VCH; John Wiley [distributor]; 2006. p. 87–98.
- Putschew A, Wischnack S, Jekel M. Occurrence of triiodinated X-ray contrast agents in the aquatic environment. *Sci. Total Environ.* 2000;255:129–34.



- Roberts G, Myatt G, Johnson W, Cross K, Blower P. LeadScope: Software for exploring large sets of screening data. *J. Chem. Inf. Model.* 2000;40:1302–14.
- Saiakhov R, Chakravarti S, Klopman G. Effectiveness of CASE Ultra expert system in evaluating adverse effects of drugs. *Mol. Inf.* 2013;32:87–97.
- Santiago-Morales J, Agüera A, Gómez MdM, Fernández-Alba AR, Giménez J, Esplugas S et al. Transformation products and reaction kinetics in simulated solar light photocatalytic degradation of propranolol using Ce-doped TiO<sub>2</sub>. *Appl. Catal. B: Environ.* 2013;129:13–29.
- Santos LHMLM, Araújo AN, Fachini A, Pena A, Delerue-Matos C, Montenegro MCBSM. Ecotoxicological aspects related to the presence of pharmaceuticals in the aquatic environment. *J. Hazard. Mat.* 2010;175:45–95.
- Schwabe U, Paffrath D, editors. *Arzneiverordnungs-Report 2013: Aktuelle Daten, Kosten, Trends und Kommentare.* Berlin, Heidelberg,: Springer-Verlag; 2013.
- Sedykh A, Saiakhov R, Klopman G. META V. A model of photodegradation for the prediction of photoproducts of chemicals under natural-like conditions. *Chemosphere* 2001;45:971–81.
- Summerhill S, Stroud T, Nagendra R, Perros-Huguet C, Trevethick M. A cell-based assay to assess the persistence of action of agonists acting at recombinant human  $\beta$ 2 adrenoceptors. *J. Pharmacol. Toxicol. Met.* 2008;58:189–97.
- Ternes TA, Hirsch R. Occurrence and Behavior of X-ray Contrast Media in Sewage Facilities and the Aquatic Environment. *Environ. Sci. Technol.* 2000;34:2741–8.
- Ternes TA, Joss A, Siegrist H. Scrutinizing Pharmaceuticals and Personal Care Products in Wastewater Treatment. *Environ. Sci. Technol.* 2004;38:392A.
- Trautwein C, Kümmerer K. Ready biodegradability of trifluoromethylated phenothiazine drugs, structural elucidation of their aquatic transformation products, and identification of environmental risks studied by LC-MS n and QSAR. *Environ. Sci. Pollut. Res.* 2012;19:3162–77.
- Trovó AG, Nogueira RFP, Agüera A, Fernandez-Alba AR, Sirtori C, Malato S. Degradation of sulfamethoxazole in water by solar photo-Fenton. Chemical and toxicological evaluation. *Water Research* 2009;43:3922–31.
- U.S Environmental Protection Agency EHAC. PBT Profiler: A Component of OPPT's P2 Framework.
- Wenzel H, Larsen HF, Clauson-Kaas J, Høiby L, Jacobsen BN. Weighing environmental advantages and disadvantages of advanced wastewater treatment of micro-pollutants using environmental life cycle assessment. *Water Sci. Technol.* 2008;57:27–32.
- Wheeler LA, Norman A, Riley R. Mutagenicity of diatrizoate and other triiodobenzoic acid derivatives in the Ames Salmonella/microsome test. *Proc. West. Pharmacol. Soc.* 1980;23:249–53.

# Curriculum Vitae

**Tushar Rastogi**, Born on 19.09.1985 in Lucknow, India.

## Education

- 05/2011-2014** Ph.D. candidate (Dr. rer. nat.) in Institute for Sustainable and Environmental Chemistry, Faculty of Sustainability Sciences at Leuphana University Lüneburg, Germany.
- 2009 – 2010** Master of Science- Process Engineering  
University of Applied sciences, Offenburg, Germany
- 2004 – 2008** Bachelor of Engineering- Chemical Engineering (First class with distinction), Maharashtra Academy of Engineering, University of Pune, India.
- 2000-2003** Secondary school certificate, Lucknow, India.

## Employment and Professional Experience

- 04/2014-09/2014** One of the supervisors of the practical experimental chemistry techniques sections for the bachelor students in the Faculty of Sustainability in the summer semester 2014.
- 05/2011-03/2014** Scientific research fellow at the Faculty of Sustainability of Leuphana University, Lüneburg.
- 06/2009 – 01/2010** Student assistant at University of Applied Sciences Offenburg. Worked under the project “Development and construction of a Laser Resonance Fluorescence System”.

## Project handled

- 05/2011-08/2013** Co-worker in the BMBF NanoPharm project (ProjectNo. 03X0094C). Involved with the experimental laboratory work, data evaluation and analysis, analyzing samples from other project partners.

## Educational Training

- 2009 (12 weeks) University of Warmia and Mazury, Poland. Learned concepts of environmental protection, water and waste treatment, activated sludge process.

2007-2008 (8 months) Centre for Materials for Electronics Technology (C-MET), Pune, India. Involved in synthesis of nanoparticles, learned various spectroscopic and microscopic tools like XRD, UV spectrometry, photoluminescence.

### **List of Publication**

**Rastogi T.**, Leder C., Kümmerer K. (2014). *Designing green derivatives of  $\beta$ -blocker Metoprolol: A tiered approach for green and sustainable pharmacy and chemistry.* Chemosphere, 111: 493-499.

**Rastogi T.**, Leder C., Kümmerer K. (2014). *Qualitative environmental risk assessment of photolytic transformation products of iodinated X-ray contrast agent diatrizoic acid,* Sci. Total Environ., 482-483: 378-388.

**Rastogi T.**, Leder C., Kümmerer K. (2015) *A sustainable chemistry solution to the presence of pharmaceuticals and chemicals in the aquatic environment – the example of re-designing  $\beta$ -blocker Atenolol,* RSC Advances 5: 27-32. DOI: 10.1039/c4ra10294k.

**Rastogi T.**, Leder C., Kümmerer K. (2015) *Addressing the Challenge of Micro-Pollutants in the Aquatic Cycle: Targeted Re-Designing the  $\beta$ -Blocker Propranolol for Environmental Biodegradability.* (Manuscript submitted in Environmental Science & Technology)

### **Contributions in Scientific Conferences**

#### **Oral presentations:**

**Rastogi T.**, Leder C., Kümmerer K. (2014). *Developing the 'Benign by Design' Approach for a Rational Design of Green Derivatives of  $\beta$ -Blockers: Propranolol as an Example.* Sustainability in Chemistry: Biannual meeting of the Division "Sustainable Chemistry" September 28-30, 2014, Erlangen, Germany

**Rastogi T.**, Leder C., Menz J., Schneider M., Kümmerer K. (2014). *Qualitative environmental risk assessment of photolytic transformation products of Iodinated X-ray contrast media (ICM) Diatrizoic acid.* SETAC Europe - 24<sup>th</sup> Annual Meeting, May 2014, Basel, Switzerland.

#### **Poster presentations:**

**Rastogi T.**, Leder C., Kümmerer K. (2014). *Rational Design of Green, (Bio) Degradable  $\beta$  Adrenergic Receptor Blocker Derivatives through Non-Targeted Synthesis: Atenolol*

*as an Example.* Sustainability in Chemistry: Biannual meeting of the Division "Sustainable Chemistry" September 28-30, 2014, Erlangen, Germany

Schneider M., Toolaram A.P., Menz J., **Rastogi T.**, Kümmerer K. (2014). *Genotoxicity and ecotoxicity screening of photolytic mixtures from the selective  $\beta$ 1-receptor blockers Atenolol and Metoprolol.* SETAC Europe - 24<sup>th</sup> Annual Meeting, Mai 2014, Basel, Switzerland.

Menz J., **Rastogi T.**, Schneider M., Kümmerer K. (2013). *Phototransformation of the beta-blockers Atenolol, Metoprolol and Propranolol – first-time application of a modified luminescent bacteria test for the initial ecotoxicity assessment of phototransformation products.* SETAC North America – 34<sup>th</sup> annual meeting, November 2013, Nashville, USA.

**Rastogi T.**, Menz J., Toolaram A.P., Leder C., Schneider M., Kümmerer K. (2013). *Identification and assessment of the Transformation Products of Metoprolol.* 3. Clustertreffen der BMBF-Foerdermaßnahmen NanoCare und NanoNature, January 2013, Frankfurt/M., Germany.

**Rastogi T.**, Menz J., Toolaram A. P., Leder C., Schneider M., Bolek R., Kümmerer K. (2012). *Photodegradation of Propranolol: Identification of transformation product, assessment of their biodegradability, bacterial toxicity and mutagenicity.* Gemeinsame Jahrestagung SETAC GLB & Fachgruppe Umweltchemie und oekotoxikologie der GDCh 2012, Leipzig, Germany.

**Rastogi T.**, Bolek R., Schneider M., Kümmerer K., (2012). *Neue photokatalytisch aktive Verbundmaterialien zur Eliminierung von Pharamzeutischen Reststoffen. Teilprojekt: Erfassung und Bewertung von Transformationsprodukten.* 2. Clustertreffen der BMBF-Foerdermaßnahmen NanoCare/NanoNature, March 2012, Frankfurt/M., Germany.

**Rastogi T.**, Bolek R., Schneider M., Kümmerer K., (2011). *Neue photokatalytisch aktive Verbundmaterialien zur Eliminierung von Pharamzeutischen Reststoffen. Teilprojekt: Erfassung und Bewertung von Transformationsprodukten.* 1. Clustertreffen BMBF-Foerdermaßnahmen NanoCare/NanoNature, May 2011, Frankfurt/M., Germany.

## **Declaration**

This PhD thesis titled “ Pharmaceuticals in the Environment: Photolysis, Identification of Transformation Products - Environmental Risk Assessment for X-ray Contrast Media and Demonstrating the Feasibility of Designing Environmentally Biodegradable Derivatives Using the Example of  $\beta$ -Blockers” has neither as a whole nor in part been submitted to assessment in a doctoral procedure at another university.

I also avouch that all information given in this appendix is true in each instance and overall.

Tushar Rastogi

Lüneburg, October 2014

## Appendix – Declarations to the individual articles

This cumulative thesis is based on four scientific articles; two of them being published in international peer-reviewed journals, while one is submitted to the international peer-reviewed journals and the other is in preparation and will be submitted soon. In the following, declarations to the contributions of the authors to the articles and the quality of the publications are given. All four publications were written by the first author Tushar Rastogi.

Articles included:

- [1] Tushar Rastogi, Christoph Leder, Klaus Kümmerer, Qualitative Environmental Risk Assessment of Photolytic Transformation Products of Iodinated X-ray Contrast Agent Diatrizoic acid, *Science of The Total Environment*, **2014**, 482–483, 378–388. <http://dx.doi.org/10.1016/j.scitotenv.2014.02.139>
- [2] Tushar Rastogi, Christoph Leder, Klaus Kümmerer, Designing green derivatives of  $\beta$ -blocker Metoprolol: A tiered approach for green and sustainable pharmacy and chemistry, *Chemosphere*, **2014**, 111, 493–499. <http://dx.doi.org/10.1016/j.chemosphere.2014.03.119>
- [3] Tushar Rastogi, Christoph Leder, Klaus Kümmerer, A sustainable chemistry solution to the presence of pharmaceuticals and chemicals in the aquatic environment – the example of re-designing  $\beta$ -blocker Atenolol. *RSC Advances*, **2015**, 5, 27-32. <http://dx.doi.org/10.1039/c4ra10294k>
- [4] Tushar Rastogi, Christoph Leder, Klaus Kümmerer, Addressing the Challenge of Micro-Pollutants in the Aquatic Cycle: Targeted Re-Designing the  $\beta$ -Blocker Propranolol for Environmental Biodegradability. *Environmental Science & Technology* (submitted), **2015**.

**Table A1: Authors' contributions to the articles and articles publication status**

Article #	Short title	Specific contributions of all authors	Author status	Weighting factor	Publication status *	Conference contributions
[1]	Qualitative Environmental Risk Assessment of Photolytic Transformation Products of Iodinated X-ray Contrast Agent Diatrizoic acid	TR: Concept, laboratory work, data evaluation and analysis, discussion of results, manuscript preparation CL: Concept, <i>In silico</i> data collection, data analysis, discussion of results, comments on the manuscript KK: Concept, discussion of results, comments of the manuscript	Co-authorship: Predominant contribution [Überwiegen der Anteil]	1.0	<b>Published</b> Science of The Total Environment, <b>2014</b> , 482–483, 378–388 <a href="http://dx.doi.org/10.1016/j.scitotenv.2014.02.139">http://dx.doi.org/10.1016/j.scitotenv.2014.02.139</a> [IF = 3.906 (5-year); Q1(Environmental sciences)]	SETAC Europe 24th Annual Meeting in Basel, Switzerland from 11-15 May 2014. <a href="http://www.basel.setac.eu">http://www.basel.setac.eu</a> (Oral presentation)
[2]	Designing green derivatives of $\beta$ -blocker Metoprolol: A tiered approach for green and sustainable pharmacy and chemistry	TR: concept, laboratory work, data evaluation and analysis, discussion of results, manuscript preparation CL: Concept, <i>In silico</i> data collection, data analysis, discussion of results, comments on the manuscript KK: Concept, discussion of results, comments of the manuscript	Co-authorship: Predominant contribution [Überwiegen der Anteil]	1.0	<b>Published</b> Chemosphere, <b>2014</b> , 111, 493–499 <a href="http://dx.doi.org/10.1016/j.chemosphere.2014.03.119">http://dx.doi.org/10.1016/j.chemosphere.2014.03.119</a> [IF = 3.867 (5-year); Q1(Environmental sciences)]	
[3]	A sustainable chemistry solution to the presence of pharmaceuticals and chemicals in the aquatic environment – the	TR: concept, laboratory work, data evaluation and analysis, discussion of results, manuscript preparation	Co-authorship: Predominant contribution [Überwiegen	1.0	<b>Published</b> RSC Advances, <b>2015</b> , 5, 27-32. <a href="http://dx.doi.org/10.103">http://dx.doi.org/10.103</a>	Sustainability in Chemistry: Biannual meeting of the Division "Sustainable Chemistry" September 28-30, 2014,

	example of re-designing $\beta$ -blocker Atenolol	CL: Concept, <i>In silico</i> data collection, data analysis, discussion of results, comments on the manuscript KK: Concept, discussion of results, comments of the manuscript	der Anteil]		9/c4ra10294k [IF = 3.708 (5-year); Q1 (Chemistry, multidisciplinary)]	Erlangen, Germany. <a href="https://www.chemie.uni-erlangen.de/suschem2014/">https://www.chemie.uni-erlangen.de/suschem2014/</a> . (Poster presentation)
[4]	Addressing the Challenge of Micro-Pollutants in the Aquatic Cycle: Targeted Re-Designing the $\beta$ -Blocker Propranolol for Environmental Biodegradability	TR: concept, laboratory work, data evaluation and analysis, discussion of results, manuscript preparation CL: Concept, <i>In silico</i> data collection, laboratory work, data analysis, discussion of results, comments on the manuscript KK: Concept, data analysis, discussion of results, comments on the manuscript	Co-authorship: Predominant contribution [Überwiegen der Anteil]	1.0	<b>Submitted</b> Environmental Science & Technology [IF = 6.326 (5-years); Q1 (Environmental sciences, Environmental engineering)]	Sustainability in Chemistry: Biannual meeting of the Division "Sustainable Chemistry" September 28-30, 2014, Erlangen, Germany. <a href="https://www.chemie.uni-erlangen.de/suschem2014/">https://www.chemie.uni-erlangen.de/suschem2014/</a> . (oral presentation)
Sum:				4.0		

\***IF** = 5-year Impact Factor, **Q** = Quartile in environmental sciences, chemistry and multidisciplinary category 2013 from ISI Web of Science (Journal Citation Reports).

*Acronyms of the individual authors:* TR = Tushar Rastogi; CL = Christoph Leder; KK = Klaus Kümmerer.

*Affiliations of authors:* Sustainable Chemistry and Material Resources, Institute of Sustainable and Environmental Chemistry, Leuphana University Lüneburg, C13, DE-21335 Lüneburg, Germany.





# Articles



# Article I

## Qualitative Environmental Risk Assessment of Photolytic Transformation Products of Iodinated X-ray Contrast Agent Diatrizoic acid

*Science of The Total Environment*, 2014, 482–483, 378–388.  
<http://dx.doi.org/10.1016/j.scitotenv.2014.02.139>





## Qualitative environmental risk assessment of photolytic transformation products of iodinated X-ray contrast agent diatrizoic acid



Tushar Rastogi, Christoph Leder, Klaus Kümmerer\*

Sustainable Chemistry and Material Resources, Institute of Sustainable and Environmental Chemistry, Leuphana University Lüneburg, C13, DE-21335 Lüneburg, Germany

### HIGHLIGHTS

- The photodegradation pathway of diatrizoic acid (DIAT) was elucidated.
- The environmental fate of photo transformation products (photo-TPs) was assessed.
- 15 photo-TPs were found to be better biodegradable than DIAT itself.
- Shortlisted photo-TPs might be less persistence and possess no bioaccumulation threats.
- A few photo-TPs were predicted to be genotoxic or mutagenic.

### ARTICLE INFO

#### Article history:

Received 21 January 2014  
Received in revised form 28 February 2014  
Accepted 28 February 2014  
Available online xxxx

#### Keywords:

Qualitative environmental risk assessment  
Iodinated contrast media  
Diatrizoic acid  
Quantitative structure–activity relationships (QSAR)  
US EPA PBT profiler

### ABSTRACT

Recent studies have confirmed that the aquatic ecosystem is being polluted with an unknown cocktail of pharmaceuticals, their metabolites and/or their transformation products (TPs). Although individual chemicals are typically present at low concentrations, they can interact with each other resulting in additive or potentially even synergistic mixture effects. Therefore it is necessary to assess the environmental risk caused by these chemicals. Data on exposure is required for quantitative risk assessment of TPs and/or metabolites. Such data are mostly missing because of the non-availability of TPs and very often metabolites for experimental testing. This study demonstrates the application of different *in silico* tools for qualitative risk assessment using the example of photodegradation TPs (photo-TPs) of diatrizoic acid (DIAT), which itself is not readily biodegradable. Its photolytic transformation was studied and the photodegradation pathway was established. The aerobic biodegradability of photo-TPs under the conditions of an aquatic environment was assessed using standardized OECD tests. The qualitative risk assessment of DIAT and selected photo-TPs was performed by the PBT approach (i.e. Persistence, Bioaccumulation and Toxicity), using experimental biodegradation test assays, applying different QSAR models with several different toxicological endpoints and *in silico* read-across approaches. The qualitative risk assessment pointed out that the photo-TPs were less persistent compared to DIAT and none of them possessed any bioaccumulation threat. However, a few photo-TPs were predicted to be active for mutagenicity and genotoxicity, which indicate the need for further testing to confirm these predictions. The present study demonstrates that *in silico* qualitative risk assessment analysis can increase the knowledge space about the environmental fate of TPs.

© 2014 Elsevier B.V. All rights reserved.

### 1. Introduction

Over the past decades, the presence of pharmaceuticals, their metabolites and/or transformation products (TPs) (often referred as micro-pollutants) in an aquatic environment are considered a major environmental problem, due to their continuous input into the aquatic ecosystem and their persistent presence even at low concentrations

( $\text{ng L}^{-1}$  to  $\mu\text{g L}^{-1}$ ) (Chang et al., 2008; Han et al., 2006; Khetan and Collins, 2007; Kormos et al., 2011; Kümmerer, 2008; Michael et al., 2013; Miège et al., 2009; Santos et al., 2010; Ternes et al., 2004).

As these micro-pollutants enter the aquatic ecosystem, they undergo various biotic and abiotic transformations which result in the formation of stable TPs. Besides these biotic and abiotic transformations of micro-pollutants, technical treatment processes like photodegradation, ozonation and chlorination can also be responsible for the formation of stable TPs (Arnold and McNeill, 2007; Boxall, 2009; Joss et al., 2005; Kanda et al., 2003). These TPs can contribute significantly to the risk posed by the parent compound if (a) they are formed with a high yield and (b) they are persistent and/or have high a toxic potential (Fattakassinos et al., 2011; Santiago-Morales et al., 2013; Trovó et al., 2009).

\* Corresponding author at: Sustainable Chemistry and Material Resources, Institute of Sustainable and Environmental Chemistry, Leuphana University Lüneburg, C.13, Scharnhorststraße 1, D-21335 Lüneburg, Germany. Tel.: +49 4131 677 2893.

E-mail addresses: [rastogi@leuphana.de](mailto:rastogi@leuphana.de), [tushar1909@gmail.com](mailto:tushar1909@gmail.com) (T. Rastogi), [cleder@leuphana.de](mailto:cleder@leuphana.de) (C. Leder), [klaus.kuemmerer@uni.leuphana.de](mailto:klaus.kuemmerer@uni.leuphana.de) (K. Kümmerer).

It is necessary to perform a risk assessment of these micro-pollutants. The research about the environmental impact of these compounds is a huge and difficult task due to lack of knowledge about their long-term effects like persistence, bioaccumulation and toxicity which certainly cannot be excluded (La Farré et al., 2008).

When carrying out an environmental risk assessment, the exposure of these micro-pollutants to the different environmental compartments needs to be estimated. Such exposure-driven assessments are carried out on the basis of available monitoring data and/or modeling. The environmental presence of TPs further adds complexity to exposure-driven risk assessment strategies. The TPs of pharmaceuticals are usually formed in low concentrations within complex matrices. This makes their isolation and purification a difficult task (Trautwein and Kümmerer, 2012). Further these compounds are often not commercially available and targeted synthesis or isolation can be expensive and time consuming, making their experimental testing rather difficult. This makes it necessary to employ other tools for the environmental risk assessment of TPs. One possibility is the usage of *in silico* tools which are based on quantitative structure–activity relationship (QSAR) calculations.

The technical guidance documents on risk assessment for chemicals within REACH (ECHA, 2012), the European chemicals regulation (European Commission, 2003a, b) and the US EPA recommend the application of *in silico* tools to perform risk assessment for chemicals, in case of a lack of information about their environmental fate and effects. The EMEA guidelines for environmental risk assessment do not explicitly mention *in silico* tools. However, it refers to the EU technical guidelines (European Medicine Agency, 2005).

According to which, the PBT approach can also be used. Substances fulfilling the PBT criteria (regarding persistence [P], bioaccumulation [B] and toxicity [T]) are of priority for risk management consideration. QSAR models should be used for a wide range of endpoints which are required for a risk assessment, including several toxicological and ecotoxicological endpoints and physico-chemical/fate parameters (including biodegradability) (European Commission, 2003b). However, as a general principle, the use of QSARs should not result in a reduction of the scientific basis on which the risk assessment is made.

One of the most widely used classes of chemicals for intravascular administration is iodinated contrast media (ICM). The worldwide consumption of ICM was about 3500 t year<sup>-1</sup> while in Germany it was about 360 t year<sup>-1</sup> (Putschew and Jekel, 2006). In the present study an attempt was made to perform a qualitative environmental risk assessment of diatrizoic acid (DIAT) and its TPs formed during photodegradation (“photo-TPs”). DIAT, which is a commonly used iodinated X-ray contrast agent, undergoes incomplete elimination in sewage treatment plants (STPs) and is reported to be present in various environmental media (Howard and Muir, 2011; Putschew et al., 2000; Ternes and Hirsch, 2000).

DIAT, itself is not biodegradable, it was however photolysed in order to check its mineralization potential and the pathway of the formation of photo-TPs was elucidated. The fate and toxicological properties of DIAT and its photo-TPs were assessed via a combination of photochemical studies with advanced chemical analysis, experimental aerobic biological degradation assays, *in silico* tools with various toxicological endpoints and *in silico* read-across approaches. According to the authors' best knowledge, until now no studies have been published addressing the fate of photo-TPs of DIAT in environment.

## 2. Material and method

### 2.1. Chemicals

Diatrizoic acid (CAS 177-96-4) was purchased from Sigma-Aldrich (Steinheim, Germany). Acetonitrile (HiPerSolv® LC-MS grade) was purchased from VWR international (Germany) and formic acid (Emsure® ACS Reag. PhEur) from Merck (Darmstadt, Germany). All

chemicals were of analytical grade and were used without further purification. All the solutions and standards for analytical measurement and photodegradation were prepared in ultrapure water (Q<sub>1</sub>: 16.6 mΩ and Q<sub>2</sub>: 18.2 mΩ).

### 2.2. Photodegradation

UV photolysis experiments of DIAT were performed in a 1 L batch photo reactor by a polychromatic medium-pressure mercury lamp (TQ150, UV Consulting Peschl, Mainz) with a Ilmasil quartz immersion tube. The batch photo reactor was provided with constant stirring and 18–20 °C temperature was maintained by a circulating cooler. The intensity of light emitted by the used UV lamp and molar extinction coefficient of DIAT for the range of 200 nm to 440 nm were summarized in Table S1 and Figure S1 in the Supplementary information (SI).

DIAT was dissolved in ultrapure water for direct photolytic experiments with no pre-treatment in order to exclude any other constituents that could interfere with the formation of TPs and/or to avoid the initiation of scavenger effects of any absorbing or photosensitizing chemical or other species during degradation.

Sampling was done after 2, 4, 8, 16, 32, 64, 128 and 256 min of irradiation time, respectively, in order to monitor the kinetics of transformation and mineralization of DIAT. The primary elimination of DIAT and photo-TPs formed during photodegradation process were monitored by HPLC–UV and LC–ESI–MS/MS (ion-trap), respectively.

The rate of the decline of DIAT during direct photolytic transformation was assumed to follow the first-order kinetics (OECD, 2008), which was confirmed by fitting a first-order curve to the experimental data.

### 2.3. Analytical methods

DIAT concentration in an aqueous solution was determined by reversed phase high performance liquid chromatography (RP-HPLC) using a Shimadzu Prominence HPLC apparatus (Duisburg, Germany) equipped with an UV/vis detector. The chromatographic column RP-C18 (CC 125/4 NUCLEODUR® 100–5 C18 ec, Macherey and Nagel, Düren, Germany) was used as a stationary phase. The chromatographic separations were performed using a binary gradient mode consisting of mobile phase 0.2% formic acid in ultrapure water (CH<sub>2</sub>O<sub>2</sub>: solution A) and 100% acetonitrile (CH<sub>3</sub>CN: solution B), as described in detail in Table S2 (SI). The flow rate, column oven temperature and injection volume were set to 0.5 mL min<sup>-1</sup>, 30 °C and 10 µL, respectively. Total running time was 25 min. DIAT was eluted at 13.7 min (retention time [t<sub>R</sub>]) and was detected by a UV/vis detector at 254 nm.

The Agilent LC 1100 series coupled to a Bruker Daltonic Esquire 6000 + ion-trap mass spectrometer (IT-MS) with electrospray ionization (ESI) interface was used for identification and structure elucidation of the formed photo-TPs. The abovementioned LC parameters were used for the elution of DIAT and photo-TPs while the MS parameters were optimized for DIAT [m/z 614.9] by a direct infusion of a 20 µg mL<sup>-1</sup> standard at a flow rate of 4 µL min<sup>-1</sup> through a syringe pump. The mass spectrometer was operated in positive polarity. The operating parameters of the source and trap were summarized in SI (Table S3). The photo-TPs formed during the UV treatment were identified by comparing 0 min photodegraded samples (i.e. DIAT itself) as reference with other photolysed samples. Their structures were elucidated by interpreting the MS/MS spectra.

DOC was measured according to ISO 8245:1999 guideline (ISO 8245, 1999) using a Shimadzu TOC-VCPN analyzer equipped with an ASI-V auto sampler.

### 2.4. Aerobic biodegradation testing

The aerobic biodegradability of DIAT and its photo-TPs after UV irradiation were investigated according to OECD guidelines by the

Closed Bottle test [CBT] 301D (OECD, 1992b) and the Manometric Respiratory Test [MRT] 301F (OECD, 1992a).

The CBT was performed with a low nutrient content and low bacterial density at room temperature ( $20 \pm 1$  °C) in the dark (Kümmerer et al., 1996). In CBT the concentration of the test compound was adjusted to  $5 \text{ mg L}^{-1}$  theoretical oxygen demand without nitrification ( $\text{ThOD}_{\text{NH}_3}$ ) for the untreated samples. The sample volume of post-treated solutions (i.e. after photolysis) was increased corresponding to the DOC reduction during photolytic treatment.

The test consisted of four different series (SI, Table S4). The blank series contained only mineral medium and inoculum. The quality control series contained readily biodegradable sodium acetate at a concentration corresponding to  $5 \text{ mg L}^{-1}$   $\text{ThOD}_{\text{NH}_3}$ , mineral medium and inoculum. The actual test series contained the respective test substance, mineral medium and inoculum. The fourth series was the toxicity control which contained the test compound and sodium acetate at the concentrations corresponding to  $5 \text{ mg L}^{-1}$   $\text{ThOD}_{\text{NH}_3}$  each. The toxicity control monitors inhibitory effects due to the toxicity of test substances against the inoculum's bacteria and in order to allow for the recognition of false negative results. All series were performed in duplicates. All the test vessels were inoculated with 2 drops of the effluent from a local municipal STP (AGL Lüneburg, Germany, 144,000 population equivalents).

The aerobic biodegradation in the CBT was monitored for 28 days by measuring oxygen concentration in the test vessels with Fibox 3 (Fiberoptical oxygen transmitter) (PreSens, Regensburg, Germany) (Friedrich et al., 2013). For qualitative reasons pH was measured at 0 and 28 days.

The MRT was performed in the dark at room temperature ( $20 \pm 1$  °C) with gentle stirring. The OxiTop® Control OC110-system (WTW GmbH, Weilheim, Germany) was used as a measuring system to monitor the microbial oxygen consumption indirectly through  $\text{CO}_2$  production during the aerobic biodegradation. The oxygen consumption was the end-point, used to calculate biodegradation.

The sample scheme and the investigated time points were equivalent to that of the CBT, except that the test compound and reference substance (sodium acetate) concentrations were adjusted to  $30 \text{ mg L}^{-1}$   $\text{ThOD}$  and 80 mL of inoculum was added to 1 L of test solution as required by the test guidelines. Furthermore, an additional sterile control for the assessment of abiotic elimination was applied. The sterile control contained the test substance and sodium azide with no inoculum.

In the present study, samples from photolysis after 0 min (parent compound, DIAT), 32 min, 128 min and 256 min irradiation have undergone CBT and MRT, respectively. A more detailed description of the testing procedures can be found elsewhere (Mahmoud and Kümmerer, 2012; Trautwein and Kümmerer, 2011). Samples were taken at the beginning (day 0) and the end of the test (day 28) for later analysis by the LC–UV–MS/MS to monitor any elimination of test compounds (i.e. DIAT and formed photo-TPs).

Substances showing at least 60% degradation in these tests are classified as “readily biodegradable” (OECD, 2006) and therefore are expected not to enter or being accumulated in the aquatic environment (Nyholm, 1991). A negative result in these tests demands the next level of testing, i.e. either a simulation test or an inherent biodegradability test, should be considered (OECD, 2006).

## 2.5. *In silico* (quantitative) structure–activity relation predictions

### 2.5.1. *In silico* prediction of photodegradation products

The photodegradation pathway of DIAT and its degradation products was predicted with the software MetaPC (Version 1.8.1, MultiCASE Inc., Beachwood, USA) (Sedykh et al., 2001) with its photodegradation dictionary in combination with the photo-TPs' structures identified and elucidated by the LC–ESI–MS/MS (Ion-trap).

Meta software predicts the transformation of chemicals under a set of different conditions with using a set of rules from literature and organized within a “dictionary” (Sedykh et al., 2001). These dictionaries are the compilation of known enzymatic transformations and based on a library of known pairs of target and transforming sequences (“transforms”). Test molecules are scanned for these target sequences. The photodegradation dictionary of the MetaPC software consists of approximately 1200 transformations that are loosely divided into 9 large subdivisions. The module was validated with 40 known industrial chemical products and had a hit/miss ratio of higher than 92%.

### 2.5.2. *In silico* prediction of environmental fate of DIAT and its photo-TPs

The ready biodegradability for DIAT and its photo-TPs were predicted by various *in silico* models listed in Table 1. The ready biodegradability of DIAT and its photo-TPs were predicted based on data for OECD 301C MITI-I test (Ministry of International Trade and Industry, Japan) (OECD, 2006) which is generally not directly comparable to CBT and MRT, but can provide orientation towards identifying the readily biodegradable and non-readily biodegradable moieties of the molecules.

The OASIS Catalogic models predicted the ready biodegradability as a numerical value between 1 and 0 which corresponds to 100% and 0% biodegradation, respectively. The numeric value of 0.6 corresponds to 60% biodegradation which is a pass criterion for ready biodegradability under MITI-I test conditions. CASE Ultra MITI-I test (OECD 301C, module AU6) predicted positive or negative alerts for the selected model.

Further, the environmental fate analyses of DIAT and photo-TPs were assessed by the PBT Profiler—A Component of OPPT's P2 Framework software developed by the Environmental Health Analysis Center under contract to the Office of Chemical Safety and Pollution Prevention, U.S. EPA (U.S. Environmental Protection Agency, 2012).

It is a screening tool developed to identify pollution prevention opportunities for chemicals without experimental data. PBT profiler identifies the chemicals that may persist and bioaccumulate in the environment based on the information published by the EPA in the Federal Register (Environmental Protection Agency, 1999a; Environmental Protection Agency, 1999b). The PBT profiler also uses a different set of criteria which is based on the scientific principles and QSAR that have been used to screen for chronic fish toxicity in EPA's New Chemical Program (Clements et al., 1993). Such screening assessments can help in the decision-making process to better focus resources.

The bioconcentration factor (BCF) in fish was also predicted for DIAT and its photo-TPs by the two models of Catalogic software listed in Table 1. Both BCF models account for a number of mitigating factors, such as molecular size, metabolism of parent chemical, water solubility and ionization. The only difference in both BCF models was that BCF base-line D/P model considers distribution coefficients (log D) and partitioning coefficients (log P) of chemicals for assessing the effect of ionization on the bioaccumulation potential. The BCF factor indicates the bioaccumulation potential of chemical species in the environment if  $\log \text{BCF} \geq 3.699$ , i.e.  $\text{BCF} > 5000$  (Arnot and Gobas, 2006).

Additionally, *in silico* toxicity (toxicity to environmental bacteria, mutagenicity and genotoxicity) for DIAT and its photo-TPs were predicted by various models of OASIS, CASE Ultra and Leadscape software listed in Table 1. Leadscape software was used with training sets from 2012 SAR Genotox Database provided by Leadscape (Roberts et al., 2000).

All the *in silico* models used in the study for environmental fate predictions have validated databases and training sets. More information about their databases, training sets and their validity criteria can be easily found elsewhere in the references provided in Table 1 for each model. Generally, the structures of chemical species are scanned by the software against the validated databases of the model, and the software calculates the activity and predicts the output in the form of alerts for that corresponding activity.

**Table 1**List of all the *in silico* models and software used for the environmental fate predictions of DIAT and its photo-TPs.

QSAR software	Models	End-points	References
Catalogic v 5.11.6 TB (OASIS)	CATABOL 301C model CATALOGIC 301C models <i>Vibrio fischeri</i> pT5 v.01 <i>Vibrio fischeri</i> pT15 v.01 <i>Vibrio fischeri</i> pT30 v.01 in vitro Ames model BCF base-line model v.02.05 BCF base-line model D/P v.01.01	Ready biodegradability according to MITI-I test Ready biodegradability according to MITI-II test Acute toxicity against <i>V. fischeri</i> after 5 min, IC50 [mg/L] Acute toxicity against <i>V. fischeri</i> after 15 min, IC50 [mg/L] Acute toxicity against <i>V. fischeri</i> after 30 min, IC50 [mg/L] Mutagenicity against <i>Salmonella Typhimurium</i> log BCF log BCF with consideration of distribution coefficients (log D) and partitioning coefficients (log P)	(Laboratory of Mathematical Chemistry B, 2012)
CASE Ultra v.1.4.5.1 (MultiCASE Inc., Beachwood, USA)	MITI-I test (OECD 301C, module AU6) Human carcinogenicity (A0J) Micronucleus formation <i>in vivo</i> composite (A7S) Chromosome aberration in vitro composite (A7U) Mutagenicity Ames (A2H) Microtox toxicity environmental bacteria (AUA).	Ready biodegradability according to MITI-I test Carcinogenicity Genotoxicity Mutagenicity Mutagenicity against <i>Salmonella Typhimurium</i> Bacterial toxicity	(Chakravarti et al., 2012; Saikhov et al., 2013)
Leadscope V. 3.0.11-1.	Bacterial mutagenesis (BM) model	Mutagenicity as a result of interaction with DNA of <i>Salmonella Typhimurium</i> or <i>Escherichia coli</i>	(Roberts et al., 2000).

### 3. Results and discussion

#### 3.1. Photolysis

The photolysis of DIAT was performed twice with three different initial concentrations i.e. 10, 25 and 150 mg L<sup>-1</sup>. It resulted in a complete primary elimination of parent compound with incomplete mineralization. The observed degree of mineralization 43%, 38% and 24% according to DOC measurement at 10, 25 and 150 mg L<sup>-1</sup> initial concentration of DIAT, respectively, indicates the formation of photo-TPs.

During 32 min of UV photodegradation, the samples showed a decrease of about 65 ± 3.6% of the initial concentration of DIAT (150 mg L<sup>-1</sup>). Afterwards, the degradation rate slowed down relatively until 128 min where 99.5 ± 0.4% of the initial concentration (150 mg L<sup>-1</sup>) was removed. This slowdown in the degradation rate after 32 min of irradiation can be assumed to be due to the presence of newly formed intermediates (photo-TPs), which might absorb the radiation, and thus, preventing the remaining parental analyte from the irradiation source.

Fig. 1a shows the time-trend for the photolytic transformation of DIAT in the laboratory experimental setup and its dependence on the initial substrate concentration. It was observed that the photodegradation of the lowest concentration (10 mg L<sup>-1</sup>) was relatively faster than that of the other two investigated concentrations. The data of photodegradation fits the first-order kinetic (OECD, 2008) with high linearity ( $r^2 > 0.97$ ) (Fig. 1b). Therefore, first-order rate constants ( $k_{obs}$ ) for the three different initial concentrations of DIAT can be obtained from the slope of each straight line (OECD, 2008). The plot of initial reaction rate ( $r_0$ ) with the initial concentration of DIAT provided a straight line with  $r^2 > 0.97$  (Fig. 1b, inset). It supported the assumption that the photolytic degradation of DIAT follows first-order kinetics.

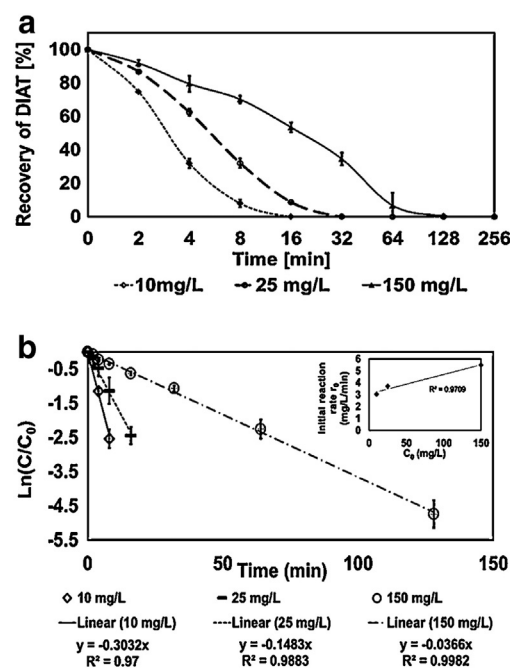
#### 3.2. Identification and structure elucidation of photo-TPs of DIAT

For the photo-TP analyses, LC-MS/MS was operated in full-scan mode and observed that a large number of photo-TPs had appeared in the degradation mixture. As the photodegradation of 10 mg L<sup>-1</sup> solution resulted in the formation of very small amounts of photo-TPs, the concentrations obtained were below instrumental quantification limits. Experiments using high initial concentration solutions were necessary to generate information about photo-TPs (kinetics and structures). Same photo-TPs were formed for both initial concentrations (25 mg L<sup>-1</sup> and 150 mg L<sup>-1</sup>) of DIAT.

A few of the photo-TPs were already reported in the literature (Hapeshi et al., 2013; Hennebel et al., 2010; Jeong et al., 2010; Sugihara et al., 2013; Velo-Gala et al., 2012). New photo-TPs that have

not been yet reported were identified as well. The elucidation of the structures of new formed photo-TPs was performed by comparing the identified structure acquired from the MS data with those predicted by the MetaPC software. The retention time ( $t_R$ ), molecular formula, extracted ion chromatogram (EIC) and the MS<sup>2</sup> fragmentation pattern of DIAT and its photo-TPs were provided in detail in SI Text S2.

Fig. 2 shows the kinetics of appearance/disappearance of photo-TPs which were formed with the relative abundance above 1% during the photolysis of DIAT (initial concentration of DIAT 150 mg L<sup>-1</sup>; n = 2). Generally, the peak area does not precisely indicate the concentration of the respective photo-TP in the photodegraded mixture as its molar extinction coefficient and ionization rate are not known. However, the estimation of the relative change of the concentration of photo-TPs during photolysis was possible thereby. The same kinetic trend of photo-TPs was observed for the 25 mg L<sup>-1</sup> DIAT subjected to photolysis. But 150 mg L<sup>-1</sup> initial concentration of DIAT was chosen for the analysis



**Fig. 1.** a) The photolytic transformation of DIAT and its dependence on the initial substrate concentration (n = 2); b) First-order plot of photodegradation of DIAT for different initial concentration and plot of calculated initial reaction rates ( $r_0$ ) against initial concentration (inset).



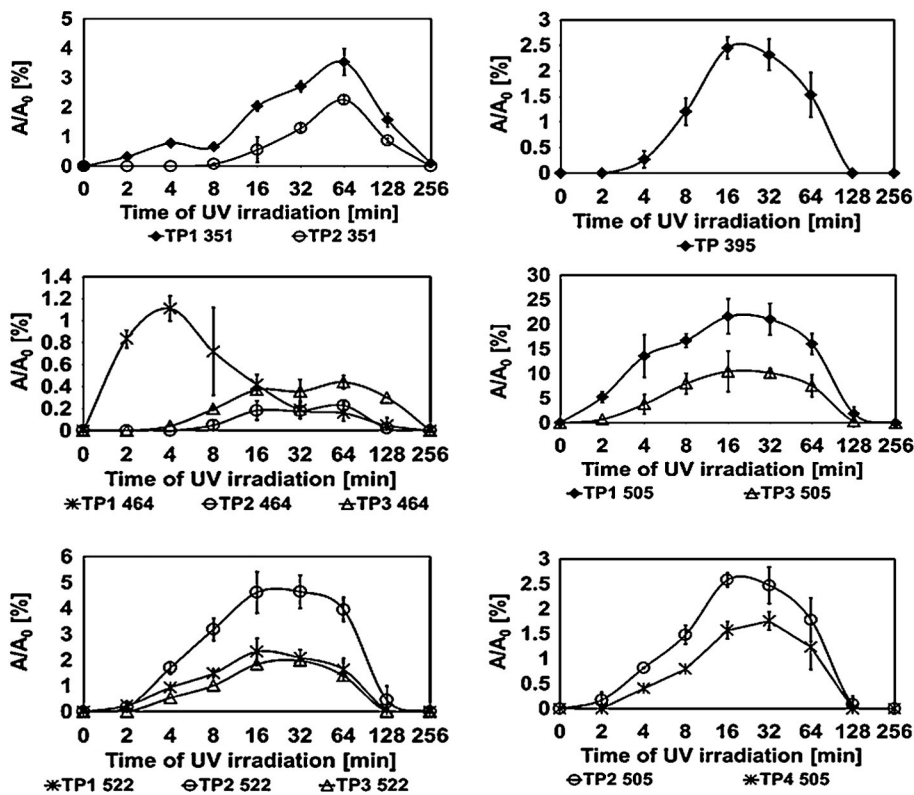


Fig. 2. Time course of appearance/disappearance of peak area of the photo-TPs of DIAT (relative abundance above 1%) measured by LC-ESI-MS in positive mode ( $A/A_0$  as  $A$  is the peak area of photo-TPs and  $A_0$  is the peak area of DIAT at 0 min) (Initial concentration of DIAT =  $150 \text{ mg L}^{-1}$ ;  $n = 2$ ).

so that all the formed photo-TPs would be quantified more precisely during MS<sup>2</sup> fragmentation.

Based on literature findings and kinetics of appearance/disappearance, a scheme of the photolytic degradation pathway was proposed (Fig. 3). The photo-TPs of DIAT could be further divided into two categories: primary and secondary photolytic degradation products. Primary photolytic degradation products were assumed to be formed from the

direct degradation of DIAT while secondary degradation products were supposed to be formed by the further degradation of primary photo-TPs.

In the present study, the preferential pathway of the photo-degradation of DIAT observed was the *ipso*-attack of hydroxyl radical ( $\cdot\text{OH}$ ) at one of the iodine sides or the carboxylic acid side (methanoate moiety) which resulted in the phenolic product. Similar findings were

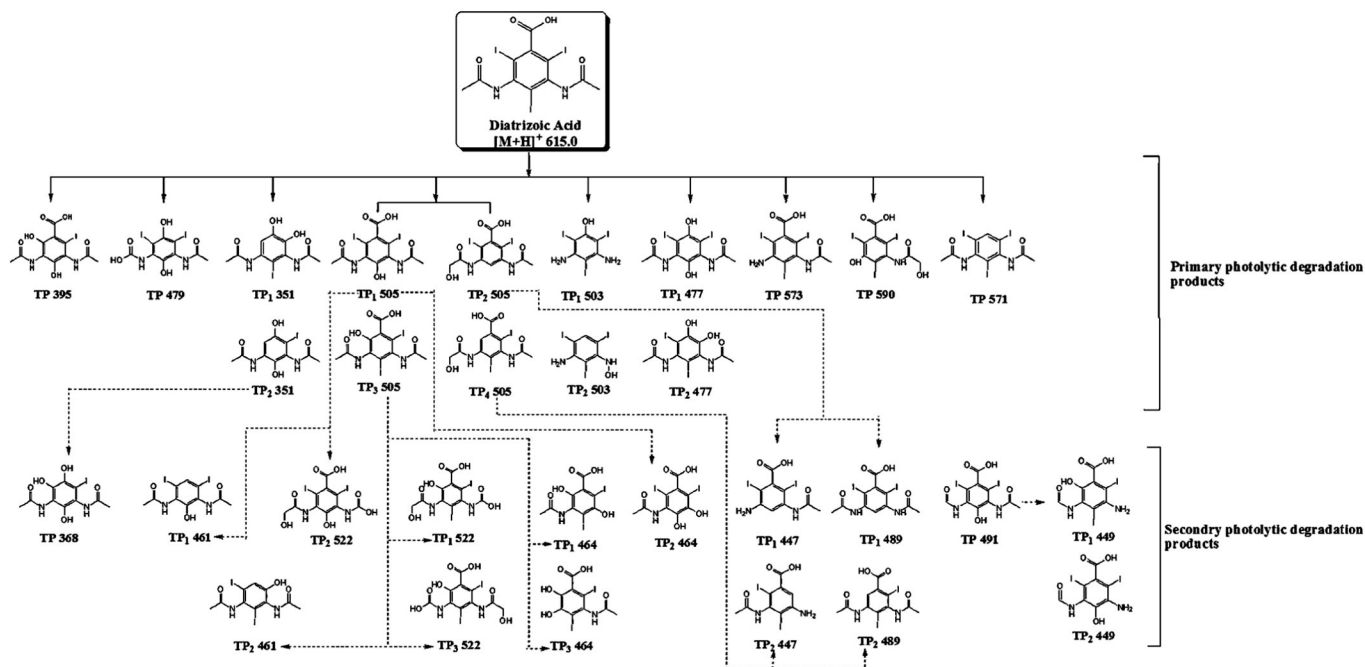


Fig. 3. Proposed tentative pathway of photolytic degradation of DIAT under UV light.

reported by Jeong et al. (2010) during the  $\gamma$ -irradiation of ICM. Kılıç and Çınar (2008) demonstrated that during the photodegradation of 4-chlorophenol (aromatic halide), the attack of OH radicals at the *ortho*- and *ipso*-carbon as the most preferred degradation mechanism ends up with the formation of the most stable degradation products 4-chlorocatechol and hydroquinone, respectively.

Fig. 4 illustrates the mechanism responsible for the photolytic degradation of the ICM under direct UV irradiation. It can be further classified into three categories: a) the *ipso*-attack of an OH radical on the iodine side, b) *ipso*-attack of an OH radical on carboxylic acid side i.e. methanoate moiety and c) homolytic cleavage of the aryl iodine or aryl methanoate bond under the presence of UV light. The mechanisms a and b resulted in the formation of the stable catechol and hydroquinone derivatives of corresponding ICM by the addition of a hydroxyl group on the aromatic ring. It was observed that the mechanisms a and b were the dominant photolytic degradation mechanisms of DIAT. They were responsible for the formation of most of the primary photolytic degradation products. Only few primary photolytic degradation products (TP<sub>2 & 4</sub> 505, TP<sub>2</sub> 503 and TP 571) were resulted through mechanism c.

Primary photolytic degradation products like TP 395 and TP<sub>1 & 3</sub> 505 were formed from DIAT by the mechanism a. DIAT, similar to other ICM, has iodine atoms at both the *ortho*- and the *para*-position which can be substituted during the photodegradation. According to Svetlichnyi et al. (2001) in case of aromatic halides, the substitution of halogen atoms by OH radicals at the *para*-position is more preferred and faster than at the *ortho*-position. Therefore, TP<sub>1</sub> 505 was assumed to be formed by the substitution of iodide at the *para*-position while TP<sub>3</sub> 505 at the *ortho*-position. The kinetics of appearance/disappearance of photo-TPs (Fig. 2) support the assumption because the formation of TP<sub>1</sub> 505 was faster than TP<sub>3</sub> 505 and also the relative peak area of TP<sub>1</sub> 505 was comparatively higher than TP<sub>3</sub> 505. Another photo-TP, TP<sub>1</sub> 503, was formed by mechanism b with simultaneous cleavage of the N–C bond of the acetyl amino side chain.

Primary photo-TPs like TP<sub>2 & 4</sub> 505, TP<sub>2</sub> 503 and TP 571 were formed due to homolytic cleavage mechanism as shown in mechanism c. TP<sub>2 & 4</sub> 505 was supposed to be formed through the homolytic cleavage of aryl iodide bond at *para*- and *ortho*-position with subsequent attachment of the hydroxyl group to the terminal carbon of acetyl amino side chain. TP<sub>2</sub> 503 and TP 571 were formed due to the homolytic breakage of aryl methanoate bond of DIAT.

The photolytic degradation of DIAT through both mechanisms a and b acting simultaneously resulted in the formation of primary photo-TPs TP<sub>2</sub> 477, TP 479 and TP<sub>1</sub> 477 which were the catechol and hydroquinone derivatives of DIAT. In contrast, the primary photo-TPs TP<sub>1 & 2</sub> 351 can be considered to be formed when DIAT degraded through all three mechanisms (a, b and c) acting simultaneously.

TP<sub>1 & 3</sub> 505 was the most abundant photo-TP (about 20%) formed during the intermediate time point of photolysis (32 min). They were further transformed (degraded) as the photolysis proceeded (Fig. 2). This further photolytic degradation of TP<sub>1 & 3</sub> 505 resulted in secondary photo-TPs like TP<sub>1-2</sub> 461, TP<sub>1-3</sub> 522 and TP<sub>1-3</sub> 464. This assumption of the formation of secondary photo-TPs from primary degradation products was based on the kinetic data of appearance/disappearance of photo-TPs (Fig. 2).

Secondary photo-TPs TP<sub>1-3</sub> 522 were assumed to be formed by the addition of an OH group at the terminal carbon of one of the acetyl amino side chains of TP<sub>1 & 3</sub> 505. TP<sub>1-3</sub> 464 was supposed to be formed by the substitution of the acetyl amino side chain of TP<sub>1 & 3</sub> 505 by the hydroxyl group. While homolytic breakage of the carboxyl moiety of TP<sub>1 & 3</sub> 505 resulted in the formation of TP<sub>1-2</sub> 461. While the formation of secondary photo-TP TP<sub>1-2</sub> 447 can be inferred from the de-acylation of the hydro-acetyl amino side chain of TP<sub>2 & 4</sub> 505.

### 3.3. Aerobic biodegradation test assays

The results of the both aerobic biodegradation tests for samples after photolysis were summarized in Table 2. The data of both biodegradation tests for the tested samples were shown in Figure S2 and S3 in SI. In both tests, the activity of inoculum in the quality control was adequate and the test assays were valid according to the established guidelines. DIAT reached about 3.5% and –4.6% biodegradation in CBT and MRT, respectively. Therefore, it can be classified as not readily biodegradable chemical according to the test guidelines (OECD, 2006). Generally, higher biodegradation is expected in MRT compared to CBT due to the higher inoculum density and bacterial diversity. In the study MRT showed less biodegradation than that the CBT. One of the reasons for such a phenomenon can be inferred from the high concentration of test substances subjected to the MRT which could inhibit the bacteria from the biodegradation.

The other pass criteria for MRT according to OECD guideline (OECD, 1992a) are a 70% removal of DOC value after 28 days. The DOC

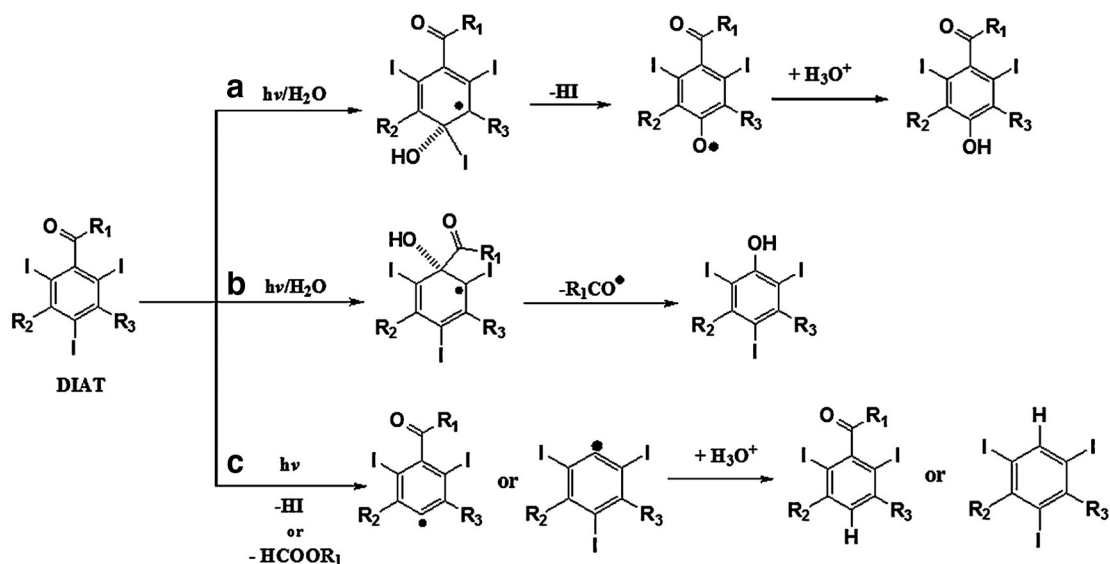


Fig. 4. Mechanisms responsible for the formation of photo-TPs of DIAT under UV light: a) *ipso*-attack of hydroxyl radical on iodine moiety; b) *ipso*-attack of hydroxyl radical on methanoate moiety and c) homolytic cleavage of the aryl iodine or aryl methanoate bond under UV light ( $R_1 = -OH$  and  $R_2 = R_3 = -NHC(=O)CH_3$ ).

**Table 2**  
Results of the investigated aerobic biodegradation test assays for DIAT and its photo-TPs.

Biodegradation test	Test sample	Biodegradation after 28 days [%]	DOC removal [%]	Parent compound elimination [%]	Photo-TPs identified to be biodegraded
CBT	0 min	3.5 ± 2.2%		20.19%	TP 395; TP <sub>3</sub> 464; TP <sub>1-2</sub> 503;
	32 min	26.2 ± 1.1%		20.17%	TP <sub>1-4</sub> 505; TP <sub>1-3</sub> 522 and TP 590
	128 min	41.2 ± 1.2%		–	
	256 min	46.6 ± 1.4%		–	
MRT	0 min	–4.6 ± 1.9%	–3.6%	11.85%	TP <sub>1-2</sub> 489; TP <sub>1-2</sub> 503; TP <sub>1-4</sub> 505;
	32 min	–0.4 ± 15.8%	2.9%	10.16%	TP <sub>1-3</sub> 522; TP 573 and TP 590
	128 min	12.3 ± 0.7%	14.4%	10.62%	
	256 min	15.1 ± 3.3%	29.6%	–	

elimination during MRT after 28 days for the samples after 0 min, 32 min, 128 min and 256 min of photolysis (Table 1) indicated the partial biodegradability of photo-TPs in the MRT.

Earlier published studies about the biodegradation of DIAT confirmed that DIAT is not readily biodegradable chemical. Haiß and Kümmerer (2006) reported that DIAT was not eliminated by sewage sludge according to OECD 303A simulation test, although it was bio-transformed into degradation products under modified Zahn–Wellens test (OECD 302B). Similar findings were reported by Kalsch (1999) and Joss et al. (2006). They reported that DIAT was not biodegraded in the activated sludge batch reactors.

An inhibitory effect was observed within the first couples of days in the toxicity control of photodegraded samples (i.e. 32 min, 128 min and 256 min samples) in both investigated aerobic biodegradation test assays. This inhibition impacted inoculum's bacteria, which were not able to degrade readily biodegradable reference substance (sodium acetate) in the investigated test assays. There was no such inhibitory effect observed in the toxicity control when the parent compound DIAT (i.e. 0 min sample) was subjected to test assays. This means that there might be a few photo-TPs present which had the toxicity against inoculum's bacteria. Therefore, bacteria required an adaptation time probably due to their slower growth rates before they could have any impact on biodegradation. After a short adaptation time (about 2–3 days) the bacteria present in the inoculum biodegraded the test mixture (in toxicity control) more than 25% in 14 days. Thus, it can be concluded that a few photo-TPs had comparatively more toxic potency than those of the parent compound.

The samples from the start to the end of each biodegradation test assays were analyzed by the LC–UV–MS/MS. The peak areas of the photo-TPs were compared for the start and end of CBT and MRT as shown in Fig. 5a and b, respectively. As mentioned earlier, the peak areas do not precisely indicate the concentration of photo-TPs. However, as biodegradation test samples were concerned, the peak areas of photo-TPs were measured with the same conditions (e.g. ionization efficiency) for 0-day and 28-day samples. Therefore their elimination through biodegradation was calculated. The LC–MS/MS results indicate that a few of the formed photo-TPs (summarized in Table 2) were comparatively better biodegradable than that of the DIAT itself.

The LC–MS/MS analysis of the sterile control of the MRT samples revealed that about 24% of DIAT was eliminated abiotically. This abiotic elimination of DIAT could be due to sorption, hydrolysis or non-biotic oxidation. In fact, DIAT was eliminated (about 20% in CBT and 11% in MRT) with no considerable oxygen consumption for the 0-min test series (see Table 2). Therefore, it could be considered that DIAT was abiotically eliminated even in the test samples similar to the sterile control. But, further investigations and tests are required to confirm and to elucidate the processes of abiotic elimination of DIAT.

### 3.4. *In silico* fate prediction and qualitative risk assessment of DIAT and its TP

#### 3.4.1. *In silico* biodegradability predictions

The structure of DIAT and its photo-TPs were analyzed by *in silico* models (see Table 1) for ready biodegradability. The predicted activating

and deactivating alerts (i.e. moieties) identified by all QSAR models were summarized in SI (Table S4). The combined predictions of all the used *in silico* models confirmed DIAT as a non-readily biodegradable chemical and indicated that a few photo-TPs might be more biodegradable as DIAT itself. The predicted better biodegradable photo-TPs were the same ones which were observed to be better biodegradable than DIAT in actual biodegradation test assays and listed in Table 2.

Both models of OASIS Catalogic software for readily biodegradability predicted the output value as  $\leq 0.3$  for DIAT (Table S4, SI). These output values were from below the pass criterion for ready biodegradability under MITI-I test conditions (i.e. biodegradation  $\geq 60\%$ ) (OECD, 2006). Therefore, DIAT can be categorized as a non-readily biodegradable chemical. Thus, it is expected to be present in aquatic environment which was confirmed by the various published studies (Putschew et al., 2000; Heberer, 2002; Seitz et al., 2006; Howard and Muir, 2011).

Case Ultra provided a marginal positive alert for DIAT and predicted acetyl moieties present on the acetamide side chain as the activating alert for ready biodegradability. This prediction by Case Ultra about the acetyl moiety as activating alert for biodegradability is supported by Haiß and Kümmerer (2006). They reported the cleavage of acetyl moiety from the acetamide side chain of DIAT as the major aerobic biodegradation mechanism, which later resulted in the formation of a stable dead end biotransformation product.

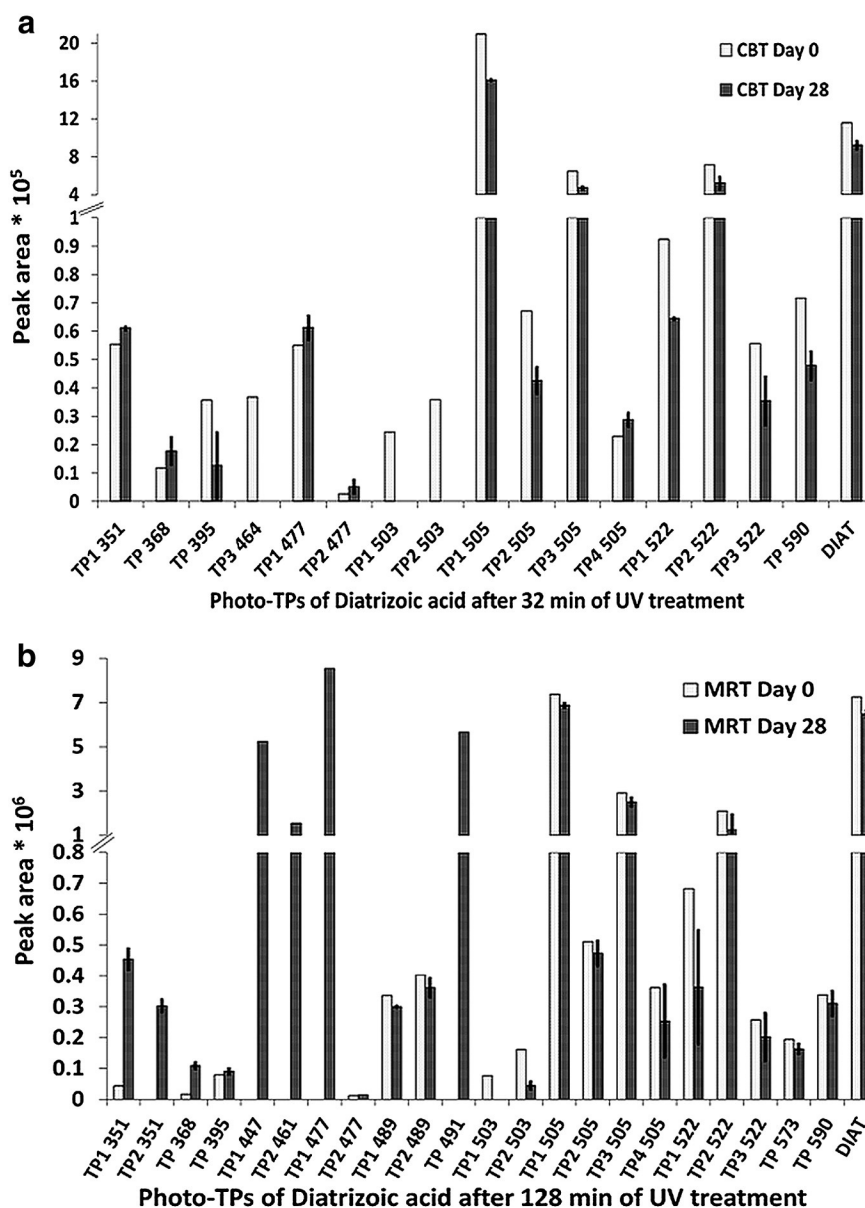
It was observed that when the photo-TPs retained the acetyl moieties during photodegradation then these moieties were predicted as activating alert moieties for ready biodegradability (see Table S4, SI). It was also observed that the resulted moieties of photo-TPs which were formed by the homolytic cleavage through the mechanism c of DIAT were predicted as deactivating alert moieties for ready biodegradability (Table S4, SI).

#### 3.4.2. *In silico* PBT profiler, bioaccumulation and air–water partitioning predictions

Escher and Fenner (2011) proposed that the TPs which are formed  $\geq 10\%$  of initial amount of parent compound during treatment are comparatively more relevant for environment fate assessment and (eco) toxicity testing. However, in the present study the photo-TPs of high activity and low yield would be missed through this approach. Therefore, in order to keep the workload manageable the photo-TPs with relative abundance  $\geq 2\%$  ( $A/A_0 \geq 2\%$ ) were selected as of main interest but the *in silico* predictions for the other remaining photo-TPs ( $A/A_0 < 2\%$ ) were also performed as summarized in SI Table S5.

Table 3 shows the predicted environmental parameters with the PBT profiler, Oasis Catalogic, Case Ultra and Leadscape software for DIAT and selected photo-TPs ( $A/A_0 \geq 2\%$ , Fig. 2). The PBT profiler predicted DIAT as a very persistent chemical. It also predicted that DIAT would not bioaccumulate in the environment but possesses a moderate chronic toxicity towards fish. These predictions were in accordance with the contrast agents that are generally designed to be very polar and persistent.

The PBT profiler predicted that the selected photo-TPs ( $A/A_0 \geq 2\%$ ) are comparatively less persistent than those DIAT and also do not possess any bioaccumulation threat to aquatic organism in the environment. It



**Fig. 5.** Peak area of the photo-TPs of DIAT at the start and end of each aerobic biodegradation test assays: a) CBT of 32 min UV irradiated samples ( $n = 2$ ); b) MRT of 128 min UV irradiated samples ( $n = 2$ ).

predicted selected photo-TPs ( $A/A_0 \geq 2\%$ ) also might have a moderate chronic toxicity towards fish similar to DIAT except TP<sub>1</sub> 351.

The log BCF predictions by OASIS Catalogic software completely supported the results of the PBT profiler about the bioaccumulation potential of DIAT and the photo-TPs. The predicted values of log BCF (OASIS software) for DIAT and its selected photo-TPs ( $A/A_0 \geq 2\%$ ) (Table 3, columns 3 and 4) were in the range from 0.469 to 0.760. According to information published by EPA (Environmental Protection Agency, 1999a), if the log BCF value for any organic compound is less than 3.699 ( $BCF < 5000$ ), then it cannot be considered as a bioaccumulative in aquatic organism. Therefore, their bioaccumulation is very unlikely.

Most of the fate predictions calculations are generally based on the log  $k_{ow}$  value of the compounds. Therefore, the log  $k_{ow}$  was predicted by Oasis Catalogic and PBT profiler for DIAT and its photo-TPs. Predictions of log  $k_{ow}$  (Table 3, columns 2 and 5) for DIAT were in accordance with the experimental values (Meylan and Howard, 1995) thus provided a basis to trust the results for the photo-TPs as predicted ('*in silico* read-across approach'). These predictions concluded DIAT as a polar compound and the selected photo-TPs ( $A/A_0 \geq 2\%$ ) might be

comparatively more polar than DIAT. Therefore the high mobility of DIAT and its photo-TPs should be expected. This is in accordance with the detection of DIAT in drinking water at a concentration range of about  $1.2 \mu\text{g L}^{-1}$  (Putschew et al., 2000).

The partitioning of DIAT and photo-TPs between water and air was predicted in terms of the Henry's Law constants (H). In the present study, the predicted H values for all compounds were very low ( $1.0 \text{ E-11} > H \leq 1.0 \text{ E-12}$ ) (Table 2, column 6) indicating that these compounds will tend to partition into the aqueous phase instead of air. Therefore, their elimination through evaporation into the atmosphere is most likely insignificant.

#### 3.4.3. *In silico* toxicity predictions

The bacterial toxicity predictions of DIAT and its selected photo-TPs ( $A/A_0 \geq 2\%$ ) were summarized in Table 3 (columns 11 and 14–16). Case Ultra predicted DIAT as a nontoxic chemical against environmental bacteria but provided ambiguous predictions for the selected photo-TPs. It provided inconclusive alerts for TP<sub>2&4</sub> 505 and out of domain (OD) alert for TP<sub>1-3</sub> 522. This indication of applicability domains can be considered

**Table 3**  
*In silico* environmental fate and toxicity predictions of DIAT and its selected photo-TPs ( $A/A_0 \geq 2\%$ , from Fig. 2) by PBT profiler and various models of Case Ultra, Catalogic and Leadscope software.

Photo-TPs	Physicochemical Properties						Toxicity predictions									
	OASIS Catalogic V.5.11.6			PBT profiler software			CASE Ultra				Leadscope		OASIS Catalogic V.5.11.6			
	log $K_{ow}$	log BCF	log BCF with ionization term	Log $K_{ow}$	Henry's Law constant (atm/m <sup>3</sup> mole)	PBT profiler estimate <sup>a</sup>	A	B	C	D	E	E	Acute toxicity against <i>V. fischeri</i> , IC <sub>50</sub> [mg/L]			
													5 min	15 min	30 min	E
DIAT	1.37	0.7268	0.7607	1.36	1.0E – 12	P <sub>3</sub> B <sub>1</sub> T <sub>2</sub>	–	–	–	–	–	–	699.6	1158.5	500.8	–
TP <sub>1</sub> 351	–0.15	0.4696	0.4733	–0.1	1.0E – 12	P <sub>2</sub> B <sub>1</sub> T <sub>3</sub>	–	+	+	–	–	+	9985.7	25,882.2	5897.6	–
TP <sub>2</sub> 351	–0.71	0.4695	0.4733	–0.7	1.0E – 12	P <sub>2</sub> B <sub>1</sub> T <sub>2</sub>	–	+	+	–	–	+	33,387.6	102,608.8	18,488.2	–
TP 395	–0.176	0.6061	0.6299	–0.1	<1E – 12	P <sub>2</sub> B <sub>1</sub> T <sub>2</sub>	–	+	–	–	–	–	11,463.8	29,553.4	6588.2	–
TP <sub>1</sub> 505	–0.284	0.6328	0.6596	–0.2	<1E – 12	P <sub>2</sub> B <sub>1</sub> T <sub>2</sub>	–	+	–	–	–	–	1476.9	2775.3	983.5	–
TP <sub>2</sub> 505	–0.369	0.5587	0.5763	–0.3	1.0E – 12	P <sub>2</sub> B <sub>1</sub> T <sub>2</sub>	–	–	–	§	–	–	21,884.9	59,505.8	12,182.1	–
TP <sub>3</sub> 505	0.911	0.6725	0.7031	0.34	1.0E – 12	P <sub>2</sub> B <sub>1</sub> T <sub>2</sub>	–	+	–	–	–	–	17,875.0	47,003.4	9900.9	–
TP <sub>4</sub> 505	0.391	0.5587	0.5763	–0.1	1.0E – 12	P <sub>2</sub> B <sub>1</sub> T <sub>2</sub>	–	–	–	§*	–	–	4396.2	9583.7	2714.2	–
TP <sub>1</sub> 522	0.194	0.576	0.5959	0.19	<1E – 11	P <sub>2</sub> B <sub>1</sub> T <sub>2</sub>	–	+	–	OD	–	–	6756.6	15,472.1	3999.7	–
TP <sub>2</sub> 522	–0.999	0.5283	0.5414	–0.9	<1E – 12	P <sub>2</sub> B <sub>1</sub> T <sub>2</sub>	–	+	–	OD	–	–	81,224.6	259,989	39,989.4	–
TP <sub>3</sub> 522	–0.367	0.576	0.5959	–0.3	<1E – 12	P <sub>2</sub> B <sub>1</sub> T <sub>2</sub>	–	+	–	OD	–	–	21,798.1	58,486.8	11,857.9	–

A– Human carcinogenicity; B– Micronucleus *in vivo* composite; C– Chromosome aberration; D– Microtox against environmental bacteria; E– Salmonella Mutagenicity; OD: Out of Domain means that the test chemical is not included in the applicability domain of the applied model; §\*: Inconclusive with asterisk symbol (\*) means both positive and deactivating alerts were found in the same molecule and therefore a clear result cannot be provided; §: Inconclusive means that the molecule contained too many unknown fragments; + : a positive alert for corresponding activity; – : a negative alert for corresponding activity.

<sup>a</sup> The output of PBT profiler can be categorized with numerical value between 1 and 3 for Persistence (P), Bioaccumulation (B) and Toxicity (T). The numerical value 3 indicates the highest and 1 the lowest level for the respective activity.

an advantage of the Case Ultra software as it does not only calculate but also evaluates the data.

Further bacterial toxicity activity was predicted by the acute toxicity against *Vibrio fischeri* models of OASIS Catalogic software. These models predicted the IC<sub>50</sub> values in mg L<sup>–1</sup> instead of alerts. OASIS models predicted a comparatively high IC<sub>50</sub> value in the range of 500 mg L<sup>–1</sup> to 1160 mg L<sup>–1</sup> for DIAT. Models predicted even higher IC<sub>50</sub> values for the selected photo-TPs ( $A/A_0 \geq 2\%$ ) than DIAT. This can be inferred as the selected photo-TPs might be less toxic than DIAT.

On the contrary, other photo-TPs (TP<sub>1</sub> 449, TP<sub>1</sub> 464, TP<sub>1&2</sub> 503, TP 571) which were formed in low yield ( $A/A_0 < 2\%$ ) were predicted by OASIS Catalogic models to be comparatively more acute toxic against *V. fischeri* than DIAT (Table S5, S1). These low yield toxic photo-TPs were supposed to be present in the samples which were subjected to experimental aerobic biodegradation test assays. Therefore, their presence in test assays could be the reason for the observed inhibitory effect in the toxicity control in test assays. Although these toxic photo-TPs were in low concentration but might interact with each other resulting in additive or synergistic activities to inhibit the inoculum's bacteria in the test assays.

The mutagenicity for DIAT and photo-TPs was predicted by Salmonella model (Table 3, columns 12, 13 and 17) and chromosome aberration model (Table 3 column 10). All three software predicted negative alerts for the DIAT for mutagenicity, i.e. DIAT could be most likely classified as a non-mutagenic chemical which was in accordance with the published literature (Wheeler et al., 1980).

The Salmonella mutagenicity model from Case Ultra and OASIS Catalogic predicted none of the selected photo-TPs to be active for the Salmonella mutagenicity activity while Leadscope's Salmonella model predicted TP<sub>1</sub> & 2 351 might be mutagenic. The difference in the prediction by different software is mainly due to difference in their training sets and databases.

The chromosome aberration model from Case Ultra also predicted TP<sub>1</sub> & 2 351 might be mutagenic. Thus, TP<sub>1</sub> & 2 351 more significantly can be assumed to be mutagenic as same alerts were predicted by two different models of different software, but still needs experimental testing to confirm these predictions.

The human carcinogenicity model of Case Ultra predicted neither DIAT nor its selected photo-TPs as carcinogens. The genotoxicity was predicted by the Micronucleus *in vivo* model of Case Ultra. It predicted DIAT as not genotoxic but adumbrated as the most of the selected

photo-TPs (TP<sub>1–2</sub> 351, TP 395, TP<sub>1</sub> & 3 505 and TP<sub>1–3</sub> 522) to be active, i.e. might be genotoxic which requires further testing to confirm.

Furthermore, it was reported that the XeCl excimer laser irradiation of DIAT resulted in the formations of cytotoxic mixtures of TPs (Grönwäller et al., 1998). Therefore it can be assumed that the photo-TPs formed during the photolysis of DIAT might also have the cytotoxic properties (read-across approach) and may cause threat to humans and the environment.

Moreover, DIAT has also been classified as nephrotoxic (Andreucci et al., 2006; Harmon et al., 2009; Messana et al., 1988) and neurotoxic (Bryan et al., 1982) chemical. On the basis of read-across approaches it might be reasonable to assume that a few of the photo-TPs may possess similar properties and can be nephrotoxic and neurotoxic as DIAT.

The results concluded from the *in silico* toxicological predictions significantly indicate the need of characterizing the photo-TPs through various experimental testing to confirm the predictions of toxicological models.

#### 4. Conclusion

The strategy of combining experimental methods and *in silico* analysis can be used for the environmental fate assessment of new compounds beforehand, as it allows very early and comparatively cheap evaluation of properties of a new compound which may contribute to a shorter time to market. This is of more importance for TPs especially that are not commercially available as they often are new chemical structure. The chemical synthesis of TPs is expensive and time consuming as would their isolation from test mixtures. Especially in the case of photo-treatment and oxidative treatment often numerous TPs are formed which makes it even more difficult to test each of them experimentally. In principle, the elucidation of the structural formula of TPs is sufficient to collect appropriate data as a basis for an environmental risk analysis.

Generally, the application of QSARs analysis within the risk assessment process may save time and financial resources. It also increases the knowledge about the fate and effects of TPs if they are released into the environment. Furthermore, their use may result in fewer experimental tests thus reducing the need for animal testing. *In silico* predictions can also be used as supporting tools for deciding the further tests and/or to optimize testing strategies.

If the experimental results of biodegradation tests and/or toxicity tests are combined with *in silico* prediction then it will increase the robustness and reliability of the results. In the present study, the results obtained from the *in silico* biodegradability predictions gave further information about the relative important photo-TPs as biodegradable photo-TPs are not of further interest for risk assessment. While *in silico* toxicity predictions of photo-TPs strongly indicate that further experimental tests are needed to characterize some of the photo-TPs for mutagenicity and genotoxicity.

The prescribed approach however, also has some limitations. First of all such *in silico* models are expert systems that rely on a high degree of expertise and experience of the user, which means there is a high risk of ending up with misleading results. Furthermore, when applying *in silico* models it should be taken into consideration that they are estimation methods that depend among other factors like the quality of the data used to establish the model and the structures to be evaluated are within the applicability domain of the individual model. Such *in silico* predictions should be considered as a complementary tool, which together with experimental test results can provide a complete understanding of the physico-chemical and (eco) toxicological characteristics of the substance. Furthermore, it should be noted that *in silico* model predictions generally only exist for discrete organic substances and not for unknown and variable compositions, complex reaction mixtures and biological materials. Therefore, the result of an *in silico* model should be evaluated for consistency with experimental data (“*in silico* testing battery”).

## Acknowledgment

Financial support from the German Ministry of Education and Research (NanoPharm, Project No. 03X0094C) is gratefully acknowledged. The authors also acknowledge Dr. Annette Haiss and B.Sc. Evgenia Logunova for planning the aerobic biodegradation tests. The authors would like to thank Dr. Mandy Schneider and Dr. Marcelo L. Wilde for their fruitful discussions. The authors also acknowledge Multicase Inc. and Leadscape Inc. for kindly providing the Case Ultra, MetaPC and Leadscape QSAR software, respectively.

## Appendix A. Supplementary data

Supplementary data to this article can be found online at <http://dx.doi.org/10.1016/j.scitotenv.2014.02.139>.

## References

- Andreucci M, Fuiano G, Presta P, Esposito P, Faga T, Bisesti V, et al. Radiocontrast media cause dephosphorylation of Akt and downstream signaling targets in human renal proximal tubular cells. *Biochem Pharmacol* 2006;72:1334–42.
- Arnold WA, McNeill K. Transformation of pharmaceuticals in the environment: photolysis and other abiotic processes. In: Petrović M, Barceló D, editors. *Comprehensive analytical chemistry analysis, fate and removal of pharmaceuticals in the water cycle*. Elsevier; 2007. p. 361–85.
- Annot JA, Gobas FA. A review of bioconcentration factor (BCF) and bioaccumulation factor (BAF) assessments for organic chemicals in aquatic organisms. *Environ Rev* 2006;14:257–97.
- Boxall ABA. Transformation products of synthetic chemicals in the environment. 2nd ed. Berlin, Heidelberg: Springer Berlin Heidelberg; 2009.
- Bryan RN, Centeno RS, Hershkowitz N, Poelstra RJ, Osato MS. Neurotoxicity of iohexol: a new nonionic contrast medium. *Radiology* 1982;145:379–82.
- Chakravarti SK, Saiakhov RD, Klopman G. Optimizing predictive performance of case ultra expert system models using the applicability domains of individual toxicity alerts. *J Chem Inf Model* 2012;52:2609–18.
- Chang H, Hu J, Wang L, Shao B. Occurrence of sulfonamide antibiotics in sewage treatment plants. *Chin Sci Bull* 2008;53:514–20.
- Clements RG, Nabholz JV, Johnson DE, Zeeman MG. The use of quantitative structure-activity relationships (qsars) as screening tools in environmental assessment. In: Gorsuch JW, Dwyer JF, Ingersoll C, La Point TW, editors. *Environmental toxicology and risk assessment*, 2nd volume. Philadelphia: ASTM; 1993. p. 555–70.
- Dimitrov S, Dimitrova N, Parkerton T, Comber M, Bonnelli M, Mekenyan O. Base-line model for identifying the bioaccumulation potential of chemicals. *SAR QSAR Environ Res* 2005;16:531–54.
- Dimitrov S, Dimitrova N, Georgieva D, Vasilev K, Hatfield T, Straka J, et al. Simulation of chemical metabolism for fate and hazard assessment. III. New developments of the bioconcentration factor base-line model. *SAR QSAR Environ Res* 2012;23:17–36.
- ECHA. Guidance on information requirements and chemical safety assessment - ECHA 2012. <http://echa.europa.eu/web/guest/guidance-documents/guidance-on-information-requirements-and-chemical-safety-assessment> (accessed November 18, 2013).
- Environmental Protection Agency. Persistent bioaccumulative toxic (PBT) chemicals; lowering of reporting thresholds for certain PBT chemicals; addition of certain PBT chemicals; community right-to-know toxic chemical reporting. Federal Register Environmental Documents USEPA; 1999a.
- Environmental Protection Agency. Category for persistent, bioaccumulative, and toxic new chemical substances. Federal Register Environmental Documents USEPA; 1999b.
- Escher BI, Fenner K. Recent advances in environmental risk assessment of transformation products. *Environ Sci Technol* 2011;45:3835–47.
- European Commission. Technical guidance document on risk assessment part II; 2003a [[http://ec.europa.eu/environment/chemicals/exist\\_subst/pdf/tgdpart2\\_2ed.pdf](http://ec.europa.eu/environment/chemicals/exist_subst/pdf/tgdpart2_2ed.pdf)].
- European Commission. Technical guidance document on risk assessment part III; 2003b [[http://echa.europa.eu/documents/10162/16960216/tgdpart3\\_2ed\\_en.pdf](http://echa.europa.eu/documents/10162/16960216/tgdpart3_2ed_en.pdf)].
- European Medicine Agency. Guideline on the environmental risk assessment of medicinal products for human use; 2005 [<http://www.iss.it/binary/farm2/cont/guideline%20Environmental%20Risk%20assessment%20medicinal%20products.1109243627.pdf>].
- Fatta-Kassinos D, Meric S, Nikolaou A. Pharmaceutical residues in environmental waters and wastewater: current state of knowledge and future research. *Anal Bioanal Chem* 2011;399:251–75.
- Friedrich J, Längin A, Kümmerer K. Comparison of an electrochemical and luminescence-based oxygen measuring system for use in the biodegradability testing according to closed bottle test (OECD 301D). *Clean-Soil, Air, Water* 2013;41:251–7.
- Grönwaller EF, Wahl HG, Kehlbach R, Rodemann HP, Claussen CD, Duda SH. Stabilität jodhaltiger röntgenkontrastmittel unter uv-laser-bestrahlung und toxizität der photoproducte. *Rofo* 1998;169:537–41.
- Haiß A, Kümmerer K. Biodegradability of the X-ray contrast compound diatrizoic acid, identification of aerobic degradation products and effects against sewage sludge micro-organisms. *Chemosphere* 2006;62:294–302.
- Han GH, Hur HG, Kim SD. Ecotoxicological risk of pharmaceuticals from wastewater treatment plants in Korea: occurrence and toxicity to daphnia magna. *Environ Toxicol Chem* 2006;25:265–71.
- Hapeshi E, Lambrianides A, Koutsoufas P, Kastanos E, Michael C, Fatta-Kassinos D. Investigating the fate of iodinated X-ray contrast media iohexol and diatrizoate during microbial degradation in an MBBR system treating urban wastewater. *Environ Sci Pollut Res* 2013;20:3592–606.
- Harmon RC, Duffy SP, Terneus MV, Ball JG, Valentovic MA. Characterization of a novel model for investigation of radiocontrast nephrotoxicity. *Nephrol Dial Transplant* 2009;24:763–8.
- Heberer T. Occurrence, fate, and removal of pharmaceutical residues in the aquatic environment: a review of recent research data. *Toxicol Lett* 2002;131:5–17.
- Hennebel T, de Corte S, Vanhaecke L, Vanherck K, Forrez L, de Gussembe B, et al. Removal of diatrizoate with catalytically active membranes incorporating microbially produced palladium nanoparticles. *Water Res* 2010;44:1498–506.
- Howard PH, Muir DCG. Identifying new persistent and bioaccumulative organics among chemicals in commerce II: pharmaceuticals. *Environ Sci Technol* 2011;45:6938–46.
- ISO 8245. Water quality—guidelines for the determination of total organic carbon (TOC) and dissolved organic carbon (DOC) 2nd ed.; 1999.
- Jeong J, Jung J, Cooper WJ, Song W. Degradation mechanisms and kinetic studies for the treatment of X-ray contrast media compounds by advanced oxidation/reduction processes. *Water Res* 2010;44:4391–8.
- Joss A, Keller E, Alder AC, Göbel A, McArdell CS, Ternes T, et al. Removal of pharmaceuticals and fragrances in biological wastewater treatment. *Water Res* 2005;39:3139–52.
- Joss A, Zabczynski S, Göbel A, Hoffmann B, Löffler D, McArdell CS, et al. Biological degradation of pharmaceuticals in municipal wastewater treatment: proposing a classification scheme. *Water Res* 2006;40:1686–96.
- Kalsch W. Biodegradation of the iodinated X-ray contrast media diatrizoate and iopromide. *Sci Total Environ* 1999;225:143–53.
- Kanda R, Griffin P, James HA, Fothergill J. Pharmaceutical and personal care products in sewage treatment works. *J Environ Monit* 2003;5:823–30.
- Khetan SK, Collins TJ. Human pharmaceuticals in the aquatic environment: a challenge to green chemistry. *Chem Rev* 2007;107:2319–64.
- Kılıç M, Çınar Z. Hydroxyl radical reactions with 4-chlorophenol as a model for heterogeneous photocatalysis. *J Mol Struct (THEOCHEM)* 2008;851:263–70.
- Kormos JL, Schulz M, Ternes TA. Occurrence of iodinated X-ray contrast media and their biotransformation products in the urban water cycle. *Environ Sci Technol* 2011;45:8723–32.
- Kümmerer K. *Pharmaceuticals in the environment: sources, fate, effects and risks*. 3rd ed. Springer-Verlag; 2008.
- Kümmerer K, Steger-Hartmann T, Baranyai A, Bürhaus I. Examination of the biodegradation of the antineoplastics cyclophosphamide and ifosfamide with the closed bottle test (OECD 301 D). *Zentralbl Hyg Umweltmed* 1996;198:215–25.
- La Farré M, Pérez S, Kantiani L, Barceló D. Fate and toxicity of emerging pollutants, their metabolites and transformation products in the aquatic environment. *TrAC Trends Anal Chem* 2008;27:991–1007.
- Laboratory of Mathematical Chemistry B. OASIS Catalogic software V. 5.11.6 TB; 2012 [<http://oasis-lmc.org/>].
- Mahmoud WMM, Kümmerer K. Captopril and its dimer captopril disulfide: Photodegradation, aerobic biodegradation and identification of transformation products by HPLC–UV and LC–ion trap–MSn. *Chemosphere* 2012;88:1170–7.

- Messana JM, Cieslinski DA, Nguyen VD, Humes HD. Comparison of the toxicity of the radiocontrast agents, iopamidol and diatrizoate, to rabbit renal proximal tubule cells in vitro. *J Pharmacol Exp Ther* 1988;244:1139–44.
- Meylan WM, Howard PH. Atom/fragment contribution method for estimating octanol-water partition coefficients. *J Pharm Sci* 1995;84:83–92.
- Michael I, Rizzo L, McArdell CS, Manaiá CM, Merlin C, Schwartz T, et al. Urban wastewater treatment plants as hotspots for the release of antibiotics in the environment: a review. *Water Res* 2013;47:957–95.
- Miège C, Choubert JM, Ribeiro L, Eusèbe M, Coquery M. Fate of pharmaceuticals and personal care products in wastewater treatment plants—conception of a database and first results. *Environ Pollut* 2009;157:1721–6.
- Nyholm N. The european system of standardized legal tests for assessing the biodegradability of chemicals. *Environ Toxicol Chem* 1991;10:1237–46.
- OECD. OECD guidelines for the testing of chemicals: ready biodegradability 301F: manometric respiratory test. OECD Pub; 1992a.
- OECD. OECD Guidelines for the testing of chemicals: ready biodegradability 301D: closed bottle test. OECD Pub; 1992b.
- OECD. Revised introduction of the OECD guidelines for testing of chemicals. OECD Pub; 2006.
- OECD. Guidelines for testing of chemicals: test no. 316: phototransformation of chemicals in water direct photolysis. Paris: OECD Pub; 2008.
- Putschew A, Jekel M. Iodinated X-ray contrast media. In: Reemtsma T, Jekel M, editors. *Organic pollutants in the water cycle: Properties, occurrence, analysis and environmental relevance of polar compounds*. Weinheim, Chichester: Wiley-VCH; John Wiley; 2006. p. 87–98.
- Putschew A, Wischnack S, Jekel M. Occurrence of triiodinated X-ray contrast agents in the aquatic environment. *Sci Total Environ* 2000;255:129–34.
- Roberts G, Myatt G, Johnson W, Cross K, Blower P. LeadScope: software for exploring large sets of screening data. *J Chem Inf Model* 2000;40:1302–14.
- Saiakhov R, Chakravarti S, Klopman G. Effectiveness of CASE ultra expert system in evaluating adverse effects of drugs. *Mol Inf* 2013;32:87–97.
- Santiago-Morales J, Agüera A, Gómez MdM, Fernández-Alba AR, Giménez J, Esplugas S, et al. Transformation products and reaction kinetics in simulated solar light photocatalytic degradation of propranolol using Ce-doped TiO<sub>2</sub>. *Appl Catal Environ* 2013;129: 13–29.
- Santos LHMLM, Araújo AN, Fachini A, Pena A, Delerue-Matos C, Montenegro MCBSM. Ecotoxicological aspects related to the presence of pharmaceuticals in the aquatic environment. *J Hazard Mater* 2010;175:45–95.
- Sedykh A, Saiakhov R, Klopman G. META V—a model of photodegradation for the prediction of photoproducts of chemicals under natural-like conditions. *Chemosphere* 2001;45:971–81.
- Seitz W, Weber WH, Jiang J, Lloyd BJ, Maier M, Maier D, et al. Monitoring of iodinated X-ray contrast media in surface water. *Chemosphere* 2006;64:1318–24.
- Sugihara MN, Moeller D, Paul T, Strathmann TJ. TiO<sub>2</sub>-photocatalyzed transformation of the recalcitrant X-ray contrast agent diatrizoate. *Appl Catal Environ* 2013;129: 114–22.
- Svetlichnyi VA, Chaikovskaya ON, Bazyl OK, Kuznetsova RT, Sokolova IV, et al. Photolysis of phenol and para-chlorophenol by UV laser excitation. *High Energy Chem* 2001;35: 258–64.
- Ternes TA, Hirsch R. Occurrence and behavior of X-ray contrast media in sewage facilities and the aquatic environment. *Environ Sci Technol* 2000;34:2741–8.
- Ternes TA, Joss A, Siegrist H. Peer Reviewed: scrutinizing pharmaceuticals and personal care products in wastewater treatment. *Environ Sci Technol* 2004;38:392A.
- Trautwein C, Kümmerer K. Incomplete aerobic degradation of the antidiabetic drug Metformin and identification of the bacterial dead-end transformation product Guanylurea. *Chemosphere* 2011;85:765–73.
- Trautwein C, Kümmerer K. Ready biodegradability of trifluoromethylated phenothiazine drugs, structural elucidation of their aquatic transformation products, and identification of environmental risks studied by LC–MSn and QSAR. *Environ Sci Pollut Res* 2012;19:3162–77.
- Trovó AG, Nogueira RFP, Agüera A, Fernandez-Alba AR, Sirtori C, Malato S. Degradation of sulfamethoxazole in water by solar photo-Fenton. *Chemical and toxicological evaluation*. *Water Res* 2009;43:3922–31.
- U.S. Environmental Protection Agency EHAC. PBT Profiler: A Component of OPPT's P2 Frame work V 2.000.2012; <http://www.pbtprofiler.net/> (accessed August 08, 2013).
- Velo-Gala I, López-Peñalver JJ, Sánchez-Polo M, Rivera-Utrilla J. Ionic X-ray contrast media degradation in aqueous solution induced by gamma radiation. *Chem Eng J* 2012; 195–6:369–76.
- Wheeler LA, Norman A, Riley R. Mutagenicity of diatrizoate and other triiodobenzoic acid derivatives in the Ames Salmonella/microsome test. *Proc West Pharmacol Soc* 1980; 23:249–53.

# Supplementary Information

For

## Qualitative Environmental Risk Assessment of Photolytic Transformation Products of Iodinated X-ray Contrast Agent Diatrizoic acid

Tushar Rastogi, Christoph Leder, Klaus Kümmerer\*

*Sustainable Chemistry and Material Resources, Institute of Sustainable and Environmental Chemistry,  
Leuphana University Lüneburg, C13, DE-21335 Lüneburg, Germany*

---

\* Corresponding author address: Chair of Sustainable Chemistry and Material Resources,  
Institute of Sustainable and Environmental Chemistry, C.13, Scharnhorststraße 1, D-21335  
Lüneburg, Germany. Tel.: +49 4131 677 2893.  
E-mail address: tushar.rastogi@leuphana.de, tushar1909@gmail.com (T. Rastogi),  
cleder@leuphana.de (C. Leder), Klaus.Kuemmerer@uni.leuphana.de (K. Kümmerer).

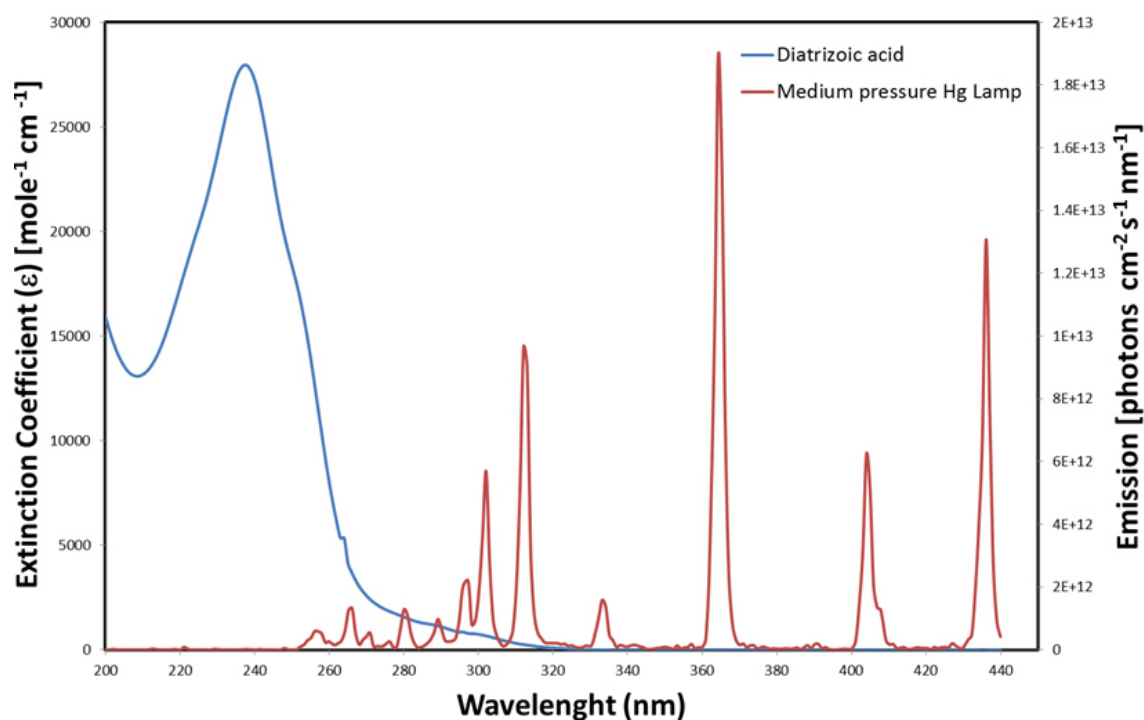


**Text S1 Supplementary Information:** Characteristic of the medium pressure UV lamp measured and absorption spectra of Diatrizoic acid (DIAT)

The emission of the used UV lamp was measured with UVpad (Opsytec Dr. Gröbel GmbH, Ettlingen, Germany) at a distance of 4 cm from the emission source in a black box in the range of 200 nm to 440 nm.

**Table S1 Supplementary Information:** The intensity of the light emitted by the UV lamp as measured by UVpad

Radiation Intensity (D)	[mJ /cm <sup>2</sup> ]
D (Total)	2057
D (VIS)	642
D (UVA)	711
D (UVB)	606
D (UVC)	98



**Figure S1 Supplementary Information:** Molar extinction coefficient of DIAT in water and emission data of medium pressure UV lamp.

**Table S2 Supplementary Information:** Gradient flow condition used to achieve the desired separation

<b>Time (min)</b>	<b>%B (Acetonitrile)</b>
0.01 to 3 min	1
3 to 13 min	1% - 15% B
13 to 15 min	15% - 5% B
15 to 20 min	5% - 1% B
20 to 25 min	1% B
25.01	stop

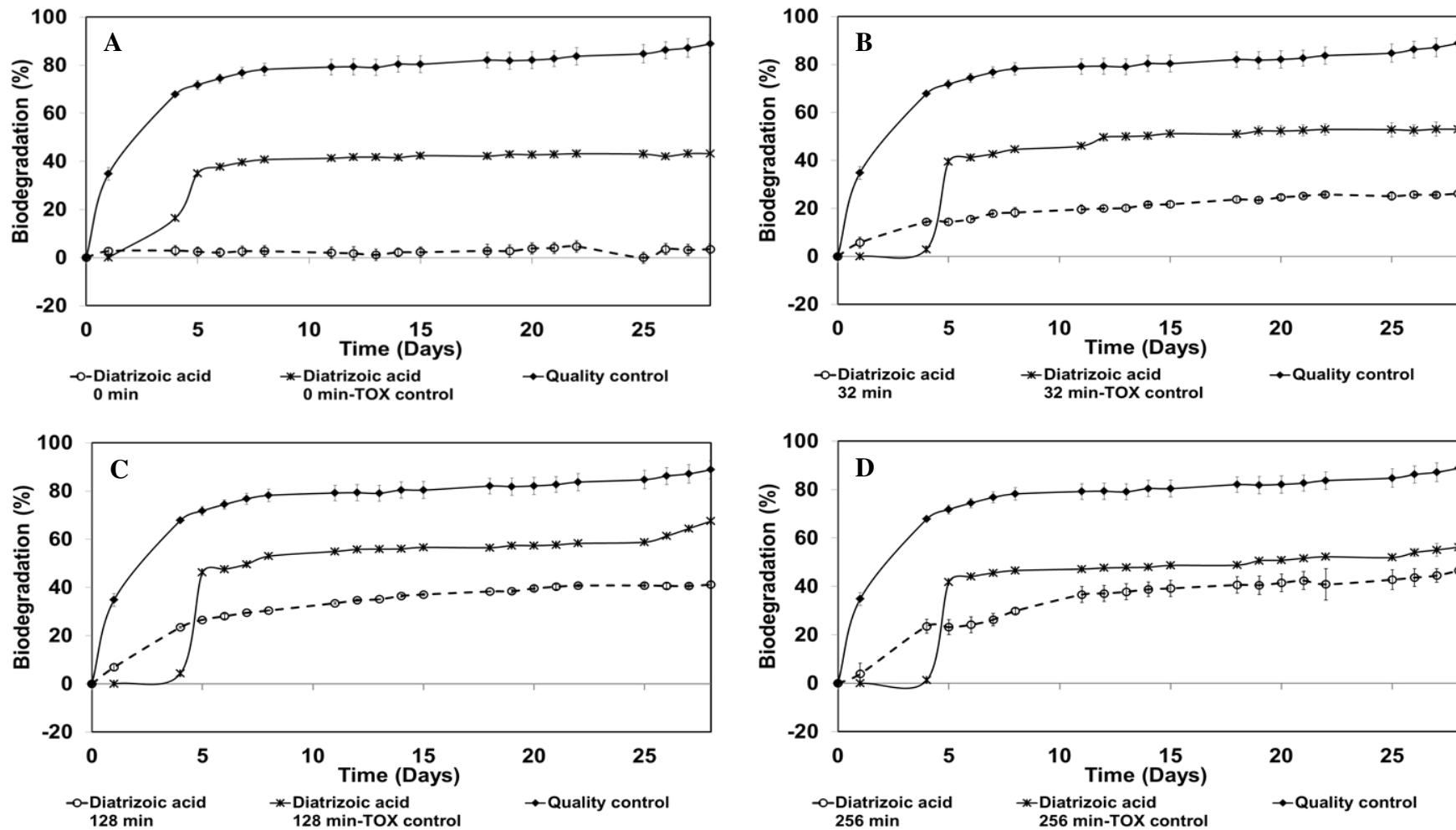
The LOD and LOQ of the above describe method was  $0.015 \mu\text{g mL}^{-1}$  and  $0.05 \mu\text{g mL}^{-1}$ . High linearity correlation [ $r^2 \geq 0.9999$ ] was obtained for calibration curve range  $150 \mu\text{g mL}^{-1}$  to  $0.1465 \mu\text{g mL}^{-1}$ .

**Table S3 Supplementary Information:** The operating parameters of the ESI and Iontrap (Bruker 6000) of the LC-ESI-IT-MS<sup>n</sup>

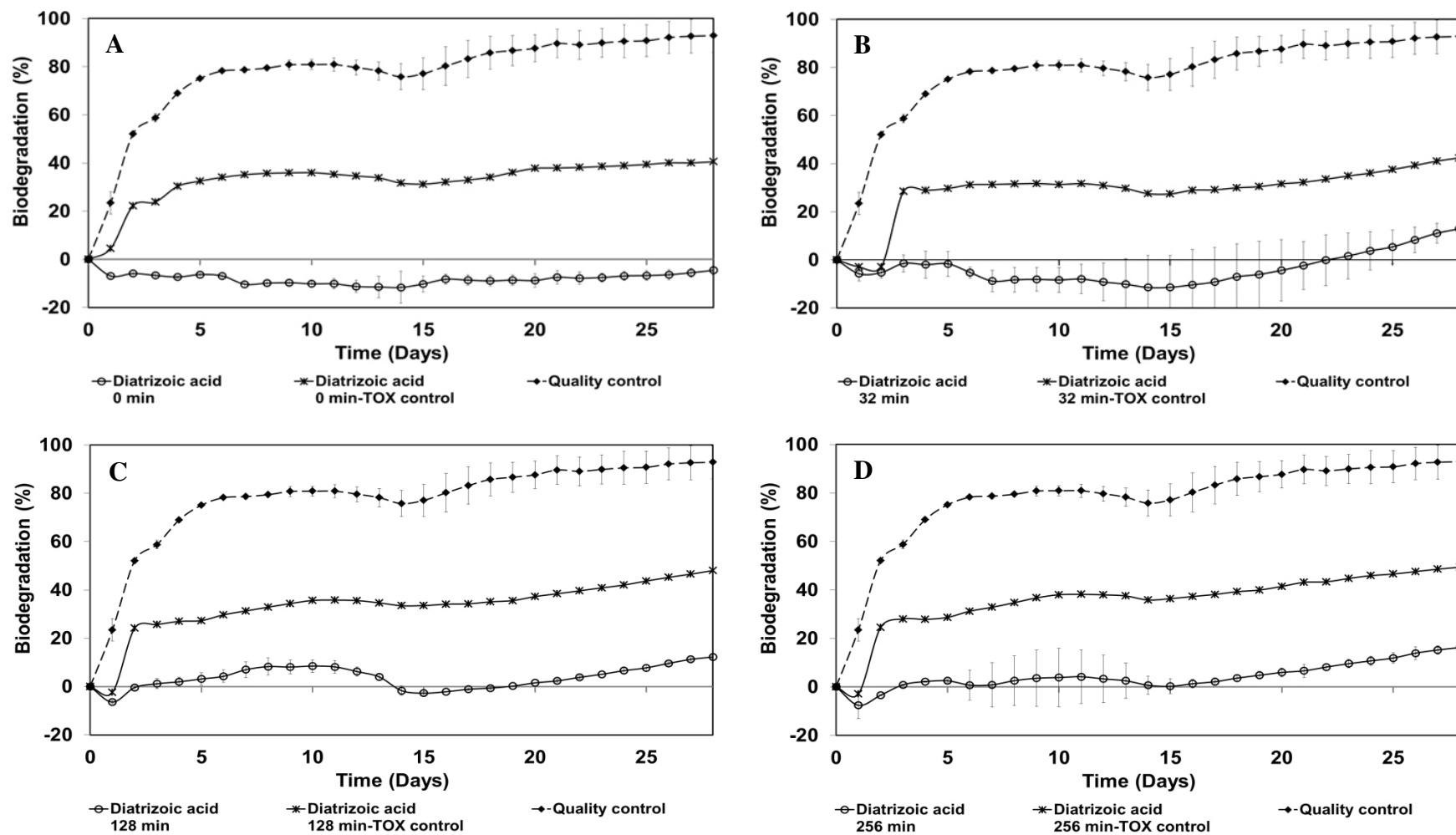
<b>Parameters</b>	<b>Metoprolol</b>
Dry gas temperature	300°C
Nebulizer pressure	30 psi
Dry gas flow	10 l min <sup>-1</sup>
end plate Offset	-500 Volt
capillary voltage	-3680Volt
skimmer	41.9 Volt
capillary exit	79.2 Volt
octopole one	10.03 Volt
octopole two	1.17 Volt
trap drive	58.2
lens one	-4.3 Volt
lens two	-77.5 Volt
target mass	614.9 m/z
maximum accumulation time	200 ms
scan range	100 m/z - 1000 m/z
fragmentation amplitude	1

**Table S4 Supplementary Information:** Composition of the aerobic biodegradation test series in the CBT (1-4) and MRT (1-5)

	1	2	3	4	5
Test series	Blank	Quality control	Test compound	Toxicity control	Sterile control
Mineral medium	+	+	+	+	+
Inoculum	+	+	+	+	
Test substance			+	+	+
Sodium acetate		+		+	
Sodium azide					+



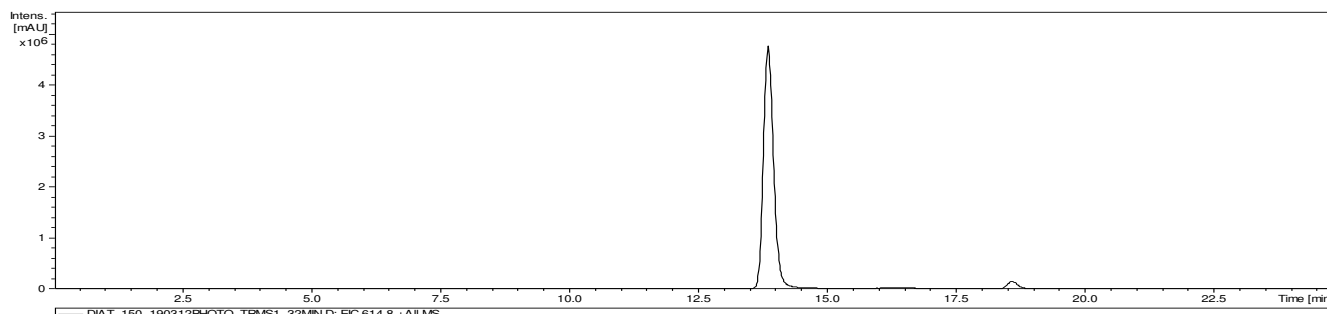
**Figure S2 Supplementary Information:** Aerobic biodegradation results of DIAT and its photo-TPs in CBT (OECD 301D) after: A) 0 min UV irradiation; B) 32 min UV irradiation; C) 128 min UV irradiation; D) 256 min UV irradiation [ $C_0 = 25 \text{ mg L}^{-1}$ ;  $n = 2$ ].



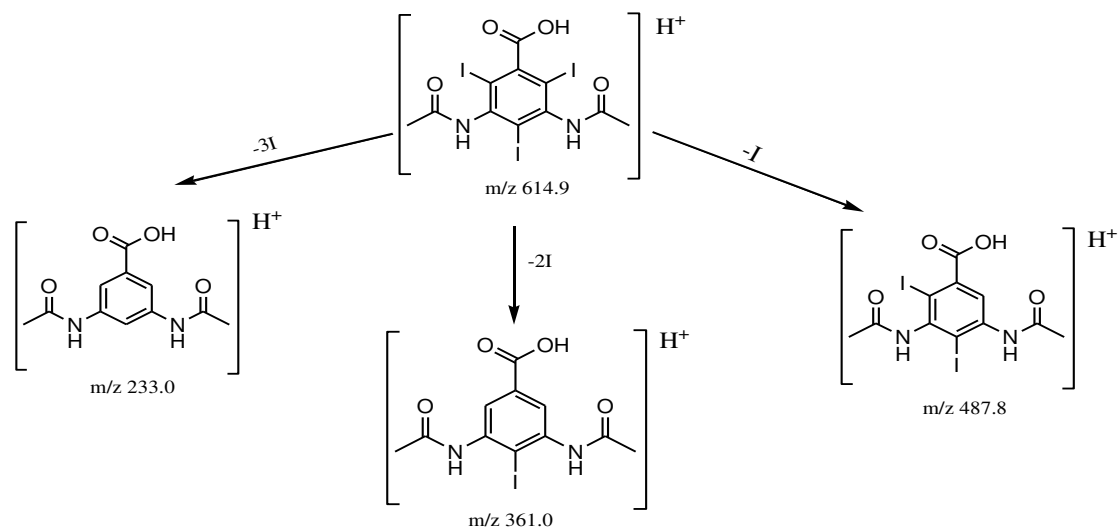
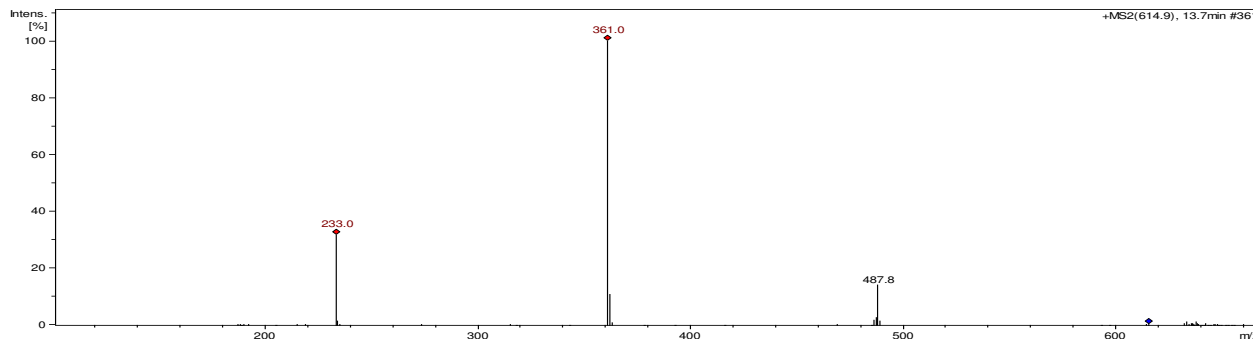
**Figure S3 Supplementary Information:** Aerobic biodegradation results of DIAT and its photo-TPs in MRT (OECD 301F) after: A) 0 min UV irradiation; B) 32 min UV irradiation; C) 128 min UV irradiation; D) 256 min UV irradiation [ $C_0 = 150 \text{ mg L}^{-1}$ ;  $n = 2$ ].

**Text S2 Supplementary Material:** The proposed structures of the fragments ions formed during the MS<sup>2</sup> fragmentation of Diatrizoic acid and its photo TPs

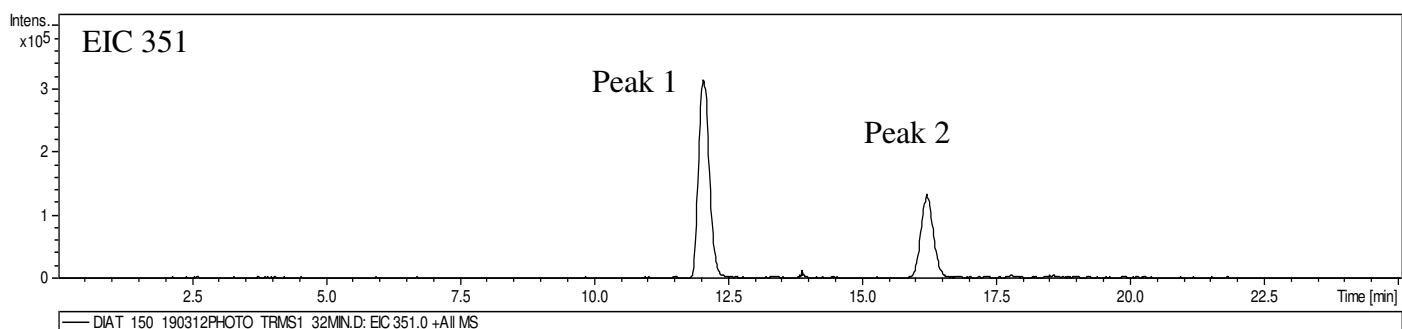
**Diatrizoic acid (m/z: 615)**



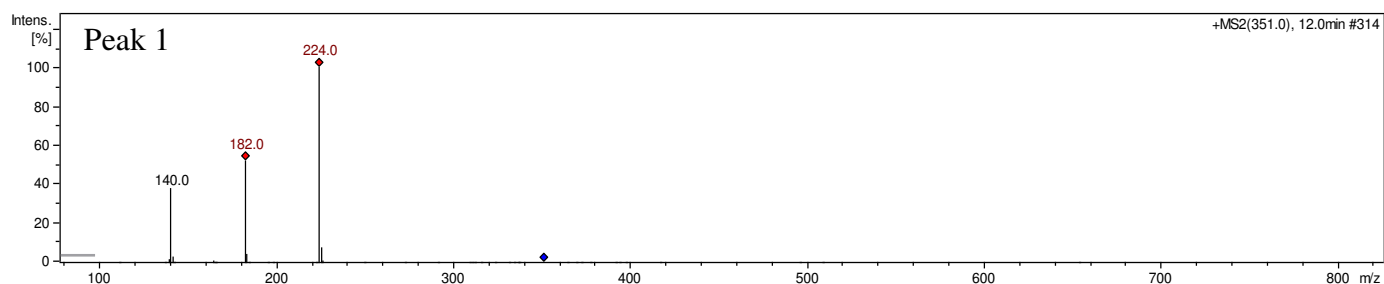
m/z	Retention time	Precursor ion/Smile code	Structure	Reference
614.9	13.7 min	[M+H] <sup>+</sup> IC1=C(C(O)=O)C(I)=C(NC(C)=O)C(I)=C1NC(C)=O		(Sugihara et al., 2013)



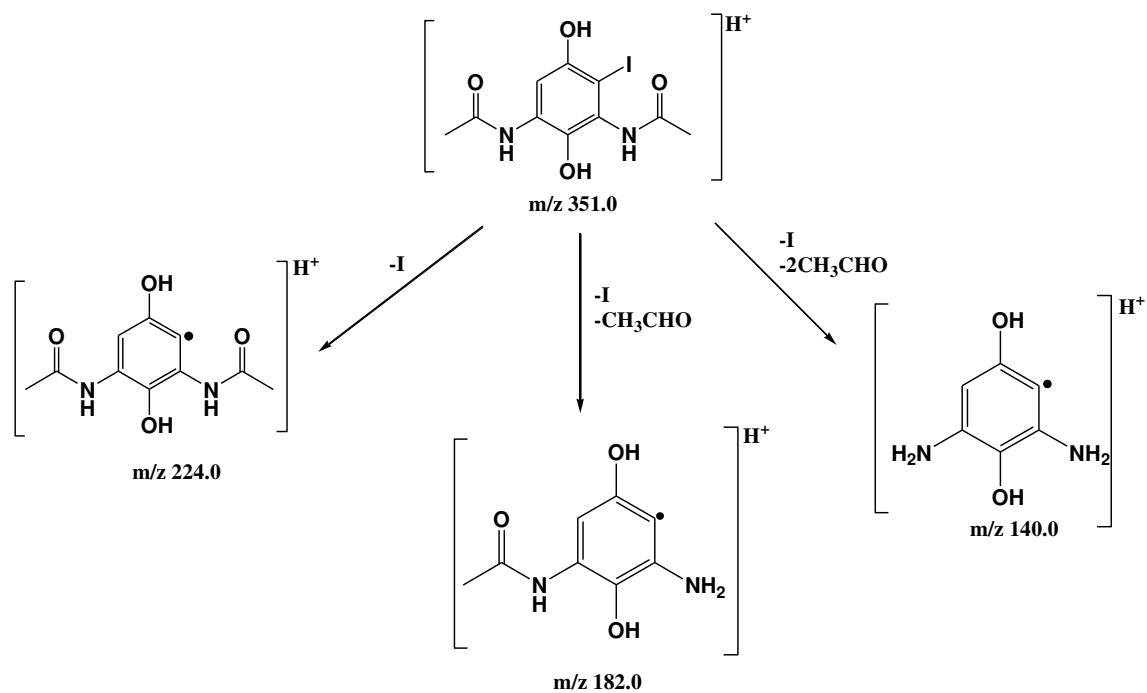
## TP 351



### Peak 1

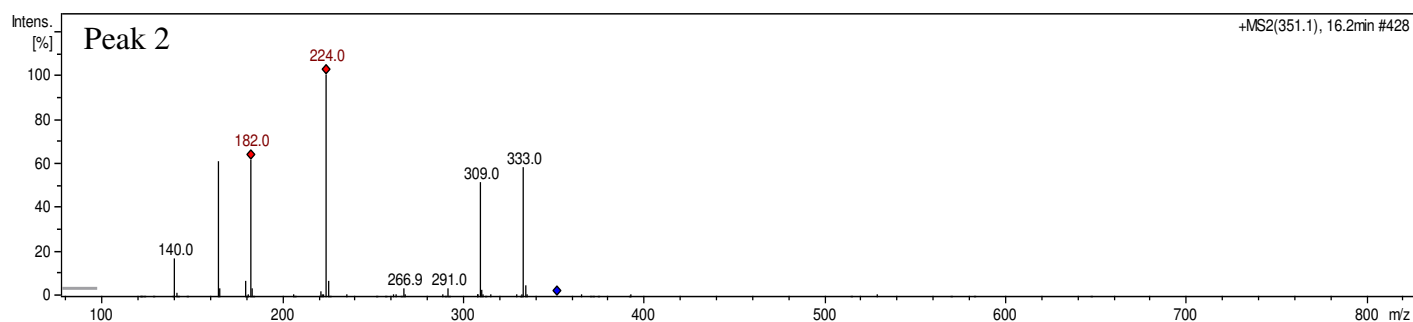


m/z	Retention time	Precursor ion/ Smiles code	Structure	Reference
351.0 TP <sub>1</sub> 351	12.0 min	$[M+H]^+$ <chem>IC1=C(O)C=C(NC(C)=O)C(O)=C1NC(C)=O</chem>		MetaPC(Sedykh et al., 2001)

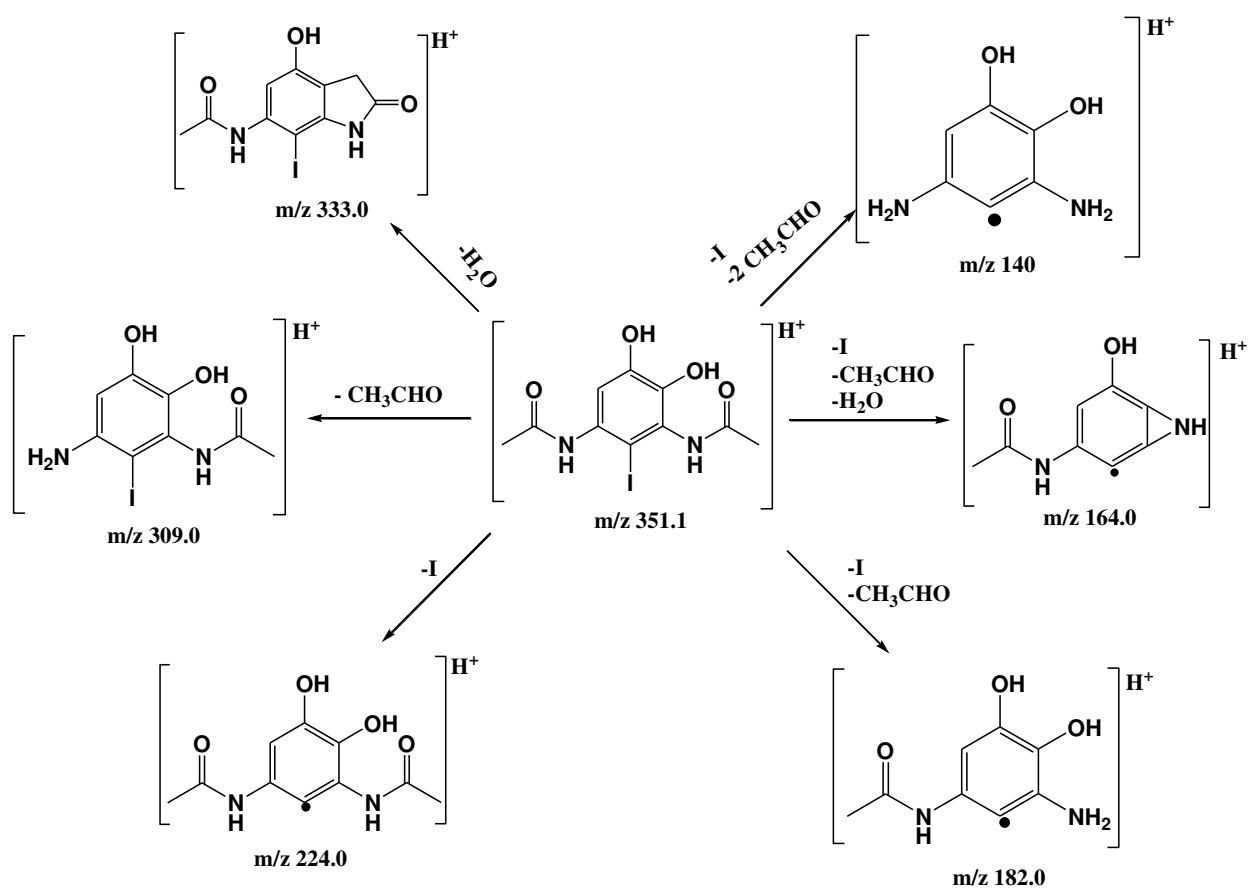




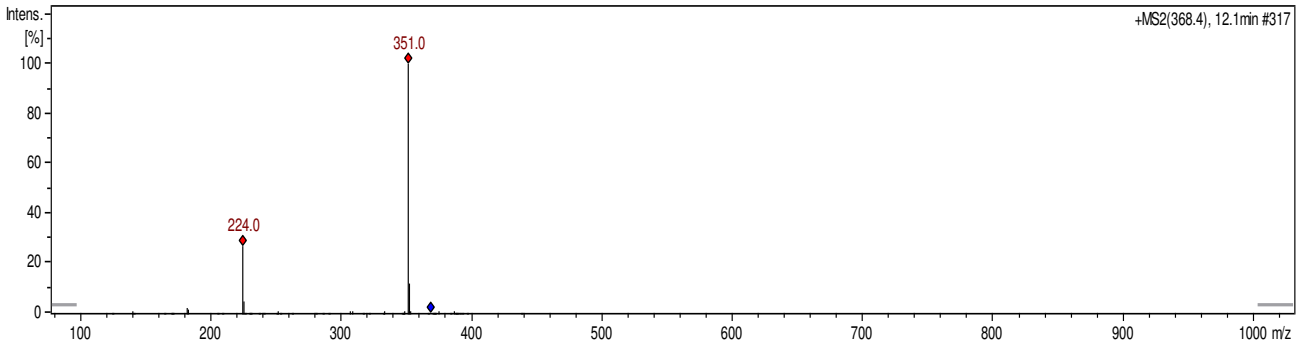
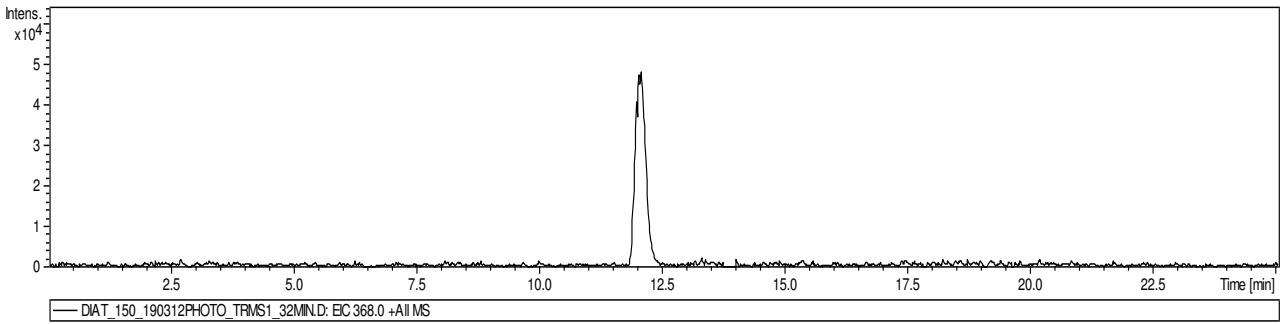
## Peak 2:



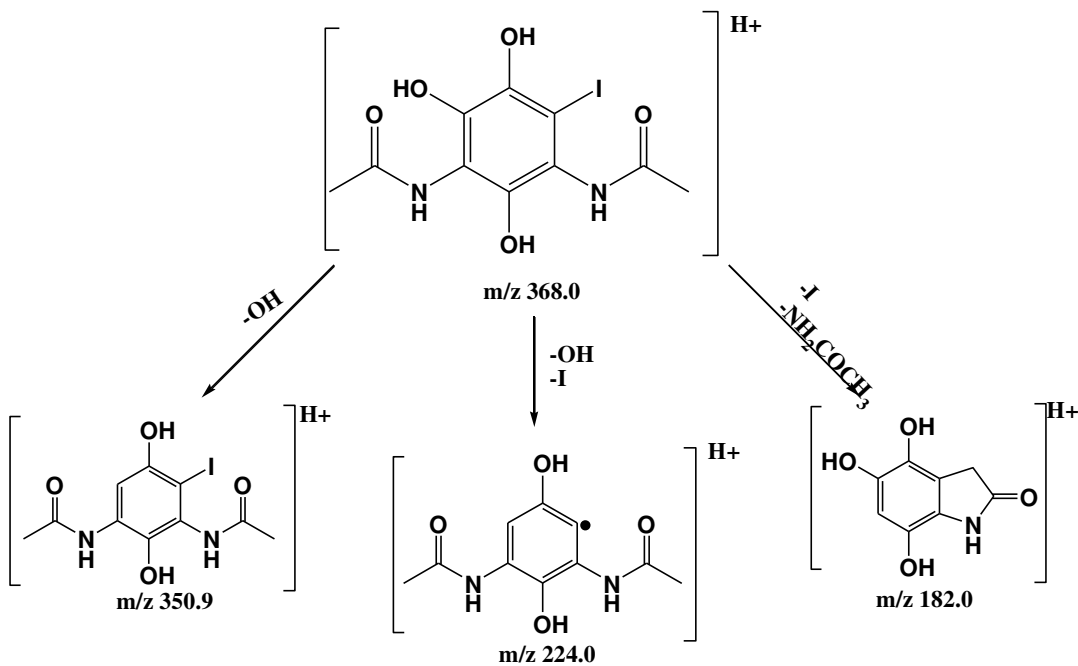
m/z	Retention time	Precursor ion/ Smiles code	Structure	Reference
351.1	16.2	[M+H] <sup>+</sup> <chem>OC1=C(O)C=C(NC(C)=O)C(I)=C1NC(C)=O</chem>		MetaPC(Sedykh et al., 2001)



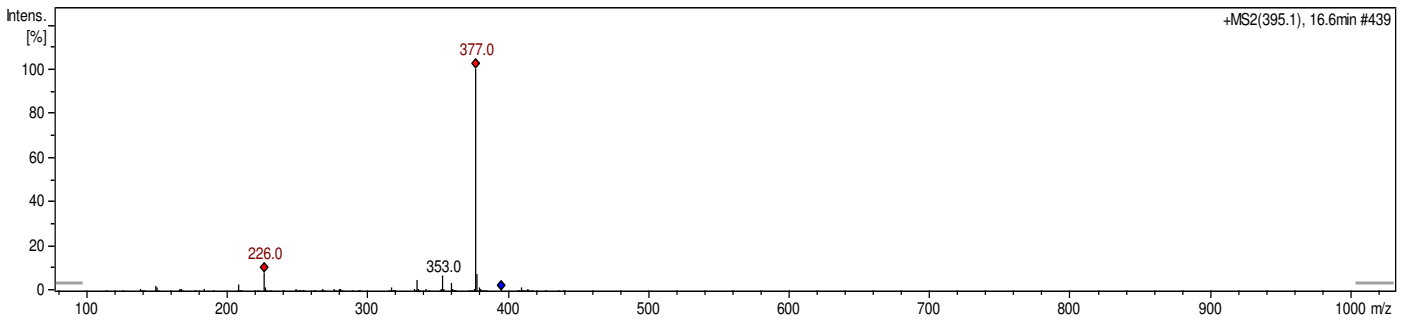
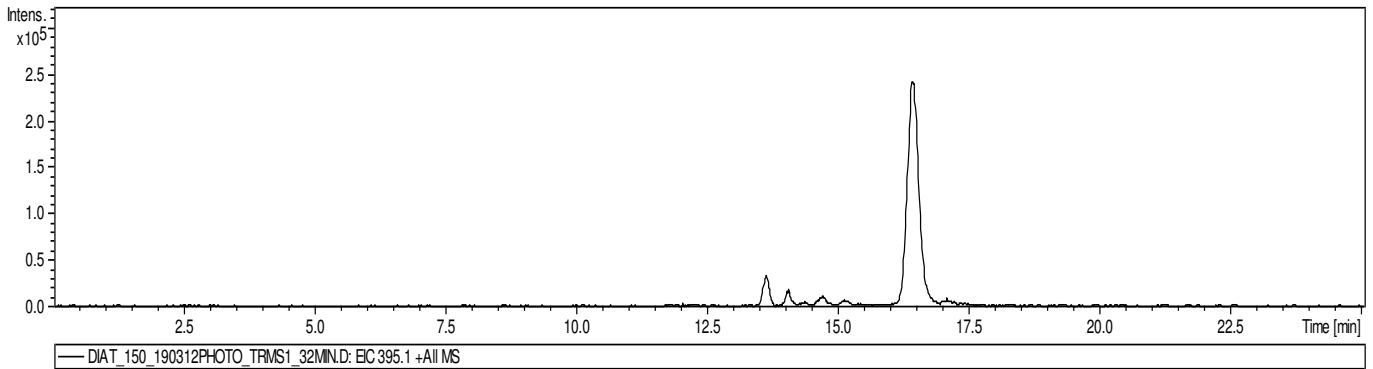
**TP 368**



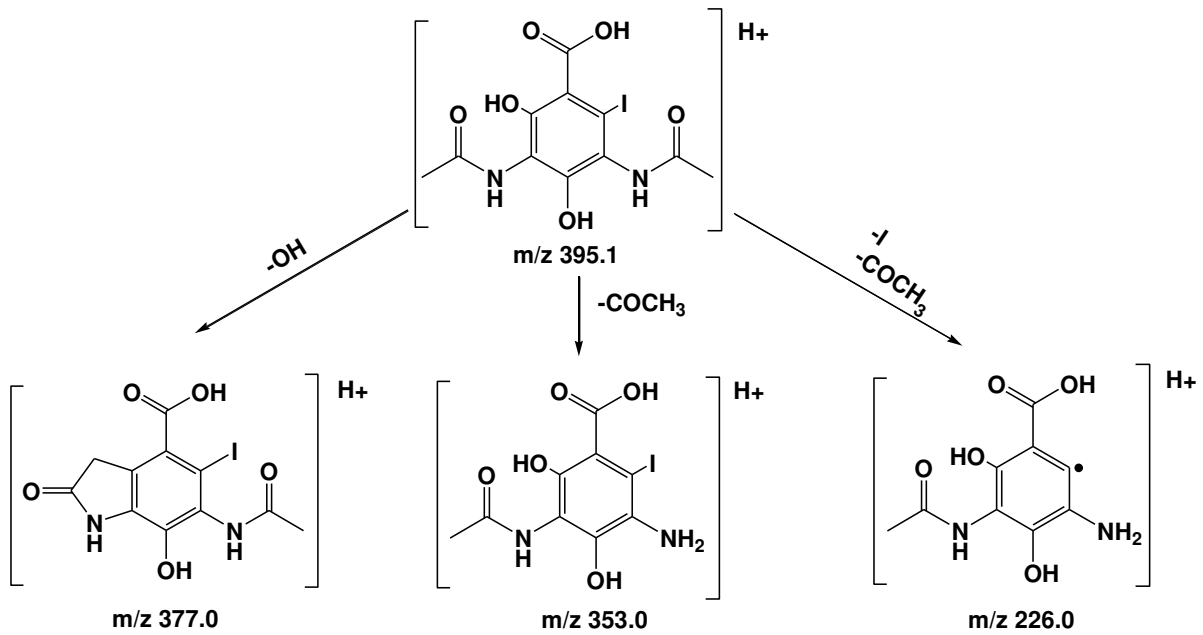
m/z	Retention time	Precursor ion/ Smiles code	Structure	Reference
368.4	12.1 min	[M+H] <sup>+</sup> <chem>IC1=C(O)C(O)=C(NC(C)=O)C(O)=C1NC(C)=O</chem>		



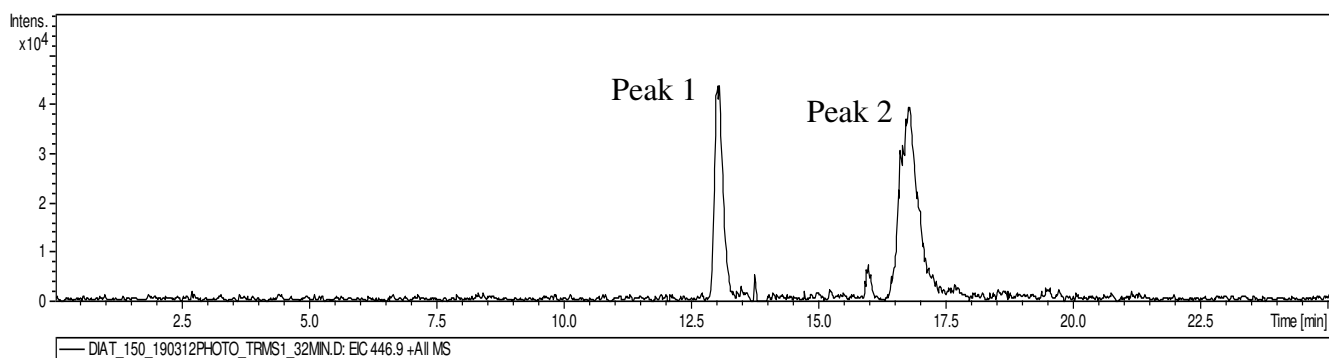
**TP 395**



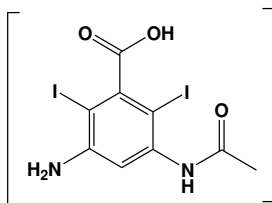
m/z	Retention time	Precursor ion/ Smiles code	Structure	Reference
395.1	16.4	[M+H] <sup>+</sup> <chem>OC1=C(NC(C)=O)C(I)=C(C(O)=O)C(O)=C1NC(C)=O</chem>		MetaPC(Sedykh et al., 2001)

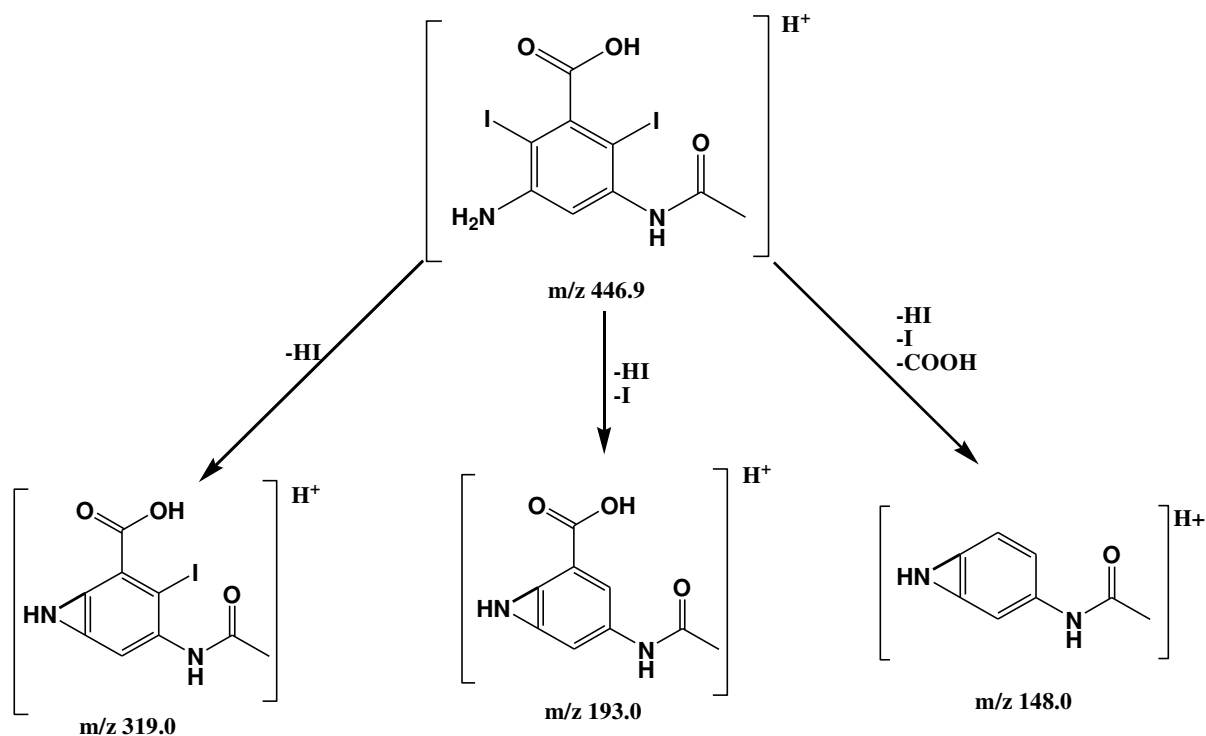


**TP 447**

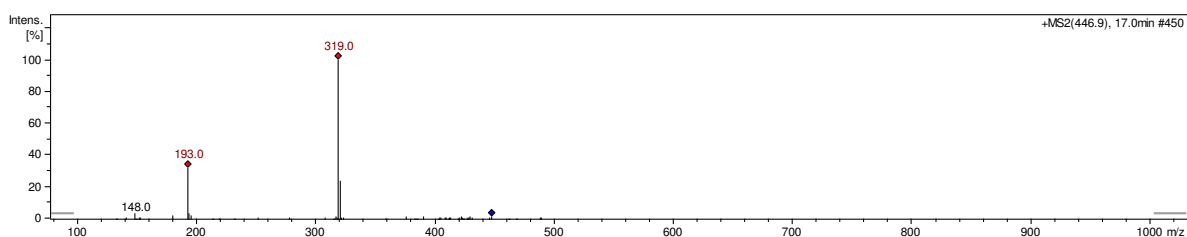


**Peak 1**

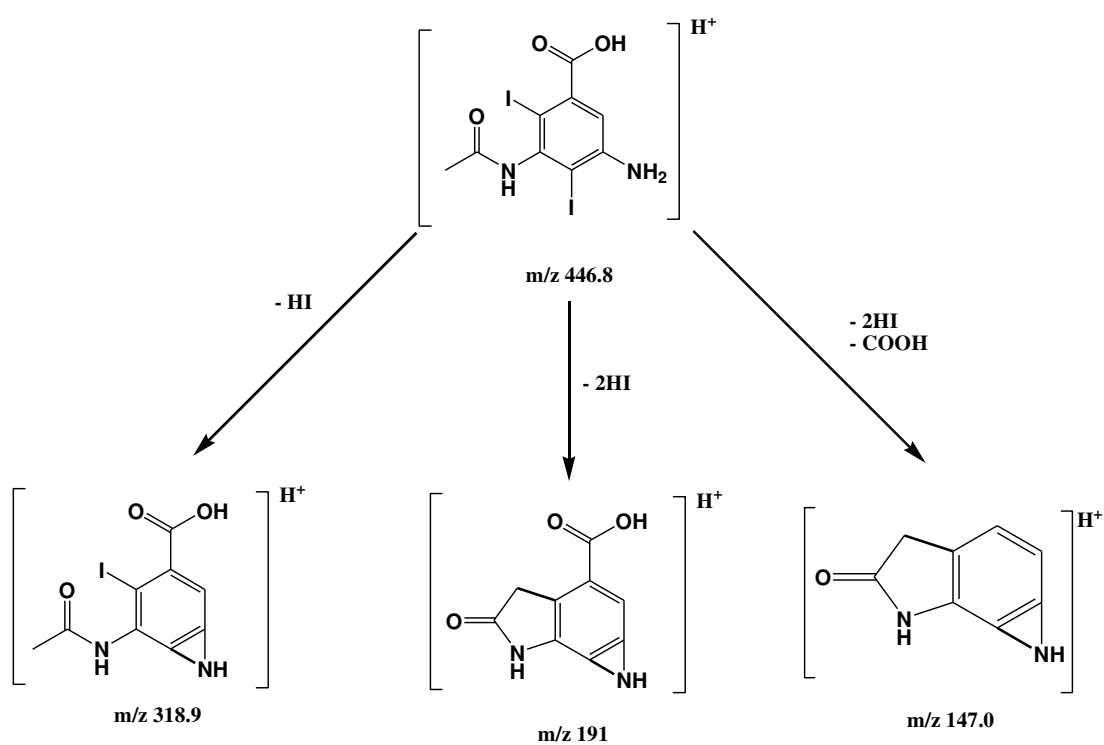
m/z	Retention time	Precursor ion/ Smiles code	Structure	Reference
446.9	13.0 min	[M+H] <sup>+</sup> <chem>IC1=C(C(O)=O)C(I)=C(N)C=C1NC(C)=O</chem>		(Hapeshi et al., 2013; Velo-Gala et al., 2012)



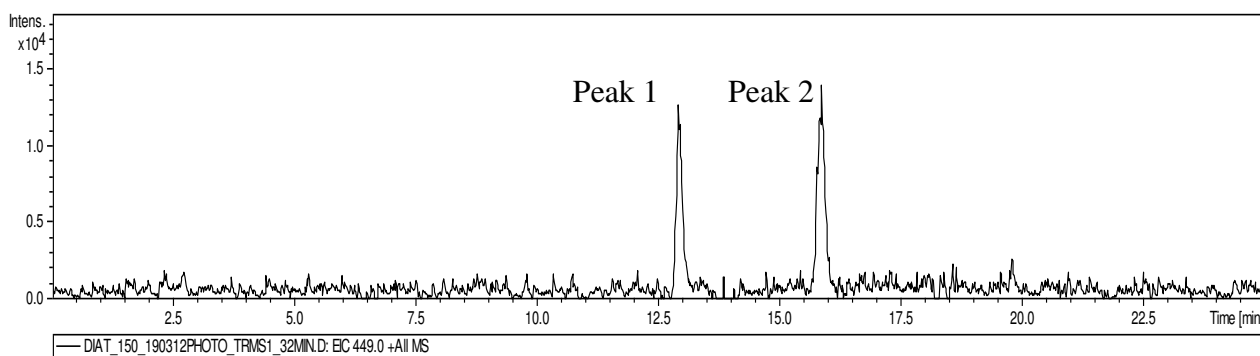
## Peak 2



m/z	Retention time	Precursor ion/ Smiles code	Structure	Reference
446.9	16.8 min	[M+H] <sup>+</sup> <chem>NC1=C(I)C(NC(C)=O)=C(I)C(C(O)=O)=C1</chem>		(Hapeshi et al., 2013; Velo-Gala et al., 2012)

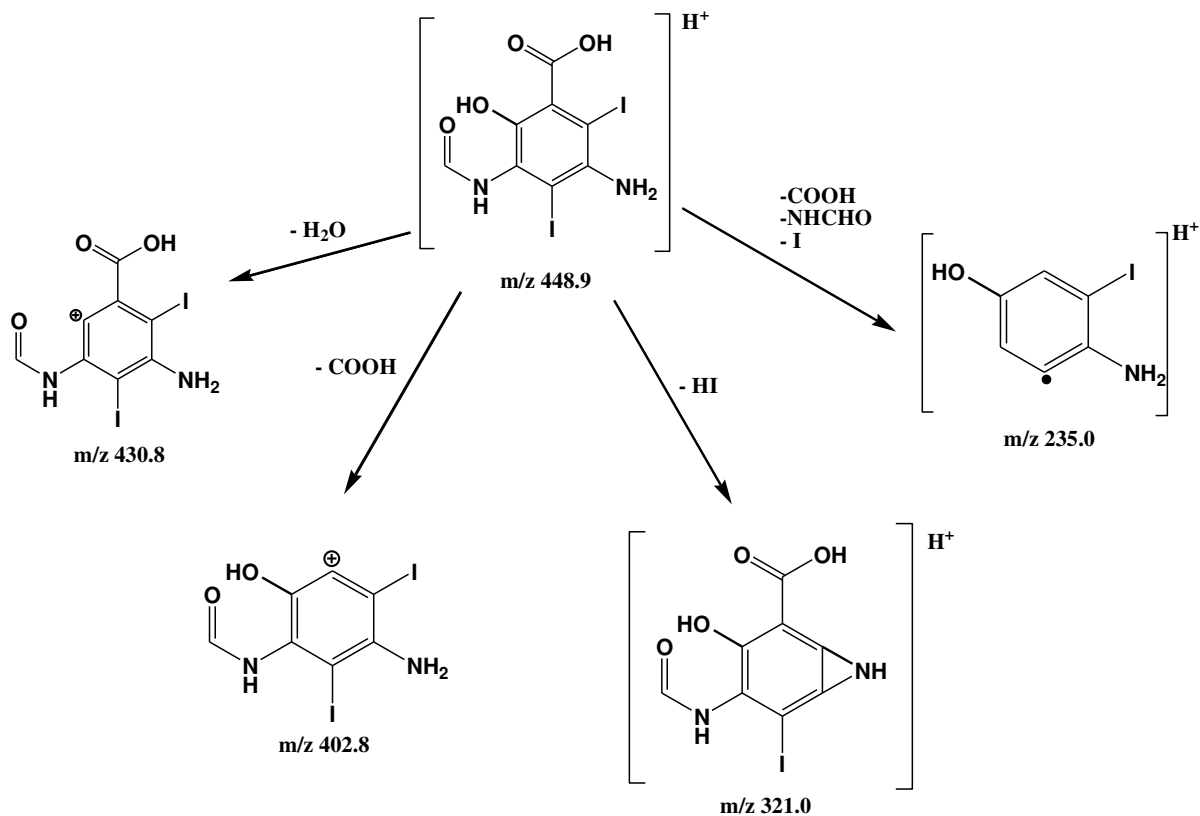


## TP 449

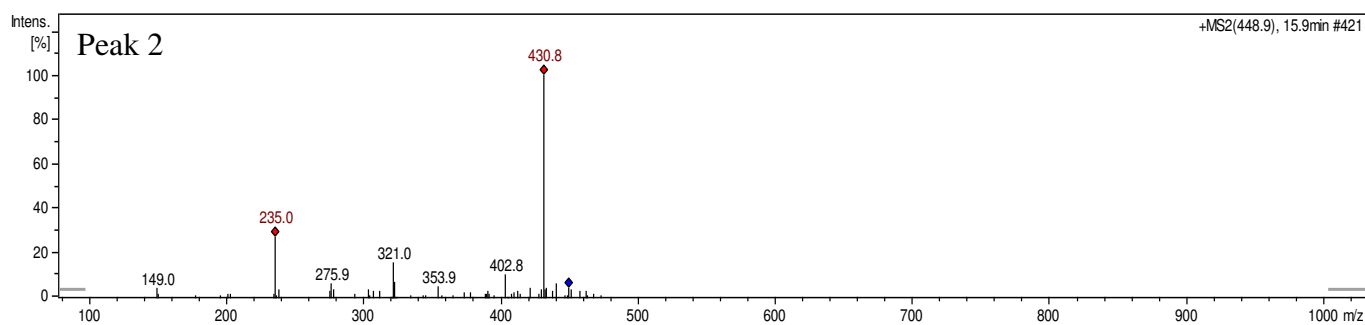


### Peak 1

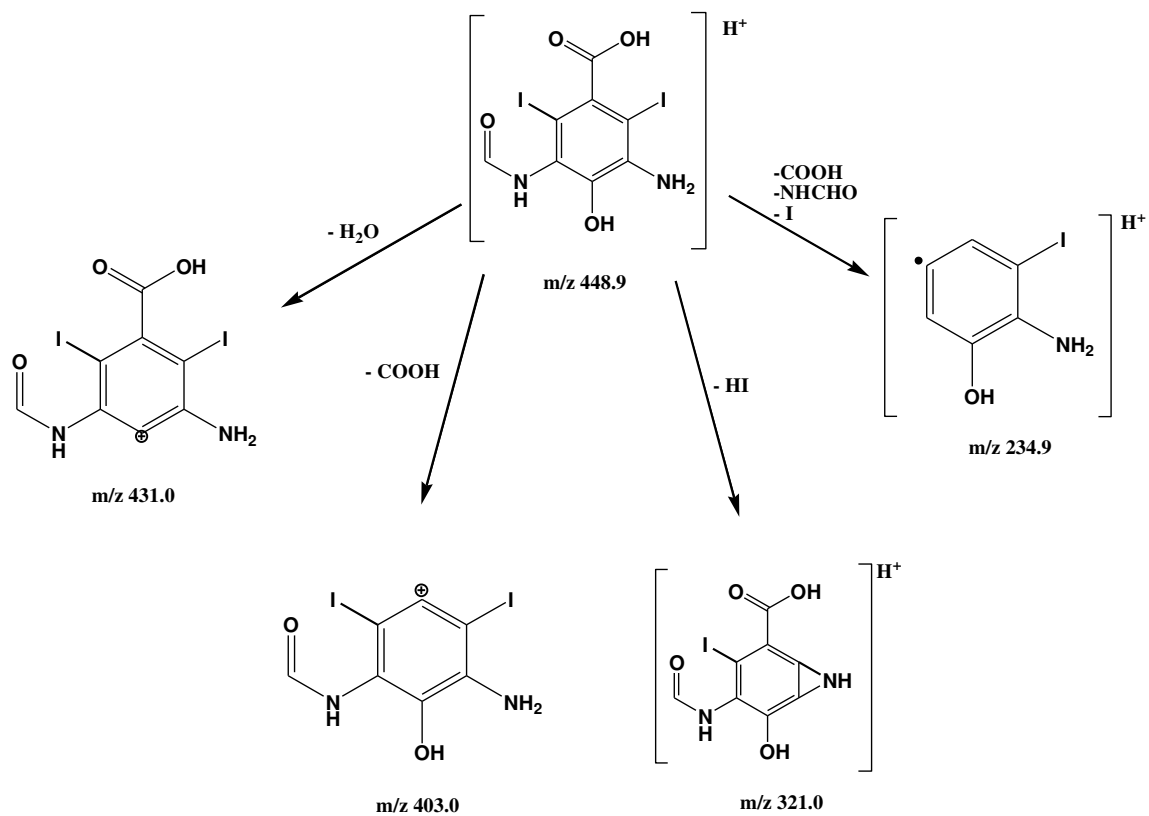
m/z	Retention time	Precursor ion/ Smiles code	Structure	Reference
448.9	12.9	[M+H] <sup>+</sup> IC1=C(C(O)=O)C(O)=C (NC=O)C(I)=C1N		MetaPC(Sedyk h et al., 2001)



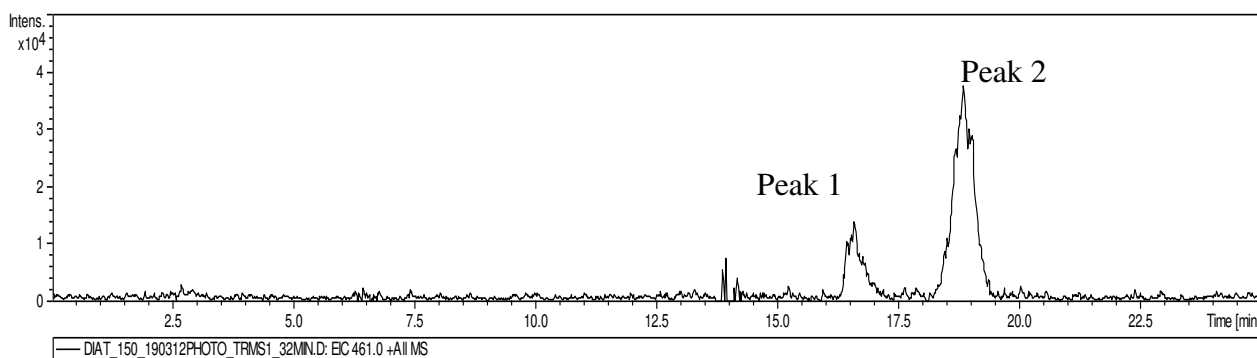
## Peak 2



m/z	Retention time	Precursor ion/ Smiles code	Structure	Reference
448.9	15.8	[M+H] <sup>+</sup> IC1=C(C(O)=O)C(I)=C(NC=O)C(O)=C1N		MetaPC(Sedykh et al., 2001)

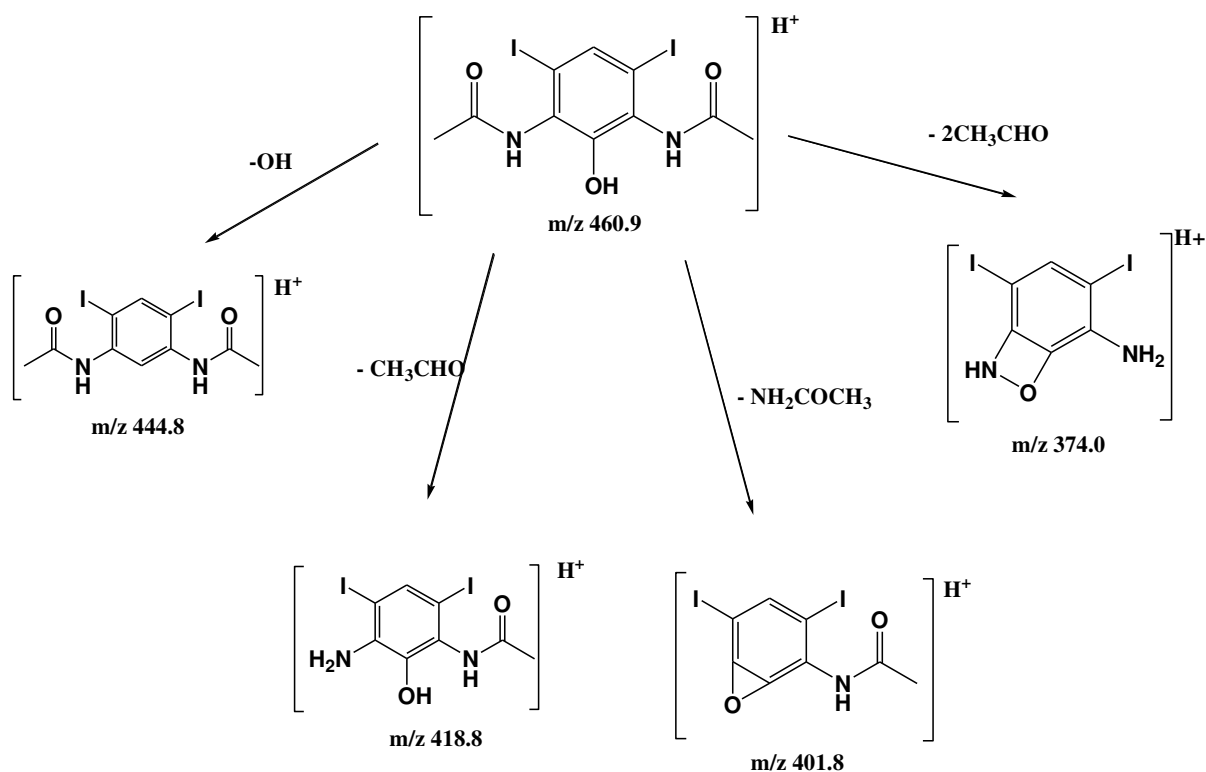


## TP 461



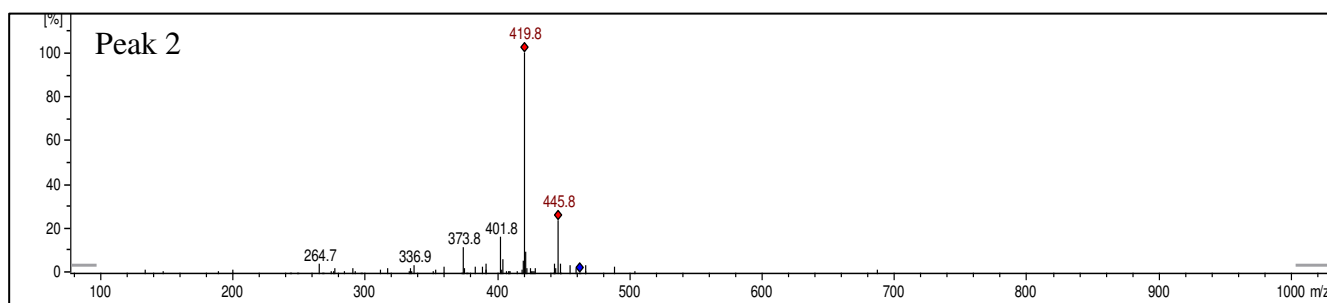
### Peak 1

m/z	Retention time	Precursor ion/ Smiles code	Structure	Reference
460.9	16.6 min	[M+H] <sup>+</sup> <chem>IC1=CC(I)=C(NC(C)=O)C(O)=C1NC(C)=O</chem>		MetaPC(Sedykh et al., 2001)

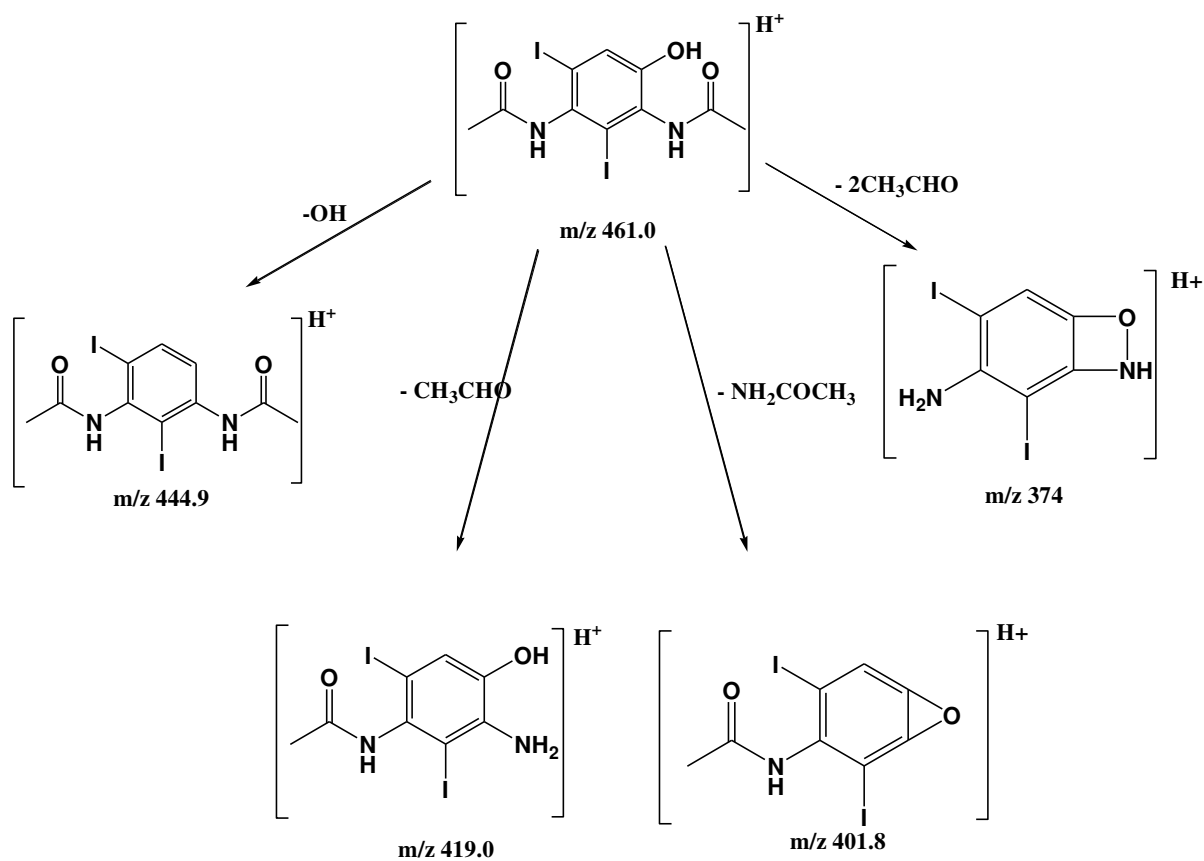




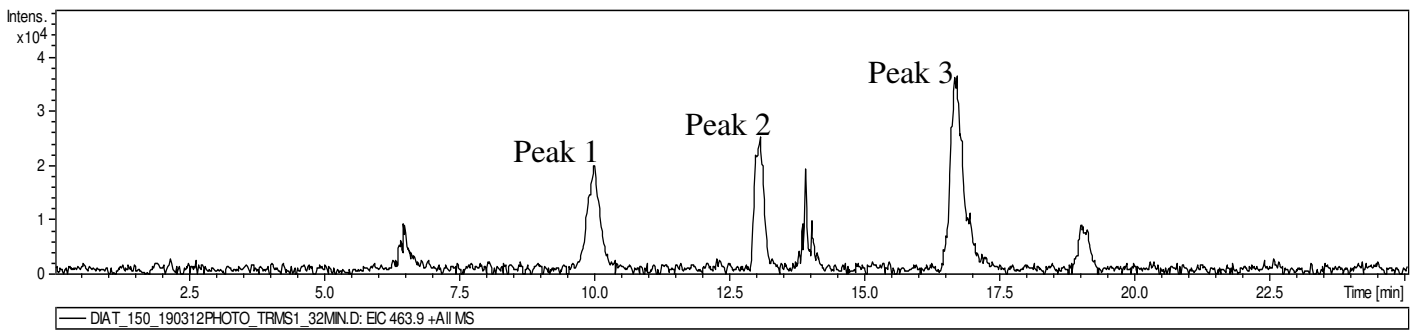
## Peak 2



m/z	Retention time	Precursor ion/ Smiles code	Structure	Reference
461.0	18.8 min	[M+H] <sup>+</sup> OC1=CC(I)=C(NC(C)=O)C(I)=C1NC(C)=O		MetaPC(Sedykh et al., 2001)



**TP 464**

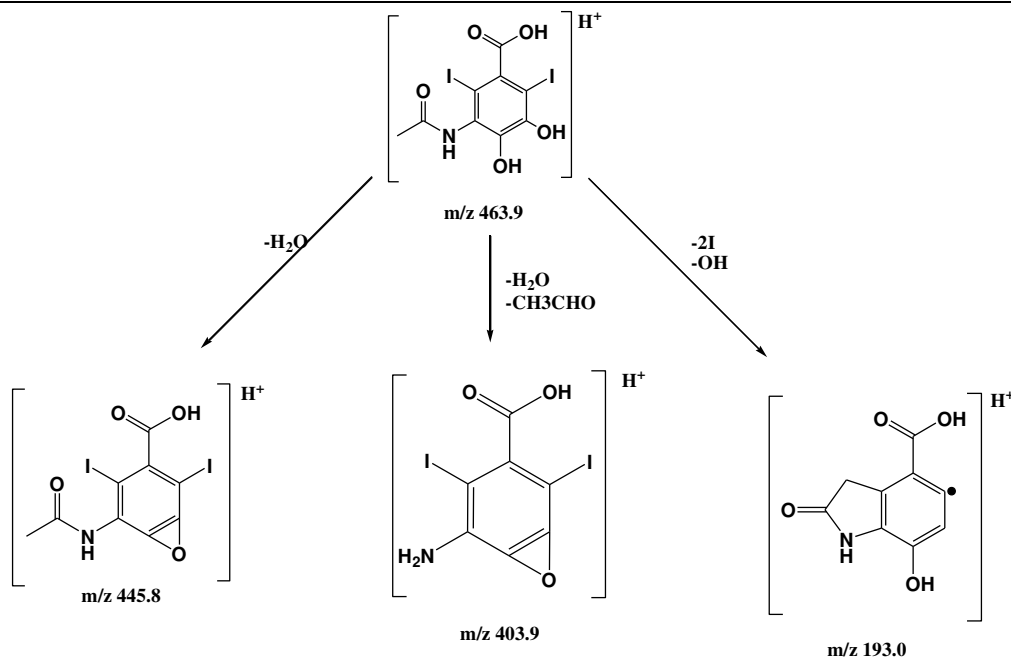


**Peak 1**

m/z	Retention time	Precursor ion/ Smiles code	Structure	Reference
463.9	10.0 min	[M+H] <sup>+</sup> <chem>IC1=C(C(O)=O)C(O)=C(NC(C)=O)C(I)=C1O</chem>	 m/z 463.9	

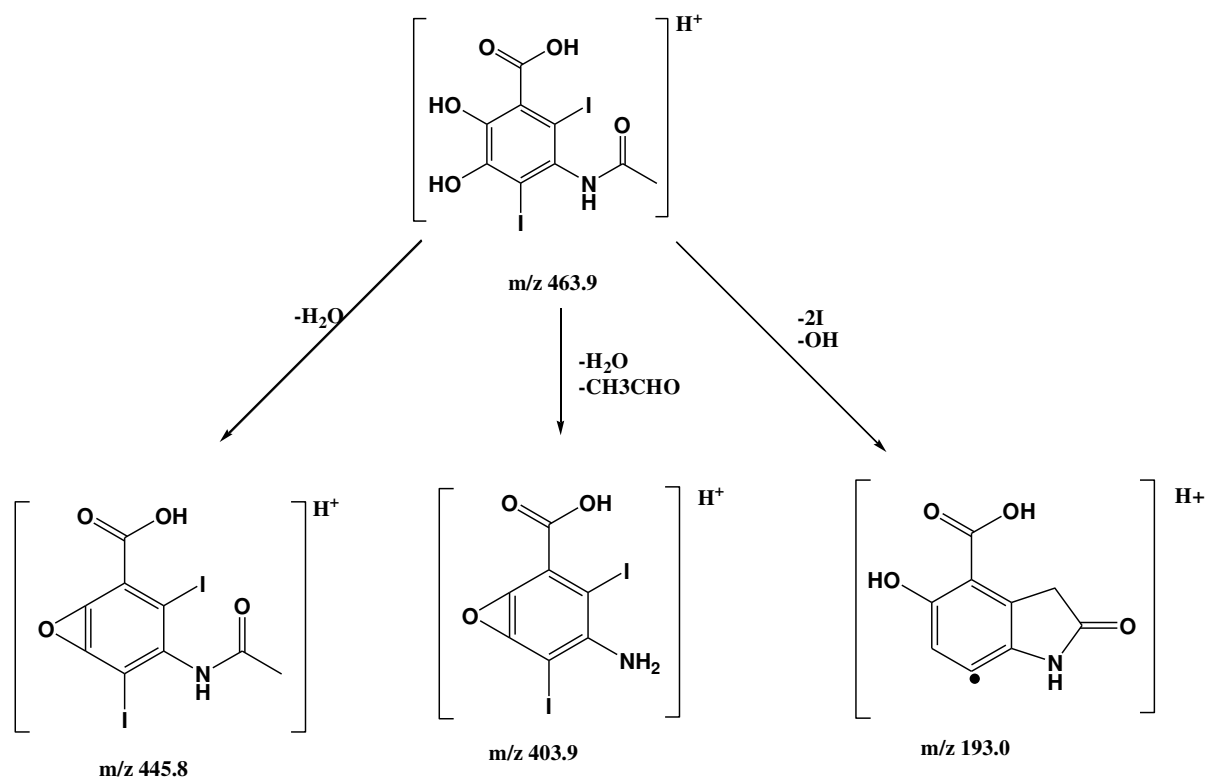
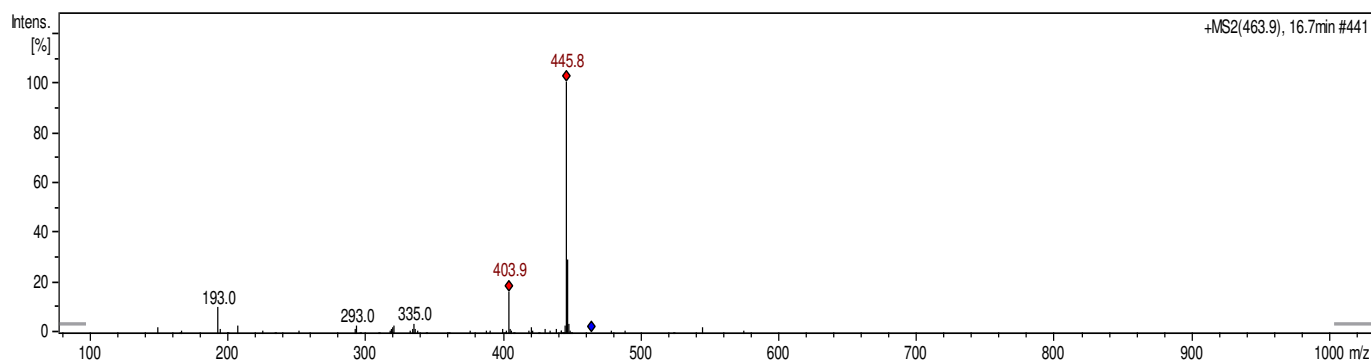
**Peak 2**

m/z	Retention time	Precursor ion/ Smiles code	Structure	Reference
463.9	13.1	[M+H] <sup>+</sup> <chem>IC1=C(C(O)=O)C(I)=C(NC(C)=O)C(O)=C1O</chem>	 m/z 463.9	

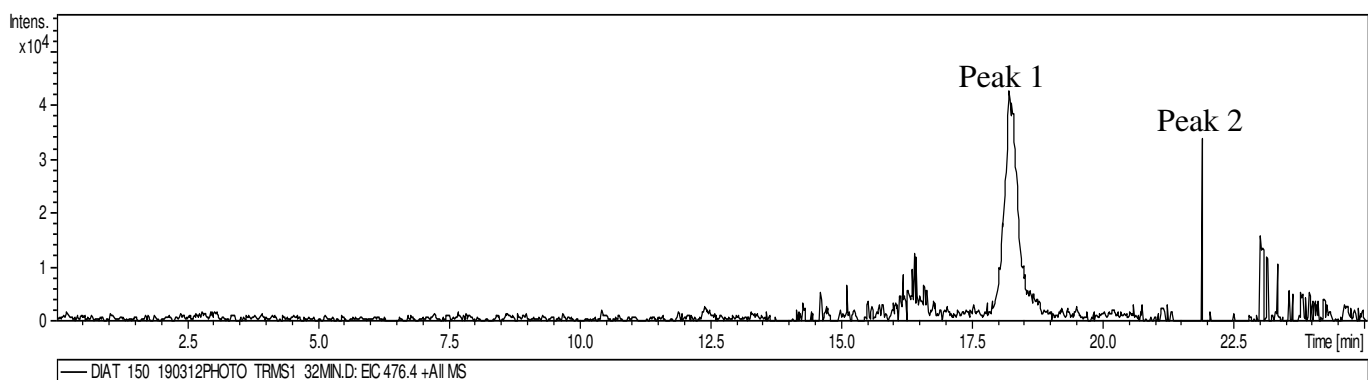


### Peak 3

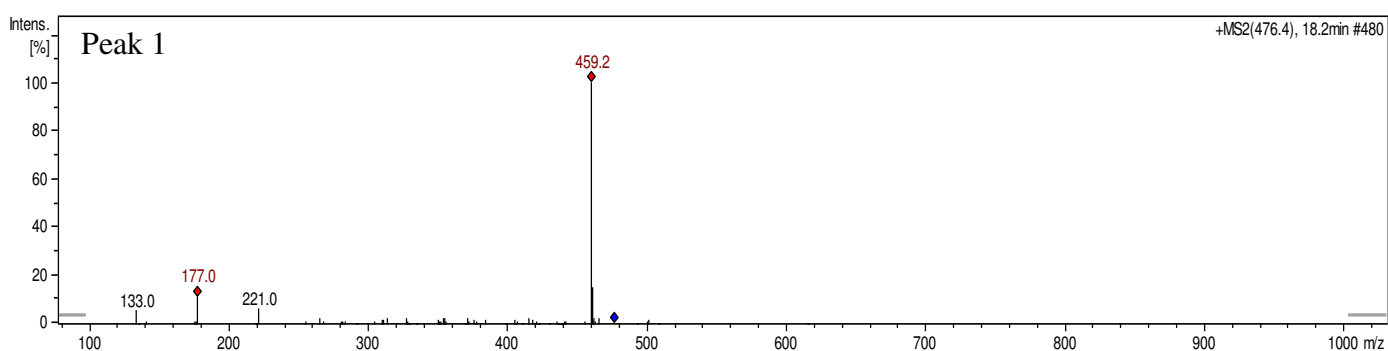
m/z	Retention time	Precursor ion/ Smiles code	Structure	Reference
463.9	16.7	[M+H] <sup>+</sup> <chem>IC1=C(C(O)=O)C(O)=C(O)C(I)=C1NC(C)=O</chem>		

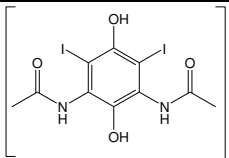


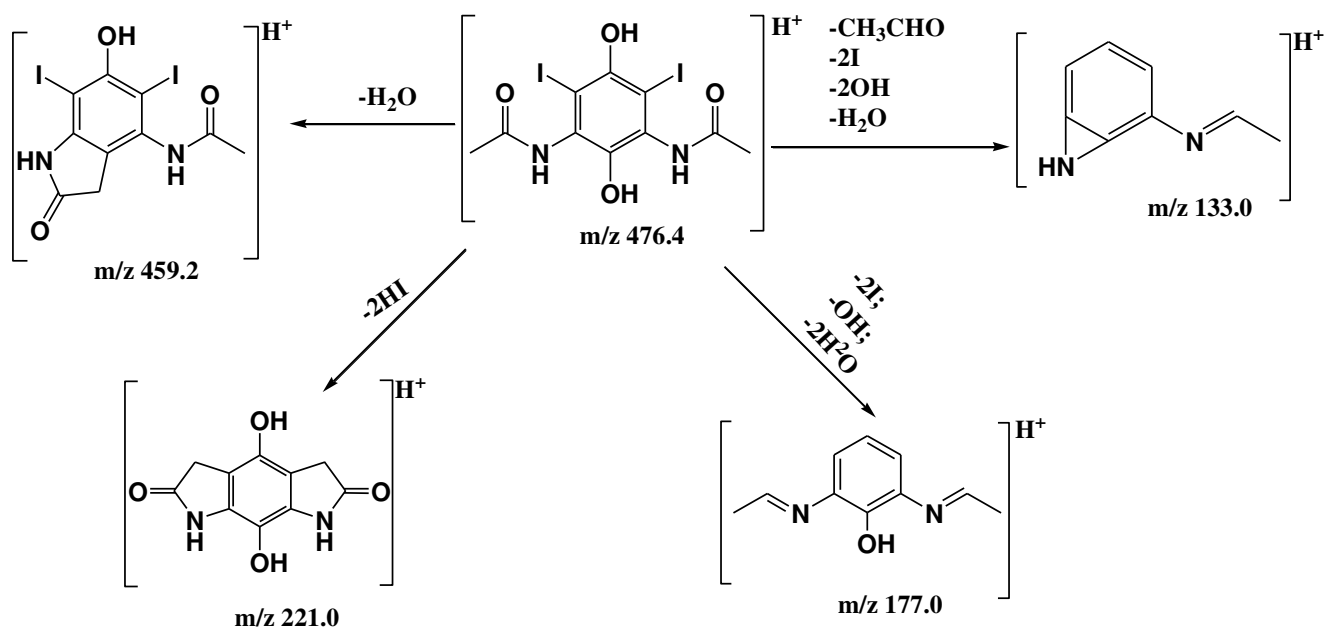
## TP 477



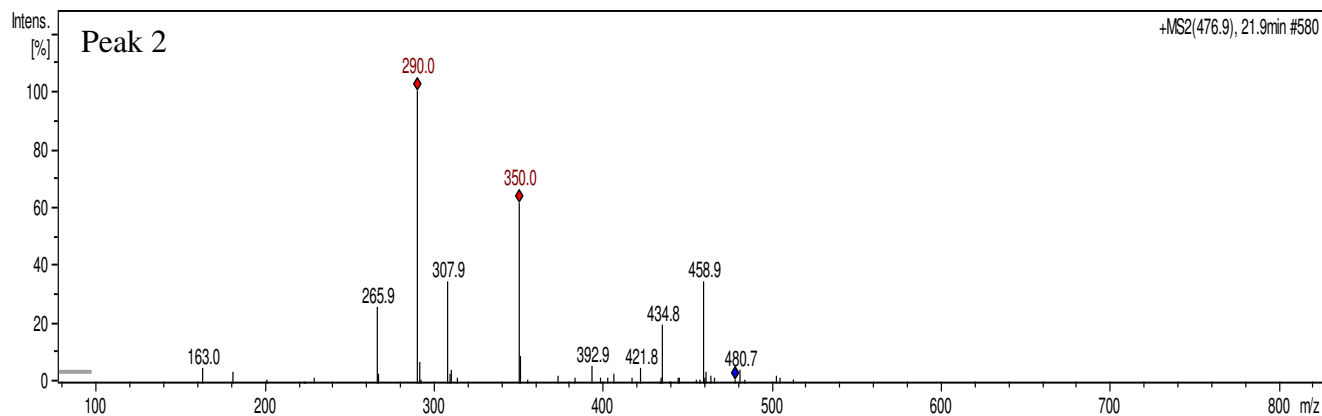
### Peak 1



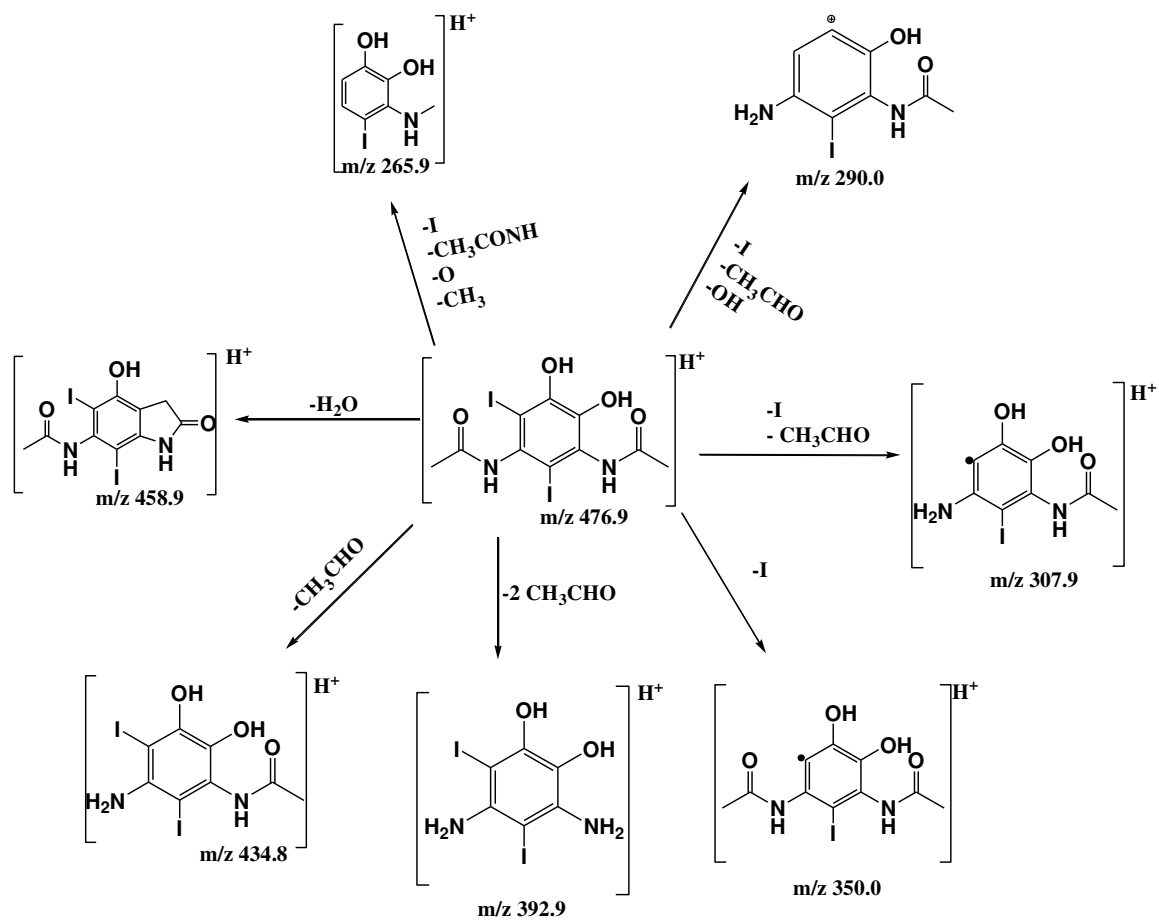
m/z	Retention time	Precursor ion/ Smiles code	Structure	Reference
476.4	18.2 min	[M+H] <sup>+</sup> OC1=C(I)C(NC(C)=O)=C(O)C(NC(C)=O)=C1 I		(Jeong et al., 2010)



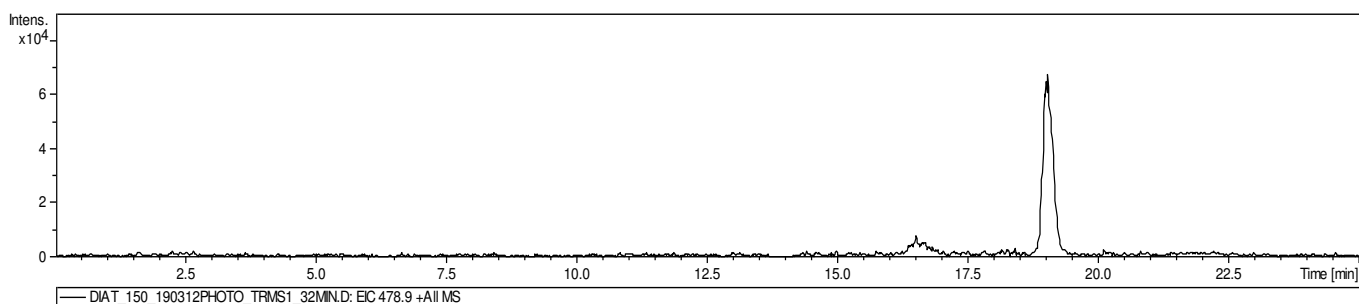
## Peak 2



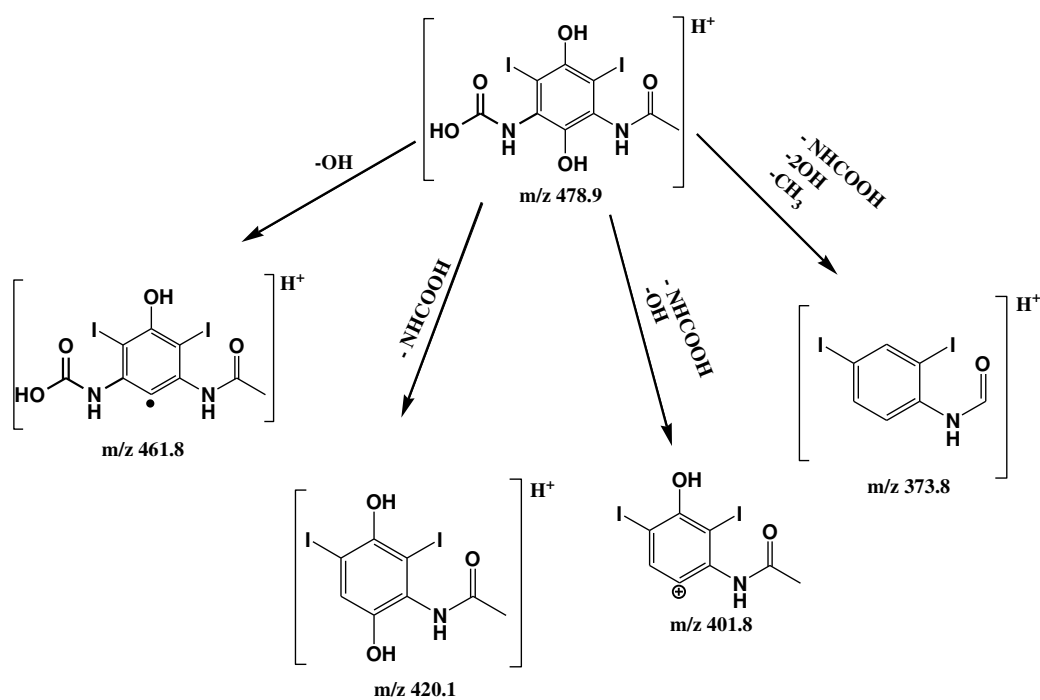
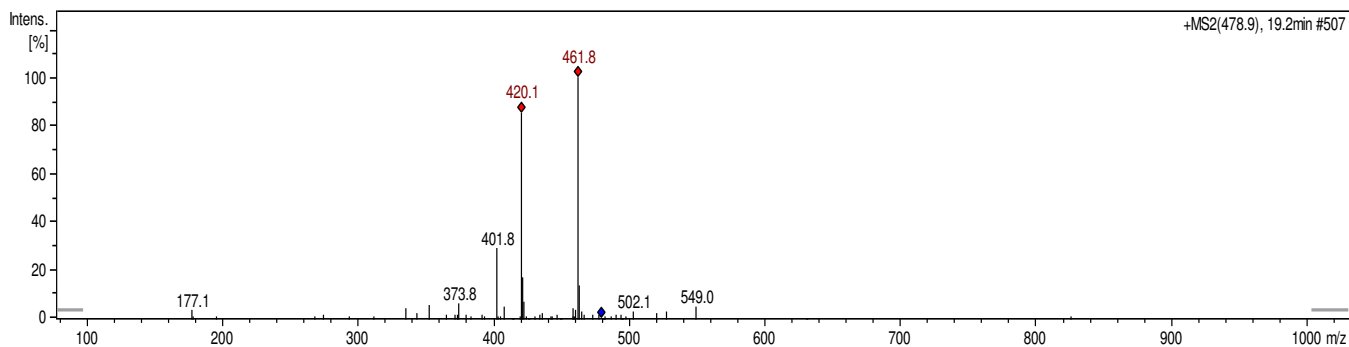
m/z	Retention time	Precursor ion/ Smiles code	Structure	Reference
476.9	21.9 min	[M+H] <sup>+</sup> <chem>OC1=C(O)C(NC(C)=O)=C(I)C(NC(C)=O)=C1I</chem>		(Jeong et al., 2010)



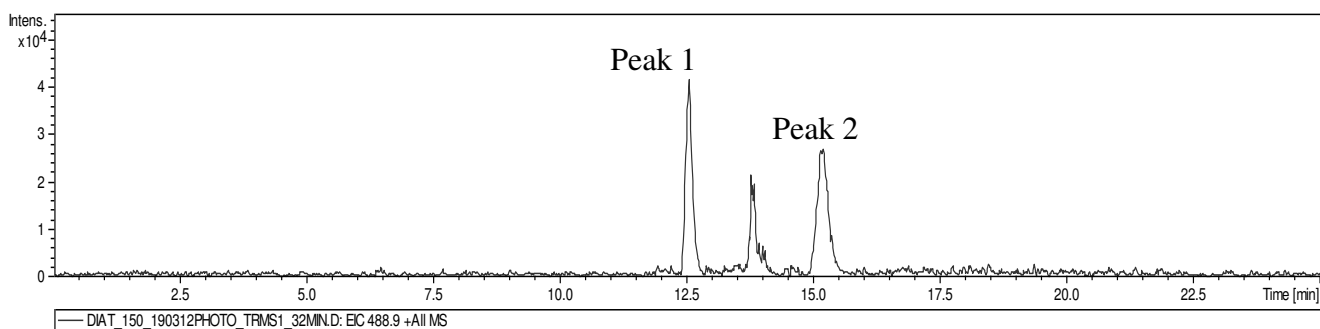
**TP 479**



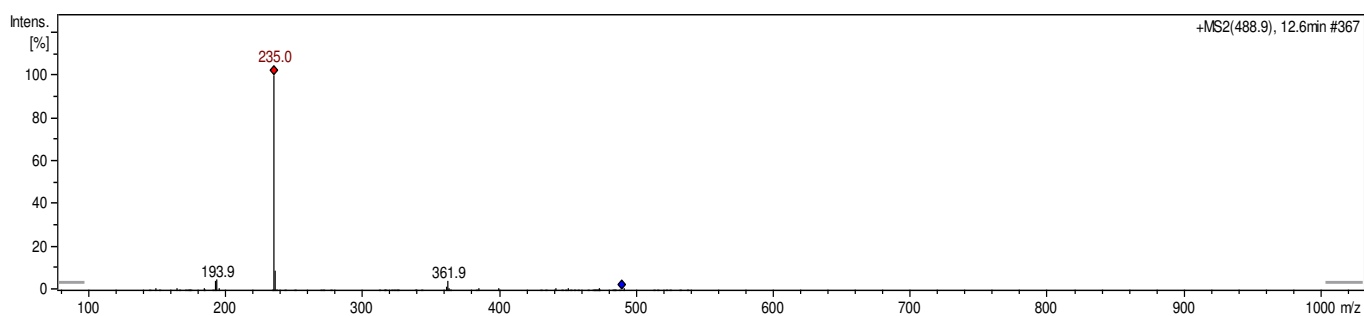
m/z	Retention time	Precursor ion/ Smiles code	Structure	Reference
478.9	19.0 min	[M+H] <sup>+</sup> OC1=C(I)C(NC(C)=O)=C(O)C(NC(O)=O)=C1I		



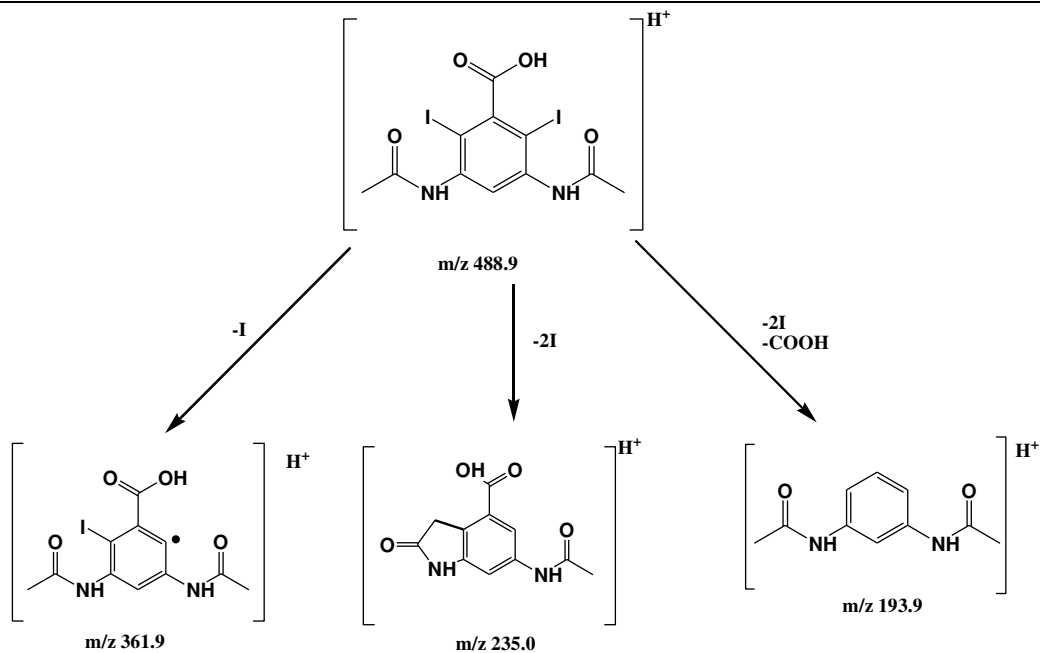
## TP 489



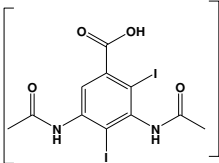
### Peak 1

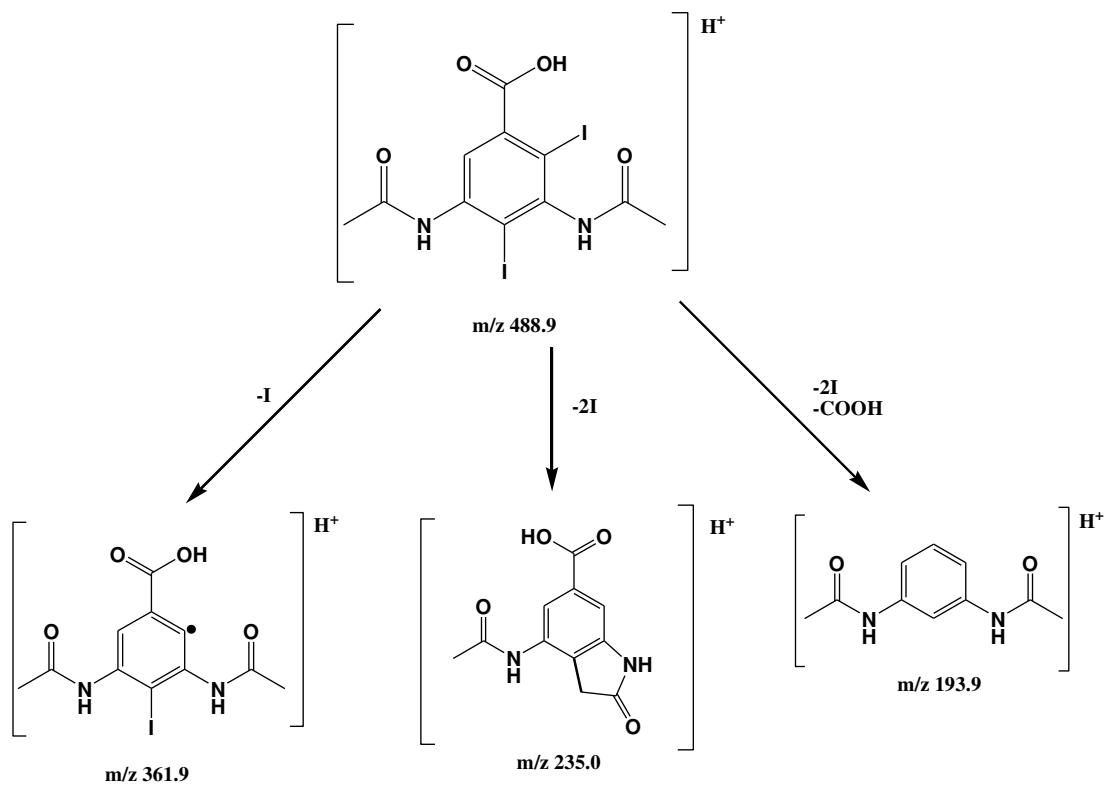


m/z	Retention time	Precursor ion/ Smiles code	Structure	Reference
488.9	12.5 min	[M+H] <sup>+</sup> <chem>IC1=C(C(O)=O)C=C(NC(C)=O)C(I)=C1NC(C)=O</chem>		(Sugihara et al., 2013; Velo-Gala et al., 2012)



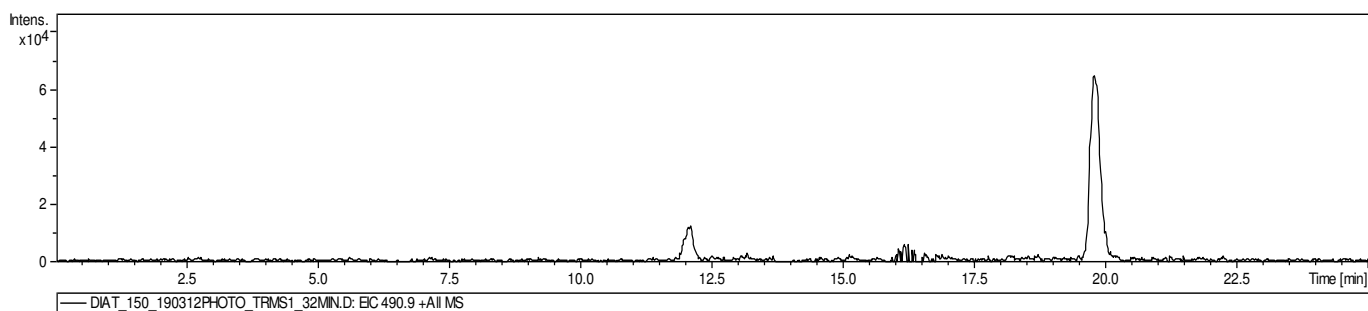
Peak 2

m/z	Retention time	Precursor ion/ Smiles code	Structure	Reference
488.9	15.1	[M+H] <sup>+</sup> <chem>IC1=C(C(O)=O)C(I)=C(NC(C)=O)C=C1NC(C)=O</chem>		(Sugihara et al., 2013; Velo-Gala et al., 2012)

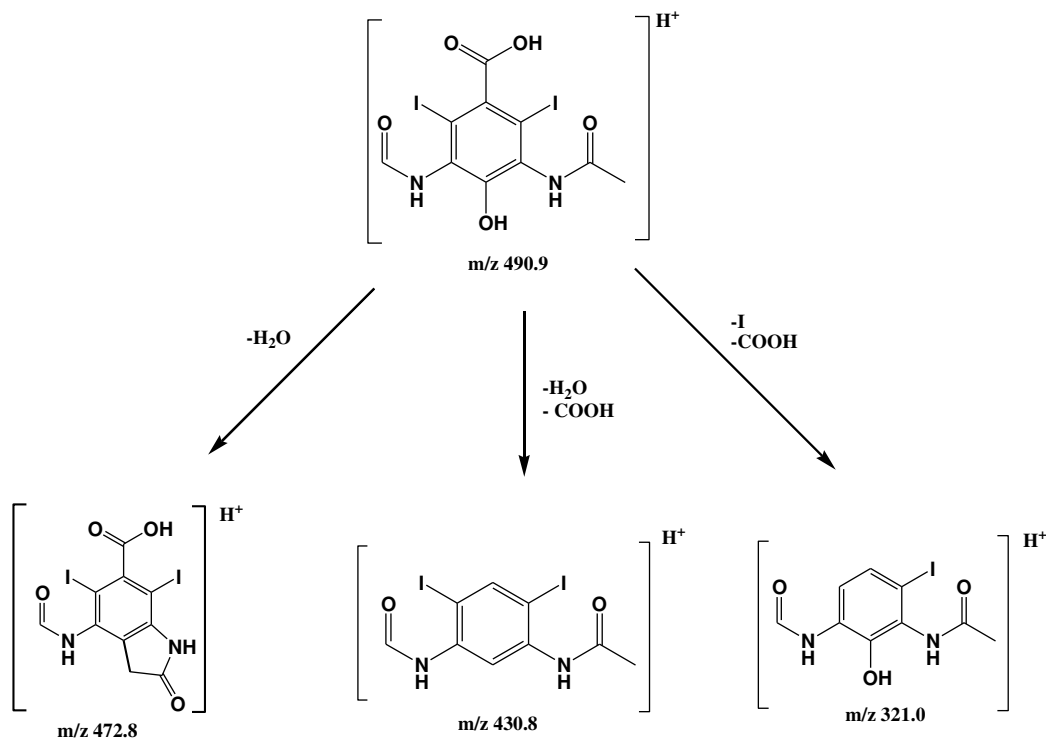
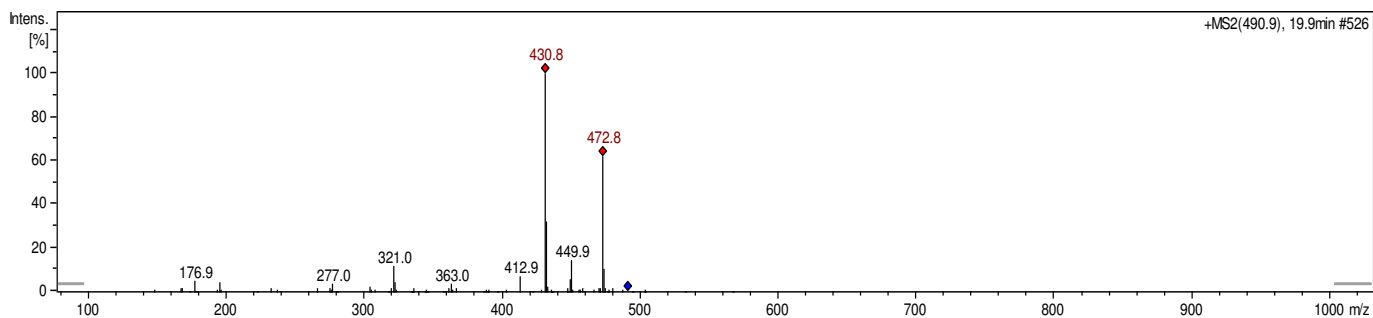




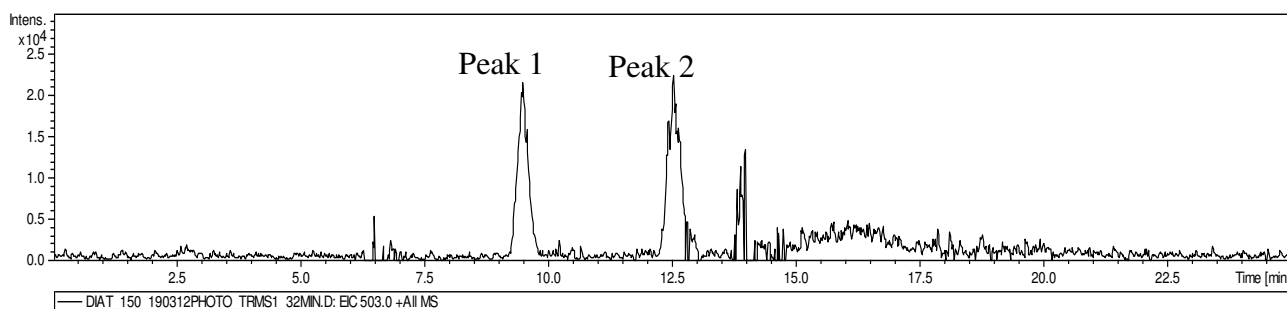
# TP 491



m/z	Retention time	Precursor ion/ Smiles code	Structure	Reference
490.9	19.8 min	$[M+H]^+$ <chem>IC1=C(C(O)=O)C(I)=C(NC=O)C(O)=C1NC(C)=O</chem>		

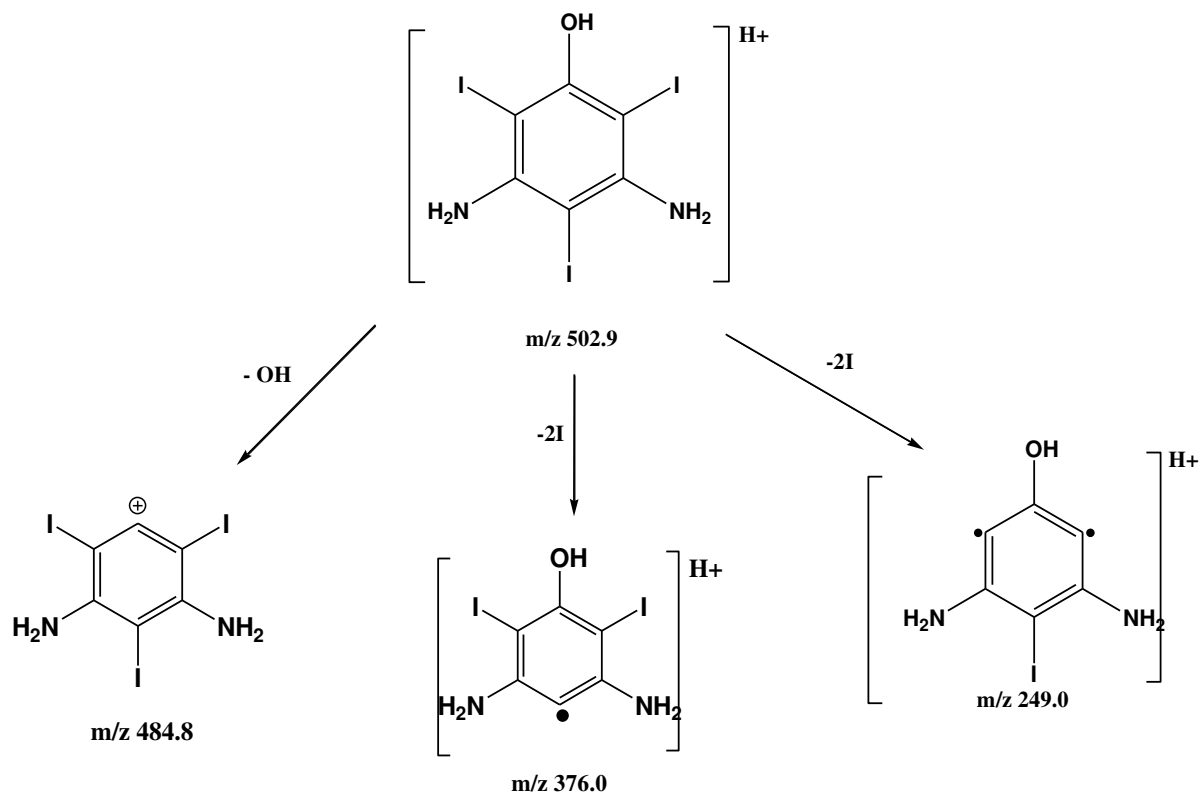


## TP 503

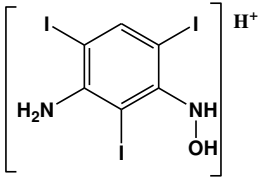


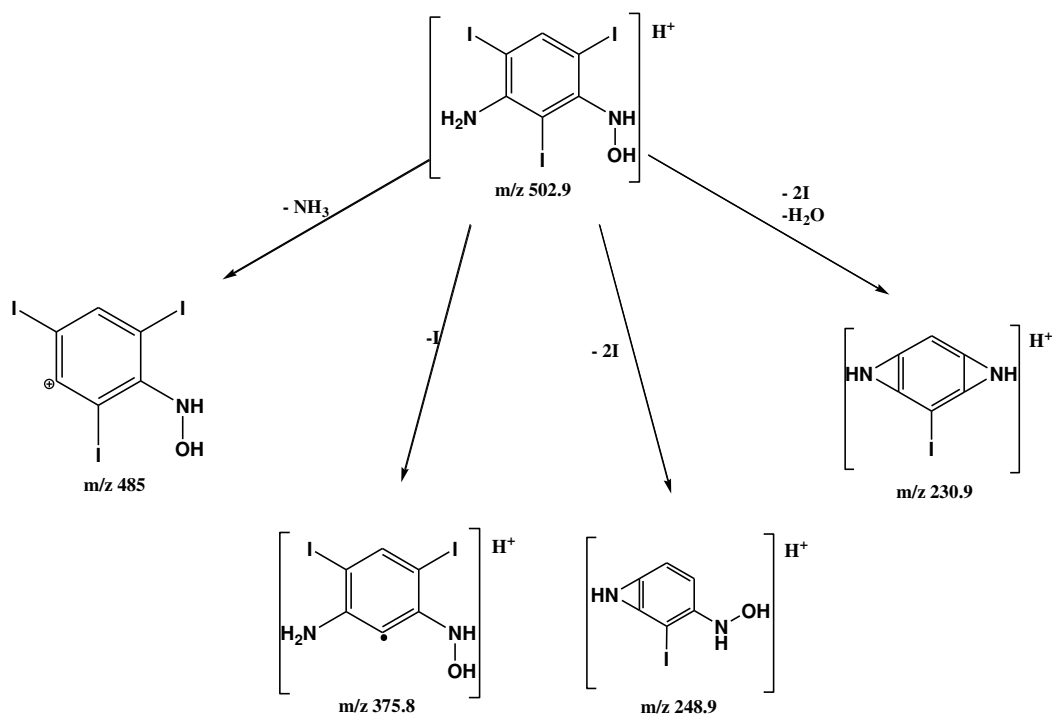
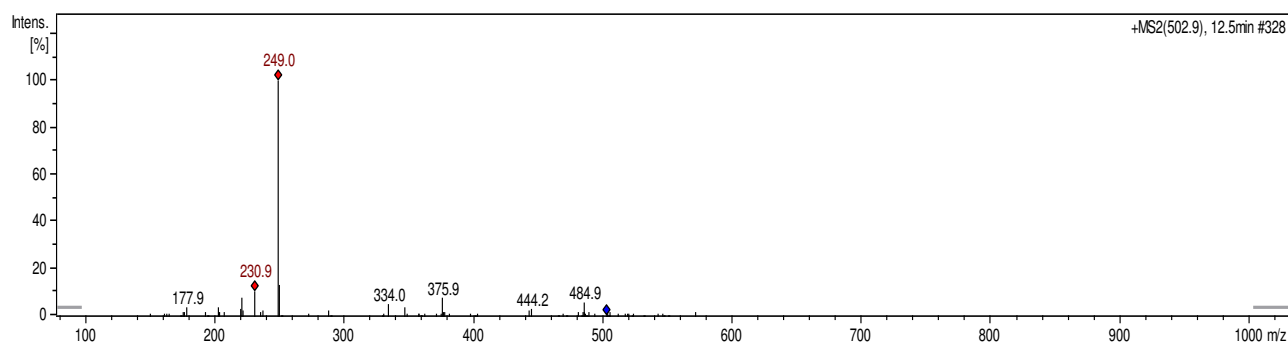
### Peak 1

m/z	Retention time	Precursor ion/ Smiles code	Structure	Reference
502.3	9.5 min	[M+H] <sup>+</sup> <chem>OC1=C(I)C(N)=C(I)C(N)=C1I</chem>		MetaPC(Sedykh et al., 2001)

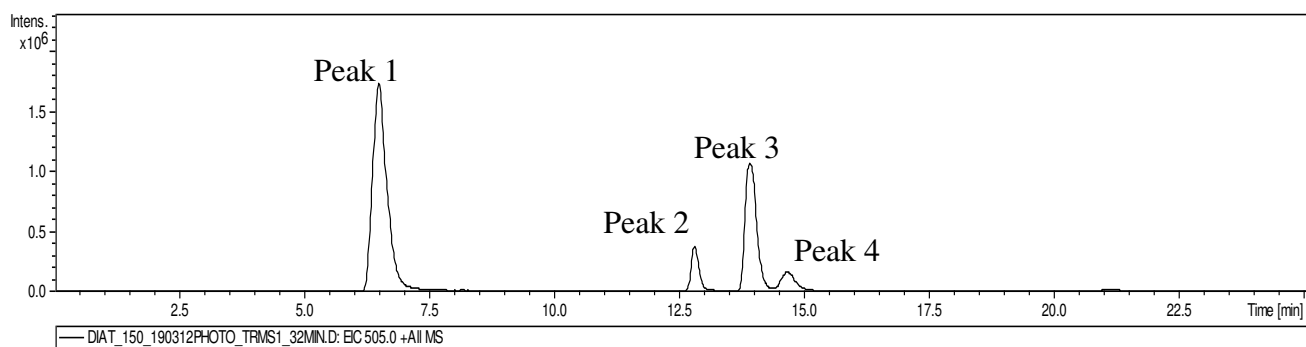


## Peak 2

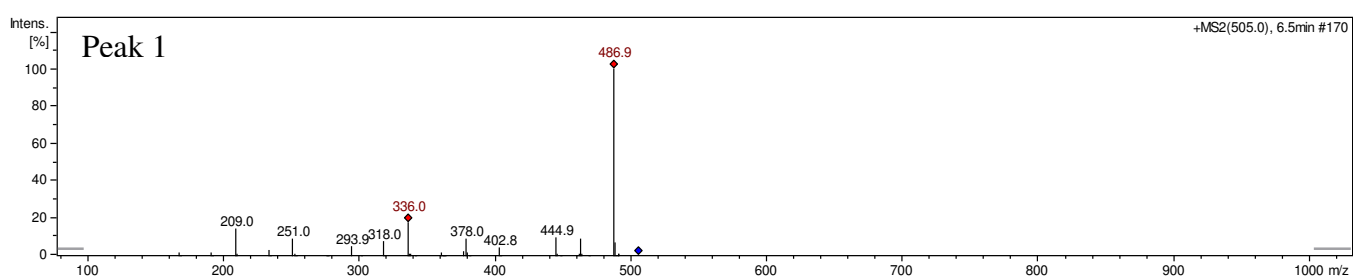
m/z	Retention time	Precursor ion/ Smiles code	Structure	Reference
502.3	12.5 min	[M+H] <sup>+</sup> IC1=CC(I)=C(N)C(I)=C 1NO		MetaPC(Sedykh et al., 2001)



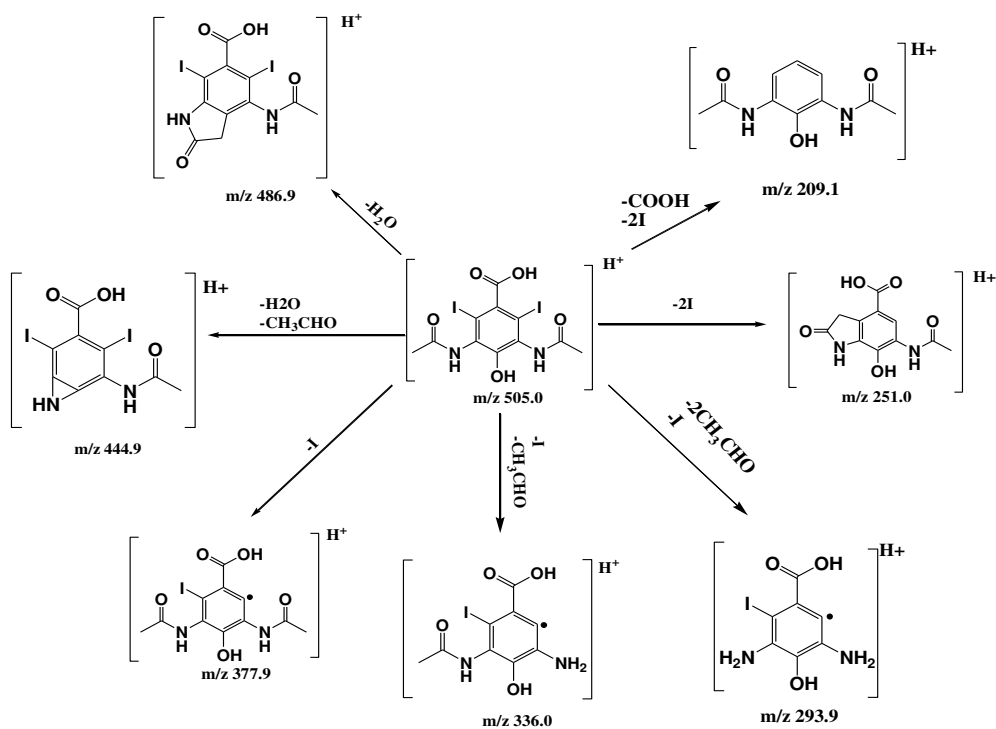
## TP 505



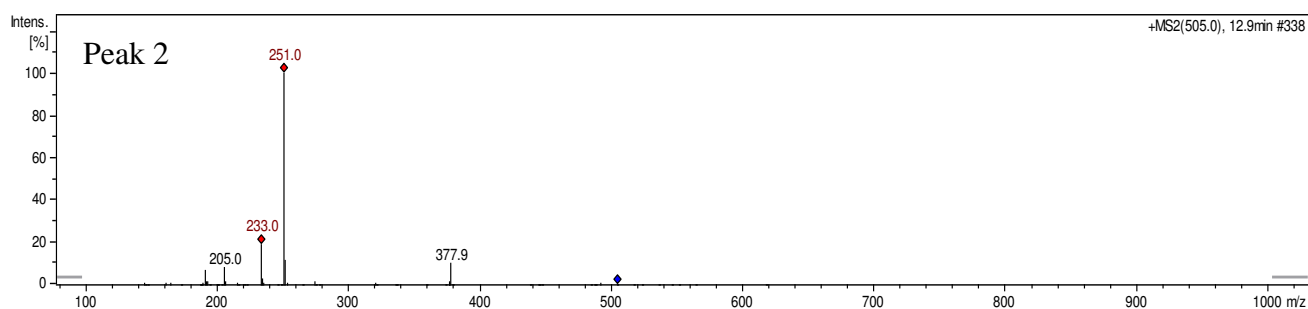
### Peak 1



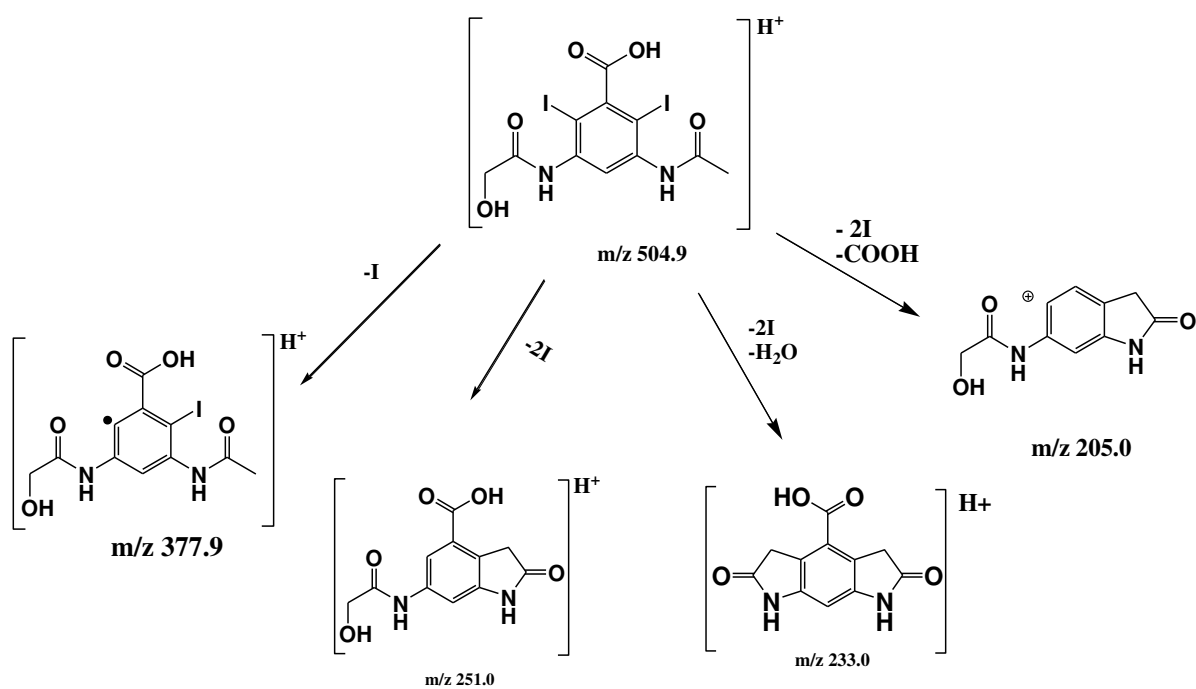
m/z	Retention time	Precursor ion/ Smiles code	Structure	Reference
505.0	6.5	[M+H] <sup>+</sup> <chem>IC1=C(C(O)=O)C(O)=C(NC(C)=O)C(I)=C1NC(C)=O</chem>		(Jeong et al., 2010)



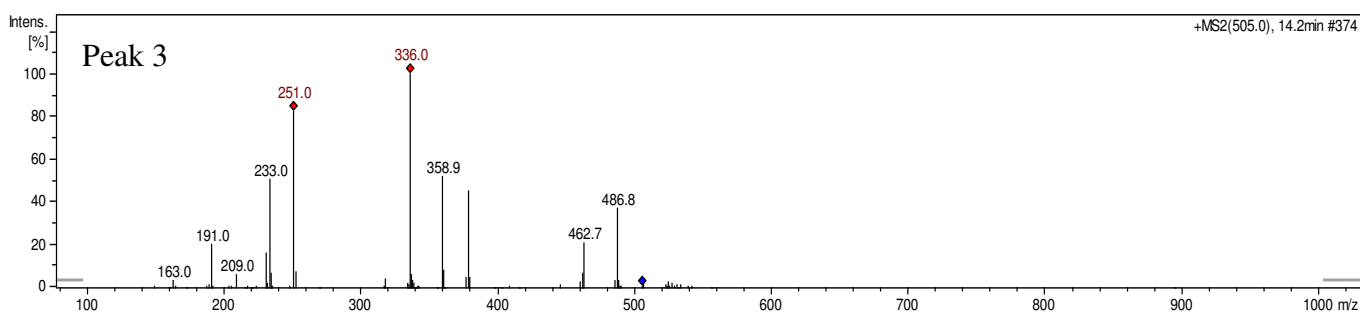
## Peak 2



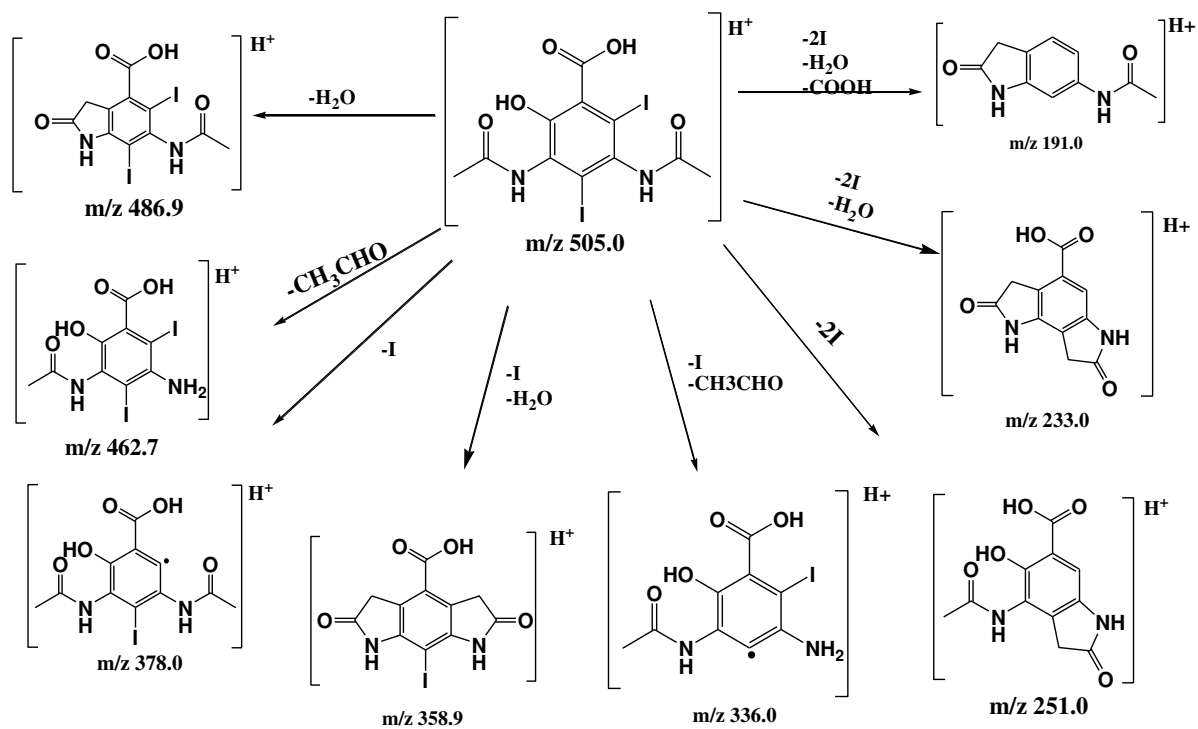
m/z	Retention time	Precursor ion/ Smiles code	Structure	Reference
505.0	12.9	[M+H] <sup>+</sup> <chem>IC1=C(C(O)=O)C=C(NC(CO)=O)C(I)=C1NC(C)=O</chem>		(Hennebel et al., 2010)



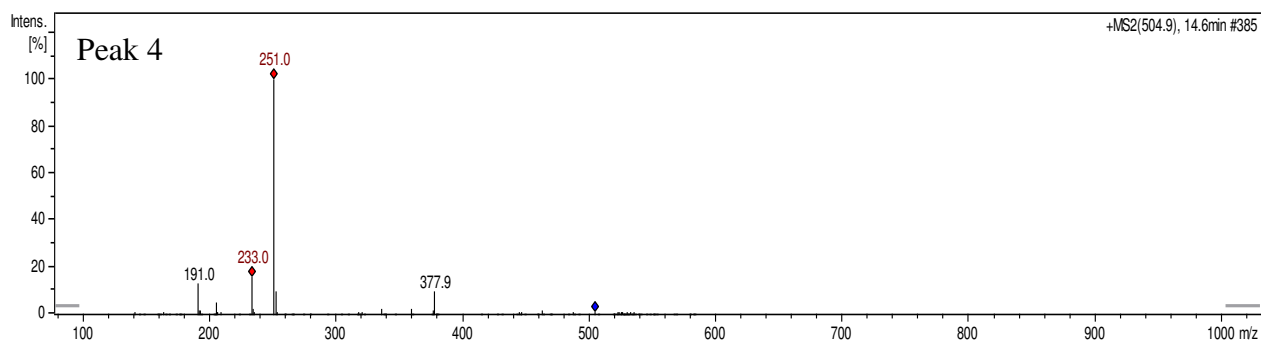
### Peak 3

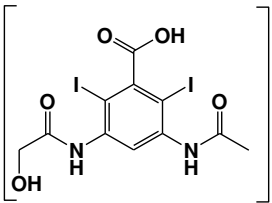


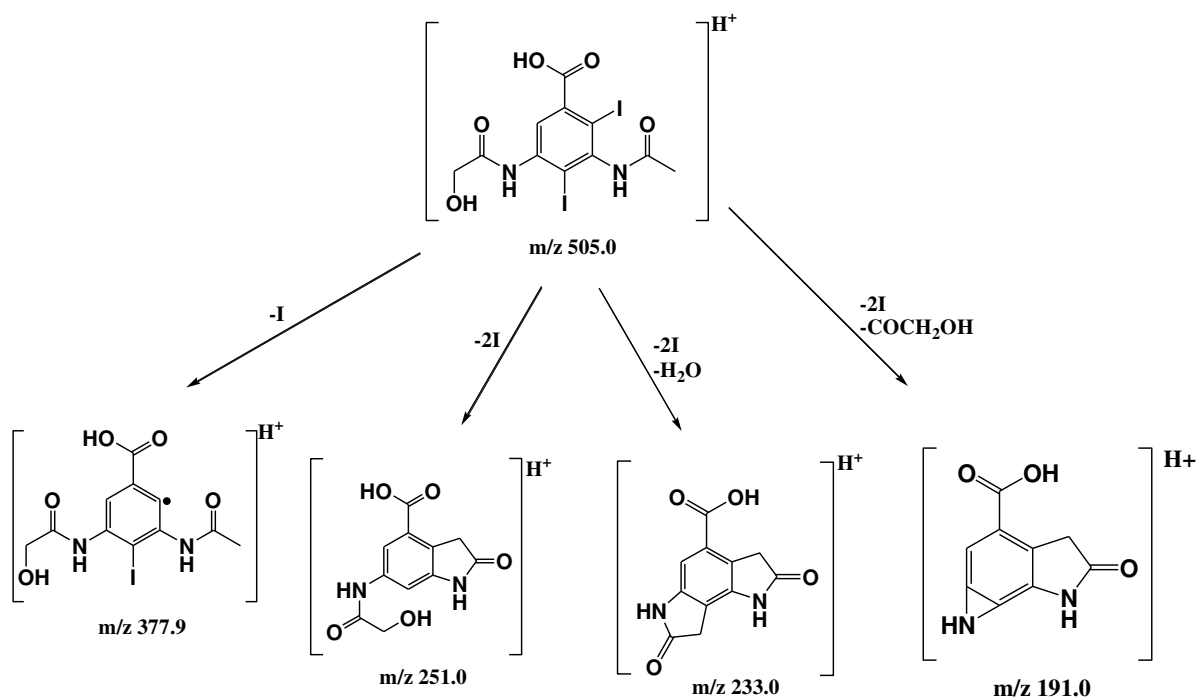
m/z	Retention time	Precursor ion/ Smiles code	Structure	Reference
505.0	14.2	[M+H] <sup>+</sup> <chem>IC1=C(C(O)=O)C(I)=C(NC(C)=O)C(O)=C1NC(C)=O</chem>		(Jeong et al., 2010)



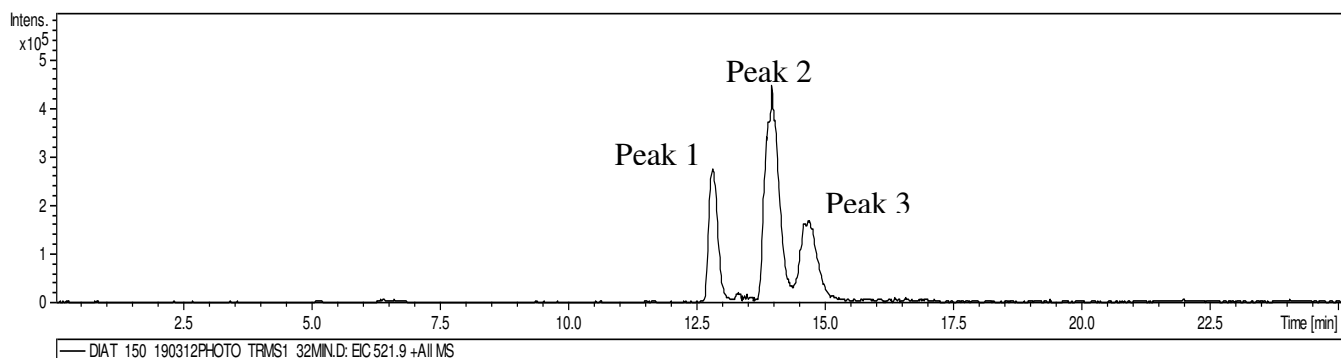
## Peak 4



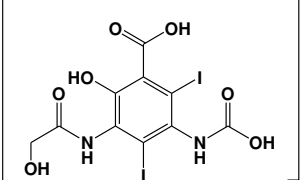
m/z	Retention time	Precursor ion/ Smiles code	Structure	Reference
504.9	14.6	[M+H] <sup>+</sup> <chem>IC1=C(C(O)=O)C(I)=C(NC(CO)=O)C=C1NC(C)=O</chem>		(Hennebel et al., 2010)

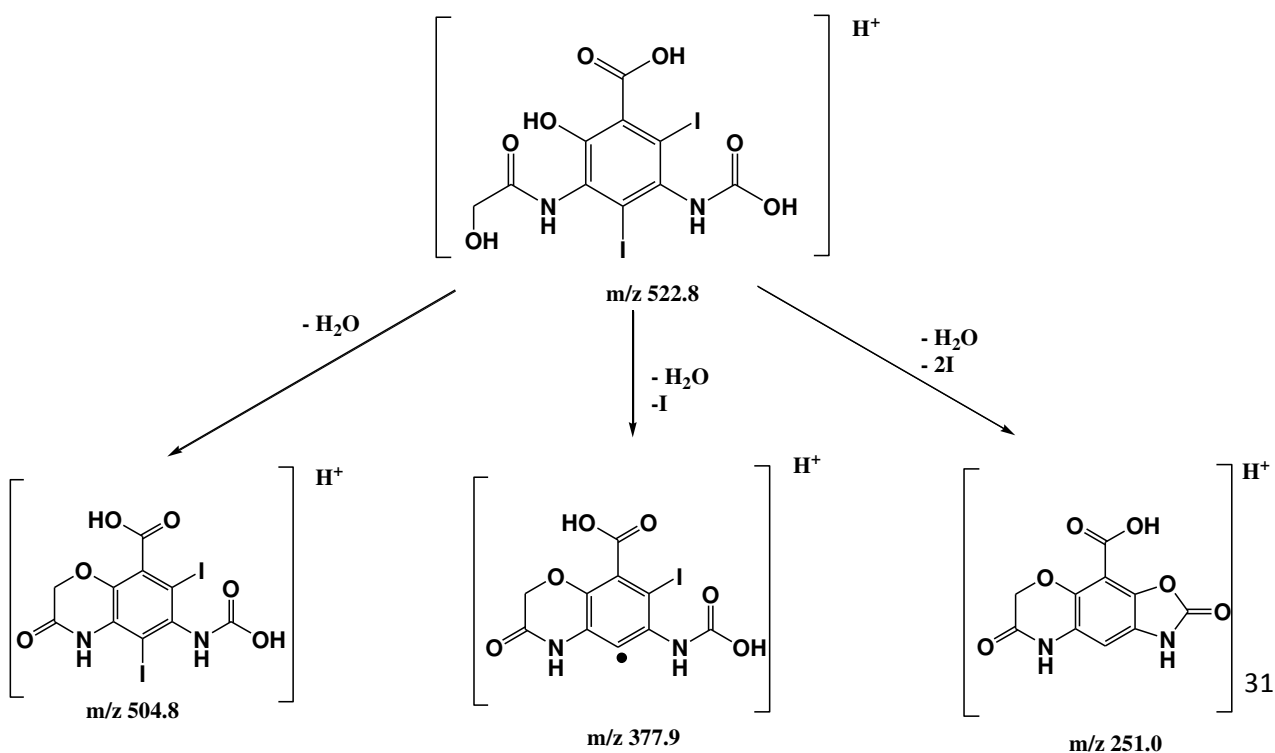
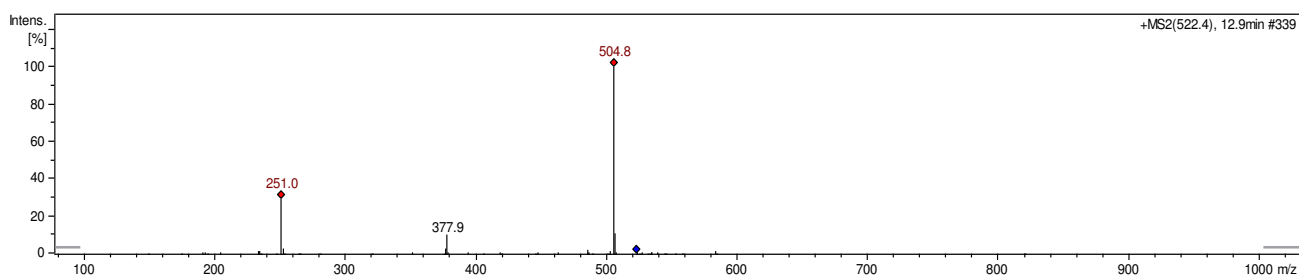


## TP 522



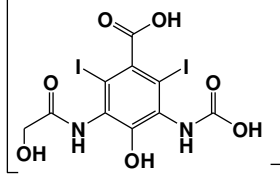
### Peak 1

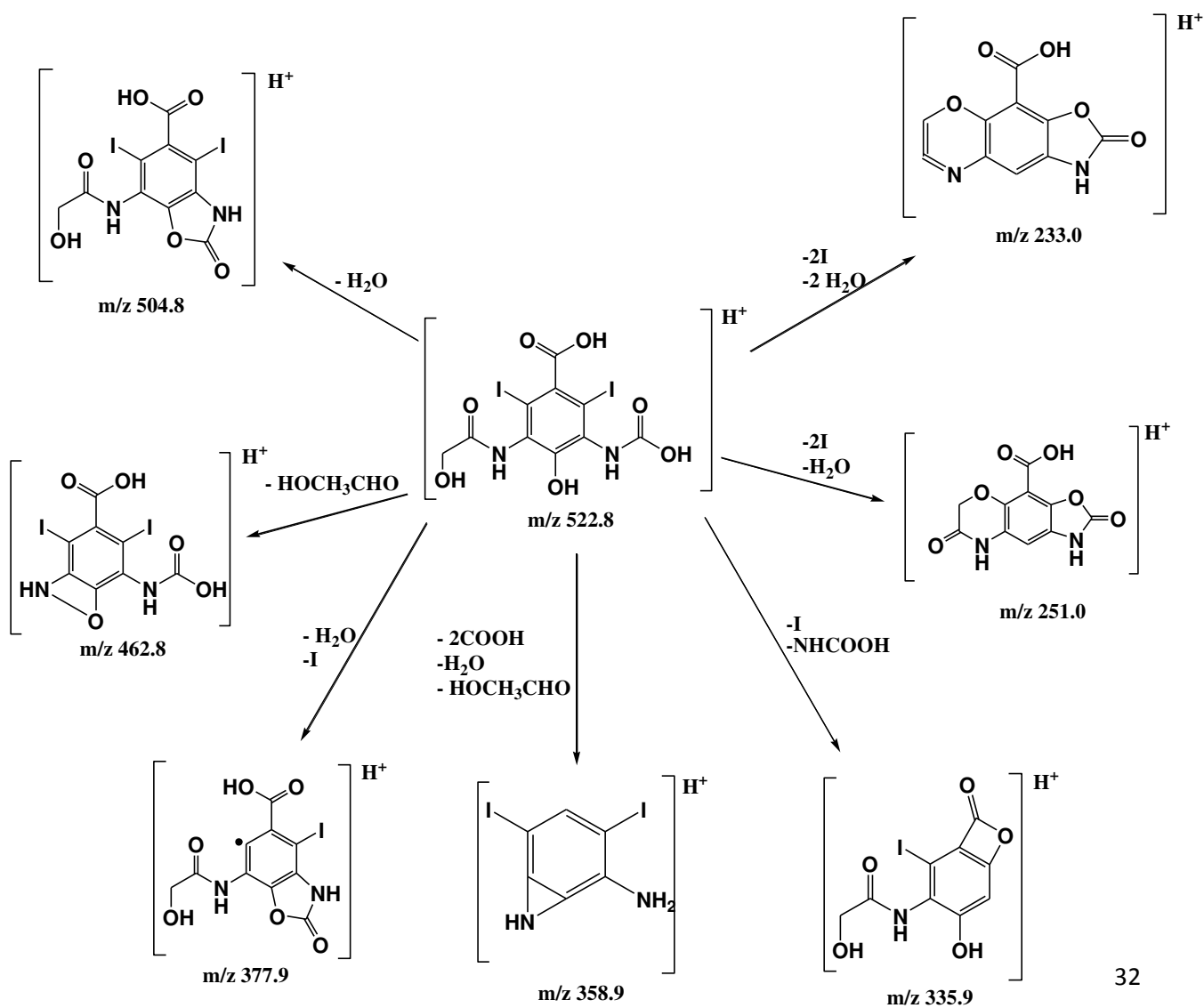
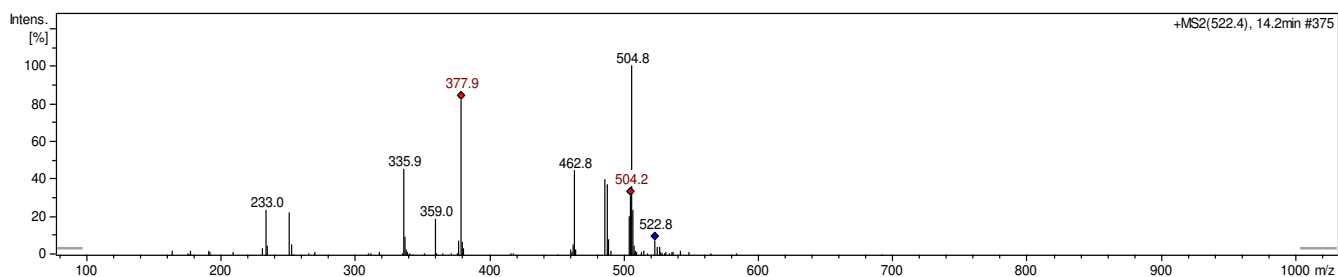
m/z	Retention time	Precursor ion/ Smiles code	Structure	Reference
522.4	12.8	[M+H] <sup>+</sup> <chem>IC1=C(C(O)=O)C(O)=C(NC(CO)=O)C(I)=C1NC(O)=O</chem>		H <sup>+</sup>



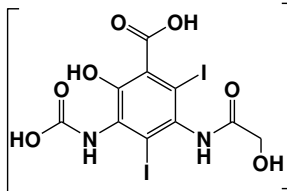


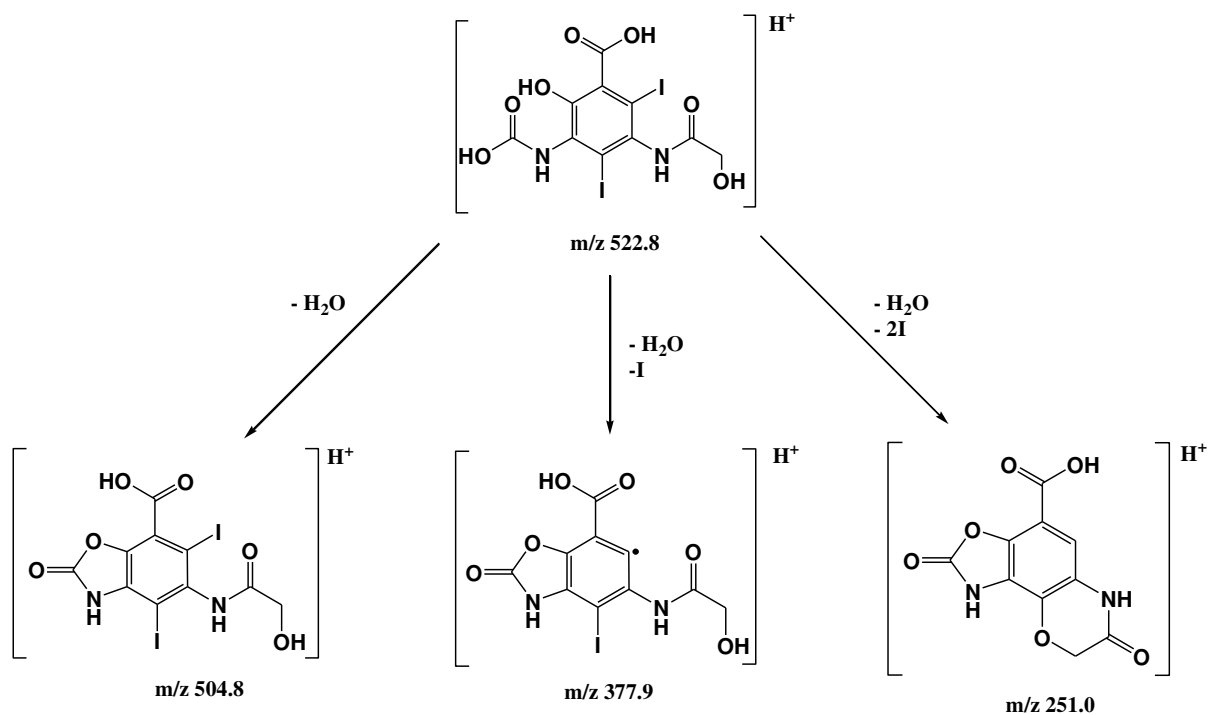
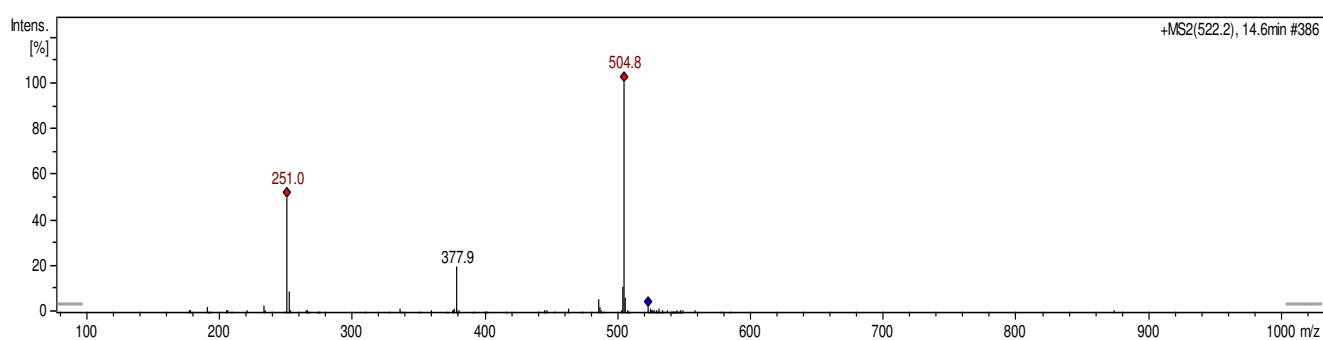
## Peak 2

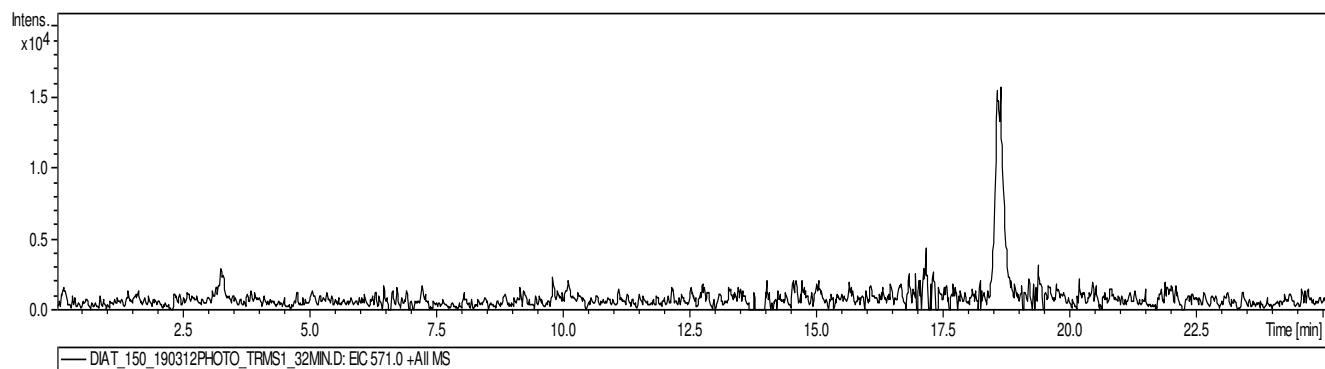
m/z	Retention time	Precursor ion/ Smiles code	Structure	Reference
522.4	13.9	[M+H] <sup>+</sup> <chem>IC1=C(C(O)=O)C(I)=C(NC(CO)=O)C(O)=C1NC(O)=O</chem>		



### Peak 3

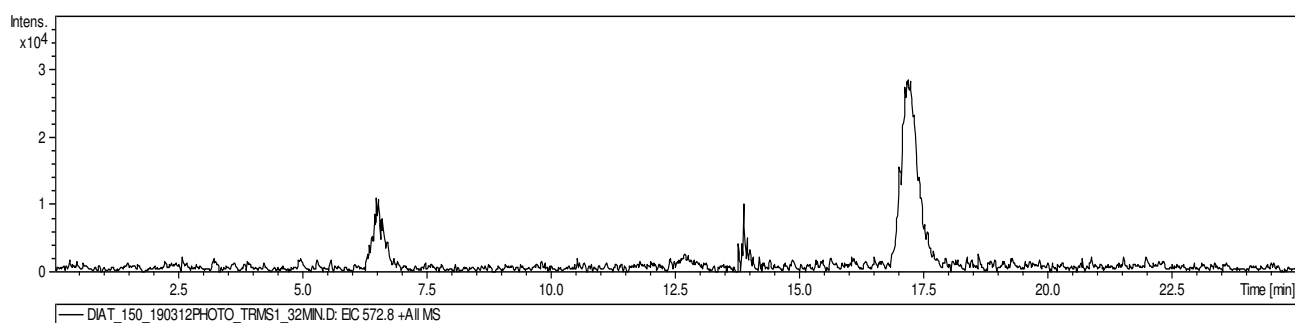
m/z	Retention time	Precursor ion/ Smiles code	Structure	Reference
522.4	14.6	[M+H] <sup>+</sup> <chem>IC1=C(C(O)=O)C(O)=C(NC(O)=O)C(I)=C1NC(CO)=O</chem>		



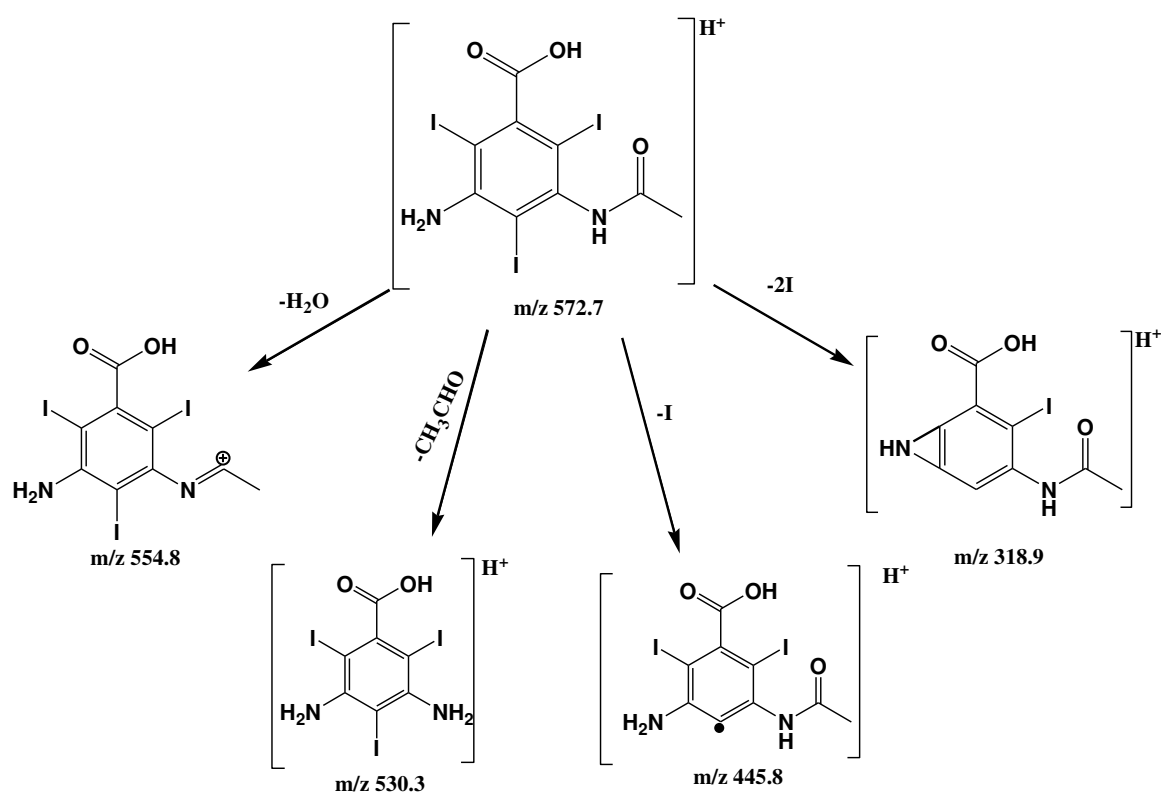
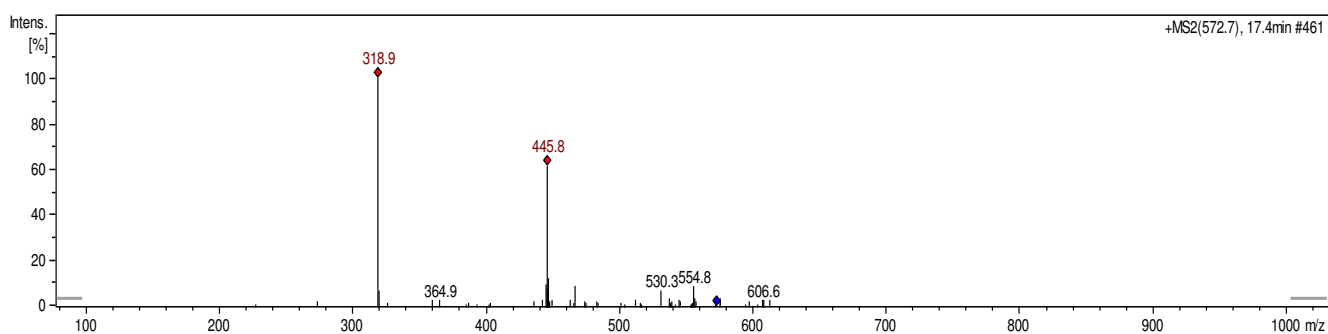


m/z	Retention time	Precursor ion/ Smiles code	Structure	Reference
571.1	18.5 min	[M+H] <sup>+</sup> <chem>IC1=CC(I)=C(NC(C)=O)C(I)=C1NC(C)=O</chem>		MetaPC(Sedykh et al., 2001)

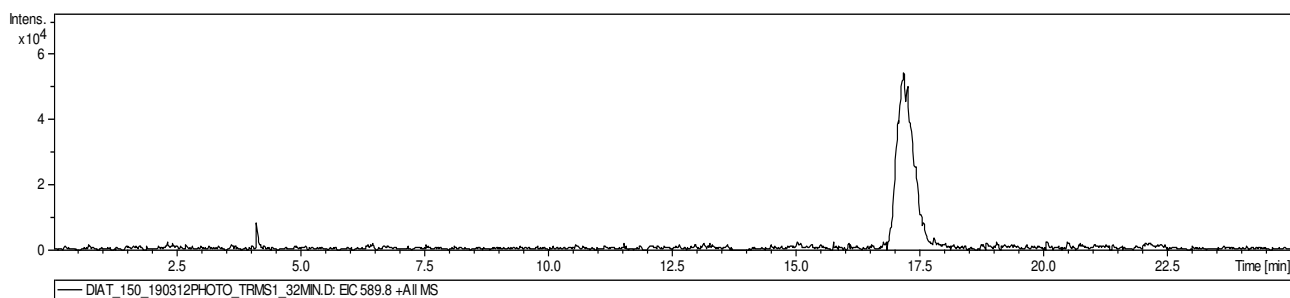
# TP 573



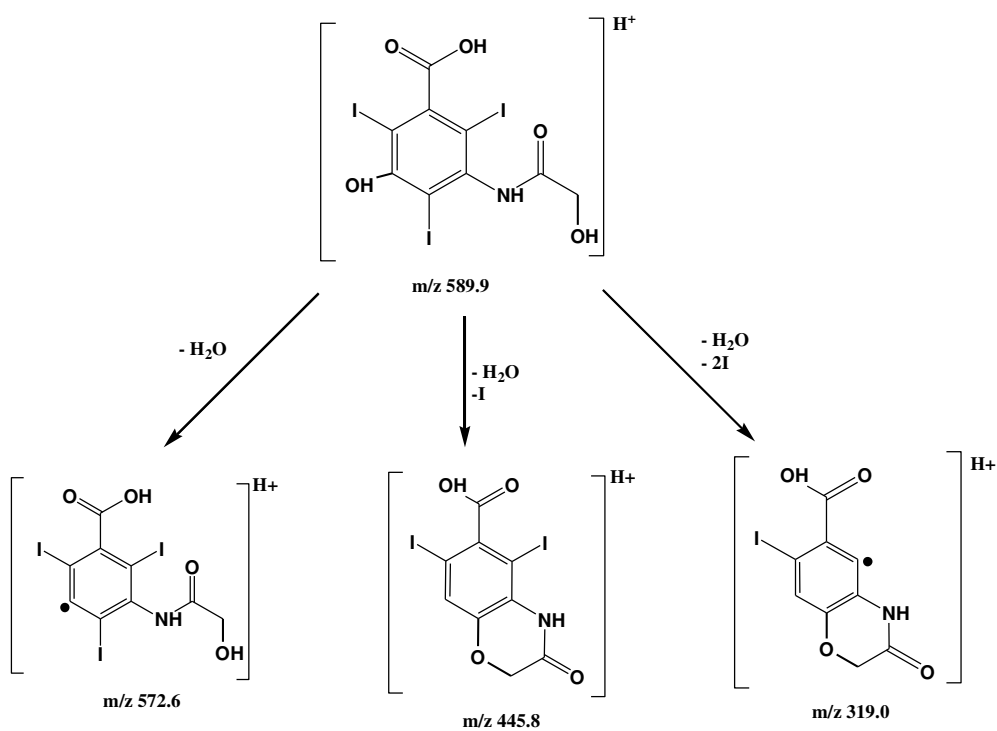
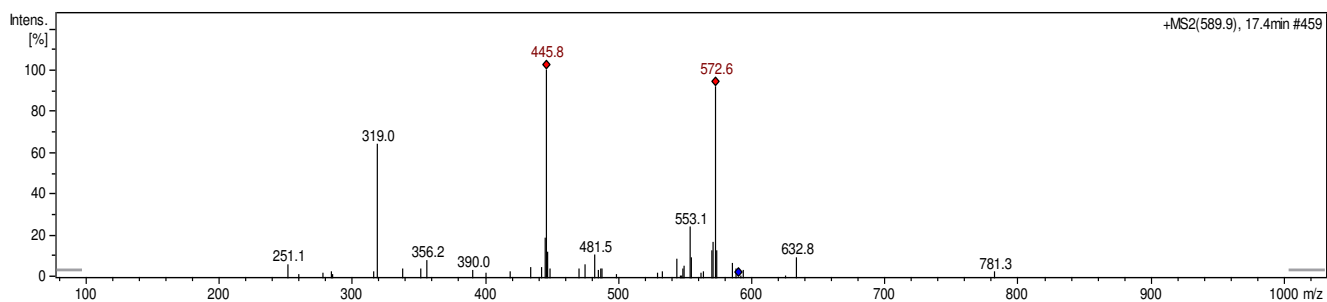
m/z	Retention time	Precursor ion/ Smiles code	Structure	Reference
572.8	17.4	[M+H] <sup>+</sup> <chem>IC1=C(C(O)=O)C(I)=C(N)C(I)=C1NC(C)=O</chem>		MetaPC(Sedykh et al., 2001)



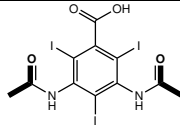
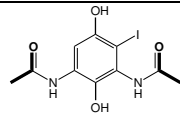
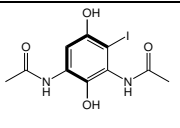
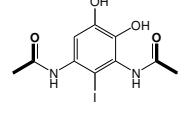
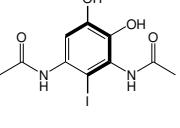
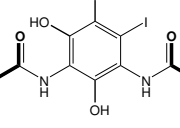
## TP 590

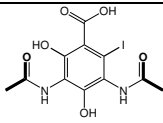
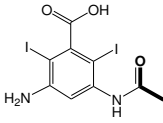
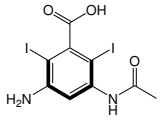
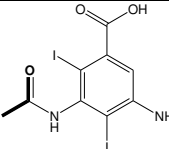
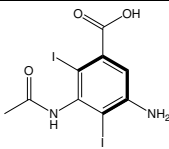
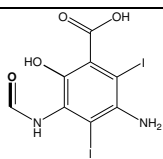
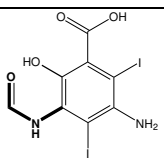
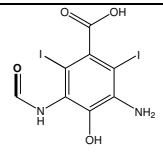
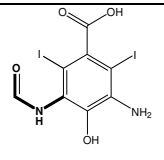
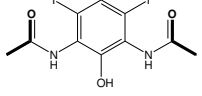
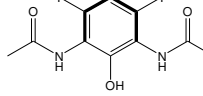
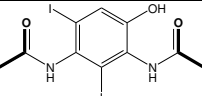
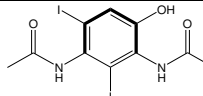


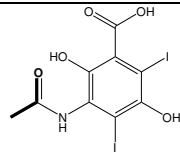
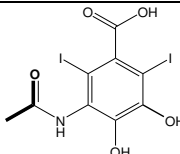
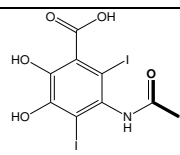
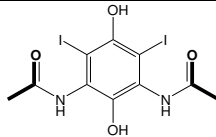
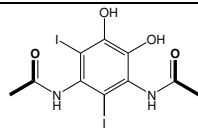
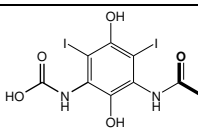
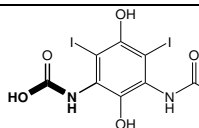
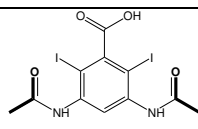
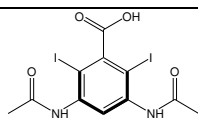
m/z	Retention time	Precursor ion/ Smiles code	Structure	Reference
589.8	17.4	[M+H] <sup>+</sup> IC1=C(C(O)=O)C(I)=C(O)C(I)=C1NC(CO)=O		



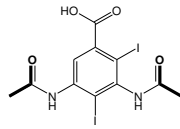
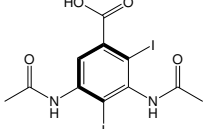
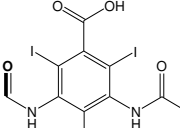
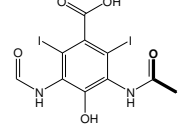
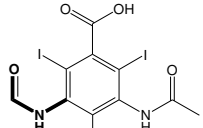
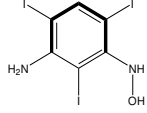
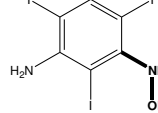
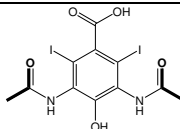
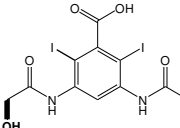
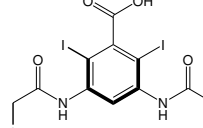
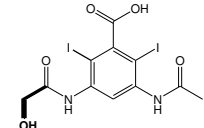
**Table S5 Supplementary Material:** QSAR predictions for DIAT and its photo-TPs for ready biodegradability by different models(CATABOL 301C model under MITI test condition, CATALOGIC 301C model, Case Ultra-Ready biodegradability under MITI test) and molecular moieties responsible for the activating and deactivating alerts.

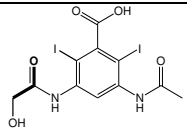
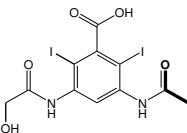
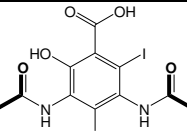
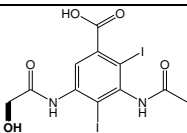
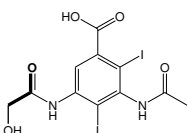
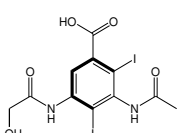
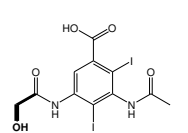
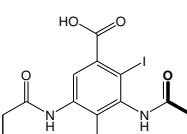
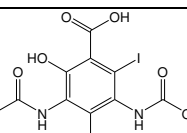
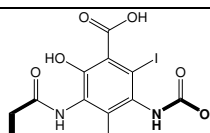
Photo-TPs	QSAR models			Moieties responsible for activating and deactivating alerts (Case Ultra)		
	Catabol 301C model §	Catalogic 301C model §	Case Ultra, MITI Ready biodegradation	Activating alert	Deactivating alert	Unknown fragment
Diat	0.3070	0.2470	MARGINAL			
TP <sub>1</sub> 351	0.3575	0.3255	INCONCLUSIVE*			
TP <sub>2</sub> 351	0.3328	0.3301	INCONCLUSIVE*			
TP 368	0.3644	0.3478	POSITIVE			

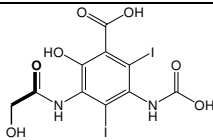
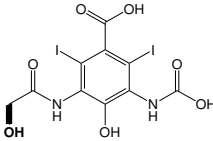
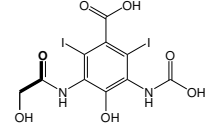
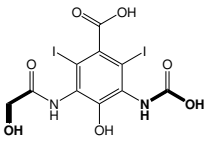
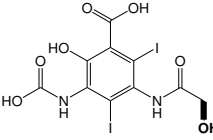
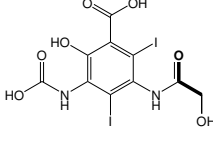
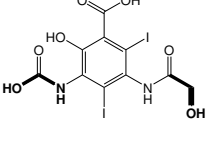
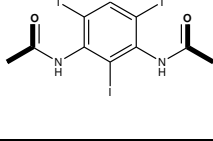
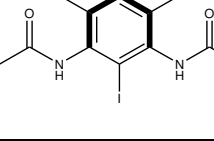
TP 395	0.3692	0.3169	POSITIVE	
TP <sub>1</sub> 447	0.3644	0.3333	INCONCLUSIVE*	 
TP <sub>2</sub> 447	0.3479	0.3343	INCONCLUSIVE*	 
TP <sub>1</sub> 449	0.0731	0.1057	POSITIVE	 
TP <sub>2</sub> 449	0.1149	0.0726	POSITIVE	 
TP <sub>1</sub> 461	0.3189	0.3143	INCONCLUSIVE*	 
TP <sub>2</sub> 461	0.3420	0.3145	INCONCLUSIVE*	 

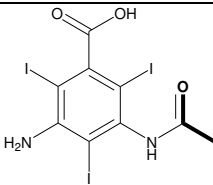
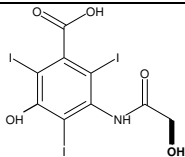
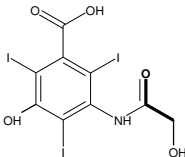
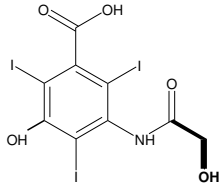
TP <sub>1</sub> 464	0.2376	0.2432	POSITIVE	
TP <sub>2</sub> 464	0.2196	0.2165	POSITIVE	
TP <sub>3</sub> 464	0.2196	0.2066	POSITIVE	
TP <sub>1</sub> 477	0.3644	0.3333	POSITIVE	
TP <sub>2</sub> 477	0.3479	0.3343	POSITIVE	
TP 479	0.2608	0.2045	POSITIVE	 
TP <sub>1</sub> 489	0.3365	0.2889	INCONCLUSIVE	 



TP <sub>2</sub> 489	0.3089	0.2777	INCONCLUSIVE		
TP 491	0.2989	0.2454	POSITIVE	 	
TP <sub>1</sub> 503	0.0254	0.0223	NEGATIVE		
TP <sub>2</sub> 503	0.0000	0.0000	NEGATIVE		 
TP <sub>1</sub> 505	0.3512	0.2921	POSITIVE		
TP <sub>2</sub> 505	0.2913	0.2512	MARGINAL	  	

				 
TP <sub>3</sub> 505	0.3217	0.2889	POSITIVE	
TP <sub>4</sub> 505	0.2632	0.2426	MARGINAL	    
TP <sub>1</sub> 522	0.1520	0.1664	MARGINAL	 

				
TP <sub>2</sub> 522	0.1882	0.1376	MARGINAL	  
TP <sub>3</sub> 522	0.1520	0.1664	MARGINAL	  
TP 571	0.3328	0.3012	MARGINAL	 

TP 573	0.2099	0.1931	POSITIVE	
TP 590	0.1686	0.1581	MARGINAL	  

§: “100% biodegradation” was assigned a numeric value of 1 and “0% biodegradation” was assigned a numeric value of 0. Out of Domain [OD] means that the test chemical is not included in the applicability domain of the applied model. ‘Inconclusive’ means a significant portion of the test chemical is covered by unknown structural fragment. Inconclusive with asterisk symbol (\*) means both positive and deactivating alerts were found in the same molecule and therefore a clear result cannot be provided.

**Table S6 Supplementary Material:** *In silico* environmental fate and toxicity predictions of DIAT and its remaining photo-TPs ( $A/A_0 < 2\%$ ) by PBT profiler and various models of Case Ultra, Catalogic and Leadscope software.

Photo-TPs	Physicochemical Properties						Toxicity predictions										
	OASIS Catalogic V.5.11.6			PBT profiler software			CASE Ultra				Leadscope		OASIS Catalogic V.5.11.6				
	log $K_{ow}$	log BCF	log BCF with ionization term	Log $K_{ow}$	Henry's Law constant (atm/m <sup>3</sup> mole)	PBT profiler estimate <sup>‡</sup>	A	B	C	D	E	E	<i>Acute toxicity against V. fischeri, IC<sub>50</sub> [mg/L]</i>				
													5 min	15 min	30 min	E	
DIAT	1.37	0.7268	0.7607	1.36	1.0E-12	P <sub>3</sub> B <sub>1</sub> T <sub>2</sub>	-	-	-	-	-	-	699.6	1158.5	500.8	-	
TP 368	-0.63	0.4819	0.4877	-0.6	<1E-12	P <sub>2</sub> B <sub>1</sub> T <sub>2</sub>	-	+	-	-	-	+	28309.5	83853.3	15485.8	-	
TP <sub>1</sub> 447	0.74	0.6586	0.688	0.73	1E-12	P <sub>2</sub> B <sub>1</sub> T <sub>2</sub>	-	-	§	-	-	+	2003.1	4044.7	1353.5	-	
TP <sub>2</sub> 447	0.93	0.6586	0.688	0.93	1E-12	P <sub>2</sub> B <sub>1</sub> T <sub>2</sub>	-	-	±	-	-	+	1321.4	2519.5	916.9	-	
TP <sub>1</sub> 449	1.494	0.7021	0.7348	1.49	1E-12	P <sub>2</sub> B <sub>1</sub> T <sub>2</sub>	-	+	OD	-	-	+	404.9	655.4	303.0	+	
TP <sub>2</sub> 449	0.3009	0.6652	0.6952	0.3	<1E-12	P <sub>2</sub> B <sub>1</sub> T <sub>1</sub>	-	+	OD	-	-	+	4899.8	11113.9	3064.0	+	
TP <sub>1</sub> 461	0.9338	0.6142	0.6394	0.93	1E-12	P <sub>2</sub> B <sub>1</sub> T <sub>2</sub>	-	§*	-	-	-	-	1343.1	2549.0	925.1	-	
TP <sub>2</sub> 461	0.9367	0.6142	0.6395	0.93	1E-12	P <sub>2</sub> B <sub>1</sub> T <sub>2</sub>	-	-	+	-	-	-	1345.9	2560.2	932.8	-	
TP <sub>1</sub> 464	1.8847	0.6715	0.702	1.88	1E-12	P <sub>2</sub> B <sub>1</sub> T <sub>2</sub>	-	+	-	-	-	-	180.6	259.4	141	-	
TP <sub>2</sub> 464	0.6917	0.5761	0.5961	0.69	<1E-12	P <sub>2</sub> B <sub>1</sub> T <sub>2</sub>	-	+	-	-	-	-	2233.2	4532.2	1479.2	-	
TP <sub>3</sub> 464	0.3632	0.6715	0.702	0.36	1E-12	P <sub>2</sub> B <sub>1</sub> T <sub>1</sub>	-	+	-	-	-	-	4357.2	9637.9	2712.3	-	
TP <sub>1</sub> 477	0.4536	0.564	0.5823	0.45	1E-10	P <sub>2</sub> B <sub>1</sub> T <sub>3</sub>	-	+	-	-	-	+	3740.7	8091.3	2374.6	-	

TP <sub>2</sub> 477	0.4565	0.564	0.5823	-0.1	1E-10	P <sub>2</sub> B <sub>1</sub> T <sub>2</sub>	-	+	-	-	-	-	3785.7	8237.0	2434.4	-
TP 479	0.3038	0.5288	0.5422	0.3	<1E-12	P <sub>2</sub> B <sub>1</sub> T <sub>3</sub>	-	+	-	-	-	+	4973.2	11087.9	3018.0	-
TP <sub>1</sub> 489	0.1954	0.6573	0.6865	0.39	1E-12	P <sub>2</sub> B <sub>1</sub> T <sub>1</sub>	-	-	-	-	-	-	4322.3	9483.1	2703.0	-
TP <sub>2</sub> 489	0.3924	0.6573	0.6865	0.19	1E-12	P <sub>2</sub> B <sub>1</sub> T <sub>1</sub>	-	-	-	-	-	-	6535.5	15170.4	3972.4	-
TP 491	0.3112	0.6903	0.7223	0.31	< 1.E-12	P <sub>2</sub> B <sub>1</sub> T <sub>1</sub>	-	+	<b>OD</b>	-	-	-	5081.9	11358.5	3113.8	-
TP <sub>1</sub> 503	2.2794	0.7744	0.7965	2.27	1E-12	P <sub>3</sub> B <sub>1</sub> T <sub>2</sub>	-	+	-	-	-	+	101.0	138.0	93.8	-
TP <sub>2</sub> 503	3.0679	1.1443	1.1594	3.06	1E-12	P <sub>2</sub> B <sub>1</sub> T <sub>3</sub>	-	-	-	±	§*	+	18.3	19.6	18.4	+
TP 571	2.5841	1.2702	1.3614	2.58	1E-12	P <sub>3</sub> B <sub>1</sub> T <sub>2</sub>	-	-	-	±	-	-	53	63	46	-
TP 573	1.3418	0.7275	0.7614	1.34	1E-12	P <sub>3</sub> B <sub>1</sub> T <sub>2</sub>	-	-	-	-	-	+	717.6	1217.3	528.7	-
TP 590	0.8628	0.6049	0.6285	0.86	1E-12	P <sub>2</sub> B <sub>1</sub> T <sub>2</sub>	-	+	-	-	-	-	1912.8	3646.7	1266.4	-

‡: The output of PBT profiler can be categorized with numerical value between 1 and 3 for Persistence (P), Bioaccumulation (B) and Toxicity (T). The numerical value 3 indicate the highest and 1 the lowest level for the respective activity.

A- Human carcinogenicity; B- Micronucleus in vivo composite; C- Chromosome aberration; D- Microtox against environmental bacteria; E- Salmonella Mutagenicity; OD: Out of Domain means that the test chemical is not included in the applicability domain of the applied model; §\*: Inconclusive with asterisk symbol (\*) means both positive and deactivating alerts were found in the same molecule and therefore a clear result cannot be provided; §: Inconclusive means that the molecule contained too many unknown fragments; + : a positive alert for corresponding activity; - : a negative alert for corresponding activity; ± : a marginal positive alert prediction for corresponding activity.

## Reference

- Hapeshi E, Lambrianides A, Koutsoftas P, Kastanos E, Michael C, Fatta-Kassinos D. Investigating the fate of iodinated X-ray contrast media iohexol and diatrizoate during microbial degradation in an MBBR system treating urban wastewater. *Environ Sci Pollut Res* 2013, 20:3592-606
- Hennebel T, Corte S de, Vanhaecke L, Vanherck K, Forrez I, Gussemme B de et al. Removal of diatrizoate with catalytically active membranes incorporating microbially produced palladium nanoparticles. *Water Research* 2010;44:1498–506.
- Jeong J, Jung J, Cooper WJ, Song W. Degradation mechanisms and kinetic studies for the treatment of X-ray contrast media compounds by advanced oxidation/reduction processes. *Water Research* 2010;44:4391–8.
- Sedykh A, Saiakhov R, Klopman G. META V-A model of photodegradation for the prediction of photoproducts of chemicals under natural-like conditions. *Chemosphere* 2001;45:971–81.
- Sugihara MN, Moeller D, Paul T, Strathmann TJ. TiO<sub>2</sub>-photocatalyzed transformation of the recalcitrant X-ray contrast agent diatrizoate. *Applied Catalysis B: Environmental* 2013;129:114–22.
- Velo-Gala I, López-Peñalver JJ, Sánchez-Polo M, Rivera-Utrilla J. Ionic X-ray contrast media degradation in aqueous solution induced by gamma radiation. *Chemical Engineering Journal* 2012;195–196:369–76.





# Article II

Designing green derivatives of  $\beta$ -blocker  
Metoprolol: A tiered approach for green and  
sustainable pharmacy and chemistry

*Chemosphere*, 2014, 111, 493–499.  
<http://dx.doi.org/10.1016/j.chemosphere.2014.03.119>





# Designing green derivatives of $\beta$ -blocker Metoprolol: A tiered approach for green and sustainable pharmacy and chemistry



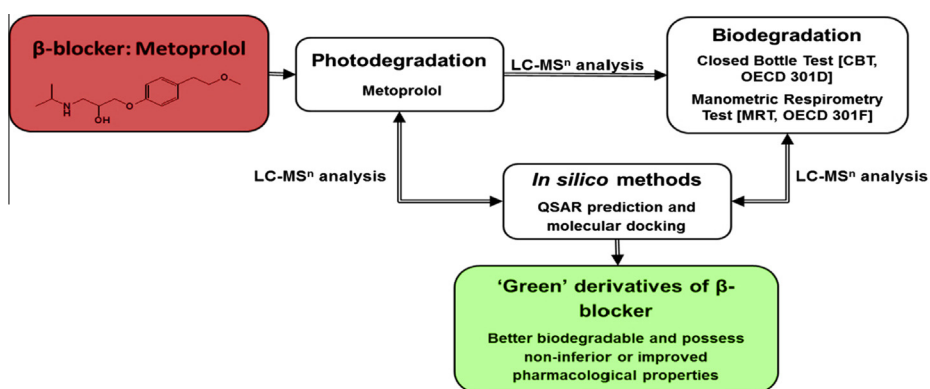
Tushar Rastogi, Christoph Leder, Klaus Kümmerer\*

Sustainable Chemistry and Material Resources, Institute of Sustainable and Environmental Chemistry, Leuphana University Lüneburg, C13, DE-21335 Lüneburg, Germany

## HIGHLIGHTS

- Biodegradation test was performed for the mixture of photo transformation products (photo-TPs) of Metoprolol (MTL).
- A few derivatives (photo-TPs) were comparatively more aerobically biodegradable.
- Better biodegradability due to addition of hydroxyl group on ring or cleavage of redundant moieties of MTL.
- Shortlisted derivatives might possess non-inferior pharmacological properties.
- A novel direction for designing greener pharmaceuticals.

## GRAPHICAL ABSTRACT



## ARTICLE INFO

### Article history:

Received 7 February 2014  
Received in revised form 26 March 2014  
Accepted 27 March 2014

Handling Editor: I. Cousins

### Keywords:

Photolysis  
(Quantitative) Structure–activity relationships (QSAR)  
Molecular docking  
Beta adrenergic receptor  
Benign by design  
Metoprolol

## ABSTRACT

The presences of micro-pollutants (active pharmaceutical ingredients, APIs) are increasingly seen as a challenge of the sustainable management of water resources worldwide due to ineffective effluent treatment and other measures for their input prevention. Therefore, novel approaches are needed like designing greener pharmaceuticals, i.e. better biodegradability in the environment. This study addresses a tiered approach of implementing green and sustainable chemistry principles for theoretically designing better biodegradable and pharmacologically improved pharmaceuticals. Photodegradation process coupled with LC–MS<sup>n</sup> analysis and *in silico* tools such as quantitative structure–activity relationships (QSAR) analysis and molecular docking proved to be a very significant approach for the preliminary stages of designing chemical structures that would fit into the “benign by design” concept in the direction of green and sustainable pharmacy. Metoprolol (MTL) was used as an example, which itself is not readily biodegradable under conditions found in sewage treatment and the aquatic environment. The study provides the theoretical design of new derivatives of MTL which might have the same or improved pharmacological activity and are more degradable in the environment than MTL. However, the *in silico* toxicity prediction by QSAR of those photo-TPs indicated few of them might be possibly mutagenic and require further testing. This novel approach of theoretically designing ‘green’ pharmaceuticals can be considered as a step forward towards the green and sustainable pharmacy field. However, more knowledge and further experience have to be collected on the full scope, opportunities and limitations of this approach.

© 2014 Elsevier Ltd. All rights reserved.

\* Corresponding author. Address: Sustainable Chemistry and Material Resources, Institute of Sustainable and Environmental Chemistry, C13, Scharnhorststraße 1, D-21335 Lüneburg, Germany. Tel.: +49 4131 677 2893.

E-mail addresses: [rastogi@leuphana.de](mailto:rastogi@leuphana.de), [tushar1909@gmail.com](mailto:tushar1909@gmail.com) (T. Rastogi), [cleder@leuphana.de](mailto:cleder@leuphana.de) (C. Leder), [Klaus.Kuemmerer@uni.leuphana.de](mailto:Klaus.Kuemmerer@uni.leuphana.de) (K. Kümmerer).

## 1. Introduction

As an established fact, the presence of pharmaceuticals as such or in form of transformation products (TPs) (often referred as micro-pollutants) in the aquatic environment has been an emerging environmental concern due to the lack of knowledge about their fate and effect especially about their persistent and toxic nature (Barceló and Petrovic, 2008; Daughton and Ternes, 1999; Dietrich et al., 2005). Therefore, these micro-pollutants are increasingly seen as a challenge of the sustainable management of water resources worldwide.

Thus, novel approaches are needed like designing greener pharmaceuticals, i.e. better biodegradability in the environment. Such an approach of designing chemicals can be called as 'start of the pipe approach' which will help to design chemical products which do not persist in environment and breakdown into innocuous compounds after their intended use. This approach is emerging from the field of green and sustainable chemistry and the concept is called the 'benign by design' concept (Kümmerer, 2007). Such approaches of designing better biodegradable chemicals will not only implement chemistry towards the sustainability but will transform the chemistry itself to be more sustainable.

The concept of 'benign by design' is becoming more and more acknowledged in recent years and became one of the important strategies within green and sustainable pharmacy (Anastas and Warner, 2000; Beach et al., 2009; Boethling, 2011; Gawande et al., 2013; Kümmerer, 2010). However, up to now only a few examples of a targeted 'greener' design of chemicals (Boethling, 2011), but none of pharmaceuticals, have been presented (Daughton, 2003; Kümmerer, 2010).

For designing 'green' pharmaceuticals it is necessary that the functionality of the pharmaceuticals should include properties required for successful application on the one hand and properties required for the ready or complete degradability of a molecule after its use, on the other hand, at the time new pharmaceuticals entities are developed.

For a more systematic approach, (Quantitative) Structure–Activity Relationships (QSAR) analysis is appreciably helpful for the direct design and assessment of new and better chemical molecules.

In the present study an attempt was made to perform a preliminary study for designing 'green' Metoprolol (MTL) derivatives. MTL, one of the highly prescribed  $\beta$ -blockers in Europe, undergoes incomplete elimination in sewage treatment plants (STPs) (Maurer et al., 2007). It is detected in different environmental samples (STPs' influent and effluent) including river water at a concentration range up to 1300 ng L<sup>-1</sup> (Santos et al., 2010).

MTL, itself not biodegradable, was photolysed in order to generate a large number of derivatives (photo-TPs). The biodegradability of MTL and its formed derivatives after the photo-treatment were assessed by aerobic biological degradation. The alterations or modifications in the non-biodegradable moieties of MTL during photolysis which render the formation of comparatively better biodegradable derivatives (photo-TPs) were identified through *in silico* QSAR analysis.

The pharmacological activity of derivatives which were found to be comparatively more biodegradable than MTL was compared with MTL by an *in silico* molecular docking analysis. Thus, combination of biodegradability and pharmacological activity analysis will allow the theoretical design of a better biodegradable and pharmacologically active derivative of MTL. Furthermore, the carcinogenicity, mutagenicity and ecotoxicity were predicted by *in silico* QSAR models in order to investigate the possibility of an additional environmental threat of those promising candidates.

Thus, this study aims to demonstrate the feasibility and opportunities of a novel approach of theoretically designing comparatively better degradable and effective pharmaceuticals through the implementation of the "green chemistry" principles. Also, the study addresses current limitations of this concept for designing 'greener' pharmaceuticals.

## 2. Experimental section

### 2.1. Photodegradation

Medium pressure mercury UV light source was used for photodegradation because MTL showed poor degradability under xenon arc lamp irradiation (Liu and Williams, 2007). Photolysis of MTL were performed in a 1L batch photo illuminated by a medium-pressure mercury lamp (TQ150, UV Consulting Peschl, Mainz) with Ilmasil quartz immersion tube. The experimental setup, procedure and characteristics of UV lamp were described in detail in Text S1 in [Supplementary Information \(SI\)](#).

MTL was degraded through direct photolytic experiments with no pre-treatment in order to exclude any other constituents that could interfere with the formation of TPs and/or to avoid the initiation of scavenger effects of any absorbing or photosensitizing chemical or other species during degradation.

### 2.2. Analysis

A Shimadzu Prominence HPLC system (Duisburg, Germany) was used to measure the primary elimination of the parent compound. The Agilent LC 1100 series coupled to a Bruker Daltonic Esquire 6000 + ion-trap mass spectrometer (IT-MS) with electrospray ionization (ESI) interface was used for identification and structure elucidation of the formed derivatives (photo-TPs). DOC was measured by Shimadzu TOC-V<sub>CPN</sub> analyzer equipped with an ASI-V auto sampler. The detail description of the LC method, operating parameters of the source and ion-trap and DOC measurement were summarized in Text S2 (SI).

### 2.3. Biodegradation

The aerobic biodegradability of MTL and its derivatives (photo-TPs) after photo-treatment were investigated according to OECD Closed Bottle Test [CBT] 301D (OECD, 1992b) and OECD Manometric Respiratory Test [MRT] 301 F (OECD, 1992a). The test principles, procedures and composition of the both investigated aerobic biodegradation test series are described in detail in Text S3 (SI).

### 2.4. *In silico* methods

#### 2.4.1. *In silico* predictions of photodegradation products, ready biodegradability and toxicological endpoints of MTL and its derivatives

The photodegradation pathway of MTL and its degradation products was predicted with the software MetaPC listed in [Table S5 \(SI\)](#) with its photodegradation dictionary in combination with the photo-TPs' structures identified and elucidated by LC-ESI-MS/MS (Ion-trap). The ready biodegradability and toxicity (toxicity to environmental bacteria, mutagenicity and genotoxicity) for MTL and its derivatives (photo-TPs) were predicted with *in silico* models listed in [Table S5](#). The above mentioned models and their output and endpoints are described in detail in Text S4 in SI.

#### 2.4.2. *In silico* molecular docking of MTL and its derivatives

Evaluation of the pharmacological properties of MTL and its derivatives (photo-TPs) was performed by molecular docking

analysis (*in silico*) with software Schrodinger Maestro Version 2012 (v.9.3). Generally, MTL is known to be a selective but not specific  $\beta_1$  adrenergic receptor antagonist (Abrahamsson et al., 1988). Thus, MTL has considerable affinity towards the  $\beta_2$  adrenergic receptor, too. Therefore, the docking experiments were performed on the  $\beta_2$  adrenergic receptor instead of  $\beta_1$  receptor as human  $\beta_1$  receptor grid is not publically available. The receptor grid and ligands are described in detail in SI as Text S5.

The docking score (output from *in silico* molecular docking analysis) indicates the binding interaction of the molecule to the protein or enzyme of interest. The lower the docking scores, the better the molecule is supposed to bind to the proteins.

The potential pharmacological activity was investigated for the derivatives (photo-TPs) which were observed to undergo biodegradation  $\geq 10\%$  in the test assays and their docking scores were compared with MTL itself. Comparable docking scores provide evidence for non-inferior pharmacological properties while comparably better scores indicate for improved pharmacological properties of the derivatives compared to MTL.

### 3. Results and discussion

#### 3.1. Photodegradation

The photolysis of MTL was performed with an initial concentration varying from 10 to 60 mg L<sup>-1</sup>. MTL solutions were exposed to UV light for 256 min. It resulted in complete primary elimination of the parent compound with incomplete mineralization. The observed low degree of mineralization (23% and 16% mineralization according to DOC measurement at 10 and 60 mg L<sup>-1</sup> initial concentration of MTL, respectively) indicates the formation of photo-TPs. The kinetic rate calculation is described in detail in SI in Text S6.

#### 3.2. Identification of photo-TPs of MTL

Several photo-TPs were identified during the photolysis process but most of them were already reported in literature (Abramović et al., 2011; Benner and Ternes, 2009; Romero et al., 2011; Song et al., 2008; Wilde et al., 2013). A few new photo-TPs were also identified which were not reported yet. The structures of the new photo-TPs which were predicted by the MetaPC software were confirmed by analyzing their MS/MS fragmentation pathways.

The data of appearance/disappearance of photo-TPs of MTL during photolysis was monitored on the basis of their peak areas and illustrated in SI (Fig. S2). Generally, the peak area does not precisely indicate the relative abundance of the respective photo-TP in the photodegraded mixture as nothing is known about its molar extinction coefficient and ionization rate in ESI. However, assuming the photo-TPs have an ionization rate similar to MTL, then it can indicate the tendency of their appearance/disappearance during the whole course of photodegradation. The retention time ( $t_R$ ), molecular formula, extracted ion chromatogram (EIC) and

the MS<sup>2</sup> fragmentation pattern of MTL and all of its photo-TPs are provided in SI (Table S7) in detail.

Several identified photo-TPs had the same respective nominal mass, but different retention and elution times were observed, respectively. In most cases, these photo-TPs exhibited the same MS<sup>2</sup> fragmentation pattern, indicating the possibility of formation of constitutional isomers.

On the basis of our results and literature finding a scheme of the photodegradation pathway scheme was proposed (Fig. S3) which is described in detail in SI as Text S6.

The limitation of analysis is the separation and allocation of the particular retention time for all isomers (constitutional isomers and enantiomers) formed during photo-degradation.

#### 3.3. Biodegradation

Both tests, CBT and MRT, were valid according to the test guidelines. The quality control and toxicity control in both tests degraded more than 60% and 25% in 14 d indicating the inoculum added in test bottles was active and MTL and its derivatives had no toxic effect against the inoculum's bacteria. The kinetic data of both biodegradation tests are shown in Fig. S4 in SI.

Table 1 summarizes the results of both aerobic biodegradation tests for samples after photolysis and classified MTL as a not readily biodegradable chemical. The standard deviation was higher in MRT as compared to CBT due to the different principle of measurement. Generally, higher biodegradation is expected in MRT compared to CBT due to the higher inoculum density and bacterial diversity. In the study MRT showed less biodegradation than the CBT. One of the reasons for such a phenomenon can be inferred from the high concentration of test substances subjected to the MRT which could inhibit the bacteria from the biodegradation. The observed negative results in the MRT in Table 1 can be inferred due to the high degradation in the blank controls. These negative results should be considered as 0% degradation of the test substances.

The other pass criterion for MRT according to OECD guideline (OECD, 1992a) is a 70% removal of DOC value after 28 d. The DOC elimination during MRT after 28 d for the samples after 0 min, 64 min, and 256 min of UV photolysis (Table 1) indicated partial biodegradability of photo-TPs in the MRT.

The samples from the start and end of each biodegradation tests were analyzed by LC-UV-MS/MS and results are summarized as Fig. S5. The LC-MS/MS results indicate that a few of the formed derivatives (summarized in Table 1) were comparatively better biodegradable than MTL itself. The insets in Fig. S5(A and B) show that MTL was not at all degraded during biodegradation testing which confirms that MTL should be classified as a non-readily biodegradable chemical. Also, LC-MS analysis indicates that the parent compound does not undergo any abiotic elimination, e.g. by hydrolysis, sorption etc.

The concentration of MTL in 32 min CBT sample at 0 d and 28 d was 1.93 mg L<sup>-1</sup> and 1.92 mg L<sup>-1</sup> respectively and derivatives were

**Table 1**

Summary of the results of investigated aerobic biodegradability test for Metoprolol (MTL) and its derivatives formed after photolysis.

Biodegradation test	Test sample (min)	Biodegradation after 28 d (%)	DOC elimination (%)	Derivatives identified to be biodegraded
CBT	0	6.3 ± 0.6		TP 134, TP 226, TP 238, TP 252, TP <sub>1-2</sub> 284, TP 300, TP 302, TP 316, TP 318 and TP 332
	32	7.8 ± 1.9		
	256	23.7 ± 0.2		
MRT	0	-12.5 ± 4	15	TP 134, TP 226, TP 238, TP 240, TP 252, TP 254, TP <sub>1-2</sub> 284, TP 300, TP 302, TP 316, TP 318 and TP 332
	64	6.8 ± 20.5	26	
	256	3.5 ± 1.2	34	

present in low concentration in the solution. Accounting 0% biodegradation of MTL, then the % biodegradation achieved during the test was most likely due to the derivatives. Therefore, it demonstrates that several derivatives are much better biodegradable than the absolute value indicated in Fig. S5. The same implies for the MRT samples, too.

According to Howard (2000) attachments of electron donating functionalities like oxygen atoms (as hydroxyl, aldehyde, carboxylic acid groups etc.) or amines to the aromatic ring of the molecule generally increases its aerobic biodegradability. Consequently, most of the derivatives, which were biodegraded in the investigated aerobic biodegradation test, were indeed hydroxylated derivatives of MTL.

One of the limitations for the investigated ready biodegradability studies is that there may be a certain degree of variation during their repeatability of the test results. The main reasons for such high variability in the repetition of biodegradation tests are (a) nature of inoculum used during biodegradation testing and/or (b) the type of measurement performed in order to monitor biodegradability. The latter point has already been addressed as a better system of the measurement is now available for the CBT (Friedrich et al., 2013). The diversity of microorganisms in the inoculum varies in different sources. However, if the use of similar sources such as certain municipal sewage treatment plants is standardized, then the variation can be much lower.

Furthermore, the stereochemistry plays an important role for biodegradability of chemical species but there are no specific rules for how to decide which enantiomer will be preferably degraded (Kümmerer et al., 2000; Müller and Kohler, 2004). The possibility of the formation of the enantiomers of certain derivatives during photodegradation cannot be excluded, which can influence the aerobic biodegradability of those derivatives in the investigated test assays. Therefore, further investigation is needed to identify which enantiomers of derivatives are more biodegradable.

### 3.4. *In silico* predictions of biodegradability of MTL and its derivatives

The structures of MTL and its derivatives (photo-TPs) were analyzed by the QSAR software with ready biodegradability models which were listed in Table S5 (SI). The predicted values or alerts from all ready biodegradability models for MTL and its derivatives (photo-TPs) are summarized in SI (Table S8).

The prediction of the selected biodegradability models confirmed MTL as a non-readily biodegradable chemical and selected

derivatives (listed in Table 1) to be comparatively better biodegradable than MTL.

Case Ultra predicted moieties like an OH group attached on  $\beta$  carbon of the ethanolamine side chain and the ether on methoxyethane side chain as the activating alert for biodegradability. The methoxybenzene moiety of MTL was predicted as the deactivating alert by Case Ultra. The moieties of MTL and its derivatives responsible for activating or deactivating alerts predictions are summarized in Table S8 in SI. The main moieties of MTL and derivatives which were predicted as activating alert by Case Ultra were alcohol, ketone, aldehyde and amine on either of the side chains.

During photodegradation processes, the methoxybenzene moiety of MTL (responsible for deactivating alert) was modified and facilitated to the formation of relatively better biodegradable derivatives especially in case of the hydroxylated derivatives.

Boethling et al. (2007) suggested that the number of substituent groups attached to the base structure (aromatic ring) have effects on biodegradability but did not provide broadly applicable generalizations about the substituent position which certainly might matter for biodegradability. Therefore, the number and position of the hydroxyl groups added to the aromatic ring might influence the ability of the molecule to undergo aerobic biodegradation.

Fig. 1 shows how the non-biodegradable moiety in the MTL structure was modified by the number and position of hydroxyl group added to it. The addition of one hydroxyl group on the aromatic ring of MTL infringed the methoxybenzene moiety of MTL at the position it was attached. Even the second deactivating alert moiety of MTL was altered due to addition of an OH group.

By two fold substitution of aromatic hydrogen atoms by OH groups, the methoxybenzene moiety was changed into the *p*-OH phenol moiety (Fig. 1), which was predicted as non-biodegradable by QSAR software Case Ultra. This was in accordance as reported by Wang and Shi (2012) that the mono substitution of phenol at *o*- or *p*-position by OH, NO<sub>2</sub>, NH<sub>2</sub>, CH<sub>3</sub>, Cl can decrease the biodegradability.

In Fig. 1, the moieties responsible for the deactivating alert in MTL were completely lost which make the molecule to undergo biodegradation and were predicted to have a positive or inconclusive\* alert (containing both activating and deactivating alert) by Case Ultra under either of the two conditions: (a) addition of OH groups with subsequent opening of the aromatic ring as in case of TP 302 and TP 318 and (b) when all 4 hydrogen atoms of the aromatic ring of MTL were substituted with the hydroxyl groups as in case of TP 332.

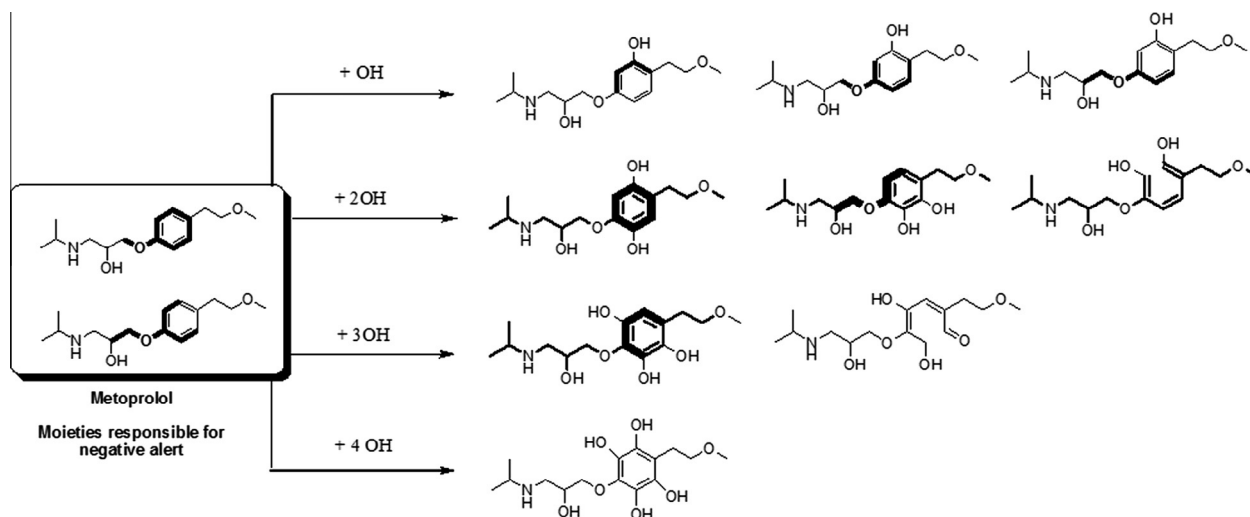


Fig. 1. Alteration of the moieties of Metoprolol (MTL) responsible for negative alert for biodegradation by the substitution of hydroxyl groups on the aromatic ring with or without opening of the ring in the derivatives (photo-TPs) during photolysis.

Lyons et al. (1984) and Nishino and Spain (1993) suggested the addition of OH groups on the aromatic ring as the first step of aerobic biodegradation pathway of the aromatic compounds like aniline and *p*-nitrophenol, respectively, which further leads to the opening of the aromatic ring forming alcohols and acids, which then finally mineralized.

It was also observed that the alteration in the basic structure of MTL caused by cleavage of redundant moieties of side chains during photolysis can lead to the formation of the comparatively better biodegradable derivatives like TP 134, TP 226, TP 238, TP 240, TP 252 and TP 254. Thus, it can be concluded that either the addition of hydroxyl groups with or without subsequent opening of the aromatic ring of MTL or removal of redundant groups from either of side chains of MTL renders the molecule to undergo aerobic biodegradation.

### 3.5. *In silico* prediction of $\beta_2$ -receptor activity of selected derivatives of MTL by molecular docking

Table 2 summarizes the docking scores and chirality of investigated chemical structures. These docking scores were due the respective chirality of the structure. The derivatives which were biodegraded ( $\geq 10\%$ ) in the test assays along with MTL, Carazolol and ICI-118,551 (genuine  $\beta_2$  adrenergic receptor antagonist) were selected for docking analysis.

As expected, MTL showed weak docking with the  $\beta_2$  receptor grid due to its selective nature towards the  $\beta_1$  subtype receptor. The docking score of the comparatively better biodegradable derivatives (photo-TPs) was higher than the reference value ( $-8.7$ ) which does not necessarily mean that these molecules will not at all bind to the receptor. They might certainly bind but probably not as good as the genuine  $\beta_2$  adrenergic receptor antagonist (ICI-118,551) would.

A few of the selected derivatives (highlighted in Table 2) have lower docking scores than MTL which suggests that these derivatives might bind better to the human  $\beta_2$  receptor compared to MTL. This means that they might possess better pharmacological properties compared to MTL.

Three derivatives which had the lowest docking score compared to MTL were di-hydroxylated MTL TP<sub>2</sub> 300 ( $-7.6$ ), tri-hydroxylated MTL TP<sub>3</sub> 316 ( $-7.8$ ) and non-hydroxylated derivate TP 238 ( $-6.9$ ). Thus, these three derivatives can be considered as promising

**Table 2**

*In silico* molecular docking of Metoprolol (MTL) and its derivatives on the human  $\beta_2$  adrenergic receptor grid (antagonized with S-Carazolol) by Schrodinger Maestro 2012 (v.9.3) software (reference docking score  $-8.7$ ).

Substance and derivatives	Docking score <sup>§</sup>	Chirality
Carazolol	$-10.4$	S
ICI 118,551	$-8.7$	R, S*
Metoprolol	$-5.3$	S
<b>TP 238</b>	<b><math>-6.9</math></b>	<b>S</b>
TP 240	$-5.4$	R
<b>TP 252</b>	<b><math>-6.7</math></b>	<b>R</b>
TP 254	$-5.1$	R
TP <sub>1</sub> 284	$-4.9$	S
<b>TP<sub>2</sub> 284</b>	<b><math>-6.0</math></b>	<b>R</b>
<b>TP<sub>1</sub> 300</b>	<b><math>-6.2</math></b>	<b>R</b>
<b>TP<sub>2</sub> 300</b>	<b><math>-7.6</math></b>	<b>R</b>
TP 302	$-4.8$	S
<b>TP<sub>1</sub> 316</b>	<b><math>-6.3</math></b>	<b>S,R*</b>
<b>TP<sub>2</sub> 316</b>	<b><math>-6.1</math></b>	<b>S</b>
<b>TP<sub>3</sub> 316</b>	<b><math>-7.8</math></b>	<b>S,R*</b>
<b>TP<sub>4</sub> 316</b>	<b><math>-6.8</math></b>	<b>R</b>
<b>TP 318</b>	<b><math>-6.3</math></b>	<b>S,R*</b>
<b>TP 332</b>	<b><math>-6.2</math></b>	<b>R</b>

<sup>§</sup> Lower the docking score better the derivatives bind to the investigated protein.

\* Presence of two chiral centers in the structure and the mentioned docking score was predicted due the stated combination of chirality.

candidates (green derivatives) who have improved biodegradability and at the same time might possess non-inferior or even improved pharmacological properties compared to MTL.

Docking results indicated the conjecture that the hydroxylation on the aromatic ring of MTL or removal of redundant elements (as in TP 238) during photolysis lead to the green derivatives which might possess non-inferior or even improved pharmacological properties compared to MTL and are better biodegradable in the environment after their intended use.

Fig. 2a illustrates the *in silico* binding interactions of MTL and TP 238 with the human  $\beta_2$  adrenergic receptor. It was observed that although MTL and TP 238 bind identically with the respective amino acids of the receptor grid but the docking score of TP 238 was improved as compared to MTL. Thus, it can be assumed that removal of redundant elements from the basic structure (like cleavage of methanol from the ether side of the MTL in case of TP 238) during photodegradation could improve the docking score (implying improved pharmacological properties) and biodegradability in the environment.

Fig. 2b illustrates the binding interactions of the constitutional isomers of one derivative (TP 300). It was observed that an alteration of the position of a hydroxyl group on the aromatic ring leads to an alteration in the interaction of amino acids of the receptor grid with TP<sub>1</sub> 300 and TP<sub>2</sub> 300 respectively, which simultaneously modulated their docking scores. This means that a small alteration in the structure of the investigated chemical species can vary their pharmacological properties to a high extent.

Furthermore, the enantiomers of respective chemical species influence their interactions with the proteins and amino acids of their respective grid (Li et al., 2012; Sabela et al., 2012). The possibility of formation of enantiomers of certain derivatives cannot be excluded which in return will have different affinities and interaction towards the amino acids of the human  $\beta_2$  adrenergic receptor. Therefore, all the isomers (either constitutional or enantiomers) formed during the photodegradation should be identified and subsequently should be taken into consideration while performing *in silico* molecular docking analysis.

The application of highly advanced analytical tools like NMR (maybe after isolation and enrichment or synthesis of the derivatives of interest) or application of analytical chiral separation methods may help to overcome this limitation. It can be concluded that isomers (constitutional and enantiomers) will influence the aerobic biodegradability and the binding affinities of the amino acids of receptor grid.

A further limitation for such studies is the lack of availability of X-ray structures of the target proteins. In this study, the structure of the human  $\beta_1$  adrenergic receptor was not publically available therefore the human  $\beta_2$  adrenergic receptor was used for *in silico* docking predictions because MTL has considerable affinity towards  $\beta_2$  adrenergic receptor as well. But, it would be interesting and worthy to perform the same *in silico* docking prediction for MTL and its derivatives with same conditions and parameters set with a human  $\beta_1$  adrenergic receptor grid in the future.

### 3.6. *In silico* prediction of toxicological endpoints of MTL and its derivatives

Further, *in silico* predictions for the toxicity of these promising candidates who have lower docking scores than MTL (green derivatives) were performed by the *in silico* models listed in Table S5 (SI). The *in silico* toxicity predictions are summarized in Table S6 in SI. These predictions strongly recommend experimental testing of the selected derivatives of MTL for genotoxicity, mutagenicity and ecotoxicity to confirm the prediction of QSAR model through experimental data.

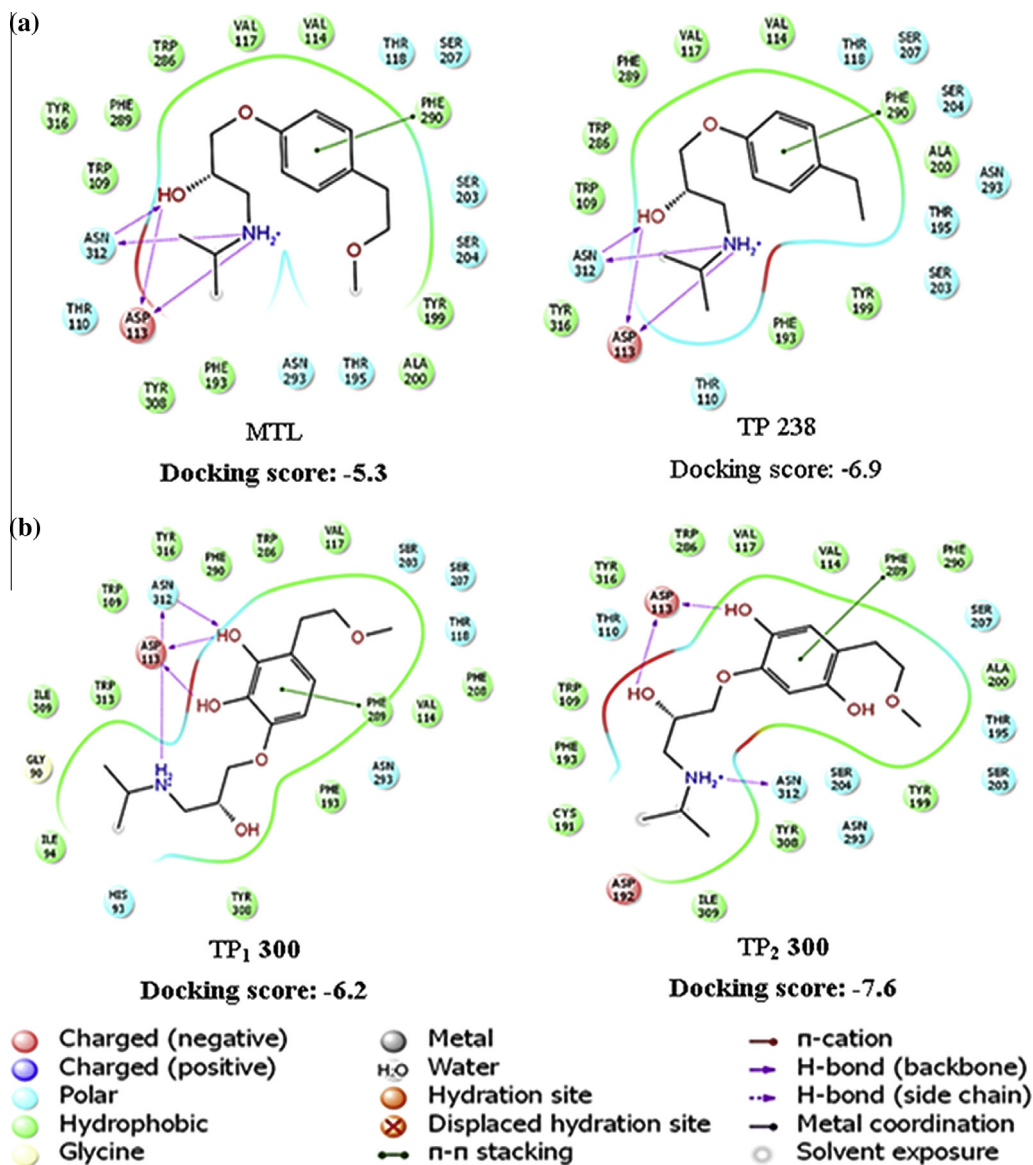


Fig. 2. An illustration of the *in silico* binding interaction of the human  $\beta_2$  adrenergic receptor grid (2RH1) with: (a) Metoprolol (MTL) and transformation product (TP) 238; (b) constitutional isomers of TP 300.

#### 4. Conclusion

The intended approach of (photo) transformation in combination with LC-MS<sup>n</sup> and *in silico* tools such as QSAR analysis and molecular docking proved to be a very powerful tool for the preliminary stages of designing chemical structures that would fit into the “benign by design” concept in the direction of green and sustainable pharmacy. The study provides evidence for the theoretical design of novel  $\beta$ -blocker derivatives which have functionality (or functional groups) in the molecules that might have properties required for a successful pharmaceutical application and for ready or complete biodegradability of a molecule after its use.

The advantage of a such tiered approach presented in the study is that it is not necessary to synthesize all the molecules that may be of interest beforehand. Only a few standard experiments and structure of promising candidates are enough for such screening purposes also with respect to pharmacological activity as well as some core endpoints of toxicity and off-target effects. Thus, it allows very early and comparatively cheap evaluation of properties

of a new compound and may contribute to a shorter time to market.

However, the authors acknowledge the fact that structures presented in the study are just theoretical designs and a lot of experiments have to be performed in respect to assess the pharmacological properties of these designs before they can be introduced for usage.

There were some limitations in the presented tiered approach (as already mentioned in earlier sections) despite the fact that it opens a novel direction in theoretically designing improved and degradable pharmaceuticals. Therefore, these limitations should be addressed and overcome in the future for a better implementation of the present approach of theoretically designing pharmaceuticals in the context of green and sustainable pharmacy.

#### Acknowledgements

Financial support from German Ministry of Education and Research (NanoPharm, Project No. 03X0094C) is gratefully



acknowledged. The authors would like to thank Dr. Mandy Schneider and Dr. Marcelo L. Wilde for their fruitful discussions. The authors also acknowledge Multicase Inc. and Leadscope Inc. for kindly providing the Case Ultra, MetaPC and Leadscope QSAR software, respectively.

## Appendix A. Supplementary material

Supplementary data associated with this article can be found, in the online version, at <http://dx.doi.org/10.1016/j.chemosphere.2014.03.119>.

## References

- Abrahamsson, T., Ek, B., Nerme, V., 1988. The  $\beta_1$ - and  $\beta_2$ -adrenoceptor affinity of atenolol and metoprolol: a receptor-binding study performed with different radioligands in tissues from the rat, the guinea pig and man. *Biochem. Pharmacol.* 37, 203–208.
- Abramović, B., Kler, S., Šojić, D., Laušević, M., Radović, T., Vione, D., 2011. Photocatalytic degradation of metoprolol tartrate in suspensions of two  $\text{TiO}_2$ -based photocatalysts with different surface area: identification of intermediates and proposal of degradation pathways. *J. Hazard. Mater.* 198, 123–132.
- Anastas, P.T., Warner, J.C., 2000. *Green Chemistry: Theory and Practice*, first ed. Oxford Univ. Press, Oxford.
- Barceló, D., Petrovic, M. (Eds.), 2008. *Emerging Contaminants from industrial and municipal waste*. Springer, Berlin Heidelberg, Berlin, Heidelberg.
- Beach, E.S., Cui, Z., Anastas, P.T., 2009. Green chemistry: a design framework for sustainability. *Energy Environ. Sci.* 2, 1038–1049.
- Benner, J., Ternes, T.A., 2009. Ozonation of Metoprolol: elucidation of oxidation pathways and major oxidation products. *Environ. Sci. Technol.* 43, 5472–5480.
- Boethling, R.S., 2011. Incorporating environmental attributes into musk design. *Green Chem.* 13, 3386–3396.
- Boethling, R.S., Sommer, E., DiFiore, D., 2007. Designing small molecules for biodegradability. *Chem. Rev.* 107, 2207–2227.
- Daughton, C.G., 2003. Cradle-to-cradle stewardship of drugs for minimizing their environmental disposition while promoting human health. I. Rationale for and avenues toward a green pharmacy. *Environ. Health Perspect.* 111, 757–774.
- Daughton, C.G., Ternes, T.A., 1999. Pharmaceuticals and personal care products in the environment: agents of subtle change? *Environ. Health Perspect.* 107, 907–938.
- Dietrich, D.R., Webb, S.F., Petry, T. (Eds.), 2005. *Hot Spot Pollutants: Pharmaceuticals in the Environment*. Elsevier Academic Press, Amsterdam, Boston.
- Friedrich, J., Längin, A., Kümmerer, K., 2013. Comparison of an electrochemical and luminescence-based oxygen measuring system for use in the biodegradability testing according to Closed Bottle Test (OECD 301D). *CLEAN – Soil, Air, Water* 41, 251–257.
- Gawande, M.B., Bonifácio, V.D.B., Luque, R., Branco, P.S., Varma, R.S., 2013. Benign by design: catalyst-free in-water, on-water green chemical methodologies in organic synthesis. *Chem. Soc. Rev.* 42, 5522–5551.
- Howard, P.H., 2000. Biodegradation. In: Mackay, D., Boethling, R.S. (Eds.), *Handbook of Property Estimation Methods for Environmental Chemicals*. Environmental and Health Sciences. Lewis Publishers, Boca Raton, pp. 281–310.
- Kümmerer, K., 2007. Sustainable from the very beginning: rational design of molecules by life cycle engineering as an important approach for green pharmacy and green chemistry. *Green Chem.* 9, 899–907.
- Kümmerer, K., 2010. Rational design of molecules by life cycle engineering. In: Kümmerer, K., Hempel, M. (Eds.), *Green and Sustainable Pharmacy*. Springer, Berlin Heidelberg, Berlin, Heidelberg, pp. 135–146.
- Kümmerer, K., Al-Ahmad, A., Bertram, B., Wiefleser, M., 2000. Biodegradability of antineoplastic compounds in screening tests: influence of glucosidation and of stereochemistry. *Chemosphere* 40, 767–773.
- Liu, Q.-T., Williams, H.E., 2007. Kinetics and degradation products for direct photolysis of  $\beta$ -blockers in water. *Environ. Sci. Technol.* 41, 803–810.
- Li, W., Liu, C., Tan, G., Zhang, X., Zhu, Z., Chai, Y., 2012. Molecular modeling study of chiral separation and recognition mechanism of  $\beta$ -adrenergic antagonists by capillary electrophoresis. *Int. J. Mol. Sci.* 13, 710–725.
- Lyons, C.D., Katz, S., Bartha, R., 1984. Mechanisms and pathways of aniline elimination from aquatic environments. *Appl. Environ. Microbiol.* 48, 491–496.
- Maurer, M., Escher, B.I., Richle, P., Schaffner, C., Alder, A.C., 2007. Elimination of  $\beta$ -blockers in sewage treatment plants. *Water Res.* 41, 1614–1622.
- Müller, T.A., Kohler, H.-P.E., 2004. Chirality of pollutants-effects on metabolism and fate. *Appl. Microbiol. Biotechnol.* 64, 300–316.
- Nishino, S.F., Spain, J.C., 1993. Cell density-dependent adaptation of *Pseudomonas putida* to biodegradation of p-nitrophenol. *Environ. Sci. Technol.* 27, 489–494.
- OECD, 1992a. *OECD Guidelines for the Testing of Chemicals: Ready Biodegradability 301F: Manometric Respiratory Test*. OECD Pub.
- OECD, 1992b. *OECD Guidelines for the Testing of Chemicals: Ready Biodegradability 301D: Closed Bottle Test*. OECD Pub.
- Romero, V., de La Cruz, N., Dantas, R.F., Marco, P., Giménez, J., Esplugas, S., 2011. Photocatalytic treatment of metoprolol and propranolol. *Catal. Today* 161, 115–120.
- Sabela, M.I., Gumede, N.J., Escuder-Gilabert, L., Martín-Biosca, Y., Bisetty, K., Medina-Hernández, M.-J., Sagrado, S., 2012. Connecting simulated, bioanalytical, and molecular docking data on the stereoselective binding of ( $\pm$ )-catechin to human serum albumin. *Anal. Bioanal. Chem.* 402, 1899–1909.
- Santos, L.H.M.L.M., Araújo, A.N., Fachini, A., Pena, A., Delerue-Matos, C., Montenegro, M.C.B.S.M., 2010. Ecotoxicological aspects related to the presence of pharmaceuticals in the aquatic environment. *J. Hazard. Mater.* 175, 45–95.
- Song, W., Cooper, W.J., Mezyk, S.P., Greaves, J., Peake, B.M., 2008. Free radical destruction of  $\beta$ -blockers in aqueous solution. *Environ. Sci. Technol.* 42, 1256–1261.
- Wang, F., Shi, J., 2012. 2D and 3D-QSBR study on biodegradation of phenol derivatives. *Bull. Environ. Contam. Toxicol.* 89, 316–321.
- Wilde, M.L., Mahmoud, W.M.M., Kümmerer, K., Martins, A.F., 2013. Oxidation-coagulation of  $\beta$ -blockers by  $\text{K}_2\text{FeVIO}_4$  in hospital wastewater: assessment of degradation products and biodegradability. *Sci. Total Environ.* 452–453, 137–147.

## Supplementary information

for

### **Designing green derivatives of $\beta$ -blocker Metoprolol: A tiered approach for green and sustainable pharmacy and chemistry**

Tushar Rastogi, Christoph Leder, Klaus Kümmerer\*

*Sustainable Chemistry and Material Resources, Institute of Sustainable and Environmental Chemistry,  
Leuphana University Lüneburg, C13, DE-21335 Lüneburg, Germany*

---

\* Corresponding author address: Chair of Sustainable Chemistry and Material Resources, Institute of Sustainable and Environmental Chemistry, C.13, Scharnhorststraße 1, D-21335 Lüneburg, Germany. Tel.: +49 4131 677 2893.  
E-mail address: rastogi@leuphana.de, tushar1909@gmail.com (T. Rastogi), cleder@leuphana.de (C. Leder), Klaus.Kuemmerer@uni.leuphana.de (K. Kümmerer).

## **Text S1 Supplementary Information: Test procedure and characteristics of UV lamp**

### **Test procedure**

The batch photo reactor used in the present study was provided with constant stirring and temperature control by a circulating cooler (WKL230, LAUDA, Berlin). According to earlier published studies (Achilleos et al., 2010; Canonica et al., 2008; Sirtori et al., 2010), the matrix of the solution subjected to photo treatment can influence the extent of photodegradation. Therefore, in the present study, MTL was dissolved in ultrapure water for photolytic experiments with no pretreatment. Ultrapure water was used in order to avoid the initiation of scavenger effect of any absorbing or photosensitizing chemical or other species during degradation and to exclusively assess the photo-TPs that were formed from the photolysis of MTL only.

Sampling was performed after 2, 4, 8, 16, 32, 64, 128 and 256 min of irradiation time, respectively, in order to monitor the kinetics of transformation and mineralization of MTL. 20 mL samples were collected at each of the above mentioned time points. The primary elimination of DIAT and photo-TPs formed during photodegradation process were monitored by HPLC-UV and LC-ESI-MS<sup>n</sup> (ion-trap), respectively. A more detailed description of the testing procedures can be found elsewhere (Khaleel et al., 2013; Mahmoud et al., 2013).

## Characteristics of UV lamp

According to the manufacturer, the total radiation flux  $\Phi$  from 200 nm to 600 nm is  $47 \text{ W m}^{-2}$  and the maximal intensities for whole spectral distribution were at following wavelengths

**Table S1 Supplementary Information:** The maximal intensities at following of medium pressure mercury lamp TQ 150 (provided by manufacturer)

Wavelength (nm)	Intensities ( $\text{W m}^{-2}$ )
254	4.0
265	1.4
302	1.8
313	4.3
366	6.4
405/408	3.2
436	4.2
546	5.1
577/579	4.7

**Text S2 Supplementary Information:** Analytical method parameters for the elution and identification of the photo-TPs of Metoprolol (MTL)

**HPLC method for the elution of MTL:**

A NUCLEODUR<sup>®</sup> RP-C18 (CC 125/4 100-5 $\mu$ m C18 ec) column and mobile phases consisting 0.1 % formic acid in ultrapure water (CH<sub>2</sub>O<sub>2</sub>: solution A) and 100 % acetonitrile (CH<sub>3</sub>CN: solution B) were used for the chromatographic separation. The flow rate, column oven temperature and injection volume was set to 0.5 mL min<sup>-1</sup>, 25 °C and 50  $\mu$ L, respectively, MTL was detected by an UV/Vis detector at 270 nm.. MTL eluted at retention time [t<sub>R</sub>] of 16.07 min. High linearity correlation [ $r^2 \geq 0.9999$ ] was obtained for calibration curve range 60  $\mu$ g mL<sup>-1</sup> to 0.1172  $\mu$ g mL<sup>-1</sup>. The gradient flow method was applied as described below:

**Table S2 Supplementary Information:** Gradient flow condition used to achieve the desired separation

Time (min)	%B (Acetonitrile)
0.01 to 2 min	1
2 to 27 min	1% - 65% B
27 to 29 min	65% - 20% B
29 to 30 min	20% - 1% B
30 to 32 min	1% B
32.01	stop

### MS parameter for the identification of photo-TPs of MTL:

The above mentioned LC parameters were used while the MS parameters were optimized for MTL [m/z 268.1] by direct infusion of a 10  $\mu\text{g mL}^{-1}$  standard at a flow rate of 4  $\mu\text{L min}^{-1}$  through a syringe pump.

**Table S3 Supplementary Information:** The operating parameters of the ESI and Iontrap (Bruker 6000) of the LC-ESI-IT-MS<sup>n</sup>

Parameters	Metoprolol
Dry gas temperature	350°C
Nebulizer pressure	30 psi
Dry gas flow	10 l min <sup>-1</sup>
end plate Offset	-500 Volt
capillary voltage	-3583 Volt
skimmer	34.8 Volt
capillary exit	137.5 Volt
octopole one	13.88 Volt
octopole two	2.35 Volt
trap drive	34.6
lens one	-1.8 Volt
lens two	-70 Volt
target mass	268 m/z
maximum accumulation time	200 ms
scan range	40 m/z - 1000 m/z
fragmentation amplitude	1

### DOC measurement:

Samples were filtered with the syringe filter (Chromafil® Xtra PES 45/25, Macherey Nagel, Düren, Germany) of 0.45  $\mu\text{m}$  pore size prior to DOC measurement.

**Text S3 Supplementary Information:** Principles and procedure of the investigated aerobic biodegradation tests

In the CBT the concentration of the test compound was adjusted to  $5 \text{ mg L}^{-1}$  Theoretical Oxygen Demand without nitrification ( $\text{ThOD}_{\text{NH}_3}$ ) for the untreated samples. The sample volume of post-treated solutions was increased according to DOC elimination during photodegradation treatment. All the test vessels were inoculated with 2 drops of the effluent from a local municipal STP (AGL Lüneburg, Germany, 144,000 population equivalents). During the test period of 28 days, the oxygen concentration in the test vessels was monitored with Fibox 3 (Fiberoptical oxygen transmitter) (PreSens, Regensburg, Germany) (Friedrich et al., 2013). For qualitative reasons pH values were also monitored at 0 and 28 d.

The MRT was conducted using the OxiTop<sup>®</sup> Control OC110-system (WTW GmbH, Weilheim, Germany) for monitoring the microbial oxygen consumption through  $\text{CO}_2$  production during the aerobic biodegradation. These measuring heads contained sodium hydroxide which removes the  $\text{CO}_2$  from the gas phase. This removal of  $\text{CO}_2$  results in a decrease in pressure in test vessels which corresponds to the oxygen consumption which is due to biodegradation. The sample scheme was equivalent to that of the CBT, except that the sample concentration was adjusted to  $30 \text{ mg L}^{-1}$  ThOD and 80 mL of inoculum were added to 1 L of test solution as required by test guidelines. Furthermore, an additional sterile control for the assessment of abiotic degradation was applied.

A more detailed description of the testing procedures can be found elsewhere (Khaleel et al., 2013; Mahmoud and Kümmerer, 2012; Trautwein and Kümmerer, 2011).

The samples subjected to the CBT and MRT after photolysis were different, i.e. samples with different UV exposure time, due the difference in the kinetics of appearance/disappearance of derivatives. This difference in kinetics was due to different initial concentration of MTL in

photo-treatments. Table S4 summarize the composition of the aerobic biodegradation test series in CBT and MRT.

**Table S4 Supplementary Information:** Composition of the aerobic biodegradation test series in the CBT (1-4) and MRT (1-5)

	1	2	3	4	5
Test series	Blank	Quality control	Test compound	Toxicity control	Sterile control
Mineral medium	+	+	+	+	+
Inoculum	+	+	+	+	
Test substance			+	+	+
Sodium acetate		+		+	
Sodium azide					+



**Text S4 Supplementary Information:** Output from various *in silico* models for used in the study

The ready biodegradability of MTL and its photo-TPs was predicted based on data for OECD 301C MITI-I test (Ministry of International Trade and Industry, Japan) (OECD, 1992) which is generally not directly comparable to investigated test (CBT and MRT), but can provide orientation towards identifying the readily biodegradable and non-readily biodegradable moieties of the molecules. The OASIS Catalogic models predict the ready biodegradability as a numerical value between 1 and 0. A numeric value of 1 corresponds to 100% biodegradation and 0 represents 0% biodegradation while numeric value of 0.6 corresponds to 60% biodegradation which is a pass criterion for ready biodegradability under MITI-I tests conditions. The output from BIOWIN models is also a number between 0 and 1 which can be interpreted as indicating ready biodegradation if the value is higher than 0.5. CASE Ultra and Leadscape software provide a positive, negative and out of domain (OD) estimations for the selected models. OD means that the test chemical is not included in the applicability domain of the model used. Often CASE Ultra software provides alerts for all its selected models like ‘Inconclusive’ and Inconclusive with asterisk symbol (\*). ‘Inconclusive’ alert means that a significant portion of the test chemical is covered by unknown structural fragments and Inconclusive with asterisk symbol (\*) means both positive and deactivating alerts were found in the same molecule and therefore a clear result cannot be given. The above mentioned models and software are described in detail elsewhere (Mahmoud et al., 2014; Mahmoud et al., 2013). Table S5 below enlisted all the *in silico* software and their respective models used in the present study.

**Table S5 Supplementary Information:** List of *in silico* software and their respective models used for the prediction of photodegradation products, ready biodegradability and toxicity of MTL and its derivatives (photo-TPs).

Activity	QSAR Software	Models	End points	References
Photodegradation products	METAPC v 1.8.1	Photodegradation	Photoproducts of chemicals under natural-like conditions	(Sedykh et al., 2001)
	CASE Ultra v.1.4.5.1	MITI-I test (OECD 301C, module AU6)	Ready biodegradability according to MITI-I test	(Chakravarti et al., 2012)
Biodegradation	EPI Suite (EPIWEB 4.1)	BIOWIN 5 and 6	Linear and nonlinear regression models predicting the Ready biodegradability according to MITI-I test	(2013).
	Catalogic v 5.11.6 TB (OASIS)	CATABOL 301C model	Ready biodegradability according to MITI-I test	(Laboratory of Mathematical Chemistry, 2012)
		CATALOGIC 301C models	Ready biodegradability according to MITI-I test	
Toxicity	CASE Ultra v.1.4.5.1 (MultiCASE Inc.)	Human carcinogenicity (A0J)	Carcinogenicity	(Chakravarti et al., 2012; Saiakhov et al., 2013)
		Micronucleus formation in vivo composite (A7S)	Genotoxicity	
		Chromosome aberration in vitro composite (A7U)	Mutagenicity	
		Mutagenicity Ames (A2H)	Mutagenicity against <i>Salmonella Typhimurium</i>	
	Microtox toxicity environmental bacteria (AUA).	Bacterial toxicity		
	Leadscope V. 3.0.11-1	Bacterial mutagenesis (BM) model	Mutagenicity as a result of interaction with DNA of <i>Salmonella Typhimurium</i> or <i>Escherichia coli</i>	
		Mammalian mutagenesis (MM)	Mutagenicity	
In vitro chromosome aberration (IVCA)		Mutagenicity		
	In vivo micronucleus (IVMN)	Genotoxicity	(Roberts et al., 2000).	

**Text S5 Supplementary Information:** *In silico* molecular docking analysis procedure

The pharmacological properties of MTL and its derivatives (photo-TPs) was evaluated by molecular docking analysis. MTL and its derivatives were docked on the x-ray structure of the human  $\beta_2$  adrenergic receptor which was crystalized with S-Carazolol. The code for the applied x-ray structure was 2RH1(Cherezov et al., 2007) and the structure was derived from RCSB protein database(RCSB Protein Data Bank). The derived x-ray structure was prepared with the protein preparation wizard and the receptor grid generation module from Schrodinger Maestro software. The ligands (ICI 118,551, MTL and its derivatives) were prepared with the LigPrep module including a  $pK_a$  penalty provided by the Epik module(Shelley et al., 2007). Two hydrogen bonds to Asparagine (ASN 312) and Aspartate (ASP 113) amino acids and the resulting constraints were identified and one of the two H-bond constraints was mandatory for docking by the software. The docking score was calculated with the Glide module using standard precision(Friesner et al., 2004).

The structure of MTL and its derivatives were docked on the human  $\beta_2$  adrenergic receptor crystallized with S-Carazolol to assure that the antagonistic state of the receptor was fixed. Carazolol is a high affinity antagonist of the  $\beta$ -adrenergic receptor(Innis et al., 1979) and it was also docked on the same receptor grid to validate the receptor grid for further docking screening.

ICI-118,551, a selective  $\beta_2$  adrenergic receptor antagonist(Summerhill et al., 2008), binds to the  $\beta_2$  subtype receptor with at least 100 times greater affinity than to the two other  $\beta$  adrenergic receptors ( $\beta_1$  or  $\beta_3$ ) (Emorine et al., 1989; Mauriège et al., 1988). ICI-118,551 is not therapeutically used in humans although it has been used widely in research to understand the action of the  $\beta_2$  adrenergic receptor. It is used in the present study as a control for docking on the human  $\beta_2$  receptor grid as it is genuinely a  $\beta_2$  adrenergic receptor binder. The docking score of it (-8.7) was considered as a reference score for a good binder which means any other

docking score lower than this will assumed to have an improved binding to the human  $\beta_2$  adrenergic receptor and might possess improved pharmacological properties.

## Text S6 Supplementary Information: Kinetic calculation and data

### Kinetic data for photolysis experiments:

The apparent first-order rate constant, used to calculate the rate of Metoprolol degradation, was obtained by data fitting to the following equation:

$$\frac{dc}{dt} = -k_{obs}c_0 \quad 1$$

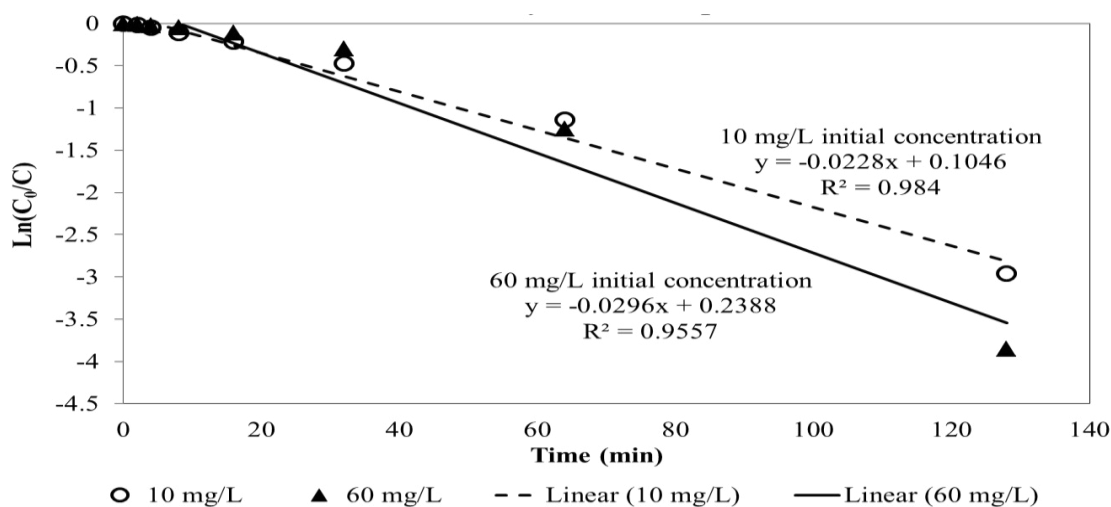
Solving it further,

$$\ln \left[ \frac{c_0}{c} \right] = -k_{obs} \cdot t \quad 2$$

where  $c$  is the MTL concentration at the time  $t$ ,  $c_0$  its initial concentration and  $k_{obs}$  the apparent first-order rate constant. The fit of the experimental data in equation 2 enabled the calculation of the pseudo-first order rate constant  $k_{obs}$ . The initial rates ( $r_0$ ) of MTL transformation were calculated as

$$r = -k_{obs} \cdot c_0 \quad 3$$

The results of kinetic calculation of both investigated initial concentration are show below:



**Figure S1 Supplementary Information:** Kinetic data of photolysis of Metoprolol for both investigated concentration

**Text S6 Supplementary Information:** Scheme of photolytic degradation pathway of MTL

Figure S2 is the data of appearance/disappearance of photo-TPs of MTL during photolysis and on its basis the photolytic degradation pathway of MTL was proposed as shown in figure S3.

Photo-TPs TP 284, TP 300, TP 314, TP 316 and TP 332 formed during photolysis processes by the attachment of hydroxyl groups (OH) on the aromatic ring and were already reported (Abramović et al., 2011). TP 300 was further transformed to TP 302 (m/z 302.1) through the opening of aromatic ring of TP 300 during UV processes and its structure was predicted by MetaPC software (Sedykh et al., 2001) and formation of the fragment ions like m/z 284.2, m/z 150.9 and m/z 134.1 during MS<sup>2</sup> fragmentation supports the proposed structure of TP 302.

Romero and co-workers (Romero et al., 2011) proposed the structure of TP 318 (m/z 318.1) as addition of OH group on the secondary amine, although it was not the preferred structure under their applied experimental conditions. So, TP 318 was proposed to be formed by substitution of three OH groups on the aromatic ring followed by ring opening.

Some photo-TPs like TP 226 (m/z 226.1), TP 254 (m/z 254.1) and TP 270 (m/z 270.1) formed during photolysis were reported as oxidation products (Benner and Ternes, 2009; Slegers et al., 2006; Wilde et al., 2013) and also as human metabolites of MTL (MA et al., 2007). TP 254 further cleaved and resulted to TP 240 (m/z 240.1) (Benner and Ternes, 2009; Wilde et al., 2013).

Another photo-TP, TP 198 (m/z 198.1) was assumed to result from TP 240 by N-dealkylation (elimination of propane) from ethanolamine side chain of TP 240. The formation of MS<sup>2</sup> product ions m/z 180.0 and m/z 152.0 supports the proposed structure of TP 198.

Photo-TPs TP 238 (m/z 238.1) and TP 252 (m/z 252.1) formed during UV processes were also reported as an oxidation products(Abramović et al., 2011; Borkar et al., 2011; Slegers et al., 2006).

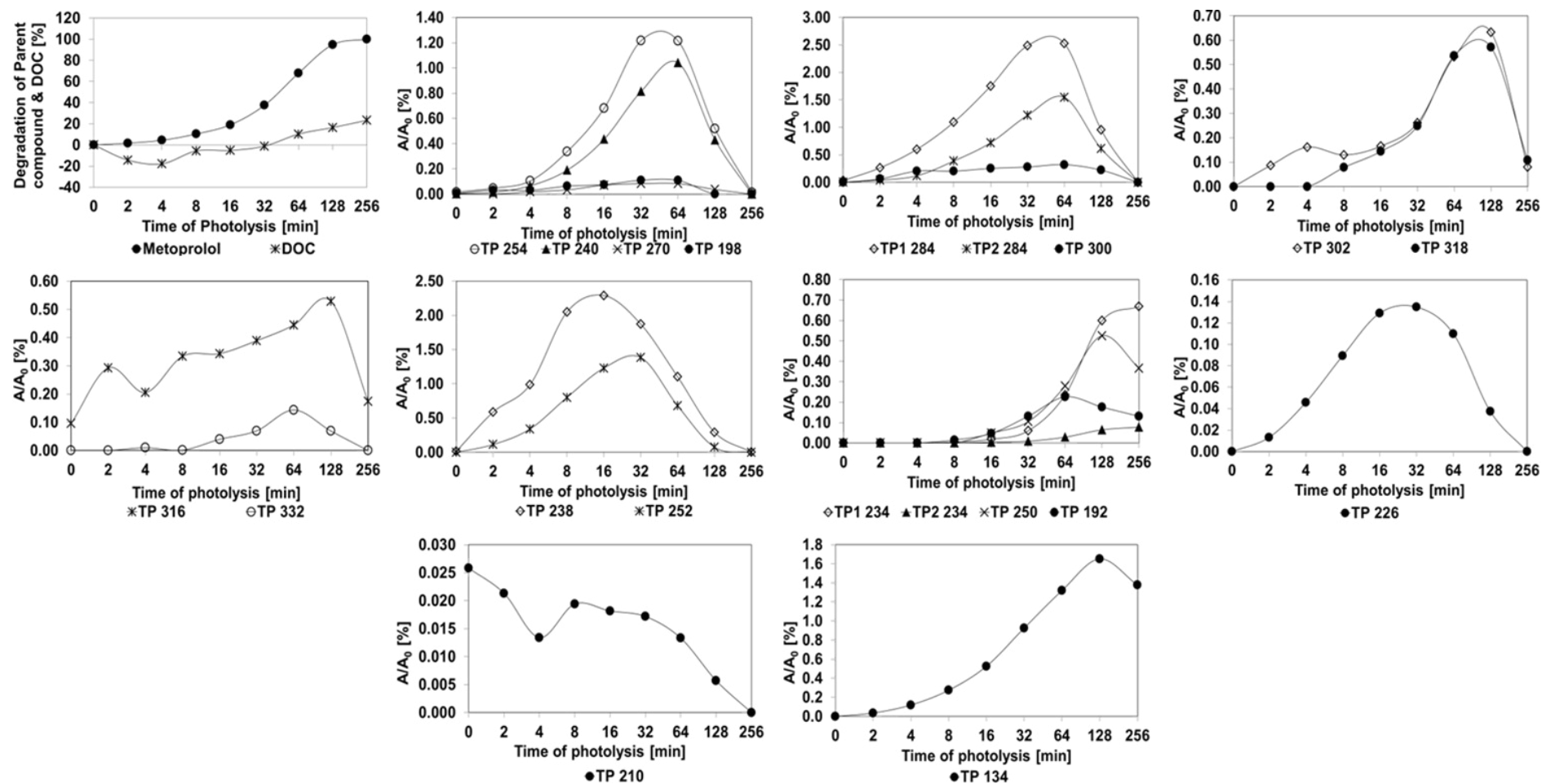
Slegers and co-workers(Slegers et al., 2006) reported the structure of TP<sub>2</sub> 234 (m/z 234.1) which was observed and assumed to be formed by the abstraction of four hydrogen atoms from TP 238.

Further attack of a hydroxyl radical on the ketone side chain of TP<sub>2</sub> 234 could be assumed for the appearance of TP 250 (m/z 250.0). The structure of TP 250 was predicted by MetaPC software(Sedykh et al., 2001) and the MS<sup>2</sup> fragment ions like m/z 232.1 (loss of water molecule) and m/z 208.1 (loss of i-propane) supported the predicted structure.

The elimination of a water molecule from the ethanolamine side chain of TP 252 leads to the unsaturated TP<sub>1</sub> 234 (m/z 234.1). Further, it can be assumed that a decarboxylation process (cleavage of acetaldehyde) on the side chain of TP<sub>1</sub> 234 resulted in the formation of TP 192 (m/z 192.0).

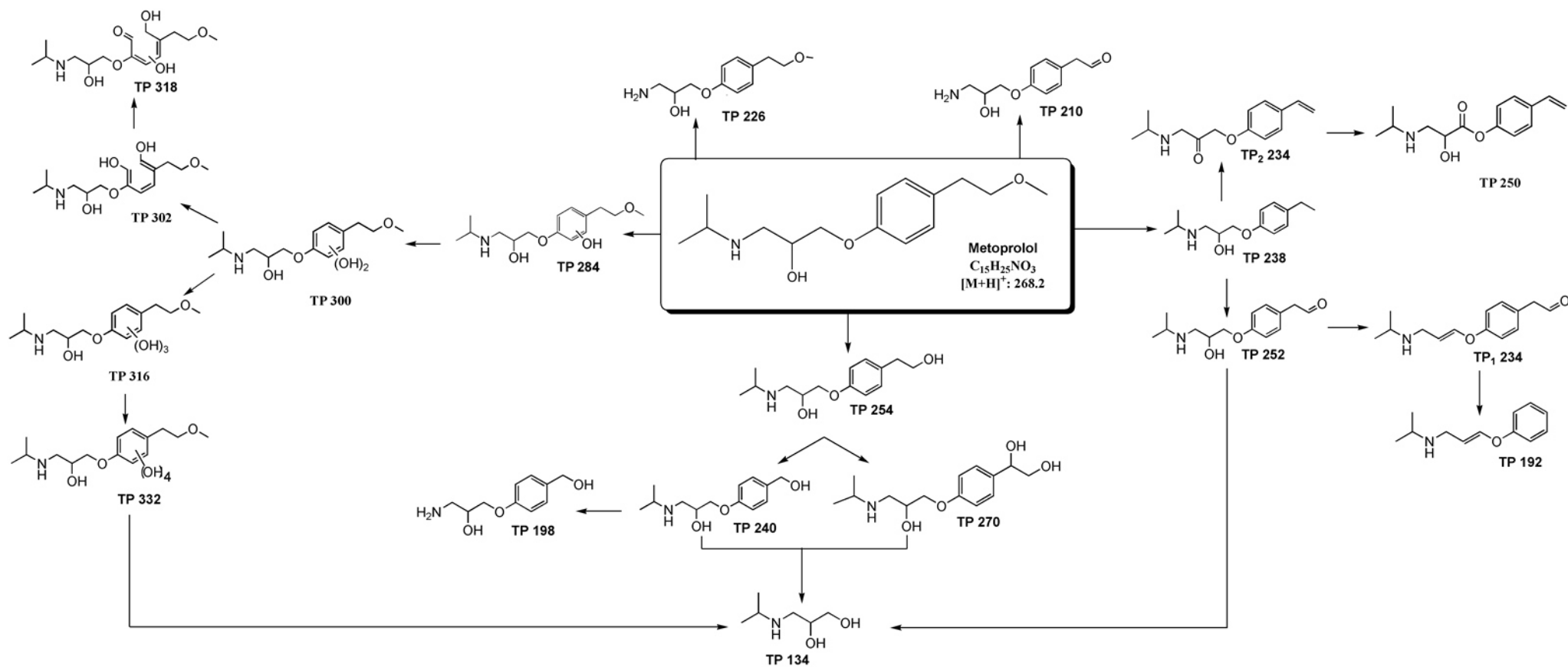
TP 210 (m/z 210.0) was formed by the N-dealkylation of secondary amines and subsequent cleavage of methanol followed by addition of OH to MTL. The MS<sup>2</sup> product ions like m/z 192.1 and m/z 168.1 confirms the proposed structure.

TP 134 (m/z 134.2), an amino-diol intermediate, was identified as one of the dominant photo-TPs. It is generated by the cleavage of ethanolamine side chain from the aromatic ring of MTL which was also identified in previous studies of photolysis and photocatalysis (Abramović et al., 2011; Benner and Ternes, 2009; Romero et al., 2011; Song et al., 2008; Wilde et al., 2013; Yang et al., 2010).

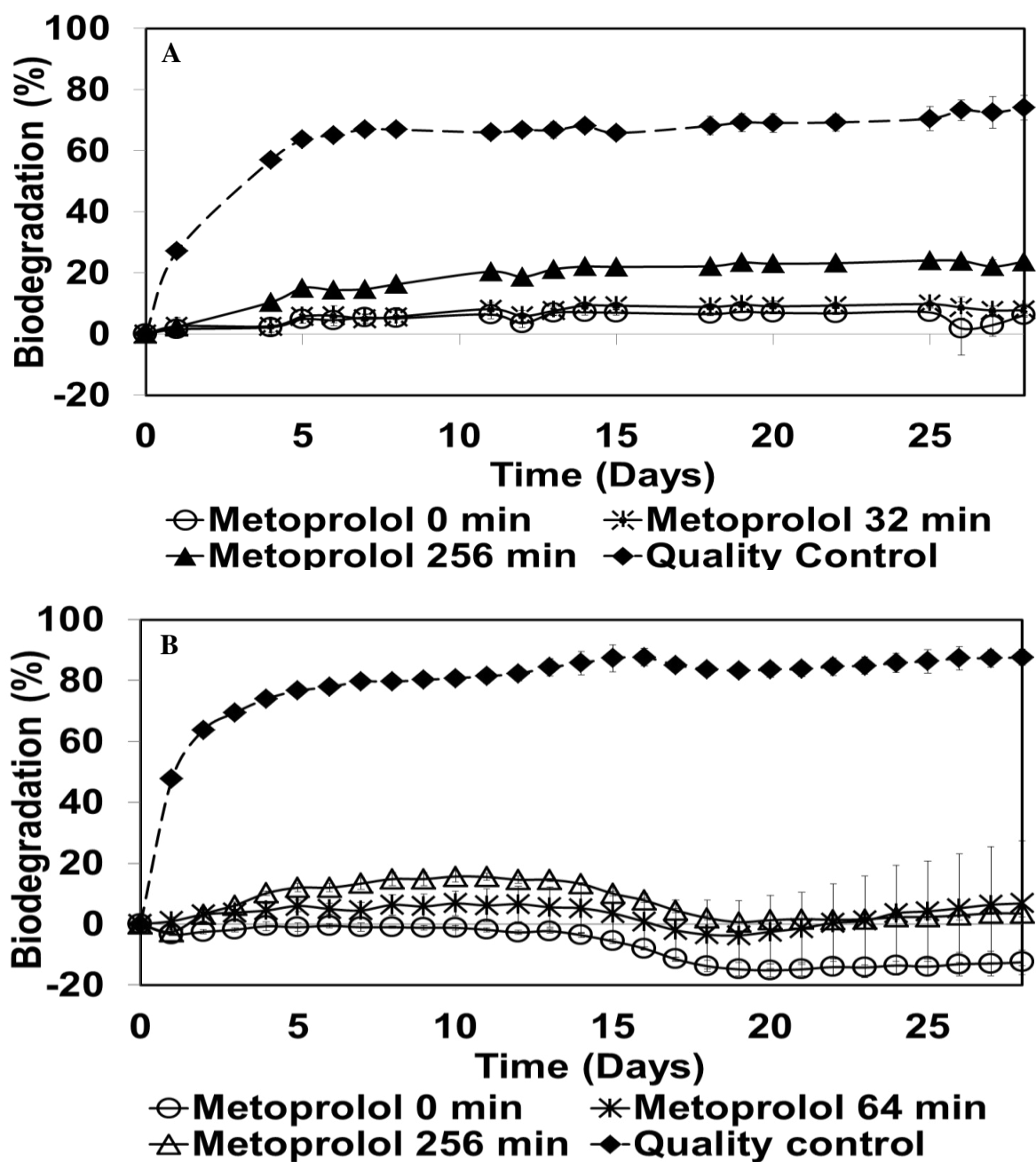


**Figure S2 Supplementary Information:** Appearance/disappearance of peak area of the photo-TPs (derivatives) of MTL during photolysis measured by LC-ESI-MS in positive mode. (Initial concentration of MTL subjected to photodegradation =  $10\text{mg L}^{-1}$ ) ( $A/A_0$  as A is the peak area of derivatives and  $A_0$  is the peak area of MTL at 0 min)

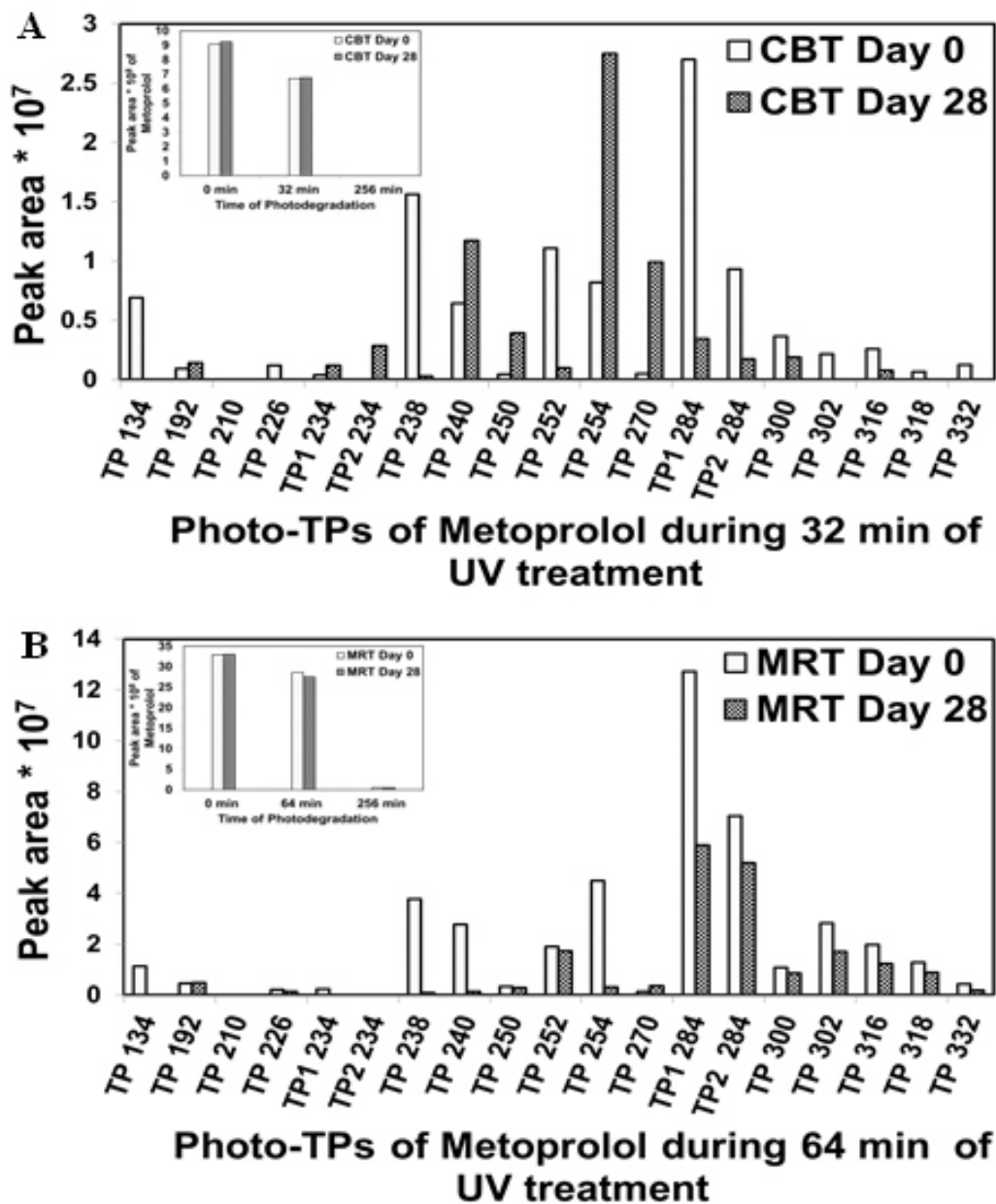




**Figure S3 Supplementary Information:** Proposed tentative scheme of degradation pathways of MTL and formation of degradation intermediate (derivatives) during photolysis under Medium pressure UV light sources



**Figure S4 Supplementary Information:** Aerobic biodegradation results of MTL and its photo-TPs (derivatives) in: A) CBT after photolysis [ $C_0 = 10 \text{ mg L}^{-1}$ ;  $n = 2$ ]; B) MRT after photolysis [ $C_0 = 60 \text{ mg L}^{-1}$ ;  $n = 2$ ].



**Figure S5 Supplementary Information:** LC-MS analysis of Biodegradation test samples: A) CBT of 32 min UV irradiated samples of MTL after day 0 and day 28; B) MRT of 64 min UV irradiated samples of MTL after day 0 and day 28

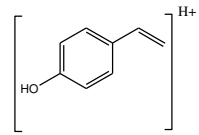
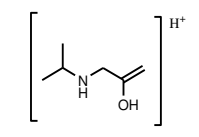
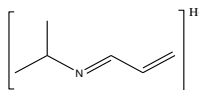
**Table S6 Supplementary Information:** *In silico* toxicity prediction by different models of Case Ultra and Leadscope QSAR for MTL and its selected derivatives (highlighted ones from Table 2)

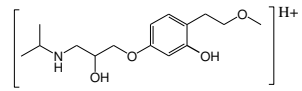
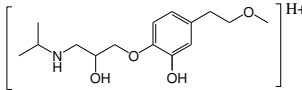
Derivatives	Case Ultra (Multicase, Inc.)					Leadscope			
	A	B (Genotoxicity)	C (Mutagenicity)	D	E	C (Mutagenicity)	D	F	B (Genotoxicity)
MTL	-	-	-	-	OD	+	-	-	-
TP 238	-	-	-	-	+	+	-	-	-
TP 252	-	-	-	-	OD	+	-	-	-
TP <sub>2</sub> 284	§*	+	-	-	OD	+	-	-	-
TP <sub>1</sub> 300	§*	+	-	-	§*	+	-	-	-
TP <sub>2</sub> 300	-	-	§*	-	OD	+	-	-	-
TP <sub>1</sub> 316	-	-	+	-	OD	+	-	+	-
TP <sub>2</sub> 316	-	+	§*	-	§*	+	-	-	-
TP <sub>3</sub> 316	-	-	-	-	OD	+	-	-	-
TP <sub>4</sub> 316	-	+	§*	-	§*	+	-	-	-
TP 318	-	-	-	§*	±	+	-	-	-
TP 332	-	+	-	-	OD	+	-	-	-

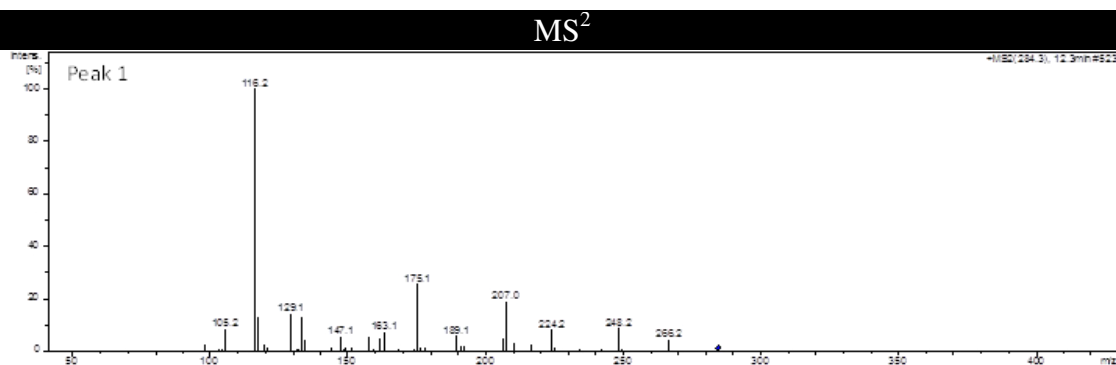
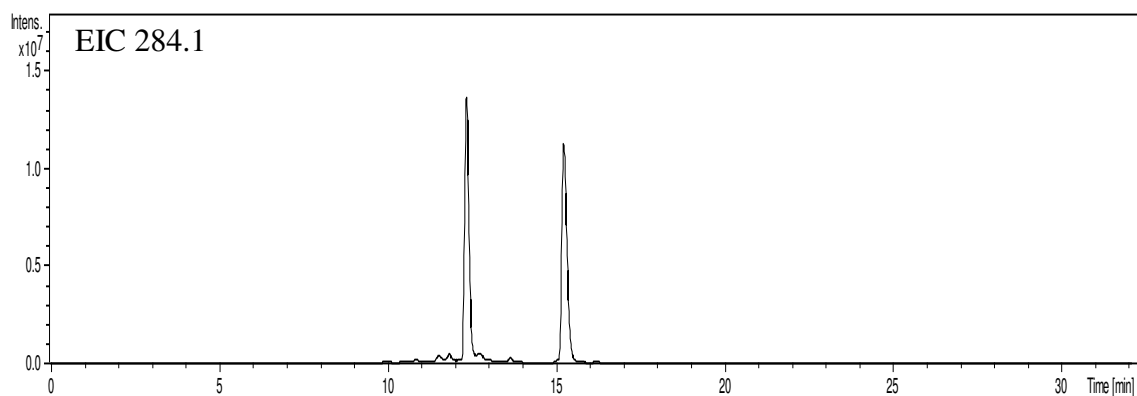
A- Human carcinogenicity; B- Micronucleus in vivo composite; C- Chromosome aberration; D- Salmonella Mutagenicity; E- Microtox against environmental bacteria; F-Mammalian mutagenesis ; OD: Out of Domain means that the test chemical is not included in the applicability domain of the applied model; §\*: Inconclusive with asterisk symbol (\*) means both positive and deactivating alerts were found in the same molecule and therefore a clear result cannot be provided; + : a positive alert for corresponding activity; - : a negative alert for corresponding activity ; ±: positive alert with low signal (marginal positive) for corresponding activity.

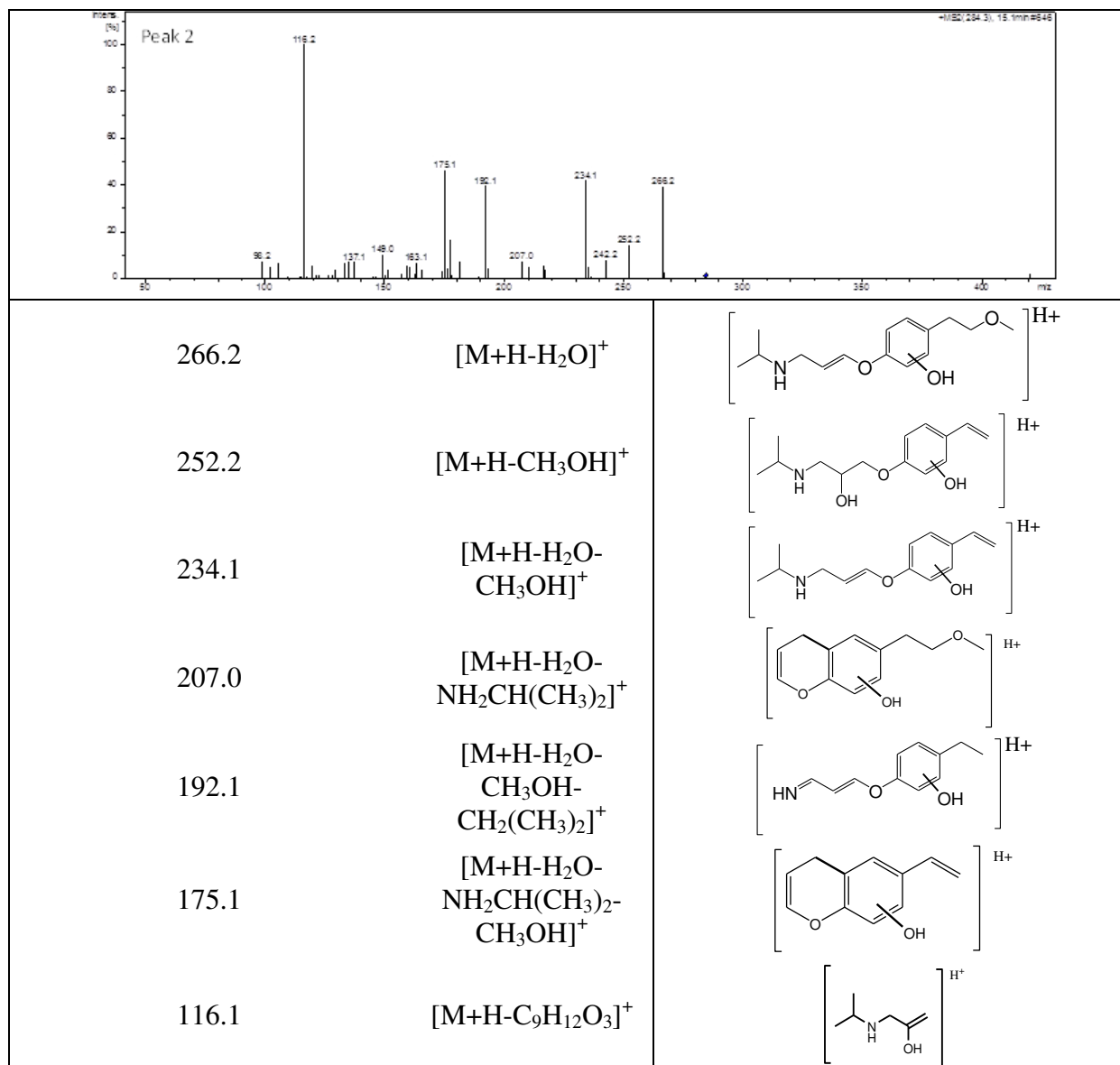
**Table S7 Supplementary Information:** The proposed structures of the fragments formed during the MS<sup>2</sup> fragmentation for Metoprolol and its photo TPs

Fragments (m/z)	Retention time (min)	Precursor ion/ Product ion	Proposed structural composition	Reference
Metoprolol (m/z 268.1)	16.1	[M+H] <sup>+</sup>		(Abramović et al., 2011; Benner and Ternes, 2009; Borkar et al., 2011; Slegers et al., 2006; Song et al., 2008; Wilde et al., 2013)
<b>MS<sup>2</sup></b>				
250		[M+H-H <sub>2</sub> O] <sup>+</sup>		
226.1		[M+H-CH(CH <sub>3</sub> ) <sub>2</sub> ] <sup>+</sup>		
218.0		[M+H-H <sub>2</sub> O-CH <sub>3</sub> OH] <sup>+</sup>		
191.0		[M+H-H <sub>2</sub> O-NH <sub>2</sub> CH(CH <sub>3</sub> ) <sub>2</sub> ] <sup>+</sup>		
176.0		[M+H-H <sub>2</sub> O-CH <sub>3</sub> OH-CH(CH <sub>3</sub> ) <sub>2</sub> ] <sup>+</sup>		
159.0		[M+H-H <sub>2</sub> O-CH <sub>3</sub> OH-NH <sub>2</sub> CH(CH <sub>3</sub> ) <sub>2</sub> ] <sup>+</sup>		
131.0		[M+H-H <sub>2</sub> O-CH <sub>3</sub> CH <sub>2</sub> OCH <sub>3</sub> -NH <sub>2</sub> CH(CH <sub>3</sub> ) <sub>2</sub> ] <sup>+</sup>		

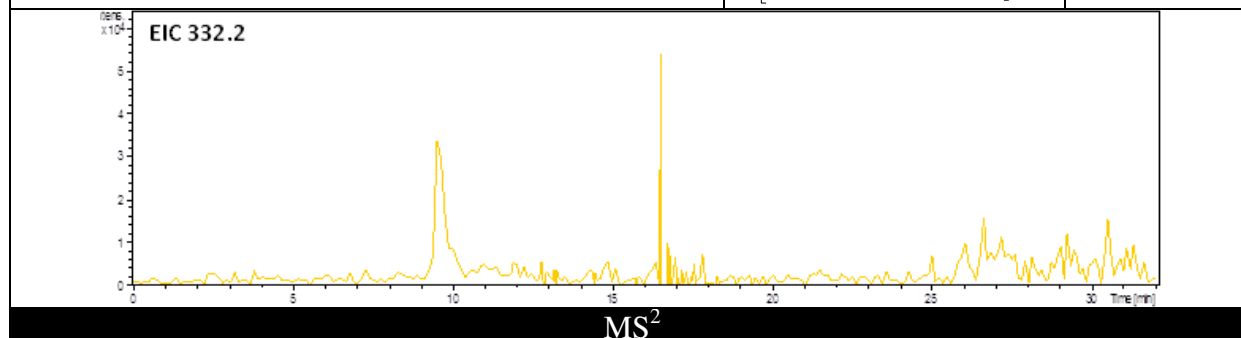
121.0	$[M+H-H_2O-CH_3OH-NH_2CH_2CH(CH_3)_2]^+$	
116.1	$[M+H-HOC_6H_4CH_2CH_2OCH_3]^+$	
98.2	$[M+H-H_2O-HOC_6H_4CH_2CH_2OCH_3]^+$	

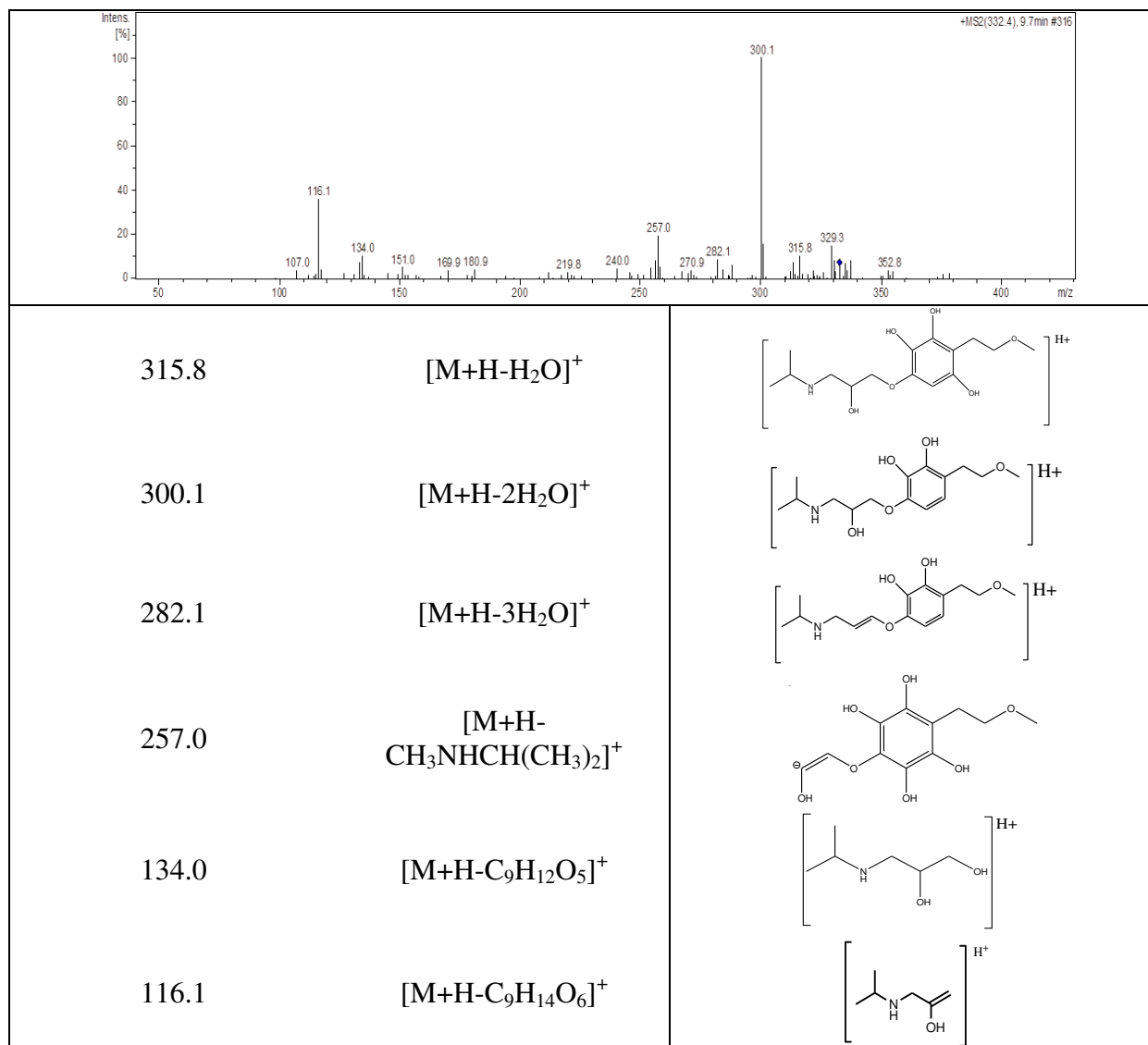
Fragments (m/z)	Retention time (min)	Precursor ion/Product ion	Proposed structural composition	Reference
TP <sub>1-2</sub> 284 (m/z 284.1)	12.3 and 15.1	$[M+H]^+$	<p>TP<sub>1</sub> 284</p>  <p>and</p> <p>TP<sub>2</sub> 284</p> 	(Abramović et al., 2011; Benner and Ternes, 2009)



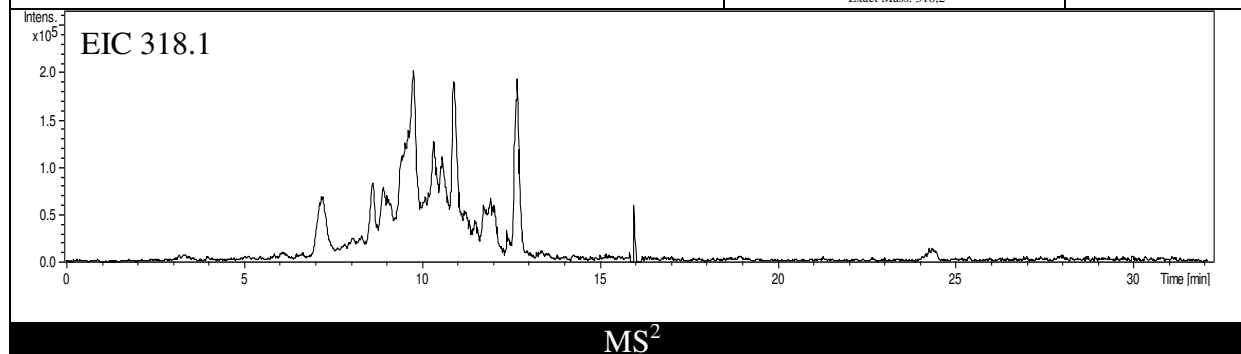


Fragments (m/z)	Retention time (min)	Precursor ion/Product ion	Proposed structural composition	Reference
TP 332 (m/z 332.2)	9.7	$[M+H]^+$	<chem>CC(C)NCC(O)COc1c(O)c(O)c(O)c(O)c1CO</chem> $H^+$	(Abramović et al., 2011)

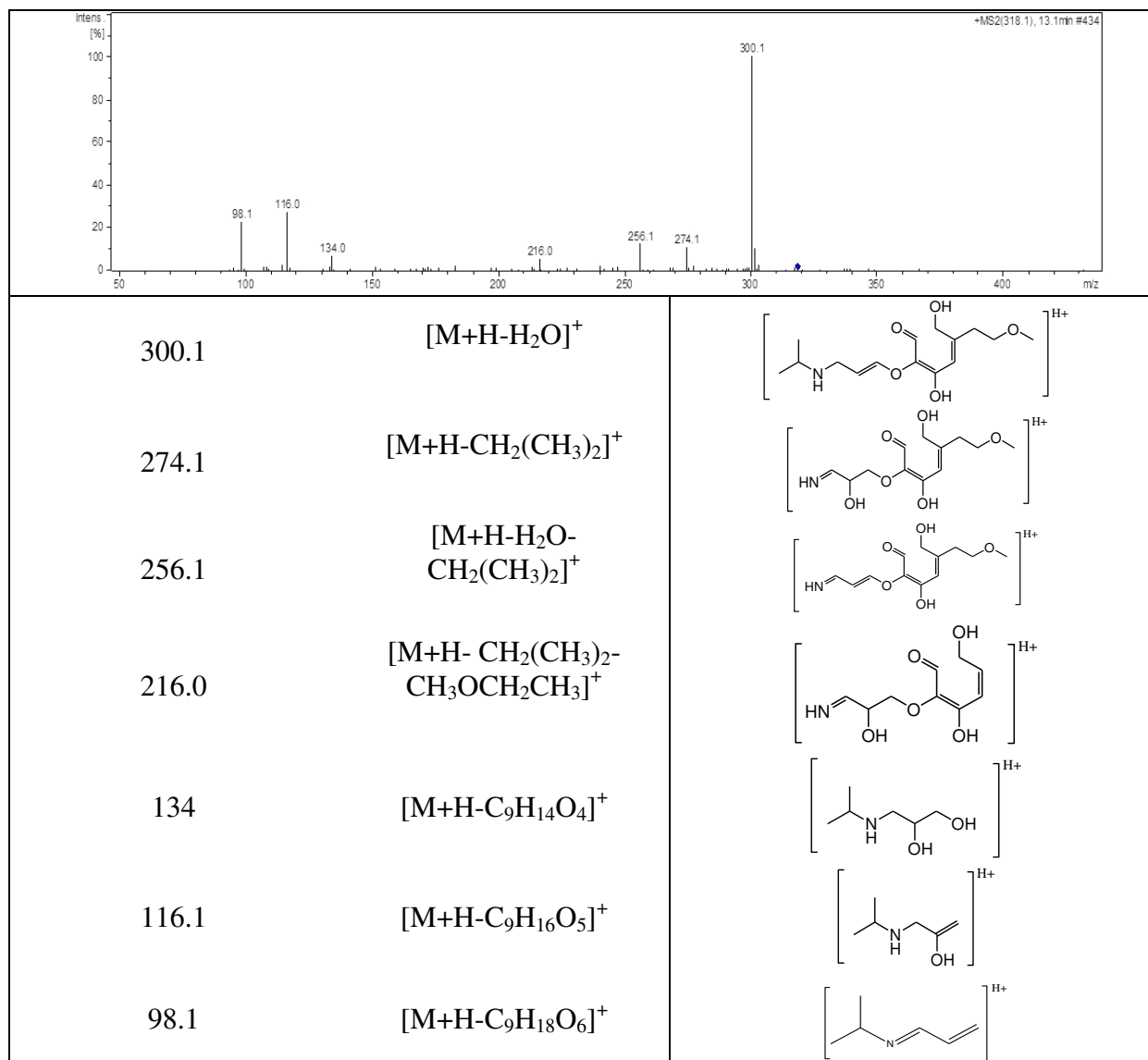




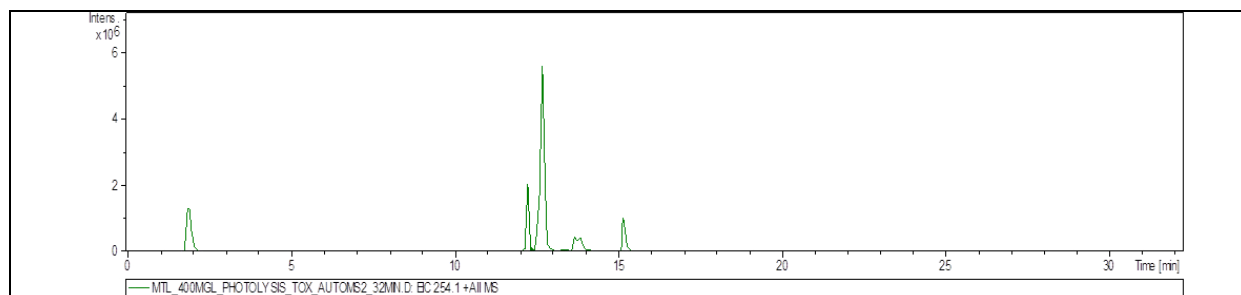
Fragments (m/z)	Retention time (min)	Precursor ion/Product ion	Proposed structural composition	Reference
TP 318 (m/z 318.1)	Several peaks were observed	$[M+H]^+$	 $C_{15}H_{28}NO_6^+$ Exact Mass: 318.2	(Romero et al., 2011)



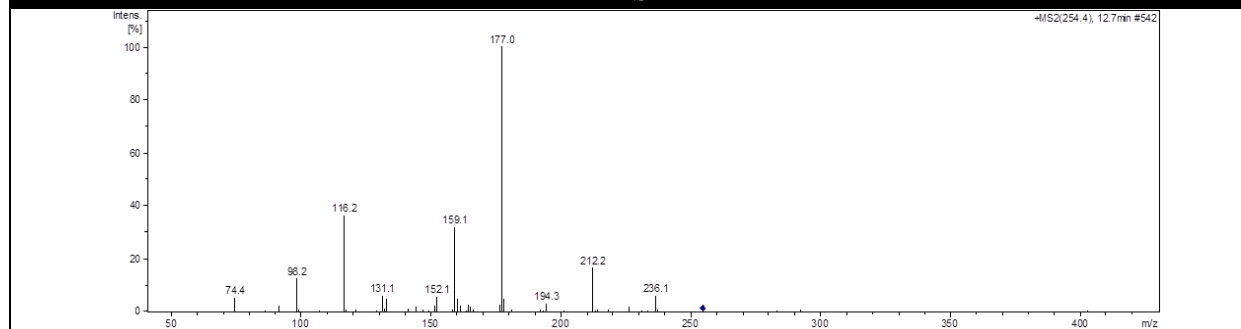




Fragments (m/z)	Retention time (min)	Precursor ion/Product ion	Proposed structural composition	Reference
TP 254 (m/z 254.1)	12.7	$[M+H]^+$		(Abramović et al., 2011; Benner and Ternes, 2009; MA et al., 2007; Slegers et al., 2006; Wilde et al., 2013)

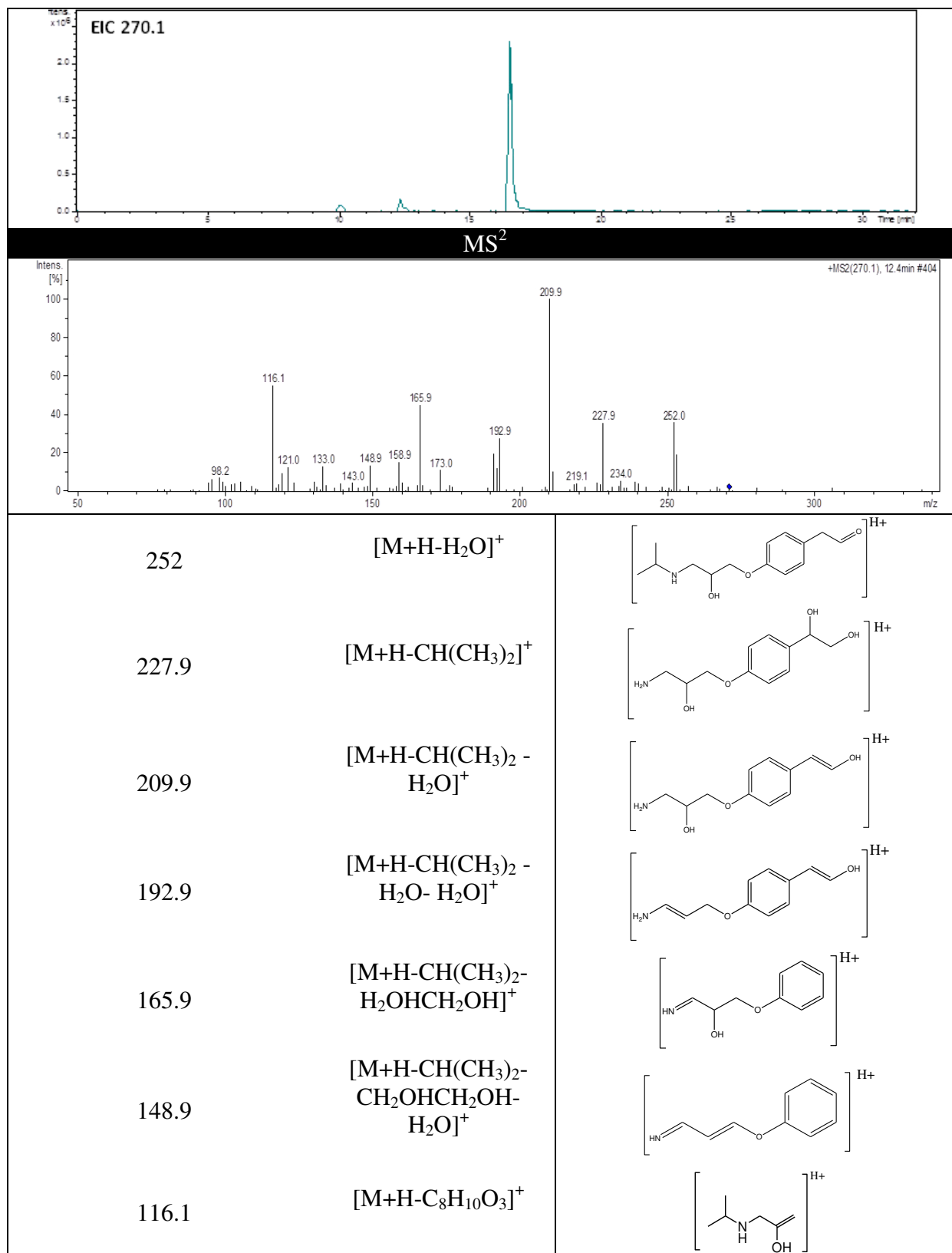


MS<sup>2</sup>

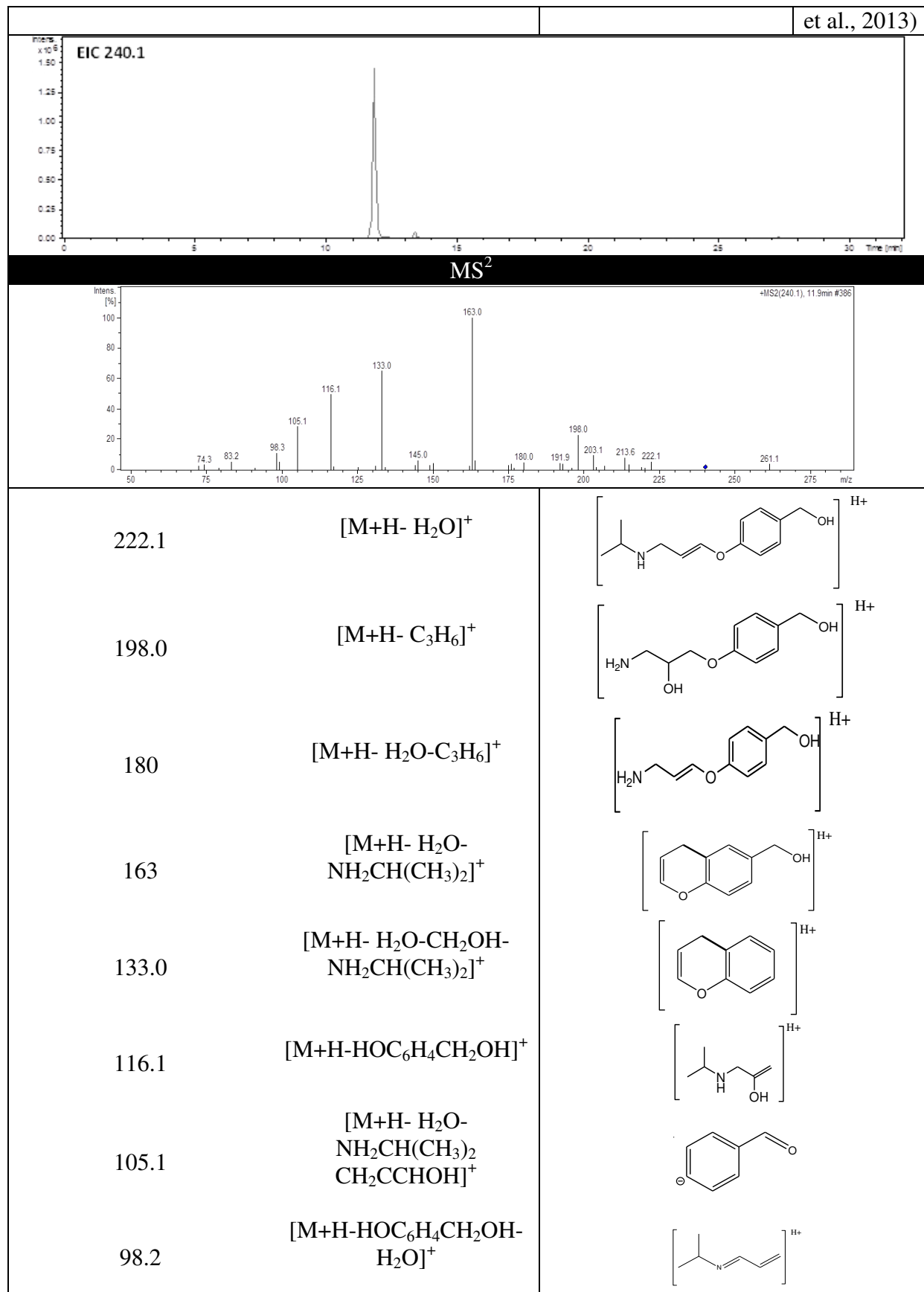


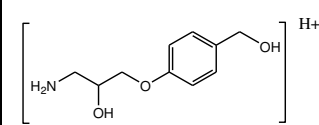
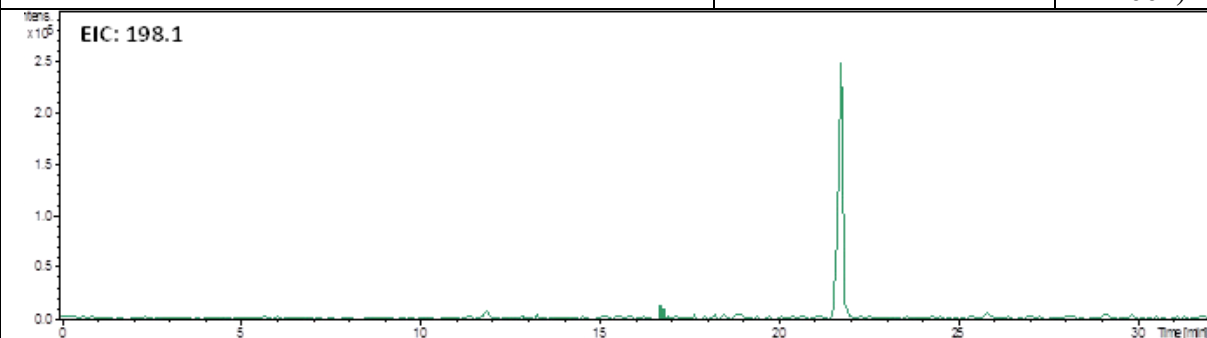
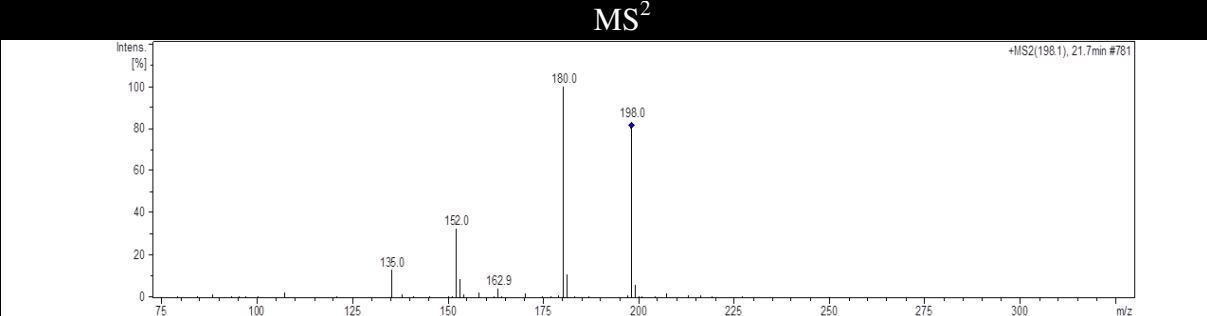
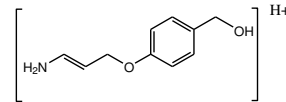
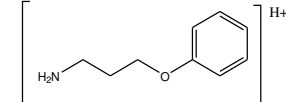
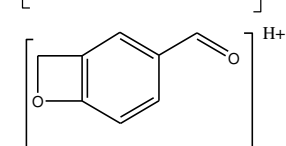
236.1	$[M+H-H_2O]^+$	
212.2	$[M+H-CH_2(CH_3)_2]^+$	
194.3	$[M+H-H_2O-CH_2(CH_3)_2]^+$	
177	$[M+H-H_2O-NH_2CH(CH_3)_2]^+$	
159.1	$[M+H-H_2O-NH_2CH(CH_3)_2-H_2O]^+$	
116.1	$[M+H-C_8H_{10}O_2]^+$	
98.2	$[M+H-C_8H_{10}O_2-H_2O]^+$	

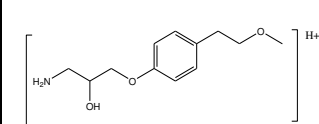
Fragments (m/z)	Retention time (min)	Precursor ion/Product ion	Proposed structural composition	Reference
TP 270 (m/z 270.1)	12.4	$[M+H]^+$		(Benner and Ternes, 2009; MA et al., 2007)

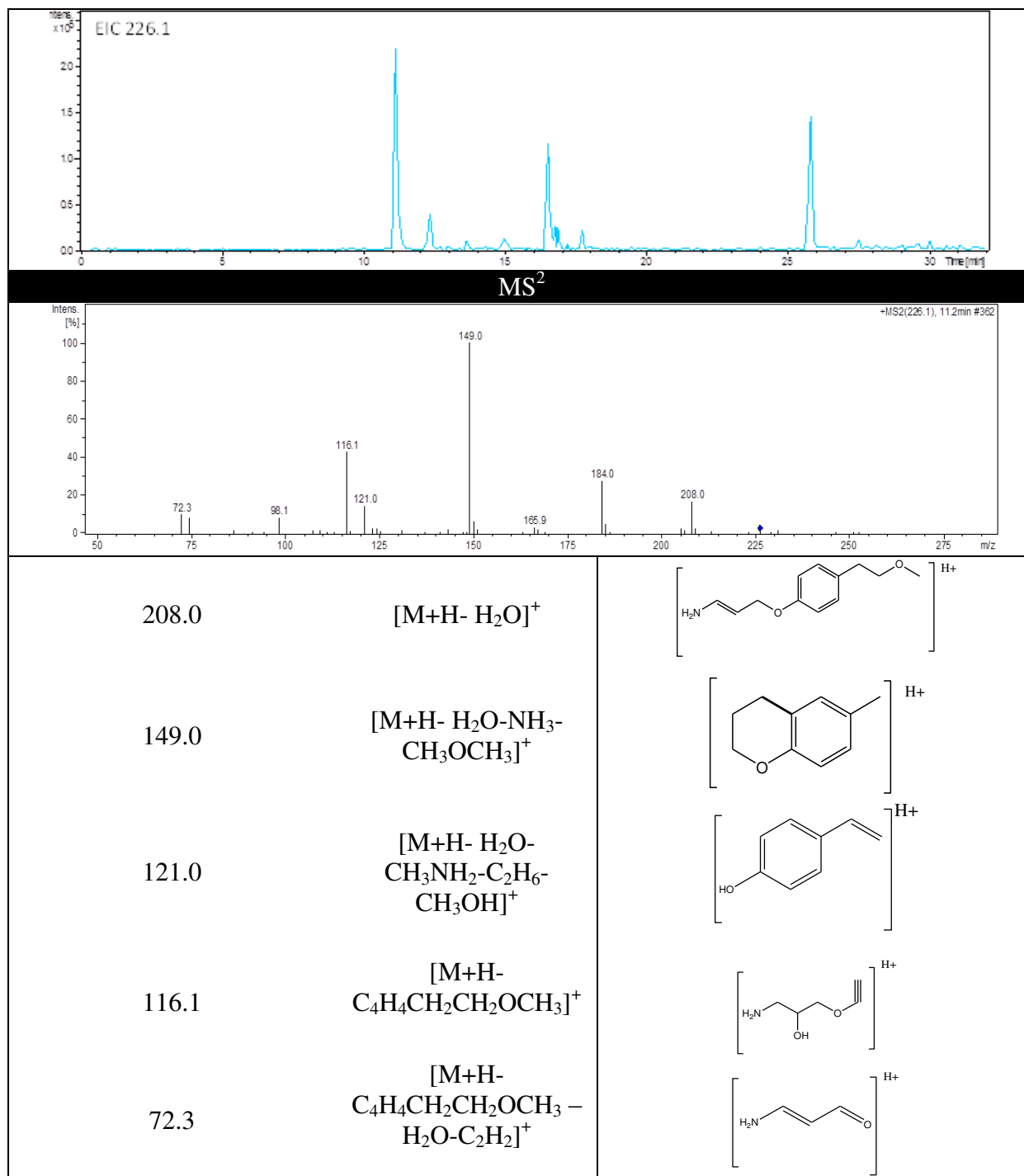


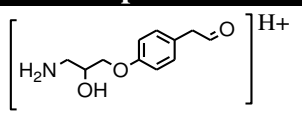
Fragments (m/z)	Retention time (min)	Precursor ion/Product ion	Proposed structural composition
TP 240 (m/z 240.1)	11.9	$[M+H]^+$	(Benner and Ternes, 2009; Wilde

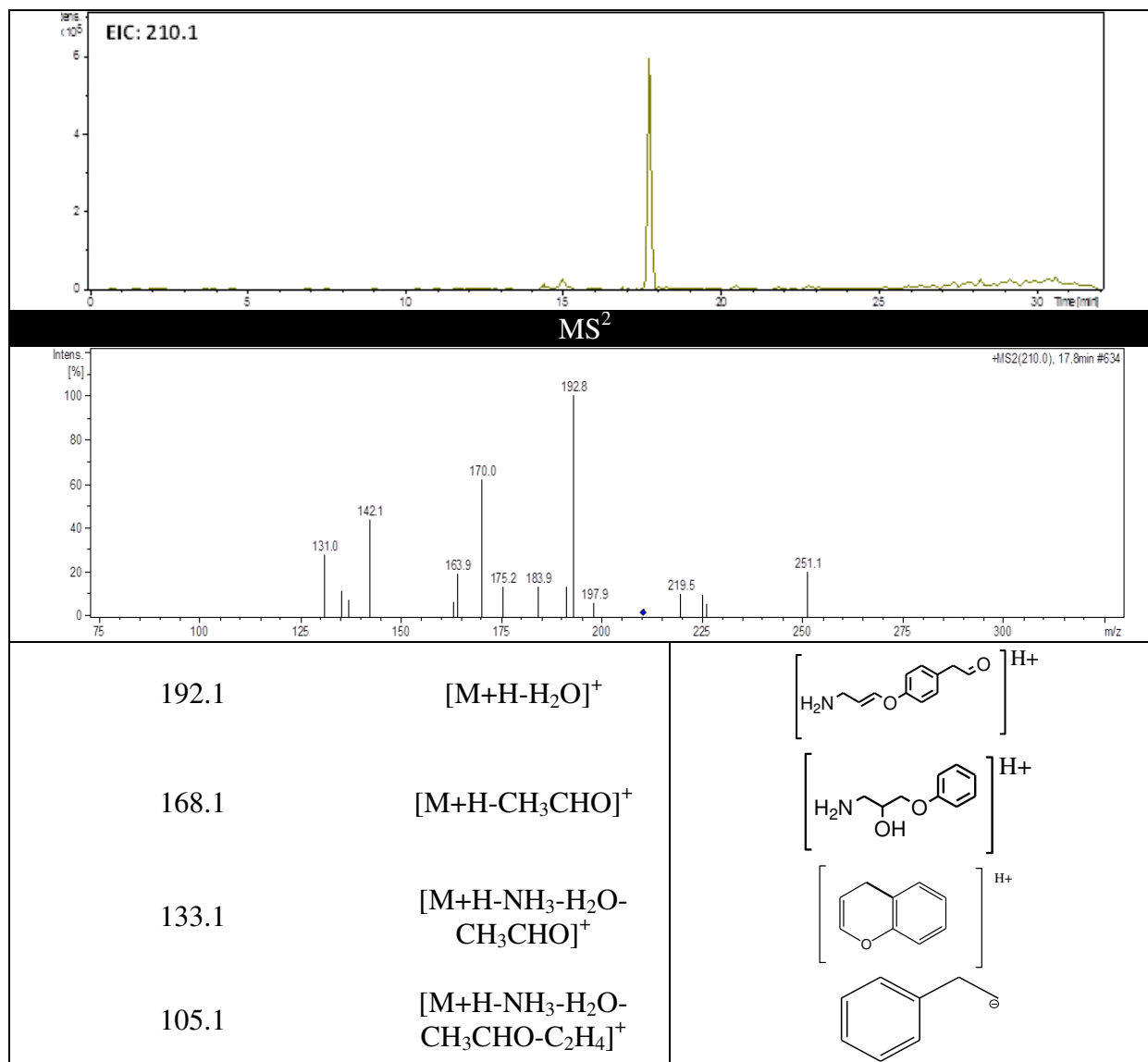


Fragment (m/z)	Retention time (min)	Precursor ion/Product ion	Proposed structural composition	Reference
TP 198 (m/z 198.1)	21.7	$[M+H]^+$		MetaPC software (Sedykh et al., 2001)
				
				
180.0		$[M+H-H_2O]^+$		
152.0		$[M+H-H_2O-CH_3OH]^+$		
135.0		$[M+H-NH_2CH_2CH_2(OH)]^+$		

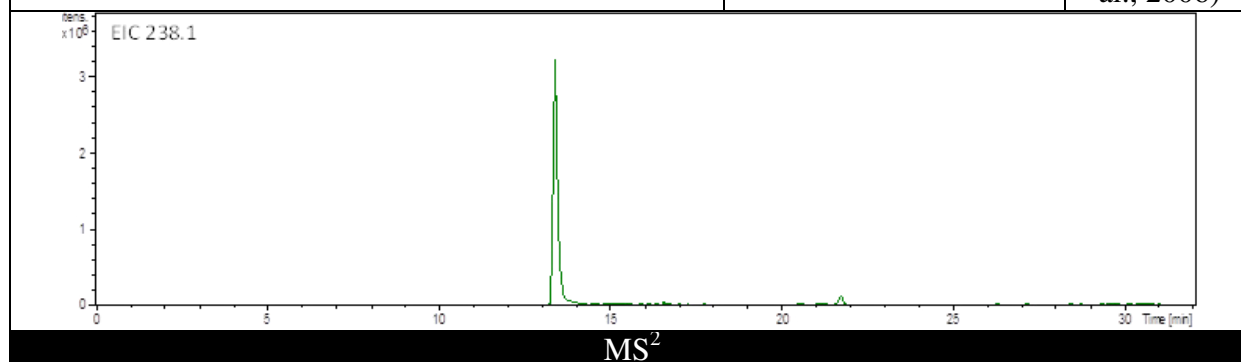
Fragment (m/z)	Retention time (min)	Precursor ion/Product ion	Proposed structural composition	Reference
TP 226 (m/z 226.1)	11.2	$[M+H]^+$		(Benner and Ternes, 2009; Borkar et al., 2011; MA et al., 2007; Slegers et al., 2006; Song et al., 2008; Wilde et al., 2013)

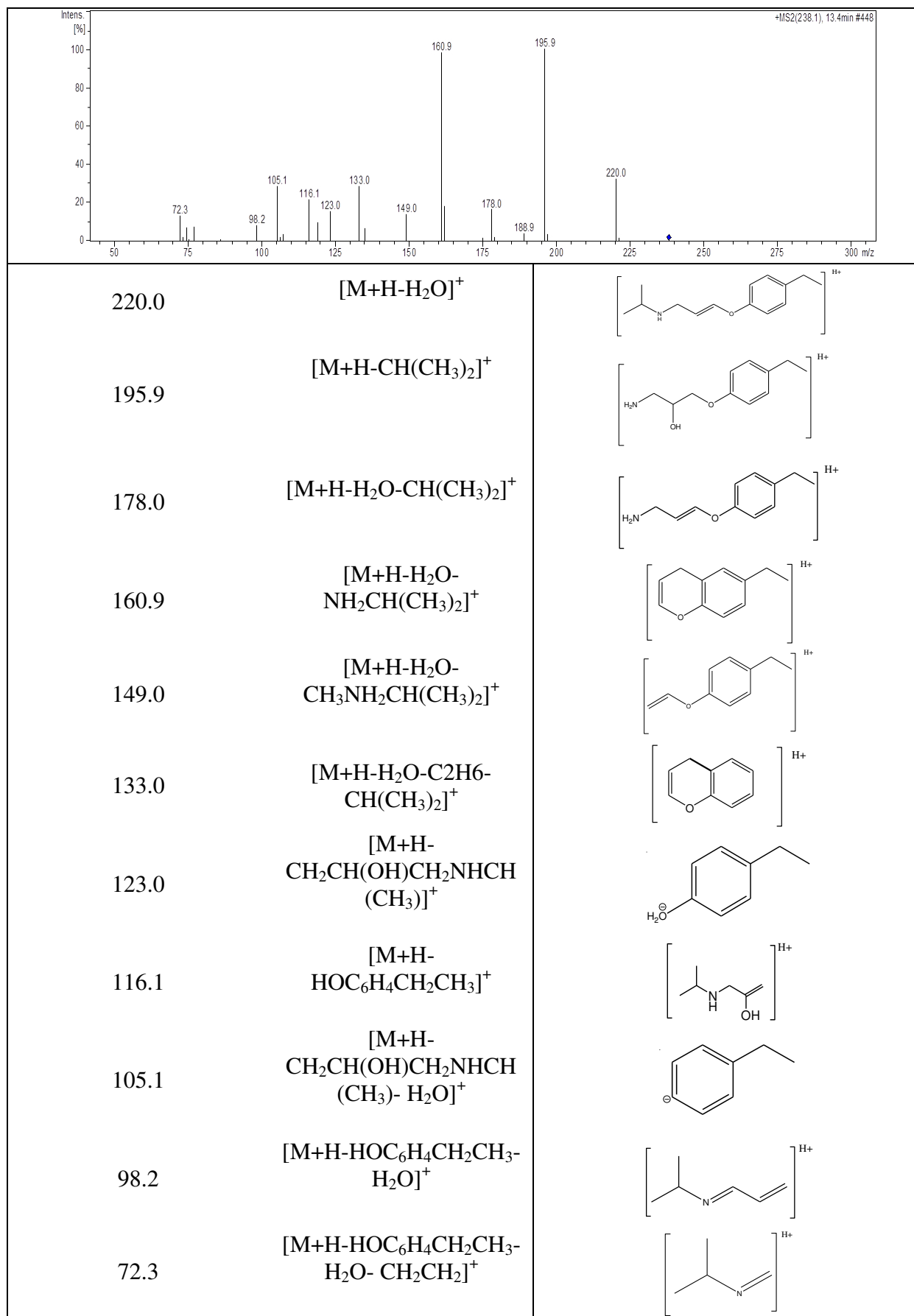


Fragments (m/z)	Retention time (min)	Precursor ion/Product ion	Proposed structural composition	Reference
TP 210 (m/z 210.0)	14.5	$[M+H]^+$		

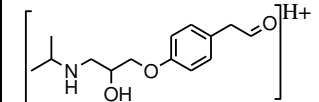
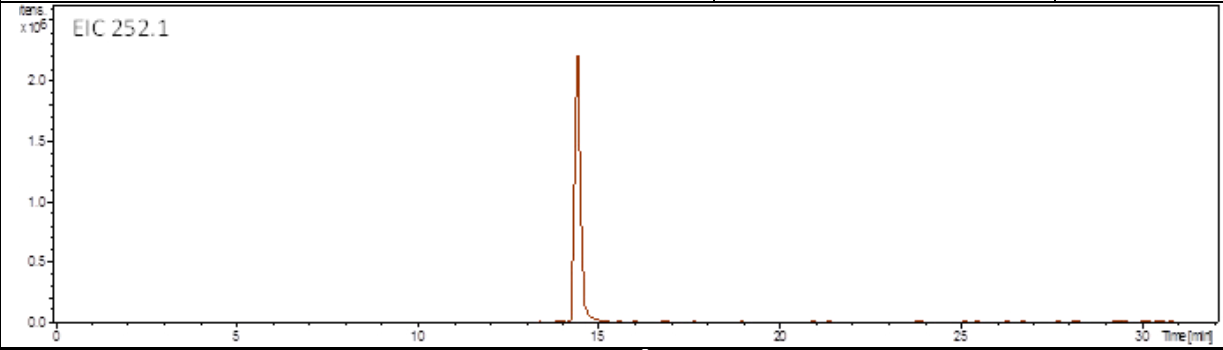
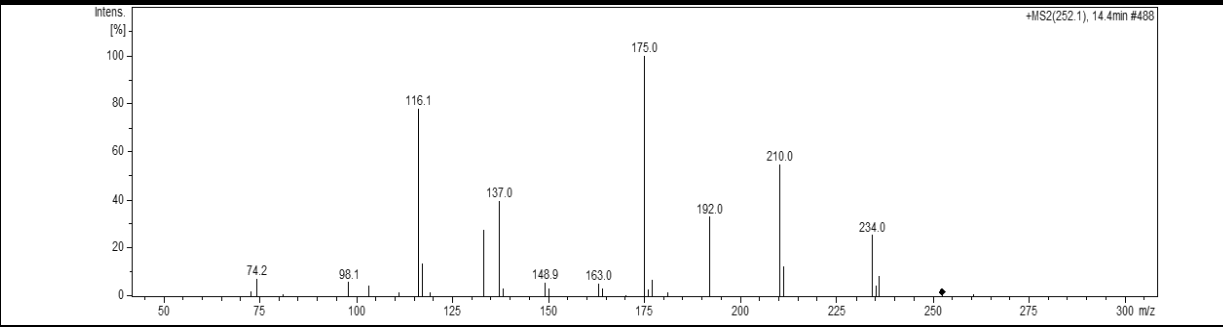
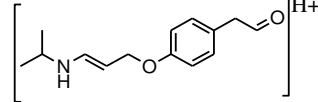
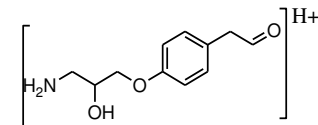
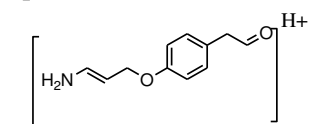
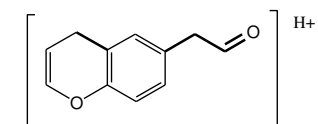
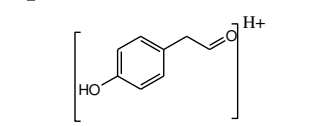
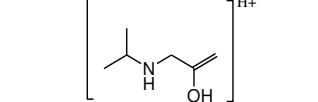


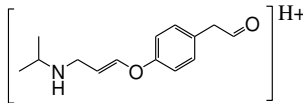
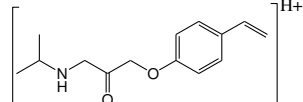
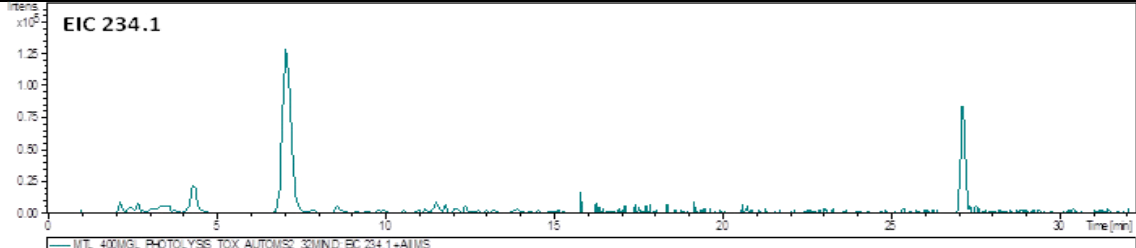
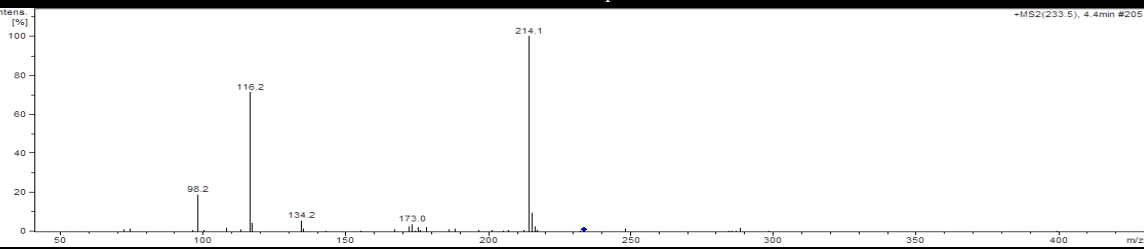
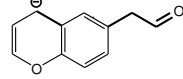
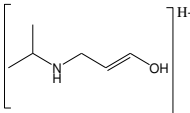
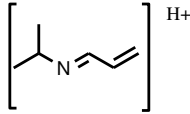
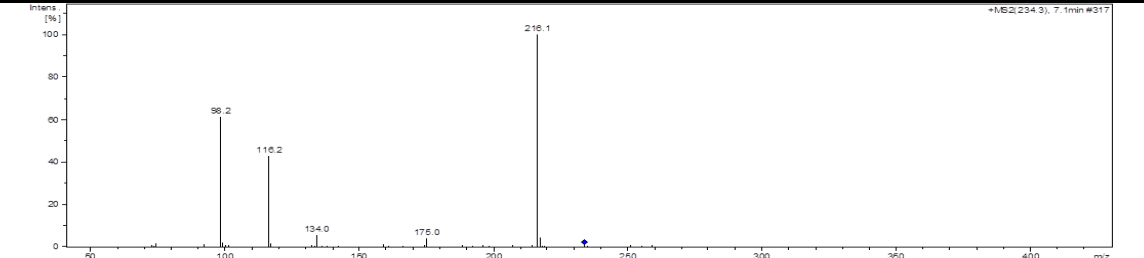
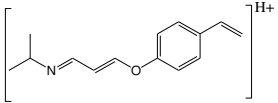
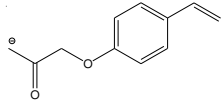
Fragments (m/z)	Retention time (min)	Precursor ion/Product ion	Proposed structural composition	Reference
TP 238 (m/z 238.1)	13.4	$[M+H]^+$		(Abramović et al., 2011; Borkar et al., 2011; Slegers et al., 2006)

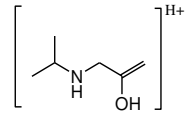
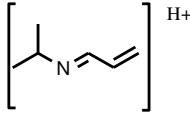


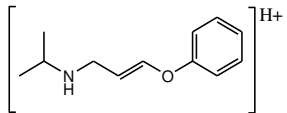
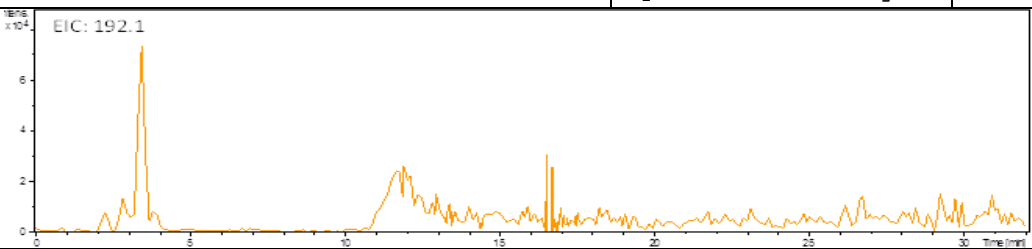
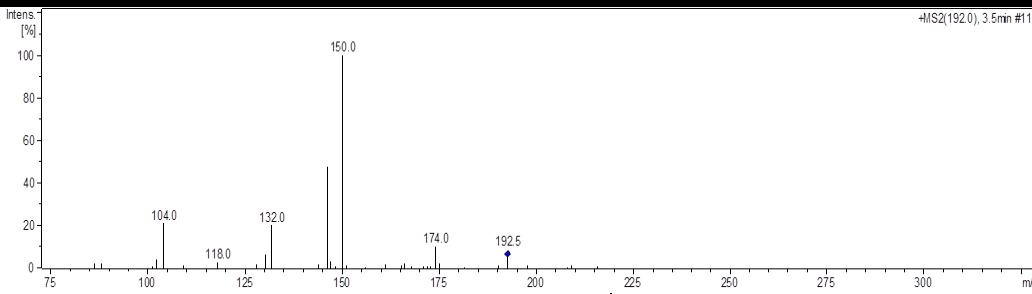
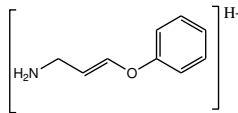
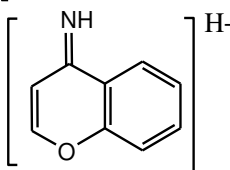


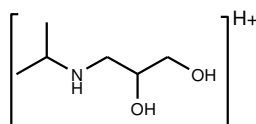


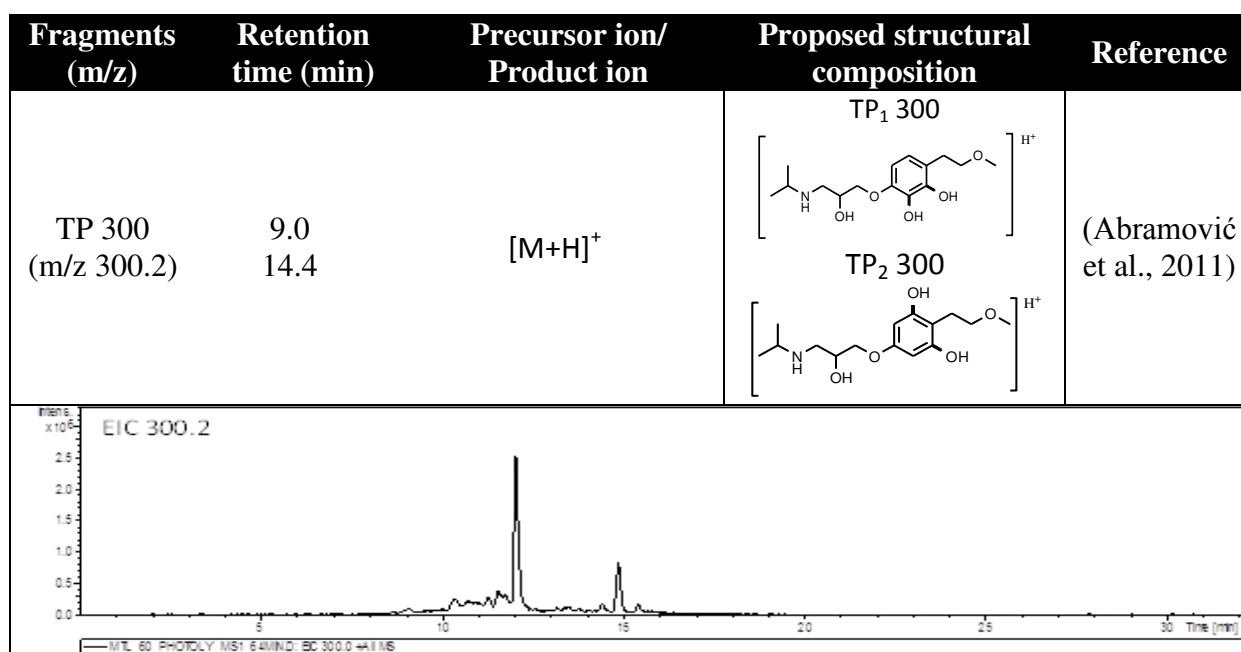
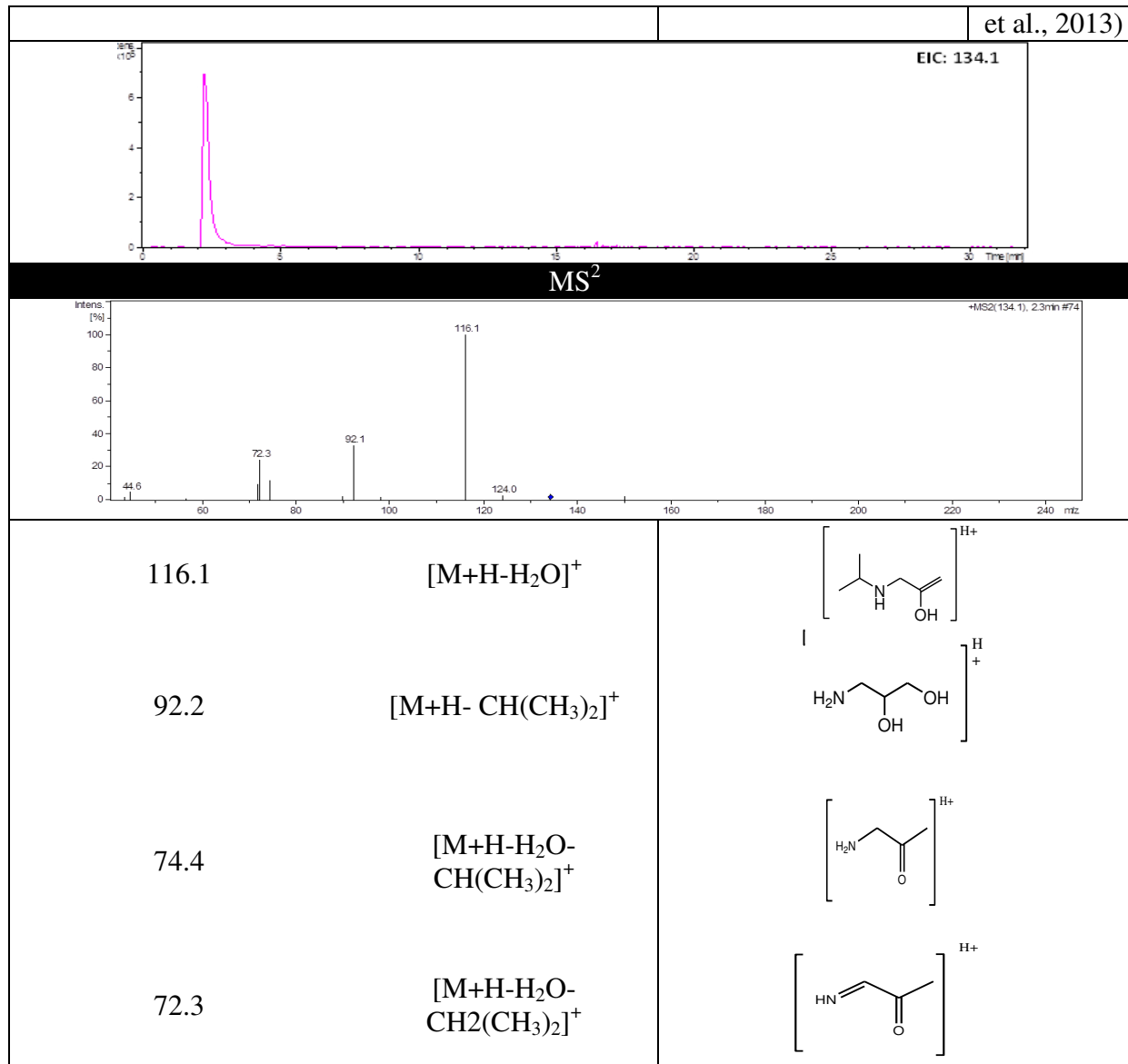
Fragment (m/z)	Retention time (min)	Precursor ion/Product ion	Proposed structural composition	Reference
TP 252 (m/z 252.1)	14.4	$[M+H]^+$		(Abramović et al., 2011)
				
<b>MS<sup>2</sup></b>				
				
234.0		$[M+H-H_2O]^+$		
210.0		$[M+H-CH(CH_3)]^+$		
192.0		$[M+H-CH(CH_3)_2-H_2O]^+$		
175.0		$[M+H-CH(CH_3)_2-H_2O-NH_3]^+$		
137.0		$[M+H-CH_2CH_2-CH_2N(OH)CH(CH_3)_2]^+$		
116.1		$[M+H-H_2O-HOC_6H_4CH_2CH_2]^+$		

Fragment (m/z)	Retention time (min)	Precursor ion/Product ion	Proposed structural composition	Reference
TP 234 (m/z 234.1)	4.4 7.1	[M+H] <sup>+</sup>	TP <sub>1</sub> 234  H <sup>+</sup> and TP <sub>2</sub> 234  H <sup>+</sup>	(Slegers et al., 2006)
				
<b>MS<sup>2</sup> of TP<sub>1</sub> 234</b>				
				
173.0		[M+H-NH <sub>2</sub> CH(CH <sub>3</sub> ) <sub>2</sub> ] <sup>+</sup>		
116.2		[M+H-C <sub>8</sub> H <sub>8</sub> O] <sup>+</sup>	 H <sup>+</sup>	
98.2		[M+H-C <sub>8</sub> H <sub>8</sub> O-H <sub>2</sub> O] <sup>+</sup>	 H <sup>+</sup>	
<b>MS<sup>2</sup> of TP<sub>2</sub> 234</b>				
				
216.1		[M+H-H <sub>2</sub> O] <sup>+</sup>	 H <sup>+</sup>	
175.0		[M+H-NH <sub>2</sub> CH(CH <sub>3</sub> ) <sub>2</sub> ] <sup>+</sup>		

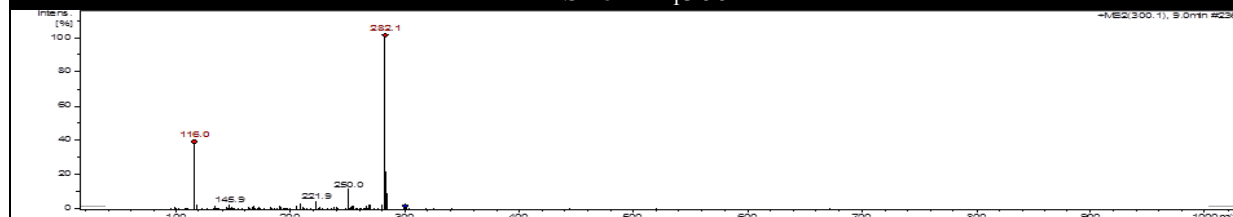
116.1	$[M+H-C_8H_8O]^+$	
98.2	$[M+H-C_8H_8O-H_2O]^+$	

Fragments (m/z)	Retention time (min)	Precursor ion/Product ion	Proposed structural composition	Reference
TP 192 (m/z 192.1)	3.5	$[M+H]^+$		
				
<b>MS<sup>2</sup></b>				
				
150.0		$[M+H-CH_2(CH_3)_2]^+$		
146.0		$[M+H-CH_2(CH_3)_2-2H_2]^+$		

Fragments (m/z)	Retention time (min)	Precursor ion/Product ion	Proposed structural composition	Reference
TP 134 (m/z 134.2)	2.5	$[M+H]^+$		(Abramović et al., 2011; Benner and Ternes, 2009; Romero et al., 2011; Slegers et al., 2006; Song et al., 2008; Wilde

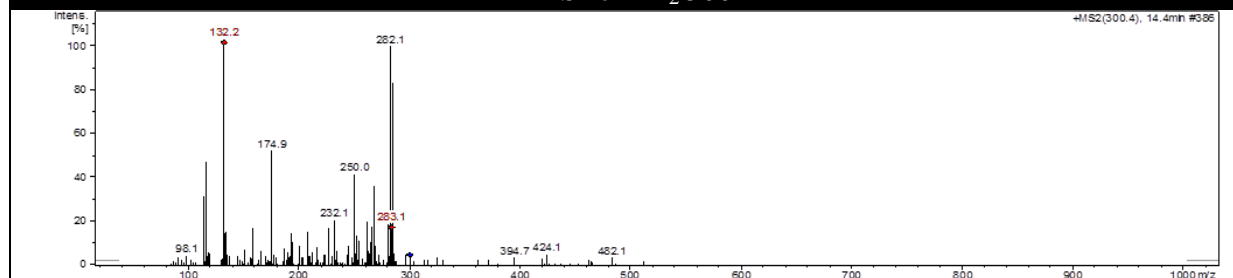


MS<sup>2</sup> of TP<sub>1</sub>300



282.2	[M+H-H <sub>2</sub> O] <sup>+</sup>	
250.1	[M+H-H <sub>2</sub> O-CH <sub>3</sub> OH] <sup>+</sup>	
222.1	[M+H-H <sub>2</sub> O-CH <sub>3</sub> OH-CH <sub>2</sub> (CH <sub>3</sub> ) <sub>2</sub> ] <sup>+</sup>	
116.1	[M+H-C <sub>9</sub> H <sub>12</sub> O <sub>4</sub> ] <sup>+</sup>	

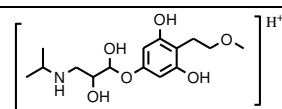
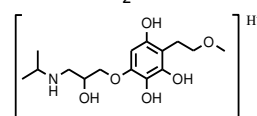
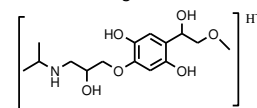
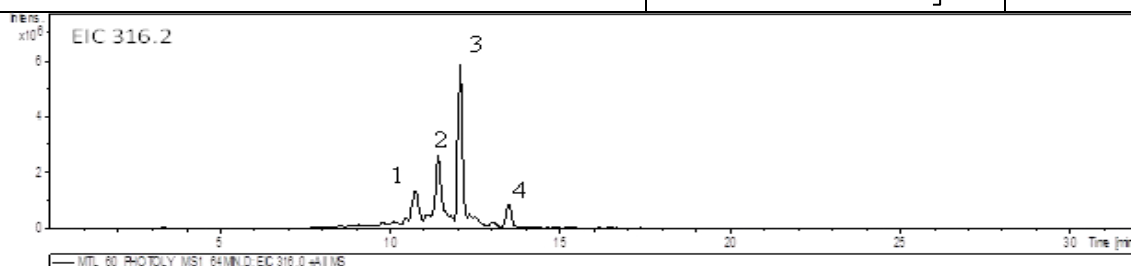
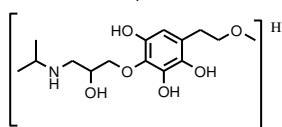
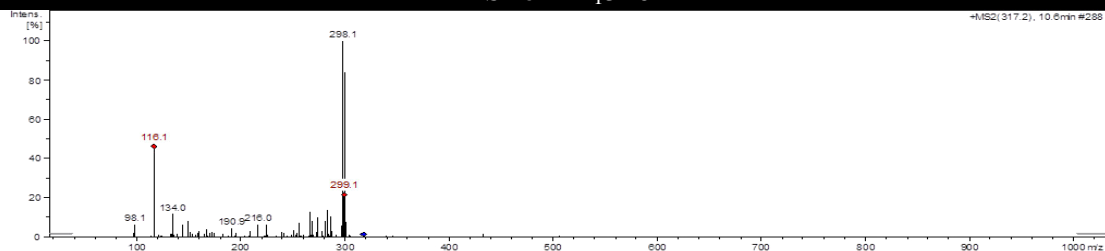
MS<sup>2</sup> of TP<sub>2</sub>300



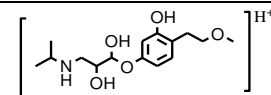
282.2	[M+H-H <sub>2</sub> O] <sup>+</sup>	
268.2	[M+H-CH <sub>3</sub> OH] <sup>+</sup>	
250.0	[M+H-H <sub>2</sub> O-CH <sub>3</sub> OH] <sup>+</sup>	
132.1	[M+H-C <sub>9</sub> H <sub>12</sub> O <sub>5</sub> ] <sup>+</sup>	
116.1	[M+H-C <sub>9</sub> H <sub>12</sub> O <sub>4</sub> ] <sup>+</sup>	

Fragments (m/z)	Retention time (min)	Precursor ion/Product ion	Proposed structural composition	Reference
TP 316 (m/z 316.2)	10.6 11.6 12.4	[M+H] <sup>+</sup>	TP <sub>1</sub> 316	(Abramović et al., 2011)

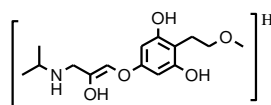
13.6

TP<sub>2</sub> 316TP<sub>3</sub> 316TP<sub>4</sub> 316MS<sup>2</sup> of TP<sub>1</sub>316

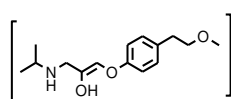
300.2

[M+H-O]<sup>+</sup>

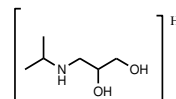
298.2

[M+H-H<sub>2</sub>O]<sup>+</sup>

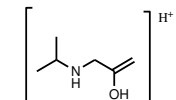
266

[M+H-H<sub>2</sub>O-O-O]<sup>+</sup>

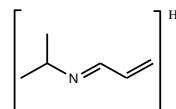
134.1

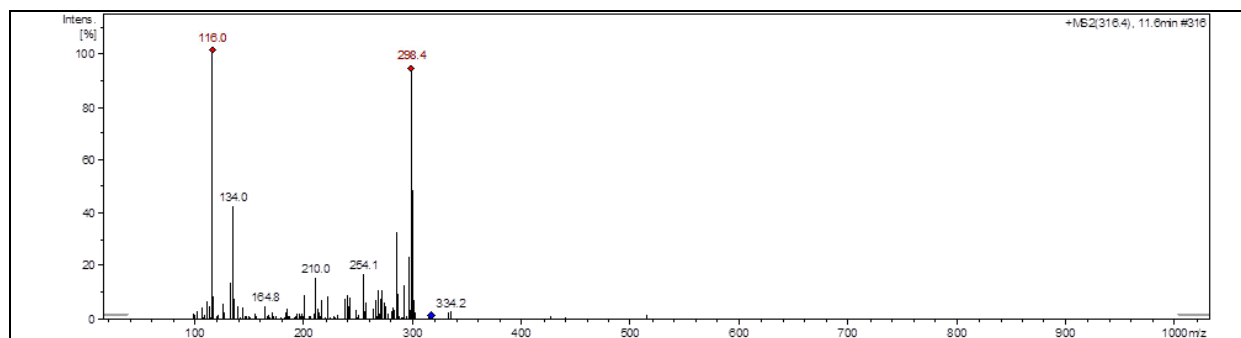
[M+H-C<sub>9</sub>H<sub>12</sub>O<sub>4</sub>]<sup>+</sup>

116.1

[M+H-C<sub>9</sub>H<sub>12</sub>O<sub>4</sub>-H<sub>2</sub>O]<sup>+</sup>

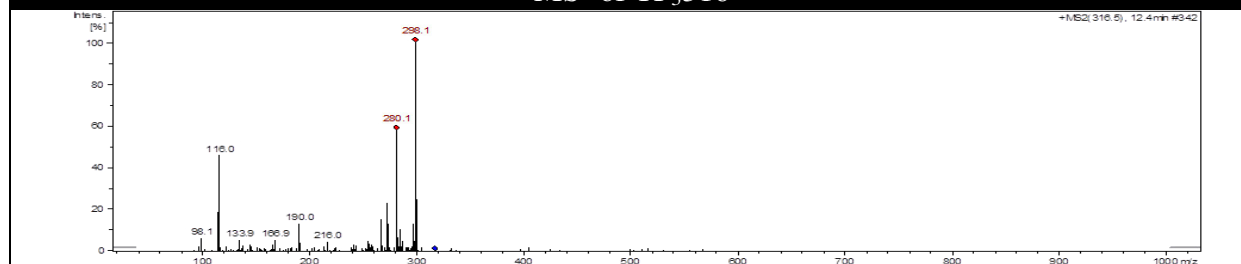
98.2

[M+H-C<sub>9</sub>H<sub>12</sub>O<sub>4</sub>-2H<sub>2</sub>O]<sup>+</sup>MS<sup>2</sup> of TP<sub>2</sub>316

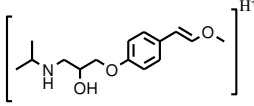
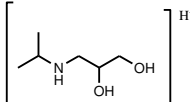
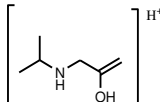
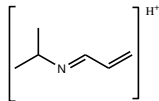


300.2	$[M+H-O]^+$	
298.2	$[M+H-H_2O]^+$	
284.2	$[M+H-2O]^+$	
254.1	$[M+H-2O-CH_3OH]^+$	
210.1	$[M+H-2O-CH_3OH-CH_2(CH_3)_2]^+$	
134.1	$[M+H-C_9H_{12}O_4]^+$	
116.1	$[M+H-C_9H_{12}O_4-H_2O]^+$	

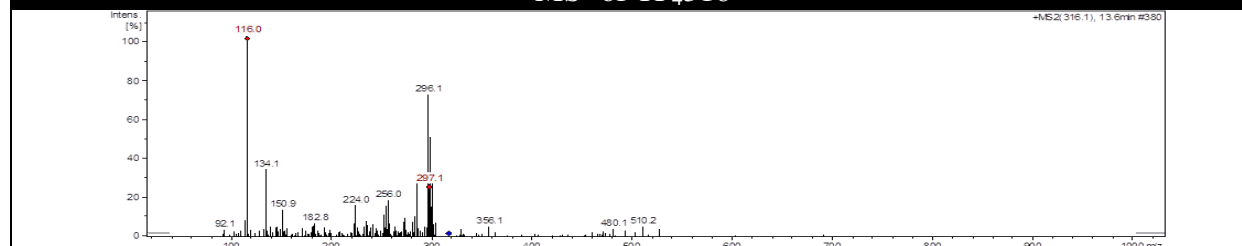
MS<sup>2</sup> of TP<sub>316</sub>

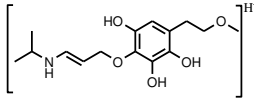
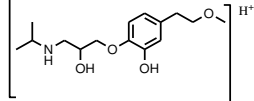
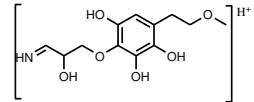
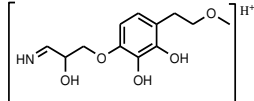
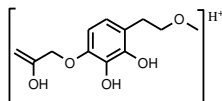
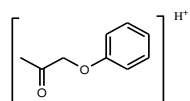
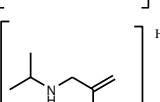


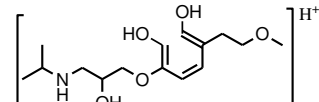
298.2	$[M+H-H_2O]^+$	
280.1	$[M+H-2H_2O]^+$	
272.1	$[M+H-CH_2(CH_3)_2]^+$	

266.2	$[M+H-2O-H_2O]^+$	
134.1	$[M+H-C_9H_{12}O_4]^+$	
116.1	$[M+H-C_9H_{12}O_4-H_2O]^+$	
98.1	$[M+H-C_9H_{12}O_4-2H_2O]^+$	

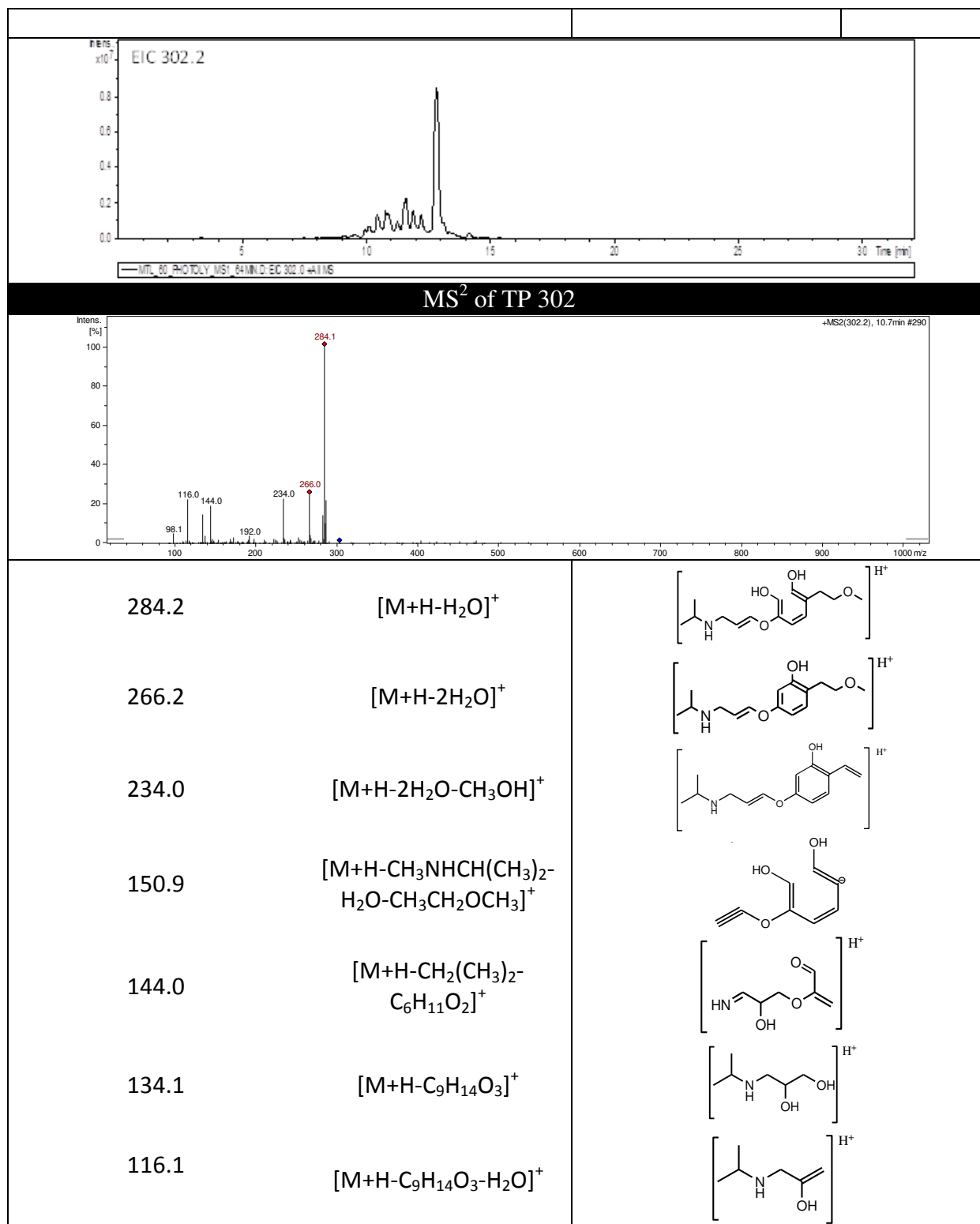
MS<sup>2</sup> of TP<sub>4316</sub>



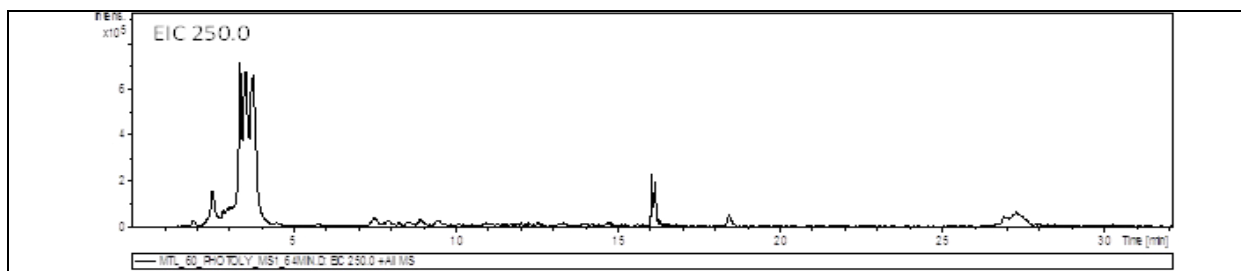
298.2	$[M+H-H_2O]^+$	
284.2	$[M+H-2O]^+$	
272.1	$[M+H-CH_2(CH_3)_2]^+$	
256.1	$[M+H-CH_2(CH_3)_2-O]^+$	
241.0	$[M+H-NH_2CH(CH_3)_2-O]^+$	
151.1	$[M+H-NHCH(CH_3)_2-3O-CH_3CH_2OCH_3]^+$	
116.1	$[M+H-C_9H_{12}O_5]^+$	

Fragments (m/z)	Retention time (min)	Precursor ion/Product ion	Proposed structural composition	Reference
TP 302 (m/z 302.2)	10.7	$[M+H]^+$		MetaPC software (Sedykh et al., 2001)

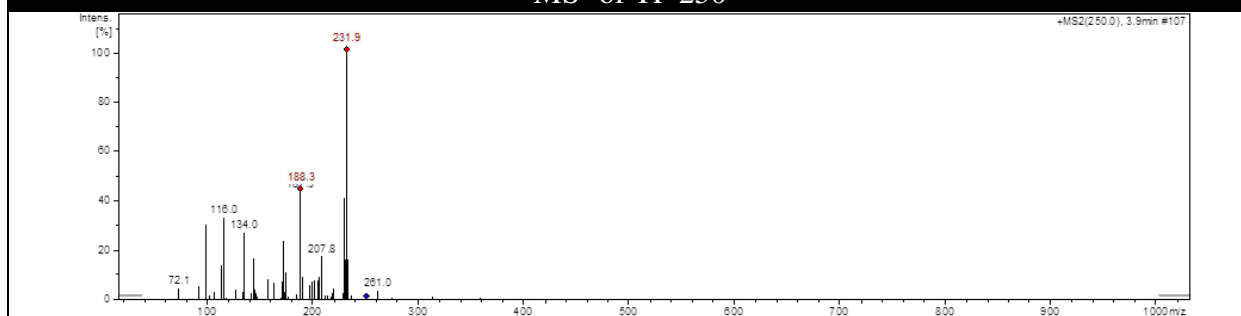


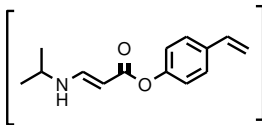
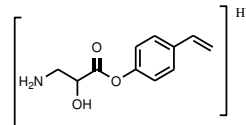
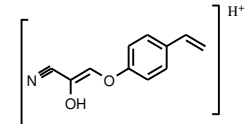
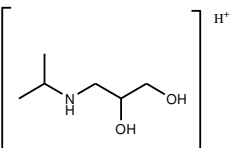
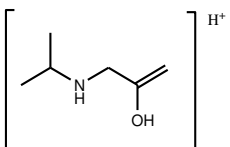
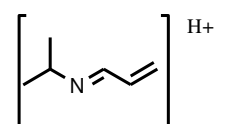


Fragments (m/z)	Retention time (min)	Precursor ion/Product ion	Proposed structural composition	Reference
TP 250 (m/z 250.0)	3.9	$[M+H]^+$	<chem>CC(C)NC(=O)C(O)C1=CC=C(C=C1)C=C</chem>	MetaPC software (Sedykh et al., 2001)

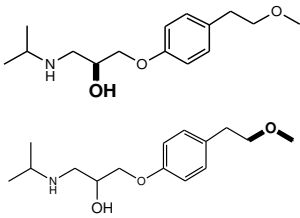
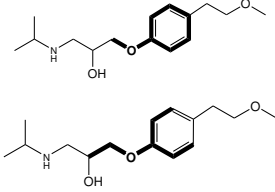
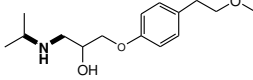
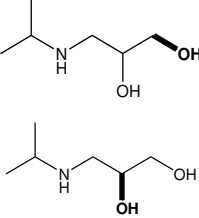
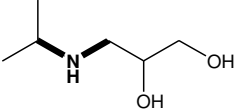
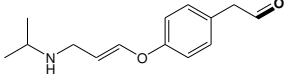
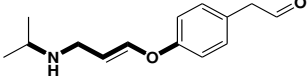


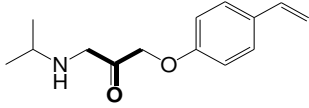
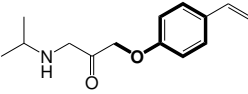
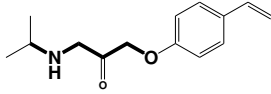
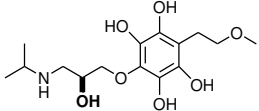
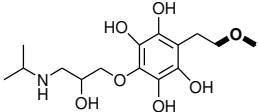
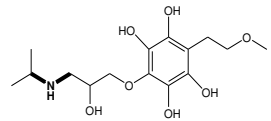
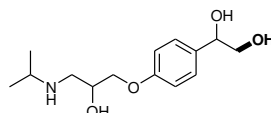
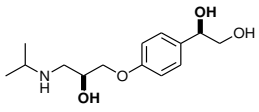
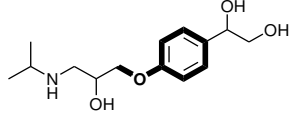
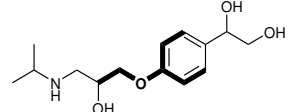
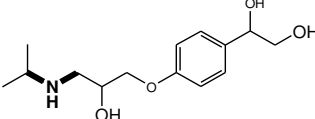
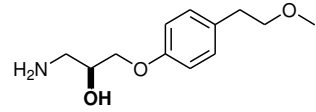
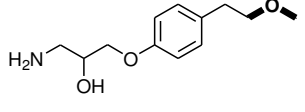
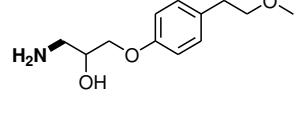
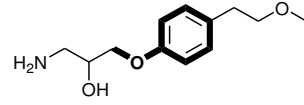
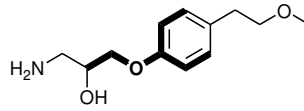
MS<sup>2</sup> of TP 250

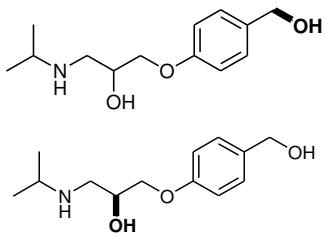
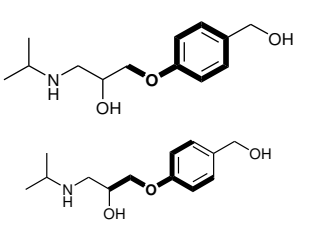
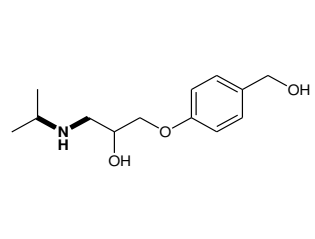
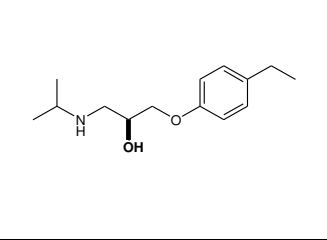
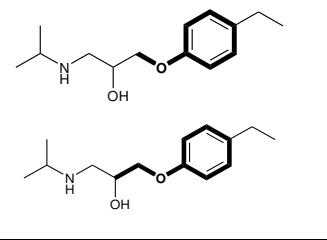
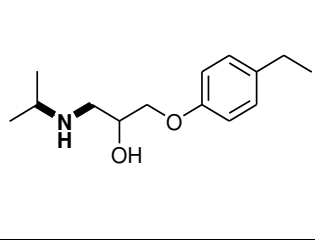
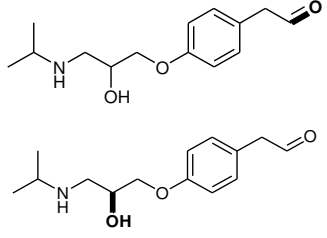
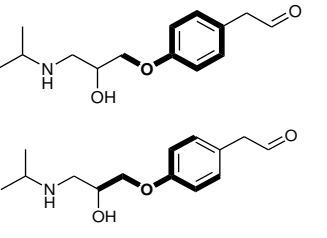
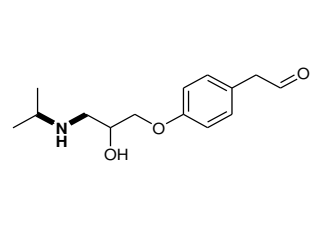
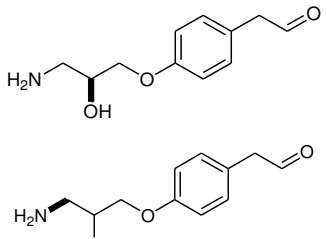
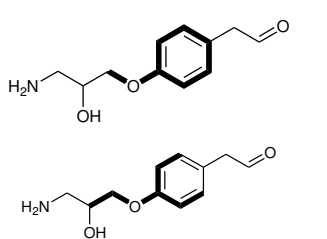



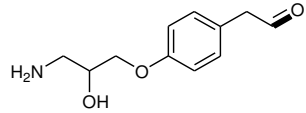
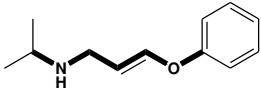
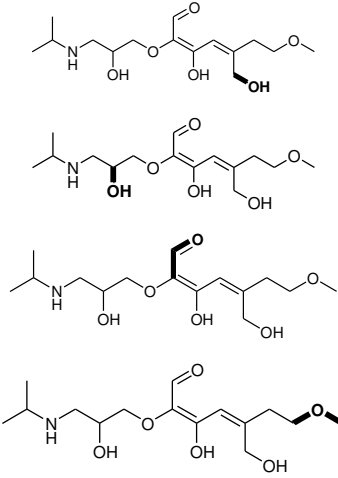
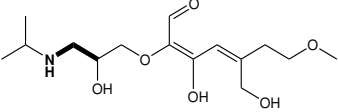
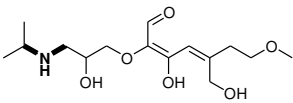
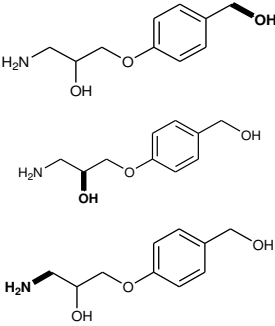
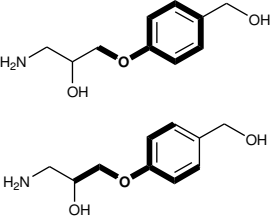
232.1	$[M+H-H_2O]^+$	
208.1	$[M+H-CH(CH_3)_2]^+$	
188.1	$[M+H-CH_2(CH_3)_2-H_2O]^+$	
134.1	$[M+H-C_8H_8O]^+$	
116.1	$[M+H-C_8H_8O-H_2O]^+$	
98.1	$[M+H-C_8H_8O-2H_2O]^+$	

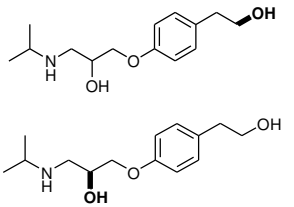
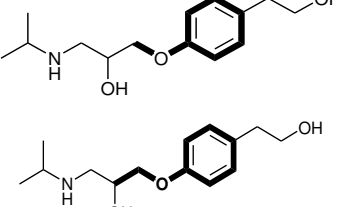
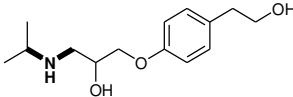
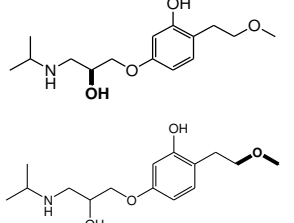
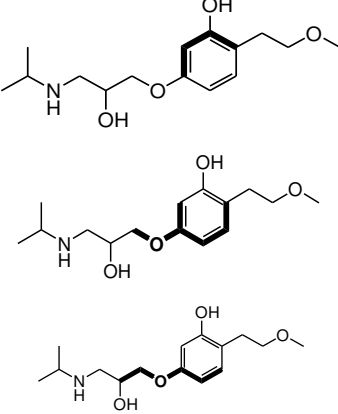
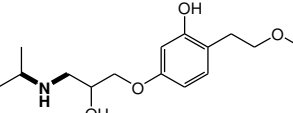
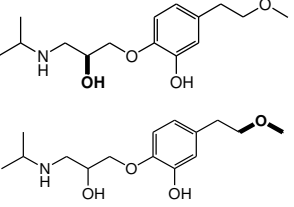
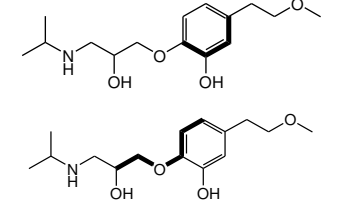
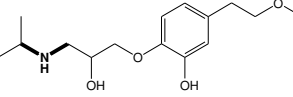
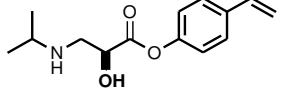
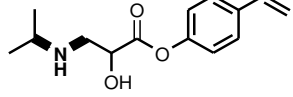
**Table S8 Supplementary Information:** QSAR predictions for Metoprolol and its derivatives (photo-TPs) for biodegradation activity by different models- 1: CATABOL 301C model under MITI test condition, 2: CATALOGIC 301C model; 3: BioWin 5 (linear model) for MITI Biodegradation probability; 4: BioWin 6 (non-linear model) for MITI Biodegradation probability; 5: Case Ultra-Readily biodegradability under MITI test (OECD 301C)

Photo-TPs	QSAR models					Multicase activating and deactivating alerts highlighted		
	1 <sup>§</sup>	2 <sup>§</sup>	3 <sup>‡</sup>	4 <sup>‡</sup>	5	Activating alert	Deactivating alert	Unknown fragment
Metoprolol	0.352	0.52	0.33	0.15	inconclusive*			
TP 134	0.54	0.75	0.67	0.75	positive			
TP <sub>1</sub> 234	0.296	0.35	0.65	0.59	inconclusive			

TP <sub>2</sub> 234	0.39	0.52	0.47	0.27	marginally positive			
TP 332	0.38	0.534	0.37	0.11	positive	 		
TP 270	0.30	0.499	0.69	0.66	inconclusive*	 	 	
TP 226	0.29	0.493	0.51	0.38	inconclusive*	  	 	

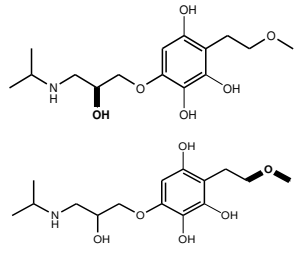
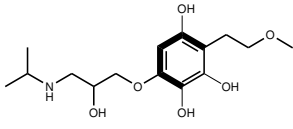
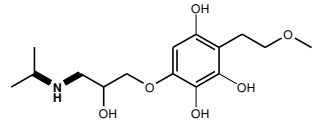
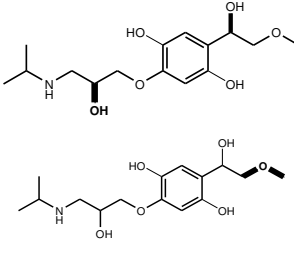
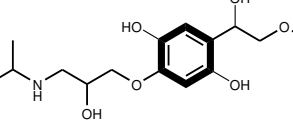
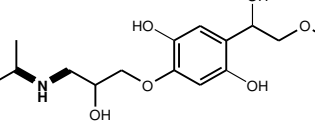
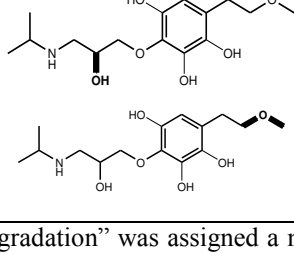
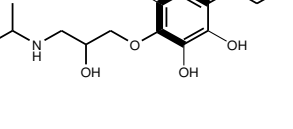
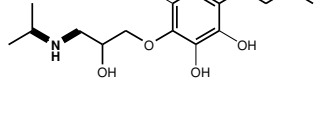
TP 240	0.41	0.555	0.53	0.43	inconclusive*			
TP 238	0.35	0.532	0.37	0.23	inconclusive*			
TP 252	0.38	0.54	0.74	0.75	inconclusive*			
TP 210	0.311	0.43	0.92	0.92	inconclusive*			

								
TP 192	0.34	0.33	0.43	0.28	OD			
TP 318	0.762	0.879	0.76	0.54	inconclusive			
TP 198	0.332	0.440	-	-	inconclusive*			

TP 254	0.38	0.54	0.53	0.44	inconclusive*			
TP <sub>1</sub> 284	0.326	0.472	-	-	inconclusive*			
TP <sub>2</sub> 284	0.376	0.543	-	-	inconclusive*			
TP 250	0.610	0.691	0.51	0.34	positive			

TP <sub>1</sub> 300	0.341	0.488	0.35	0.13	inconclusive*	
TP <sub>2</sub> 300	0.348	0.503	0.35	0.13	inconclusive*	
TP 302	0.261	0.457	0.46	0.12	positive	
TP <sub>1</sub> 316	0.623	0.796	0.36	0.13	inconclusive*	



TP <sub>2</sub> 316	0.368	0.527	0.36	0.12	inconclusive*			
TP <sub>3</sub> 316	0.383	0.526	0.51	0.27	inconclusive*			
TP <sub>4</sub> 316	0.383	0.545	0.36	0.12	inconclusive*			

§: "100% biodegradation" was assigned a numeric value of 1 and "0% biodegradation" was assigned a numeric value of 0. ‡: "Readily biodegradable" was assigned a numeric value of 1 and "not readily biodegradable" was assigned a numeric value of 0. (0 to 1 is the probability range to undergo biodegradation). Out of Domain [OD] means that the test chemical is not included in the applicability domain of the model used. 'Inconclusive' means a significant portion of the test chemical is covered by unknown structural fragment. Inconclusive with asterisk symbol (\*) means both positive and deactivating alerts were found in the same molecule and therefore a clear result cannot be given.

## References

- EPA/OPPT/Exposure Assessment Tools and Models/Estimation Program Interface (EPI) Suite Version 3.12 (August 17, 2004), 2013.  
<<http://www.epa.gov/oppt/exposure/pubs/episuite.htm>> (retrieved 10.07.13).
- Abramović, B., Kler, S., Šojić, D., Laušević, M., Radović, T., Vione, D., 2011. Photocatalytic degradation of metoprolol tartrate in suspensions of two TiO<sub>2</sub>-based photocatalysts with different surface area: Identification of intermediates and proposal of degradation pathways. *Journal of Hazardous Materials* 198, 123–132.
- Achilleos, A., Hapeshi, E., Xekoukoulotakis, N.P., Mantzavinos, D., Fatta-Kassinos, D., 2010. Factors affecting diclofenac decomposition in water by UV-A/TiO<sub>2</sub> photocatalysis. *Chemical Engineering Journal* 161, 53–59.
- Benner, J., Ternes, T.A., 2009. Ozonation of metoprolol: elucidation of oxidation pathways and major oxidation products. *Environ. Sci. Technol.* 43, 5472–5480.
- Borkar, R.M., Raju, B., Srinivas, R., Patel, P., Shetty, S.K., 2011. Identification and characterization of stressed degradation products of metoprolol using LC/Q-TOF-ESI-MS/MS and MS<sup>n</sup> experiments. *Biomed. Chromatogr.* 26, 720–736.
- Canonica, S., Meunier, L., Gunten, U. von, 2008. Phototransformation of selected pharmaceuticals during UV treatment of drinking water. *Water Research* 42, 121–128.
- Chakravarti, S.K., Saiakhov, R.D., Klopman, G., 2012. Optimizing Predictive Performance of CASE Ultra Expert System Models Using the Applicability Domains of Individual Toxicity Alerts. *J. Chem. Inf. Model.* 52, 2609–2618.
- Cherezov, V., Rosenbaum, D.M., Hanson, M.A., Rasmussen, S.G.F., Thian, F.S., Kobilka, T.S., Choi, H.-J., Kuhn, P., Weis, W.I., Kobilka, B.K., Stevens, R.C., 2007. High-resolution crystal structure of an engineered human 2-adrenergic G protein coupled receptor. *Science* 318, 1258–1265.
- Emorine, L., Marullo, S., Briend-Sutren, M., Patey, G., Tate, K., Delavier-Klutchko, C., Strosberg, A., 1989. Molecular characterization of the human beta 3-adrenergic receptor. *Science* 245, 1118–1121.
- Friedrich, J., Längin, A., Kümmerer, K., 2013. Comparison of an electrochemical and luminescence-based oxygen measuring system for use in the biodegradability testing according to Closed Bottle Test (OECD 301D). *CLEAN – Soil, Air, Water* 41, 251–257.
- Friesner, R.A., Banks, J.L., Murphy, R.B., Halgren, T.A., Klicic, J.J., Mainz, D.T., Repasky, M.P., Knoll, E.H., Shelley, M., Perry, J.K., Shaw, D.E., Francis, P., Shenkin, P.S., 2004.

- Glide: A New Approach for Rapid, Accurate Docking and Scoring. 1. Method and Assessment of Docking Accuracy. *J. Med. Chem.* 47, 1739–1749.
- Innis, R.B., Corrêa, F.M.A., Snyder, S.H., 1979. Carazolol, an extremely potent  $\beta$ -adrenergic blocker: Binding to  $\beta$ -receptors in brain membranes. *Life Sciences* 24, 2255–2264.
- Khaleel, N.D.H., Mahmoud, W.M.M., Hadad, G.M., Abdel-Salam, R.A., Kümmerer, K., 2013. Photolysis of sulfamethoxypyridazine in various aqueous media: Aerobic biodegradation and identification of photoproducts by LC-UV-MS/MS. *Journal of Hazardous Materials* 244–245, 654–661.
- Laboratory of Mathematical Chemistry, B., 2012. OASIS Catalogic software V.5.11.6TB. <<http://oasis-lmc.org/>>(retrieved 10.07.13).
- MA, B., HUANG, H.-h., CHEN, X.-y., SUN, Y.-m., LIN, L.-h., ZHONG, D.-f., 2007. Biotransformation of metoprolol by the fungus *Cunninghamella blakesleeana*. *Acta Pharmacologica Sinica* 28, 1067–1074.
- Mahmoud, W.M.M., Kümmerer, K., 2012. Captopril and its dimer captopril disulfide: Photodegradation, aerobic biodegradation and identification of transformation products by HPLC-UV and LC-ion trap-MSn. *Chemosphere* 88, 1170–1177.
- Mahmoud, W.M.M., Toolaram, A.P., Menz, J., Leder, C., Schneider, M., Kümmerer, K., 2014. Identification of phototransformation products of thalidomide and mixture toxicity assessment: An experimental and quantitative structural activity relationships (QSAR) approach. *Water Research* 49, 11–22.
- Mahmoud, W.M.M., Trautwein, C., Leder, C., Kümmerer, K., 2013. Aquatic photochemistry, abiotic and aerobic biodegradability of thalidomide: Identification of stable transformation products by LC-UV-MSn. *Science of The Total Environment* 463–464, 140–150.
- Mauriège, P., Pergola, G. de, Berlan, M., Lafontan, M., 1988. Human fat cell beta-adrenergic receptors: beta-agonist-dependent lipolytic responses and characterization of beta-adrenergic binding sites on human fat cell membranes with highly selective beta 1-antagonists. *J. Lipid Res.* 29, 587–601.
- OECD, 1992. OECD Guidelines for the Testing of Chemicals. Organisation of Economic Cooperation and Development.
- RCSB Protein Data Bank. RCSB Protein Data Bank - RCSB PDB. <<http://www.rcsb.org/pdb/home/home.do>> (retrieved 06.06.13).
- Roberts, G., Myatt, G., Johnson, W., Cross, K., Blower, P., 2000. LeadScope: Software for Exploring Large Sets of Screening Data. *J. Chem. Inf. Model.* 40, 1302–1314.

- Romero, V., La Cruz, N. de, Dantas, R.F., Marco, P., Giménez, J., Esplugas, S., 2011. Photocatalytic treatment of metoprolol and propranolol. *Catalysis Today* 161, 115–120.
- Saiakhov, R., Chakravarti, S., Klopman, G., 2013. Effectiveness of CASE Ultra expert system in evaluating adverse effects of drugs. *Mol. Inf.* 32, 87–97.
- Sedykh, A., Saiakhov, R., Klopman, G., 2001. META V. A model of photodegradation for the prediction of photoproducts of chemicals under natural-like conditions. *Chemosphere* 45, 971–981.
- Shelley, J.C., Cholleti, A., Frye, L.L., Greenwood, J.R., Timlin, M.R., Uchimaya, M., 2007. Epik: a software program for pK a prediction and protonation state generation for drug-like molecules. *J. Comput. Aided Mol. Des.* 21, 681–691.
- Sirtori, C., Agüera, A., Gernjak, W., Malato, S., 2010. Effect of water-matrix composition on Trimethoprim solar photodegradation kinetics and pathways. *Water Research* 44, 2735–2744.
- Slegers, C., Maquille, A., Deridder, V., Sonveaux, E., Habib Jiwan, J.-L., Tilquin, B., 2006. LC–MS analysis in the e-beam and gamma radiolysis of metoprolol tartrate in aqueous solution: Structure elucidation and formation mechanism of radiolytic products. *Radiation Physics and Chemistry* 75, 977–989.
- Song, W., Cooper, W.J., Mezyk, S.P., Greaves, J., Peake, B.M., 2008. Free Radical Destruction of  $\beta$ -Blockers in Aqueous Solution. *Environ. Sci. Technol* 42, 1256–1261.
- Summerhill, S., Stroud, T., Nagendra, R., Perros-Huguet, C., Trevethick, M., 2008. A cell-based assay to assess the persistence of action of agonists acting at recombinant human  $\beta$ 2 adrenoceptors. *Journal of Pharmacological and Toxicological Methods* 58, 189–197.
- Trautwein, C., Kümmerer, K., 2011. Incomplete aerobic degradation of the antidiabetic drug Metformin and identification of the bacterial dead-end transformation product Guanylurea. *Chemosphere* 85, 765–773.
- Wilde, M.L., Mahmoud, W.M.M., Kümmerer, K., Martins, A.F., 2013. Oxidation–coagulation of  $\beta$ -blockers by K<sub>2</sub>FeVIO<sub>4</sub> in hospital wastewater: Assessment of degradation products and biodegradability. *Science of The Total Environment* 452–453, 137–147.
- Yang, H., An, T., Li, G., Song, W., Cooper, W.J., Luo, H., Guo, X., 2010. Photocatalytic degradation kinetics and mechanism of environmental pharmaceuticals in aqueous suspension of TiO<sub>2</sub>: A case of [beta]-blockers. *Journal of Hazardous Materials* 179, 834–839.

# Article III

A sustainable chemistry solution to the presence of pharmaceuticals and chemicals in the aquatic environment – the example of re-designing  $\beta$ -blocker Atenolol

*RSC Advances*, 2015, 5, 27-32.

<http://dx.doi.org/10.1039/c4ra10294k>





CrossMark  
click for updates

Cite this: *RSC Adv.*, 2015, 5, 27

Received 12th September 2014  
Accepted 13th November 2014

DOI: 10.1039/c4ra10294k

www.rsc.org/advances

# A sustainable chemistry solution to the presence of pharmaceuticals and chemicals in the aquatic environment – the example of re-designing $\beta$ -blocker Atenolol†

Tushar Rastogi, Christoph Leder and Klaus Kümmerer\*

Micro-pollutants in general as well as pharmaceuticals in the environment (PIE) in particular are obstacles for sustainable chemistry and can be seen as one of the major challenges of the sustainable management of water resources and a threat to health, water and food safety. Recent research has shown that this problem cannot be solved with advanced effluent treatment. Therefore, new approaches are urgently needed. This includes the new design of molecules or the re-design of existing molecules that present the functionality needed for their application and that are improved with regards to their biodegradability in the environment after their intended use. This paper presents a new approach for generating, identifying and testing biodegradable and drug-like molecules.

Micro-pollutants have gained much attention in the scientific community. They are increasingly seen as one of the major challenges to the sustainable management of water resources and a threat to health, water, and food safety. Due to their targeted design for bioactivity and stability, pharmaceuticals are the main cause of micro-pollutants to the aquatic environment.<sup>1–4</sup> The most extensively discussed strategies for the prevention of the input of pharmaceuticals into the aquatic environment are advanced effluent treatment processes. However, these advanced effluent treatment processes have their own specific limitations and drawbacks such as the formation of toxic and stable reaction products and their very limited possibility of application on the global scale.<sup>5–7</sup>

The tenth principle of green chemistry is ‘Design for Degradation’.<sup>8</sup> This means that ‘Chemical products should be designed so that at the end of their function they break down into innocuous degradation products and do not persist in the

environment’ as stated by the American Chemical Society on their webpage.<sup>9</sup> In other words, the goal is to design pharmaceutically active ingredients (APIs) that can mineralize at a reasonable rate and more or less completely in normal effluent treatment and in the aquatic environment. The concept of the benign by design is the key element in this respect.<sup>10,11</sup> It is an important concept within green and sustainable pharmacy and chemistry and very promising in terms of sustainability.<sup>12</sup> The concept of benign by design can be applied on two levels: the design of completely new molecules or the re-design of existing molecules. In both cases, small alterations in the chemical structure of an API may have a significant impact on the one hand, on its activity, solubility and polarity and on the other hand on biodegradability. Therefore it is reasonable to assume that a set of functionalities exists that can foster both and need to be explain in detail. Re-designing such biodegradable drugs is a challenge that is addressed in the research presented here.

The present study focuses on the re-design of the existing API  $\beta$ -blocker Atenolol (ATL), a selective  $\beta_1$  blocker and reported to be largely excreted as unchanged from the human body.<sup>13</sup> In 2012, 45.7 million defined daily dose (DDD) of ATL [accounting for 75 mg of pure ATL taken either oral or parenteral<sup>14</sup>] were prescribed in Germany.<sup>15</sup> This corresponds to a total amount of 3.43 tonnes of ATL consumed by individuals in Germany who were insured by public health insurance in 2012. ATL is not biodegradable and has been frequently detected in the aquatic environment including drinking water at concentrations up to  $120 \mu\text{g L}^{-1}$ .<sup>2</sup>

Atenolol was used as an example to incorporate the additional attribute biodegradability while preserving its substructures responsible for  $\beta$  adrenergic receptor blocker activity. An aromatic ring and a  $\beta$ -ethanolamine moiety are considered essential substructures of  $\beta$ -blockers responsible for their receptor blocking activity.<sup>16,17</sup>

The very first step in designing biodegradable  $\beta$ -blocker derivatives is to generate new molecules that possess substructures (both aromatic ring and  $\beta$ -ethanolamine) responsible for their specific action as  $\beta$ -blockers. New drug-like

*Institute of Sustainable and Environmental Chemistry, Leuphana University Lüneburg, C13, DE-21335 Lüneburg, Germany. E-mail: tushar.rastogi@leuphana.de; tushar1909@gmail.com; cleder@leuphana.de; Klaus.Kuemmerer@uni.leuphana.de; Tel: +49 4131 677 2893*

† Electronic supplementary information (ESI) available: Experimental procedures, LC-MS/MS data and spectra of the derivatives, QSAR prediction, biodegradation study results. See DOI: 10.1039/c4ra10294k

derivatives (photo-transformation products, photo-TPs) were generated by direct photolysis of ATL with no pre-treatment and no other oxidizing agents in order to exclude any other constituents that could interfere with the formation of derivatives (photo-TPs). Photolysis of ATL resulted in numerous derivatives. The kinetics of formation of derivatives (photo-TPs) and proposed molecular structures and reaction pathways were elucidated by ion-trap LC-MS/MS and by using the photo-degradation dictionary of *in silico* MetaPC software (MultiCASE Inc.). *In silico* predicted molecular structures were compared to the corresponding MS/MS spectra measured by LC-ESI-MS<sup>n</sup> (ion-trap).

In the next step, aerobic biodegradation tests (Closed Bottle Test [CBT] OECD 301D<sup>18</sup> and the Manometric Respiratory Test [MRT] OECD 301 F<sup>19</sup>) were applied to the resulting mixture of photolytic treatment for the assessment of the derivatives' biodegradability in the environment. CBT was employed because it is the most stringent biodegradation test with low bacterial density and diversity in order to avoid any false positive results. Thereby, the derivatives (photo-TPs) that had improved biodegradability compared to the parent compound and that still possessed an aromatic ring and a  $\beta$ -ethanolamine moiety were selected. The ones that were found to be biodegradable were further assessed with the help of QSAR tools in order to get further insights.

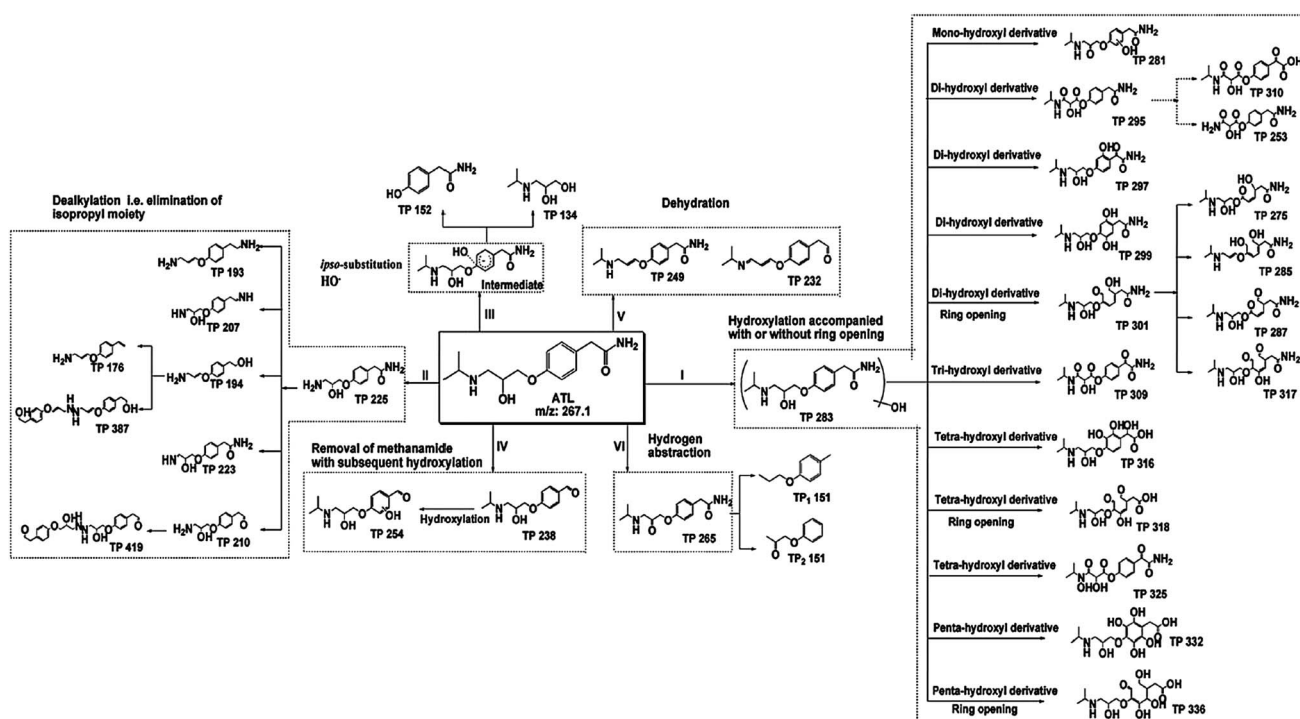
In addition, the detainment of the drug-like properties (absorption, distribution, metabolism and excretion; ADME) of the better biodegradable derivatives (photo-TPs) that retained the aromatic ring and a  $\beta$ -ethanolamine moiety similar to ATL were investigated. The final step was an *in silico* toxicity assessment of those biodegradable and drug-like derivatives.

**Proposed structures of derivatives:** The structures as well as reaction pathways are illustrated in Scheme 1. Six major pathways were found to be involved in the formation of the derivatives:

(I) The observed major pathway was hydroxylation by the attack of electrophilic hydroxyl radical ( $\text{HO}^\bullet$ ) at the aromatic ring of ATL molecule, which was also reported by Ji *et al.*<sup>20</sup> However, Medana *et al.*<sup>21</sup> mentioned that the attack of  $\text{HO}^\bullet$  on the benzene ring of ATL is preferred, but not limited to it. This could be the reason for the formation of various derivatives such as TP 295, TP 310, *etc.* Further attack of  $\text{HO}^\bullet$  on mono-hydroxyl derivatives of ATL (TP 283) results in the formation of di-, tri-, tetra- and even penta-hydroxyl derivatives of ATL, as shown in Scheme 1.  $\text{HO}^\bullet$  attack on the benzene ring often leads to ring opening, which results in the formation of two aldehyde moieties or an aldehyde and an alcohol moiety, respectively.<sup>22</sup> The derivatives that were found, such as TP 275, TP 285, TP 317, TP 318 and TP 336 are likely to be formed through this proposed mechanism.

(II) Another pathway observed during photolysis was dealkylation, *i.e.* cleavage of isopropyl moiety from the isopropyl-amino-propoxy side chain of ATL, which results in the formation of TP 225, as shown in Scheme 1. The subsequent elimination of  $\text{NO}_2$  from TP 225 through the formation of a nitroso intermediate could lead to the formation of TP 210.<sup>23</sup> TP 225 could also be a precursor of TP 193; TP 207; TP 223 and TP 194. Coupling reactions were observed, reaction that resulted in the formation of dimers of TP 194 and TP 210 as TP 387 and TP 419, respectively (Scheme 1).<sup>23</sup>

(III) An *ipso* substitution of  $\text{HO}^\bullet$  on a carbon atom of the aromatic ring<sup>20</sup> resulted in an intermediate radical (resonance-



Scheme 1 Proposed pathways of the generation of derivatives (photo-TPs).



stabilized carbon-centered radical) which later resulted in derivatives such as TP 134 and TP 152, as shown in Scheme 1.

(IV) The loss of the methanamide radical ( $\text{CONH}_2^\cdot$ ) from the acetamide side chain of ATL was observed, which finally was oxidized to benzaldehyde and resulted in TP 238. Further electrophilic  $\text{HO}^\cdot$  attack either on the *ortho*- and *meta*-position of aromatic ring of TP 238 resulted in a hydroxylated benzaldehyde derivative TP 254 (Scheme 1).

(V) Another pathway could be the dehydration, *i.e.* elimination of water from the isopropyl-amino-propoxy side chain of ATL, as shown in Scheme 1. This mechanism would result in the formation of TP 249, which was also reported as UVA-UVB photo-TP of ATL.<sup>24</sup> Removal of the amino group from the acetamide side chain of TP 249 through the formation of a nitroso intermediate result in TP 232.

(VI) The pathway leading to TP 265 could be hydrogen abstraction from the alcoholic moiety of the isopropyl-amino-propoxy side chain. TP 265 broke down further to TP<sub>1&2</sub> 151 during photolysis (Scheme 1).

**Biodegradability:** The LC-MS analysis of sterile controls of MRT indicates that ATL was not abiotically eliminated, *e.g.* by hydrolysis, sorption *etc.* Samples from the start and the end of both biodegradation tests were analyzed through LC-UV-MS/MS, as illustrated in Fig. S3 (in ESI<sup>†</sup>). Both biodegradation tests, CBT and MRT, classified ATL as not readily biodegradable chemical. The LC-MS/MS analysis confirmed that ATL was not transformed or eliminated during biodegradation tests. These findings are in accordance with the presence of ATL in the aquatic environment. However, it was found that a few of the formed derivatives (summarized in ESI Table S6<sup>†</sup>) were better biodegradable than ATL.

Biodegradable derivatives were then analyzed *in silico* by QSAR models (summarized in Table S5 in ESI<sup>†</sup>) for ready biodegradability to get a further insight of the structural alterations. The software package Case Ultra (Multicase Inc.) identifies the structural changes in the derivatives (photo-TPs) molecules that would modulate their biodegradability. The predictions and moieties of the derivatives that increase or reduce biodegradability are summarized in Table S9 in ESI<sup>†</sup>. This knowledge contributes to a better understanding of processes, which in turn could be the basis of a rational design of better biodegradable compounds in the future in accordance with the benign by design approach.

Case Ultra software predicted that the methoxybenzene moiety at the aromatic ring weakens the biodegradability of ATL, as shown in Scheme 2. It also predicted moieties such as an OH group attached to the  $\beta$ -carbon of the ethanolamine side chain and the acetyl moiety on the acetamide side chain to assist biodegradability (Scheme 2). Moreover, the derivatives (photo-TPs) that were predicted to be better biodegradable were the same ones which were observed to be, according to analytical results, better biodegradable than ATL in the biodegradation test assays. Additionally, other moieties in the derivatives (photo-TPs) molecule such as alcohol, ketone, aldehyde and amine functionalities were predicted by Case Ultra software to foster biodegradability. This is also in accordance with the general understanding for biodegradability.<sup>12,25</sup>

The structural alterations at the aromatic ring and side chains of ATL during photolysis that modulated the biodegradability of derivatives (photo-TPs) are summarized below.

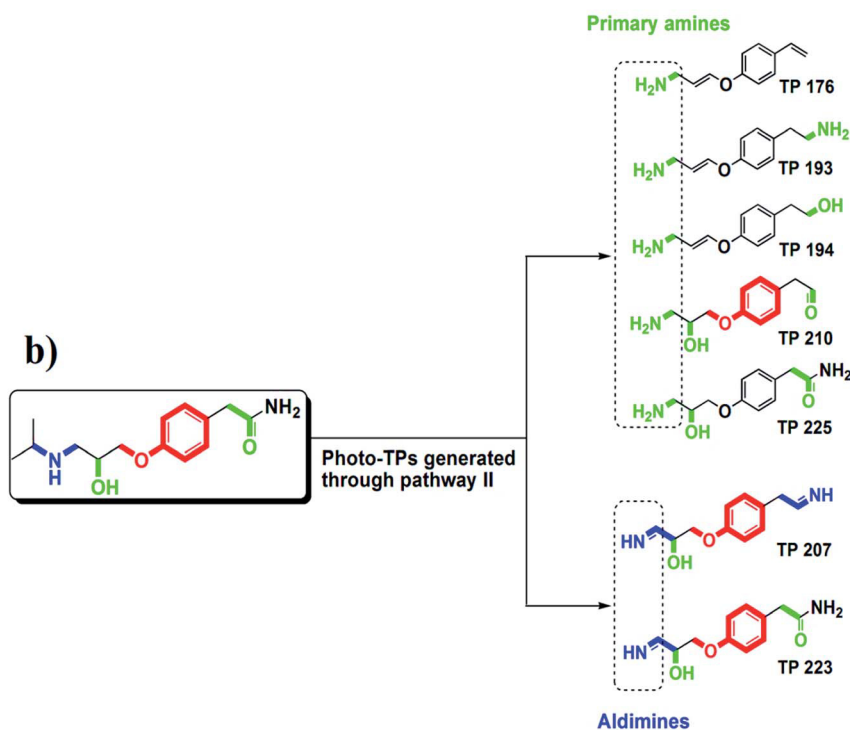
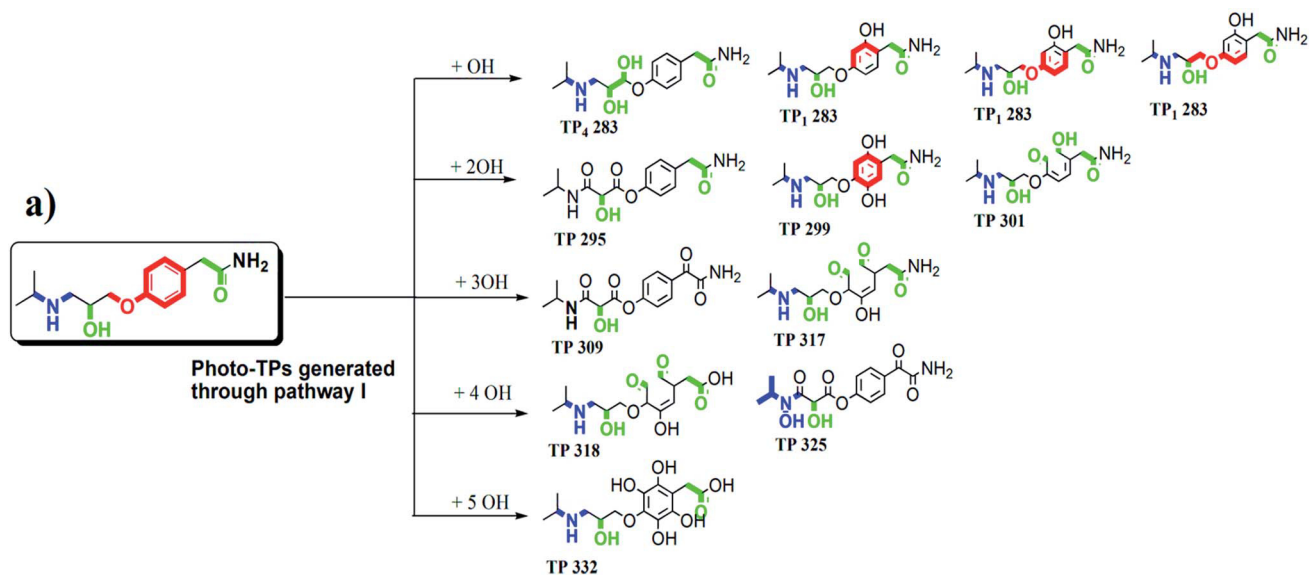
**Changes at the benzene ring:** It was observed that the methoxybenzene moiety that weakens biodegradability was altered during photolysis of ATL, which resulted in the modulation of the biodegradability of the respective derivatives (photo-TPs). This alteration was mainly due to the attachment of functionalities like hydroxyl groups on a benzene ring according to the proposed photo-transformation pathway I *i.e.* hydroxylation (Scheme 2a). This phenomenon can be explained by the fact that the attachment of electron donating functionalities like oxygen or amine to the aromatic ring of the molecule often increases the aerobic biodegradability of the molecule whereas the attachment of electron withdrawing functionalities do reduce it.<sup>26,27</sup>

The attachment of hydroxyl groups at the aromatic ring of ATL was often accompanied by ring-opening, which results in the formation of moieties such as alcohols and aldehydes that assist biodegradability. These modifications in the structure of derivatives such as TP 301, TP 317 and TP 318 provided a positive alert for biodegradation, as shown in Scheme 2a. This phenomenon *i.e.* the opening of the benzene ring due to the attachment of hydroxyl groups is considered the first step of aerobic biodegradation of aromatic compounds, which first turned into alcohols and acids and then subsequently mineralizes.<sup>28,29</sup>

The di-substitution of hydroxyl groups on the benzene ring of ATL without ring opening resulted into *p*-OH phenol moiety for TP 299 (Scheme 2a). This *p*-OH phenol moiety of TP 299 was predicted to deter biodegradability, which is in accordance with the fact that substitutions of OH,  $\text{NO}_2$ ,  $\text{NH}_2$ ,  $\text{CH}_3$  and Cl groups at *o*- or *p*-position of a phenol alter the biodegradable phenol moieties to non-biodegradable substituted phenol.<sup>30</sup>

**Changes at the side chains:** When a hydroxyl group was attached to an  $\alpha$ -carbon atom of the isopropyl-amino-propoxy side chain by replacing the hydrogen atom as in TP<sub>4</sub> 283, the predicted moiety that weakens the biodegradability of ATL molecule was completely lost, and a new moiety was formed. This new moiety in TP<sub>4</sub> 283 was predicted to assist biodegradation (Scheme 2a). Moieties that were predicted to reduce biodegradability of ATL were lost when two electron donating functionalities like oxygen were attached at the  $\alpha$ - and  $\gamma$ -carbon atoms of the propoxy side chain as in TP 295 (Scheme 2a). The addition of three oxygen atoms to isopropyl-amino-propoxy and acetamide side chains of ATL (as in TP 309 and TP 325) also altered the biodegradability reducing moieties of ATL into the biodegradability assisting moieties.

The second major photo-transformation pathway that could be assumed to alter the biodegradability of the derivatives was pathway II *i.e.* dealkylation. The dealkylation pathway resulted in primary amines and aldimines derivatives. Scheme 2b shows the structural changes due to the photo-transformation pathway II in an ATL molecule, which would assist the biodegradability of the resulting derivatives. The primary amine moiety (in TP 176, TP 193, TP 194, TP 210 and TP 225) that was



- Red:** Moieties lowering biodegradability of the molecule  
**Green:** Moieties increasing biodegradability of the molecule  
**Blue:** Moieties recognized as unknown structure i.e. not included in the applicability domain of the model

**Scheme 2** Observed structural changes responsible for the improved biodegradability of derivatives (photo-TPs) generated through (a) pathway I i.e. hydroxylation; (b) pathway II i.e. dealkylation.

formed was predicted to be responsible for the biodegradation, as shown in Scheme 2b. This is in accordance with the observation that primary amines are considered to be easily and rapidly biodegraded through the alkyl amine dehydrogenase pathway during biodegradation.<sup>31</sup> TP 207 and TP 223 had the aldimine moiety that could not be classified by the software, as this functionality is not included in the applicability domain of

the model. Therefore, no reliable prediction is possible for these derivatives.

In general, it is difficult to quantify the effect of one certain structural alteration on biodegradability in total. However, the experimental results and QSAR predictions as well as the results of the other studies indicate that there are structural alterations that foster biodegradability. Therefore, the results presented

here can serve as a good starting point for the rational design of improved biodegradable compounds.

**Assessment of drug-likeness:** The software package Schrödinger QikProp 3.8 (Schrödinger, LLC) was employed for this assessment. It predicts the drug-likeness of the derivatives according to their ADME (absorption, distribution, metabolism and excretion) properties, which are described in detail as Text S5 in ESI.† The QikProp predictions for the drug-likeness of the observed biodegradable derivatives are summarized in Table S7 in ESI.†

Biodegradable derivatives such as TP 176, TP 193 and TP 194 lack the  $\beta$ -ethanolamine moiety, which is an indispensable substructure of the pharmacophore of  $\beta$ -blockers. Therefore, these three derivatives were not further considered. QikProp software predicted that derivatives like TP 225, TP<sub>1-7</sub> 283, TP<sub>1</sub> 295, TP 299, TP<sub>2</sub> 309 and TP 325 to be drug-like but less orally available. This means that these derivatives also had to be omitted and that they were not considered for the further development of new ATL derivatives.

The biodegradable derivatives such as TP<sub>1-6</sub> 301, TP 317, and TP 318, which were formed by the opening of the aromatic ring due to the attachment of hydroxyl group, were predicted to be less drug-like and less orally available. These derivatives (photo-TPs) also lack the other essential substructure (benzene ring) responsible for their specific action as  $\beta$ -blockers. Therefore, these derivatives were also not further considered due to their unsatisfactory ADME properties prediction and activity.

The results show that remaining biodegradable derivatives such as TP 207, TP 210, TP 223, TP 238 and TP<sub>2</sub> 295 were predicted to be drug-like and orally available (Table S7, ESI†). These derivatives also possess both essential substructures (aromatic ring and  $\beta$ -ethanolamine) of  $\beta$ -blockers. Thus, it can be concluded that the attachment or the removal of certain groups from either one of the side chains might not change the drug-likeness while opening of the aromatic ring decreases the drug-likeness and oral availability of the derivatives. Thus, derivatives such as TP 207, TP 210, TP 223, TP 238 and TP<sub>2</sub> 295 might be considered to be the leading candidates for biodegradable drug-like molecules.

**Toxicity assessment:** Another important prerequisite for drug-like substances and APIs is that they should not be toxic. First of all, mutagenicity, genotoxicity and carcinogenicity have to be absent. Therefore, *in silico* predictions for these toxicity endpoints for the leading candidates (biodegradable drug-like derivatives) of ATL were performed by employing the QSAR toxicity models summarized in Table S5 in ESI.† The predictions of these QSAR models are summarized in Table S10 in ESI.†

The predictions indicate that some of the leading candidates such as TP 207, TP 210, TP 223 and TP 238, as shown in Fig. 1, are possibly neither carcinogenic, genotoxic nor mutagenic in mammals, while TP<sub>2</sub> 295 was predicted to be a carcinogenic. Therefore, TP<sub>2</sub> 295 will not be considered to be a leading candidate for the development of new biodegradable ATL-derived entities anymore. However, the chromosome aberration model of Leadscape software provided a positive alert for all of the leading candidates mentioned above. Therefore, the next step would be to synthesize all

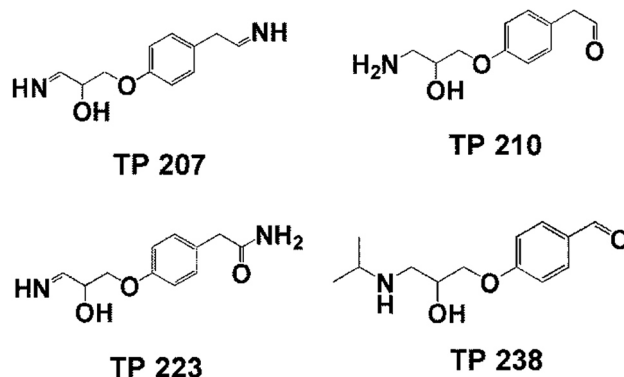


Fig. 1 The shortlisted leading candidates, which were comparatively biodegradable and predicted to be drug-like, orally available, non-carcinogenic, non-genotoxic and non-mutagenic.

these shortlisted biodegradable drug-like leading candidates and test them through various experimental assays to confirm the toxicity prediction and to investigate their pharmacological potency.

Fig. 1 summarizes the leading candidates which are observed to be comparatively more biodegradable, drug-like and non-toxic. However, some of these shortlisted derivatives possess non-preferred functional groups such as aldehydes (non-preferred due to their toxicological potency and adverse effect in the human body) or imines (non-preferred due to their instability). Therefore, a comprehensive study is needed for the pharmacological, pharmacokinetic and toxicological assessment of these leading derivatives.

The limitation of this approach for re-designing ATL into biodegradable derivatives is the uncertainty of the pharmacological potency of the modified structures, which needs to be further investigated. However, a similar approach of re-designing existing pharmaceuticals was recently demonstrated for the alternative  $\beta$ -blocker Metoprolol.<sup>32</sup> This study concluded that it was possible to design new drug-like molecules of Metoprolol, which might have similar or non-inferior pharmacological properties with the additional attribute of biodegradability through small alterations of its structure during photolysis. Therefore, a thorough investigation of the pharmacological potency of the new derivatives of ATL is critically required. In addition, in the present study, photolysis was used as a method for the generation of derivatives, but other derivatisation processes (such as ozonation, Fenton reaction *etc.*) are the possible alternatives for the future studies.

Furthermore, the approach presented here can be used to re-design existing pharmaceuticals as demonstrated, though it has to be confirmed with various other pharmaceuticals before being generalized. Further, it could be integrated into the lead optimization process of drug development as an addition to the pre-clinical development of novel pharmaceuticals. However, this was not the task of this initial work and this integration has to be explored in further studies.

## Conclusions

Generally, studies like this will increase the knowledge about the role of the attachment of certain functionalities to the parent drug in order to improve its biodegradability while conserving pharmacological properties, an approach that was, in the past, neglected issue in drug development. A future goal should be to perform more of such studies with several other known pharmaceuticals in order to deepen the understanding concerning the approach as well as in order to understand the significance of the different functional groups that could alter the both biodegradability and activity of APIs.

## Acknowledgements

The financial support from the German Ministry of Education and Research (NanoPharm, Project no. 03X0094C) is gratefully acknowledged. The authors also acknowledge Multicase Inc. and Leadscope Inc. for kindly providing the Case Ultra, MetaPC as well as the Leadscope QSAR software.

## Notes and references

- Emerging Contaminants from Industrial and Municipal Waste, in *Handbook of environmental chemistry*, ed. D. Barceló, M. Petrovic and A. G. Kostianoy, Springer, Berlin, 2008, vol. 5.
- L. H. M. L. M. Santos, A. N. Araújo, A. Fachini, A. Pena, C. Delerue-Matos and M. C. B. S. M. Montenegro, *J. Hazard. Mater.*, 2010, **175**, 45.
- I. Michael, L. Rizzo, C. S. McArdell, C. M. Manaia, C. Merlin, T. Schwartz, C. Dagot and D. Fatta-Kassinos, *Water Res.*, 2013, **47**, 957.
- K. Kümmerer, *Annu. Rev. Environ. Resour.*, 2010, **35**, 57.
- O. A. H. Jones, P. G. Green, N. Voulvoulis and J. N. Lester, *Environ. Sci. Technol.*, 2007, **41**, 5085.
- H. Wenzel, H. F. Larsen, J. Clauson-Kaas, L. Høiby and B. N. Jacobsen, *Water Sci. Technol.*, 2008, **57**, 27.
- Pharmaceuticals in the Environment: Sources, Fate, Effects and Risks*, ed. K. Kümmerer, Springer-Verlag, Berlin, Heidelberg, 5th edn, 2008.
- P. T. Anastas and J. C. Warner, *Green chemistry: Theory and practice*, Oxford Univ. Press, New York, 1998, p. 30.
- American Chemical Society, *12 Principles of Green Chemistry*, 2014, <http://www.acs.org/content/acs/en/greenchemistry/what-is-green-chemistry/principles/12-principles-of-green-chemistry.html>.
- K. Kümmerer, *Green Chem.*, 2007, **9**, 899.
- K. Kümmerer, in *Handbook of Green Chemistry, Green Processes, Designing Safer Chemicals*, ed. P. T. Anastas, R. Boethling and A. Votchkova, Wiley-VCH, Weinheim, 2012, p. 215.
- K. Kümmerer, in *Green and sustainable pharmacy*, ed. K. Kümmerer and M. Hempel, Springer, Berlin, Heidelberg, 2010, p. 135.
- P. R. Reeves, J. McAinsh, D. A. McIntosh and M. J. Winrow, *Xenobiotica*, 1978, **8**, 313.
- WHO – ATC/DDD Index 2014, [http://www.whocc.no/atc\\_ddd\\_index/?code=C07AB03](http://www.whocc.no/atc_ddd_index/?code=C07AB03), 2014.
- Arzneiverordnungs-Report 2013: Aktuelle Daten, Kosten, Trends und Kommentare*, ed. U. Schwabe and D. Paffrath, Springer-Verlag, Berlin, Heidelberg, 2013.
- A. Gringauz, *Introduction to medicinal chemistry: How drugs act and why*, Wiley-VCH, New York, 1997.
- F. Gorre and H. Vandekerckhove, *Acta Cardiol.*, 2010, **65**, 565.
- OECD, *OECD Guidelines for the Testing of Chemicals: Ready Biodegradability 301D: Closed Bottle Test*, OECD Pub., 1992.
- OECD, *OECD Guidelines for the Testing of Chemicals: Ready Biodegradability 301F: Manometric Respiratory Test*, OECD Pub., 1992.
- Y. Ji, L. Zhou, C. Ferronato, X. Yang, A. Salvador, C. Zeng and J.-M. Chovelon, *J. Photochem. Photobiol., A*, 2013, **254**, 35.
- C. Medana, P. Calza, F. Carbone, E. Pelizzetti, H. Hidaka and C. Baiocchi, *Rapid Commun. Mass Spectrom.*, 2008, **22**, 301.
- J. Benner and T. A. Ternes, *Environ. Sci. Technol.*, 2009, **43**, 5472.
- M. L. Wilde, W. M. M. Mahmoud, K. Kümmerer and A. F. Martins, *Sci. Total Environ.*, 2013, **452–453**, 137.
- V. Andrisano, R. Gotti, A. Leoni and V. Cavrini, *J. Pharm. Biomed. Anal.*, 1999, **21**, 851.
- R. S. Boethling, E. Sommer and D. DiFiore, *Chem. Rev.*, 2007, **107**, 2207.
- P. H. Howard, in *Handbook of property estimation methods for environmental chemicals: Environmental and health sciences*, ed. D. Mackay and R. S. Boethling, Lewis Publishers, Boca Raton, 2000, p. 281.
- P.-G. Rieger, H.-M. Meier, M. Gerle, U. Vogt, T. Groth and H.-J. Knackmuss, *J. Biotechnol.*, 2002, **94**, 101.
- C. Lyons, S. Katz and R. Bartha, *Appl. Environ. Microbiol.*, 1984, **48**, 491.
- S. F. Nishino and J. C. Spain, *Environ. Sci. Technol.*, 1993, **27**, 489.
- F. Wang and J. Shi, *Bull. Environ. Contam. Toxicol.*, 2012, **89**, 316.
- C. G. Ginkel, A. Louwerse and B. Togh, *Biodegradation*, 2008, **19**, 129.
- T. Rastogi, C. Leder and K. Kümmerer, *Chemosphere*, 2014, **111**, 493.

## Supporting Information

for

### **A Sustainable Chemistry Solution to the Presence of Pharmaceuticals and Chemicals in the Aquatic Environment- the Example of Re-Designing $\beta$ -blocker Atenolol**

**Tushar Rastogi, Christoph Leder, Klaus Kümmerer\***

*Sustainable Chemistry and Material Resources, Institute of Sustainable and Environmental Chemistry,  
Leuphana University Lüneburg, C13, DE-21335 Lüneburg, Germany*

---

\* Corresponding author email address: [Klaus.Kuemmerer@uni.leuphana.de](mailto:Klaus.Kuemmerer@uni.leuphana.de)

## Table of Contents

Text S1 Supporting Information: Generation of photo-transformation products (photo TPs) of ATL and characteristics of UV lamp .....	1
Text S2 Supporting Information: Analytical method parameters for chromatography and identification of derivatives (photo-TPs) of Atenolol (ATL).....	3
Text S3 Supporting Information: Principles and procedure of the investigated aerobic biodegradation tests.....	5
Text S4 Supporting Information: Detailed description and output from various <i>in silico</i> models used in the present study.....	7
Text S5 Supporting Information: Detailed description of the drug-likeness prediction software QikProp 3.8. ....	11
Text S6 Supporting Information: Results of photolysis and generation of derivatives (photo-TPs) of ATL. ....	13
Figure S2 Supporting Information: Aerobic biodegradation results of ATL and its derivatives (photo-TPs).....	16
Figure S3 Supporting Information: LC-MS analysis of biodegradation test samples for photo TPs at the beginning and the end of the tests, respectively: a) CBT; b) MRT; c) Atenolol in CBT and MRT.....	17
Table S6 Supporting Information: Summary of the results of investigated aerobic biodegradability test for Atenolol and its derivatives mixture.....	18
Table S7 Supporting Information: <i>In silico</i> drug-likeness prediction of the biodegradable derivatives (photo-TPs) of Atenolol through the ADME prediction software QikProp .....	19
Table S8 Supporting Information: The proposed structures of the fragments formed during the MS <sup>2</sup> fragmentation for Atenolol and its derivatives (photo-TPs) .....	20
Table S9 Supporting Information: QSAR predictions for Atenolol and its derivatives (photo-TPs) for biodegradability different models .....	61
Table S10 Supporting Information: <i>In silico</i> toxicity prediction by different QSAR models of Case Ultra, Leadscope and OASIS Catalogic for Atenolol and its biodegradable derivatives	73
Reference.....	76

**Text S1 Supporting Information:** Generation of photo-transformation products (photo TPs) of ATL and characteristics of UV lamp

### **Test procedure**

Photolysis: ATL was dissolved in ultrapure water for direct photolytic experiments with no pre-treatment in order to exclude any other constituents that could interfere with the formation of derivatives and/or to avoid the initiation of scavenger effects of any absorbing or photosensitizing chemical or other species during degradation. Photolysis of ATL was performed in a 1L batch photo reactor irradiated by 150 W medium-pressure mercury lamp (TQ150, UV Consulting Peschl, Mainz) with Ilmasil quartz immersion tube as described elsewhere in detail.<sup>1,2</sup> The batch photo reactor was provided with constant stirring and the temperature in the reactor was maintained between 18-20 °C through temperature control by a circulating cooler (WKL230, LAUDA, Berlin).

Sampling: In order to monitor the kinetics of transformation and mineralization of ATL, samples (20 mL) were collected after 2, 4, 8, 16, 32, 64, 128 and 256 min of irradiation time respectively. The primary elimination of ATL and formation of photo-transformation products (photo-TPs) was monitored by HPLC-UV-Vis and LC-ESI-MS<sup>n</sup> (ion-trap), respectively.

## Characteristics of UV lamp

According to the manufacturer, the total radiation flux  $\Phi$  from 200 nm to 600 nm is  $47 \text{ W m}^{-2}$  and the maximal intensities for whole spectral distribution were at following wavelengths

**Table S1 Supporting Information:** The maximal intensities at following of medium pressure mercury lamp TQ 150 (as provided by manufacturer)

Wavelength (nm)	Intensities ( $\text{W m}^{-2}$ )
254	4.0
265	1.4
302	1.8
313	4.3
366	6.4
405/408	3.2
436	4.2
546	5.1
577/579	4.7



**Text S2 Supporting Information:** Analytical method parameters for chromatography and identification of derivatives (photo-TPs) of Atenolol (ATL)

**HPLC method for the elution of ATL:**

A Shimadzu Prominence HPLC system (Duisburg, Germany) was used to measure the elimination of ATL. A NUCLEODUR<sup>®</sup> RP-C18 (CC 125/4 100-5 $\mu$ m C18 ec) column and mobile phases consisting of 0.1 % formic acid in ultrapure water (CH<sub>2</sub>O<sub>2</sub>: solution A) and 100 % acetonitrile (CH<sub>3</sub>CN: solution B) were used for the chromatographic separation. The flow rate, column oven temperature and injection volume was set to 0.5 mL min<sup>-1</sup>, 25 °C and 50  $\mu$ L, respectively. ATL eluted at retention time [ $t_R$ ] 10.9 min. High linearity correlation [ $r^2 \geq 0.9999$ ] was obtained for calibration curve range from 0.0978  $\mu$ g mL<sup>-1</sup> to 200  $\mu$ g mL<sup>-1</sup>. A gradient flow method was used as describe in Table S2.

**Table S2 Supporting Information:** Gradient flow condition used to achieve the desired separation

Time (min)	%B (Acetonitrile)
0.01 to 2 min	1
2 to 27 min	1% - 65% B
27 to 29 min	65% - 20% B
29 to 30 min	20% - 1% B
30 to 32 min	1% B
32.01	stop

**MS parameter for the identification of derivatives of ATL:**

An Agilent LC 1100 series coupled to a Bruker Daltonic Esquire 6000+ ion-trap mass spectrometer (IT-MS) with electrospray ionization (ESI) interface was used for identification and structure elucidation of ATL and the formed derivatives (photo-TPs). The above mentioned LC parameters were used while the MS parameters were optimized for ATL [m/z

267.1] by direct infusion of a 10  $\mu\text{g mL}^{-1}$  standard at a flow rate of 4  $\mu\text{L min}^{-1}$  through a syringe pump. The mass spectrometer was operated in positive polarity. The photo-TPs were identified by comparing 0 min samples (i.e. ATL) as reference with other samples. Their supposed structures were elucidated by interpreting the MS<sup>n</sup> spectra.

**Table S3 Supporting Information:** The operating parameters of the ESI and ion-trap (Bruker 6000) of the LC-ESI-IT-MS<sup>n</sup>

Parameters	Metoprolol
Dry gas temperature	350°C
Nebulizer pressure	30 psi
Dry gas flow	10 L min <sup>-1</sup>
end plate Offset	-500 Volt
capillary voltage	-3583 Volt
skimmer	40 Volt
capillary exit	111.0 Volt
octopole one	12.00 Volt
octopole two	1.70 Volt
trap drive	38.2
lens one	-5.0 Volt
lens two	-60 Volt
target mass	267 m/z
maximum accumulation time	200 ms
scan range	40 m/z - 1000 m/z
fragmentation amplitude	1

**DOC measurement:**

Dissolved Organic Carbon (DOC) was measured by Shimadzu TOC-V<sub>CPN</sub> analyzer equipped with an ASI-V auto sampler. DOC was measured according to ISO 8245: 1999 guideline<sup>3</sup> using a Shimadzu TOC-VCPN analyzer equipped with an ASI-V auto sampler. Samples were filtered with the syringe filter (Chromafil® Xtra PES 45/25, Macherey Nagel, Düren, Germany) of 0.45 $\mu\text{m}$  pore size prior to DOC measurement.

**Text S3 Supporting Information:** Principles and procedure of the investigated aerobic biodegradation tests

The aerobic biodegradability of ATL and its derivatives was investigated according to the OECD guidelines through Closed Bottle test [CBT] 301D<sup>4</sup> and Manometric Respiratory Test [MRT] 301 F.<sup>5</sup>

In CBT the concentration of the test compound was adjusted to 5 mg L<sup>-1</sup> Theoretical Oxygen Demand without nitrification (ThOD<sub>NH3</sub>) for untreated samples. The sample volume of post-treated solutions was increased according to DOC elimination during photodegradation treatment in order to have sufficient organic carbon related to the LOQ (limit of quantification) of the method used for the measurement of the endpoint parameter (oxygen consumption/oxygen concentration in test solution).

The test consisted of four different series that were run in duplicates, respectively. The blank series contained only mineral medium and inoculum. The quality control series contained readily biodegradable sodium acetate at a concentration corresponding to 5 mg L<sup>-1</sup> ThOD<sub>NH3</sub>, mineral medium and inoculum. The actual test series contained the respective test substance, mineral medium and inoculum. The fourth series was the toxicity control which contained the test compound and sodium acetate at concentrations corresponding to 5 mg L<sup>-1</sup> ThOD<sub>NH3</sub> each. The toxicity control monitors inhibitory effects due to the toxicity of test substances against the inoculum's bacteria and in order to allow for the recognition of false negative results. All the test vessels were inoculated with 2 drops of the effluent from a local municipal STP (AGL Lüneburg, Germany, 144,000 population equivalents).

The aerobic biodegradation in CBT was monitored for 28 days by measuring oxygen concentration in the test vessels with Fibox 3 (Fiberoptical oxygen transmitter) (PreSens, Regensburg, Germany).<sup>6</sup> For quality assessments pH was measured at 0 and 28 days.

MRT was conducted using the OxiTop<sup>®</sup> Control OC110-system (WTW GmbH, Weilheim, Germany) for monitoring the microbial oxygen consumption through CO<sub>2</sub> production during

the aerobic biodegradation. These measuring heads contained sodium hydroxide which removes the CO<sub>2</sub> from the gas phase. The removal of CO<sub>2</sub> results in a decrease in pressure in test vessels which corresponds to the oxygen consumption which is due to biodegradation. The scheme was equivalent to that of CBT, except that the sample concentration was adjusted to 30 mg L<sup>-1</sup> ThOD and 80 mL of inoculum were added to 1 L of test solution as required by test guidelines. Furthermore, an additional sterile control for the assessment of abiotic degradation was applied. The sterile control contained the test substance and sodium azide with no inoculum. A more detailed description of the testing procedures can be found elsewhere.<sup>1,2</sup>

The samples after 0 min, 32 min and 256 min of photolysis were tested in CBT while samples after 0 min, 64 min and 256 min were tested in MRT. The difference in the irradiation time of samples for both tests was due the difference in the kinetics of formation of the derivatives. This difference in the kinetic was due to the different starting concentration of ATL in the treatment. Table S4 summarizes the composition of the aerobic biodegradation test series in CBT and MRT.

Substances showing at least 60% degradation (based on oxygen consumption) in these tests are classified as readily biodegradable according to test guideline<sup>7</sup> and therefore are expected not to being accumulated in the aquatic environment.<sup>8</sup>

**Table S4 Supporting Information:** Composition of the aerobic biodegradation test series in the CBT (1-4) and MRT (1-5)

Test series	1 Blank	2 Quality control	3 Test compound	4 Toxicity control	5 Sterile control
Mineral medium	+	+	+	+	+
Inoculum	+	+	+	+	
Test substance			+	+	+
Sodium acetate		+		+	
Sodium azide					+

**Text S4 Supporting Information:** Detailed description and output from various *in silico* models used in the present study.

Photo-TPs: The photodegradation pathway of ATL and resulting photo-TPs (“derivatives”) products was established by using a combination of chemical analysis (LC-ESI-ion-trap-MS/MS structure elucidation, see above, S2) and *in silico* prediction by the software MetaPC (Version 1.8.1, MultiCASE Inc., Beachwood, USA<sup>[9]</sup>, Table S5, SI) using its photodegradation dictionary. *In silico* predictions were compared to the corresponding MS<sup>n</sup> spectra measured by LC-ESI-MS/MS (ion-trap).

The dictionary is a compilation of known rules for photo reactions of chemicals. Generally, the dictionaries of MetaPC software are based on a library of known pairs of target and transform sequences. Meta program uses respective dictionaries to predict the transformation of chemicals under a set of different conditions such as mammalian metabolism, aerobic and anaerobic degradation and photodegradation. The structures of investigated molecules are scanned for their target sequences which are gradually replaced by the relevant transform sequences of the respective dictionary to create a set of predicted TPs.<sup>9</sup> The photodegradation dictionary of the MetaPC software is loosely divided into 9 large subdivisions which consist of approximately 1200 transformations in total. The photodegradation dictionary module was validated with 40 known industrial chemical products and had a hit/miss ratio of higher than 92%. MetaPC is an efficient model for the evaluation of the photo-induced degradation processes that take place in diluted conditions in oxygenated aqueous solutions.

Biodegradability: The *in silico* models used to predict the aerobic biodegradability of ATL and its derivatives (photo-TPs) are summarized in Table S5. As all *in silico* models and approaches have their limitations, therefore a combination of several software packages that rely on different data sets and underlying algorithms/statistics has been applied (“*in-silico* testing battery”). The ready biodegradability of ATL and its derivatives was predicted based

on data for OECD 301C MITI-I test (Ministry of International Trade and Industry, Japan)<sup>7</sup>, which is generally not fully comparable to CBT and MRT, as models for the CBT are not available. However, these predictions can provide at least an orientation towards identifying certain structural alterations in the derivatives molecules which would modulate their biodegradability.

The OASIS Catalogic models predict the ready biodegradability as a numerical value between 1 and 0. A numeric value of 1 corresponds to 100% biodegradation and 0 represents 0% biodegradation while numeric value of 0.6 corresponds to 60% biodegradation which is the pass criterion for ready biodegradability under MITI-I tests conditions. The output from BIOWIN models is also a number between 0 and 1 which can be interpreted as indicating ready biodegradation if the value is higher than 0.5.

Toxicity: Toxicity against environmental bacteria (against *Vibrio fischeri* an often used test organism for this purpose), mutagenicity and genotoxicity for ATL and its derivatives (photo-TPs) were predicted *in silico* by various models of OASIS Catalogic (Laboratory for Mathematical chemistry, Bulgaria), CASE Ultra (MultiCASE Inc., USA) and Leadscope software (Leadscope, Inc., USA), which are listed in Table S5. Leadscope software was used with training sets from 2012 SAR Genetox Database as provided by Leadscope.<sup>10</sup> The mutagenicity was predicted by *in vitro* model for bacterial mutagenicity of OASIS Catalogic. This model identifies chemicals, which are able to elicit mutagenicity as a result of interaction with DNA of *Salmonella typhimurium* or *Escherichia coli*. Micronucleus formation (A7S) for genotoxicity and chromosome aberration (A7U) and mutagenicity Ames (A2H) models for mutagenicity were used from Case Ultra software for prediction.

CASE Ultra, Leadscope and OASIS Catalogic software provide positive, negative and out of domain (OD) estimations for the selected models. OD means that the test chemical is not included in the applicability domain of the applied model. In such cases there are no

predictions made or even if provided by the software they should be discarded. The advantage of Case Ultra software is that it does not only calculate the activity but also evaluates the data and predict the moieties of the molecule which could be responsible for the activating and deactivating activity. Often CASE Ultra software provides alerts for all its selected models like ‘Inconclusive’ and Inconclusive with asterisk symbol (\*). ‘Inconclusive’ alert means that a significant portion of the test chemical is covered by unknown structural fragments and Inconclusive with asterisk symbol (\*) means both positive and deactivating alerts were found in the same molecule. In both cases therefore a clear result cannot be provided.

All the *in silico* models used in the study have validated databases and training sets. More information about their databases, training sets and their validity criteria can be easily found elsewhere in the references provided in Table S5 for each model. Generally, the structures of chemical species are scanned by the software against these validated databases of the model, and the software calculates the activity and predicts the output in the form of alerts for that corresponding activity. The above mentioned models and software are described in detail elsewhere.<sup>1,2,11</sup> Table S5 below enlisted all the *in silico* software and their respective models used in the present study.

**Table S5 Supporting Information:** List of *in silico* software and their respective models used for the prediction of photodegradation products, ready biodegradability and toxicity of ATL and its photo-TPs.

Activity	QSAR Software	Models	End points	References
Photodegradation products	METAPC v 1.8.1	Photodegradation	Photoproducts of chemicals under natural-like conditions	9
	CASE Ultra v.1.4.5.1	MITI-I test (OECD 301C, module AU6)	Ready biodegradability according to MITI-I test	12
Biodegradation	EPI Suite (EPIWEB 4.1)	BIOWIN 6	Nonlinear regression models predicting the Ready biodegradability according to MITI-I test	13
	Catalogic v 5.11.6 TB (OASIS)	CATABOL 301C model	Ready biodegradability according to MITI-I test	14
		CATALOGIC 301C models	Ready biodegradability according to MITI-I test	
Toxicity	CASE Ultra v.1.4.5.1 (MultiCASE Inc.)	Human carcinogenicity (A0J)	Carcinogenicity	12,15
		Micronucleus formation in vivo composite (A7S)	Genotoxicity	
		Chromosome aberration in vitro composite (A7U)	Mutagenicity	
		Mutagenicity Ames (A2H)	Mutagenicity against <i>Salmonella Typhimurium</i>	
		Microtox toxicity environmental bacteria (AUA).	Bacterial toxicity	
	Leadscope V. 3.0.11-1	Bacterial mutagenesis (BM) model	Mutagenicity as a result of interaction with DNA of <i>Salmonella Typhimurium</i> or <i>Escherichia coli</i>	SAR Genotox Database 2012 10
		Mammalian mutagenesis (MM)	Mutagenicity	
In vitro chromosome aberration (IVCA)		Mutagenicity		
Catalogic v 5.11.6 TB (OASIS)	In vivo micronucleus (IVMN)	Genotoxicity		
Catalogic v 5.11.6 TB (OASIS)	<i>in vitro</i> Ames model	Mutagenicity against <i>Salmonella Typhimurium</i>	14	



**Text S5 Supporting Information:** Detailed description of the drug-likeness prediction software QikProp 3.8.

The software package QikProp 3.8 developed by Jorgensen<sup>16</sup> was used to predict drug-likeness of the biodegradable derivatives (photo-TPs) of ATL. QikProp is a quick, accurate, easy-to-use absorption, distribution, metabolism, and excretion (ADME) prediction program. QikProp software (part of Schrödinger software package, Schrödinger, Germany) predicts the drug-likeness through the calculation of various physically significant descriptors and pharmaceutically relevant properties of organic, ligand-like molecules. The software database has ~710 compounds including about 500 drugs and related heterocycles.<sup>17</sup> In addition to predicting molecular properties, QikProp provides ranges for comparing a particular molecule's property with those of 95% of known drugs. Below the properties or descriptors used to predict the drug-likeness of the biodegradable derivatives (photo-TPs) of ATL are explained in detail.

The drug-likeness of chemical molecule is predicted through the '**#stars**' property. The '**#stars**' property of QikProp measures the number of property or descriptor values that fall outside the 95% range of similar values for known drugs. The properties and descriptors which are included in the determination of #stars are mentioned in the technical information manual of QikProp software.<sup>17</sup> The range for #stars predictions is between 0-5. A large number of stars suggest that a molecule is less drug-like than molecules with few stars.

The **RuleOfFive** number gives the number of violations of Lipinski's rule of five.<sup>18</sup> Compounds that satisfy this rule-of-five are considered drug-like. The rules are: molecular weight of molecule < 500, octanol/water partition coefficient ( $\log P_{o/w}$ ) < 5, hydrogen bond donors  $\leq 5$ , hydrogen bond acceptors  $\leq 10$ . The **RuleOfThree** number is the counting of violations of Jorgensen's rule of three. Compound that satisfy this rule-of-three are considered as orally available. The three rules are: aqueous solubility ( $\log S$ ) > -5.7, apparent

Caco-2 cell permeability  $> 22$  nm/s, number of likely metabolic reactions  $< 7$ . Molecules satisfying these rules are considered orally available. Compounds with fewer (and preferably no) violations of both rules are more likely to be considered drug-like and orally available molecule, respectively.

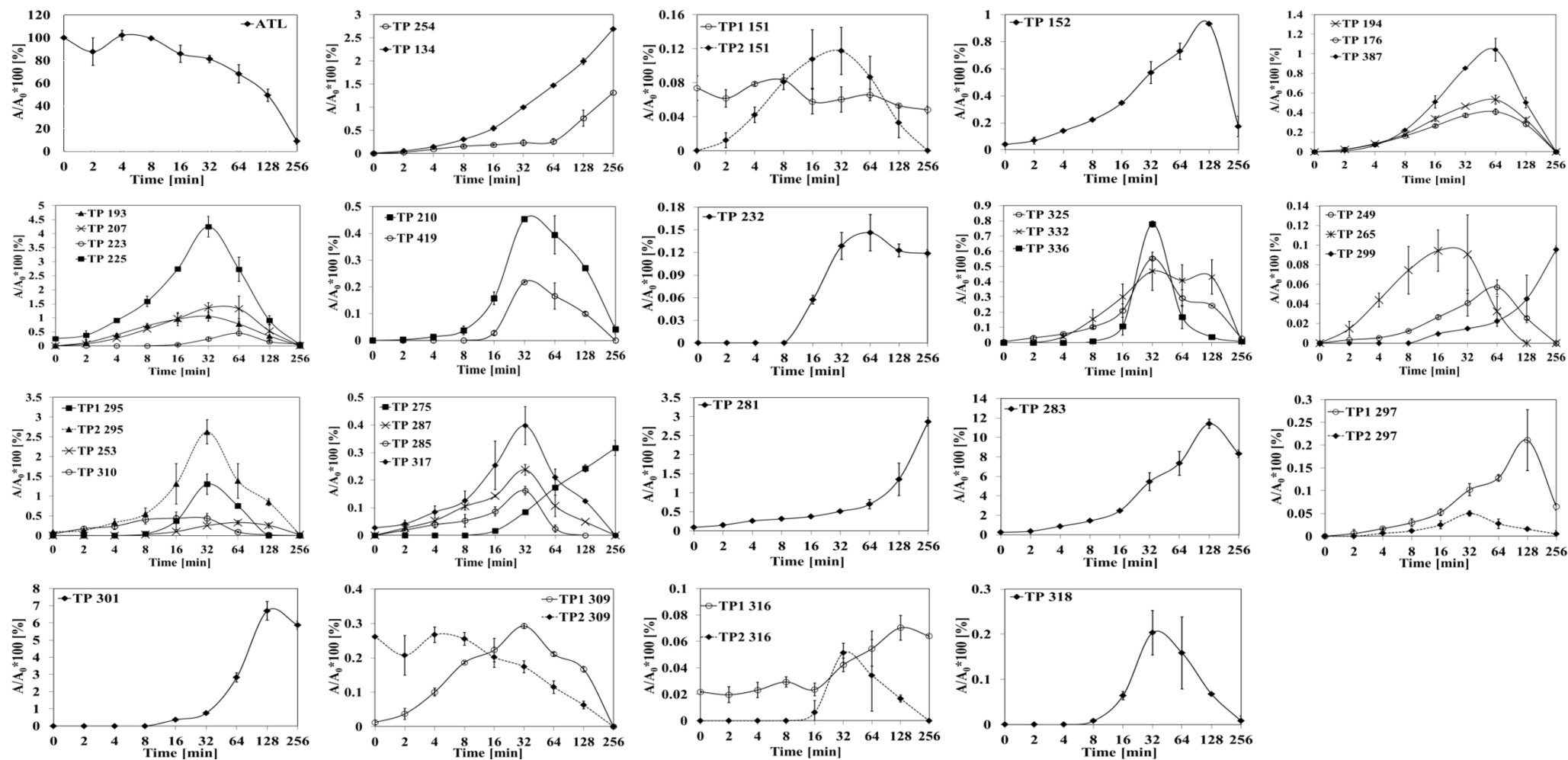
**Text S6 Supporting Information:** Results of photolysis and generation of derivatives (photo-TPs) of ATL.

ATL solutions (initial concentration varying from 10 to 60 mg L<sup>-1</sup>) were exposed to UV light for 256 min. This resulted in the complete primary elimination of the parent compound with incomplete mineralization as measured according to HPLC-UV and DOC analysis, respectively. New peaks were observed in the total ion chromatogram (TIC) during LC-MS analysis at different irradiation time points confirms the formation of derivatives. Several derivatives (photo-TPs) of ATL identified during the photolysis have already been reported in literature.<sup>19-27</sup> New derivatives that have not yet been reported were identified as well. The retention time ( $t_R$ ), molecular formula, extracted ion chromatogram (EIC) and the MS<sup>2</sup> fragmentation pattern of ATL and its derivatives (photo-TPs) are provided in detail in SI Table S8.

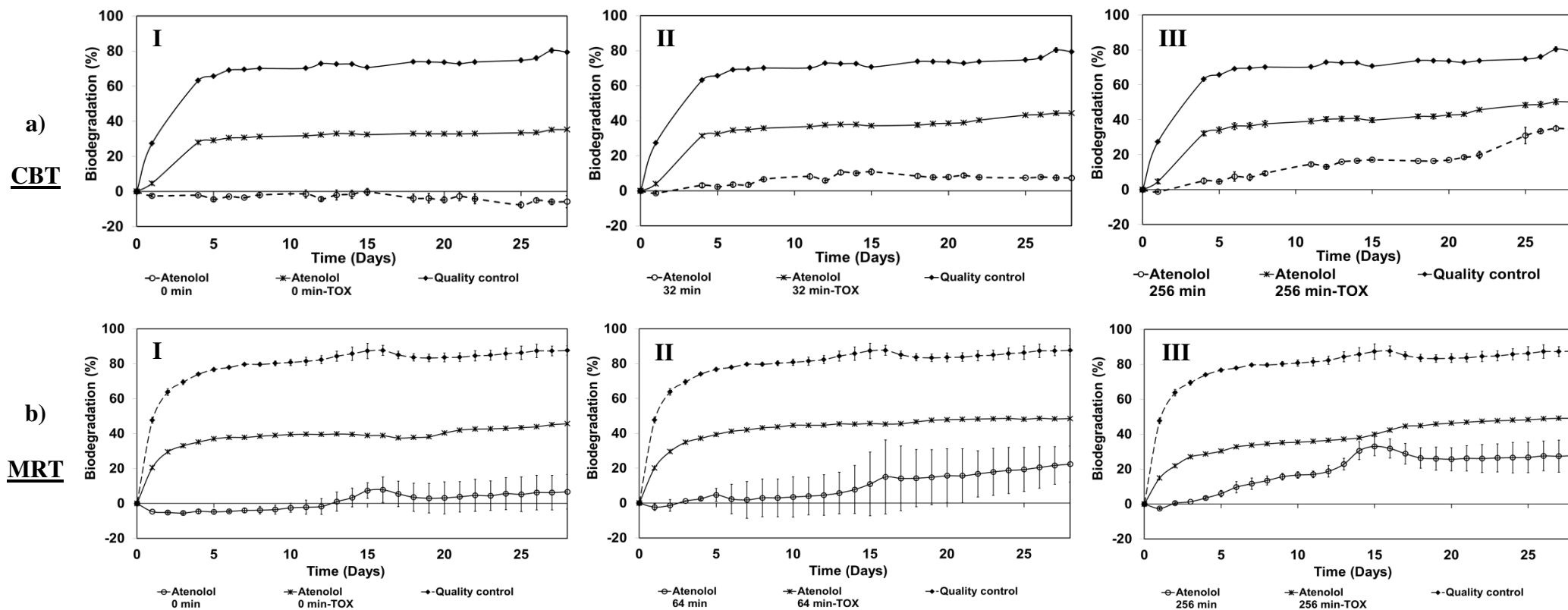
According to LC-MS/MS data, several identified derivatives (photo-TPs) had the same respective nominal mass with different retention times. The retention time gives some information of the polarity of the individual compound. The chromatographic material was a non-polar C18 material. Therefore, lower retention times indicate a higher polarity of the analyte which may in some cases also correlate with a lower log P<sub>ow</sub>. In most cases these derivatives exhibited the same MS<sup>2</sup> fragmentation pattern, indicating the possibility of formation of constitutional isomers. The same phenomena of the formation of constitutional isomers were reported earlier.<sup>20,21,24</sup>

The kinetics of the appearance/disappearance of derivatives (photo-TPs) formed during photolysis was monitored and is illustrated in Figure S1. Generally, the peak area does not precisely indicate the concentration of the respective derivative in the photodegraded mixture as its molar extinction coefficient and ionization rate is not known. However, determination of

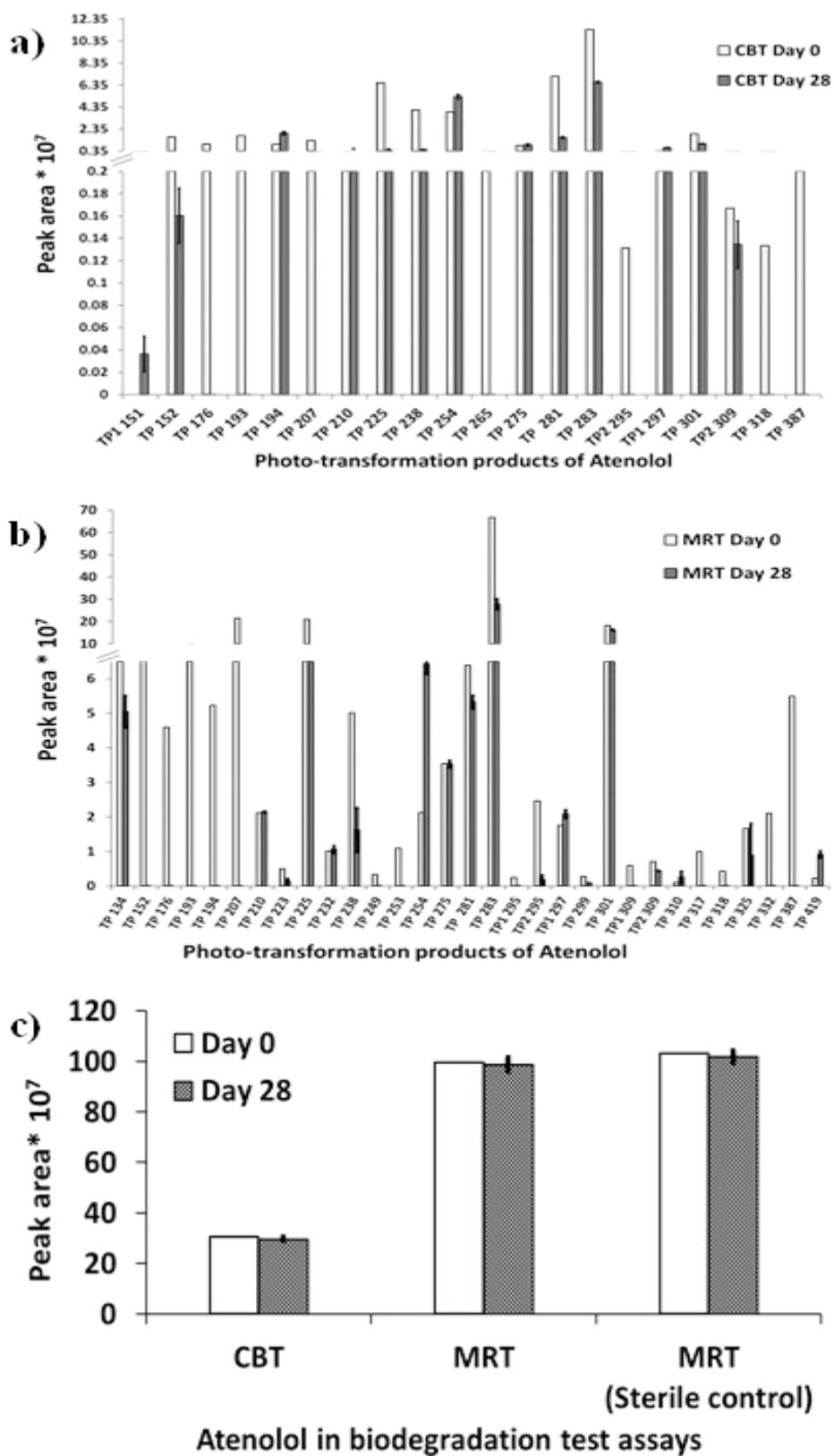
relative change of the concentration of individual derivatives during photolysis is possible thereby.



**Figure S1 Supporting Information:** Appearance/disappearance of peak area of the derivatives (photo-TPs) of ATL during photolysis measured by LC-ESI-MS in positive mode. (Initial concentration of ATL =  $10\text{mg L}^{-1}$ ;  $n = 2$ ) ( $A/A_0$  as  $A$  is the peak area of derivatives and  $A_0$  is the peak area of ATL at 0 min)



**Figure S2 Supporting Information:** Aerobic biodegradation results of ATL and its derivatives (photo-TPs) in: a) CBT after photolysis at **I**- 0 min, **II**- 32 min and **III**- 256 min [ $C_0 = 10 \text{ mg L}^{-1}$ ;  $n = 2$ ]; b) MRT after photolysis at **I**- 0 min, **II**- 64 min and **III**- 256 min [ $C_0 = 60 \text{ mg L}^{-1}$ ;  $n = 2$ ].



**Figure S3 Supporting Information:** LC-MS analysis of biodegradation test samples for photo TPs at the beginning and the end of the tests, respectively: a) CBT; b) MRT; c) Atenolol in CBT and MRT.

**Table S6 Supporting Information:** Summary of the results of investigated aerobic biodegradability test for Atenolol and its derivatives mixture

<b>Biodegradation test</b>	<b>Test Sample</b>	<b>Biodegradation after 28 d [%]</b>	<b>DOC removal [%]</b>	<b>Derivatives (photo-TPs) identified to be biodegraded</b>
<b>CBT</b>	0 min	$-6 \pm 4 \%$	-	TP 134; TP 152; TP 176; TP 193; TP 207; TP 225; TP <sub>1&amp;2</sub> 238; TP 265; TP 281; TP 283; TP <sub>2</sub> 295; TP 301; TP <sub>2</sub> 309; TP 318; TP 387
	32 min	$8 \pm 1 \%$	-	
	256 min	$35 \pm 2 \%$	-	
<b>MRT</b>	0 min	$7 \pm 10 \%$	9 %	TP 134; TP <sub>1</sub> 151; TP 152; TP 176; TP 193; TP 194; TP 207; TP 223; TP 225; TP <sub>1&amp;2</sub> 238; TP 249; TP 253; TP 281; TP 283; TP <sub>2</sub> 295; TP 299; TP 301; TP <sub>1&amp;2</sub> 309; TP 317; TP 318; TP 325; TP 332; TP 387
	64 min	$22 \pm 10 \%$	23 %	
	256 min	$28 \pm 9 \%$	34 %	

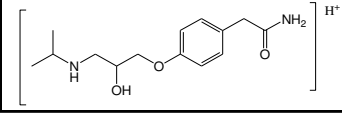
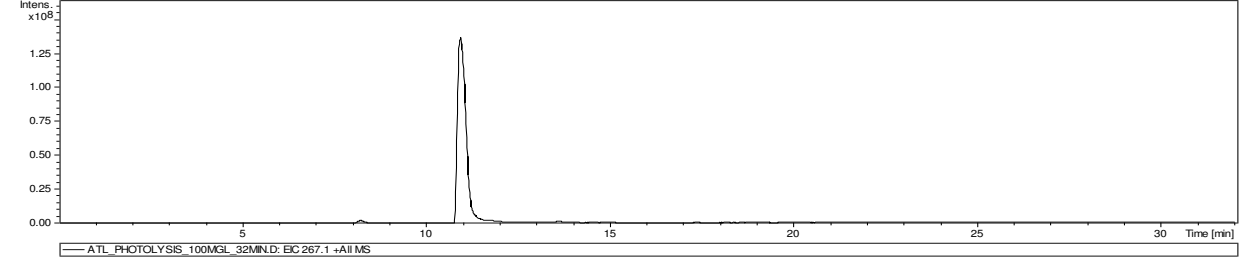
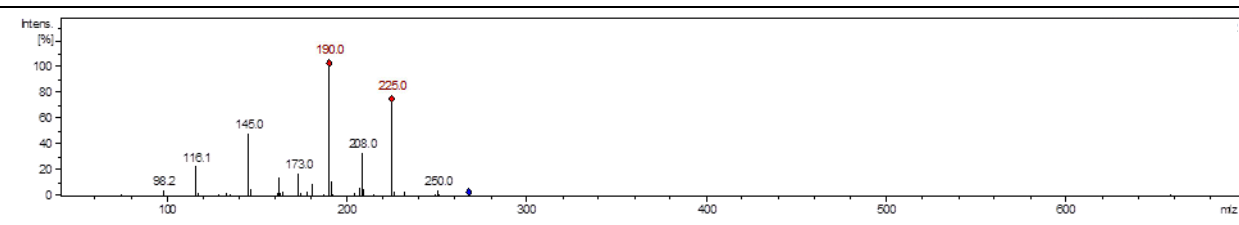
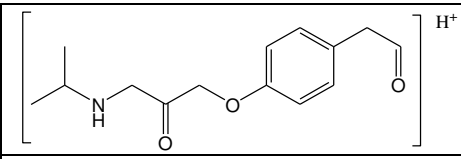
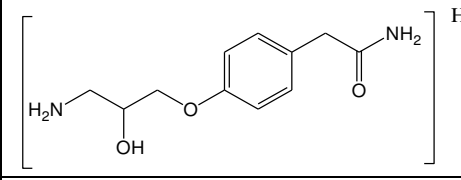
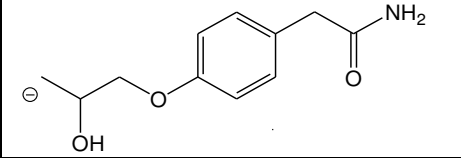
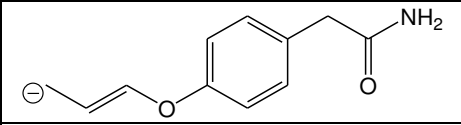
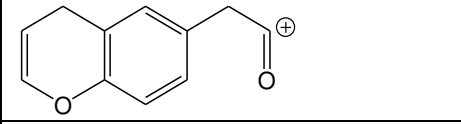
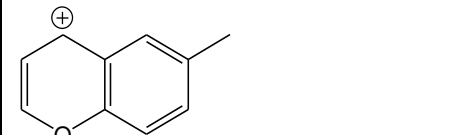


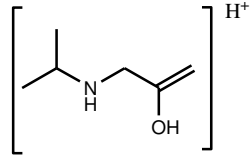
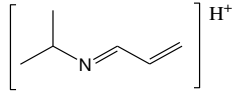
**Table S7 Supporting Information:** *In silico* drug-likeness prediction of the biodegradable derivatives (photo-TPs) of Atenolol through the ADME prediction software QikProp

<b>Substance and Photo-TPs</b>	<b>Drug-likeness [#star]*</b>	<b>No. of violation of Lipinski's rule of five<sup>‡</sup></b>	<b>No. of violation of Jorgensen's rule of three<sup>‡</sup></b>
ATL	0	0	0
TP 176	1	0	0
TP 193	0	0	0
TP 194	0	0	0
TP 207	0	0	0
TP 210	0	0	0
TP 223	0	0	0
TP 225	0	0	1
TP 238	0	0	0
TP <sub>1-7</sub> 283	0	0	1
TP <sub>1</sub> 295	0	0	1
TP <sub>2</sub> 295	0	0	0
TP 299	0	1	2
TP <sub>1</sub> 301	1	0	1
TP <sub>2</sub> 301	1	0	1
TP <sub>3</sub> 301	0	0	1
TP <sub>4</sub> 301	0	0	1
TP <sub>5</sub> 301	1	0	1
TP <sub>6</sub> 301	0	0	1
TP <sub>2</sub> 309	0	0	1
TP 317	3	0	2
TP 318	2	0	1
TP 325	0	0	1
TP 332	2	1	2

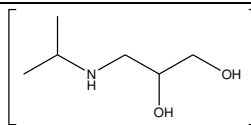
\* predict the drug-likeness in range of 0-5, 0 suggests that molecule is more drug-like while 5 suggest less drug-likeness of the molecule. <sup>‡</sup> Molecules with fewer (and preferably no) violations are more likely to be considered as drug-like and orally available molecules, respectively.

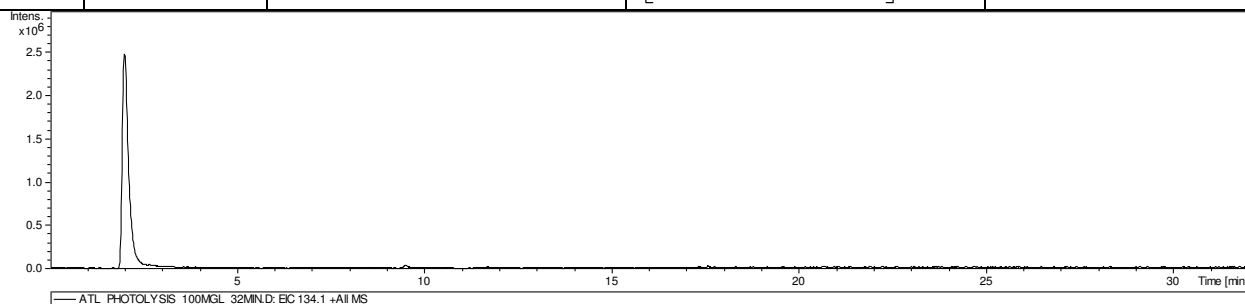
**Table S8 Supporting Information:** The proposed structures of the fragments formed during the MS<sup>2</sup> fragmentation for Atenolol and its derivatives (photo-TPs), not all mesomeric structures shown (References: if already documented in literature)

m/z	Retention time	Precursor/ Product ion	Structure	References
ATL 267.1	10.9	[M+H] <sup>+</sup>		20,24,27
				
<b>MS<sup>2</sup></b>				
				
250.0		[M+H-NH <sub>3</sub> ] <sup>+</sup>		
225.0		[M+H-C(CH <sub>3</sub> ) <sub>2</sub> ] <sup>+</sup>		
208.0		[M+H-NH <sub>2</sub> C(CH <sub>3</sub> ) <sub>2</sub> ] <sup>+</sup>		
190.0		[M+H-NH <sub>2</sub> C(CH <sub>3</sub> ) <sub>2</sub> -H <sub>2</sub> O] <sup>+</sup>		
173.0		[M+H-NH <sub>2</sub> C(CH <sub>3</sub> ) <sub>2</sub> -H <sub>2</sub> O-NH <sub>2</sub> ] <sup>+</sup>		
145.0		[M+H-NH <sub>2</sub> C(CH <sub>3</sub> ) <sub>2</sub> -H <sub>2</sub> O-CO-NH <sub>2</sub> ] <sup>+</sup>		

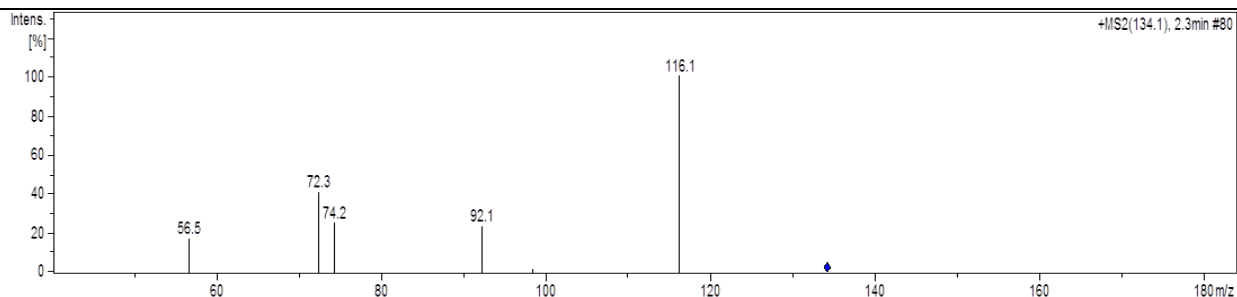
116.1	$[M+H-HOC_6H_4CH_2CONH_2]^+$	
98.2	$[M+H-HOC_6H_4CH_2CONH_2-H_2O]^+$	

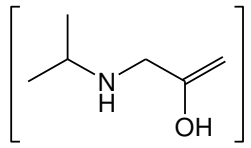
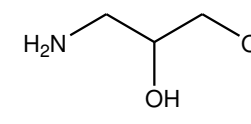
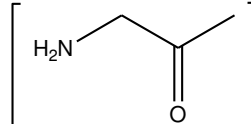
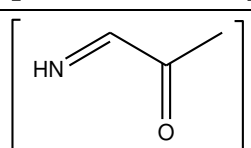
### TP 134

m/z	Retention time	Precursor/ Product ion	Structure	References
134.1	2.0	$[M+H]^+$		20,24,26,27 MetaPC software

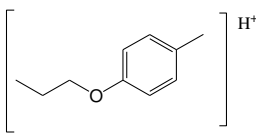
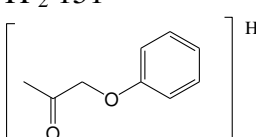
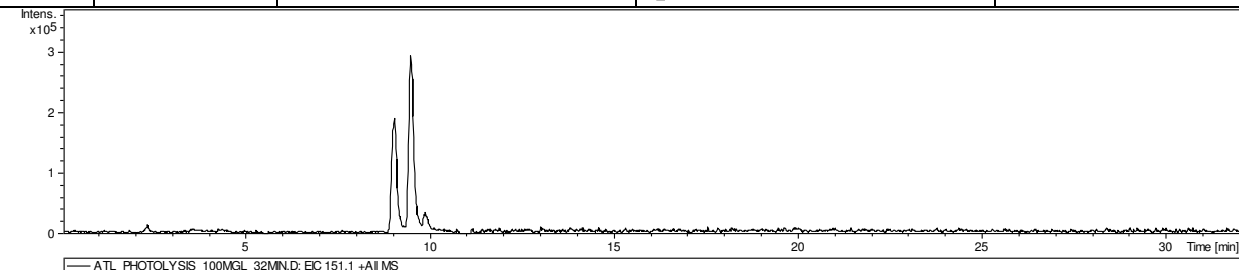
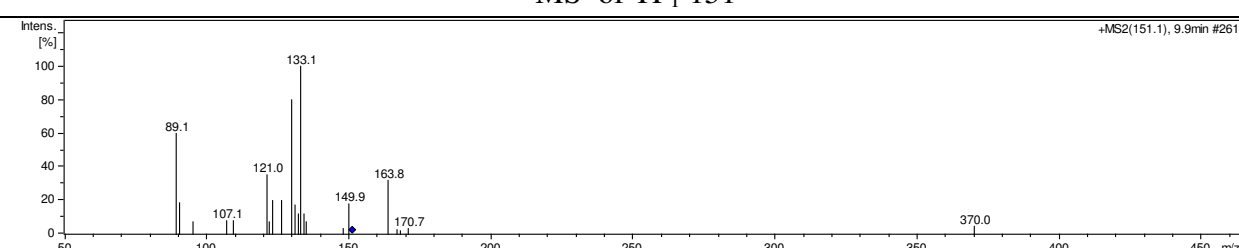
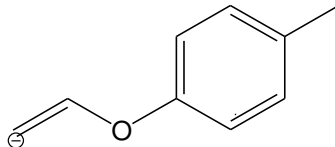
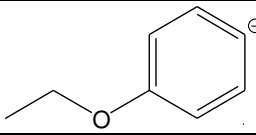
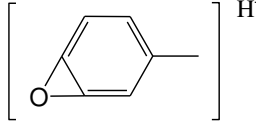


### MS<sup>2</sup>



116.1	$[M+H-H_2O]^+$	
92.1	$[M+H-CH(CH_3)_2]^+$	
74.2	$[M+H-H_2O-CH(CH_3)_2]^+$	
72.3	$[M+H-H_2O-CH_2(CH_3)_2]^+$	

# TP 151

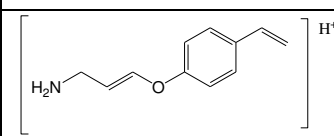
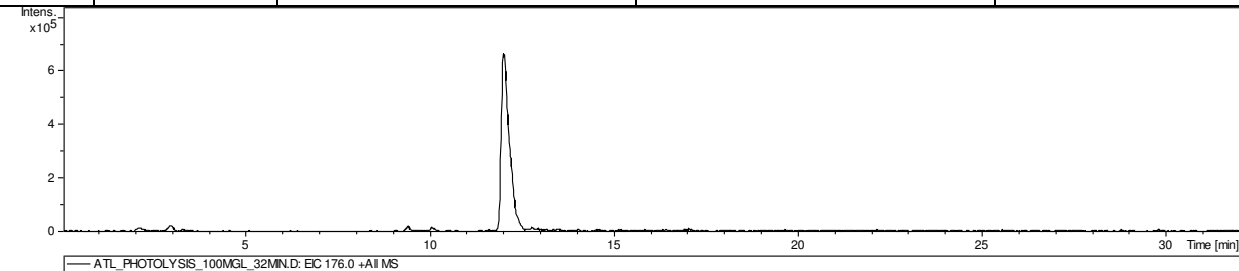
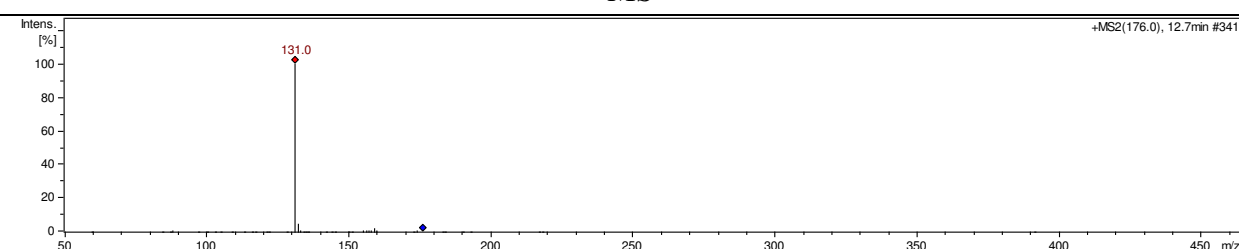
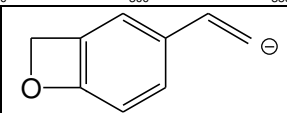
m/z	Retention time	Precursor/ Product ion	Structure	References
151.1	9.1 min and 9.5 min	$[M+H]^+$	<p>TP<sub>1</sub> 151</p>  <p>TP<sub>2</sub> 151</p> 	
 <p>ATL_PHOTOLYSIS_100MGL_32MIND: EC 151.1 +All MS</p>				
MS <sup>2</sup> of TP <sub>1</sub> 151				
 <p>+MS2(151.1), 9.9min #261</p>				
133.1		$[M+H-CH_3]^+$		
121.0		$[M+H-2CH_3]^+$		
107.1		$[M+H-CH_3CH_2CH_3]^+$		
MS <sup>2</sup> of TP <sub>2</sub> 151				

134.0	$[M+H-H_2O]^+$	
106.1	$[M+H-CH_3CHO]^+$	
95.3	$[M+H-CH_3COCH_3]^+$	

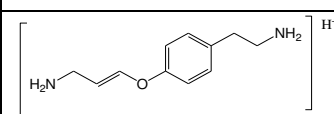
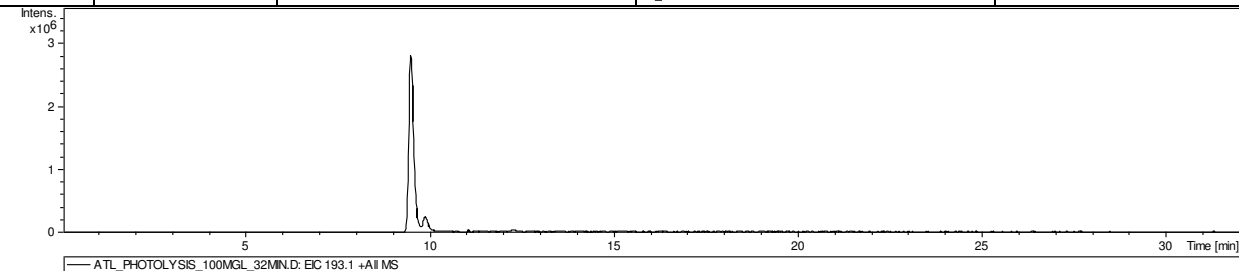
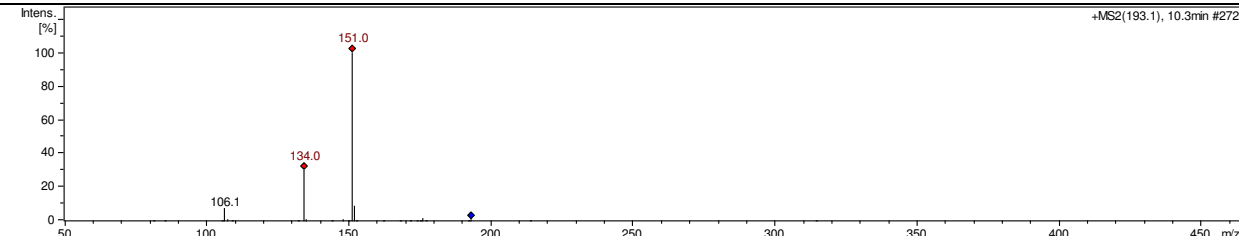
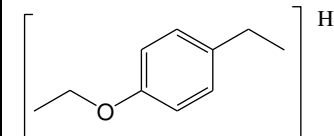
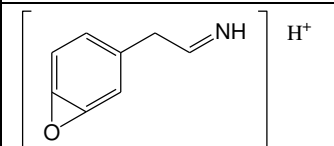
### TP 152

m/z	Retention time	Precursor/ Product ion	Structure	References
152.1	11.7	$[M+H]^+$		19,20,23,24,26,27 MetaPC software
<b>MS<sup>2</sup></b>				
107.1		$[M+H-CHONH_2]^+$		

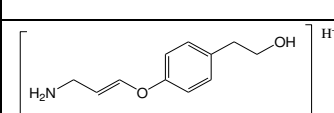
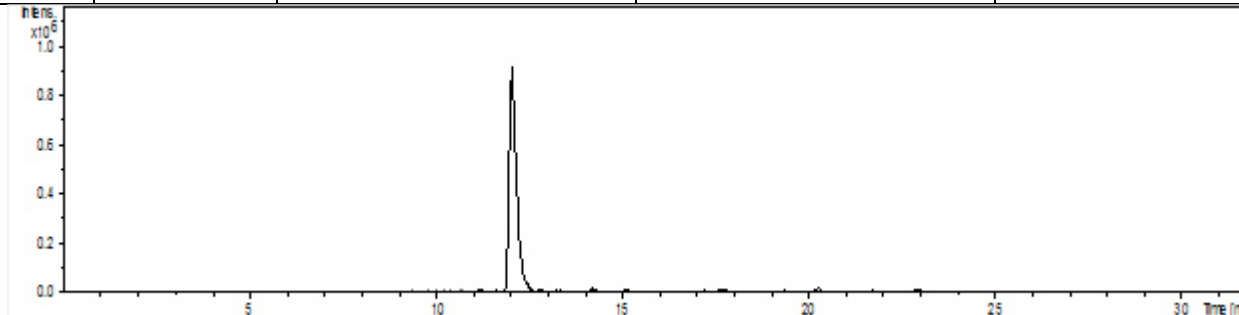
### TP 176

m/z	Retention time	Precursor/ Product ion	Structure	References
176.0	12.0	$[M+H]^+$		
<p>Intens. <math>\times 10^5</math></p>  <p>ATL_PHOTOLYSIS_100MGL_32MIN.D: EC 176.0 +All MS</p>				
$MS^2$				
<p>Intens. [%]</p>  <p>+MS2(176.0), 12.7min #341</p>				
131.0		$[M+H-CH_3CH_2NH_2]^+$		

### TP 193

m/z	Retention time	Precursor/ Product ion	Structure	References
193.1	9.5 min	$[M+H]^+$		
 <p>ATL_PHOTOLYSIS_100MGL_32MIN.D: EC:193.1 +All MS</p>				
<b>MS<sup>2</sup></b>				
 <p>+MS2(193.1), 10.3min #272</p>				
151.0		$[M+H-NH_3-CH_3NH_2]^+$		
134.0		$[M+H-CH_3CH_2CH_2NH_2]^+$		

### TP 194

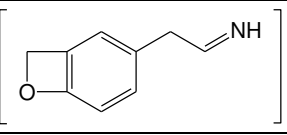
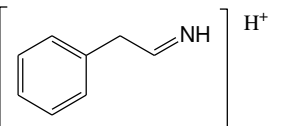
m/z	Retention time	Precursor/ Product ion	Structure	References
194.1	12.0	$[M+H]^+$		27 MetaPC software
 <p>ATL_PHOTOLYSIS_100MGL_32MIN.D: EC:194.0 +All MS</p>				

MS <sup>2</sup>		
176.0	$[M+H-H_2O]^+$	
131.0	$[M+H-CH_3OH-CH_3NH_2]^+$	

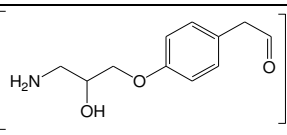
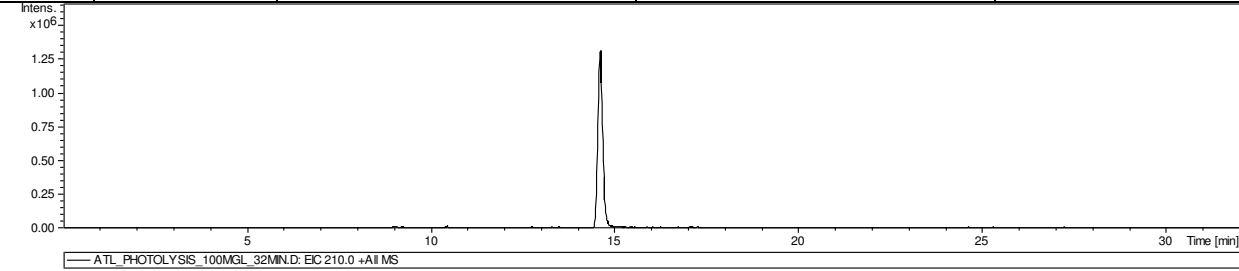
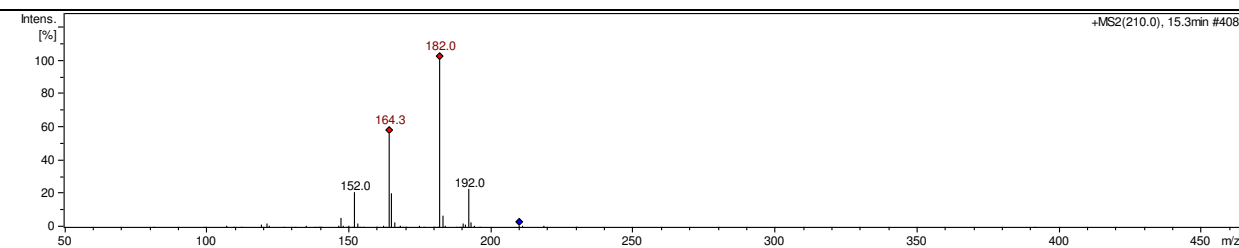
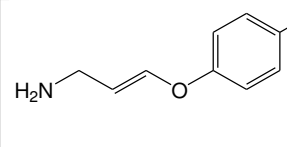
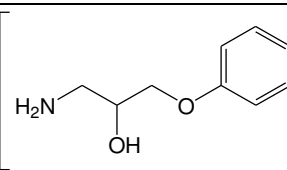
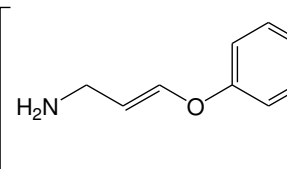
### TP 207

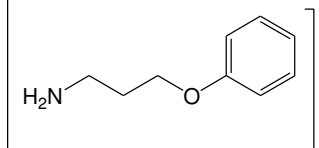
m/z	Retention time	Precursor/ Product ion	Structure	References
207.1	9.2	$[M+H]^+$		
MS <sup>2</sup>				
190.9		$[M+H-O]^+$		
165.0		$[M+H-O-2NH_3]^+$		



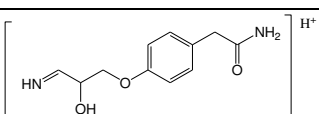
148.0	$[M+H-CH_2NH-CH_3OH]^+$	 $H^+$
120.1	$[M+H-C_3H_7NO_2]^+$	 $H^+$

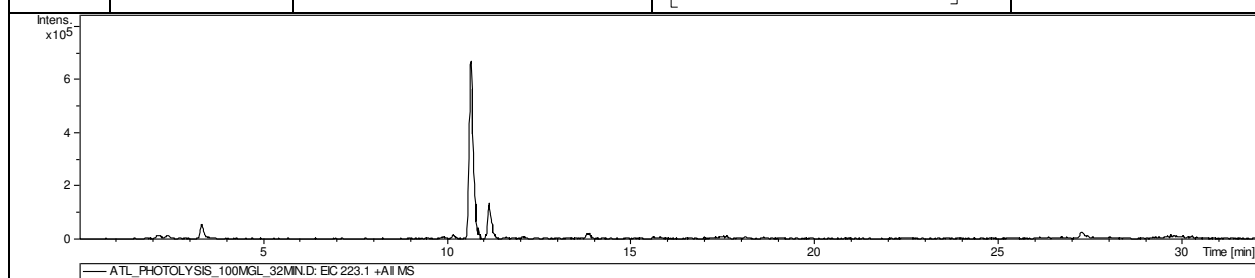
### TP 210

m/z	Retention time	Precursor/ Product ion	Structure	References
210.0	14.6	$[M+H]^+$	 $H^+$	27
 <p>ATL_PHOTOLYSIS_100MGL_32MIN.D: EC 210.0 +All MS</p>				
<b>MS<sup>2</sup></b>				
 <p>+MS2(210.0), 15.3min #408</p>				
192.0		$[M+H-H_2O]^+$	 $H^+$	
182.0		$[M+H-HCHO]^+$	 $H^+$	
164.3		$[M+H-H_2O-HCHO]^+$	 $H^+$	

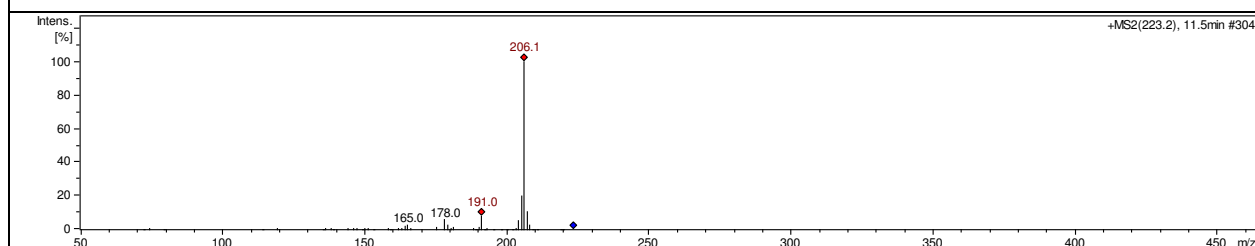
152.0	$[M+H-O-CH_3CHO]^+$	
-------	---------------------	--

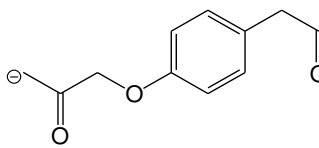
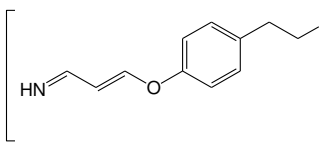
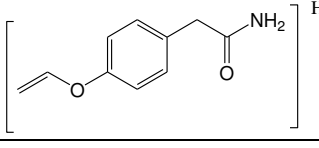
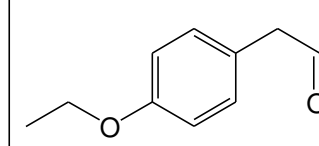
**TP 223**

m/z	Retention time	Precursor/ Product ion	Structure	References
223.1	10.7	$[M+H]^+$		MetaPC software



**MS<sup>2</sup>**

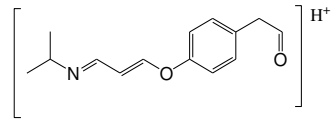
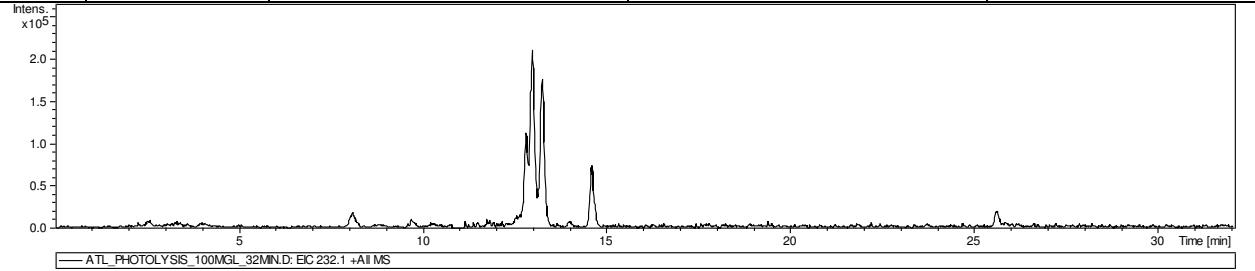
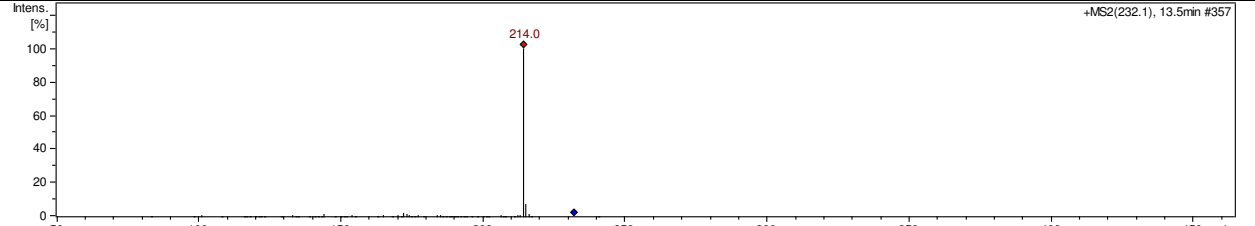
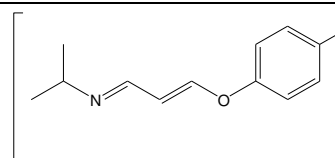


206.1	$[M+H-NH_3]^+$	
191.0	$[M+H-H_2O-O]^+$	
178.0	$[M+H-CH_3NH_2-H_2O]^+$	
165.0	$[M+H-CH_2NH-H_2O-NH_3]^+$	

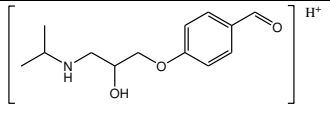
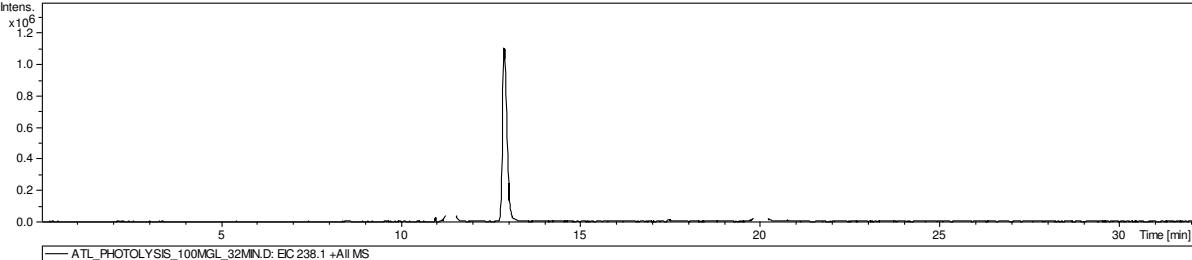
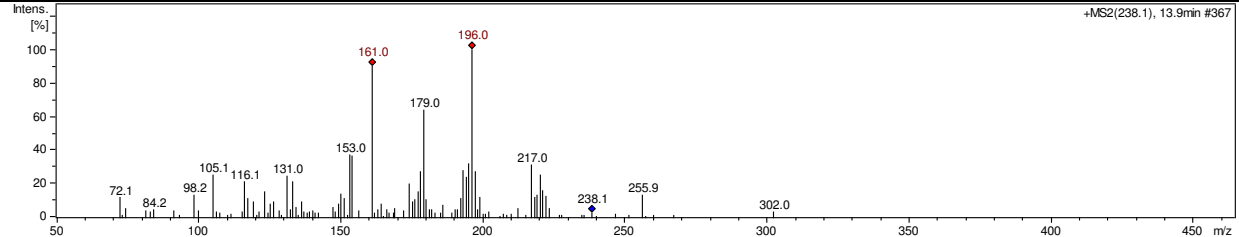
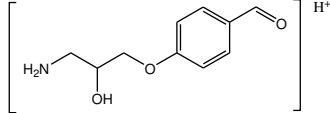
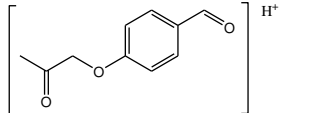
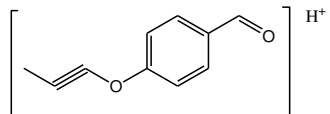
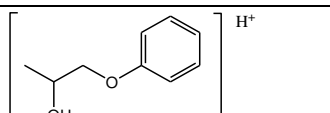
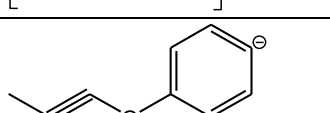
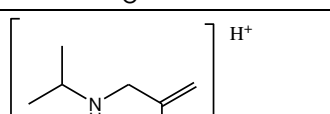
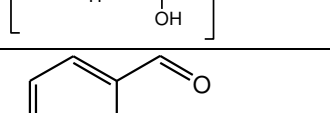
TP 225

m/z	Retention time	Precursor/ Product ion	Structure	References
225.1	5.5 min	$[M+H]^+$		24,27 MetaPC software
<b>MS<sup>2</sup></b>				
208.0		$[M+H-NH_3]^+$		
190.0		$[M+H-NH_3-H_2O]^+$		
180.0		$[M+H-CHONH_2]^+$		
162.1		$[M+H-CHONH_2-H_2O]^+$		
144.9		$[M+H-CHONH_2-H_2O-NH_3]^+$		
74.3		$[M+H-HOC_6H_4CH_2CONH_2]^+$		

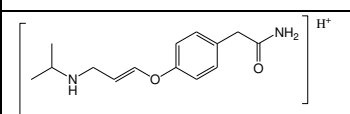
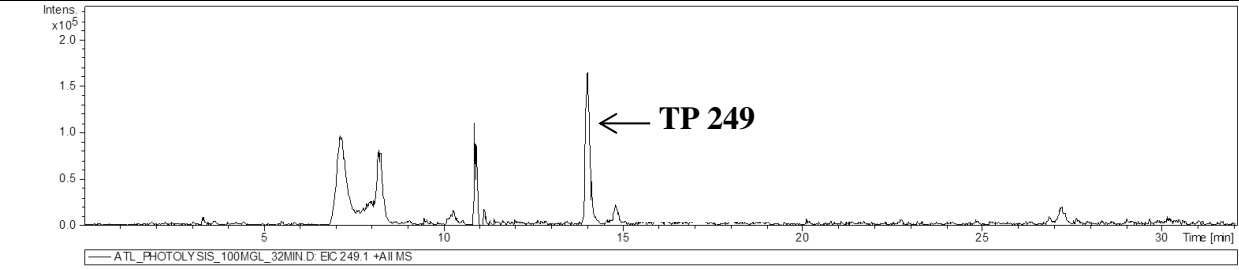
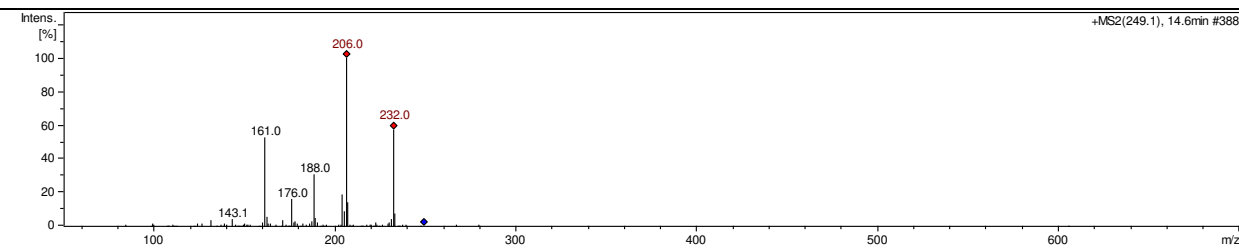
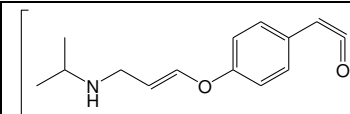
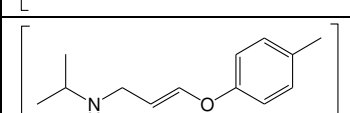
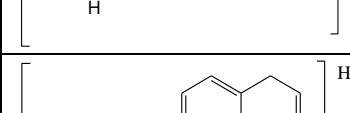
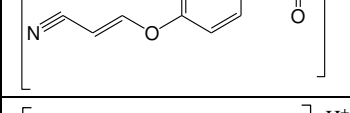
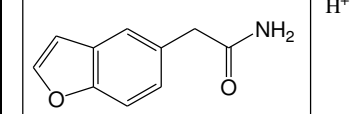
**TP 232**

m/z	Retention time	Precursor/ Product ion	Structure	References
232.1	13.2	$[M+H]^+$		
 <p style="text-align: center;">ATL_PHOTOLYSIS_100MGL_32MIN.D: EIC 232.1 +All IIS</p>				
<p><b>MS<sup>2</sup></b></p>				
				
214.0		$[M+H-H_2O]^+$		

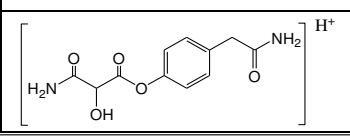
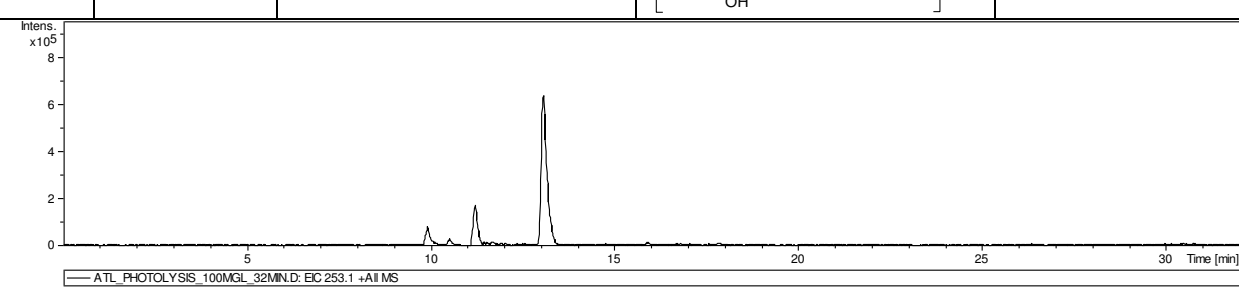
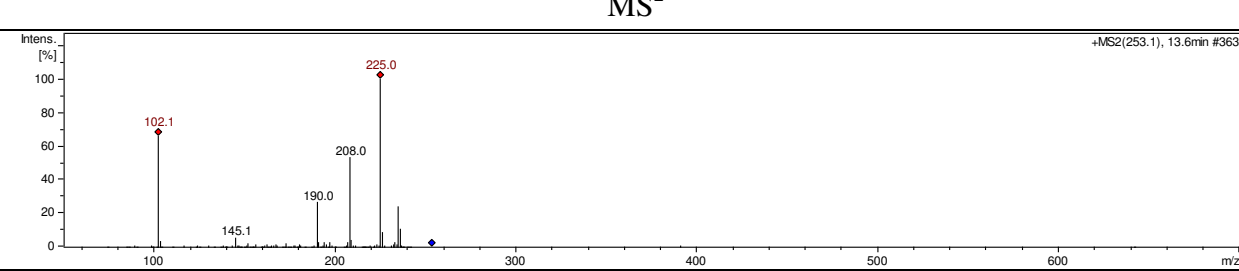
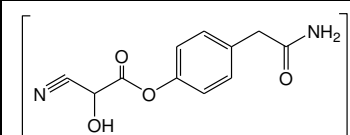
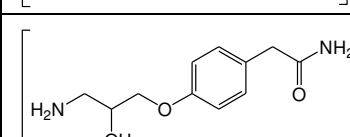
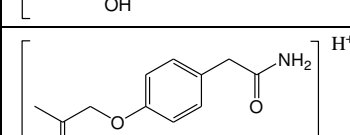
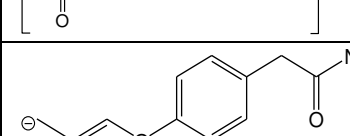
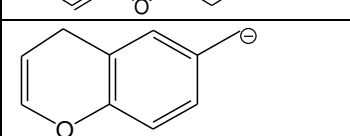
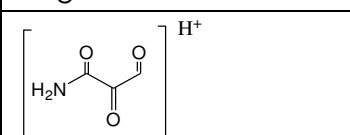
TP 238

m/z	Retention time	Precursor/ Product ion	Structure	References
238.1	12.9 min	$[M+H]^+$		24,26 21
 <p>ATL_PHOTOLYSIS_100MGL_32MIN.D: EC 238.1 +All MS</p>				
<b>MS<sup>2</sup> of TP 238</b>				
 <p>+MS2(238.1), 13.9min #367</p>				
196.0		$[M+H-CH(CH_3)_2]^+$		
179.0		$[M+H-CH(CH_3)_2NH_2]^+$		
161.0		$[M+H-CH(CH_3)_2NH_2-H_2O]^+$		
153.0		$[M+H-CH(CH_3)_2NH_2-HCHO]^+$		
131.0		$[M+H-CH(CH_3)_2NH_2-H_2O-HCHO]^+$		
116.1		$[M+H-HOC_6H_4CHO]$		
105.0		$[M+H-H_2OC_2H_6-CH_2NHCH(CH_3)_2-OH]^+$		

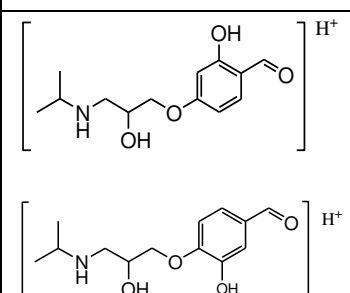
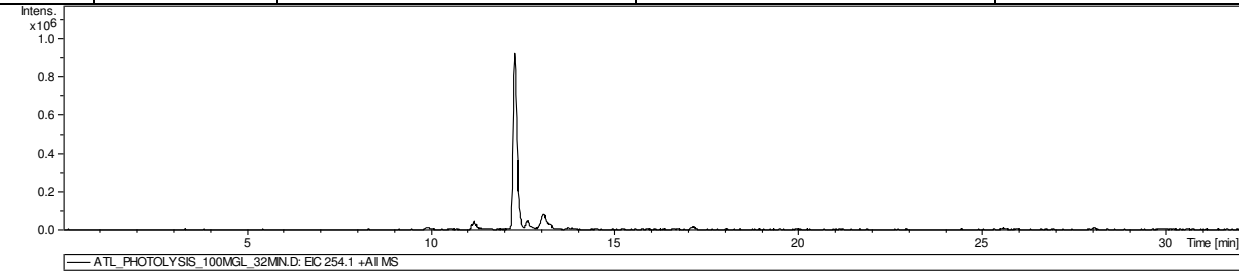
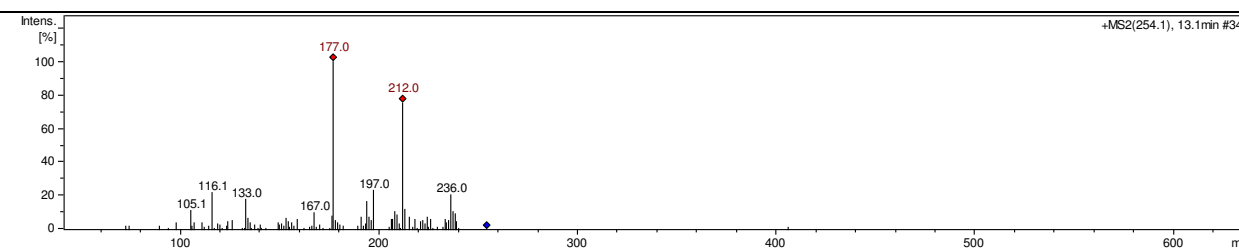
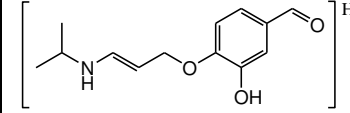
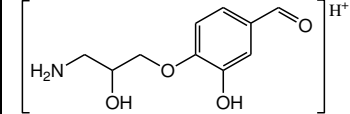
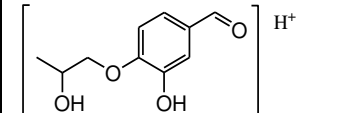
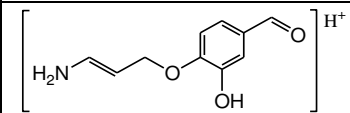
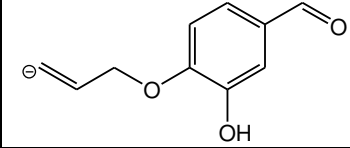
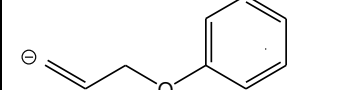
**TP 249**

m/z	Retention time	Precursor/ Product ion	Structure	References
249.1	14.0	$[M+H]^+$		19 MetaPC software
				
<b>MS<sup>2</sup></b>				
				
232.0		$[M+H-NH_3]^+$		
206.0		$[M+H-HCONH_2]^+$		
188.0		$[M+H-CH(CH_3)_2-NH_2]^+$		
176.0		$[M+H-CH_3NHCH(CH_3)_2]^+$		
161.0		$[M+H-NHCH(CH_3)_2-NH_3-H_2O]^+$		

TP 253

m/z	Retention time	Precursor/ Product ion	Structure	References
253.1	13.1	$[M+H]^+$		
 <p>ATL_PHOTOLYSIS_100MGL_32MIN.D: EC 253.1 +All MS</p>				
<b>MS<sup>2</sup></b>				
 <p>+MS2(253.1), 13.6min #363</p>				
235.0		$[M+H-H_2O]^+$		
225.0		$[M+H-2O]^+$		
208.0		$[M+H-2O-NH_3]^+$		
190.0		$[M+H-2O-NH_3-H_2O]^+$		
142.1		$[M+H-2O-NH_3-H_2O-HCONH_2]^+$		
102.1		$[M+H-C_8H_9NO_2]^+$		

TP 254

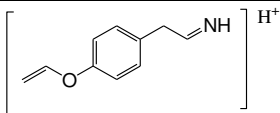
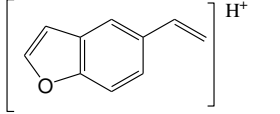
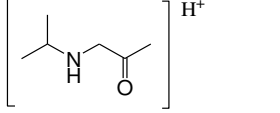
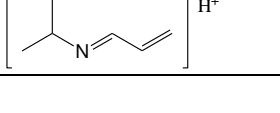
m/z	Retention time	Precursor/ Product ion	Structure	References
254.1	12.3	$[M+H]^+$		26 20,21,28
 <p>ATL_PHOTOLYSIS_100MGL_32MIN.D: EC 254.1 +All MS</p>				
<b>MS<sup>2</sup></b>				
 <p>+MS2(254.1), 13.1min #349</p>				
236.0		$[M+H-H_2O]^+$		
212.0		$[M+H-CH(CH_3)_2]^+$		
197.0		$[M+H-NHCH(CH_3)_2]^+$		
194.0		$[M+H-H_2O-CH(CH_3)_2]^+$		
177.0		$[M+H-NH_2CH(CH_3)_2-H_2O]^+$		
133.0		$[M+H-NH_2CH(CH_3)_2-H_2O-HCHO-O]^+$		



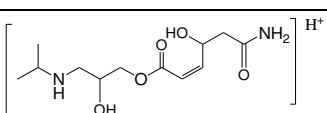
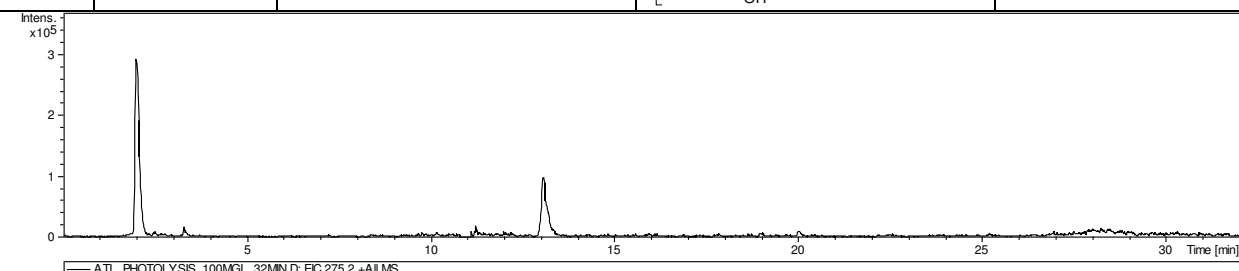
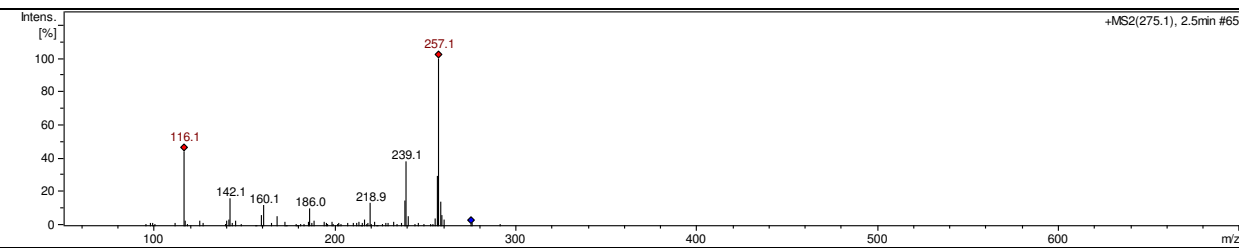
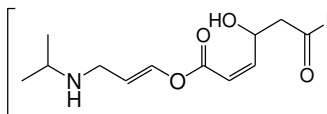
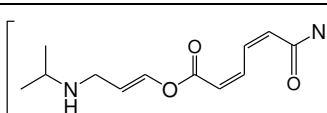
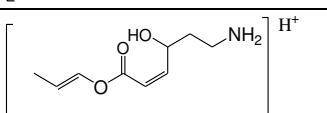
116.1	$[M+H-C_7H_6O_3]^+$	
105.1	$[M+H-C_5H_{13}NO-H_2O-HCHO]^+$	

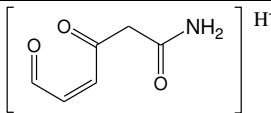
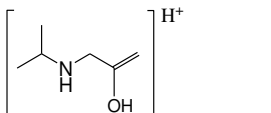
### TP 265

m/z	Retention time	Precursor/ Product ion	Structure	References
265.1	9.4	$[M+H]^+$		MetaPC software
<b>MS<sup>2</sup></b>				
249.0		$[M+H-H_2O]^+$		
237.0		$[M+H-2O]^+$		
225.0		$[M+H-CH(CH_3)_2]^+$		
208.0		$[M+H-CHNH(CH_3)_2]^+$		
190.0		$[M+H-H_2O-CH_3CONH_2]^+$		

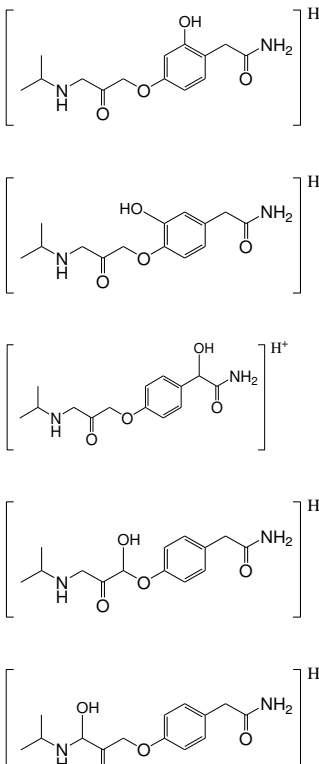
162.0	$[M+H-2H_2O-CH_3NHCH(CH_3)_2]^+$	
145.0	$[M+H-2H_2O-CH_3NHCH(CH_3)_2-NH_3]^+$	
116.1	$[M+H-C_8H_9NO_2]^+$	
98.1	$[M+H-C_8H_9NO_2-H_2O]^+$	

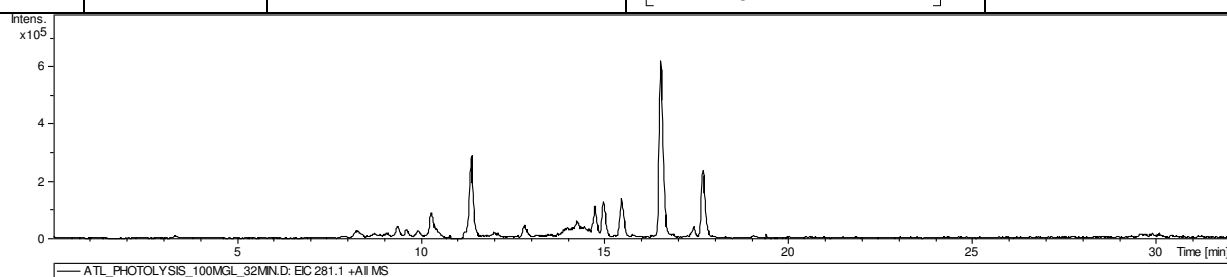
### TP 275

m/z	Retention time	Precursor/ Product ion	Structure	References
275.2	2.0 min	$[M+H]^+$		
 <p>ATL_PHOTOLYSIS_100MGL_32MIND: EIC 275.2 +All MS</p>				
<b>MS<sup>2</sup></b>				
 <p>+MS2(275.1), 2.5min #65</p>				
257.1		$[M+H-H_2O]^+$		
239.1		$[M+H-2H_2O]^+$		
186.0		$[M+H-H_2O-NHCH(CH_3)_2-O]^+$		

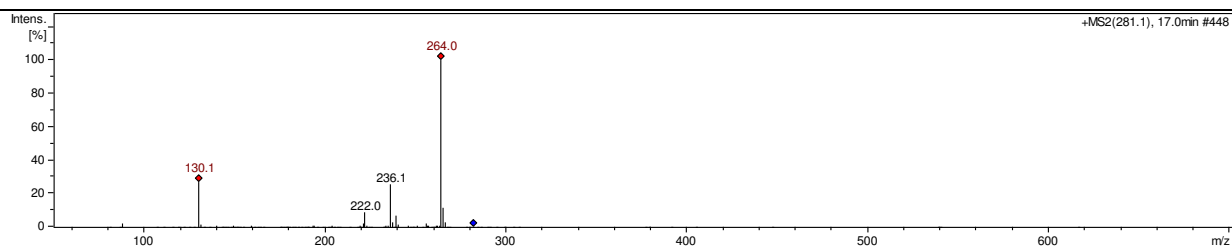
142.1	$[M+H-C_6H_{15}NO_2]^+$	
116.1	$[M+H-C_6H_9NO_4]^+$	

### TP 281

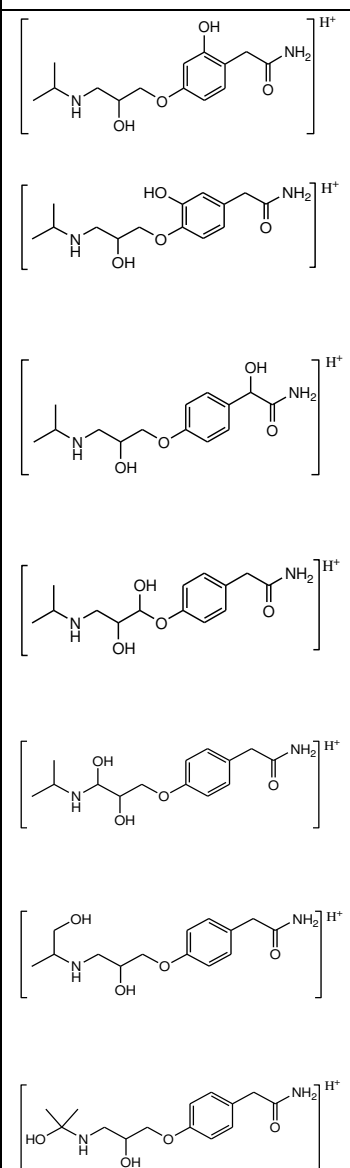
m/z	Retention time	Precursor/ Product ion	Structure	References
281.2	several peaks	$[M+H]^+$		20,21,24 MetaPC software

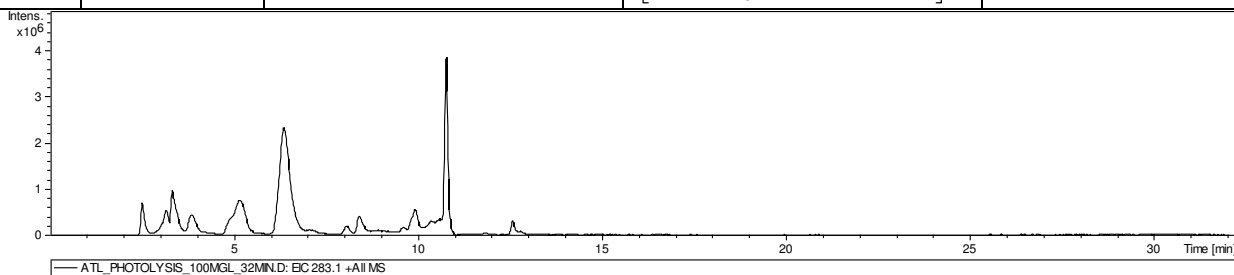


### MS<sup>2</sup>

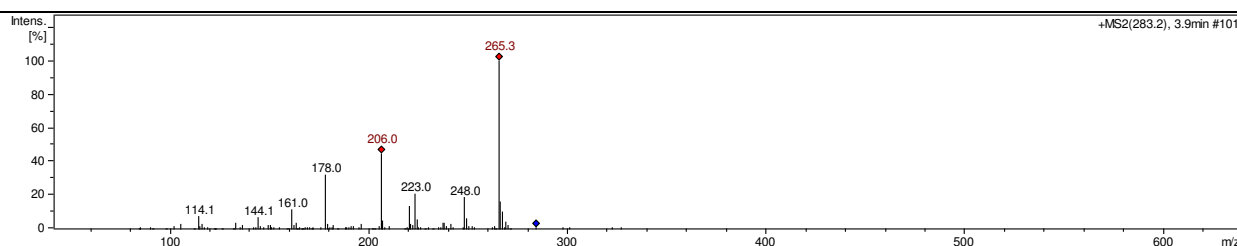


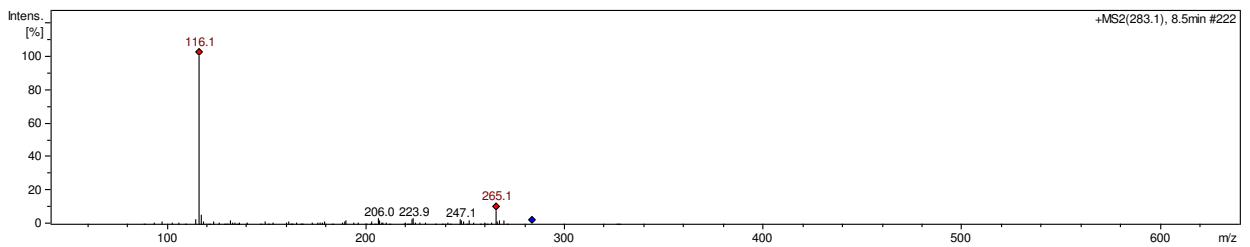
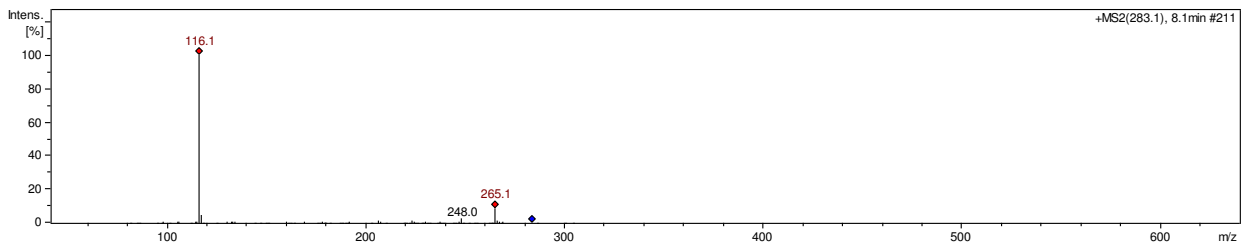
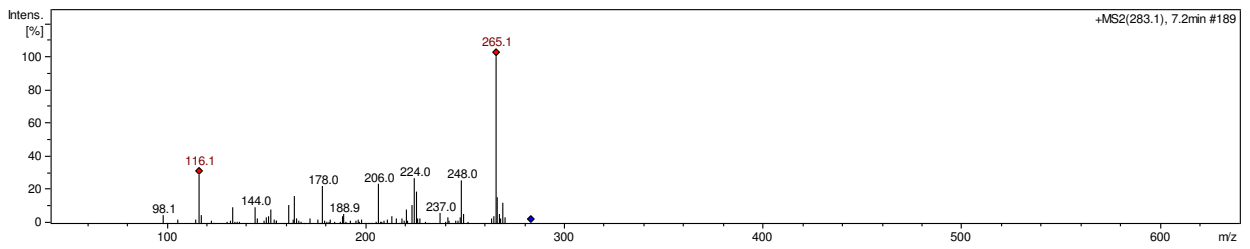
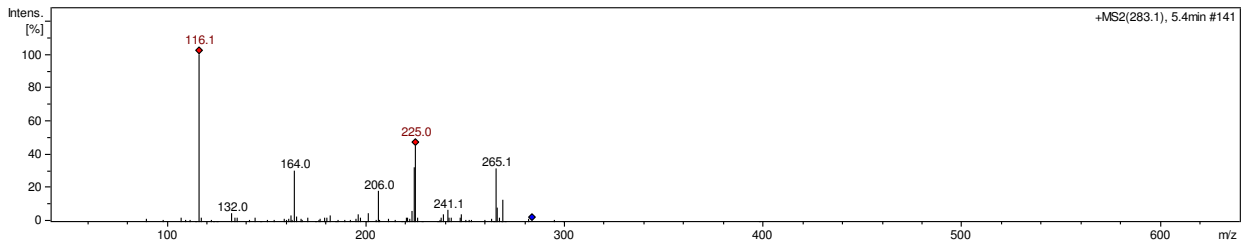
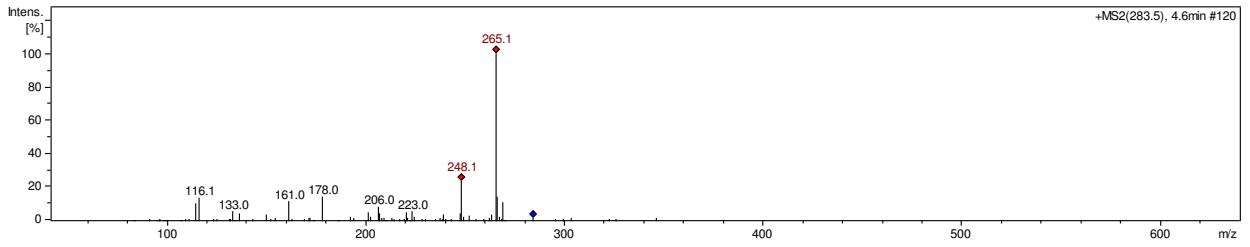
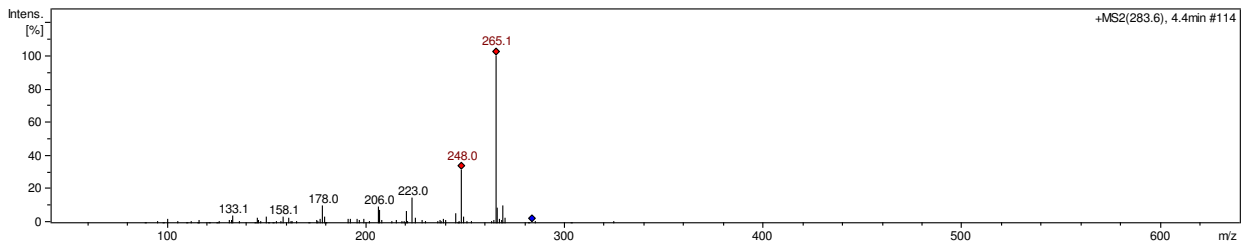
264.0	$[M+H-NH_3]^+$	
239.0	$[M+H-CH(CH_3)_2]^+$	
236.1	$[M+H-HCONH_2]^+$	
222.0	$[M+H-NH_2CH(CH_3)_2]^+$	
130.1	$[M+H-C_8H_9NO_2]^+$	

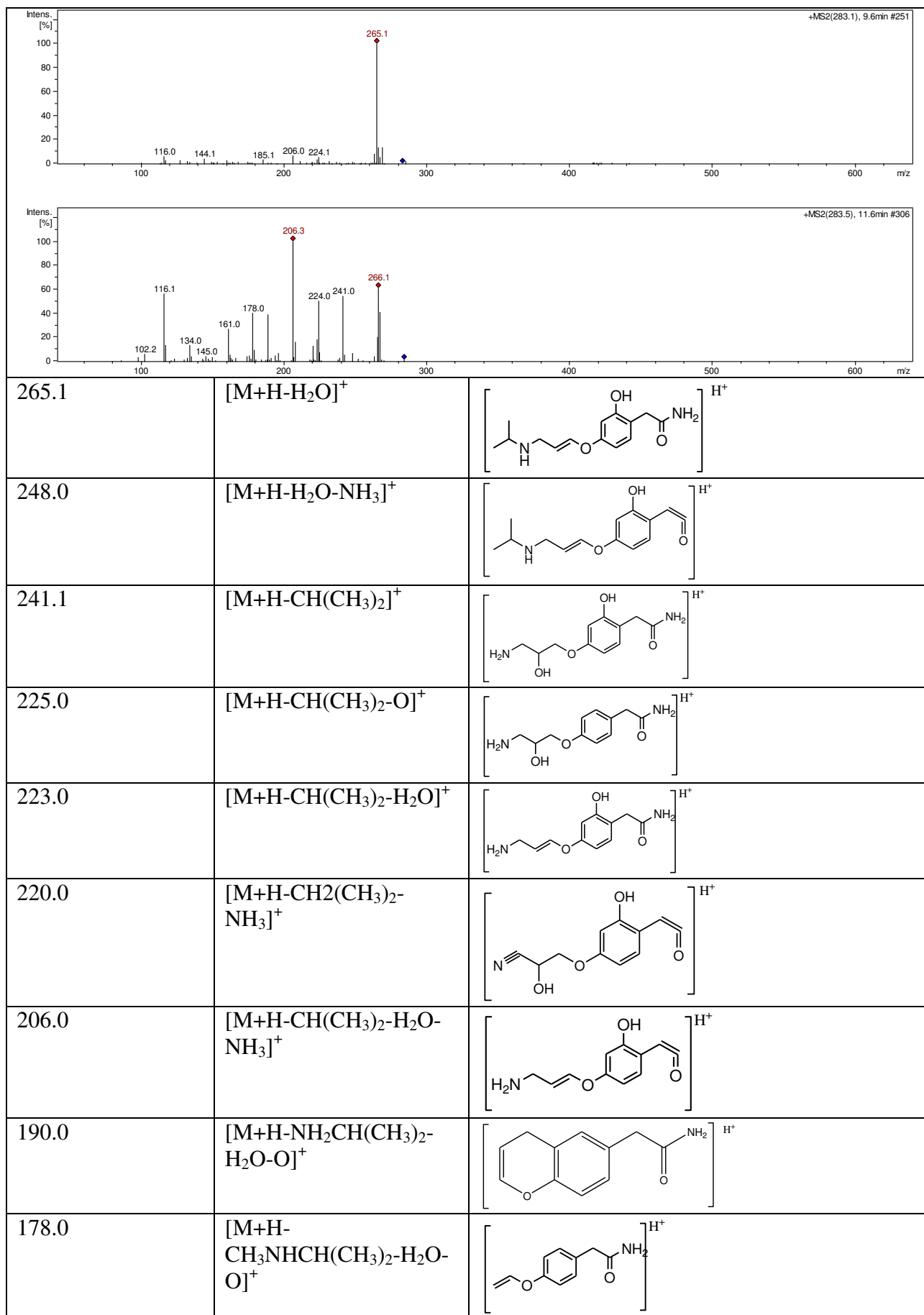
m/z	Retention time	Precursor/ Product ion	Structure	References
283.2	several peaks	$[M+H]^+$		20–22,24,26–28 MetaPC software

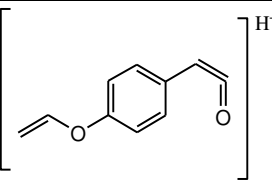
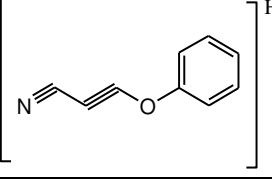
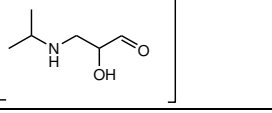
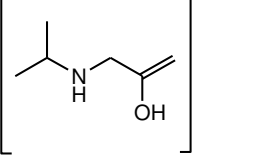
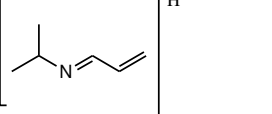


MS<sup>2</sup>

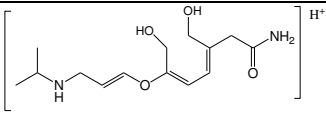
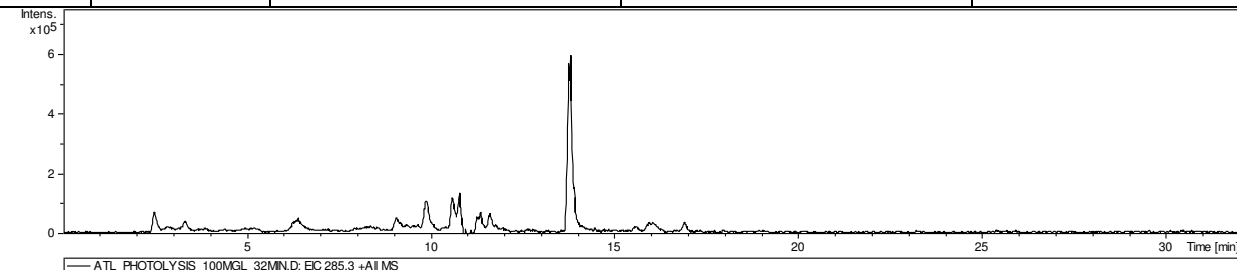






161.0	$[M+H-CH_3NHCH(CH_3)_2-H_2O-O-NH_3]^+$	
144.0	$[M+H-CH_2(CH_3)_2-H_2O-O-CH_3CONH_2]^+$	
132.0	$[M+H-C_8H_{11}NO_2]^+$	
116.1	$[M+H-C_8H_{11}NO_3]^+$	
98.2	$[M+H-C_8H_{11}NO_3-H_2O]^+$	

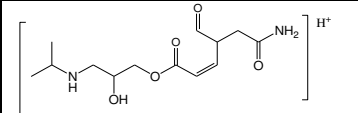
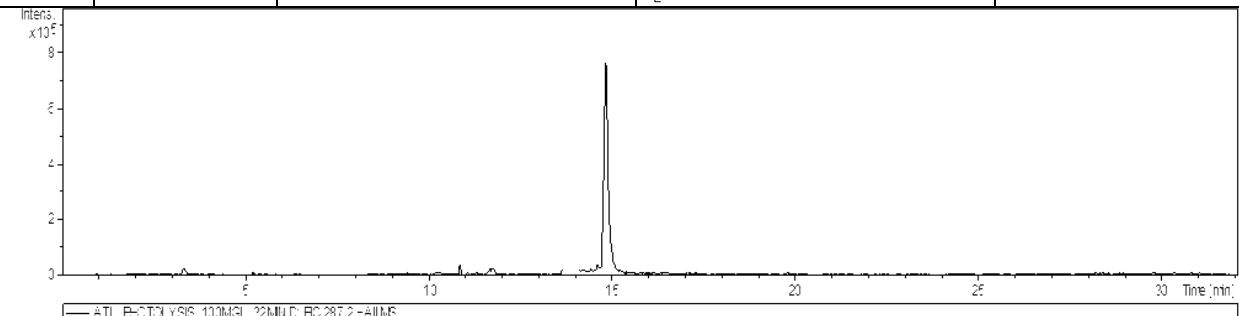
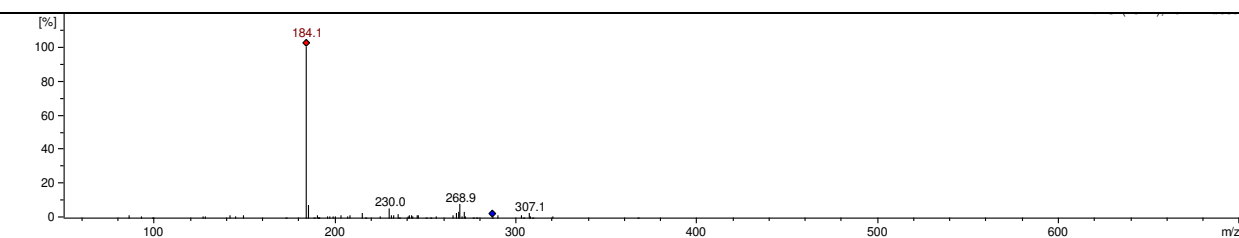
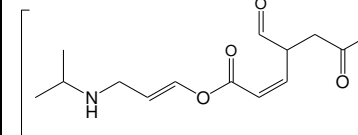
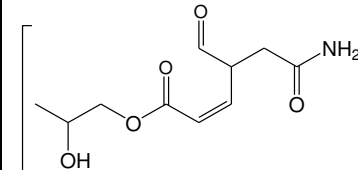
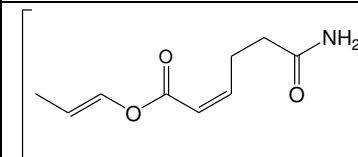
### TP 285

m/z	Retention time	Precursor/ Product ion	Structure	References
285.3	13.8	$[M+H]^+$		
 <p>Intens. x10<sup>5</sup></p> <p>Time [min]</p> <p>ATL_PHOTOLYSIS_100MGL_32MIN.D: EC 285.3 +All MS</p>				
<b>MS<sup>2</sup></b>				
NO MS2 fragment observed				

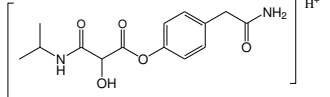
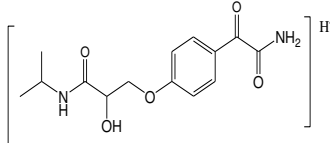
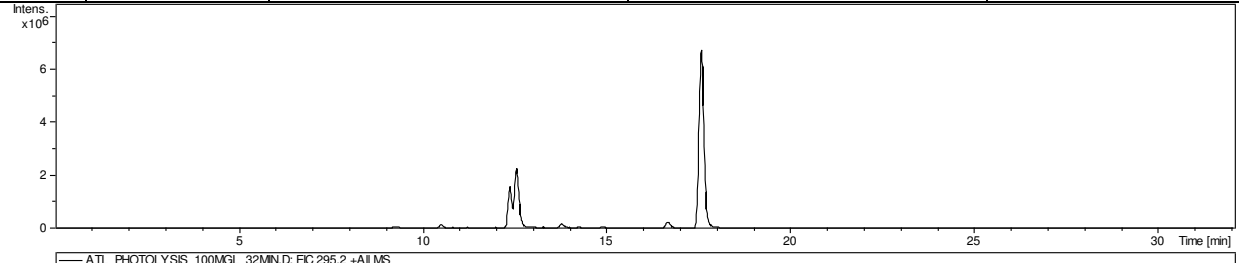
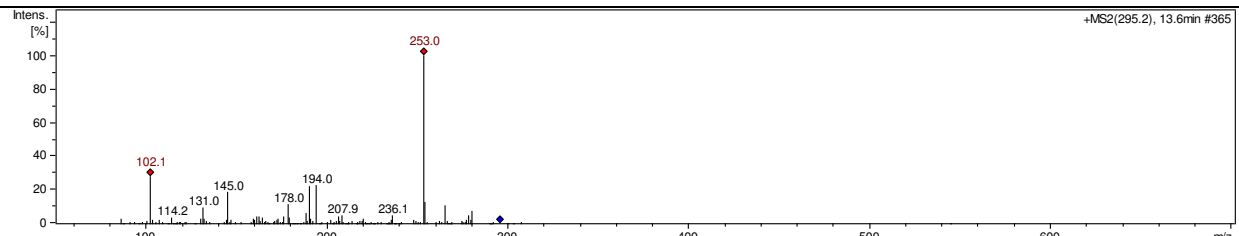
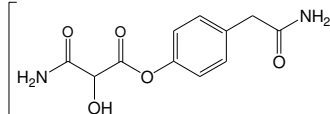
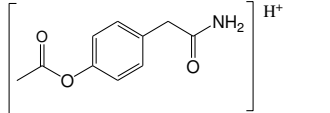
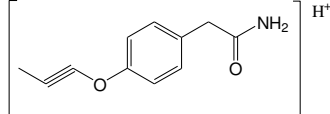
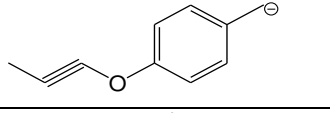
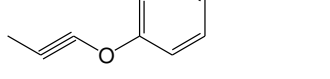
### TP 287

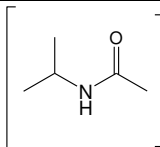
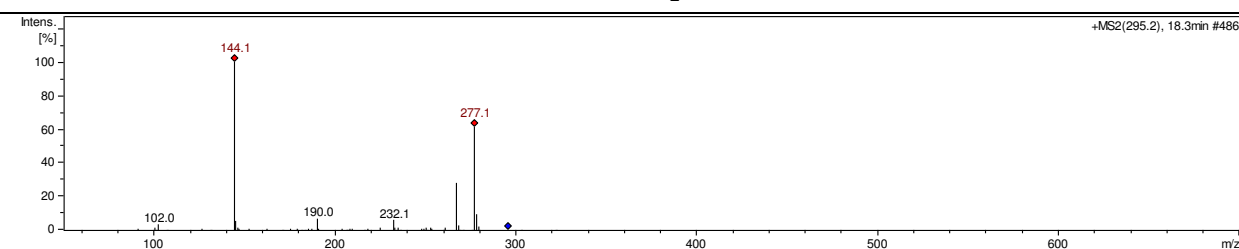
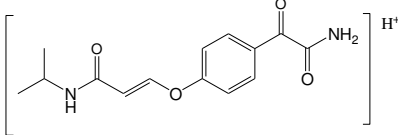
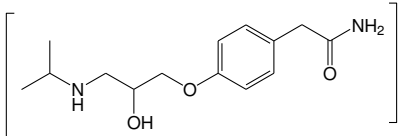
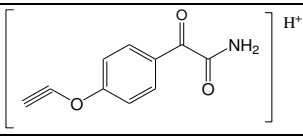
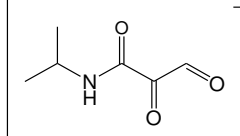
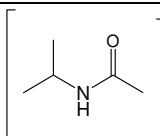
m/z	Retention time	Precursor/ Product ion	Structure	References



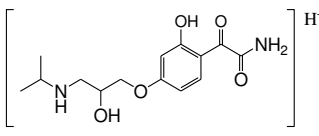
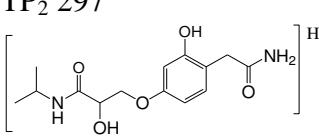
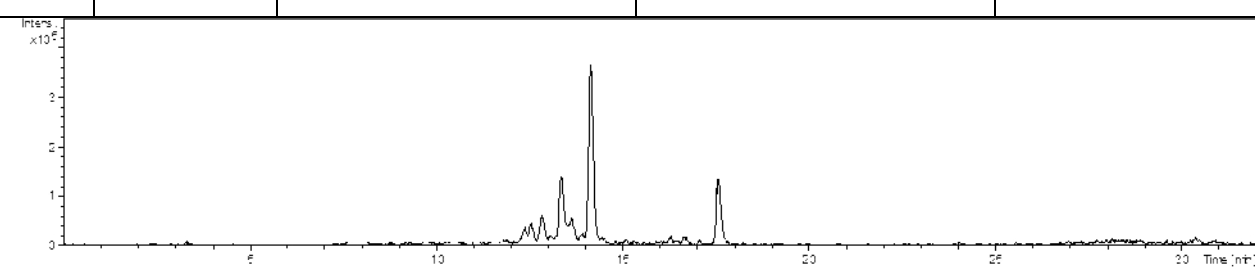
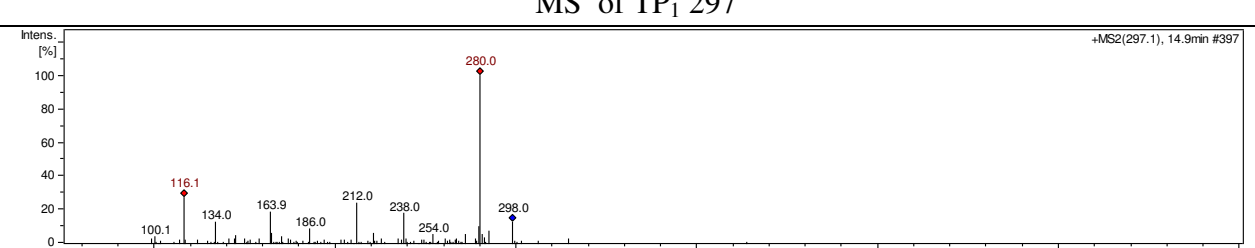
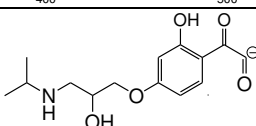
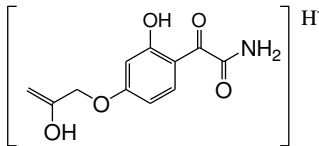
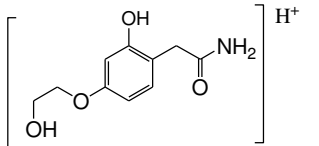
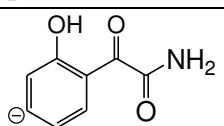
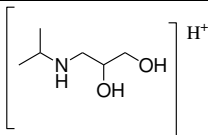
287.3	14.8 min	$[M+H]^+$	
			
$MS^2$			
			
268.9		$[M+H-H_2O]^+$	
230.0		$[M+H-NH_2CH(CH_3)_2]^+$	
184.1		$[M+H-NH_2CH(CH_3)_2-H_2O-HCHO]^+$	

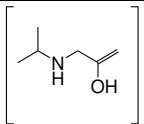
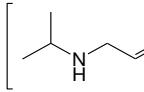
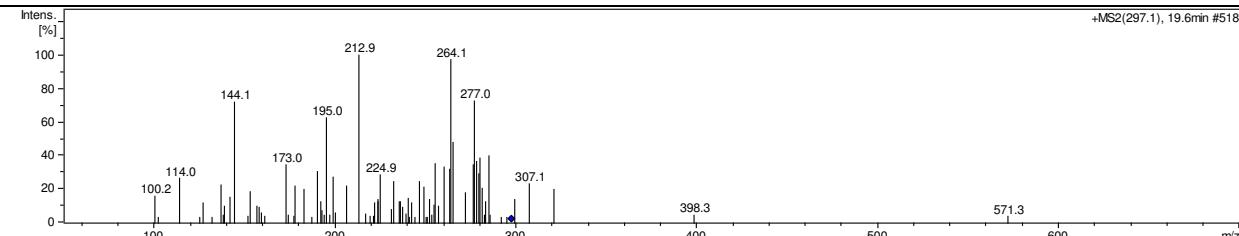
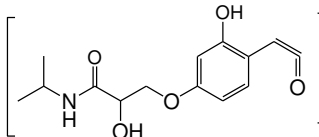
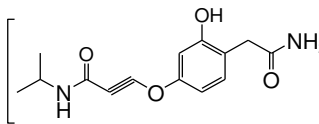
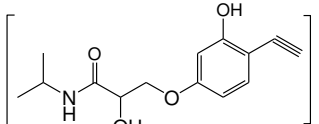
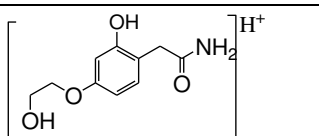
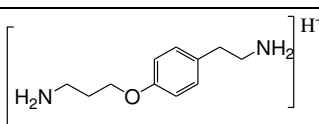
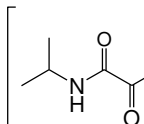
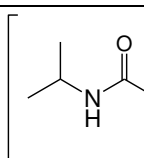
**TP 295**

m/z	Retention time	Precursor/ Product ion	Structure	References
295.2	12.6 min	$[M+H]^+$	<p><b>TP<sub>1</sub> 295</b></p>  <p><b>TP<sub>2</sub> 295</b></p> 	29
 <p>ATL_PHOTOLYSIS_100MGL_32MIN.D: EC 295.2 +All MS</p>				
<b>MS<sup>2</sup> of TP<sub>1</sub> 295</b>				
 <p>+MS2(295.2), 13.6min #365</p>				
253.0		$[M+H-CH(CH_3)_2]^+$		
194.0		$[M+H-2H_2O-NHCH(CH_3)_2]^+$		
190.0		$[M+H-2H_2O-NHCH(CH_3)_2-H_2O]^+$		
145.0		$[M+H-2H_2O-NHCH(CH_3)_2-H_2O-HCONH_2]^+$		
131.0		$[M+H-2H_2O-NHCH(CH_3)_2-H_2O-CH_3CONH_2]^+$		

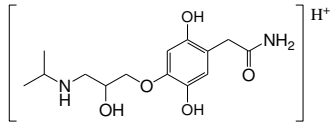
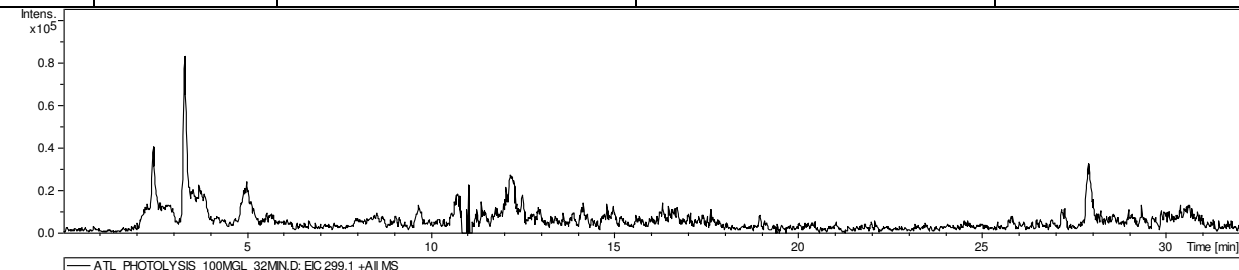
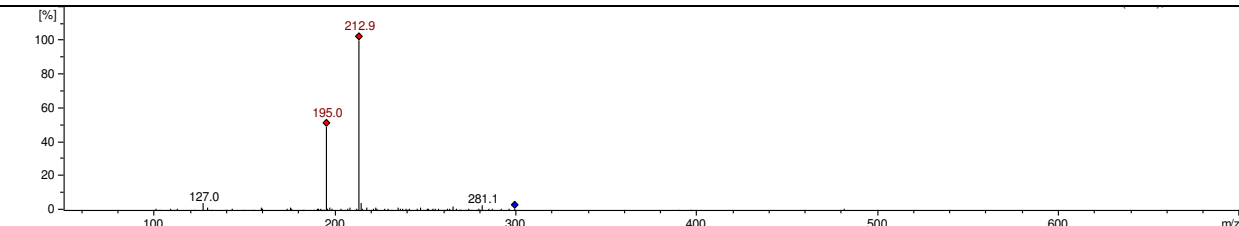
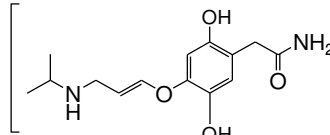
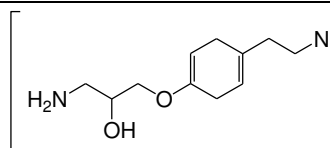
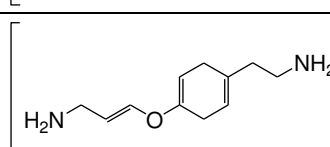
102.1	$[M+H-C_9H_{11}NO_3]^+$	 $H^+$
<b>MS<sup>2</sup> of TP<sub>2</sub> 295</b>		
		
277.1	$[M+H-H_2O]^+$	 $H^+$
267.1	$[M+H-2O]^+$	 $H^+$
190.1	$[M+H-2H_2O-CH_3NHCH(CH_3)_2]^+$	 $H^+$
144.1	$[M+H-C_8H_9NO_2]^+$	 $H^+$
102.0	$[M+H-C_9H_{11}NO_4]^+$	 $H^+$

**TP 297**

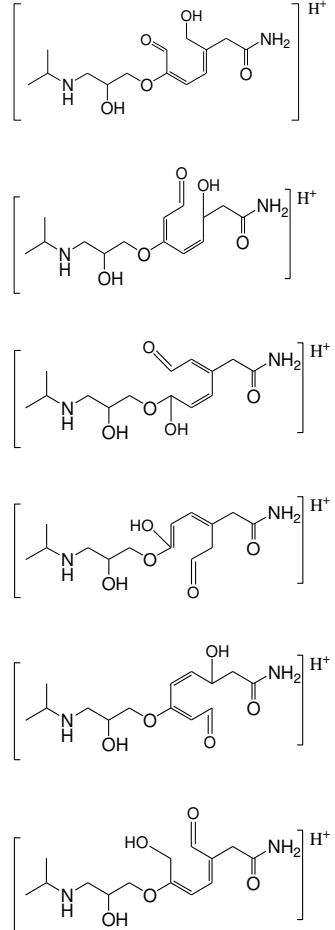
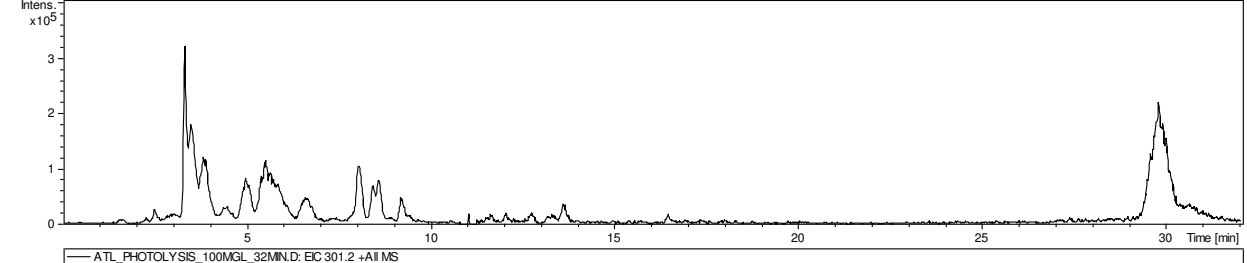
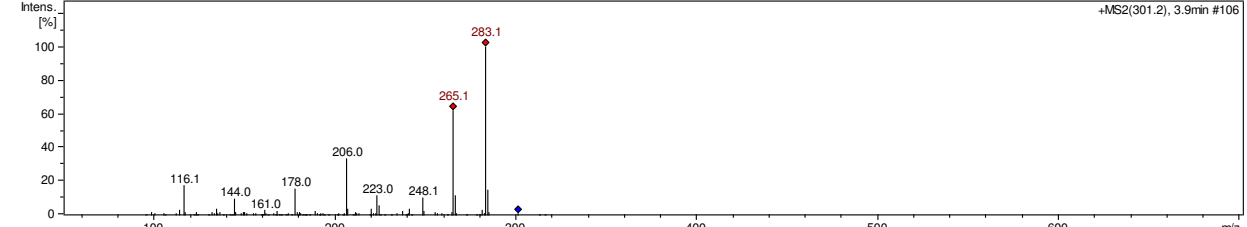
m/z	Retention time	Precursor/ Product ion	Structure	References
297.1	14.1 min  17.6 min	$[M+H]^+$	<p>TP<sub>1</sub> 297</p>  <p>TP<sub>2</sub> 297</p> 	20
 <p>ATL_F-CTCLYSIS_100M3L_20MIN.D: EC 297.1 -AMME</p>				
<b>MS<sup>2</sup> of TP<sub>1</sub> 297</b>				
 <p>+MS2(297.1), 14.9min #397</p>				
280.0		$[M+H-NH_3]^+$		
238.0		$[M+H-NH_2CH(CH_3)_2]^+$		
212.0		$[M+H-O-CH_3NHCH(CH_3)_2]^+$		
163.9		$[M+H-C_6H_{15}NO_2]^+$		
134.0		$[M+H-C_8H_7NO_3]^+$		

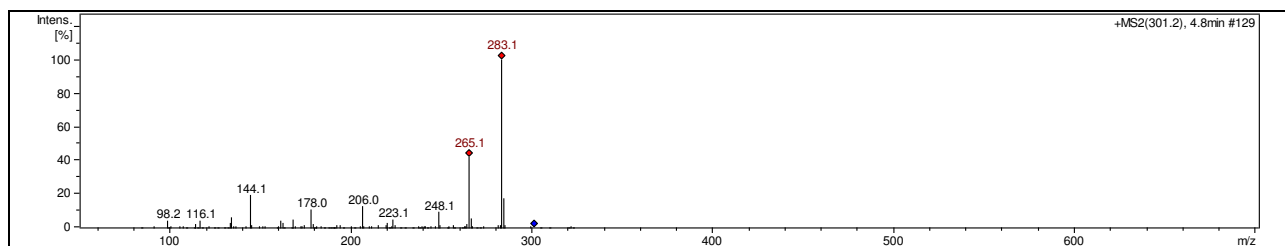
116.1	$[M+H-C_8H_7NO_3-H_2O]^+$	
100.1	$[M+H-C_8H_7NO_3-2H_2O]^+$	
<b>MS<sup>2</sup> of TP<sub>2</sub> 297</b>		
		
280.2	$[M+H-NH_3]^+$	
277.0	$[M+H-H_2O]^+$	
264.0	$[M+H-H_2O-NH_3]^+$	
212.9	$[M+H-HCHO-NH_2CH(CH_3)_2]^+$	
195.0	$[M+H-CH(CH_3)_2-H_2O-3O]^+$	
144.1	$[M+H-C_8H_{13}NO_2]^+$	
114.0	$[M+H-C_8H_{13}NO_2-H_2O-O]^+$	

TP 299

m/z	Retention time	Precursor/ Product ion	Structure	References
299.1	3.3 min	$[M+H]^+$		20,24,26
 <p>ATL_PHOTOLYSIS_100MGL_32MIN.D: EIC 299.1 +All MS</p>				
<b>MS<sup>2</sup></b>				
				
281.1		$[M+H-H_2O]^+$		
212.9		$[M+H-2H_2O-CH(CH_3)_2-O]^+$		
195.0		$[M+H-3H_2O-CH(CH_3)_2-O]^+$		

**TP 301**

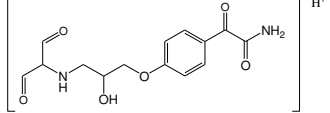
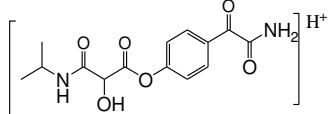
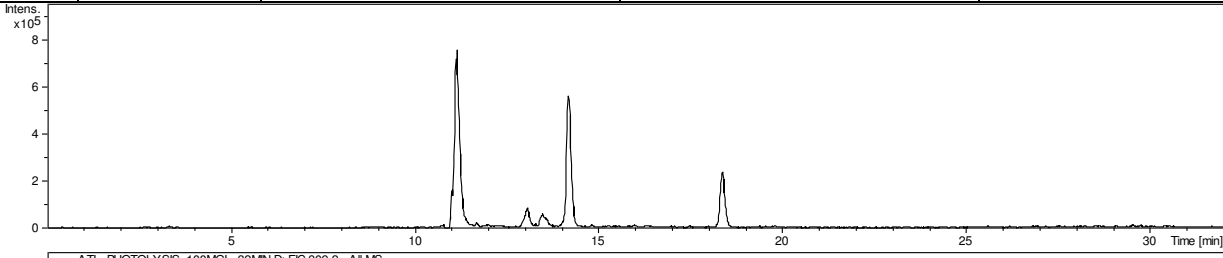
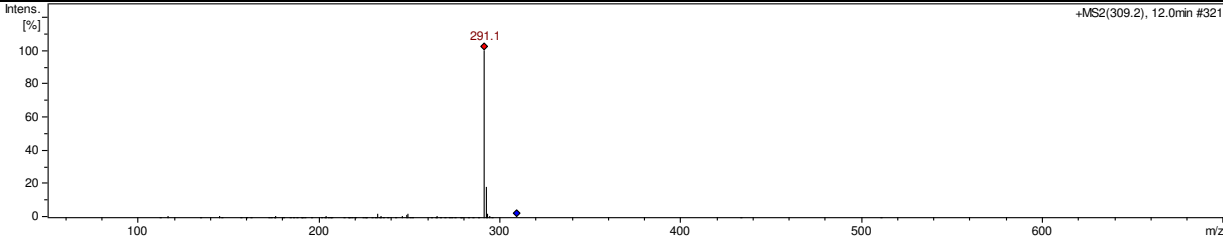
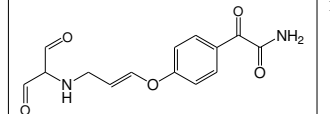
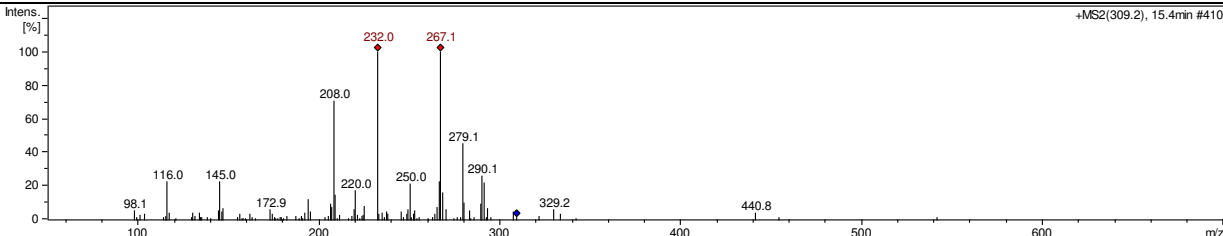
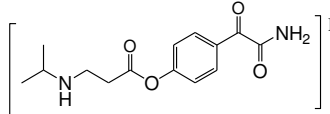
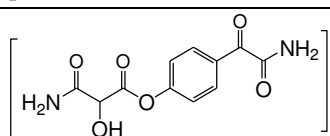
m/z	Retention time	Precursor/ Product ion	Structure	References
301.2	several Peaks	[M+H] <sup>+</sup>		
 <p style="text-align: center;">— ATL_PHOTOLYSIS_100MGL_32MIND_EC 301.2 +All MS</p>				
<b>MS<sup>2</sup></b>				
 <p style="text-align: right;">+MS2(301.2), 3.9min #106</p>				

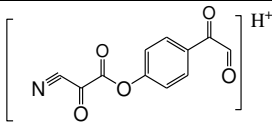
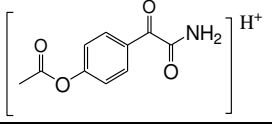
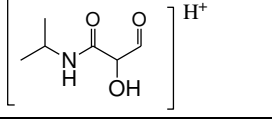
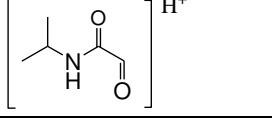


283.1	$[M+H-H_2O]^+$	
265.1	$[M+H-2H_2O]^+$	
248.1	$[M+H-2H_2O-NH_3]^+$	
223.1	$[M+H-CH_2(CH_3)_2-2H_2O]^+$	
178.0	$[M+H-NH_2CH(CH_3)_2-2H_2O-CH_3OH]^+$	
144.0	$[M+H-CH_2(CH_3)_2-C_5H_9NO_2]^+$	
134.0	$[M+H-C_8H_{11}NO_3]^+$	
116.1	$[M+H-C_8H_{11}NO_3-H_2O]^+$	

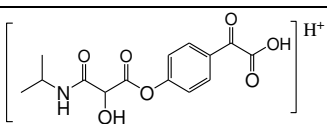
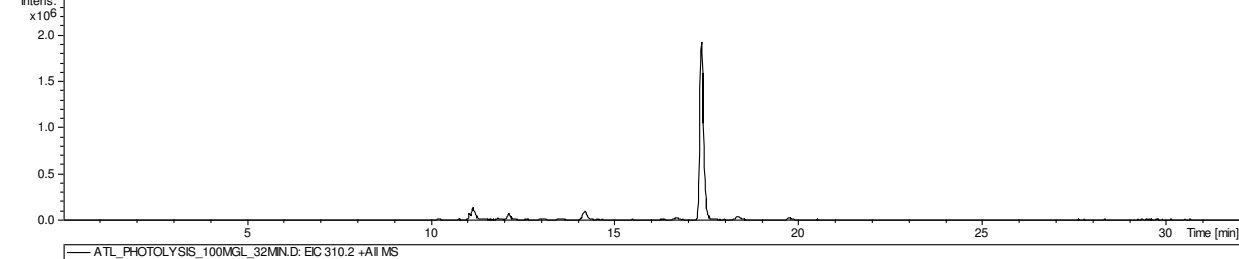
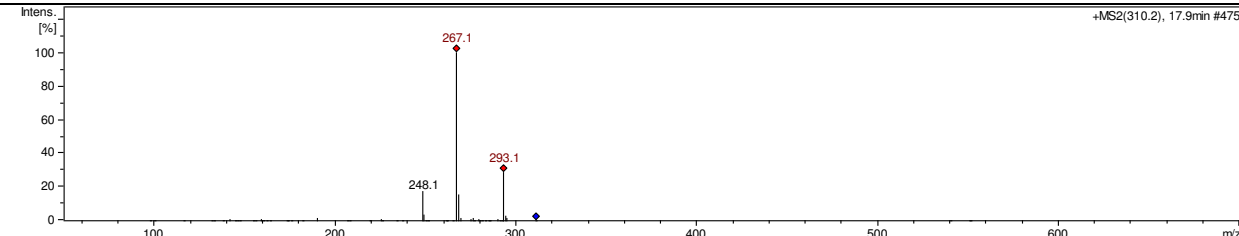
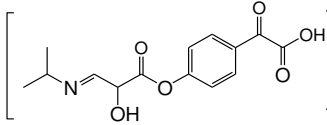
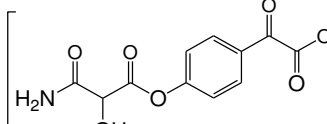
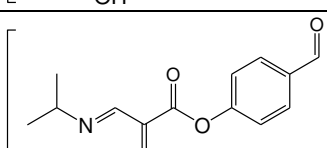


**TP 309**

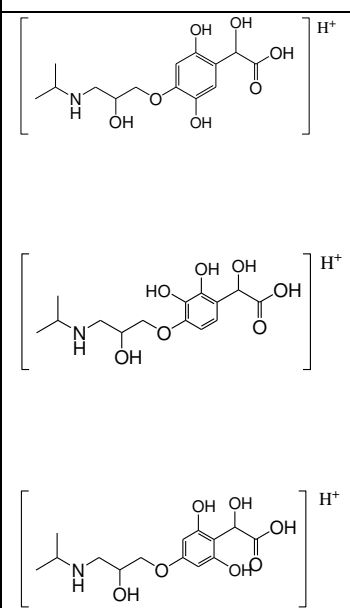
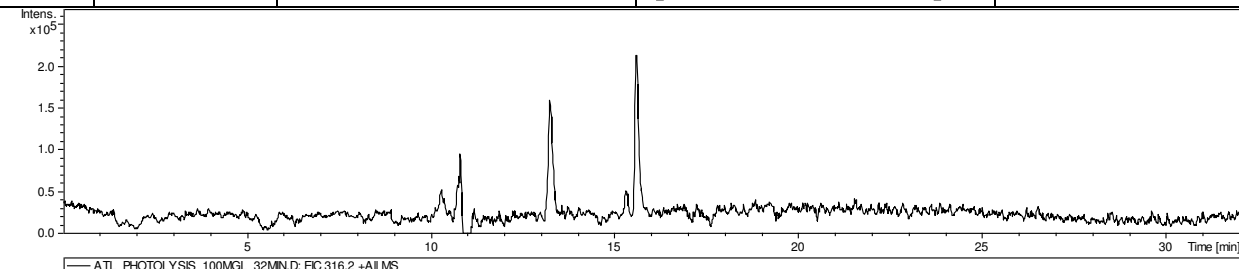
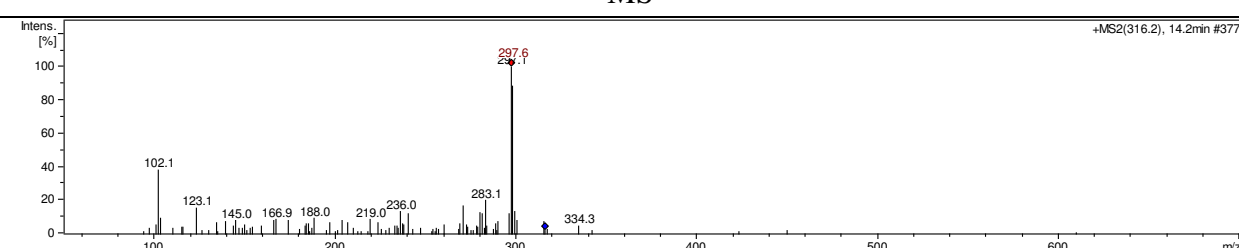
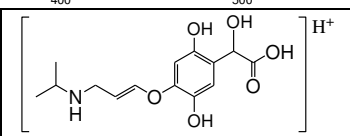
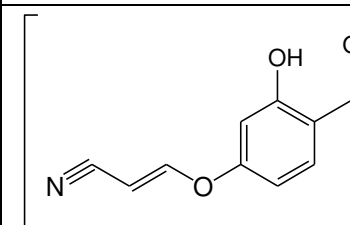
m/z	Retention time	Precursor/ Product ion	Structure	References
309.2	TP <sub>1</sub> 309 11.2  TP <sub>2</sub> 309 14.2	[M+H] <sup>+</sup>	<p>TP<sub>1</sub> 309</p>  <p>TP<sub>2</sub> 309</p> 	29
 <p>ATL_PHOTOLYSIS_100MGL_32MIN.D: EC 309.2 +All MS</p>				
MS <sup>2</sup> of TP <sub>1</sub> 309				
 <p>+MS2(309.2), 12.0min #321</p>				
291.1		[M+H-H <sub>2</sub> O] <sup>+</sup>		
MS <sup>2</sup> of TP <sub>2</sub> 309				
 <p>+MS2(309.2), 15.4min #410</p>				
279.1		[M+H-2O] <sup>+</sup>		
267.1		[M+H-CH <sub>2</sub> (CH <sub>3</sub> ) <sub>2</sub> ] <sup>+</sup>		

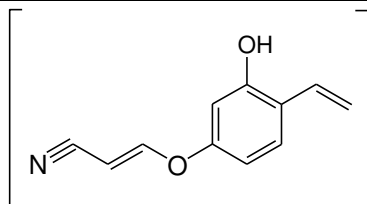
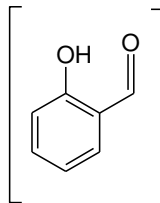
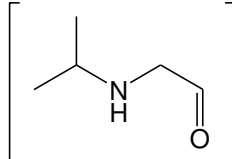
232.0	$[M+H-H_2O-CH_2(CH_3)_2-NH_3]^+$	
208.0	$[M+H-NH_2CH(CH_3)_2-HCHO-H_2O]^+$	
145.0	$[M+H-C_8H_7NO_3]^+$	
116.0	$[M+H-C_8H_7NO_3-HCHO]^+$	

### TP 310

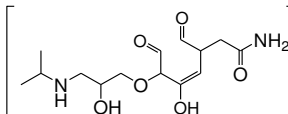
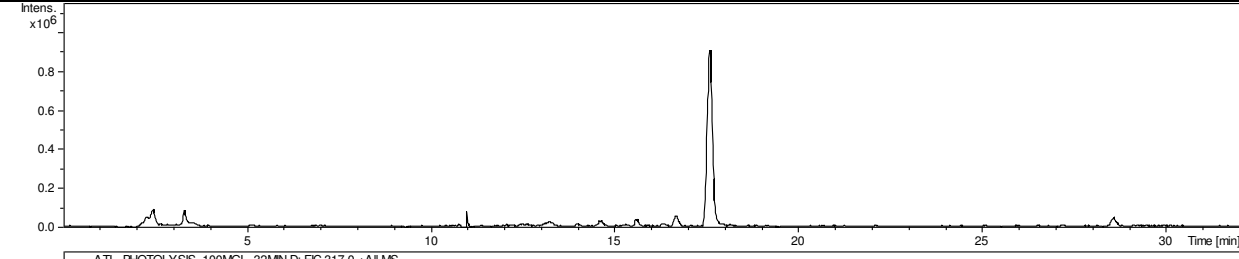
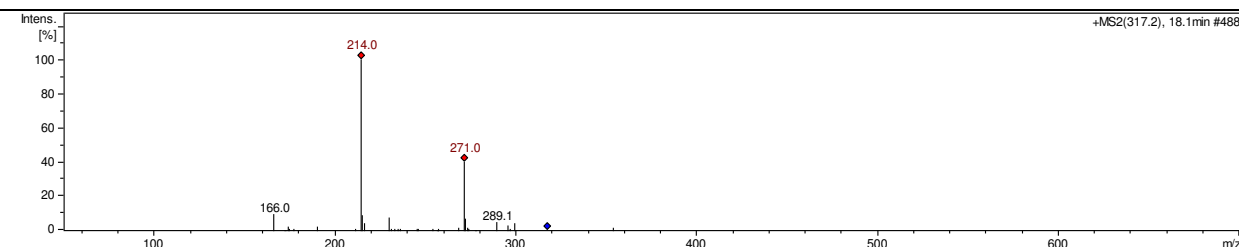
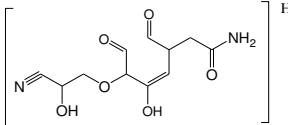
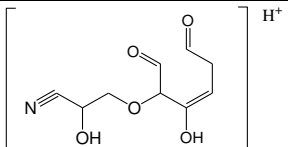
m/z	Retention time	Precursor/ Product ion	Structure	References
310.2	17.3 min	$[M+H]^+$		
				
<b>MS<sup>2</sup></b>				
				
293.1		$[M+H-H_2O]^+$		
267.1		$[M+H-CH(CH_3)_2]^+$		
248.1		$[M+H-H_2O-HCOOH]^+$		

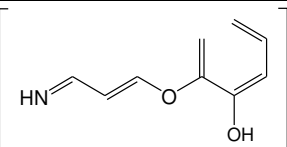
TP 316

m/z	Retention time	Precursor/ Product ion	Structure	References
316.2	13.2	$[M+H]^+$		
 <p>ATL_PHOTOLYSIS_100MGL_32MIN.D: EIC 316.2 +All MS</p>				
<b>MS<sup>2</sup></b>				
 <p>+MS2(316.2), 14.2min #377</p>				
297.6		$[M+H-H_2O]^+$		
236.0		$[M+H-2H_2O-CH_2(CH_3)_2]^+$		

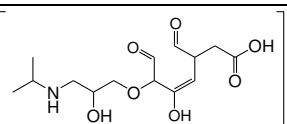
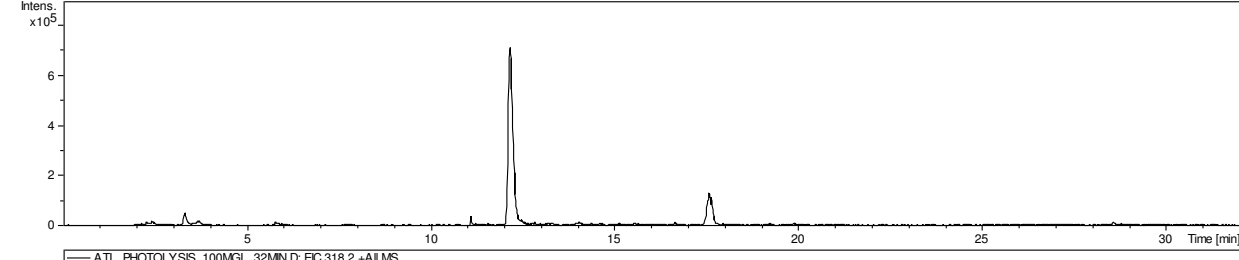
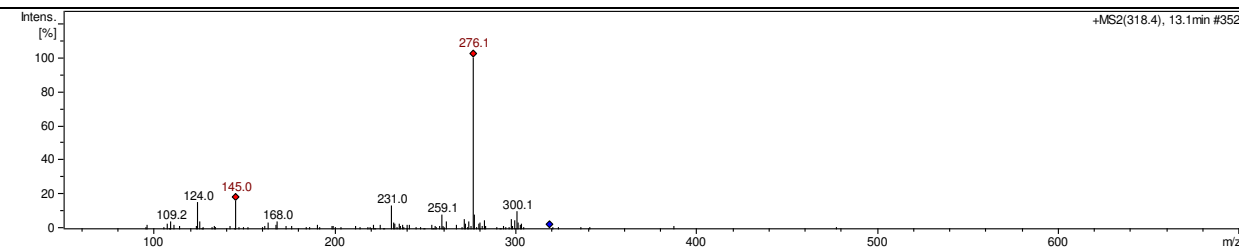
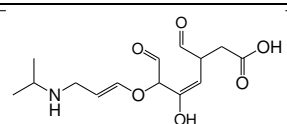
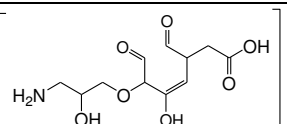
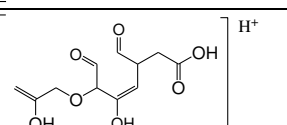
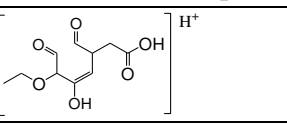
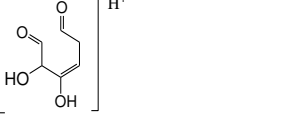
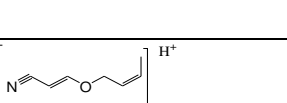
188.0	$[M+H-3H_2O-CH_2(CH_3)_2-HCOOH]^+$	
123.1	$[M+H-C_6H_{15}NO_2-H_2O-HCOOH]^+$	
102.1	$[M+H-C_9H_{12}O_6]^+$	

### TP 317

m/z	Retention time	Precursor/ Product ion	Structure	References
317.2	17.6	$[M+H]^+$		
				
<b>MS<sup>2</sup></b>				
				
271.0		$[M+H-CH(CH_3)_2]^+$		
214.0		$[M+H-CH(CH_3)_2-CH_3CONH_2]^+$		

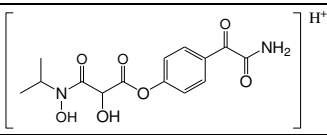
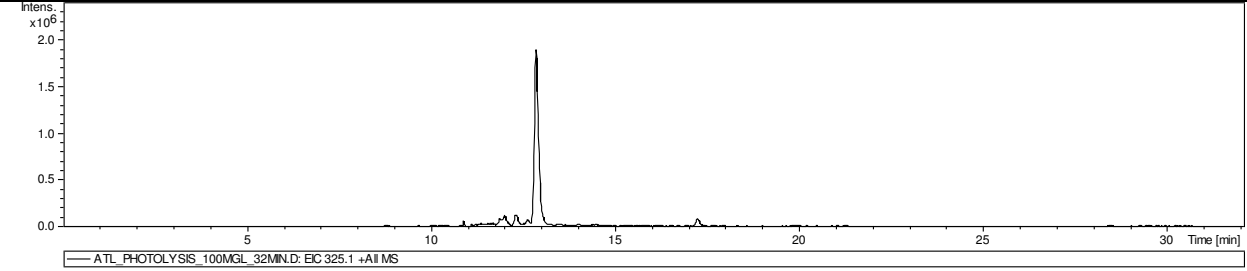
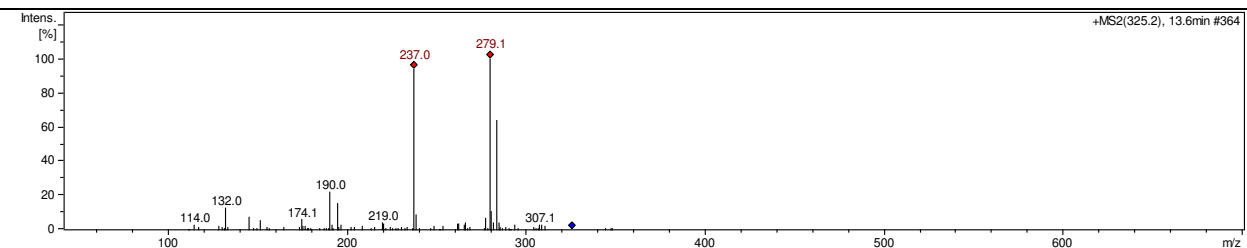
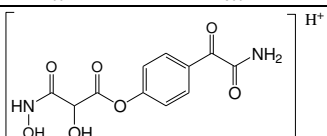
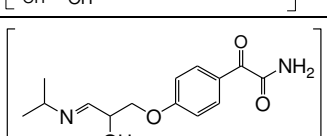
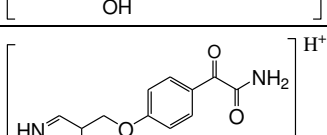
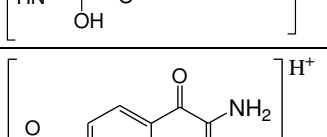
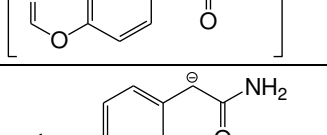
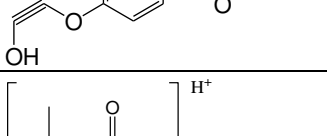
166.0	$[M+H-CH(CH_3)_2-CH_3CONH_2-3H_2O]^+$	
-------	---------------------------------------	--

### TP 318

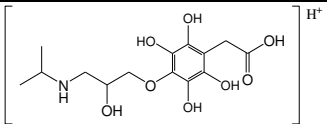
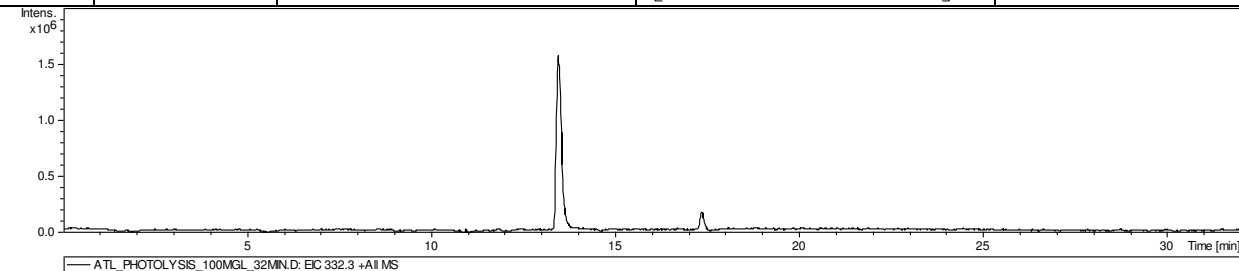
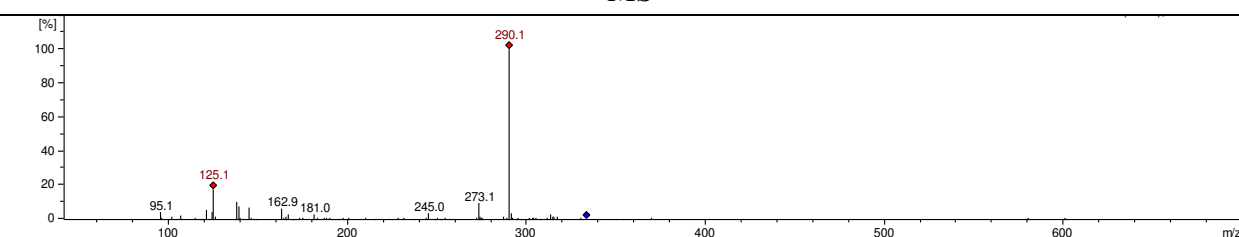
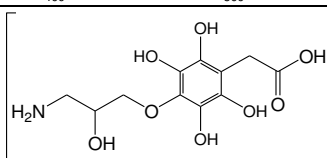
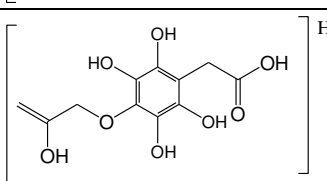
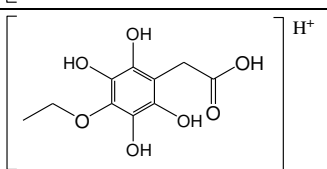
m/z	Retention time	Precursor/ Product ion	Structure	References
318.2	12.2	$[M+H]^+$		
 <p>ATL_PHOTOLYSIS_100MGL_32MIN.D: EIC 318.2 +All MS</p>				
<b>MS<sup>2</sup></b>				
 <p>+MS2(318.4), 13.1min #352</p>				
300.1		$[M+H-H_2O]^+$		
276.0		$[M+H-CH(CH_3)_2]^+$		
259.1		$[M+H-NH_2CH(CH_3)_2]^+$		
231.0		$[M+H-CH_3NHCH(CH_3)_2-H_2O]^+$		
145.0		$[M+H-CH_3NHCH(CH_3)_2-CH_3CH_2OH-CH_3COOH]^+$		
124.0		$[M+H-NH_2CH(CH_3)_2-CH_3COOH-2HCHO]^+$		

--	--	--

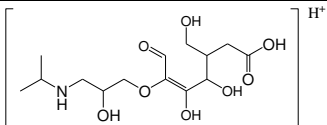
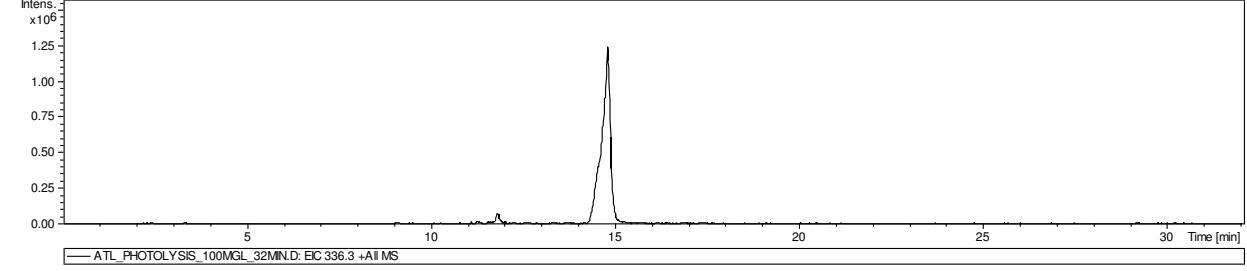
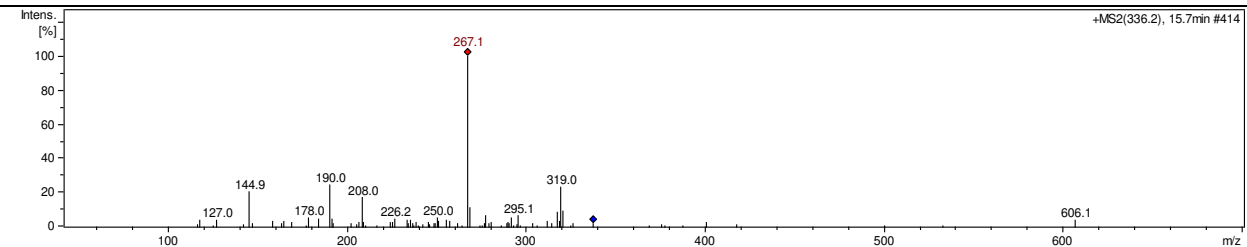
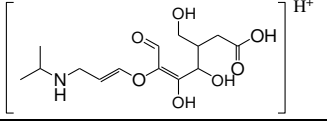
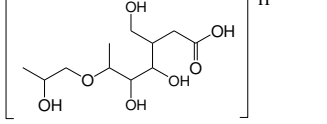
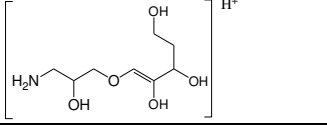
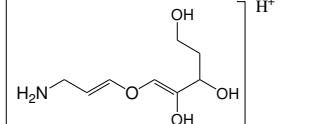
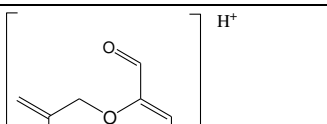
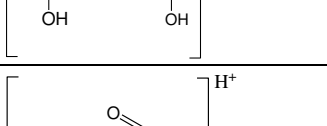
**TP 325**

m/z	Retention time	Precursor/ Product ion	Structure	References
325.2	12.9min	$[M+H]^+$		
 <p>ATL_PHOTOLYSIS_100MG.L_32MIN.D: EC 325.1 +All MS</p>				
<b>MS<sup>2</sup></b>				
 <p>+MS2(325.2), 13.6min #364</p>				
283.0		$[M+H-CH(CH_3)_2]^+$		
279.1		$[M+H-H_2O-2O]^+$		
237.0		$[M+H-CH(CH_3)_2-H_2O-2O]^+$		
194.0		$[M+H-C_5H_{11}NO_3]^+$		
190.0		$[M+H-C_4H_9NO_2-2H_2O]^+$		
132.0		$[M+H-C_9H_8NO_4]^+$		

TP 332

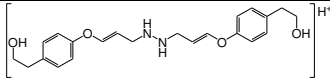
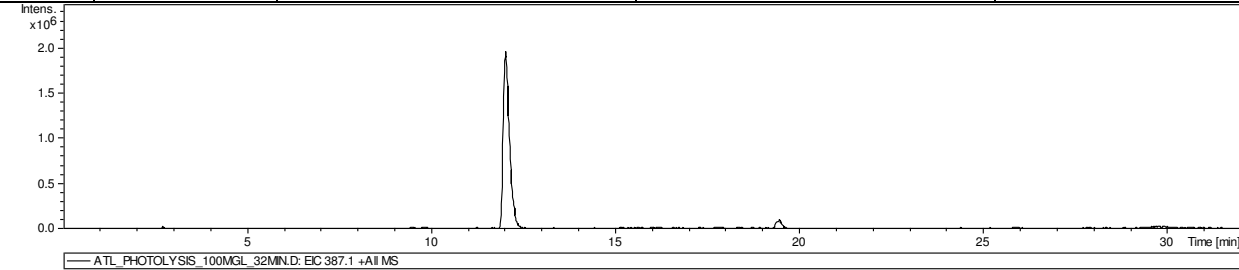
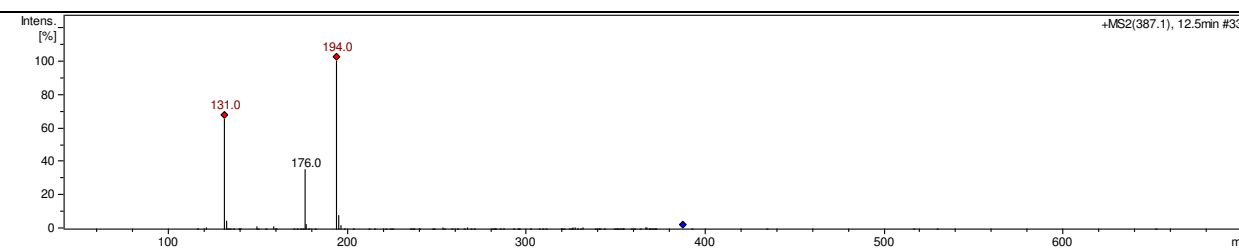
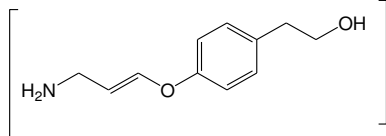
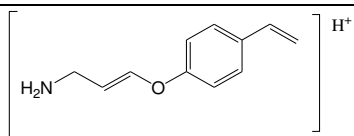
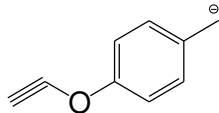
m/z	Retention time	Precursor/ Product ion	Structure	References
332.3	13.5 min	$[M+H]^+$		
 <p>ATL_PHOTOLYSIS_100MGL_32MIN.D: EIC 332.3 +All MS</p>				
<b>MS<sup>2</sup></b>				
				
290.1		$[M+H-CH(CH_3)_2]^+$		
273.1		$[M+H-NH_2CH(CH_3)_2]^+$		
245.0		$[M+H-CH_3NHCH(CH_3)_2-H_2O]^+$		

TP 336

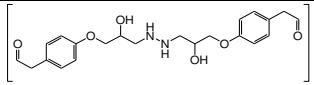
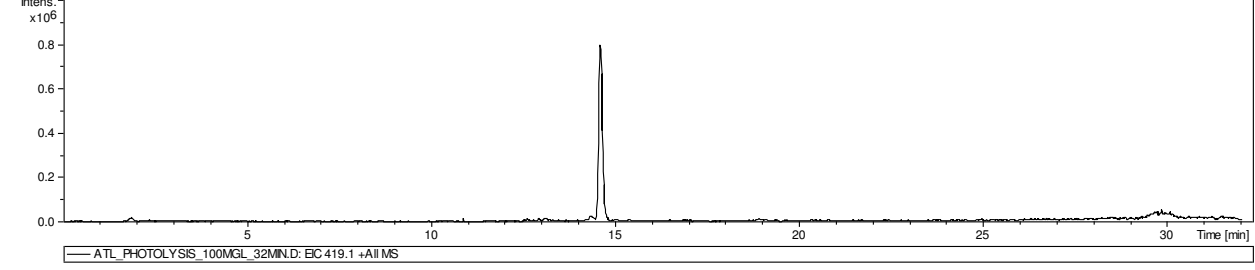
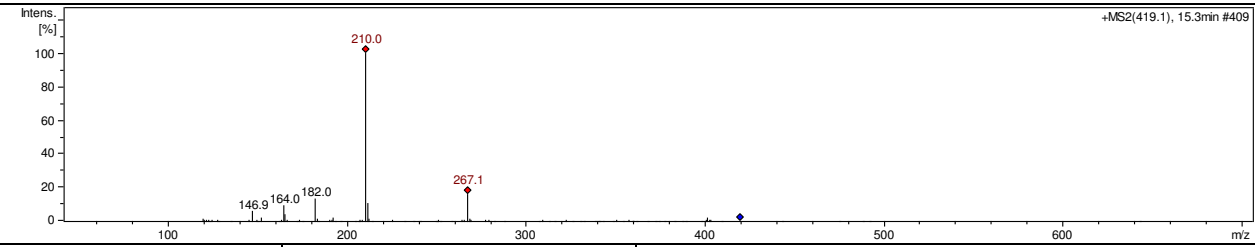
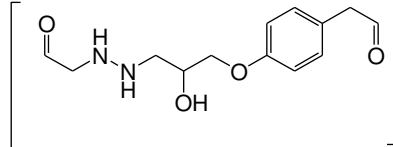
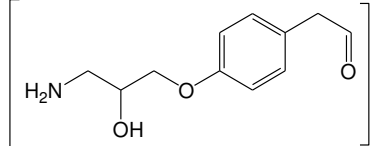
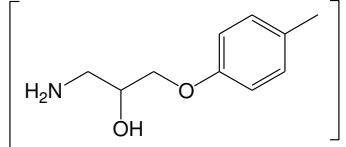
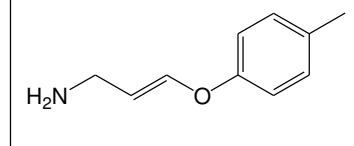
m/z	Retention time	Precursor/ Product ion	Structure	References
336.3	14.8 min	$[M+H]^+$		
 <p>ATL_PHOTOLYSIS_100MGL_32MIN.D: EC 336.3 +All MS</p>				
<b>MS<sup>2</sup></b>				
 <p>+MS2(336.2), 15.7min #414</p>				
319.0		$[M+H-H_2O]^+$		
267.0		$[M+H-NH_2CH(CH_3)_2-O]^+$		
208.0		$[M+H-CH(CH_3)_2-CH_3COOH-HCHO]^+$		
190.0		$[M+H-CH(CH_3)_2-CH_3COOH-HCHO-H_2O]^+$		
144.9		$[M+H-NH_2CH(CH_3)_2-CH_3COOH-HOCH_2CH_2CH_2OH]^+$		
127.0		$[M+H-NH_2CH(CH_3)_2-CH_3COOH-HOCH_2CH_2CH_2OH-H_2O]^+$		



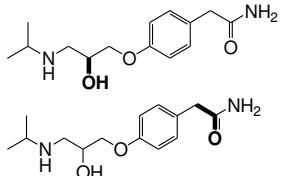
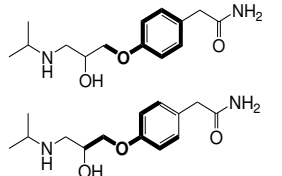
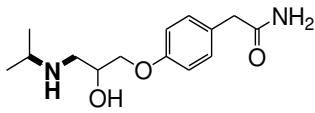
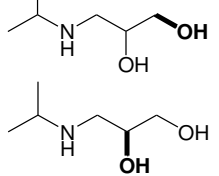
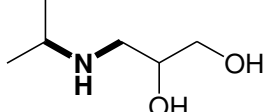
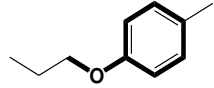
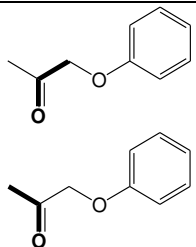
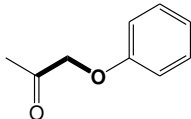
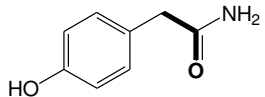
TP 387

m/z	Retention time	Precursor/ Product ion	Structure	References
387.1	12.0 min	$[M+H]^+$		27
 <p>ATL PHOTOLYSIS_100MGL_32MIN.D: EIC 387.1 +All MS</p>				
<b>MS<sup>2</sup></b>				
 <p>+MS2(387.1), 12.5min #332</p>				
194.0		$[M+H-C_{11}H_{15}NO_2]^+$		
176.0		$[M+H-C_{11}H_{15}NO_2-H_2O]^+$		
131.0		$[M+H-C_{11}H_{15}NO_2-CH_3OH-CH_3NH_2]^+$		

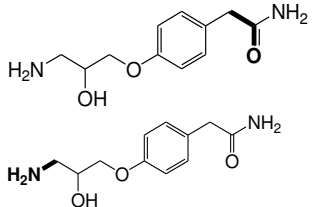
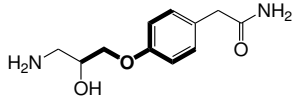
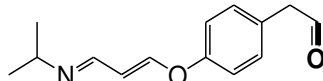
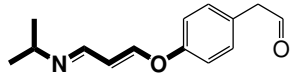
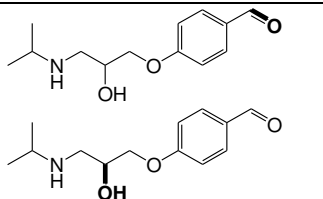
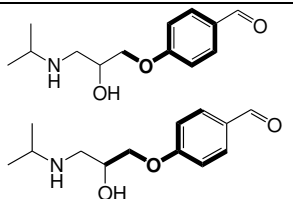
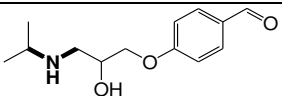
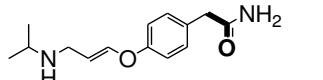
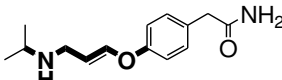
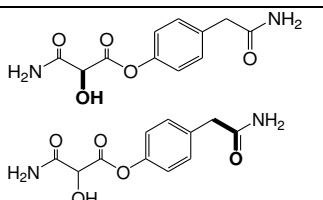
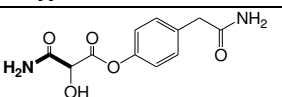
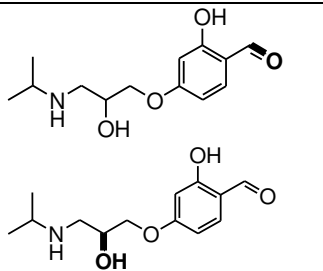
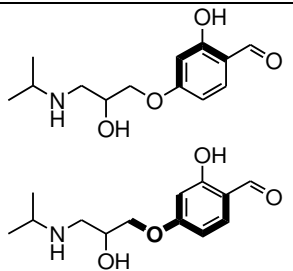
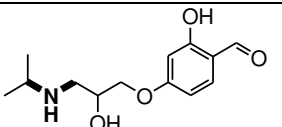
TP 419

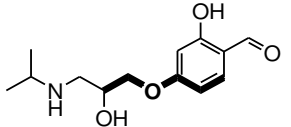
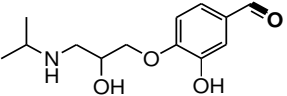
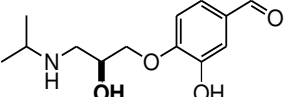
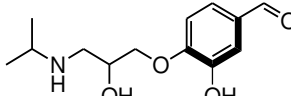
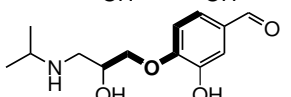
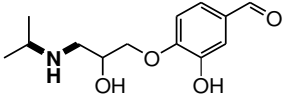

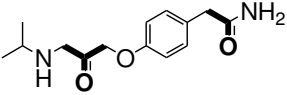
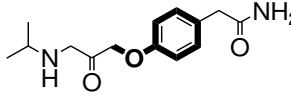
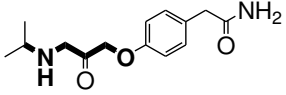
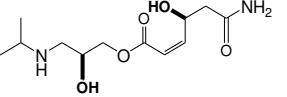
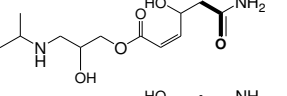
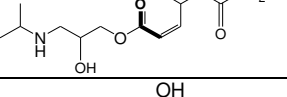
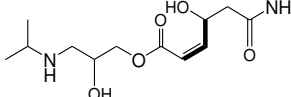
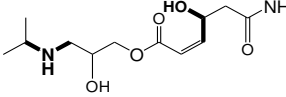
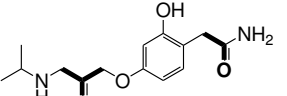
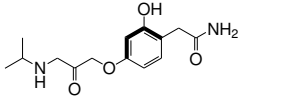
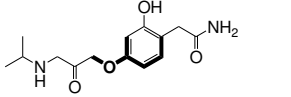
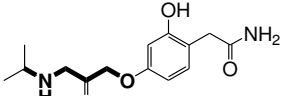
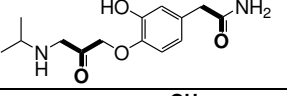
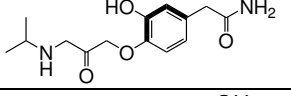
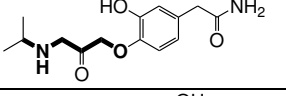
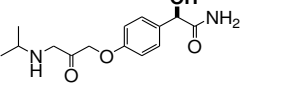
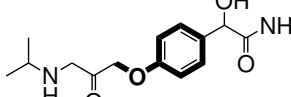
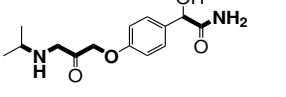
m/z	Retention time	Precursor/ Product ion	Structure	References
419.1	14.6 min	$[M+H]^+$		27
 <p>ATL_PHOTOLYSIS_100MGL_32MIN.D: EC 419.1 +All MS</p>				
<b>MS<sup>2</sup></b>				
 <p>+MS2(419.1), 15.3min #409</p>				
267.0		$[M+H-C_9H_{12}O_2]^+$		
210.0		$[M+H-C_{11}H_{15}NO_3]^+$		
182.0		$[M+H-C_{11}H_{15}NO_3-HCHO]^+$		
164.0		$[M+H-C_{11}H_{15}NO_3-HCHO-H_2O]^+$		

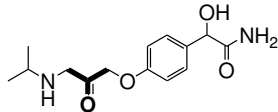
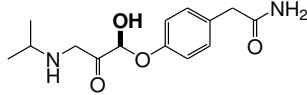
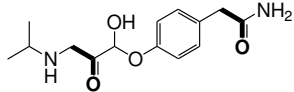
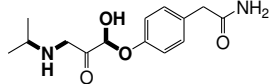
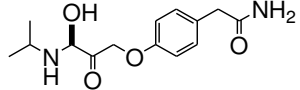
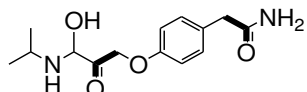
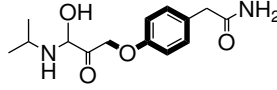
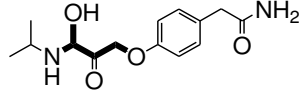
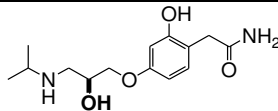
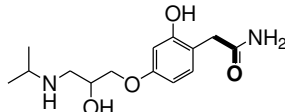
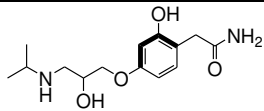
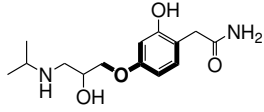
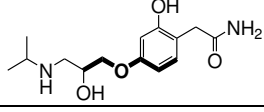
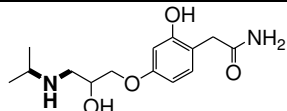
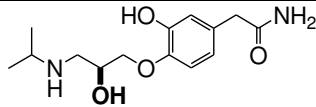
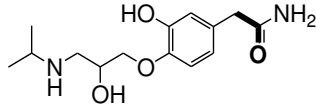
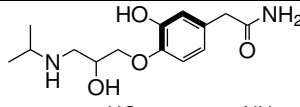
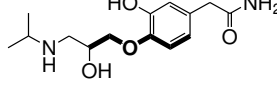
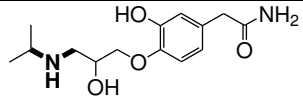
**Table S9 Supporting Information:** QSAR predictions for Atenolol and its derivatives (photo-TPs) for biodegradability different models- 1: CATABOL 301C model under MITI test condition, 2: CATALOGIC 301C model; 3: BioWin 6 (non-linear model) for MITI Biodegradation probability; 4: Case Ultra-Readily biodegradability under MITI test (OECD 301C); bonds and hetero atoms in bold: structural alerts as provided by Case Ultra

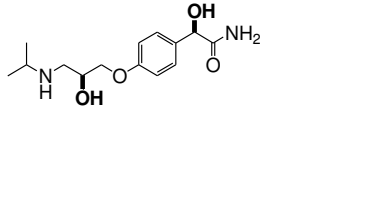
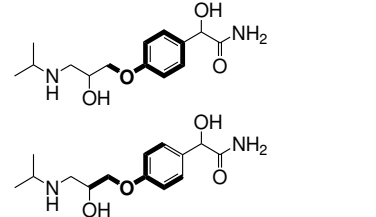
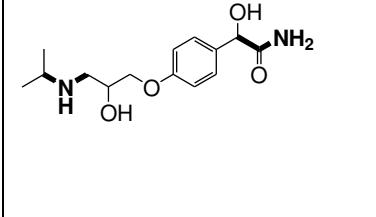
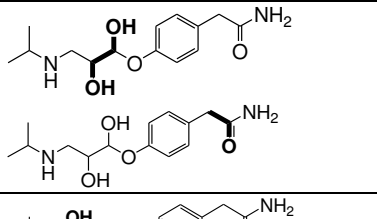
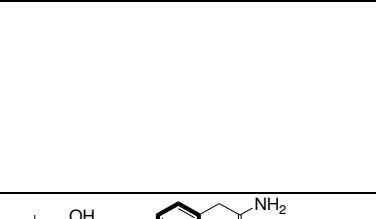
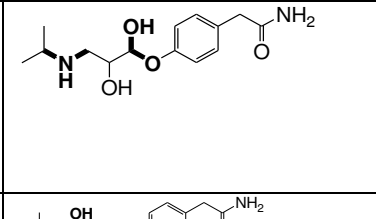
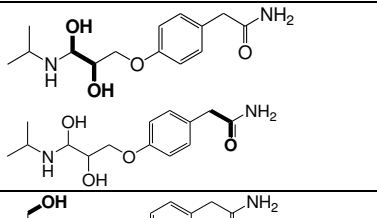
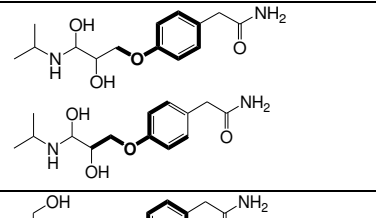
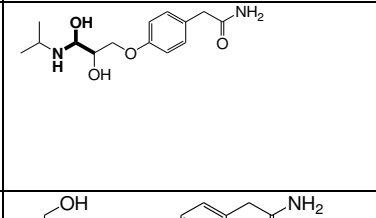
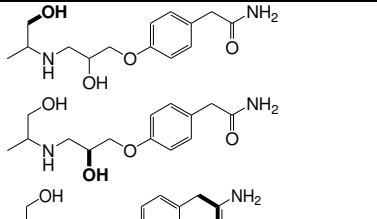
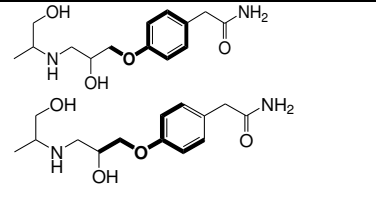
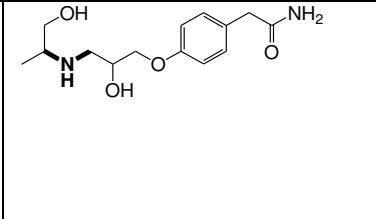
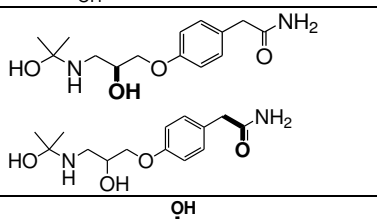
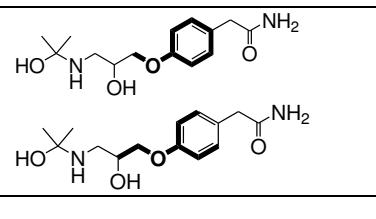
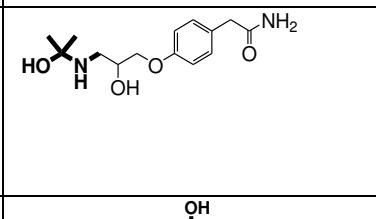
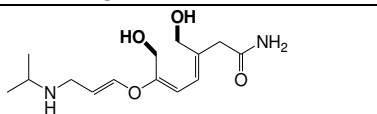
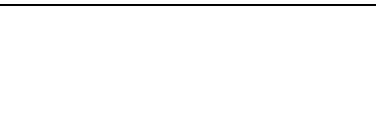
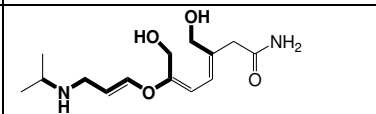
Derivatives	QSAR models				Multicase activating and deactivating alerts highlighted		
	1 <sup>§</sup>	2 <sup>§</sup>	3 <sup>‡</sup>	4	Activating alert	Deactivating alert	Unknown fragment
Atenolol	0.3168	0.4445	0.235	Inconclusive*			
TP 134	0.5375	0.7462	0.751	+			
TP <sub>1</sub> 151	0.0230	0.0298	0.765	-			
TP <sub>2</sub> 151	0.8113	0.8360	0.802	+			
TP 152	0.6327	0.5554	0.473	+			

TP 176	0.2742	0.2626	0.391	Inconclusive			
TP 193	0.2110	0.2072	0.269	Inconclusive			
TP 194	0.2493	0.2479	0.565	Inconclusive			
TP 207	0.4173	0.6278	0.351	Inconclusive			
TP 210	0.3108	0.4270	0.916	Inconclusive*			
TP 223	0.3423	0.5465	0.477	Inconclusive*			
TP 225	0.2594	0.3897	0.524	Inconclusive*			

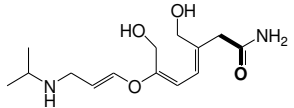
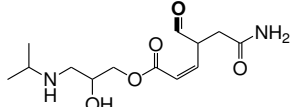
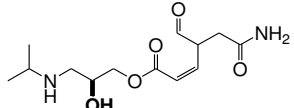
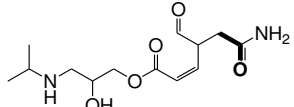
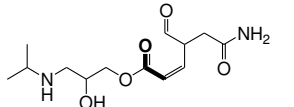
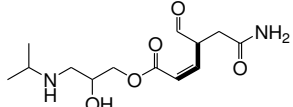
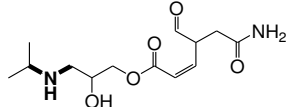
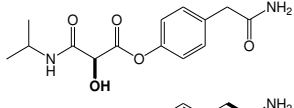
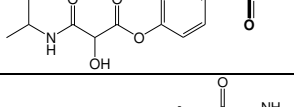
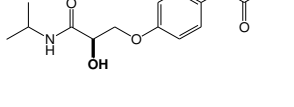
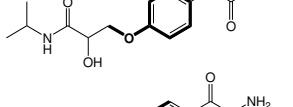
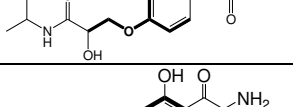
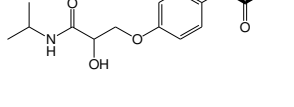
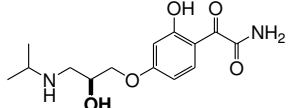
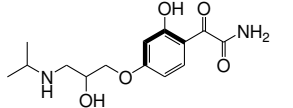
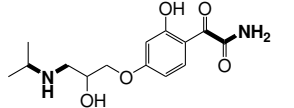
							
TP 232	0.3363	0.3789	0.524	Inconclusive			
TP 238	0.4097	0.5552	0.838	Inconclusive*			
TP 249	0.2473	0.2970	0.126	Inconclusive			
TP 253	0.5645	0.5914	0.673	+			
TP <sub>1</sub> 254	0.4300	0.5588	0.824	Inconclusive*			

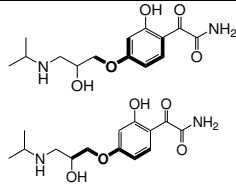
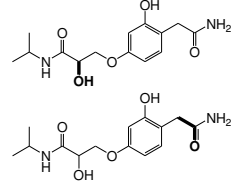
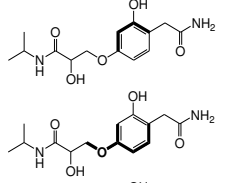
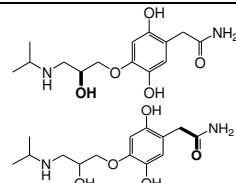
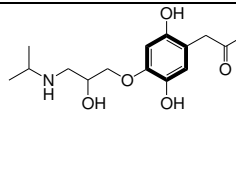
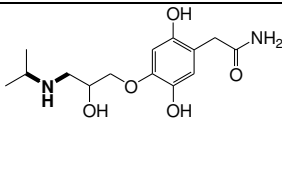
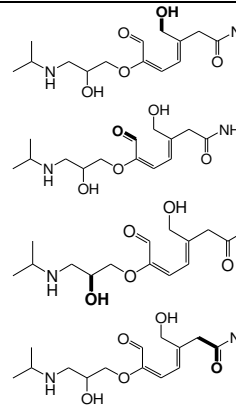

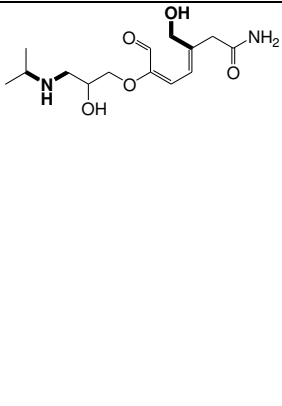
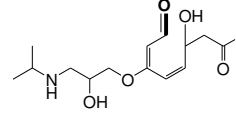
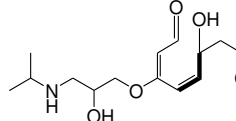
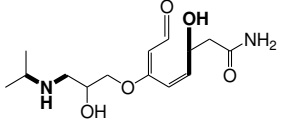
							
TP <sub>2</sub> 254	0.4316	0.5764	0.824	Inconclusive*	 	 	 
TP 265	0.3168	0.4445	0.233	±			
TP 275	0.6058	0.6427	0.679	Inconclusive*	  		
TP <sub>1</sub> 281	0.3320	0.4625	0.216	±		 	
TP <sub>2</sub> 281	0.3348	0.4998	0.216	±			
TP <sub>3</sub> 281	0.3207	0.4087	0.434	Inconclusive			

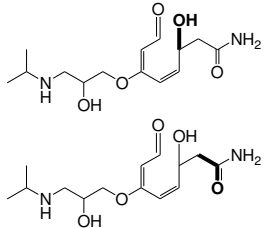
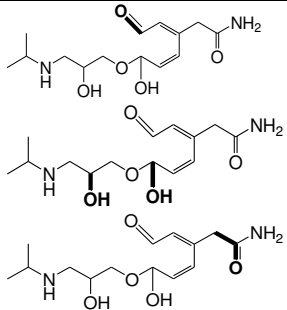
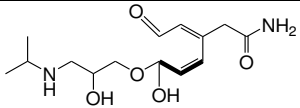
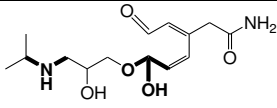
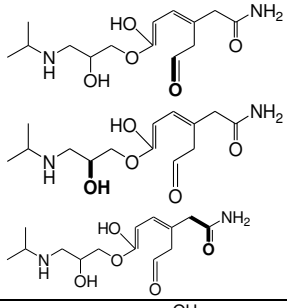
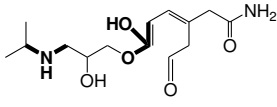
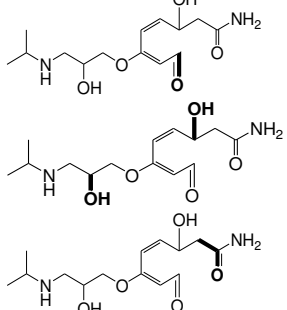
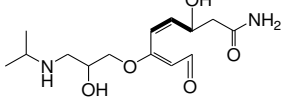
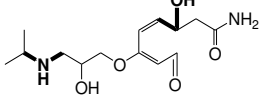
							
TP <sub>4</sub> 281	0.5935	0.6340	0.235 ±		 		
TP <sub>5</sub> 281	0.3484	0.4995	0.235	Inconclusive	 		
TP <sub>1</sub> 283	0.3320	0.4625	0.219	Inconclusive*	 	  	
TP <sub>2</sub> 283	0.3348	0.4998	0.219	Inconclusive*	 	 	

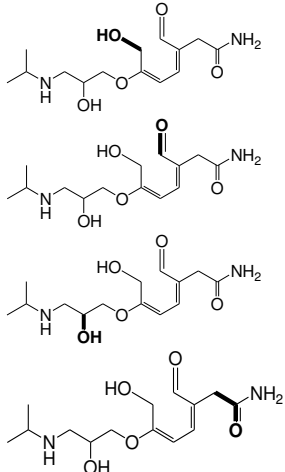
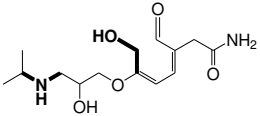
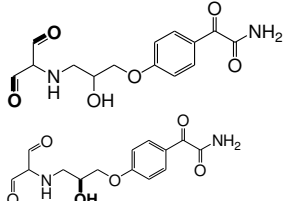
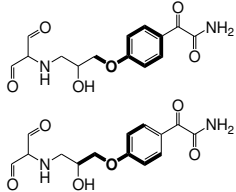
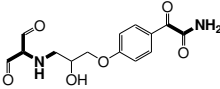
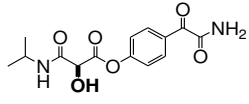
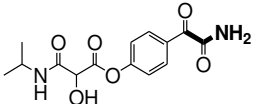
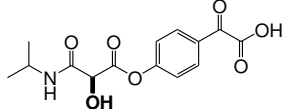
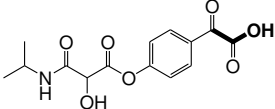
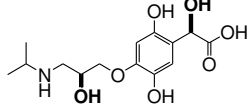
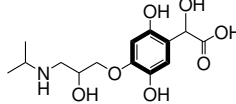
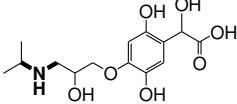
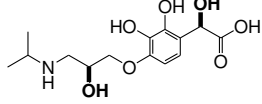
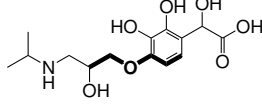
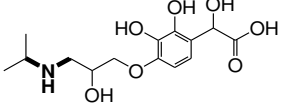
TP <sub>3</sub> 283	0.3207	0.4087	0.437	Inconclusive*			
TP <sub>4</sub> 283	0.5935	0.6340	0.237	+			
TP <sub>5</sub> 283	0.3484	0.4977	0.237	Inconclusive*			
TP <sub>6</sub> 283	0.2974	0.4255	0.443	Inconclusive*			
TP <sub>7</sub> 283	0.3484	0.4720	0.242	Inconclusive			
TP 285	0.3773	0.4178	0.196	Inconclusive			



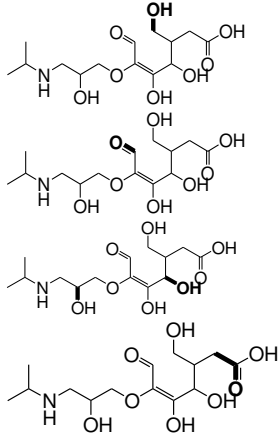
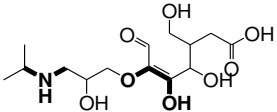
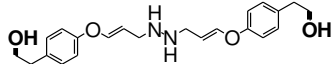
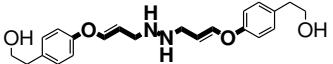
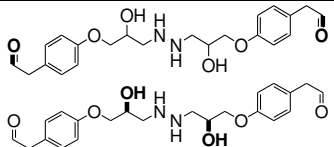
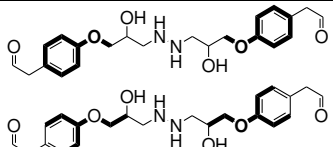
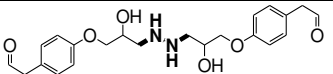
							
TP 287	0.6029	0.6565	0.895	Inconclusive*	   	 	
TP <sub>1</sub> 295	0.4790	0.5279	0.365	+	 		
TP <sub>2</sub> 295	0.2144	0.3712	0.246	Inconclusive*	  		
TP <sub>1</sub> 297	0.3408	0.4719	0.175	Inconclusive*	 		

							
TP <sub>2</sub> 297	0.2372	0.3734	0.282	Inconclusive*			
TP 299	0.3521	0.5297	0.203	Inconclusive*			
TP <sub>1</sub> 301	0.4161	0.4743	0.672	+			
TP <sub>2</sub> 301	0.3538	0.3786	0.553	Inconclusive*			

							
TP <sub>3</sub> 301	0.7786	0.8535	0.553	Inconclusive			
TP <sub>4</sub> 301	0.4663	0.6603	0.672	Inconclusive			
TP <sub>5</sub> 301	0.3538	0.3786	0.553	Inconclusive*			

TP <sub>6</sub> 301							
	0.4161	0.4743	0.672	+			
TP <sub>1</sub> 309				Inconclusive			
	0.2678	0.4518	0.96				
TP <sub>2</sub> 309				+			
	0.3888	0.5348	0.303				
TP 310				+			
	0.6000	0.6979	0.352				
TP <sub>1</sub> 316				Inconclusive*			
	0.3044	0.5433	0.446				
TP <sub>2</sub> 316				Inconclusive*			
	0.2973	0.5039	0.446				

TP <sub>3</sub> 316	0.2914	0.5071	0.446	Inconclusive*			
TP 317	0.2919	0.5230	0.912	+			
TP 318	0.3137	0.6750	0.928	±			
TP 325	0.3888	0.5348	0.102	Inconclusive			
TP 332	0.4295	0.5857	0.208	±			

TP 336				Inconclusive			
	0.3661	0.5533	0.846				
TP 387				Inconclusive			
	0.1945	0.1613	0				
TP 419				Inconclusive*			
	0.0612	0.0981	0				

§: “100% biodegradation” was assigned a numeric value of 1 and “0% biodegradation” was assigned a numeric value of 0. ‡: “Readily biodegradable” was assigned a numeric value of 1 and “not readily biodegradable” was assigned a numeric value of 0. (0 to 1 is the probability range to undergo biodegradation). Out of Domain [OD] means that the test chemical is not included in the applicability domain of the model used. ‘Inconclusive’ means a significant portion of the test chemical is covered by unknown structural fragments. Inconclusive with asterisk symbol (\*) means both positive and deactivating alerts were found in the same molecule and therefore a clear result cannot be provided. + : a positive alert for corresponding activity; - : a negative alert for corresponding activity ; ±: positive alert with low signal (marginal positive) for corresponding activity.

**Table S10 Supporting Information:** *In silico* toxicity prediction by different QSAR models of Case Ultra, Leadscope and OASIS Catalogic for Atenolol and its biodegradable derivatives (photo-TPs)

Derivatives	CASE Ultra					Leadscope				OASIS Catalogic V.5.11.6
	A (A0J)	B (A7S)	C (A7U)	D (AUA)	E (A2H)	B	C	E	F	E
Atenolol	-	§*	-	OD	-	-	+	-	-	-
TP 176	±	OD	OD	‡*	-	OD	OD	-	+	+
TP 193	±	OD	OD	‡*	-	OD	-	-	+	+
TP 194	±	OD	OD	‡*	+	OD	OD	-	+	+
TP 207	OD	OD	OD	OD	OD	-	-	-	-	-
TP 210	-	-	-	-	-	-	+	-	-	-
TP 223	OD	§*	-	OD	-	-	OD	-	-	-
TP 225	OD	§*	-	-	-	-	+	-	-	-
TP 238	-	-	-	OD	-	-	+	-	-	-
TP <sub>1</sub> 283	-	§*	-	OD	-	-	+	-	-	-

TP <sub>2</sub> 283	§*	+	-	OD	-	-	+	-	-	-
TP <sub>3</sub> 283	-	§*	-	OD	-	-	+	-	-	-
TP <sub>4</sub> 283	-	+	-	OD	-	-	+	-	-	-
TP <sub>5</sub> 283	OD	§*	-	OD	-	-	+	-	-	-
TP <sub>6</sub> 283	-	§*	-	OD	-	-	-	-	-	-
TP <sub>7</sub> 283	OD	§*	-	OD	-	-	+	-	-	-
TP <sub>1</sub> 295	+	+	-	-	-	OD	OD	-	OD	-
TP <sub>2</sub> 295	+	§*	-	+	-	-	+	-	+	-
TP 299	-	+	-	OD	-	-	+	-	-	-
TP <sub>1</sub> 301	-	+	-	‡*	§*	-	+	-	-	-
TP <sub>2</sub> 301	-	+	-	‡*	-	-	+	-	-	-
TP <sub>3</sub> 301	OD	+	-	‡*	-	-	+	-	-	-
TP <sub>4</sub> 301	OD	+	OD	‡*	-	-	+	-	-	-
TP <sub>5</sub> 301	-	+	-	‡*	-	-	+	-	-	-
TP <sub>6</sub> 301	-	+	-	‡*	§*	-	+	-	-	-
TP <sub>2</sub> 309	+	+	-	+	-	-	+	-	+	-



TP 317	OD	+	-	OD	-	-	+	-	-	-
TP 318	OD	-	-	OD	-	-	+	-	-	-
TP 325	+	+	OD	+	-	-	+	-	+	-
TP 332	-	+	-	OD	-	-	+	-	-	-

A- Human carcinogenicity; B- Micronucleus in vivo composite; C- Chromosome aberration in vitro CHO cells; D- Microtox against environmental bacteria; E- Salmonella Mutagenicity; F- Mammalian Mutagenicity; OD: Out of Domain means that the test chemical is not included in the applicability domain of the applied model; §\*: Inconclusive with asterisk symbol (\*) means both positive and deactivating alerts were found in the same molecule and therefore a clear result cannot be provided; §: Inconclusive means that the molecule contained too many unknown fragments; + : a positive alert for corresponding activity; - : a negative alert for corresponding activity; ±: Marginal positive; ‡\* : positive alert with low statistical significance.

## Reference

1. W. M. M. Mahmoud, C. Trautwein, C. Leder and K. Kümmerer, *Sci. Total Environ.*, 2013, **463–464**, 140.
2. T. Rastogi, C. Leder and K. Kümmerer, *Sci. Total Environ.*, 2014, **482–483**, 378.
3. ISO 8245, *Water quality -- Guidelines for the determination of total organic carbon (TOC) and dissolved organic carbon (DOC)*, 1999.
4. OECD, *OECD Guidelines for the Testing of Chemicals: Ready Biodegradability 301D: Closed Bottle Test*, OECD Pub., 1992.
5. OECD, *OECD Guidelines for the Testing of Chemicals: Ready Biodegradability 301F: Manometric Respiratory Test*, OECD Pub., 1992.
6. J. Friedrich, A. Längin and K. Kümmerer, *CLEAN – Soil, Air, Water*, 2013, **41**, 251.
7. OECD, *Revised introduction of the OECD guidelines for testing of chemicals, Section 3*, Organisation of Economic Cooperation and Development, 2006.
8. N. Nyholm, *Environ. Toxicol. Chem.*, 1991, **10**, 1237.
9. A. Sedykh, R. Saiakhov and G. Klopman, *Chemosphere*, 2001, **45**, 971.
10. G. Roberts, G. Myatt, W. Johnson, K. Cross and P. Blower, *J. Chem. Inf. Model.*, 2000, **40**, 1302.
11. W. M. M. Mahmoud, A. P. Toolaram, J. Menz, C. Leder, M. Schneider and K. Kümmerer, *Water Research*, 2014, **49**, 11.
12. S. K. Chakravarti, R. D. Saiakhov and G. Klopman, *J. Chem. Inf. Model.*, 2012, **52**, 2609.
13. EPA, "OPPT/Exposure Assessment Tools and Models/Estimation Program Interface (EPI) Suite Version 3.12, <http://www.epa.gov/oppt/exposure/pubs/episuite.htm>, 2013.
14. Laboratory of Mathematical Chemistry Bulgaria, *OASIS Catalogic software V.5.11.6TB*, 2012.
15. R. Saiakhov, S. Chakravarti and G. Klopman, *Mol. Inf.*, 2013, **32**, 87.
16. W. L. Jorgensen, *Small-Molecule Drug Discovery Suite 2013-3: QikProp*, Schrödinger, New York, 2013.
17. W. L. Jorgensen, "QikProp 3.8. User Manual", [http://helixweb.nih.gov/schrodinger-2013.3-docs/qikprop/qikprop\\_user\\_manual.pdf](http://helixweb.nih.gov/schrodinger-2013.3-docs/qikprop/qikprop_user_manual.pdf), 2014.
18. C. A. Lipinski, F. Lombardo, B. W. Dominy and P. J. Feeney, *Advan. Drug Delivery Rev.*, 2001, **46**, 3.
19. V. Andrisano, R. Gotti, A. Leoni and V. Cavrini, *J. Pharm. Biomed. Anal.*, 1999, **21**, 851.
20. C. Medana, P. Calza, F. Carbone, E. Pelizzetti, H. Hidaka and C. Baiocchi, *Rapid Commun. Mass Spectrom.*, 2008, **22**, 301.
21. J. Radjenovic, C. Sirtori, M. Petrovic, D. Barceló and S. Malato, *Applied Catalysis B: Environ.*, 2009, **89**, 255.
22. E. Marco-Urrea, J. Radjenović, G. Caminal, M. Petrović, T. Vicent and D. Barceló, *Water Research*, 2010, **44**, 521.

23. E. Isarain-Chavez, C. Arias, P. L. Cabot, F. Centellas, R. M. Rodriguez, J. A. Garrido and E. Brillas, *Applied Catalysis B: Environ.*, 2010, **96**, 361.
24. K. S. Tay, N. A. Rahman and M. R. B. Abas, *Microchem. J.*, 2011, **99**, 312.
25. Y. Chen, H. Li, Z. Wang, H. Li, T. Tao and Y. Zuo, *Water Research*, 2012, **46**, 2965.
26. Y. Ji, L. Zhou, C. Ferronato, X. Yang, A. Salvador, C. Zeng and J.-M. Chovelon, *J. Photochem. Photobiol. A: Chem.*, 2013, **254**, 35.
27. M. L. Wilde, W. M. M. Mahmoud, K. Kümmerer and A. F. Martins, *Sci. Total Environ.*, 2013, **452–453**, 137.
28. Y. Ji, C. Zeng, C. Ferronato, J.-M. Chovelon and X. Yang, *Chemosphere*, 2012, **88**, 644.
29. V. Kumar, R. P. Shah, S. Malik and S. Singh, *J. Pharma. Biomed. Anal.*, 2009, **49**, 880.



# Article IV

Addressing the Challenge of Micro-Pollutants  
in the Aquatic Cycle: Targeted Re-Designing  
the  $\beta$ -Blocker Propranolol for Environmental  
Biodegradability

*Environmental Science & Technology, 2015, submitted*



1 Addressing the Challenge of Micro-Pollutants in the Aquatic  
2 Cycle: Targeted Re-Designing the  $\beta$ -Blocker Propranolol for  
3 Environmental Biodegradability

4 Tushar Rastogi, Christoph Leder, Klaus Kümmerer\*

5 *Sustainable Chemistry and Material Resources, Institute of Sustainable and Environmental Chemistry,*  
6 *Leuphana University Lüneburg, C13, DE-21335 Lüneburg, Germany*

---

\* Corresponding author: Chair of Sustainable Chemistry and Material Resources, Institute of Sustainable and Environmental Chemistry, C.13, Scharnhorststraße 1, D-21335 Lüneburg, Germany. Tel.: +49 4131 677 2893. E-mail address: Klaus.Kuemmerer@uni.leuphana.de (K. Kümmerer)

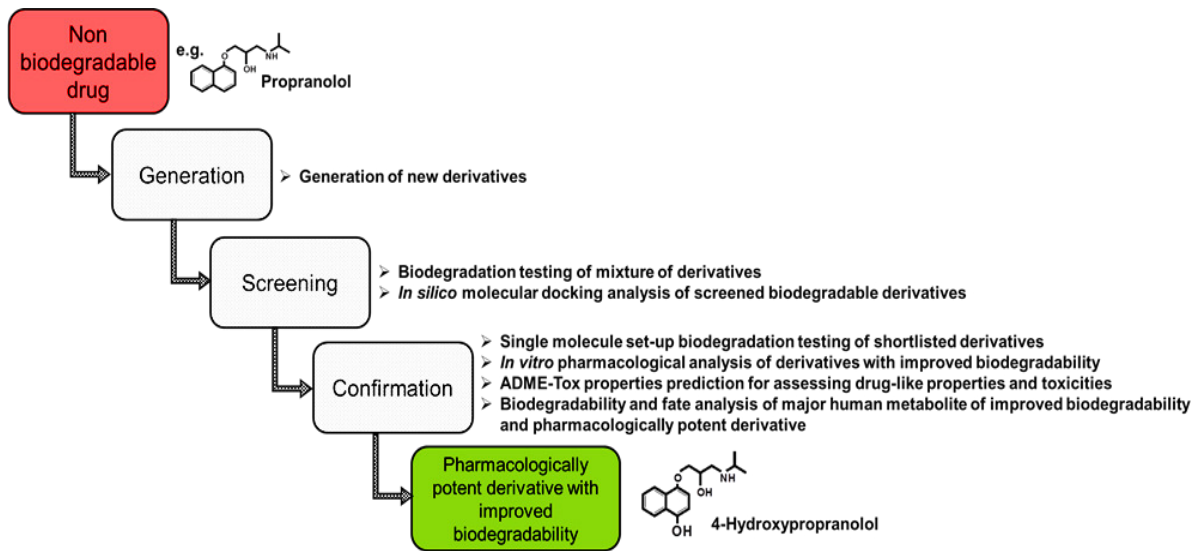
Other e-mail addresses: tushar.rastogi@leuphana.de, tushar1909@gmail.com (T. Rastogi), cleder@leuphana.de (C. Leder).

## 7 **Abstract**

8 Worldwide, contamination of aquatic systems with micro-pollutants, including  
9 pharmaceuticals, is one of the key environmental problems facing humanity. Although micro-  
10 pollutants are present at low concentrations, many of them raise considerable toxicological  
11 concerns, particularly when present as components of complex mixtures. Regarding effluent  
12 treatment, no technology works well and is also not a sustainable solution because of energy  
13 consumption, typically low efficiency and efficacy, as well as follow-up problems created by  
14 formation of often unknown products resulting from incomplete degradation which can be of  
15 even higher toxicity. Therefore, an alternative that might overcome these environmental  
16 problems is the design of new pharmaceutical molecules or the re-design of existing  
17 pharmaceutical molecules that offer the functionality needed for their application but have  
18 improved biodegradability in the environment after having been used as intended. This proof  
19 of concept study provides an approach for the rational re-design of a given pharmaceutical  
20 (Propranolol as an example) in order to generate biodegradable and pharmacologically active  
21 derivatives. The study demonstrated the feasibility that small molecular changes in the non-  
22 biodegradable pharmaceutical molecule with intact drug moiety could incorporate additional  
23 attributes such as biodegradability while retaining pharmacological potency which in turn will  
24 contribute to the protection of water resources in a truly sustainable manner.



25 TOC/Abstract art



26

## 27 **Introduction**

28 Clean water is fundamental for water quality, food security, health, societal well-being and  
29 economic growth. However, worldwide, freshwater systems, including drinking water, are  
30 contaminated by such micro-pollutants, derived from personal care products, pesticides,  
31 pharmaceuticals, etc. and the unwanted products of their incomplete degradation, which have  
32 undetermined chemical structure and unknown toxicity.<sup>1-4</sup> Although present at low  
33 concentrations, many of these molecules raise considerable toxicological concerns,  
34 particularly as they are present as complex mixtures, making chemical pollution a key  
35 environmental problem of our era.<sup>5-8</sup> The presence of active pharmaceutical ingredients  
36 (APIs) in the aquatic environment is increasingly seen as one of the major challenges to the  
37 sustainable management of water resources worldwide because of the expense and  
38 ineffectiveness of input prevention measures.<sup>9-11</sup> Therefore, it is urgently necessary to  
39 encourage the design of APIs of increased environmental biodegradability, which was  
40 historically not considered necessary.

41 The tenth principle of green chemistry is 'Design for Degradation'.<sup>12</sup> This principle relates to  
42 the design of molecules of improved biodegradability. Accordingly, the functionality of a  
43 pharmaceutical should not only include the properties required for successful application as a  
44 pharmaceutical per se, but also properties required for the fast and easy degradability in the  
45 environment of a molecule after its use if it has not been completely metabolized in the  
46 human body. The concept of the benign by design is the key element in this respect.<sup>13, 14</sup> The  
47 concept of benign by design can be applied on two levels: the design of completely new  
48 molecules or the re-design of existing molecules. However, the feasibility of 'Design for  
49 Degradation' has not yet been demonstrated for pharmaceuticals, nor is a proper working  
50 scheme yet available. The present study demonstrates the feasibility of this principle for  
51 pharmaceuticals.

52 The present study is a proof of concept and focuses on the re-design of the  $\beta$ -blocker class of  
53 APIs. Propranolol (PPL), a non-selective  $\beta$ -blocker<sup>15</sup> which binds to both  $\beta_1$  and  $\beta_2$  adrenergic  
54 receptors<sup>16</sup> as the essential step of its activity, was selected as an example for the  
55 investigations. In 2012, a total amount of 3.216 tonnes of PPL was consumed by individuals  
56 in Germany who were insured by public health insurance.<sup>17, 18</sup> PPL has been also reported as a  
57 non-biodegradable and highly persistent chemical<sup>19</sup> and was detected in sewage treatment  
58 plant effluent at concentrations ranging from 30 to 373 ng L<sup>-1</sup>.<sup>20</sup>

59 The goal of this proof of concept was to incorporate additional attribute biodegradability into  
60 PPL molecule through small molecular alteration in its structure while conserving its  
61 substructures responsible for  $\beta$  adrenergic receptor blocker activity. An aromatic ring and a  $\beta$ -  
62 ethanolamine moiety are considered the essential substructures of  $\beta$ -blockers responsible for  
63 their receptor blocking activity.<sup>21, 22</sup> The challenge is the generation and selection of such drug  
64 derivatives.

65 The very first step in designing biodegradable  $\beta$ -blocker derivatives is to generate new  
66 molecules that possess substructures providing their specific action as  $\beta$ -blockers. New  
67 derivatives (photo-derivatives, PDs) were generated by direct photolysis of PPL; this resulted  
68 in numerous derivatives. In the next step, aerobic biodegradation tests employing different  
69 bacterial densities (Closed Bottle Test [CBT] and Manometric Respiratory Test [MRT]) were  
70 applied to the mixtures resulting from photolytic treatment in order to assess the derivatives'  
71 biodegradability in the environment. Thereby, the PDs that had improved biodegradability  
72 compared to the parent compound and that still possessed an aromatic ring and a  $\beta$ -  
73 ethanolamine moiety were selected. The ones that were found to be biodegradable were  
74 further assessed with the help of *in silico* molecular docking and *in vitro* analysis for the  
75 investigation of their pharmacological activity.

76 In addition, the retention of drug-like properties (absorption, distribution, metabolism and  
77 excretion; ADME) of a derivative which was pharmacologically active with improved  
78 biodegradability was investigated. The final step was *in silico* toxicity  
79 (mutagenicity/genotoxicity) assessment for the improved biodegradable yet  
80 pharmacologically active derivatives. The biodegradability of human metabolite of this  
81 derivative was also investigated. Thus, the present study is the proof of concept for  
82 demonstrating a working scheme for the generation and targeted selection of biodegradable  
83 and pharmacologically-active derivatives of a non-biodegradable  $\beta$ -blocker drug PPL.

## 84 **Experimental**

### 85 **Chemicals**

86 ( $\pm$ )-Propranolol hydrochloride (CAS 318-96-9) and Isoprenaline hydrochloride (CAS 51-30-  
87 9) were purchased from Sigma-Aldrich (Steinheim, Germany). ( $\pm$ )-4-hydroxy-Propranolol  
88 hydrochloride (CAS 10476-53-6), 5-Hydroxy-Propranolol hydrochloride (CAS 62117-35-5),  
89 (rac)-7-hydroxy-Propranolol (CAS 81907-81-5) and 4-Hydroxy Propranolol  $\beta$ -D-Glucuronide  
90 (CAS 94731-13-2) were purchased from Santa Cruz Biotechnology, Inc. All the solutions and  
91 standards for analytical measurement and photodegradation were prepared in ultrapure water  
92 ( $Q_1$ :16.6 m $\Omega$  and  $Q_2$ : 18.2m $\Omega$ ).

### 93 **Photolytic generation of photo-derivatives of Propranolol**

94 New photo-derivatives (PDs) were generated through UV exposure. Propranolol (PPL)  
95 solution was exposed to a medium pressure mercury lamp (TQ150, UV Consulting Peschl,  
96 Mainz) for 256 min in a 1L batch photo reactor. PPL was dissolved in ultrapure water for  
97 direct photolytic experiments with no pre-treatment in order to exclude any other constituents  
98 that could interfere with the formation of derivatives and/or to avoid the initiation of  
99 scavenger effects of any absorbing or photosensitizing chemical or other species during

100 degradation. The experimental setup, procedure and characteristics of UV lamp were  
101 described in detail in Text S1 in Supporting Information (SI).

## 102 **Analysis**

103 A Shimadzu Prominence HPLC system (Duisburg, Germany) was used to measure the  
104 primary elimination of the parent compound (PPL). The Agilent LC 1100 series coupled to a  
105 Bruker Daltonic Esquire 6000+ ion-trap mass spectrometer (IT-MS) with electrospray  
106 ionization interface was used for identification and structure elucidation of the formed photo-  
107 derivatives (PDs). DOC was measured by Shimadzu TOC-V<sub>CPN</sub> analyzer equipped with an  
108 ASI-V auto sampler. The detail description of the LC method, operating parameters of the  
109 source and ion-trap and DOC measurement were summarized in Text S2 in SI.

## 110 **Biodegradation**

111 The aerobic biodegradability of PPL and the mixture of its generated photo-derivatives (PDs)  
112 were investigated according to OECD guidelines through Closed Bottle Test [CBT] 301D<sup>23</sup>  
113 and Manometric Respiratory Test [MRT] 301 F.<sup>24</sup> The CBT was employed as the most  
114 stringent biodegradation test working at low bacterial densities and diversities in order to  
115 avoid any false positive results. The MRT works with higher bacterial densities and  
116 diversities. The ready biodegradability of 4-, 5- and 7- Hydroxypropranolol was tested  
117 through the CBT only. The test principles, procedures and composition of the both  
118 investigated aerobic biodegradation test series are described in detail in Text S3 (SI).

## 119 ***In silico* analysis**

### 120 **Molecular docking**

121 Photo-derivatives (PDs) of PPL which were observed to be improved biodegradable in  
122 aerobic biodegradation assays were considered to be relevant for assessing their  
123 pharmacological potency. The prediction of the pharmacological properties of PPL and its  
124 relatively biodegradable PDs was performed by *in silico* molecular docking with Schrodinger  
125 Maestro Version 2012 (v.9.3) software. PPL is known to have a considerable affinity towards

126 both  $\beta_1$  and  $\beta_2$  adrenergic receptor.<sup>16</sup> As the human  $\beta_1$  adrenergic receptor crystal structure  
127 was not publically available, PPL and its derivatives were docked on the structures of the  
128 turkey  $\beta_1$  and human  $\beta_2$  adrenergic receptors.

129 The x-ray structures of both  $\beta_1$  and  $\beta_2$  adrenergic receptor were derived from RCSB protein  
130 database.<sup>25</sup> The codes for the applied x-ray structures of the turkey  $\beta_1$  receptor was 2YCW<sup>26</sup>  
131 and 2RH1 for the human  $\beta_2$  receptor,<sup>27</sup> respectively. The receptor grid and ligands preparation  
132 are described in detail in SI as Text S4.

133 The docking score (output from *in silico* molecular docking analysis) estimates the binding  
134 interaction of the molecule (ligands) to the protein or enzyme of interest. The lower the  
135 docking scores, the better the molecule is supposed to bind to the protein and in return  
136 provides an indication of the pharmacological potency of the investigated molecules. In order  
137 to identify the PDs which have comparable binding ability as compared to PPL, their docking  
138 scores were evaluated.

139 However, in order to keep the workload manageable, the derivatives with docking score  $\leq -8$   
140 (less than - 8) were selected as of main interest to shortlist the pharmacologically comparable  
141 biodegradable derivatives and to perform further analysis.

#### 142 **ADME properties prediction**

143 The ADME (absorption, distribution, metabolism and excretion) properties prediction prior to  
144 expensive experimental procedures of pharmacokinetic and/or clinical trials can eliminate  
145 unnecessary testing of compounds that are doomed to fail, which will significantly reduce the  
146 amount of wasted time and resources, and streamline the overall drug development process.  
147 Therefore, in the present study, ADME properties were predicted using Schrödinger's  
148 QikProp 3.8 software developed by Jorgensen and co-workers<sup>28</sup> for the improved  
149 biodegradable and pharmacologically potent derivative shortlisted after the experimental  
150 assessment.

151 Thus, incorporating ADME properties predictions as a part of the ‘green’ drug development  
152 process will result in lead derivatives that are more likely exhibiting satisfactory ADME  
153 performances during experimental clinical trials. In the present study, the ADME properties  
154 of the lead candidate were also compared with PPL and the known selective  $\beta_1$  blockers  
155 Atenolol and Metoprolol. The information about the database of the software and various  
156 ADME properties, which were predicted by QikProp, are summarized and described in detail  
157 in Text S5 in SI.

### 158 **Toxicity prediction**

159 The toxicological end points such as carcinogenicity, mutagenicity and genotoxicity were  
160 predicted for the improved biodegradable and pharmacologically potent derivative by the  
161 various models of OASIS Catalogic (Laboratory for Mathematical chemistry, Bulgaria),  
162 CASE Ultra v.1.4.5.1 (MultiCASE Inc., USA) and Leadscape software (Leadscape, Inc.).

163 The mutagenicity assessment as suggested by the recently implemented ICH M7 guideline by  
164 the combination of statistical and rule-based models from different software packages CASE  
165 Ultra v. 1.5.2.0<sup>29</sup> and Leadscape Model Applier v. 1.8.6 (Leadscape, Inc.).<sup>30</sup> The above  
166 mentioned software’s models and their outputs and endpoints are described in detail in SI in  
167 Text S6.

### 168 ***In vitro* pharmacological assay**

169 *In vitro* pharmacological analysis was performed through the PathHunter® eXpress  $\beta$ -  
170 Arrestin Human and Ortholog GPCR kits (DiscoverX Corporation, USA). The kit contains a  
171 genetically modified CHO-K1 cell line expressing the human  $\beta_1$  adrenergic receptor.<sup>31</sup> The kit  
172 monitors GPCR (G protein-coupled receptors) activity by detecting the interaction of  $\beta$ -  
173 Arrestin with the activated GPCR using  $\beta$ -galactosidase ( $\beta$ -gal) enzyme fragment  
174 complementation.<sup>32</sup> Isoprenaline hydrochloride, an agonist for the  $\beta_1$  adrenergic receptor, was  
175 used as a positive control in the test assay. PPL and 4-OH PPL were tested in the assay for

176 their antagonistic activity. The principle and working procedure of the *in vitro* assay is  
177 detailed described in SI in Text S7.

## 178 **Results and Discussion**

### 179 **Generation of photo-derivatives**

180 In total, 16 photo-derivatives (PDs) of PPL were observed to be formed during photolysis.  
181 According to the LC-MS/MS data (Table S11, SI), several of the identified PDs were  
182 constitutional isomers. Formation of constitutional isomers of PPL derivatives was previously  
183 reported.<sup>33–36</sup> On the basis of observed results and literature finding a scheme as well as  
184 reaction pathways of the generation of PDs of PPL are illustrated in Figure S1 (under Text S8,  
185 SI). The attachment of hydroxyl radical (HO<sup>•</sup>) on the aromatic naphthalene ring of PPL was  
186 observed to be the major mechanism for the synthesis of derivatives of PPL. This attachment  
187 of HO<sup>•</sup> often resulted in the opening of the naphthalene ring which ends up forming the  
188 alcohol and/or aldehyde moieties.

189 The other two mechanisms which were observed for the generation of derivatives were the  
190 dealkylation (elimination of isopropyl moiety from the side chain) and/or the cleavage of  
191 ethanolamine side chain from the aromatic ring. The observed mechanism for the generation  
192 of PDs were also reported earlier.<sup>34, 36, 37</sup> The detailed description of the results and structures  
193 of PDs are described in detail in Text S8 and Table S11 in SI.

### 194 **Biodegradability screening of photo-derivatives**

195 The mixture of PDs of PPL resulting from photo treatment was submitted to two aerobic  
196 biodegradation test assays and the results are summarized in Figure S2 and S3, and Table S7  
197 in SI. The results of both aerobic biodegradation assays confirmed that PPL is not at all  
198 biodegradable. LC-MS/MS analyses of samples from each biodegradation test confirmed  
199 these findings (Figure S3, SI), which were also supported by data in the literature, i.e. that



200 PPL was not eliminated through biodegradation, hydrolysis, sorption or abiotic oxidation.  
201 Therefore, it can be concluded that the degradation observed to have been achieved during the  
202 biodegradation tests was due to the PDs. All the PDs with improved biodegradability (Table  
203 S7) were found to be hydroxylated derivatives of PPL, with or without the opening of the  
204 naphthalene ring as identified after photo treatment. This phenomenon is consistent with the  
205 observation that attachments of electron-donating functionalities such as oxygen atoms (e.g.  
206 hydroxyl, aldehyde, carboxylic acid groups, etc.) or amines to the aromatic ring of a molecule  
207 generally increase its aerobic biodegradability.<sup>38</sup>

208 Also, the addition of hydroxyl groups onto the aromatic ring is considered the first step of the  
209 aerobic biodegradation pathway of aromatic compounds (such as aniline and the *p*-  
210 nitrophenol), leading to the opening of the aromatic ring to form alcohols and acids, which  
211 then subsequently mineralize.<sup>39, 40</sup> Stereochemistry also plays an important role for  
212 biodegradability. However, there are no specific rules for determining which enantiomer will  
213 be preferably degraded.<sup>41, 42</sup> Therefore, formation of enantiomers of certain derivatives of  
214 different biodegradability cannot be excluded.

### 215 **Pharmacological potency screening of photo-derivatives (*in silico*)**

216 The binding interactions between chemical species and the amino acids of the receptor grid  
217 have been reported to be stereoselective.<sup>43, 44</sup> Therefore, all the identified PDs with improved  
218 biodegradability (Table S7), including all their possible constitutional and enantiomeric  
219 isomers, were *in silico* docked on the turkey  $\beta_1$  and human  $\beta_2$  adrenergic receptors to estimate  
220 their pharmacological potency. As expected, PPL showed good docking with both receptor  
221 grids due to its non-selective nature towards the  $\beta_1$  and  $\beta_2$  subtype receptors.<sup>15</sup> The results of  
222 molecular docking of PPL and PDs are summarized in Table 1. The docking results indicate  
223 that the hydroxylation on the naphthalene ring of PPL (as in PD<sub>1-7</sub> 276) and the opening of the  
224 ring (as in PD 266) during photolysis lead to derivatives which may have comparable or even

225 improved pharmacological potency as compared to PPL. The binding interactions of the  
226 turkey  $\beta_1$  adrenergic receptor grid generated by *in silico* docking software with both  
227 enantiomers (R and S) of PPL, 4-OH PPL and 7-OH PPL are detailed described in SI as Text  
228 S9.

229 The docking results showed that small changes are possible without losing pharmacological  
230 potency, even on the moieties responsible for the particular mode of action of the parent  
231 compound. The only condition is that such small molecular changes should not disturb or  
232 rupture the drug moieties of the molecule. Such changes in the molecule with intact drug  
233 moiety could incorporate additional attributes into the molecule (such as biodegradability)  
234 while conserving its pharmacological potency. Thus, derivatives such as PD<sub>1-7</sub> 276 and PD  
235 266 (Table 1) could be considered new lead derivatives that might have pharmacological  
236 potency and are, at the same time, comparably improved environmentally biodegradable.  
237 Therefore, further experimental analyses were performed to confirm their properties such as  
238 biodegradability and pharmacological potency.

### 239 **Confirmation of biodegradability**

240 To confirm the properties of the shortlisted lead (proposed to be pharmacologically active)  
241 PDs, it was necessary to test them in a single molecule set-up in the respective test assays.  
242 Three hydroxyl derivatives of PPL (i.e. 4-OH PPL, 5-OH PPL and 7-OH PPL), commercially  
243 available as racemic mixtures, were tested for their biodegradability in the CBT along with  
244 PPL. The highest % of biodegradation was observed for 4-OH PPL (23 %), while the other  
245 selected derivatives showed no biodegradation (Figure S5 in SI). These observations of  
246 biodegradation of the lead PDs were in accordance with Boethling et al.<sup>45</sup> There, the authors  
247 suggested that the number of substituent groups attached to the base structure (aromatic ring)  
248 will affect biodegradability.

249 LC-UV-MS/MS analysis of the CBT samples (Figure 1a) shows that there was no elimination  
250 of PPL itself or of 5-OH PPL or 7-OH PPL during the test. Dissolved organic carbon (DOC)  
251 measurements supported these results (no decrease in DOC). In contrast 4-OH PPL was  
252 completely primarily eliminated and a mineralization of 48% was observed. Hence, these  
253 analyses confirmed that 4-OH PPL has an improved biodegradability and will be much more  
254 mineralized compared to PPL and the other lead derivatives (5- and 7-OH PPL) under aerobic  
255 environmental biodegradation conditions and might not accumulate in the aquatic  
256 environment.

257 However, the incomplete mineralization of 4-OH PPL indicates the formation of  
258 biodegradation transformation products (bioTPs) during the test. This is confirmed by the  
259 detection of three bioTPs (bioTP<sub>1-6</sub> 290, bioTP 272 and bioTP 134, Figure 1b) that were  
260 formed during biodegradation testing of 4-OH PPL. Several peaks were observed with the  
261 same MS<sup>2</sup> fragmentation pattern during LC-MS/MS analysis for the specific mass m/z 290  
262 (bioTP 290), indicating the formation of constitutional isomers of bioTP 290 (see Table S11  
263 in SI).

264 These proposed structures, which are not commercially available, were characterized *in silico*  
265 for ready biodegradability (Table S8, SI). BioTP 134 and bioTP 272 were predicted with  
266 positive alerts for ready biodegradability while constitutional isomers of bioTP<sub>1-6</sub> 290 were  
267 predicted either with ‘out of domain’ or ‘inconclusive’ predictions. This means that these  
268 isomers of bioTP<sub>1-6</sub> 290 were not included in the applicability domain of the model, or there  
269 were positive alerts but the calculated probability fell below the classification threshold  
270 (50.0%) of the respective model.

271 For greater safety, bacterial mutagenicity was therefore assessed for all bioTPs, as suggested  
272 in the only guideline, the very recently implemented ICH M7,<sup>46</sup> and as acknowledged for this  
273 purpose by the U.S. FDA and the European Medical Agency (EMA). As *in silico* predictions

274 are somewhat uncertain, therefore several software packages were applied for individual  
275 endpoints ('*in silico* testing battery') when the compounds and/or tests for reliable predictions  
276 were not available. Therefore, the proposed structures of all bioTPs of 4-OH PPL were  
277 characterized for bacterial mutagenicity as per ICH M7 guideline by the combination of  
278 statistical and rule-based models from different software packages (Table S8).

279 The *in silico* mutagenicity predictions of the statistical models of CASE Ultra software  
280 package reported that all bioTPs would be non-mutagenic. The rule-based model 'Expert rules  
281 for genotoxicity' from CASE Ultra provided a positive alert for genotoxicity due to the  
282 presence of naphthalene analogs (Table S8). However, this model also provided the same  
283 positive alert for PPL due to the presence of the naphthalene ring, but this prediction was  
284 overruled because PPL is a known non-genotoxic compound. Thus, on the basis of *in silico*  
285 read-across approach, these predictions by the expert rule model might be overruled for the  
286 bioTPs. Therefore, these bioTPs may be non-mutagenic, as is PPL itself.

287 Both the statistical and expert models of Leadscope provided a negative prediction for all  
288 bioTPs except bioTP<sub>2</sub> 290 (Table S8). This bioTP<sub>2</sub> 290 was predicted with an indeterminate  
289 alert. The negative prediction for all bioTPs except bioTP<sub>2</sub> 290 indicates that they might be  
290 non-mutagenic. The indeterminate alerts for bioTP<sub>2</sub> 290 for both the expert and statistically  
291 based models indicate that there was insufficient evidence or conflicting data to provide a  
292 positive or negative alert with confidence. However, the ICH M7 genotox consensus  
293 predicted that all the bioTPs, including bioTP<sub>2</sub> 290, might be non-mutagenic.

#### 294 **Confirmation of pharmacological activity (*in vitro*)**

295 Based on the encouraging results for 4-OH PPL as described above, the pharmacological  
296 potency of 4-OH PPL as a  $\beta_1$  adrenergic receptor antagonist was assessed *in vitro* by  
297 comparing it with PPL. Figures 2a and 2b show the dose response curve for PPL and 4-OH  
298 PPL, respectively. The graph shows the inhibition of the  $\beta_1$  adrenergic receptor triggering due

299 to the addition of agonist isoprenaline in the test assay. Increasing doses of both PPL and 4-  
300 OH PPL reduces the agonistic activity in the test assay. Such a phenomenon was expected  
301 from PPL, as PPL is a known antagonistic drug for the  $\beta_1$  adrenergic receptors. 4-OH PPL  
302 also showed a similar dose response (reduction of agonistic activity) which confirms that it is  
303 most likely also an antagonistic chemical for  $\beta_1$  adrenergic receptor.

304 However, the  $EC_{50}$  value of 4-OH PPL was higher than PPL in the *in vitro* assay. That  
305 indicates the respective extents of blocking of the  $\beta_1$  adrenergic receptors by both 4-OH PPL  
306 and PPL are different. In a t-test performed for the  $EC_{50}$  values of PPL and 4-OH PPL, no  
307 statistically significant difference was found. This is in accordance with the *in vivo* data from  
308 Fitzgerald et al.,<sup>47</sup> who reported that 4-OH PPL is approximately pharmacologically  
309 equipotent to the parent drug PPL as a  $\beta$ -adrenoceptor blocking agent *in vivo*.

310 To this point it can be concluded that 4-OH PPL is a pharmacologically active  $\beta_1$  adrenergic  
311 receptor blocking molecule of improved biodegradability that will not accumulate in the  
312 aquatic environment.

### 313 **Assessment of drug-like properties (*in silico* ADME properties)**

314 In order to augment the data already established for 4-OH PPL as a  $\beta_1$  blocker, ADME  
315 properties (absorption, distribution, metabolism and excretion) of 4-OH PPL were assessed by  
316 a software package QikProp 3.8 (see Table S9, SI), and compared with non-selective  $\beta$ -  
317 blocker PPL and selective  $\beta_1$ -blocker Atenolol (ATL) and Metoprolol (MTL). The predictions  
318 for drug-like properties for 4-OH PPL were in the recommended range of the software and  
319 comparable with PPL and selected  $\beta_1$ -blockers (see Table S9, SI). Predictions for Lipinski's  
320 rule of five and for Jorgensen's rule of three properties showed no violation by 4-OH PPL,  
321 similar to ATL, MTL and PPL. This further supports that 4-OH PPL is a drug-like molecule  
322 and most likely to be orally available. The predicted partition coefficient ( $\log P_{o/w}$ ) values

323 were within the recommended range and indicate that 4-OH PPL is more hydrophilic than  
324 PPL.

325 The inhibitory concentration ( $IC_{50}$ ) values for the blockage of the human Ether-à-go-go-  
326 Related Gene (hERG)  $K^+$  channel were predicted by the Qikprop software. It was observed  
327 that the predicted value was below the recommended range for 4-OH PPL but however  
328 comparable to both PPL and MTL (Table S9). The Qikprop software predicted apparent  
329 Caco-2 cell permeability and apparent MDCK cell permeability (P Caco and P MDCK) for 4-  
330 OH PPL less than PPL and MTL but was still in the recommended range (see Table S9, ESI).

331 The Qikprop software predicted 4-OH PPL to have a high human oral absorption, similar to  
332 PPL. The skin permeability prediction for 4-OH PPL was in the recommended range and  
333 comparable to the other investigated  $\beta$ -blockers. The predicted brain/blood partition  
334 coefficient (log BB) was lower than that for PPL, which is a satisfactory indication that 4-OH  
335 PPL will tend to partition in the blood instead of the brain.

### 336 **Toxicity assessment (*in silico* toxicity prediction)**

337 In addition to their pharmacological activity, efficacy and efficiency drugs should also be  
338 non-toxic. First of all, mutagenicity, genotoxicity and carcinogenicity have to be absent.  
339 Therefore, 4-OH PPL was assessed and compared with PPL for mutagenicity by an '*in silico*  
340 testing battery' (with different software packages for individual endpoints) described in detail  
341 in Text S6 in SI. The results of *in silico* mutagenicity assessment as suggested by the ICH M7  
342 guideline for PPL and 4-OH PPL are summarized in Table S10. The statistical mutagenicity  
343 models of CASE Ultra predicted 4-OH PPL might be non-mutagenic while the rule-based  
344 model predicted 4-OH PPL to be mutagenic. This rule-based model predicted a positive alert  
345 due the presence of a naphthalene analog in the 4-OH PPL. However, both the statistical and  
346 expert models from the Leadscape predicted PPL and 4-OH PPL might be non-mutagenic.

347 Predictions by other models indicated that the 4-OH PPL is probably not a carcinogen, nor  
348 genotoxic or mutagenic.

#### 349 **Human metabolite 4-hydroxypropranolol Glucuronide**

350 It has been reported that 4-OH PPL generally undergoes sequential metabolism to 4-  
351 hydroxypropranolol glucuronide (4-OH PPL GLU).<sup>48</sup> Therefore, if 4-OH PPL is administered  
352 as a drug, it will be excreted in part as 4-OH PPL GLU. In this study, it was found that the  
353 metabolite 4-OH PPL GLU was 22 % degraded in the CBT (Figure S6a), according to oxygen  
354 consumption, and partially mineralized to 36%, according to DOC elimination. Furthermore,  
355 by employing LC-MS/MS it was demonstrated that 4-OH PPL GLU was completely cleaved  
356 back into the biodegradable parent compound 4-OH PPL, as shown in Figure S6b in SI. Such  
357 a behavior is reported in the literature for glucuronides of other pharmaceuticals such as  
358 Diclofenac. Lee et al.<sup>49</sup> reported that Diclofenac glucuronide, a major metabolite of  
359 Diclofenac, deconjugated to equimolar Diclofenac during microbial degradation testing.

360 The reformed parent compound 4-OH PPL undergoes further elimination and transformations  
361 into the three already identified bioTPs (bioTP 134, bioTP 272 and bioTP<sub>1-6</sub> 290) (Figure 1b  
362 and Table S8). Thus, 4-OH PPL GLU will not persist in the environment after its release and  
363 strengthens the potential that 4-OH PPL can be a greener  $\beta$ -blocker derivative.

364 4-OH PPL can be considered a lead structure for an environmentally-friendly  $\beta_1$  adrenergic  
365 receptor blocker, although it must be taken into account that further analysis such as bio-  
366 distribution, pharmacokinetic and/or clinical trials should be carried out for 4-OH PPL. Thus,  
367 after successful trials it can be labeled and used as a  $\beta_1$  adrenergic receptor blocker drug with  
368 the additional advantage of being improved biodegradable after its release to the aquatic  
369 environment.

370 The study demonstrated the feasibility and provided a working scheme for rationally re-  
371 designing  $\beta$ -blockers. This approach promises a solution to the global challenge of micro-

372 pollutants in the aquatic system even if there is no sewage treatment available. It may also  
373 lead to new drug candidates useful for patients and industries, and can therefore be called a  
374 sustainable solution in the broadest sense. The authors acknowledge that the tiered approach  
375 to rationally re-designing pharmaceuticals presented here should also be tested for additional  
376 classes of drugs. This might lead to innovative follow-up studies and will widen the  
377 knowledge and experience in order to integrate environmental aspects into drug design and  
378 development.



379 **Acknowledgement**

380 Financial support from German Ministry of Education and Research (NanoPharm, Project No.  
381 03X0094C) is gratefully acknowledged. The authors also acknowledge Multicase Inc. and  
382 Leadscope Inc. for kindly providing the CASE Ultra, MetaPC and Leadscope QSAR  
383 software, respectively.

384 **Supporting Information**

385 Additional supporting information is available on descriptive experimental methodology,  
386 supporting results, tables and figure.

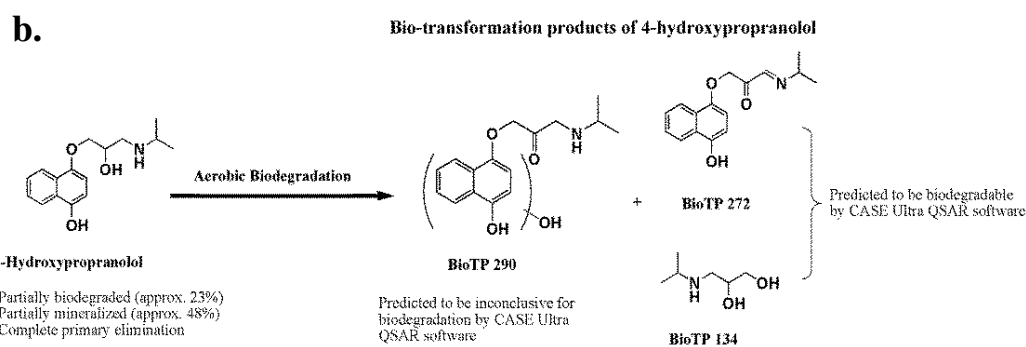
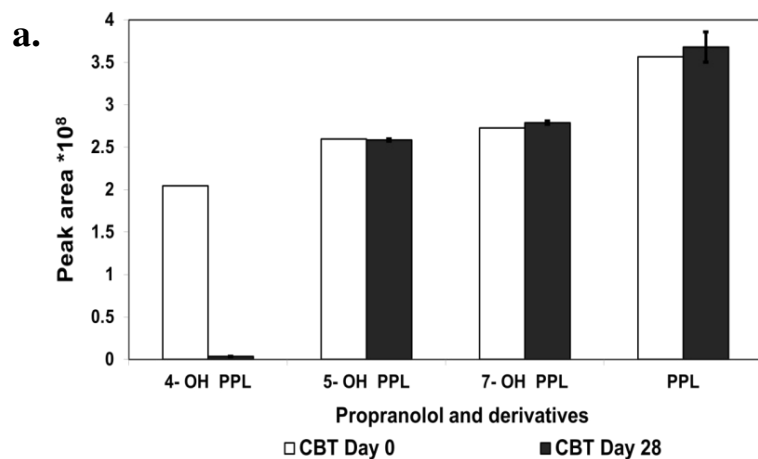
387 **Reference**

- 388 (1) Schwarzenbach, R.; Escher, B.; Fenner, K.; Hofstetter, T.; Johnson, C. A.; Urs von  
389 Gunten, W. B. The challenge of micropollutants in aquatic systems. *Science* **2006**, *313*  
390 (5790), 1072–1077.
- 391 (2) Fenner, K.; Canonica, S.; Wackett, L. P.; Elsner, M. Evaluating Pesticide Degradation  
392 in the Environment: Blind Spots and Emerging Opportunities. *Science* **2013**, *341*  
393 (6147), 752–758.
- 394 (3) Lambropoulou, D. A., Nollet, L. M. L., Eds. *Transformation products of emerging*  
395 *contaminants in the environment. Analysis, processes, occurrence, effects and risks*;  
396 John Wiley & Sons Inc: United Kingdom, 2014.
- 397 (4) Trautwein, C.; Berset, J. D.; Wolschke, H.; Kümmerer, K. Occurrence of the  
398 antidiabetic drug Metformin and its ultimate transformation product Guanylurea in  
399 several compartments of the aquatic cycle. *Environ. Int.* **2014**, *70* (0), 203–212.
- 400 (5) Richardson, S. D.; Ternes, T. A. Water Analysis: Emerging Contaminants and Current  
401 Issues. *Anal. Chem.* **2014**, *86* (6), 2813–2848.
- 402 (6) Brodin, T.; Fick, J.; Jonsson, M.; Klaminder, J. Dilute Concentrations of a Psychiatric  
403 Drug Alter Behavior of Fish from Natural Populations. *Science* **2013**, *339* (6121), 814–  
404 815.
- 405 (7) Loos, R.; Carvalho, R.; António, D. C.; Comero, S.; Locoro, G.; Tavazzi, S.; Paracchini,  
406 B.; Ghiani, M.; Lettieri, T.; Blaha, L.; Jarosova, B.; Voorspoels, S.; Servaes, K.;  
407 Haglund, P.; Fick, J.; Lindberg, R. H.; Schwesig, D.; Gawlik, B. M. EU-wide  
408 monitoring survey on emerging polar organic contaminants in wastewater treatment  
409 plant effluents. *Water Res.* **2013**, *47* (17), 6475–6487.
- 410 (8) Mompelat, S.; Le Bot, B.; Thomas, O. Occurrence and fate of pharmaceutical products  
411 and by-products, from resource to drinking water: Pharmaceutical products in the  
412 environment: trends toward lowering presence and impact. *Environ. Int.* **2009**, *35* (5),  
413 803–814.
- 414 (9) Jones, O. A. H.; Green, P. G.; Voulvoulis, N.; Lester, J. N. Questioning the excessive  
415 use of advanced treatment to remove organic micropollutants from wastewater. *Environ.*  
416 *Sci. Technol.* **2007**, *41* (14), 5085–5089.
- 417 (10) Wenzel, H.; Larsen, H. F.; Clauson-Kaas, J.; Højbye, L.; Jacobsen, B. N. Weighing  
418 environmental advantages and disadvantages of advanced wastewater treatment of  
419 micro-pollutants using environmental life cycle assessment. *Water Sci. Technol.* **2008**,  
420 *57* (1), 27–32.
- 421 (11) Kümmerer, K. *Pharmaceuticals in the Environment. Sources, Fate, Effects and Risks*,  
422 3rd ed.; Springer-Verlag: Berlin, Heidelberg, 2008.
- 423 (12) Anastas, P. T.; Warner, J. C. *Green chemistry. Theory and practice*; Oxford Univ.  
424 Press: New York, 1998.

- 425 (13) Kümmerer, K. Sustainable from the very beginning: rational design of molecules by life  
426 cycle engineering as an important approach for green pharmacy and green chemistry.  
427 *Green Chem.* **2007**, 9 (8), 899–907.
- 428 (14) Kümmerer, K. Drugs. In *Handbook of Green Chemistry, Green Processes, Designing*  
429 *Safer Chemicals*; Anastas, P. T., Boethling, R., Votchkova, A., Eds.; Handbook of  
430 Green Chemistry 9; Wiley-VCH: Weinheim, 2012; pp 215–280.
- 431 (15) Black, J. W.; Crowther, A. F.; Shanks, R. G.; Smith, L. H.; Dornhorst, A. C. A new  
432 adrenergic: Beta-receptor antagonist. *The Lancet* **1964**, 283 (7342), 1080–1081.
- 433 (16) Lechat, P. Clinical pharmacology of beta-blockers in cardiology: trial results and  
434 clinical applications. *Hot Topics in Cardiology* **2006** (1), 7–44.
- 435 (17) WHOCC. WHOCC - ATC/DDD Index.  
436 [http://www.whocc.no/atc\\_ddd\\_index/?code=C07AA05](http://www.whocc.no/atc_ddd_index/?code=C07AA05) (accessed September 9, 2014).
- 437 (18) Schwabe, U., Paffrath, D., Eds. *Arzneiverordnungs-Report 2013. Aktuelle Daten,*  
438 *Kosten, Trends und Kommentare*; Springer-Verlag: Berlin, Heidelberg, 2013.
- 439 (19) Bendz, D.; Paxéus, N. A.; Ginn, T. R.; Loge, F. J. Occurrence and fate of  
440 pharmaceutically active compounds in the environment, a case study: Høje River in  
441 Sweden. *J. Hazard. Mat.* **2005**, 122 (3), 195–204.
- 442 (20) Santos, L. H. M. L. M.; Araújo, A. N.; Fachini, A.; Pena, A.; Delerue-Matos, C.;  
443 Montenegro, M. C. B. S. M. Ecotoxicological aspects related to the presence of  
444 pharmaceuticals in the aquatic environment. *J. Hazard. Mat.* **2010**, 175 (1–3), 45–95.
- 445 (21) Gringauz, A. *Introduction to medicinal chemistry. How drugs act and why*; Wiley-  
446 VCH: New York, 1997.
- 447 (22) Gorre, F.; Vandekerckhove, H. Beta-blockers: focus on mechanism of action. Which  
448 beta-blocker, when and why? *Acta Cardiol.* **2010**, 65 (5), 565–570.
- 449 (23) OECD. *OECD Guidelines for the Testing of Chemicals. Ready Biodegradability 301D:*  
450 *Closed Bottle Test*; OECD Pub., 1992.
- 451 (24) OECD. *OECD Guidelines for the Testing of Chemicals. Ready Biodegradability 301F:*  
452 *Manometric Respiratory Test*; OECD Pub., 1992.
- 453 (25) RCSB Protein Data Bank. RCSB Protein Data Bank - RCSB PDB.  
454 <http://www.rcsb.org/pdb/home/home.do> (accessed June 6, 2013).
- 455 (26) Moukhametzianov, R.; Warne, T.; Edwards, P. C.; Serrano-Vega, M. J.; Leslie, A. G.  
456 W.; Tate, C. G.; Schertler, G. F. X. Two distinct conformations of helix 6 observed in  
457 antagonist-bound structures of a beta1-adrenergic receptor. *Proc. Natl. Acad. Sci. U.S.A.*  
458 **2011**, 108 (20), 8228–8232.
- 459 (27) Cherezov, V.; Rosenbaum, D. M.; Hanson, M. A.; Rasmussen, S. G. F.; Thian, F. S.;  
460 Kobilka, T. S.; Choi, H.-J.; Kuhn, P.; Weis, W. I.; Kobilka, B. K.; Stevens, R. C. High-  
461 Resolution Crystal Structure of an Engineered Human 2-Adrenergic G Protein Coupled  
462 Receptor. *Science* **2007**, 318 (5854), 1258–1265.

- 463 (28) Jorgensen, W. L. *Small-Molecule Drug Discovery Suite 2013-3: QikProp*; Schrödinger:  
464 New York, 2013.
- 465 (29) Saiakhov, R.; Chakravarti, S.; Sedykh, A. An improved workflow to perform in silico  
466 mutagenicity assessment of impurities as per ICH M7 guideline. *Toxicol. Letters* **2014**,  
467 *229, Supplement (0)*, S164.
- 468 (30) Leadscope. A new ICH M7 compliant expert alert system to predict the mutagenic  
469 potential of impurities. [http://www.leadscope.com/white\\_papers/ICHM7-WhitePaper-](http://www.leadscope.com/white_papers/ICHM7-WhitePaper-0314.pdf)  
470 *0314.pdf* (accessed April 9, 2015).
- 471 (31) DiscoverX. PathHunter® CHO-K1 ADRB1  $\beta$ -Arrestin Cell Line.  
472 <http://www.discoverx.com/product-data-sheets-3-tab/93-0488c2> (accessed April 24,  
473 2014).
- 474 (32) DiscoverX. PathHunter®  $\beta$ -Arrestin GPCR Assay Platform.  
475 [http://www.discoverx.com/technologies-platforms/enzyme-fragment-complementation-](http://www.discoverx.com/technologies-platforms/enzyme-fragment-complementation-technology/pathhunter-efc-cell-based-assay-platform/protein-protein-interactions/gpcrs-b-arrestin)  
476 *technology/pathhunter-efc-cell-based-assay-platform/protein-protein-interactions/gpcrs-*  
477 *b-arrestin* (accessed April 24, 2014).
- 478 (33) Liu, Q.-T.; Williams, H. E. Kinetics and Degradation Products for Direct Photolysis of  
479  $\beta$ -Blockers in Water. *Environ. Sci. Technol.* **2007**, *41* (3), 803–810.
- 480 (34) Benner, J.; Ternes, T. A. Ozonation of Propranolol: Formation of Oxidation Products.  
481 *Environ. Sci. Technol.* **2009**, *43* (13), 5086–5093.
- 482 (35) Santiago-Morales, J.; Agüera, A.; Gómez, M. d. M.; Fernández-Alba, A. R.; Giménez,  
483 J.; Esplugas, S.; Rosal, R. Transformation products and reaction kinetics in simulated  
484 solar light photocatalytic degradation of propranolol using Ce-doped TiO<sub>2</sub>. *Appl. Catal.*  
485 *B: Environ.* **2013**, *129*, 13–29.
- 486 (36) Wilde, M. L.; Montipó, S.; Martins, A. F. Degradation of  $\beta$ -blockers in hospital  
487 wastewater by means of ozonation and Fe<sup>2+</sup>/ozonation. *Water Res.* **2014**, *48*, 280–295.
- 488 (37) Wilde, M. L.; Mahmoud, W. M. M.; Kümmerer, K.; Martins, A. F. Oxidation–  
489 coagulation of  $\beta$ -blockers by K<sub>2</sub>FeVIO<sub>4</sub> in hospital wastewater: Assessment of  
490 degradation products and biodegradability. *Sci. Total Environ.* **2013**, *452–453* (0), 137–  
491 147.
- 492 (38) Howard, P. H. Biodegradation. In *Handbook of property estimation methods for*  
493 *environmental chemicals: Environmental and health sciences*; Mackay, D., Boethling,  
494 R. S., Eds.; Lewis Publishers: Boca Raton, 2000; pp 281–310.
- 495 (39) Lyons, C.; Katz, S.; Bartha, R. Mechanisms and pathways of aniline elimination from  
496 aquatic environments. *Appl. Environ. Microbiol.* **1984**, *48* (3), 491–496.
- 497 (40) Nishino, S. F.; Spain, J. C. Cell density-dependent adaptation of *Pseudomonas putida* to  
498 biodegradation of p-nitrophenol. *Environ. Sci. Technol.* **1993**, *27* (3), 489–494.
- 499 (41) Kümmerer, K.; Al-Ahmad, A.; Bertram, B.; Wießler, M. Biodegradability of  
500 antineoplastic compounds in screening tests: influence of glucosidation and of  
501 stereochemistry. *Chemosphere* **2000**, *40* (7), 767–773.

- 502 (42) Müller, T. A.; Kohler, H.-P. E. Chirality of pollutants-effects on metabolism and fate.  
503 *Appl. Microbiol. Biotechnol.* **2004**, *64* (3), 300–316.
- 504 (43) Sabela, M. I.; Gumede, N. J.; Escuder-Gilabert, L.; Martín-Biosca, Y.; Bisetty, K.;  
505 Medina-Hernández, M.-J.; Sagrado, S. Connecting simulated, bioanalytical, and  
506 molecular docking data on the stereoselective binding of (±)-catechin to human serum  
507 albumin. *Anal. Bioanal. Chem.* **2012**, *402* (5), 1899–1909.
- 508 (44) Li, W.; Liu, C.; Tan, G.; Zhang, X.; Zhu, Z.; Chai, Y. Molecular Modeling Study of  
509 Chiral Separation and Recognition Mechanism of  $\beta$ -Adrenergic Antagonists by  
510 Capillary Electrophoresis. *Int. J. Mol.Sci.* **2012**, *13* (12), 710–725.
- 511 (45) Boethling, R. S.; Sommer, E.; DiFiore, D. Designing Small Molecules for  
512 Biodegradability. *Chem. Rev.* **2007**, *107* (6), 2207–2227.
- 513 (46) ICH. *Assessment and control of DNA reactive (mutagenic) impurities in*  
514 *pharmaceuticals to limit potential carcinogenic risk M7. ICH M7 Genotoxic impurities*  
515 *Version 4*, 2014.
- 516 (47) Fitzgerald, J. D.; O'Donnell, S. R. Pharmacology of 4-hydroxypropranolol, a metabolite  
517 of propranolol. *Br. J. Pharmacol.* **1971**, *43* (1), 222–235.
- 518 (48) Walle, T.; Conradi, E. C.; Walle, U. K.; Fagan, T. C.; Gaffney, T. E. 4-  
519 Hydroxypropranolol and its glucuronide after single and long-term doses of  
520 propranolol. *Clin. Pharmacol. Ther.* **1980**, *27* (1), 22–31.
- 521 (49) Lee, H.-J.; Lee, E.; Yoon, S.-H.; Chang, H.-R.; Kim, K.; Kwon, J.-H. Enzymatic and  
522 microbial transformation assays for the evaluation of the environmental fate of  
523 diclofenac and its metabolites. *Chemosphere* **2012**, *87* (8), 969–974.



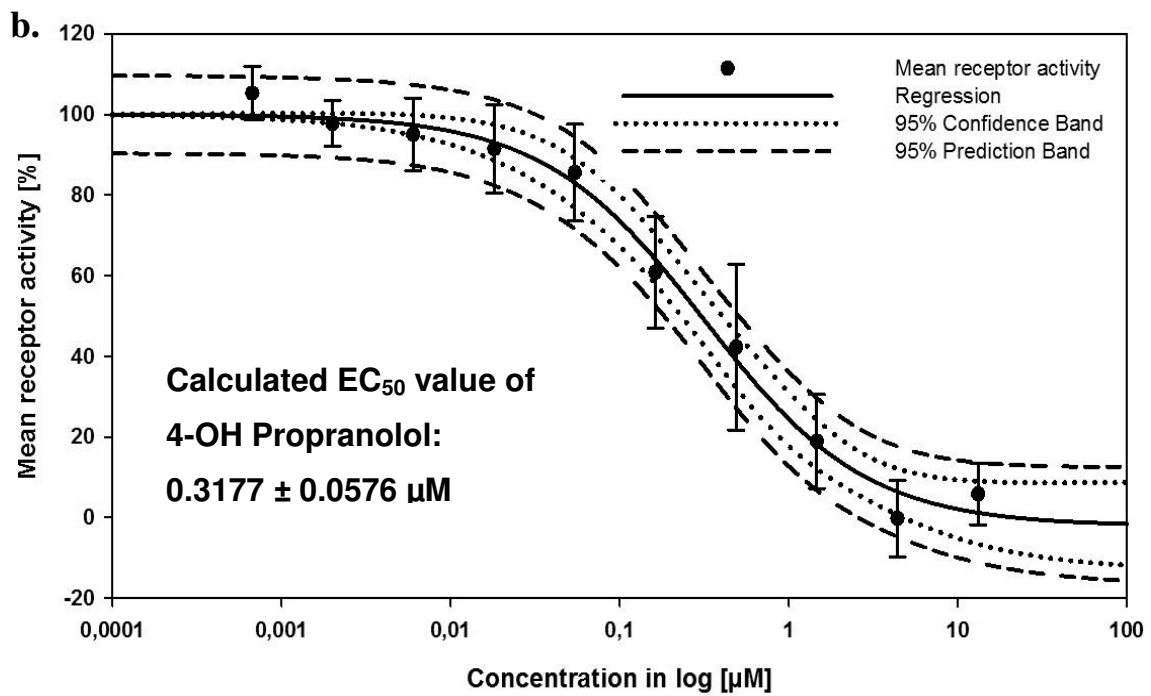
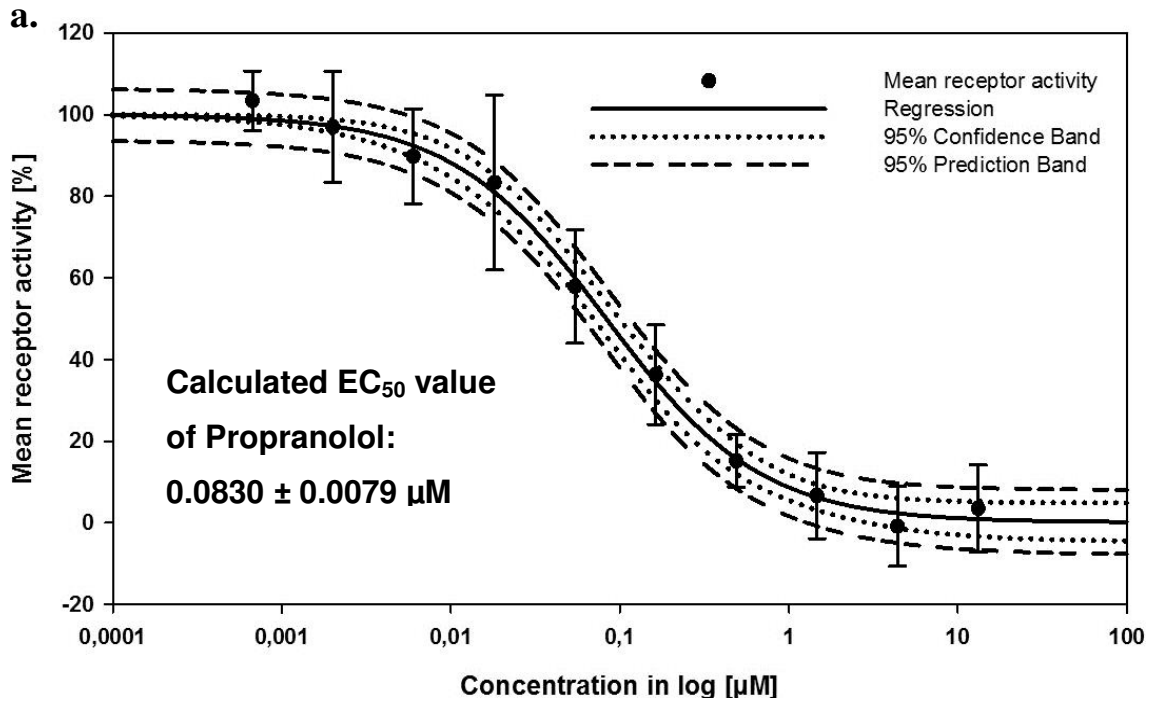
524

525

526 **Figure 1:** a) Results of LC-MS of CBT samples of Propranolol and hydroxyl derivatives of

527 Propranolol (n=2); b) Proposed biodegradation pathways and biodegradation transformation

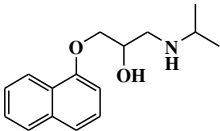
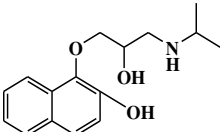
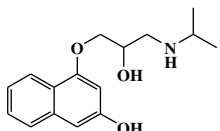
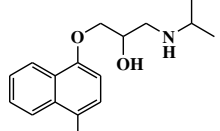
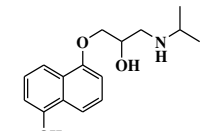
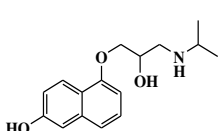
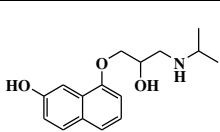
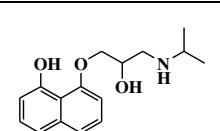
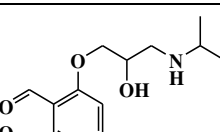
528 products of 4-Hydroxypropranolol.



529

530 **Figure 2:** *In vitro* analysis of the pharmacological potency of tested chemicals as  $\beta$  adrenergic  
531 receptor antagonists: a) Propranolol and b) 4-Hydroxypropranolol [n=3].

532 **Table 1:** Summary of the results of *in silico* molecular docking of the biodegradable  
 533 derivatives and Propranolol for both  $\beta_1$  and  $\beta_2$  adrenergic receptors which had the docking  
 534 score less than -8 (cut-off < -8).

Derivatives	Structure	$\beta_1$ docking score	$\beta_2$ docking score
Propranolol		-8.6 (R); -9.1 (S)	-9.2 (R); -9.2 (S)
PD <sub>1</sub> 276 (2- OH PPL)		-8.2 (R); -8.5 (S)	-8.1 (R); -8.3 (S)
PD <sub>2</sub> 276 (3- OH PPL)		-8.0 (R); -8.9 (S)	-9.4 (R);
PD <sub>3</sub> 276 (4- OH PPL)		-9.2 (R); -9.3 (S)	-8.9 (R); -9.6 (S)
PD <sub>4</sub> 276 (5- OH PPL)		-8.2 (R)	-8.9 (R)
PD <sub>5</sub> 276 (6- OH PPL)		-9.6 (S)	-8.6 (R); -9.1 (S)
PD <sub>6</sub> 276 (7- OH PPL)		-8.6 (R); -9.7 (S)	-8.3 (R); -9.0 (S)
PD <sub>7</sub> 276 (8- OH PPL)		-9.6 (R); -9.1 (S)	-9.1 (R); -9.0 (S)
PD 266		-8.4 (R); -8.4 (S)	-8.1 (R); -8.5 (S)

The docking scores of Propranolol and biodegradable derivatives predicted by the molecular docking software correspond particularly to the mentioned chirality of the molecule.



1 Supporting Information

2 for

3 Addressing the Challenge of Micro-Pollutants in the Aquatic  
4 Cycle: Targeted Re-Designing the  $\beta$ -Blocker Propranolol for  
5 Environmental Biodegradability

6 Tushar Rastogi, Christoph Leder, Klaus Kümmerer\*

7 *Sustainable Chemistry and Material Resources, Institute of Sustainable and Environmental Chemistry,*

8 *Leuphana University Lüneburg, C13, DE-21335 Lüneburg, Germany*

9 Pages: 79  
10 Texts: 9  
11 Figures: 6  
12 Tables: 11

---

\* Corresponding author: E-mail address: Klaus.Kuemmerer@uni.leuphana.de (K. Kümmerer)  
Other e-mail addresses: tushar.rastogi@leuphana.de, tushar1909@gmail.com (T. Rastogi),  
clleder@leuphana.de (C. Leder).

## 13 **Table of content**

14	<b>Experimental methods</b> .....	S3
15	Text S1 Supporting Information: Generation of photo-derivatives (PDs) of Propranolol and	
16	characteristics of UV lamp. ....	S3
17	Text S2 Supporting Information: Analytical method parameter for the elution and	
18	identification of the derivatives of Propranolol. ....	S4
19	Text S3 Supporting Information: Principles and procedure of the investigated aerobic	
20	biodegradation tests. ....	S5
21	Text S4 Supporting Information: <i>In silico</i> molecular docking of PPL and its PDs. ....	S7
22	Text S5 Supporting Information: <i>In silico</i> ADME properties predictions. ....	S7
23	Text S6 Supporting Information: <i>In silico</i> toxicity predictions. ....	S10
24	Text S7 Supporting Information: <i>In vitro</i> pharmacological assay. ....	S13
25	<b>Supporting results</b> .....	S14
26	Text S8 Supporting Information: Results of photolysis and generation of photo-derivatives	
27	(PDs) of PPL. ....	S14
28	Text S9 Supporting Information: Additional results for the pharmacological potency	
29	screening of photo-derivatives ( <i>in silico molecular docking</i> ). ....	S18
30	<b>Figures</b>	
31	Figure S1 Supporting Information: Proposed scheme of generation of photo-derivatives	
32	(PDs). ....	S14
33	Figure S2 Supporting Information: Aerobic biodegradation results of PPL and the mixture	
34	of photo-derivatives .....	S15
35	Figure S3 Supporting Information: LC-MS analysis of biodegradation test samples. ....	S16
36	Figure S4 Supporting Information: An illustration of the interaction of the turkey $\beta$ 1	
37	adrenergic receptor grid (2YCW) generated by <i>in silico</i> docking. ....	S20
38	Figure S5 Supporting Information: Aerobic biodegradation results of CBT of Propranolol	
39	and various hydroxyl derivatives of Propranolol .....	S21

40	Figure S6 Supporting Information: Result of CBT of 4-Hydroxypropranolol	
41	Glucuronide .....	S26
42	<b>Tables</b>	
43	Table S7 Supporting Information: Summary of the results of the investigated aerobic	
44	biodegradability test .....	S17
45	Table S8 Supporting Information: <i>In silico</i> biodegradability predictions and mutagenicity	
46	assessment .....	S22
47	Table S9 Supporting Information: ADME properties prediction of 4-OH PPL.....	S23
48	Table S10 Supporting Information: <i>In silico</i> mutagenicity assessment suggested by ICH M7	
49	guideline .....	S24
50	Table S11 Supporting Information: Proposed structures of the fragments formed during the	
51	MS <sup>2</sup> fragmentation.....	S27
52	<b>Reference</b> .....	S75

## 55 **Experimental methods**

56 **Text S1 Supporting Information:** Generation of photo-derivatives (PDs) of Propranolol and  
57 characteristics of UV lamp.

### 58 **Test procedure**

59 The generation of the photo-derivatives was performed in batch photo reactor which was  
60 constantly stirred and the temperature of the reaction mixture in the reactor was maintained  
61 between 18-20 °C through temperature control by a circulating cooler. The photolysis of PPL  
62 was performed with an initial concentration varying from 10 to 60 mg L<sup>-1</sup> under UV light for  
63 256 min. Sampling was performed after 2, 4, 8, 16, 32, 64, 128 and 256 min of irradiation  
64 time, respectively, in order to monitor the kinetics of transformation and mineralization of  
65 PPL. 15 mL samples were collected at each of the above mentioned time points. The primary  
66 elimination of PPL and the photo-derivatives (PDs) formed during the photolysis process  
67 were monitored by HPLC-UV and LC-ESI-MS/MS (ion-trap), respectively. A more detailed  
68 description of the testing procedures can be found elsewhere.<sup>1, 2</sup> The characteristics of the UV  
69 lamp are summarized in Table S1.

### 70 **Characteristics of UV lamp**

71 According to the manufacturer, the total radiation flux  $\Phi$  from 200 nm to 600 nm is 47 W m<sup>-2</sup>.

72 **Table S1 Supporting Information:** The maximal intensities at following of medium  
73 pressure mercury lamp TQ 150 (provided by manufacturer).

Wavelength (nm)	Intensities (W m <sup>-2</sup> )
254	4.0
265	1.4
302	1.8
313	4.3
366	6.4
405/408	3.2
436	4.2
546	5.1
577/579	4.7

74

75 **Text S2 Supporting Information:** Analytical method parameter for the elution and  
76 identification of the derivatives of Propranolol.

77 A Shimadzu Prominence HPLC system (Duisburg, Germany) was used to measure the  
78 primary elimination of the parent compound. A NUCLEODUR<sup>®</sup> RP-C18 (CC 125/4 100-  
79 5 $\mu$ m C18 ec) column and mobile phases consisting of 0.1 % formic acid in ultrapure water  
80 (CH<sub>2</sub>O<sub>2</sub>: solution A) and 100 % acetonitrile (CH<sub>3</sub>CN: solution B) were used for the  
81 chromatographic separation. The flow rate, column oven temperature and injection volume  
82 were set to 0.5 mL min<sup>-1</sup>, 25 °C and 50  $\mu$ L, respectively. PPL eluted at retention time [t<sub>R</sub>] 19.2  
83 min. High linearity correlation [ $r^2 \geq 0.9999$ ] was obtained for calibration curve range 200  $\mu$ g  
84 mL<sup>-1</sup> to 0.0978  $\mu$ g mL<sup>-1</sup>. The gradient flow method was applied as described in Table S2.

85 **Table S2 Supporting Information:** Gradient flow condition used to achieve the desired  
86 separation.

Time (min)	%B (Acetonitrile)
0.01 to 2 min	1
2 to 27 min	1% - 65% B
27 to 29 min	65% - 20% B
29 to 30 min	20% - 1% B
30 to 32 min	1% B
32.01	stop

87

#### 88 **LC-MS/MS method for the identification of derivatives of PPL:**

89 The Agilent LC 1100 series coupled to a Bruker Daltonic Esquire 6000+ ion-trap mass  
90 spectrometer (IT-MS) with electrospray ionization (ESI) interface was used for identification  
91 and structure elucidation of the formed derivatives. The above mentioned LC parameters were  
92 used while the MS parameters were optimized for PPL [m/z 260.1] by direct infusion of a 10  
93  $\mu$ g mL<sup>-1</sup> standard at a flow rate of 4  $\mu$ L min<sup>-1</sup> through a syringe pump. The mass spectrometer  
94 was operated in positive polarity. The PDs (photo-derivatives) formed during the UV  
95 treatment were identified by comparing 0 min photodegraded samples (i.e. PPL) as reference  
96 with other photolysed samples. Their structures were elucidated by interpreting the MS/MS  
97 spectra. The optimized parameters of MS are summarized in Table S3.

98 **Table S3 Supporting Information:** The operating parameters of the ESI and ion-trap  
 99 (Bruker 6000) of the LC-ESI-IT-MS<sup>n</sup>.

Parameters	Values
Dry gas temperature	350°C
Nebulizer pressure	30 psi
Dry gas flow	10 L min <sup>-1</sup>
end plate Offset	-500 Volt
capillary voltage	-3583 Volt
skimmer	40 Volt
capillary exit	110.5 Volt
octopole one	12.00 Volt
octopole two	1.70 Volt
trap drive	37.7
lens one	-5.0 Volt
lens two	-60 Volt
target mass	260 m/z
maximum accumulation time	200 ms
scan range	40 m/z - 1000 m/z
fragmentation amplitude	1

100

101 **DOC measurement:**

102 DOC was measured according to ISO 8245: 1999 guideline<sup>3</sup> using a Shimadzu TOC-VCPN  
 103 analyzer equipped with an ASI-V auto sampler. Samples were filtered with the syringe filter  
 104 (Chromafil® Xtra PES 45/25, Macherey Nagel, Düren, Germany) of 0.45µm pore size prior  
 105 to DOC measurement.

106 **Text S3 Supporting Information:** Principles and procedure of the investigated aerobic  
 107 biodegradation tests.

108 The aerobic biodegradability of PPL and its generated photo-derivatives were investigated  
 109 according to OECD Closed Bottle Test [CBT] 301D<sup>4</sup> and Manometric Respiratory Test  
 110 [MRT] 301 F.<sup>5</sup>

111 The CBT was performed in the dark at room temperature (20 ± 1 °C) with low bacterial  
 112 density. In CBT the concentration of the test compound was adjusted to 5 mg L<sup>-1</sup> theoretical  
 113 oxygen demand without nitrification (ThOD<sub>NH3</sub>) for the untreated samples. The aerobic

114 biodegradation in the CBT was monitored for 28 days by measuring oxygen concentration in  
115 the test vessels with Fibox 3 (PreSens, Regensburg, Germany).<sup>6</sup>

116 CBT consisted of four different series. The blank series contained only mineral medium and  
117 inoculum. The quality control series contained readily biodegradable sodium acetate at a  
118 concentration corresponding to  $5 \text{ mg L}^{-1} \text{ ThOD}_{\text{NH}_3}$ , mineral medium and inoculum. The  
119 actual test series contained the respective test substance, mineral medium and inoculum. The  
120 fourth series was the toxicity control which contained the test compound and sodium acetate  
121 at the concentrations corresponding to  $5 \text{ mg L}^{-1} \text{ ThOD}_{\text{NH}_3}$  each. The toxicity control monitors  
122 inhibitory effects due to the toxicity of test substances against the inoculum's bacteria and in  
123 order to allow for the recognition of false negative results. All series were performed in  
124 duplicates. All the test vessels were inoculated with 2 drops of the effluent from a local  
125 municipal STP (AGL Lüneburg, Germany, 144,000 population equivalents).

126 The MRT was also performed in the dark at room temperature ( $20 \pm 1 \text{ }^\circ\text{C}$ ) with gentle  
127 stirring. The OxiTop® Control OC110-system (WTW GmbH, Weilheim, Germany) was used  
128 as a measuring system to monitor the microbial oxygen consumption indirectly through  $\text{CO}_2$   
129 production during the aerobic biodegradation. The oxygen consumption was the endpoint  
130 used to calculate biodegradation.

131 These measuring heads contained sodium hydroxide which removes the  $\text{CO}_2$  from the gas  
132 phase. This removal of  $\text{CO}_2$  results in a decrease in pressure in test vessels which corresponds  
133 to the oxygen consumption which is due to biodegradation. The sample scheme was  
134 equivalent to that of the CBT, except an additional sterile control for the assessment of abiotic  
135 degradation was applied. The sterile control contained the test substance and sodium azide  
136 with no inoculum.

137 The concentrations of the test compound in MRT were adjusted to  $30 \text{ mg L}^{-1} \text{ ThOD}$  and 80  
138 mL of inoculum was added to 1 L of test solution as required by test guidelines. All the test  
139 vessels in both tests were inoculated with the effluent from a local municipal STP (AGL  
140 Lüneburg, Germany, 144,000 population equivalents). For qualitative reasons, pH was  
141 measured at 0 and 28 d for both investigated test assays.

142 The sample volume of post-treated samples (i.e. after photolysis) was increased corresponding  
143 to the DOC reduction during photolytic treatment. The samples after 0 min, 32 min and 256  
144 min of photolysis were tested in CBT while samples after 0 min, 64 min and 256 min were  
145 tested in MRT. The difference in the irradiation time of samples for both tests was due the  
146 difference in the kinetics of formation of the photo-derivatives (PDs). This difference in the  
147 kinetic was due to the different starting concentration of PPL in the photo-treatment.

148 Samples were taken at the beginning (day 0) and the end of the test (day 28) for later analysis  
149 by LC-UV-MS/MS to monitor any elimination of test compounds (i.e. PPL and PDs). A more  
150 detailed description of the testing procedures can be found elsewhere.<sup>1,7</sup>

151 Substances showing at least 60% degradation in these tests are classified as readily  
152 biodegradable<sup>8</sup> and therefore are expected not to enter or being accumulated in the aquatic  
153 environment.<sup>9</sup>

154 **Text S4 Supporting Information:** *In silico* molecular docking of PPL and its photo-  
155 derivatives.

156 The pharmacological property of PPL and its photo-derivatives with improved  
157 biodegradability was evaluated by molecular docking analysis. PPL and its improved  
158 biodegradable PDs were docked on the x-ray structures of both  $\beta_1$  and  $\beta_2$  adrenergic receptors  
159 which were crystallized with S-Carazolol to assure that the antagonistic state of the receptor  
160 was fixed. Carazolol is a high affinity antagonist of the  $\beta$ -adrenergic receptor.<sup>10</sup> All the  
161 improved biodegradable PDs including their constitutional isomers were docked to both  
162 receptors grids in order not to oversight any improved biodegradable derivative which might  
163 have non-inferior or comparable pharmacological potency as compared to PPL.

164 The derived x-ray structures were prepared with the protein preparation wizard and the  
165 receptor grid generation module from Schrodinger Maestro software. The ligands (PPL and its  
166 PDs) were prepared with the LigPrep module including a  $pK_a$  penalty provided by the Epik  
167 module.<sup>11</sup> The resulting constraints due to the hydrogen bonds of the investigated ligands with  
168 Asparagine (ASN) and Aspartate (ASP) amino acid of both receptors were identified. It was a  
169 constraint of the docking software that at least one of the two above mentioned hydrogen  
170 bonds should be formed. The docking score was calculated with the Glide module using  
171 standard precision.<sup>12</sup> Comparable docking scores provides evidence for non-inferior  
172 pharmacological properties while comparably lower scores indicate for possibly improved  
173 pharmacological potency of the derivatives compared to PPL.

174 **Text S5 Supporting Information:** *In silico* ADME properties predictions.

175 ADME properties were predicted using Schrödinger's QikProp 3.8 software developed by  
176 Jorgensen and co-workers<sup>13</sup> for the improved biodegradable and pharmacologically potent  
177 derivative shortlisted after the experimental assessment. The software database has ~710  
178 compounds including about 500 drugs and related heterocyclics.<sup>14</sup> In addition to predicting  
179 molecular properties, QikProp provides ranges for comparing a particular molecule's property



180 with those of 95% of known drugs. Various ADME properties, which were predicted by  
181 QikProp, are summarized and described in detail in Table S4.

182 The RuleOfFive number gives the number of violations of Lipinski's rule of five.<sup>15</sup>  
183 Compounds that satisfy this rule-of-five are considered drug-like. The rules are: molecular  
184 weight of molecule < 500, octanol/water partition coefficient ( $\log P_{o/w}$ ) < 5, hydrogen bond  
185 donors  $\leq 5$ , hydrogen bond acceptors  $\leq 10$ . The RuleOfThree number is the counting of  
186 violations of Jorgensen's rule of three.<sup>16</sup> Compound that satisfy this rule-of-three are  
187 considered as orally available.

188 The Qikprop software predicts the inhibitory concentration ( $IC_{50}$ ) values for the blockage of  
189 the hERG K<sup>+</sup> channel. The human Ether-à-go-go-Related Gene (hERG) encodes the protein  
190 of potassium (K) channel expressed in the heart. This ion channel contributes the electrical  
191 activity that coordinates the heart's beating.<sup>17, 18</sup> When the ability of the channel to conduct  
192 electrical current across cell membranes is inhibited or compromised, either by application of  
193 drugs or by rare mutations,<sup>19</sup> it could result in a potentially fatal disorder. It is has already  
194 been reported that a number of clinically successful drugs (such as some antihistamines and  
195 antibiotics) have the tendency to inhibit the hERG channel and create an associated risk of  
196 sudden death as a side-effect.<sup>20</sup> Thus, this phenomenon has made hERG inhibition an  
197 important antitarget that must be avoided during drug development.

198 The Qikprop software predicted apparent Caco-2 cell permeability and apparent MDCK cell  
199 permeability in nm/sec for non-active transport of chemicals. Caco-2 cells are a model for the  
200 gut-blood barrier<sup>21, 22</sup> and widely used across the pharmaceutical industry as an *in vitro* model  
201 of the human small intestinal mucosa to predict the absorption of orally administered drugs.<sup>23</sup>  
202 MDCK cells are considered to be a good mimic for the blood-brain barrier and used as a  
203 screening tool to increase the throughput of membrane permeability screening in early drug  
204 discovery stages.<sup>24</sup>

205 The Qikprop software uses a knowledge-based set of rules, including checking for suitable  
206 values of percent human oral absorption, number of metabolites, number of rotatable bonds,  
207 partition coefficient, solubility and cell permeability of the chemical, for the assessment of  
208 human oral absorption.

209 **Table S4 Supporting Information:** Detailed description of QikProp properties and  
 210 descriptors (ADME) used in the study.

<b>ADME properties or descriptor</b>	<b>Description</b>	<b>Range or recommended values</b>
Rule of five	Number of violations of Lipinski's rule of five. Compounds that satisfy these five rules are considered drug-like.	Fewer or preferably no violations
Rule of three	Number of violations of Jorgensen's rule of three. The three rules are: aqueous solubility > -5.7, apparent Caco-2 cell permeability > 22 nm/s, Number of likely metabolic reactions < 7. Molecule satisfying these rules are considered orally available	Fewer or preferably no violations
log P <sub>o/w</sub>	Predicted octanol/water partition coefficient.	-2.0 to 6.5
log S	Predicted aqueous solubility in mol dm <sup>-3</sup>	-6.5 to 0.5
log HERG	Predicted IC <sub>50</sub> value for blockage of HERG K <sup>+</sup> channels.	Concern below -5
P Caco	Predicted apparent Caco-2 cell permeability in nm/sec for non-active transport. Caco-2 cells are a model for the gut-blood barrier.	<25 poor and >500 great
log BB	Predicted brain/blood partition coefficient for orally delivered drugs	-3.0 to 1.2
P MDCK	Predicted apparent MDCK cell permeability in nm/sec for non-active transport. MDCK cells are considered to be a good mimic for the blood-brain-barrier.	<25 poor and >500 great
log K <sub>p</sub>	Predicted skin permeability.	-8.0 to -1.0
Human-oral absorption	Predicted human oral absorption. The assessment uses a knowledge-based set of rules, including checking for suitable values of number of metabolites, number of rotatable bonds, logP, solubility and cell permeability.	1, 2, or 3 for low, medium, or high respectively
log K <sub>hsa</sub>	Prediction of binding to human serum albumin	-1.5 to 1.5
CNS	Predicted central nervous system activity	-2 (inactive) to 2 (active)

211 **Text S6 Supporting Information:** *In silico* toxicity predictions.

212 Table S5 summarizes all the models used in the study for predicting toxicological end points  
213 such as carcinogenicity, mutagenicity and genotoxicity by OASIS Catalogic CASE Ultra and  
214 Leadscope software. The statistical and rule-based models from different software packages  
215 CASE Ultra v. 1.5.2.0 and Leadscope Model Applier v. 1.8.6 for predicting mutagenicity as  
216 per ICH M7 are also described in Table S5. Also the prediction for ready biodegradability of  
217 the proposed biodegradation transformation product was performed by CASE Ultra v.1.5.2.0  
218 software. One of the Leadscope Model applier's models ICH M7 Genotox Consensus model  
219 predicts the overall value based on any available experimental data on the test compound as  
220 well as the prediction results from the two ICH M7 statistical models and the expert model.  
221 CASE Ultra, Leadscope and OASIS Catalogic software provide positive, negative and out of  
222 domain (OD) estimations for the selected models. OD means that the test chemical is not  
223 included in the applicability domain of the applied model. Inconclusive alert provided by the  
224 CASE Ultra v.1.5.2.0 software means that there were positive alerts but the calculated  
225 probability falls below the classification threshold (50.0%) of the respective model.  
226 Additionally, Leadscope Model Applier software provided an indeterminate prediction. An  
227 indeterminate prediction is provided by software when both the expert model as well as the  
228 statistical based QSAR models is in situations where there is insufficient evidence or  
229 conflicting data to reach a positive/negative call with confidence.

230 All the *in silico* models used in the study have validated databases and training sets. More  
231 information about their databases, training sets and their validity criteria can be easily found  
232 elsewhere in the references provided in Table S8 for each model. The above mentioned  
233 models and software are described in detail elsewhere.<sup>1, 2, 25</sup> Table S5 below enlisted all the *in*  
234 *silico* software and their respective models applied in the present study.

235 **Table S5 Supporting Information:** List of *in silico* software and their respective models used for predicting ready biodegradability and toxicity.

QSAR Software	Models	End points	References
CASE Ultra v.1.4.5.1 (MultiCASE Inc.)	Human carcinogenicity (A0J)	Carcinogenicity	26, 27
	Micronucleus formation in vivo composite (A7S)	Genotoxicity	
	Chromosome aberration in vitro composite (A7U)	Mutagenicity	
	Mutagenicity Ames (A2H)	Mutagenicity against <i>Salmonella Typhimurium</i>	
CASE Ultra v. 1.5.2.0 (MultiCASE Inc.)	MITI Ready biodegradability	Ready biodegradability	28
	Salmonella mutagenicity TA 97,98,100, 1535-1538 (Statistical model)	Bacterial Mutagenicity	
	A-T mutation E coli and TA102 (Statistical model)	Bacterial Mutagenicity	
	Expert rules for genotoxicity (Rule based model)	Genotoxicity	
	E.coli mutagenicity (all strains) (Statistical model)	Bacterial Mutagenicity	
	Salmonella mutagenicity (TA97,98,100,1535-1538) (Statistical model)	Bacterial Mutagenicity	

	Bacterial mutagenesis (BM) model	Mutagenicity as a result of interaction with DNA of <i>Salmonella Typhimurium</i> or <i>Escherichia coli</i>	
Leadscope V. 3.0.11-1	Mammalian mutagenesis (MM)	Mutagenicity	29
	In vitro chromosome aberration (IVCA)	Mutagenicity	
	In vivo micronucleus (IVMN)	Genotoxicity	
	ICH M7 Genetox Consensus (Overall value)	Genetox Consensus	
Leadscope Model Applier Version: 1.8.6	E Coli - Sal 102 A-T mutagenicity (Statistical model)	Mutagenicity	30
	Salmonella mutagenicity (Statistical model)	Mutagenicity	
	Bacterial Mutation (Expert model)	Mutagenicity	
Catalogic v 5.11.6 TB (OASIS)	<i>in vitro</i> Ames model (mutagenicity v.04)	Mutagenicity against <i>Salmonella Typhimurium</i>	31

236 **Text S7 Supporting Information:** *In vitro* pharmacological assay.

237 *In vitro* pharmacological analysis was performed through the PathHunter® eXpress  $\beta$ -  
238 Arrestin Human and Ortholog GPCR kits (DiscoverX Corporation, USA). In this system,  
239 GPCR cells are engineered to co-express the ProLink™ (PK, small enzyme fragment) tagged  
240 GPCR and the enzyme acceptor (EA) tagged  $\beta$ -Arrestin. Upon activation, the EA tagged  $\beta$ -  
241 Arrestin induces binding to the PK tagged GPCR resulting in the formation of an active  $\beta$ -gal  
242 enzyme. This resulting functional enzyme hydrolyzes the substrate to generate a  
243 chemiluminescent signal which can be measured using a standard chemiluminescence reader.  
244 The detailed technology principle of the PathHunter® kit can be found elsewhere.<sup>32</sup>

245 Isoprenaline hydrochloride, an agonist for the  $\beta_1$  adrenergic receptor, was used as a positive  
246 control in the test assay. PPL and 4-OH PPL were tested in the assay for their antagonistic  
247 activity. The starting concentration of the agonist was  $22 \times EC_{80}$  value while the starting  
248 concentrations of the antagonists were  $1100 \times IC_{50}$  value. The same  $IC_{50}$  value for 4-OH PPL  
249 was assumed in order to compare its pharmacological potency to the parent compound. The  
250 starting concentrations of agonistic and antagonistic chemicals are summarized in Table S6.

251 The cells were incubated for 48 hours at 37 °C and 5 % CO<sub>2</sub> environment in a 96-well plate  
252 before measuring the antagonistic activity of the compound. The whole detailed working  
253 procedure is described in the user manual of PathHunter® eXpress kit.<sup>33</sup>

254 **Table S6 Supporting Information:** Starting concentration of agonistic and antagonistic  
255 chemicals for *in vitro* test assays.

Characteristic	Substance	IC <sub>50</sub> [nM]	Reference	Starting concentration [μM]
Agonist	Isoprenaline hydrochloride	200 (EC <sub>80</sub> value)	34	4.4
	Propranolol	12	35	13.2
Antagonist	4-hydroxy Propranolol	12		13.2

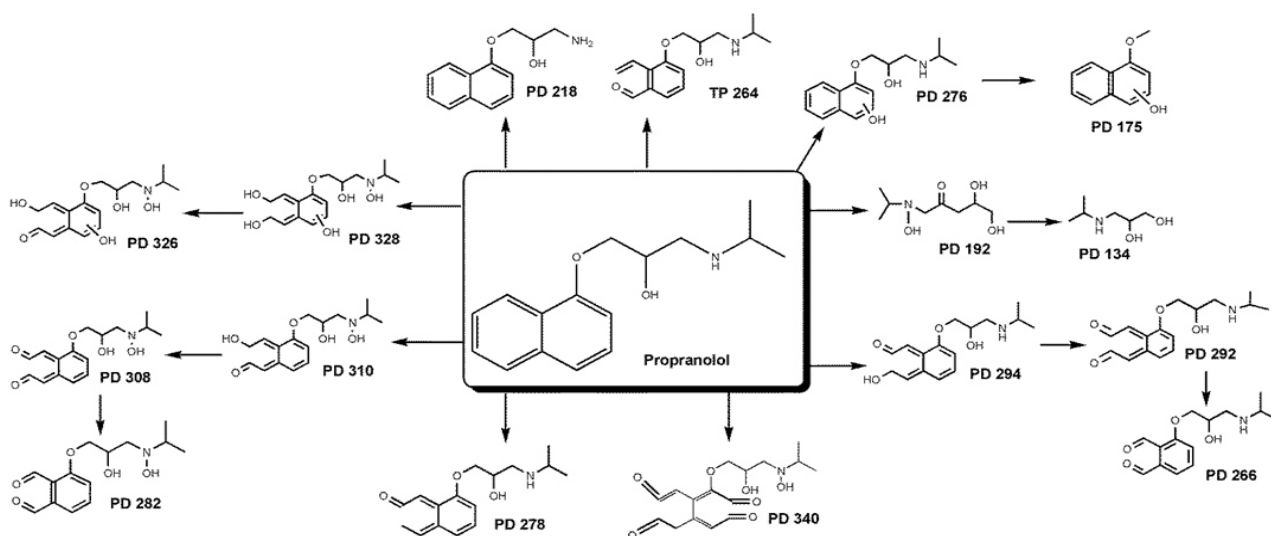
## 256 Supporting results

257 **Text S8 Supporting Information:** Results of photolysis and generation of photo-derivatives  
258 (PDs) of PPL.

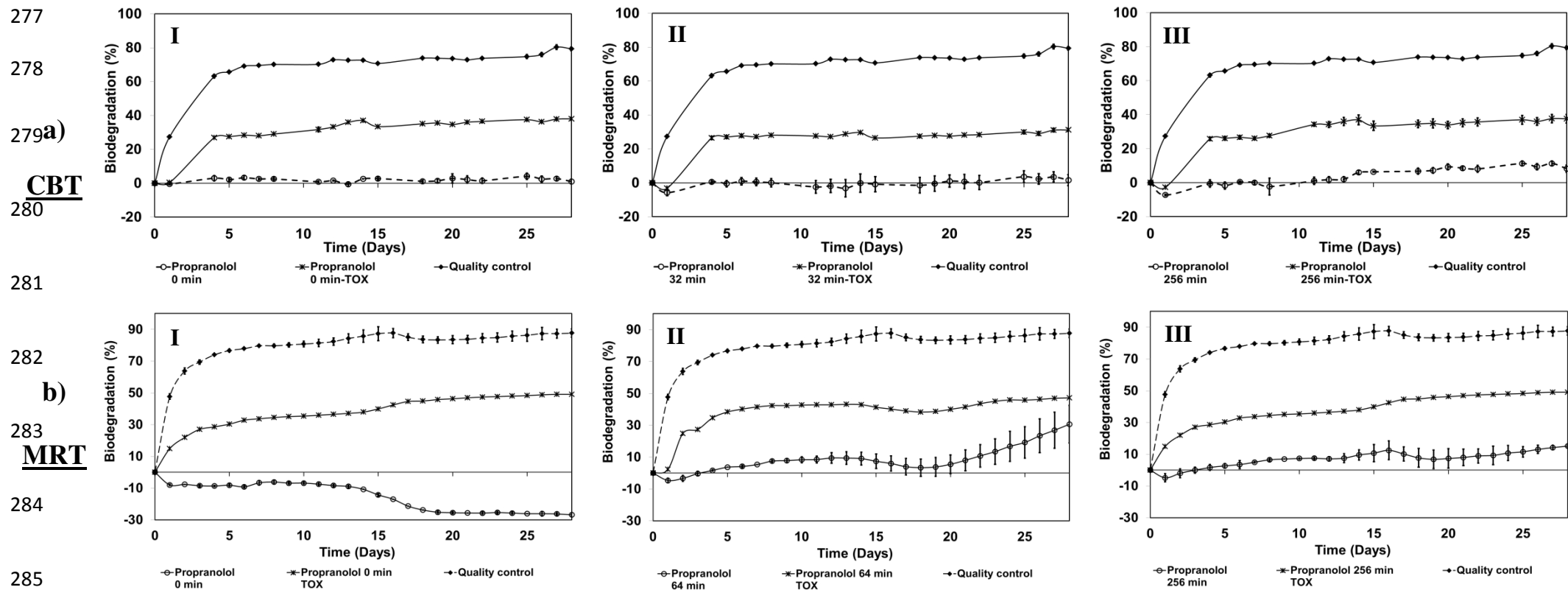
259 The photolysis of PPL was performed with an initial concentration varying from 10 to 60 mg  
260 L<sup>-1</sup>. PPL solutions were exposed to UV light for 256 min which resulted in complete primary  
261 elimination of the parent compound with incomplete mineralization.

262 New peaks were observed in the total ion chromatogram (TIC) during LC-MS analysis at  
263 different irradiation time which confirmed the formation of derivatives. In total, 16 photo-  
264 derivatives (PDs) were observed to be formed during the photolysis. Out of these 13 PDs  
265 were identified as the mono- or poly- hydroxylated derivatives of PPL with or without the  
266 subsequent opening of the Naphthalene ring of PPL molecule.

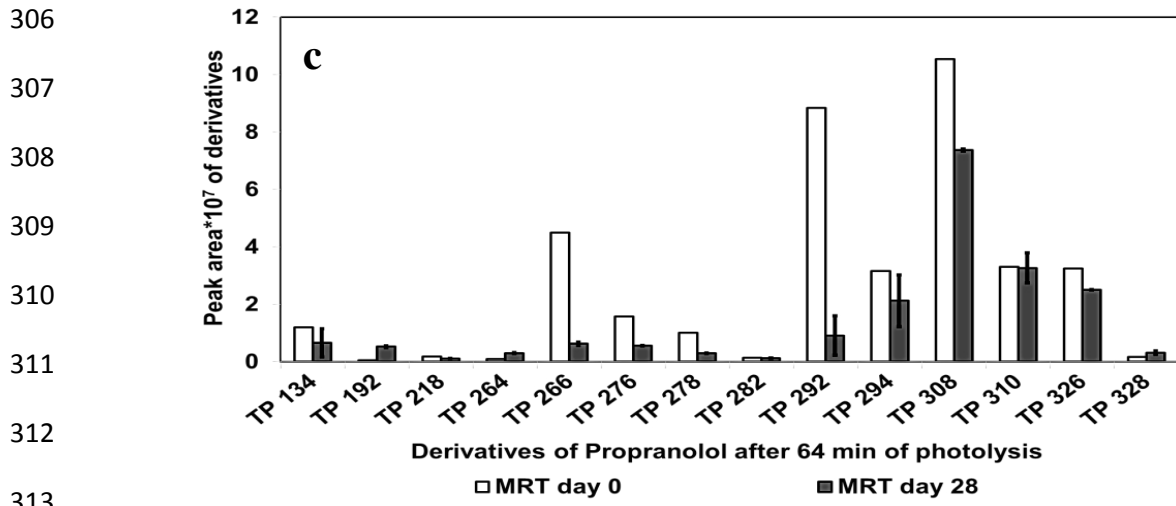
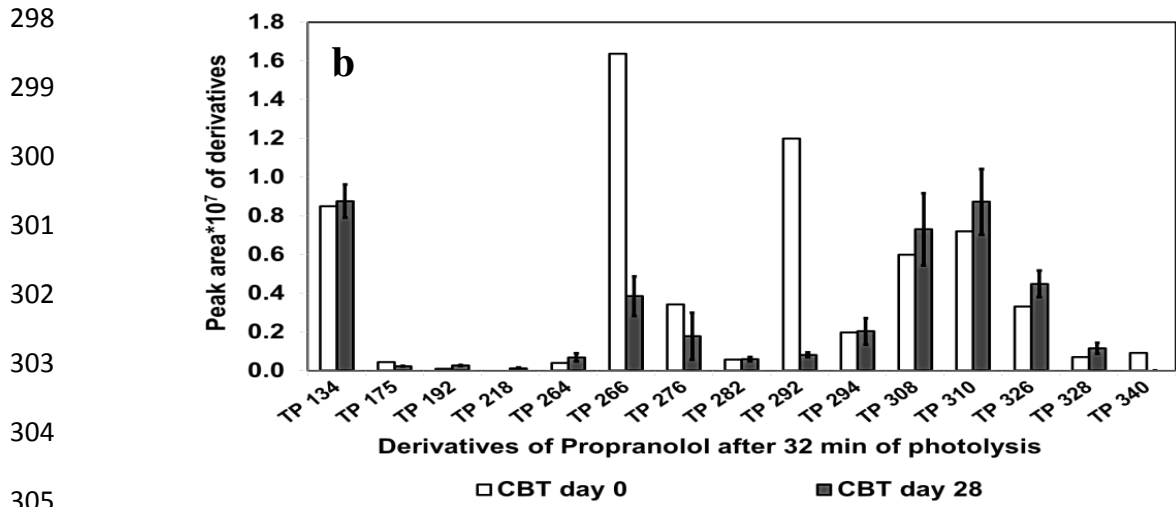
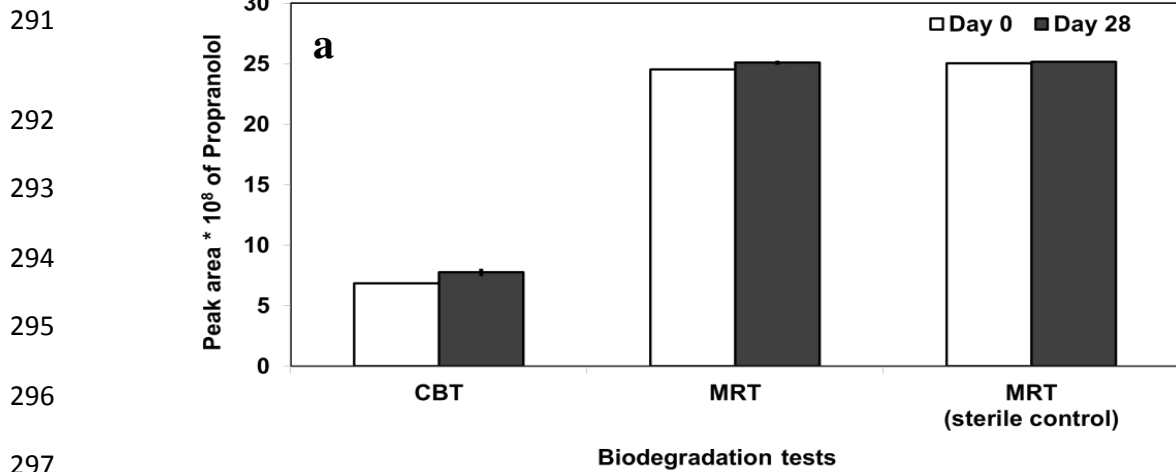
267 Several identified PDs of PPL were already reported in literature.<sup>36-44</sup> According to LC-  
268 MS/MS data, several identified PDs had the same respective nominal mass but eluted at  
269 different times. In most cases, these derivatives exhibited the same MS<sup>2</sup> fragmentation  
270 pattern, indicating the possibility of formation of constitutional isomers. The same phenomena  
271 of the formation of constitutional isomers of PPL derivatives were also reported earlier.<sup>37, 39,</sup>  
272 <sup>42, 44</sup> The retention time (t<sub>R</sub>), molecular formula, the possible structure of constitutional  
273 isomers of certain derivatives, extracted ion chromatogram (EIC) and the MS<sup>2</sup> fragmentation  
274 pattern of PPL and its PDs were provided in detail Table S11.



275 **Figure S1 Supporting Information:** Proposed scheme of generation of photo-derivatives  
276 (PDs).







314 **Figure S3 Supporting Information:** LC-MS analysis of biodegradation test samples: a) CBT  
 315 and MRT results of PPL after day 0 and day 28; b) CBT of 32 min UV irradiated samples of  
 316 PPL after day 0 and day 28; c). MRT of 64 min UV irradiated samples of PPL after day 0 and  
 317 day 28.

318 **Table S7 Supporting Information:** Summary of the results of the investigated aerobic biodegradability test for Propranolol and its mixture of  
 319 photo-derivatives (PDs).

<b>Biodegradation test</b>	<b>Test Sample</b>	<b>Biodegradation after 28 d [%]</b>	<b>DOC removal [%]</b>	<b>Derivatives identified with improved degraded</b>
<b>CBT</b>	0 min	1 ± 1 %	-	
	32 min	2 ± 3 %	-	PD 266; PD 276; PD 292 and PD 340
	256 min	8 ± 2%	-	
<b>MRT</b>	0 min	-27 ± 1 %*	3 %	PD 266; PD 276; PD 278; PD 292; PD 294; PD 308 and PD 326
	64 min	31 ± 12%	30 %	
	256 min	15 ± 1%	27 %	

\*The observed negative results in the MRT can be inferred due to the high degradation in the blank controls. The negative results are within the normally occurring fluctuations of this biological test system and have to be considered as 0 % degradation of the test substances.

320 **Text S9 Supporting Information:** Additional results for the pharmacological potency  
321 screening of photo-derivatives (*in silico molecular docking*).

322 An illustration of the binding interaction of the turkey  $\beta_1$  adrenergic receptor grid (2YCW)  
323 generated by *in silico* docking with both enantiomers of PPL, 4-OH PPL and 7-OH PPL is  
324 shown below as Figure S4.

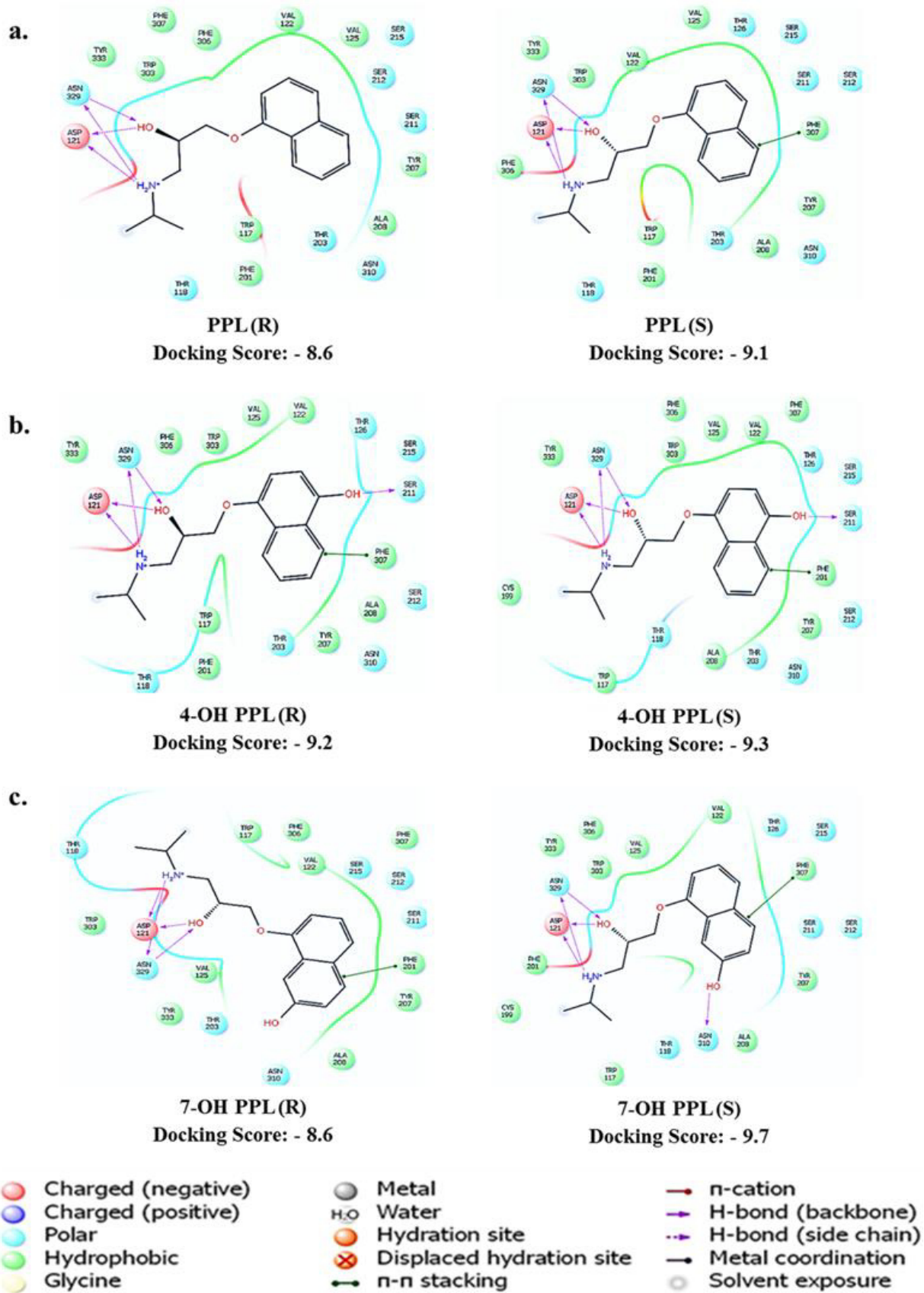
325 The binding interaction of both enantiomers of PPL with turkey  $\beta_1$  adrenergic receptors  
326 illustrated as Figure S4a. It was observed that the side chains of both enantiomers of PPL have  
327 identical hydrogen bonds with asparagine (ASN 329) and aspartate (ASP 121) amino acids of  
328 the  $\beta_1$  adrenergic receptor. Additional  $\Pi$ - $\Pi$  stacking of the naphthalene ring with the  
329 phenylalanine (PHE 307) amino acid in the (S)-PPL modulates its binding interaction and  
330 results in a lower docking score. This means that the (S)-PPL would be pharmacologically  
331 more potent than the (R)-PPL. This is in accordance with the finding that (S)-PPL is more  
332 potent in blocking  $\beta$  adrenergic receptors than (R)-PPL.<sup>45</sup>

333 The PD<sub>3</sub> 276 (i.e. 4-OH PPL) is a known human metabolite of PPL.<sup>46</sup> The binding interaction  
334 of enantiomers of this PPL's human metabolite PD 4-OH PPL with turkey  $\beta_1$  receptors is  
335 shown in Figure S4b. The hydroxyl group on the aromatic ring of both R and S enantiomers  
336 of 4-OH PPL formed an additional hydrogen bond with the serine (SER 211) amino acid,  
337 which in return altered their docking scores compared to PPL. The side chains of both  
338 enantiomers (R and S) of 4-OH PPL had identical binding with the ASN and ASP amino acid  
339 and naphthalene ring moiety of both have identical  $\Pi$ - $\Pi$  stacking with the PHE amino acid of  
340 the receptor, resulting in similar docking scores for both. This means that both enantiomers of  
341 4-OH PPL may be pharmacologically equipotent in blocking  $\beta$  adrenergic receptors.

342 Figure S4c illustrates the interaction of another constitutional isomer of mono- hydroxyl PD  
343 of PPL, i.e. 7-OH PPL (PD<sub>6</sub> 276). Although the side chains of both enantiomers of 7-OH PPL  
344 had identical binding with ASP and ASN amino acids, and the naphthalene rings of both

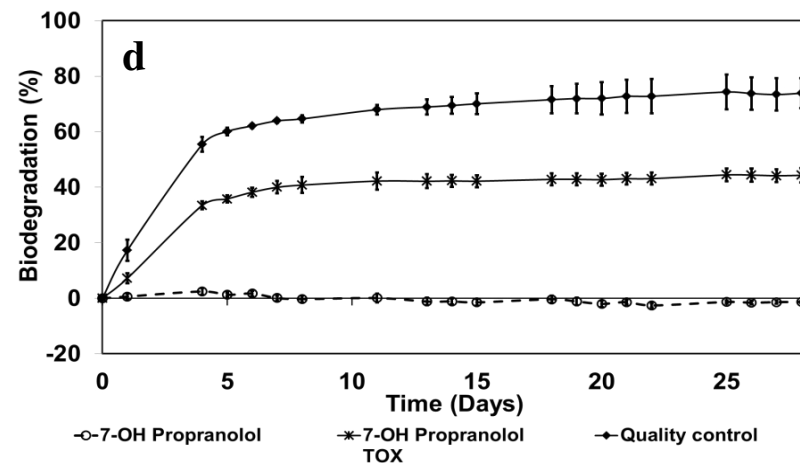
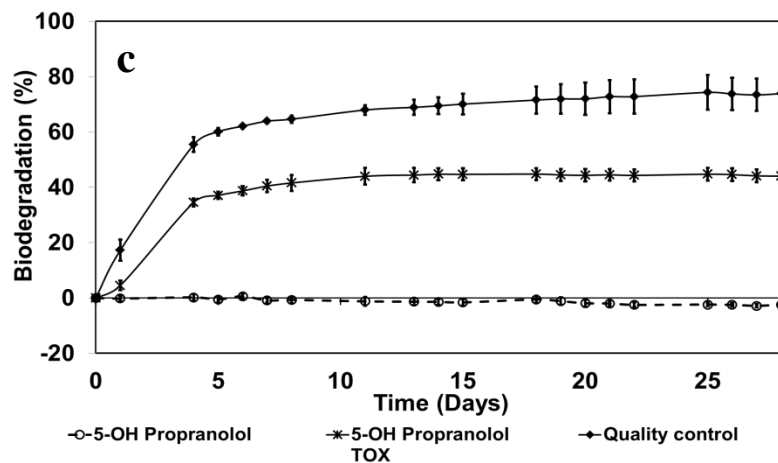
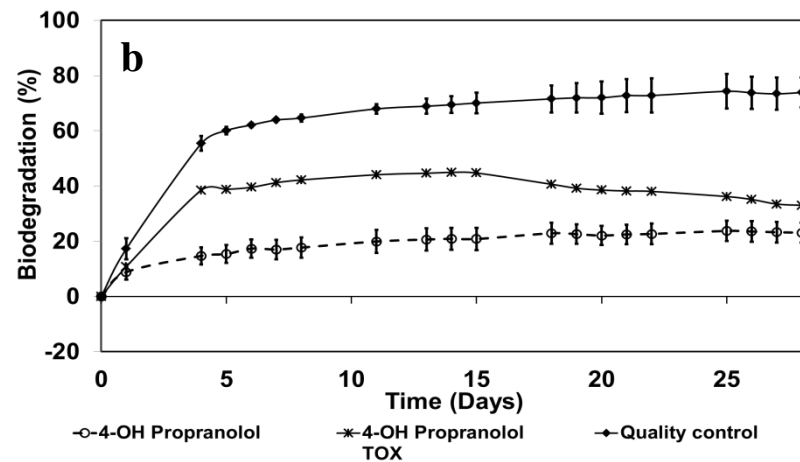
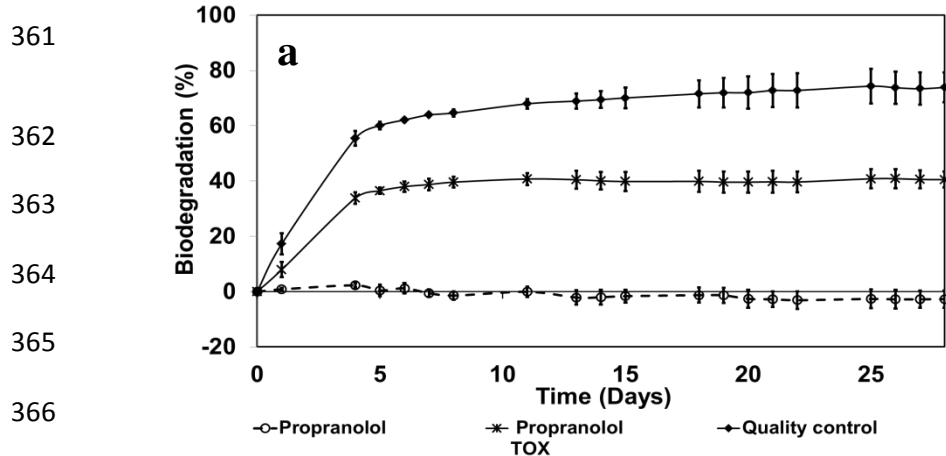
345 enantiomers had identical  $\Pi$ - $\Pi$  stacking with the PHE 307 amino acid, their docking scores  
346 were different. However, an additional hydrogen bond was formed between the hydroxyl  
347 group of the aromatic ring of S-7-OH PPL with the ASN amino acid, but this was not the case  
348 for the R enantiomer. This additional hydrogen bond in the S-7-OH PPL lowered the docking  
349 score, so S-7-OH PPL might have greater pharmacological potency compared to R-7-OH  
350 PPL.

351 It can also be seen in Figures S4b and S4c that a small alteration in the position of the  
352 hydroxyl group on the aromatic ring could modulate the interactions of the molecule with  
353 amino acids of the receptor, affecting its docking scores. Thus, different isomers of the same  
354 derivative (either constitutional or enantiomeric isomers) would have different affinities and  
355 binding interactions with the amino acids of the adrenergic receptors, which could in turn  
356 affect the overall docking score of those chemicals.



357

358 **Figure S4 Supporting Information:** An illustration of the interaction of the turkey  $\beta 1$   
 359 adrenergic receptor grid (2YCW) generated by in silico docking with both enantiomers of a)  
 360 Propranolol; b) 4-Hydroxypropranolol and c) 7-Hydroxypropranolol.



375 **Figure S5 Supporting Information:** Aerobic biodegradation results of CBT of Propranolol and various hydroxyl derivatives of Propranolol: a)  
376 Propranolol; b) 4-hydroxy Propranolol; c) 5-hydroxy Propranolol; d) 7-hydroxy Propranolol [n = 2]. The test was valid according to OECD  
377 guidelines<sup>8</sup> and no inhibitory effects were observed in the toxicity control for these derivatives. Thus, these tested lead candidates were not toxic  
378 against inoculum's bacteria.

379 **Table S8 Supporting Information:** *In silico* biodegradability predictions and mutagenicity assessment suggested by ICH M7 guideline with a  
 380 combination of statistical and rule-based models for Propranolol and bio-transformation products (bioTPs) of 4-Hydroxypropranolol by CASE Ultra  
 381 v. 1.5.2.0 and Leadscope Model Applier v.1.8.6 software.

	CASE Ultra v.1.5.2.0	CASE Ultra v.1.5.2.0 (MultiCase Inc.)					Leadscope Model Applier Version: 1.8.6 (Leadscope Inc.)			
	MITI Ready biodegradation	Salmonella mutagenicity TA 97,98,100, 1535-1538	A-T site mutation (E. coli/ S.typhimurium TA102)	Expert rules for genotoxicity	E.coli mutagenicity (all strains)	Salmonella mutagenicity (TA97,98,100, 1535-1538)	ICH M7 Genetox Consensus (Genetox Consensus)	E Coli - Sal 102 A-T mutagenicity	Salmonella mutagenicity	Bacterial Mutation
	(Statistical model)	(Statistical model)	(Statistical model)	(Rule-based model)	(Statistical model)	(Statistical model)	(Overall value)*	(Statistical model)	(Statistical model)	(Expert model)
PPL	§	-	§	-	-	-	-	-	-	-
4-OH PPL	§	-	-	+	-	-	-	-	-	-
4-OH PPL GLU	§	-	-	-	-	-	-	-	-	-
BioTP 134	+	-	-	-	-	-	-	-	-	-
BioTP 272	+	OD	§	+	-	+	-	-	-	-
BioTP <sub>1</sub> 290	OD	-	-	+	-	-	-	-	-	-
BioTP <sub>2</sub> 290	OD	-	-	+	-	-	-	#	-	#
BioTP <sub>3</sub> 290	OD	-	-	+	-	+	-	-	-	-
BioTP <sub>4</sub> 290	§	-	-	+	-	-	-	-	-	-
BioTP <sub>5</sub> 290	§	-	-	+	-	-	-	-	-	-
BioTP <sub>6</sub> 290	OD	-	-	+	-	+	-	-	-	-

OD: Out of Domain means that the test chemical is not included in the applicability domain of the applied model; §: Inconclusive means that there were positive alerts but the calculated probability falls below the classification threshold (50.0%) of the respective model; + : a positive alert for corresponding activity; - : a negative alert for corresponding activity

\*: overall value based on any available experimental data on the test compound as well as the prediction results from the two ICH M7 statistical models and the expert model; - : a negative prediction call indicates that there is evidence that the test compound is negative for corresponding activity; #: An indeterminate prediction call for both the expert alerts as well as the statistical based QSAR models in situations where there is insufficient evidence or conflicting data to reach a positive/negative call with confidence.

382

383 **Table S9 Supporting Information:** ADME properties prediction through QikProp software for the environmentally friendly  $\beta$ 1 adrenergic receptor  
 384 blocker 4-Hydroxypropranolol and comparison with Propranolol and selective  $\beta$ 1-blockers Atenolol and Metoprolol.

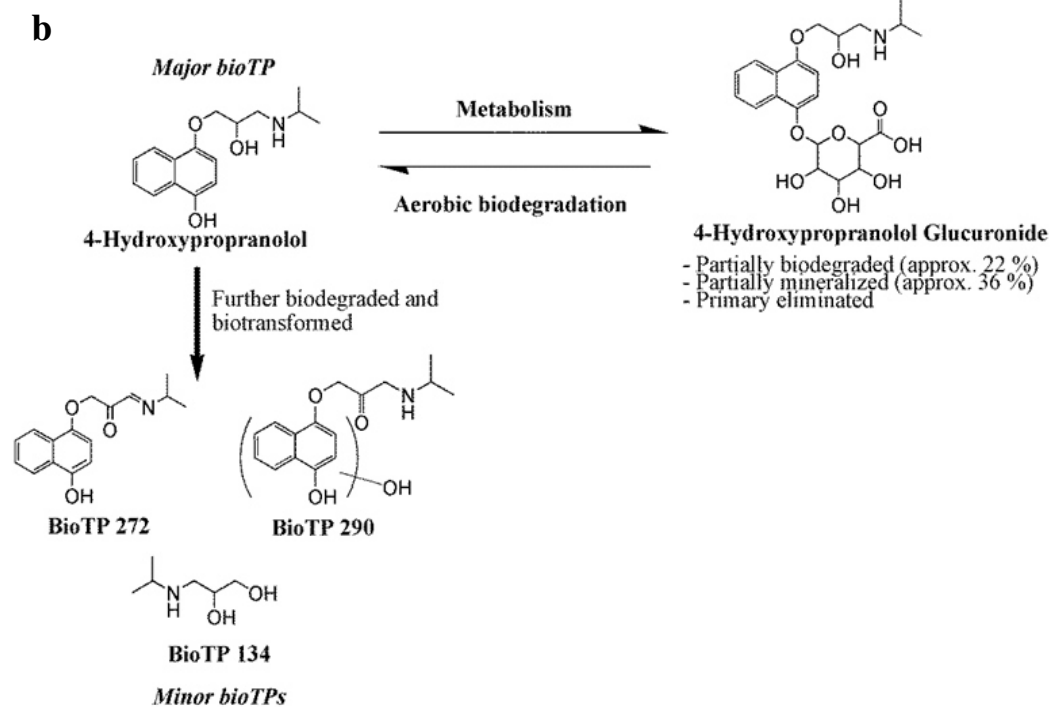
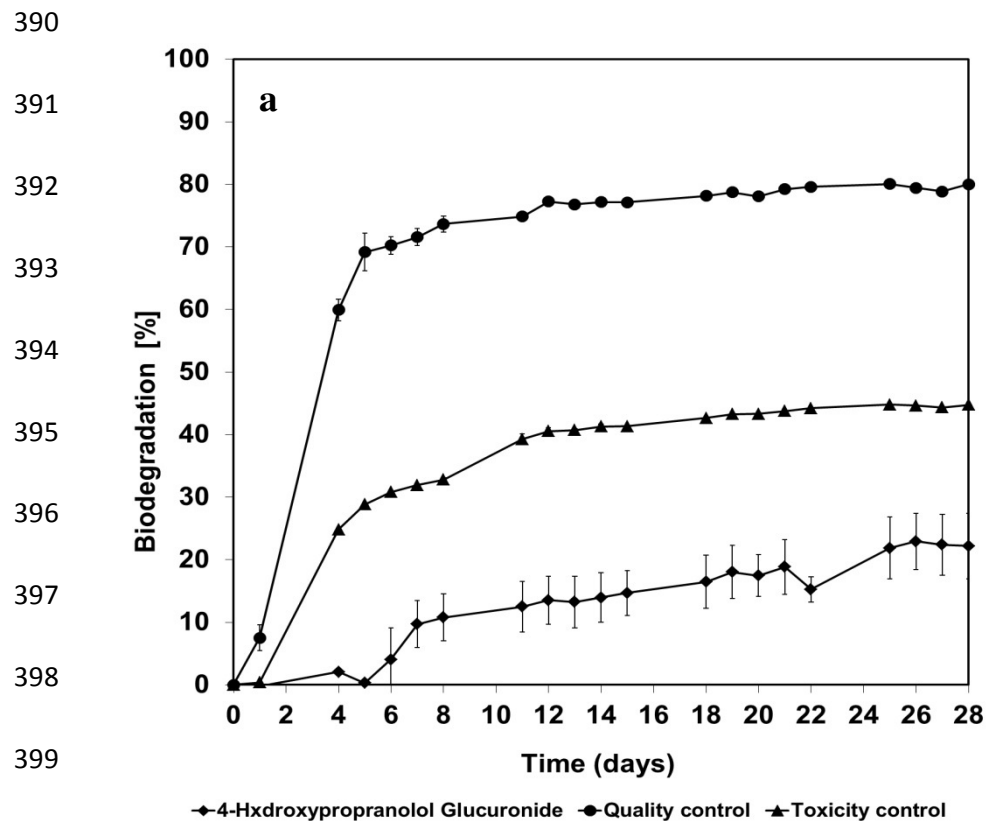
<b>ADME properties</b>	<b>Description</b>	<b>Range or recommended values</b>	<b>Atenolol</b>	<b>Metoprolol</b>	<b>Propranolol</b>	<b>4-Hydroxy propranolol</b>
<b>Rule of five</b>	Lipinski's rule of five.	Fewer or no violations	0	0	0	0
<b>Rule of three</b>	Jorgensen's rule of three.	Fewer or no violations	0	0	0	0
<b>log P<sub>o/w</sub></b>	Octanol/water partition coefficient.	-2.0 to 6.5	0.17	1.9	3.1	2.1
<b>log S</b>	Aqueous solubility	-6.5 to 0.5	-1.3	-1.4	-3.5	-2.1
<b>log HERG</b>	IC50 value for blockage of HERG K <sup>+</sup> channels.	Concern below -5	-4.5	-6.1	-5.9	-5.9
<b>P Caco</b>	Apparent Caco-2 cell permeability	<25 poor and >500 great	33.9	733.9	1147.9	320.7
<b>log BB</b>	Brain/blood partition coefficient	-3.0 to 1.2	-1.21	-0.22	0.22	-0.4
<b>P MDCK</b>	Apparent MDCK cell permeability	<25 poor and >500 great	32.0	391.7	635.3	160.1
<b>log K<sub>p</sub></b>	Skin permeability.	-8.0 to -1.0	-5.2	-3.2	-2.6	-3.7
<b>Human-oral absorption</b>		1, 2, or 3 for low, medium, or high respectively	2	3	3	3
<b>log K<sub>hsa</sub></b>	Binding to human serum albumin	-1.5 to 1.5	-0.76	-0.15	0.05	-0.12
<b>CNS</b>	Central nervous system activity	-2 (inactive) to 2 (active)	1	-2	1	0



385 **Table S10 Supporting Information:** *In silico* mutagenicity assessment suggested by ICH  
386 M7 guideline with a combination of statistical and rule-based models of CASE Ultra v.  
387 1.5.2.0 and Leadscope Model Applier Version: 1.8.6 and other toxicity endpoints prediction  
388 by different QSAR models of CASE Ultra v.1.4.5.1, Leadscope and OASIS Catalogic for  
389 Propranolol and 4-OH Propranolol.

QSAR Software	Models	End points	Propranolol	4-OH Propranolol
CASE Ultra v. 1.5.2.0	Salmonella mutagenicity TA 97,98,100, 1535-1538	Mutagenicity (Statistical Model)	Known negative	Negative
	A-T site mutation (E. coli/S.typhimurium TA102)	Mutagenicity (Statistical Model)	Inconclusive	Negative
	Expert rules for genotoxicity	Genotoxicity (Rule-based Model)	Known negative	Positive
	E.coli mutagenicity (all strains)	Mutagenicity (Statistical Model)	Negative	Negative
	Salmonella mutagenicity (TA97,98,100,1535-1538)	Mutagenicity (Statistical Model)	Known negative	Negative
Leadscope Model Applier Version: 1.8.6	ICH M7 Genetox Consensus	GenetoxConsensus (Overall value)	Negative	Negative
	E Coli - Sal 102 A-T mutagenicity	Mutagenicity (Statistical model)	Negative	Negative
	Salmonella mutagenicity	Mutagenicity (Statistical model)	Negative	Negative
	Bacterial Mutation	Mutagenicity (Expert model)	Negative	Negative
CASE Ultra v.1.4.5.1	Human carcinogenicity (A0J)	Carcinogenicity	Negative	Negative
	Micronucleus formation <i>in vivo</i> composite (A7S)	Genotoxicity	Positive	Negative
	Chromosome aberration <i>in vitro</i> composite (A7U)	Mutagenicity	Marginal positive	Negative
	Mutagenicity Ames (A2H)	Mutagenicity	Negative	Negative

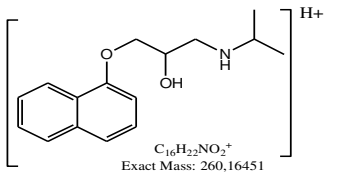
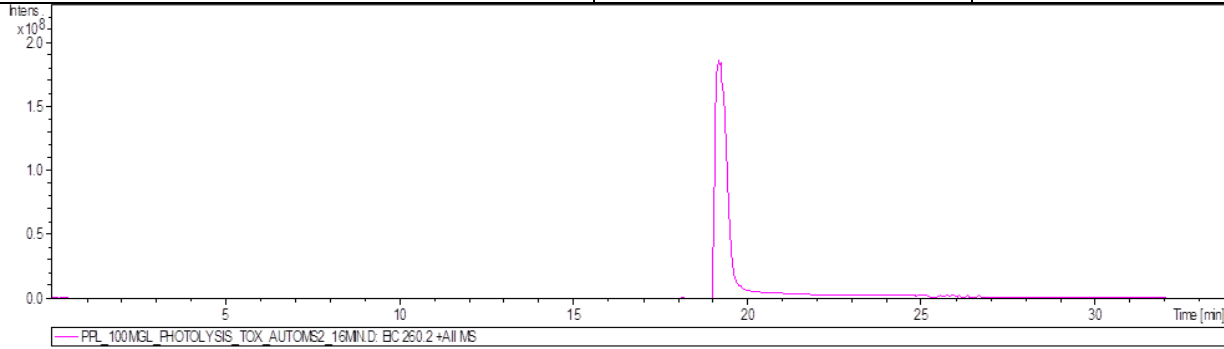
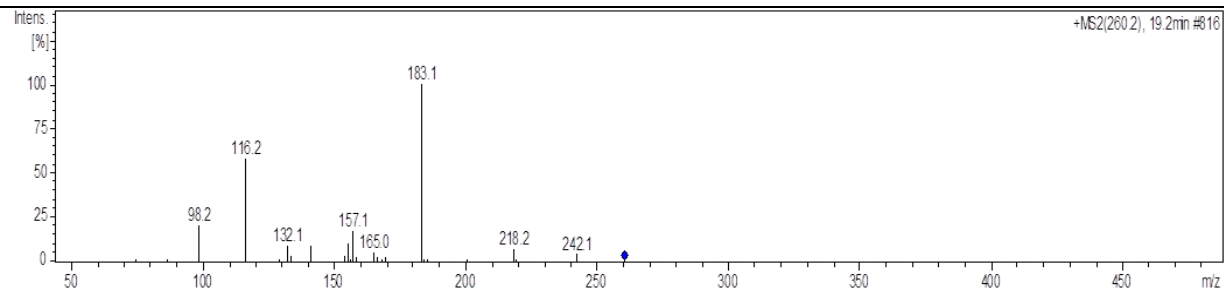
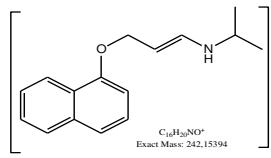
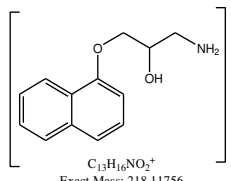
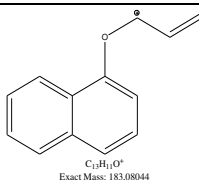
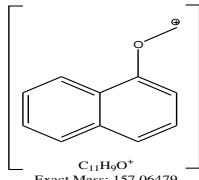
	Bacterial mutagenesis (BM) model	Mutagenicity	Negative	Negative
Leadscope	Mammalian mutagenesis (MM)	Mutagenicity	Negative	Negative
	<i>In vitro</i> chromosome aberration (IVCA)	Mutagenicity	Negative	Negative
	<i>In vivo</i> micronucleus (IVMN)	Genotoxicity	Negative	Negative
OASIS Catalogic	<i>In vitro</i> Ames model (mutagenicity v.04)	Mutagenicity	Negative	Negative

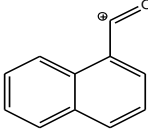
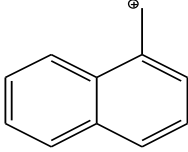
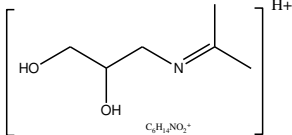
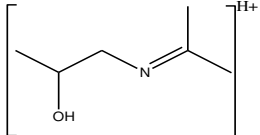
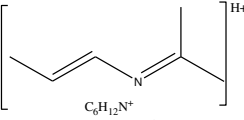


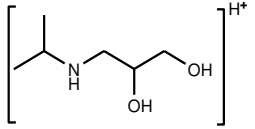
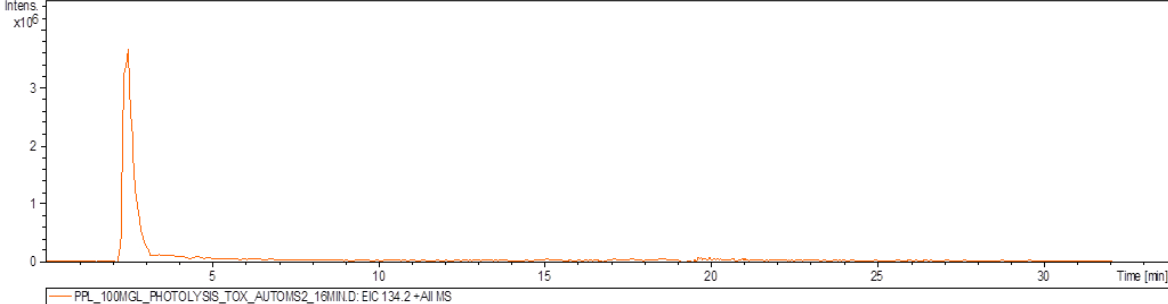
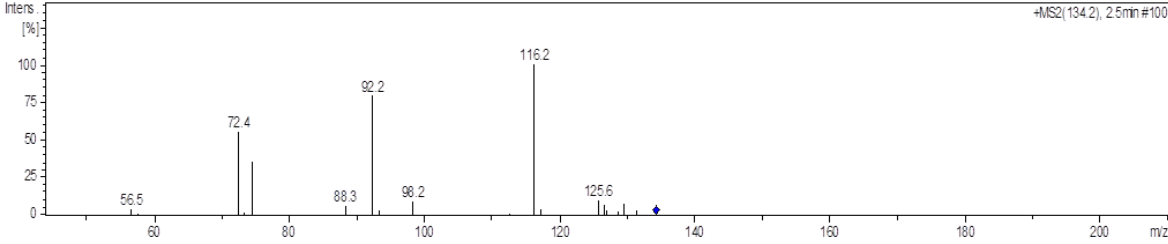
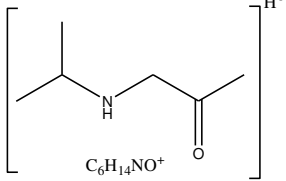
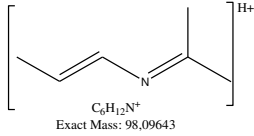
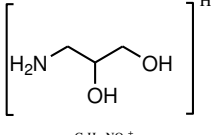
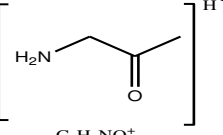
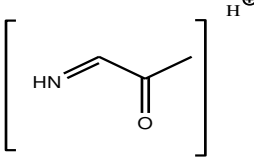
401 **Figure S6 Supporting Information:** Result of CBT of 4-Hydroxypropranolol Glucuronide: a) Kinetic of aerobic biodegradation CBT [n=2]. The  
 402 test was valid according to OECD guidelines and no inhibitory effects were observed in the toxicity control. Thus, it was not toxic against  
 403 inoculum's bacteria; b) Tentative scheme for biodegradation of 4-hydroxypropranolol Glucuronide, a metabolite of 4-hydroxypropranolol.

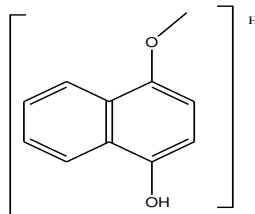
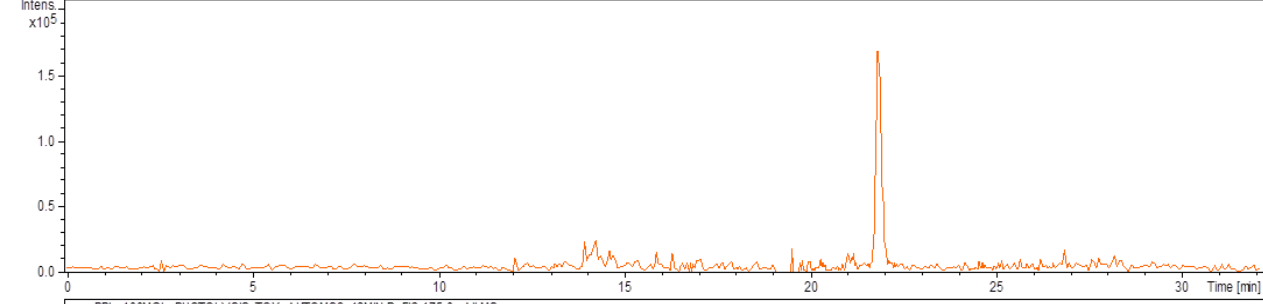
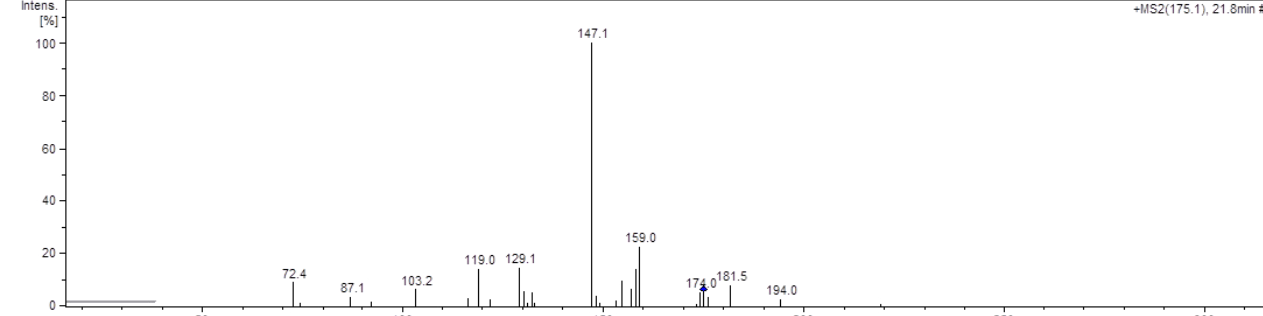
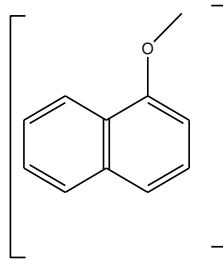
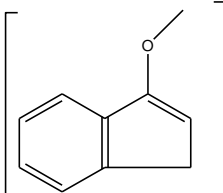
404 **Table S11 Supporting Information:** Proposed structures of the fragments formed during the  
 405 MS<sup>2</sup> fragmentation of Propranolol and its photo-derivatives.

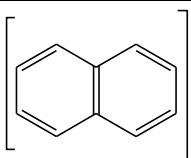
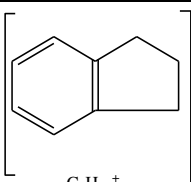
406 **Propranolol (PPL; m/z: 260)**

Fragments (m/z)	Retention time (min)	Precursor ion/Product ion	Structure	Reference
260.2	19.2	[M+H] <sup>+</sup>	 <chem>CC(C)NCC(O)COc1ccc2ccccc12</chem> $C_{16}H_{22}NO_2^+$ Exact Mass: 260.16451	43, 38, 42, 44, 47
 PPL_100MGL_PHOTOLYSIS_TOX_AUTOME2_16MIN.D: EIC 260.2 +All MS				
<b>MS<sup>2</sup></b>				
 +MS2(260.2), 19.2min #816				
242.1		[M+H- H <sub>2</sub> O] <sup>+</sup>	 <chem>CC(C)NCC=COc1ccc2ccccc12</chem> $C_{16}H_{20}NO^+$ Exact Mass: 242.15394	
218.2		[M+H-CH(CH <sub>3</sub> ) <sub>2</sub> ] <sup>+</sup>	 <chem>CC(O)COc1ccc2ccccc12</chem> $C_{13}H_{16}NO_3^+$ Exact Mass: 218.11756	
183.1		[M+H-H <sub>2</sub> O-NHCH(CH <sub>3</sub> ) <sub>2</sub> ] <sup>+</sup>	 <chem>COc1ccc2ccccc12</chem> $C_{11}H_{10}O^+$ Exact Mass: 183.08044	
157.1		[M+H-HOCH <sub>2</sub> CH <sub>2</sub> NHCH(CH <sub>3</sub> ) <sub>2</sub> ] <sup>+</sup>	 <chem>Oc1ccc2ccccc12</chem> $C_{11}H_9O^+$ Exact Mass: 157.06479	

155.2	Rearrangement of the m/z 157.1	 <p><math>C_{11}H_7O^+</math> Exact Mass: 155,04914</p>
141.1	$[M+H-$ HOCH <sub>2</sub> HOCH <sub>2</sub> CH <sub>2</sub> NH CH(CH <sub>3</sub> ) <sub>2</sub> ] <sup>+</sup>	 <p><math>C_{11}H_9^+</math> Exact Mass: 141,06988</p>
132.1	$[M+H-C_{10}H_8]^+$	 <p><math>C_6H_{14}NO_2^+</math> Exact Mass: 132,10191</p>
116.2	$[M+H-C_{10}H_8-H_2O]^+$	 <p><math>C_6H_{14}NO^+</math> Exact Mass: 116,10699</p>
98.2	$[M+H-C_{10}H_8-H_2O-$ H <sub>2</sub> O] <sup>+</sup>	 <p><math>C_6H_{12}N^+</math> Exact Mass: 98,09643</p>

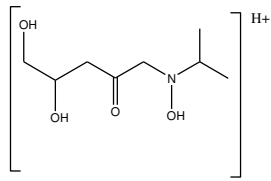
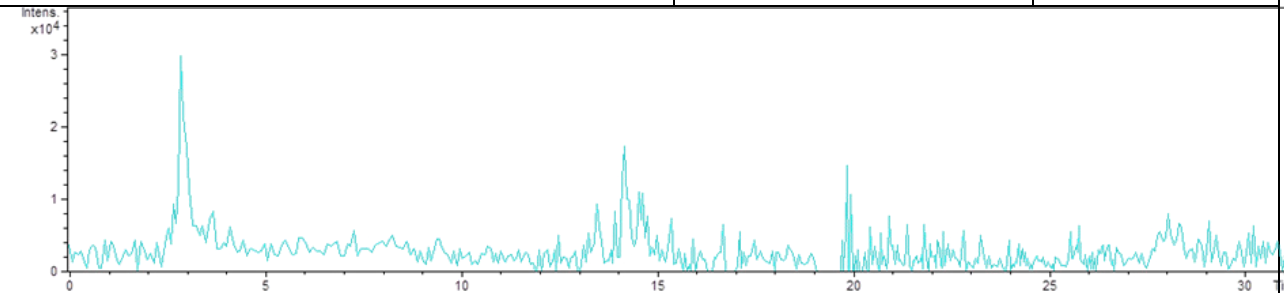
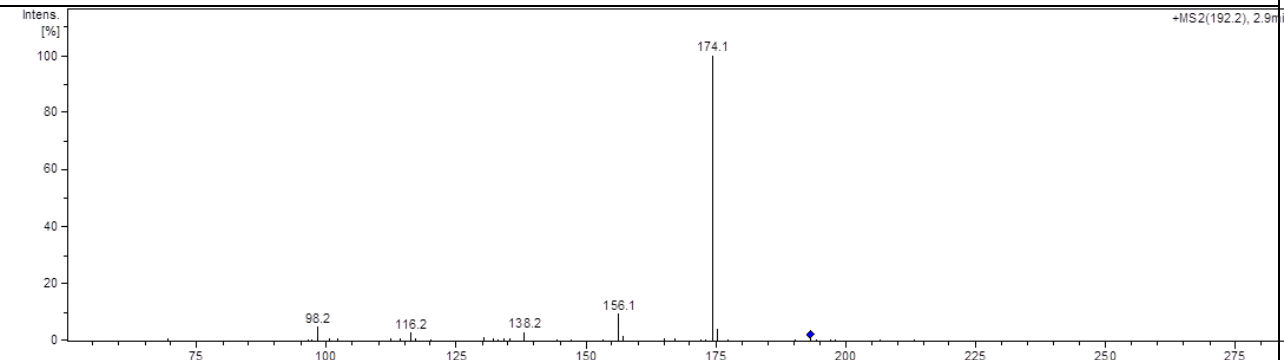
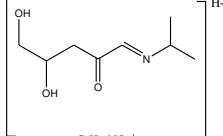
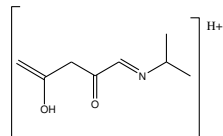
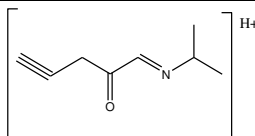
Fragments (m/z)	Retention time (min)	Precursor ion/Product ion	Structure	Reference
134.2	2.5	$[M+H]^+$	 $C_6H_{16}NO_2^+$ Exact Mass: 134,11756	42, 44, 40
				
$MS^2$				
				
116.2		$[M+H-H_2O]^+$	 $C_6H_{14}NO^+$ Exact Mass: 116,10699	
98.2		$[M+H-H_2O-H_2O]^+$	 $C_6H_{12}N^+$ Exact Mass: 98,09643	
92.2		$[M+H-CH(CH_3)_2]^+$	 $C_3H_{10}NO_2^+$ Exact Mass: 92,0706	
74.4		$[M+H-H_2O-CH(CH_3)_2]^+$	 $C_3H_8NO^+$ Exact Mass: 74,06004	
72.4		$[M+H-H_2O-CH_2(CH_3)_2]^+$	 $C_3H_6NO^+$ Exact Mass: 72,04439	

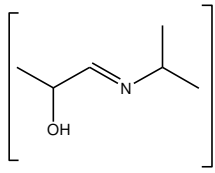
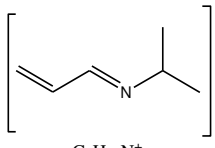
Fragments (m/z)	Retention time (min)	Precursor ion/Product ion	Structure	Reference
175.1	21.8	[M+H] <sup>+</sup>	 <p data-bbox="861 548 1117 604">C<sub>11</sub>H<sub>11</sub>O<sub>2</sub><sup>+</sup> Exact Mass: 175,07536</p>	MetaPC software
 <p data-bbox="159 929 1428 952">PPL_100MGL_PHOTOLYSIS_TOX_AUTOMS2_16MIN.D: EIC 175.0 +All MS</p>				
MS <sup>2</sup>				
 <p data-bbox="1292 1019 1436 1041">+MS2(175.1), 21.8min #914</p>				
159.0	[M+H-H <sub>2</sub> O] <sup>+</sup>		 <p data-bbox="989 1624 1212 1680">C<sub>11</sub>H<sub>11</sub>O<sup>+</sup> Exact Mass: 159,08044</p>	
147.1	[M+H-CH <sub>3</sub> OH] <sup>+</sup>		 <p data-bbox="989 1915 1212 1971">C<sub>10</sub>H<sub>11</sub>O<sup>+</sup> Exact Mass: 147,08044</p>	

<p>129.1</p>	<p><math>[M+H-CH_3OH-H_2O]^+</math></p>	 <p><math>C_{10}H_9^+</math> Exact Mass: 129,06988</p>
<p>119.0</p>	<p><math>[M+H-CH_3OH-CH_3OH]^+</math></p>	 <p><math>C_9H_{11}^+</math> Exact Mass: 119,08553</p>

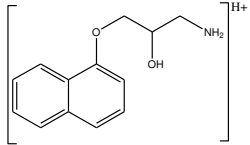
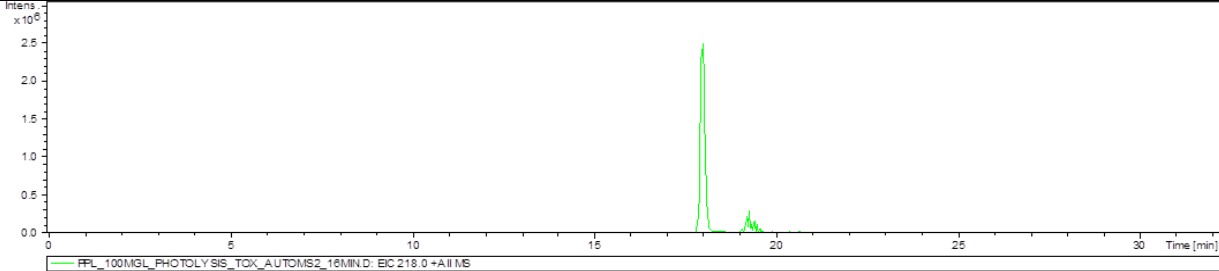
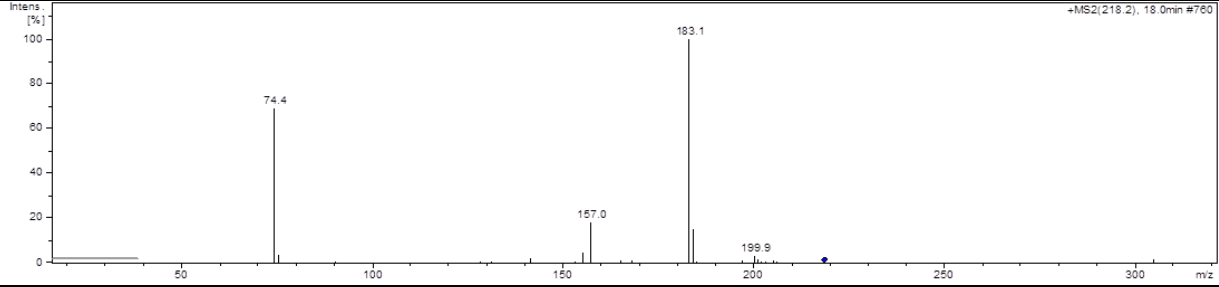
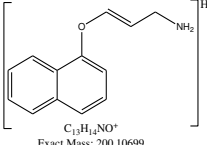
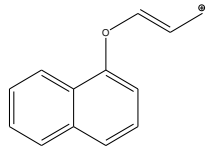
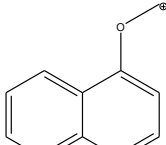
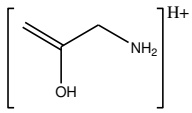
410

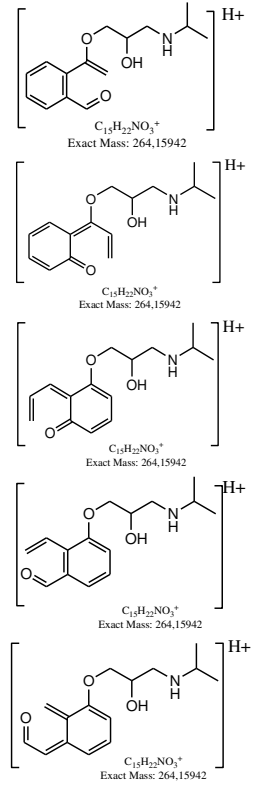
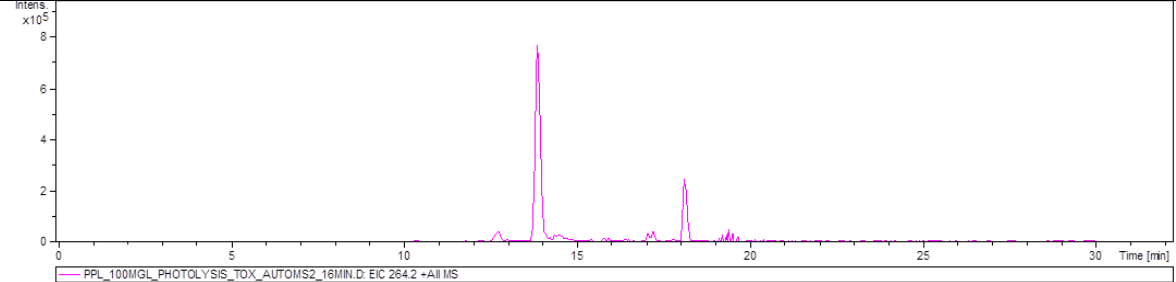
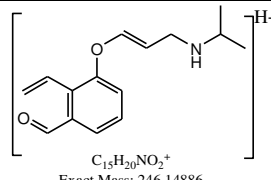
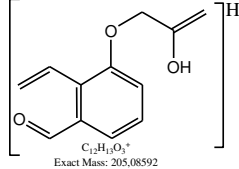


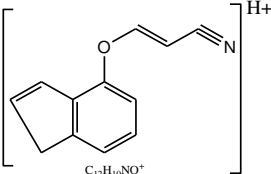
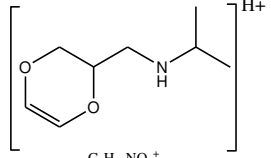
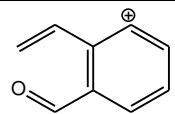
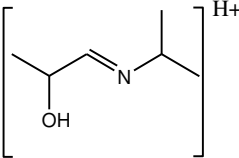
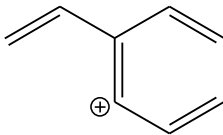
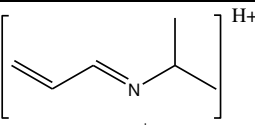
Fragments (m/z)	Retention time (min)	Precursor ion/Product ion	Structure	Reference
192.2	2.0	[M+H] <sup>+</sup>	 <p><math>C_8H_{18}NO_4^+</math> Exact Mass: 192.12303</p>	MetaPC software
 <p>PPL_100MGL_PHOTOLYSIS_TOX_AUTOMS2_16MIN.D: EIC 193.0 +All MS</p>				
<b>MS<sup>2</sup></b>				
 <p>-MS2(192.2), 2.9min</p>				
174.1		[M+H-H <sub>2</sub> O] <sup>+</sup>	 <p><math>C_8H_{16}NO_3^+</math> Exact Mass: 174.11247</p>	
156.1		[M+H-H <sub>2</sub> O-H <sub>2</sub> O] <sup>+</sup>	 <p><math>C_8H_{14}NO_2^+</math> Exact Mass: 156.10191</p>	
138.2		[M+H-H <sub>2</sub> O-H <sub>2</sub> O-H <sub>2</sub> O] <sup>+</sup>	 <p><math>C_8H_{12}NO^+</math> Exact Mass: 138.09134</p>	

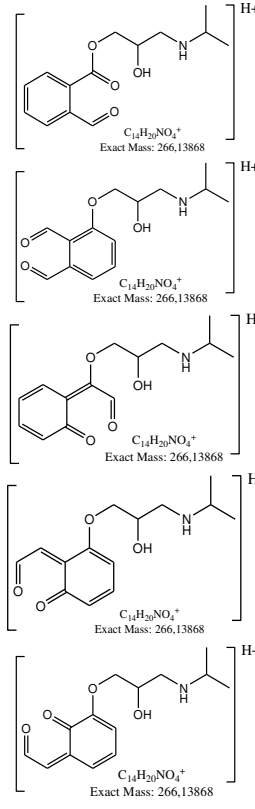
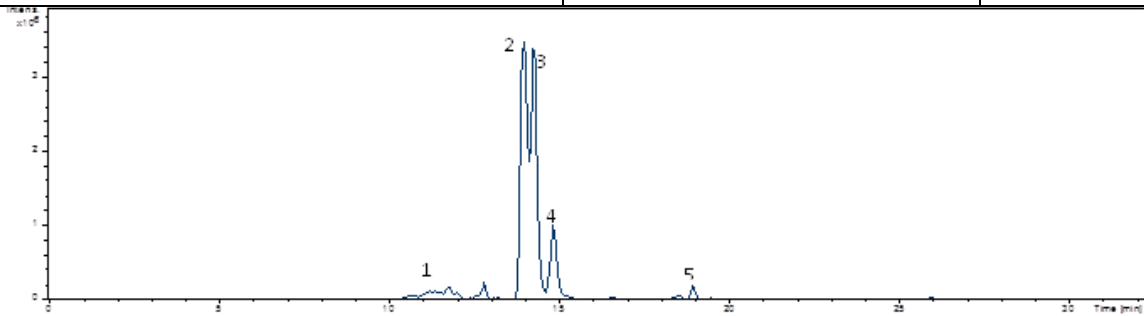
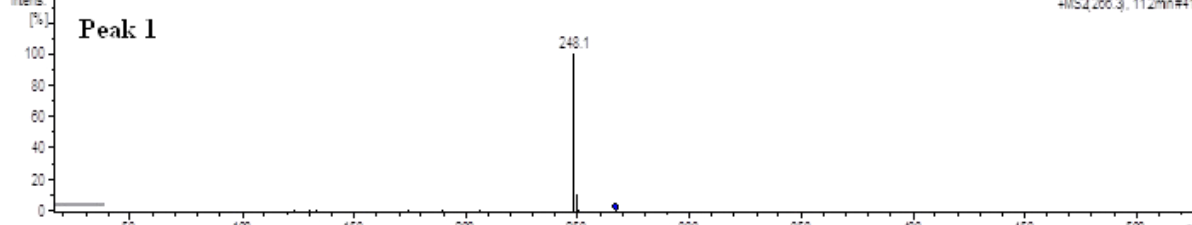
<p>116.2      <math>[M+H-H_2O-H_2O-H_2O-C_2H_2]^+</math></p>	 <p><math>C_6H_{14}NO^+</math> Exact Mass: 116,10699</p>
<p>98.2      <math>[M+H-H_2O-H_2O-H_2O-C_2H_2-H_2O]^+</math></p>	 <p><math>C_6H_{12}N^+</math> Exact Mass: 98,09643</p>

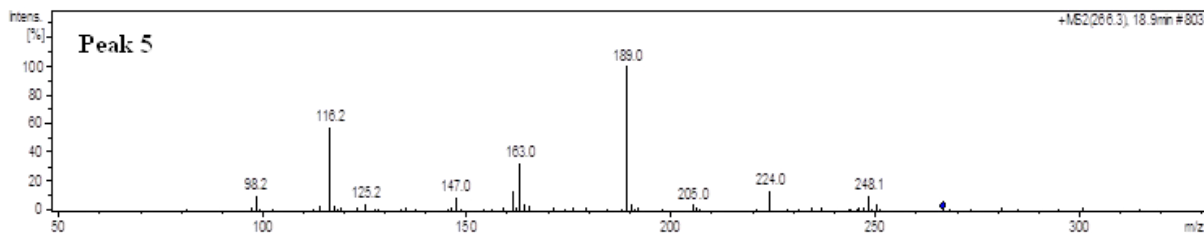
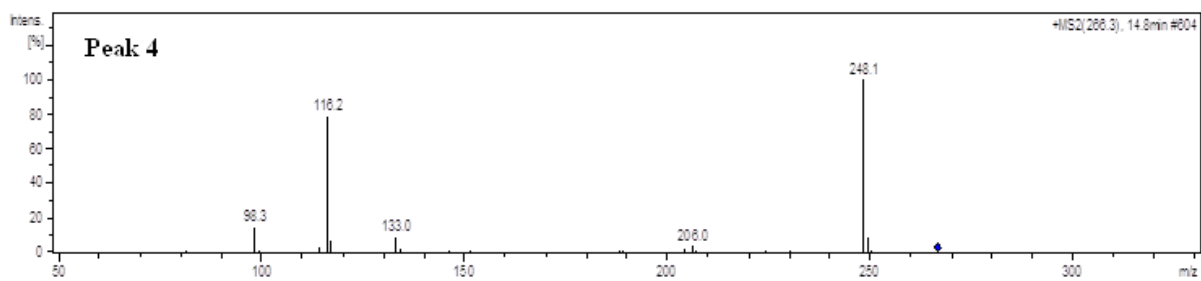
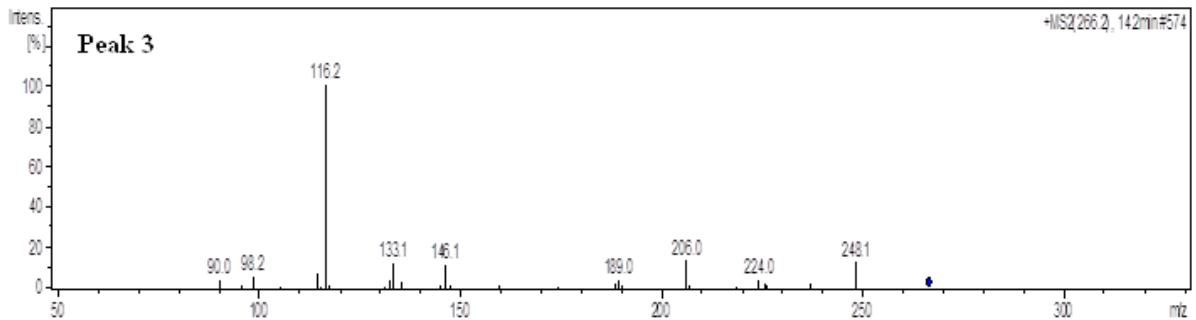
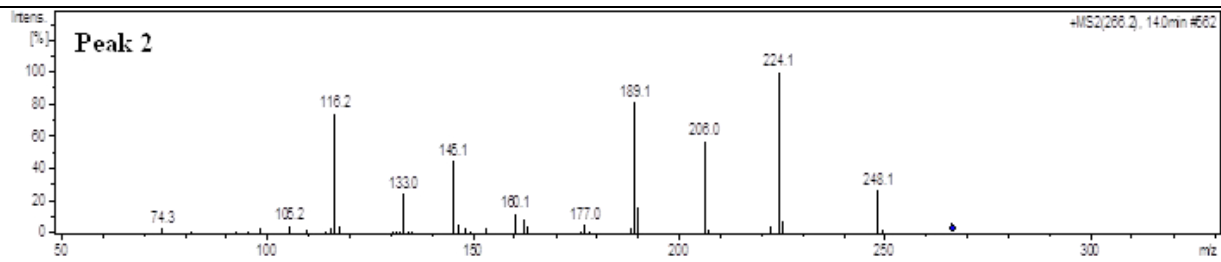
412

Fragments (m/z)	Retention time (min)	Precursor ion/Product ion	Structure	Reference
218.2	18.0	$[M+H]^+$	 <p><math>C_{13}H_{16}NO_2^+</math> Exact Mass: 218,11756</p>	MetaPC software
 <p>IPIL_100MGL_PHOTOLYSIS_TOX_AUTOMS2_18MIN.D: EIC 218.0 +All MS</p>				
$MS^2$				
 <p>+MS2(218.2), 18.0min #760</p>				
199.9		$[M+H-H_2O]^+$	 <p><math>C_{13}H_{14}NO^+</math> Exact Mass: 200,10699</p>	
183.1		$[M+H-H_2O-NH_3]^+$	 <p><math>C_{13}H_{14}O^+</math> Exact Mass: 183,08044</p>	
157.0		$[M+H-CH_2(OH)CH_2NH_2]^+$	 <p><math>C_{11}H_{10}O^+</math> Exact Mass: 157,06479</p>	
74.4		$[M+H-C_{10}H_8O]^+$	 <p><math>C_3H_8NO^+</math> Exact Mass: 74,06004</p>	

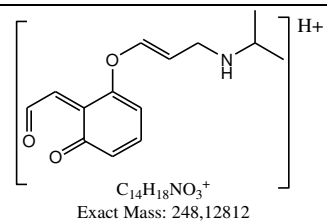
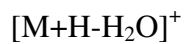
Fragments (m/z)	Retention time (min)	Precursor ion/Product ion	Structure	Reference
264.2	13.9	$[M+H]^+$	 <p> <math>C_{15}H_{22}NO_3^+</math>            Exact Mass: 264.15942         </p> <p> <math>C_{15}H_{22}NO_3^+</math>            Exact Mass: 264.15942         </p> <p> <math>C_{15}H_{22}NO_3^+</math>            Exact Mass: 264.15942         </p> <p> <math>C_{15}H_{22}NO_3^+</math>            Exact Mass: 264.15942         </p> <p> <math>C_{15}H_{22}NO_3^+</math>            Exact Mass: 264.15942         </p>	37
				
$MS^2$				
246	$[M+H-H_2O]^+$		 <p> <math>C_{15}H_{20}NO_2^+</math>            Exact Mass: 246.14886         </p>	
205	$[M+H-NHCH(CH_3)_2]^+$		 <p> <math>C_{12}H_{13}O_3^+</math>            Exact Mass: 205.08592         </p>	

184	$[M+H-H_2O-CH_2(CH_3)_2-H_2O]^+$	 <p><math>C_{12}H_{10}NO^+</math> Exact Mass: 184,07569</p>
158		 <p><math>C_8H_{16}NO_2^+</math> Exact Mass: 158,11756</p>
131	$[M+H-C_6H_{15}NO_2]^+$	 <p><math>C_9H_7O^+</math> Exact Mass: 131,04914</p>
116	$[M+H-C_9H_8O_2]^+$	 <p><math>C_6H_{14}NO^+</math> Exact Mass: 116,10699</p>
103	$[M+H-C_6H_{15}NO_2-HCHO]^+$	 <p><math>C_8H_7^+</math> Exact Mass: 103,05423</p>
98	$[M+H-C_9H_8O_2-H_2O]^+$	 <p><math>C_6H_{12}N^+</math> Exact Mass: 98,09643</p>

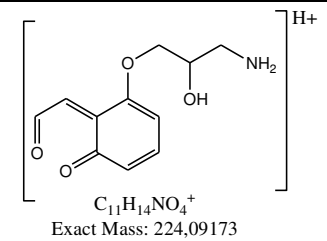
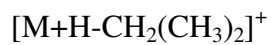
Fragments (m/z)	Retention time (min)	Precursor ion/Product ion	Structure	Reference
266.2	Multiple peaks	[M+H] <sup>+</sup>	 <p>Five chemical structures of the precursor ion [M+H]<sup>+</sup> are shown, each with the formula C<sub>14</sub>H<sub>20</sub>NO<sub>4</sub><sup>+</sup> and an exact mass of 266.13868. The structures represent different isomers of a 14-membered ring containing a hydroxyl group, a secondary amine, and a methoxy group, with varying degrees of unsaturation and ring fusion.</p>	43, 38, 42, 44
 <p>Chromatogram showing intensity versus time (min). The x-axis ranges from 0 to 30 minutes. The y-axis represents intensity. Five peaks are labeled: 1 (at ~18 min), 2 (at ~14 min), 3 (at ~14 min), 4 (at ~14 min), and 5 (at ~20 min). Peak 2 is the most prominent.</p>				
MS <sup>2</sup>				
 <p>Mass spectrum of Peak 1. The x-axis is m/z from 50 to 550. The y-axis is intensity from 0 to 100%. A single major peak is observed at m/z 248.1.</p>				

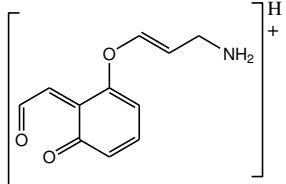
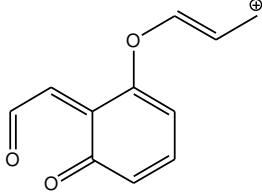
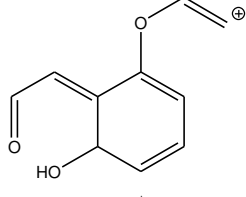
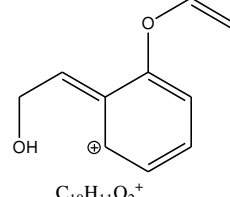
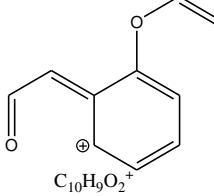
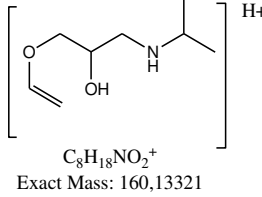


248.1

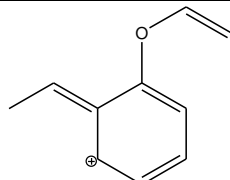
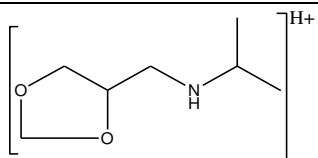
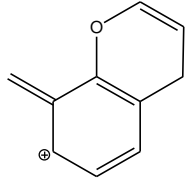
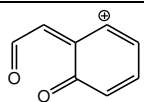
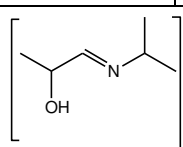
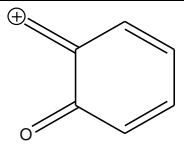
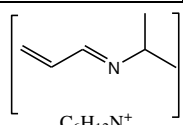


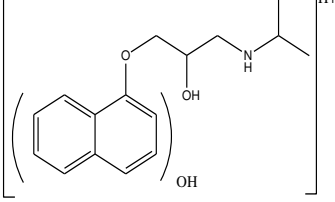
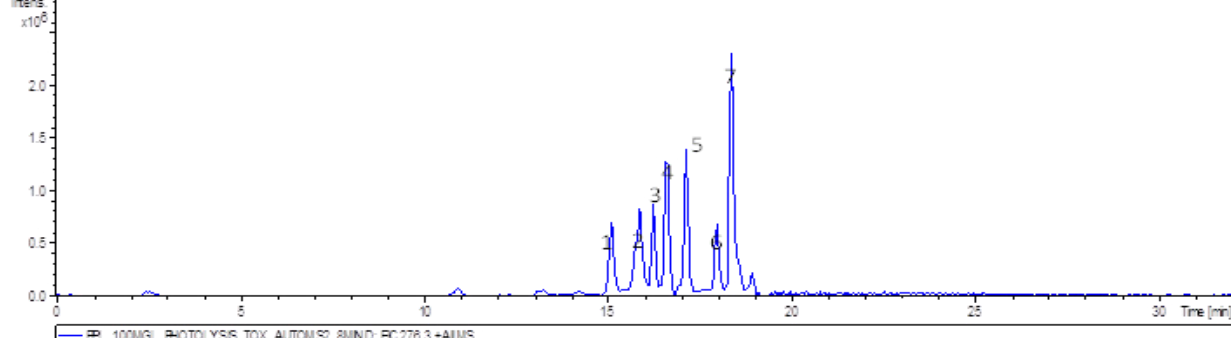
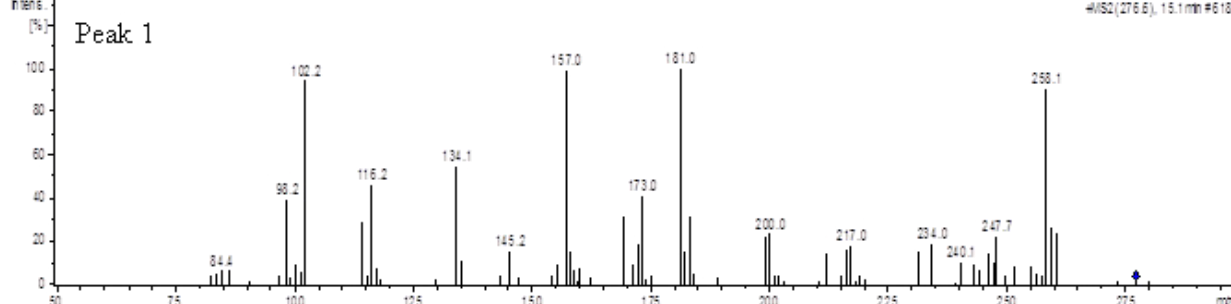
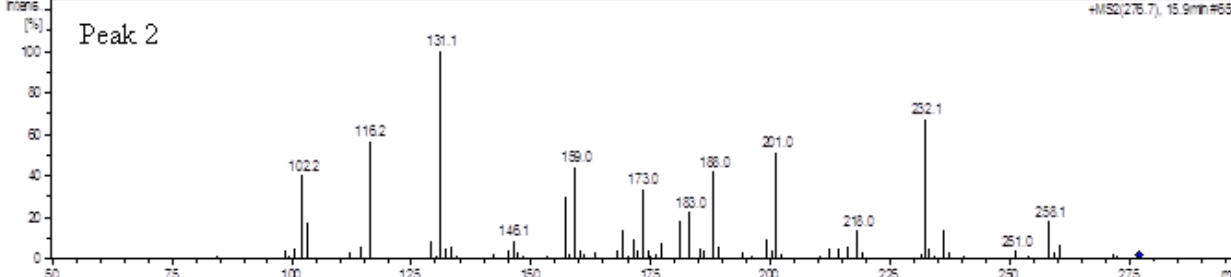
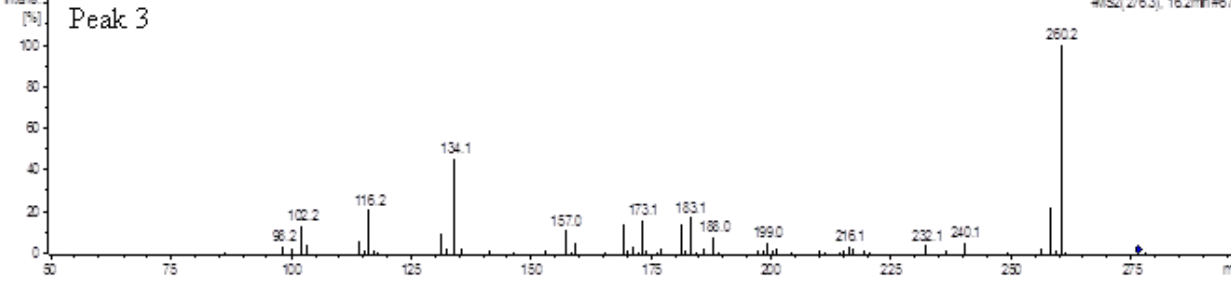
224.0

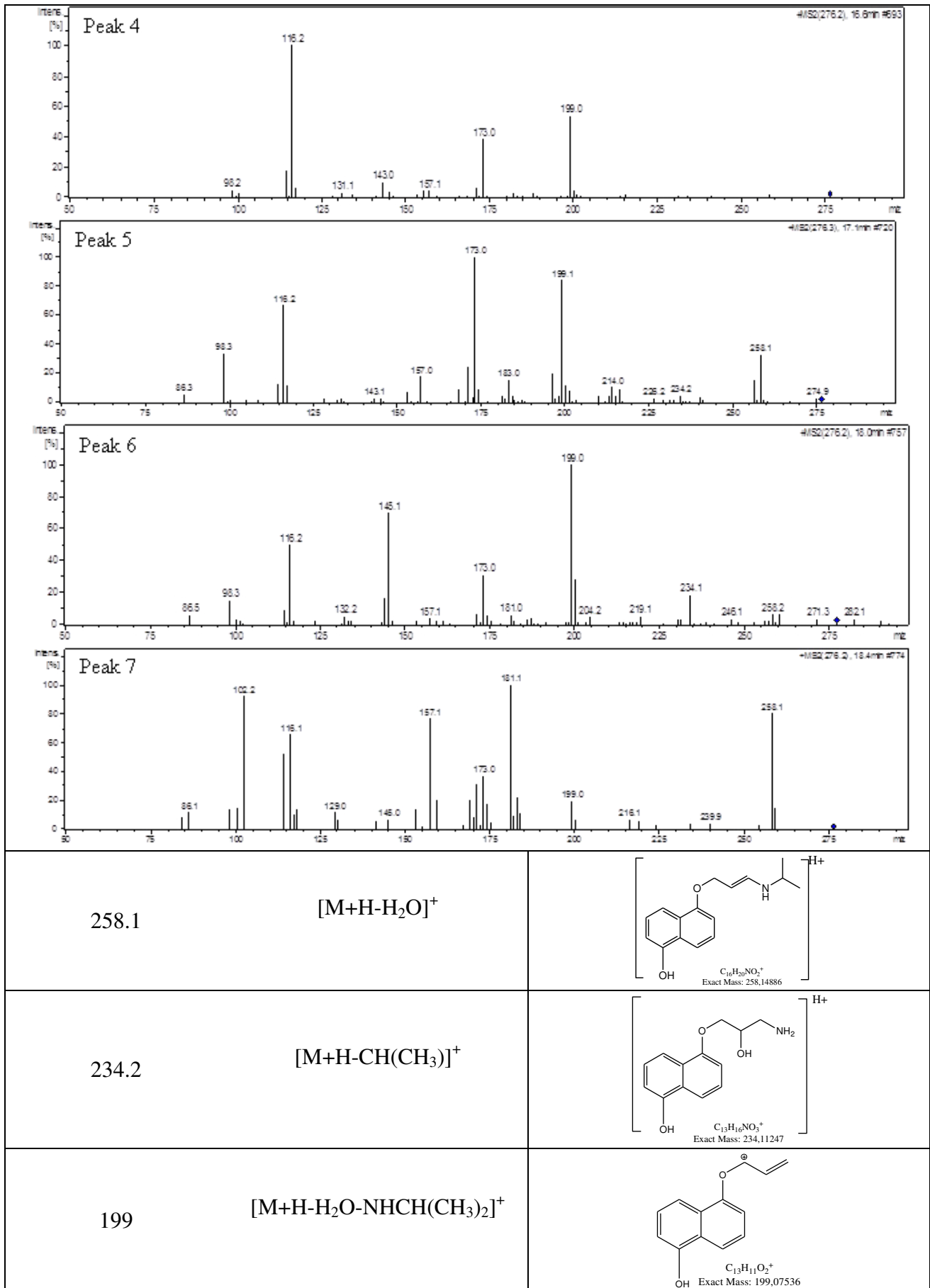


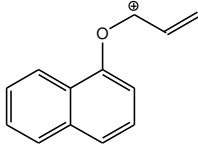
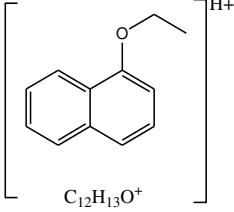
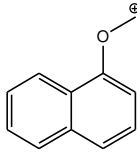
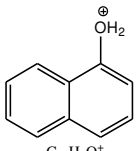
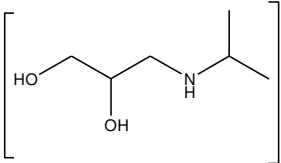
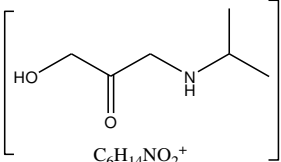
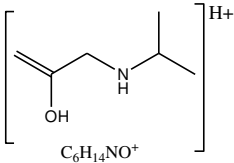
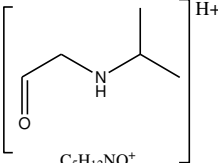
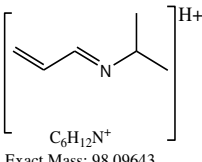
<p>206</p> <p><math>[M+H-CH_2(CH_3)_2-H_2O]^+</math></p>	 <p><math>C_{11}H_{12}NO_3^+</math> Exact Mass: 206,08117</p>
<p>189</p> <p><math>[M+H-H_2O -NHCH(CH_3)_2]^+</math></p>	 <p><math>C_{11}H_9O_3^+</math> Exact Mass: 189,05462</p>
<p>177</p> <p><math>[M+H-H_2O - CH_3NHCH(CH_3)_2]^+</math></p>	 <p><math>C_{10}H_9O_3^+</math> Exact Mass: 177,05462</p>
<p>163</p> <p><math>[M+H-H_2O - H_2O - CH_3NHCH(CH_3)_2]^+</math></p>	 <p><math>C_{10}H_{11}O_2^+</math> Exact Mass: 163,07536</p>
<p>161</p> <p>rearrangement of 163</p>	 <p><math>C_{10}H_9O_2^+</math> Exact Mass: 161,05971</p>
<p>160</p> <p><math>[M+H-C_6H_6O_2]^+</math></p>	 <p><math>C_8H_{18}NO_2^+</math> Exact Mass: 160,13321</p>

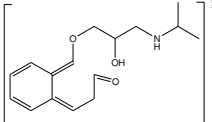
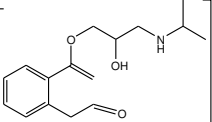
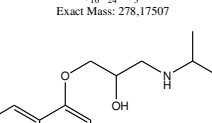
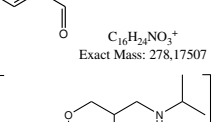
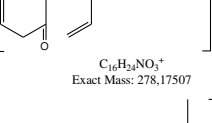
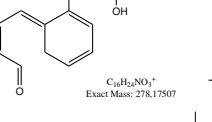
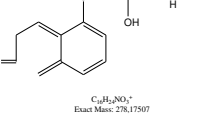
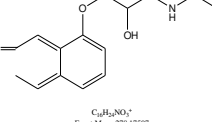
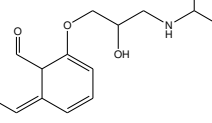
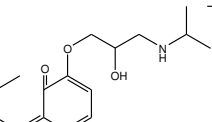


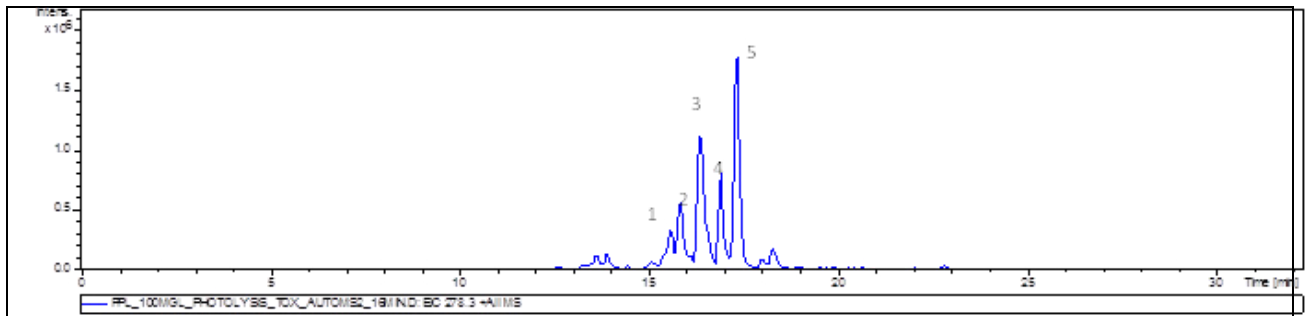
147	$[M+H-H_2O-H_2O-H_2O-CH_3NHCH(CH_3)_2]^+$	 <p><math>C_{10}H_{11}O^+</math> Exact Mass: 147,08044</p>
146	$[M+H-C_7H_8O_2]^+$	 <p><math>C_7H_{16}NO_2^+</math> Exact Mass: 146,11756</p>
145	$[M+H-H_2O-NHCH(CH_3)_2-CH_2O]^+$	 <p><math>C_{10}H_9O^+</math> Exact Mass: 145,06479</p>
133	$[M+H-C_6H_{15}NO_2]^+$	 <p><math>C_8H_5O_2^+</math> Exact Mass: 133,02841</p>
116	$[M+H-C_8H_6O_3]^+$	 <p><math>C_6H_{14}NO^+</math> Exact Mass: 116,10699</p>
105	$[M+H-C_7H_{17}NO_3]^+$	 <p><math>C_7H_5O^+</math> Exact Mass: 105,03349</p>
98	$[M+H-C_8H_8O_4]^+$	 <p><math>C_6H_{12}N^+</math> Exact Mass: 98,09643</p>

Fragments (m/z)	Retention time (min)	Precursor ion/Product ion	Structure	Reference
276.2	Multiple peaks	[M+H] <sup>+</sup>	 <p data-bbox="861 560 1053 616">C<sub>16</sub>H<sub>22</sub>NO<sub>3</sub><sup>+</sup> Exact Mass: 276,15942</p>	47, 40, 44
 <p data-bbox="231 974 654 996">PL_100MG_PHTOLYSIS_TOX_AUTOM_SE_8MIND_EC276.3+AIMS</p>				
<b>MS<sup>2</sup></b>				
 <p data-bbox="247 1064 327 1097">Peak 1</p> <p data-bbox="1268 1041 1412 1064">#MS2(276.6), 15.1min#618</p>				
 <p data-bbox="247 1384 327 1417">Peak 2</p> <p data-bbox="1268 1361 1412 1384">#MS2(276.7), 15.9min#656</p>				
 <p data-bbox="247 1682 327 1715">Peak 3</p> <p data-bbox="1268 1659 1412 1682">#MS2(276.3), 16.2min#672</p>				

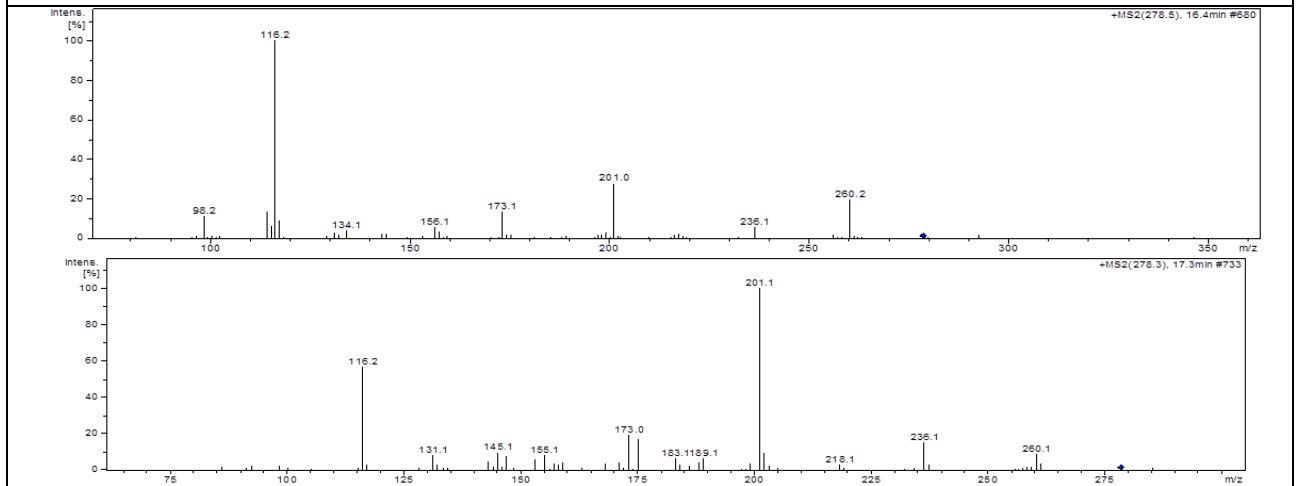


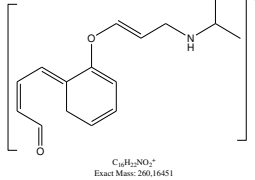
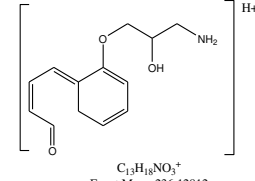
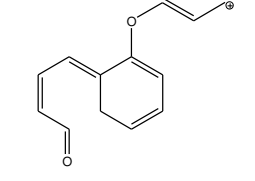
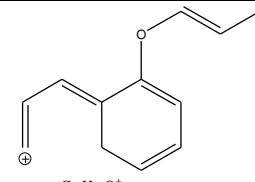
183	$[M+H-H_2O-H_2O-NHCH(CH_3)_2]^+$	 <p><math>C_{13}H_{11}O^+</math> Exact Mass: 183,08044</p>
173	$[M+H-H_2O-H_2O-NHCH(CH_3)_2]^+$	 <p><math>C_{12}H_{13}O^+</math> Exact Mass: 173,09609</p>
157	$[M+H-H_2O-H_2O-NHCH(CH_3)_2-C_2H_6]^+$	 <p><math>C_{11}H_9O^+</math> Exact Mass: 157,06479</p>
145	$[M+H-H_2O-H_2O-NHCH(CH_3)_2-C_2H_6-CH_3]^+$	 <p><math>C_{10}H_9O^+</math> Exact Mass: 145,06479</p>
134	$[M+H-C_{10}H_5O]^+$	 <p><math>C_6H_{16}NO_2^+</math> Exact Mass: 134,11756</p>
132	$[M+H-C_{10}H_7O]^+$	 <p><math>C_6H_{14}NO_2^+</math> Exact Mass: 132,10191</p>
116.2	$[M+H-C_{10}H_7O-H_2O]^+$	 <p><math>C_6H_{14}NO^+</math> Exact Mass: 116,10699</p>
102.2	$[M+H-C_{10}H_7O-H_2O-CH_3]^+$	 <p><math>C_5H_{12}NO^+</math> Exact Mass: 102,09134</p>
98.2	$[M+H-C_{10}H_7O-H_2O-CH_3-H_2O]^+$	 <p><math>C_6H_{12}N^+</math> Exact Mass: 98,09643</p>

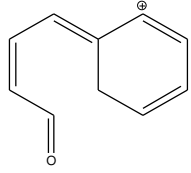
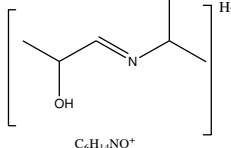
Fragments (m/z)	Retention time (min)	Precursor ion/ Product ion	Structure	Reference
278.3	Multiple peaks	[M+H] <sup>+</sup>	 <p><math>C_{16}H_{22}NO_3^+</math> Exact Mass: 278.17507</p>	MetaPC software
			 <p><math>C_{16}H_{22}NO_3^+</math> Exact Mass: 278.17507</p>	
			 <p><math>C_{16}H_{24}NO_3^+</math> Exact Mass: 278.17507</p>	
			 <p><math>C_{16}H_{24}NO_3^+</math> Exact Mass: 278.17507</p>	
			 <p><math>C_{16}H_{22}NO_3^+</math> Exact Mass: 278.17507</p>	
			 <p><math>C_{16}H_{22}NO_3^+</math> Exact Mass: 278.17507</p>	
			 <p><math>C_{16}H_{22}NO_3^+</math> Exact Mass: 278.17507</p>	
			 <p><math>C_{16}H_{22}NO_3^+</math> Exact Mass: 278.17507</p>	
			 <p><math>C_{16}H_{22}NO_3^+</math> Exact Mass: 278.17507</p>	
 <p><math>C_{16}H_{22}NO_3^+</math> Exact Mass: 278.17507</p>				



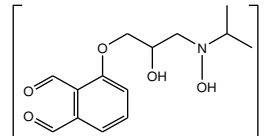
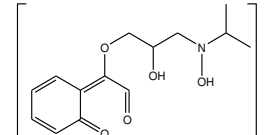
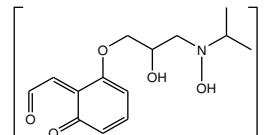
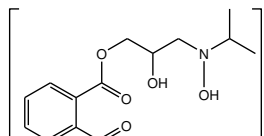
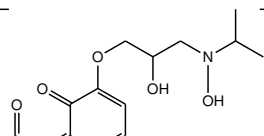
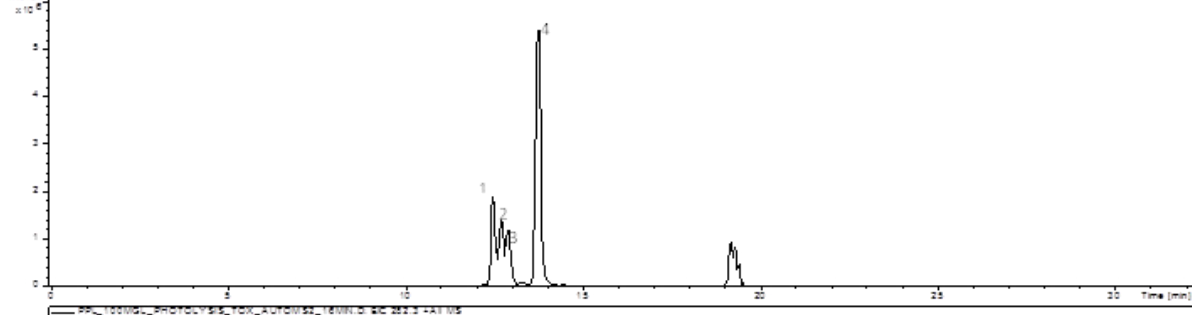
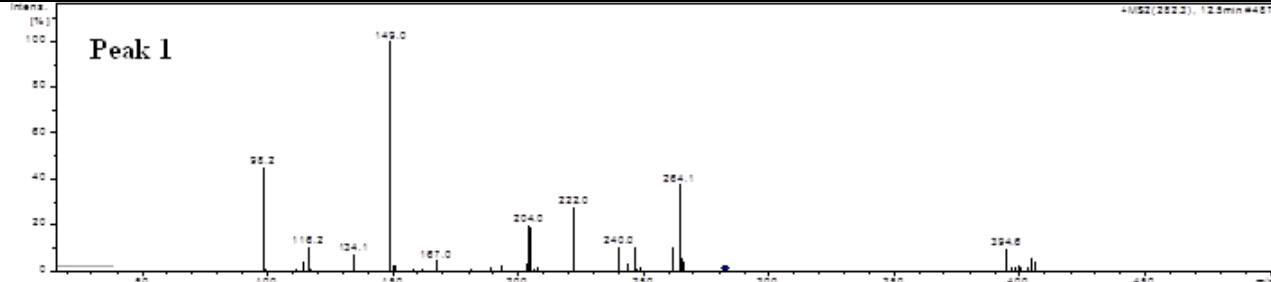
MS<sup>2</sup>



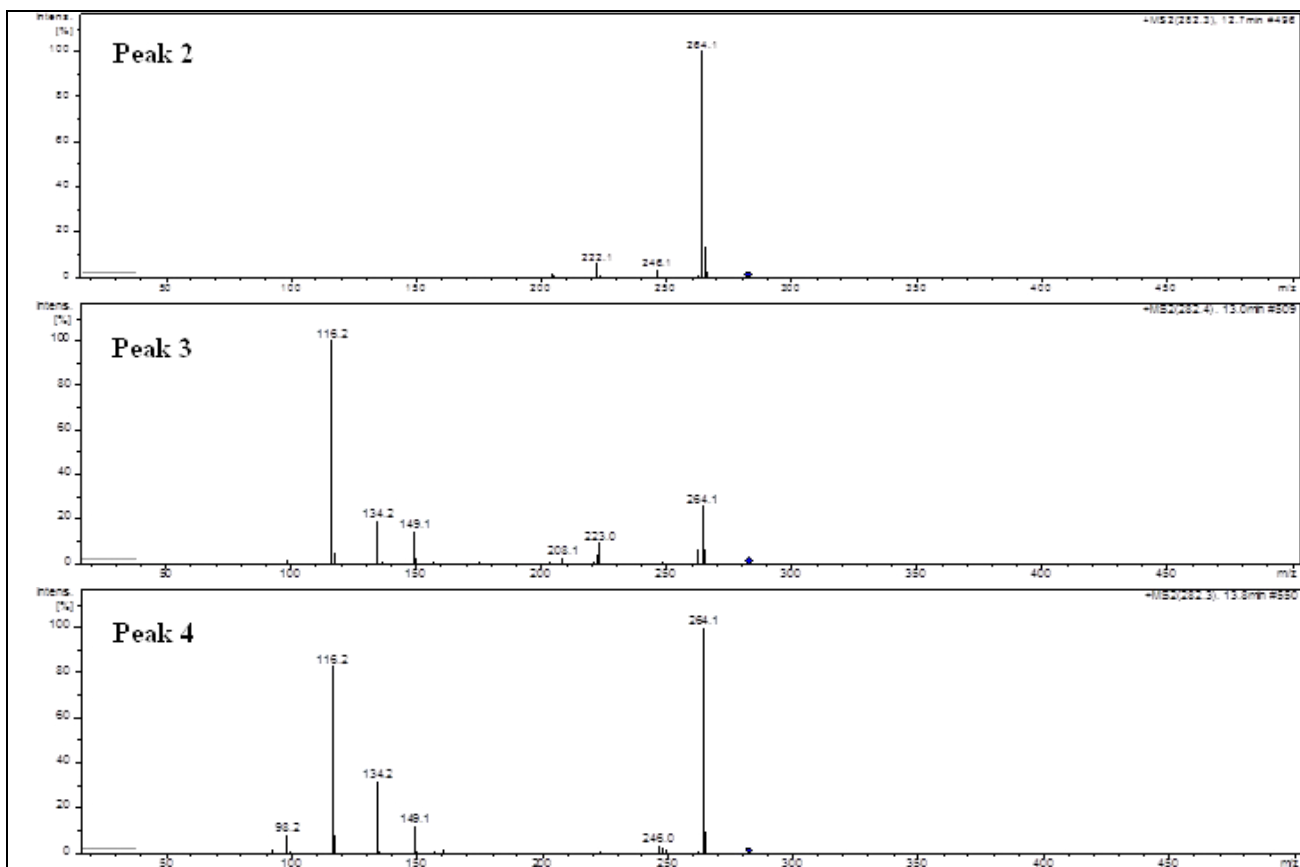
<p>260</p> <p><math>[M+H-H_2O]^+</math></p>	 <p><math>C_{10}H_{15}NO_2^+</math> Exact Mass: 260.10451</p>
<p>236</p> <p><math>[M+H-CH(CH_3)_2]^+</math></p>	 <p><math>C_{13}H_{18}NO_2^+</math> Exact Mass: 236.12812</p>
<p>201</p> <p><math>[M+H-H_2O-NHCH_2(CH_3)_2]^+</math></p>	 <p><math>C_{13}H_{13}O_2^+</math> Exact Mass: 201.09101</p>
<p>173</p> <p><math>[M+H-H_2O-NHCH_2(CH_3)_2 - HCHO]^+</math></p>	 <p><math>C_{12}H_{13}O^+</math> Exact Mass: 173.09609</p>

<p>145</p> <p><math>[M+H-C_6H_{15}NO_2]^+</math></p>	 <p><math>C_{10}H_9O^+</math> Exact Mass: 145.06479</p>
<p>116.2</p> <p><math>[M+H-C_{10}H_{10}O_2]^+</math></p>	 <p><math>C_6H_{14}NO^+</math> Exact Mass: 116.10699</p>

421

Fragments (m/z)	Retention time (min)	Precursor ion/Product ion	Structure	Reference
282.2	Multiple peaks	[M+H] <sup>+</sup>	<div style="display: flex; flex-direction: column; align-items: center;"> <div style="text-align: center;">  <p><math>C_{14}H_{20}NO_5^+</math> Exact Mass: 282,1336</p> </div> <div style="text-align: center;">  <p><math>C_{14}H_{20}NO_5^+</math> Exact Mass: 282,1336</p> </div> <div style="text-align: center;">  <p><math>C_{14}H_{20}NO_5^+</math> Exact Mass: 282,1336</p> </div> <div style="text-align: center;">  <p><math>C_{14}H_{20}NO_5^+</math> Exact Mass: 282,1336</p> </div> <div style="text-align: center;">  <p><math>C_{14}H_{20}NO_5^+</math> Exact Mass: 282,1336</p> </div> </div>	43, 38, 42, 44
				
<b>MS<sup>2</sup></b>				
				

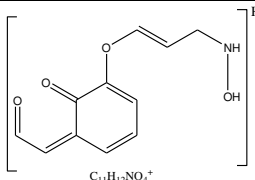
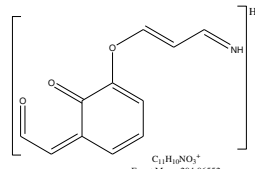
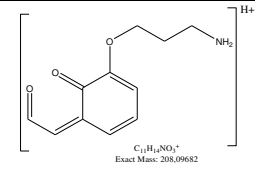
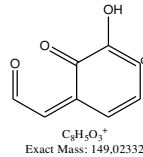
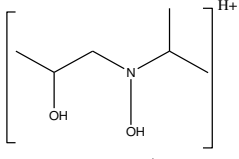
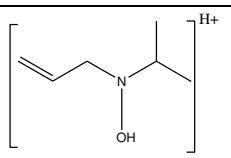
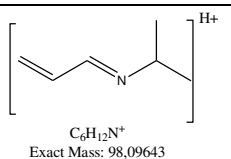


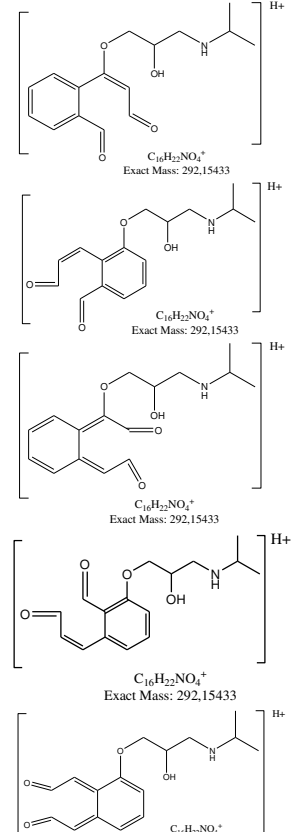
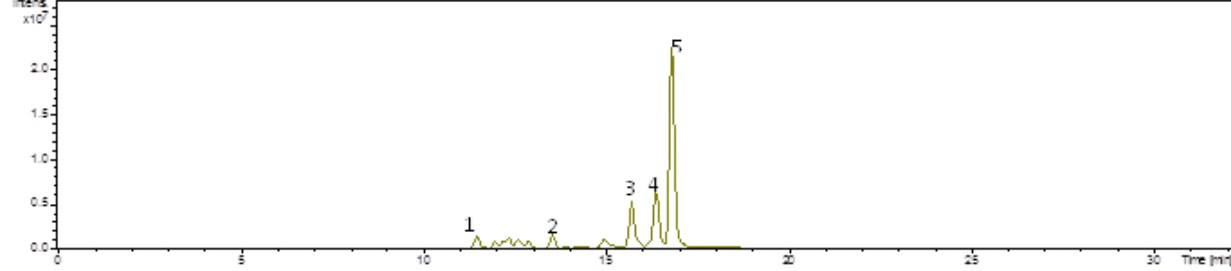
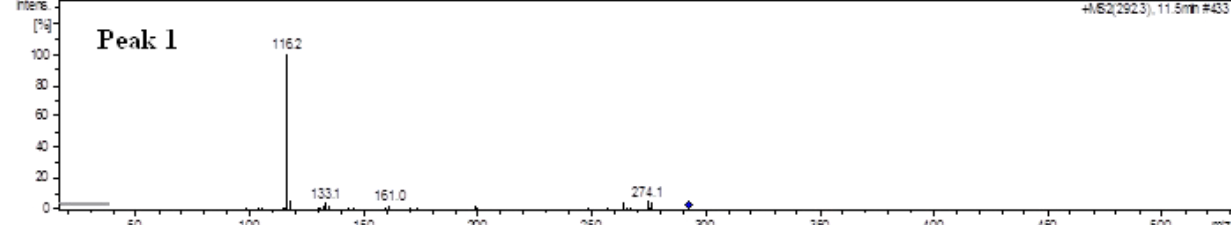
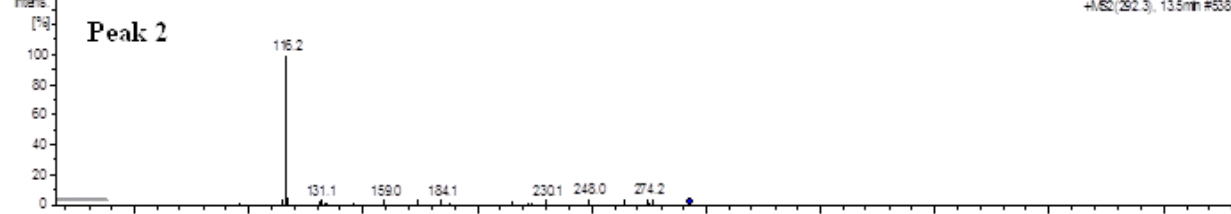


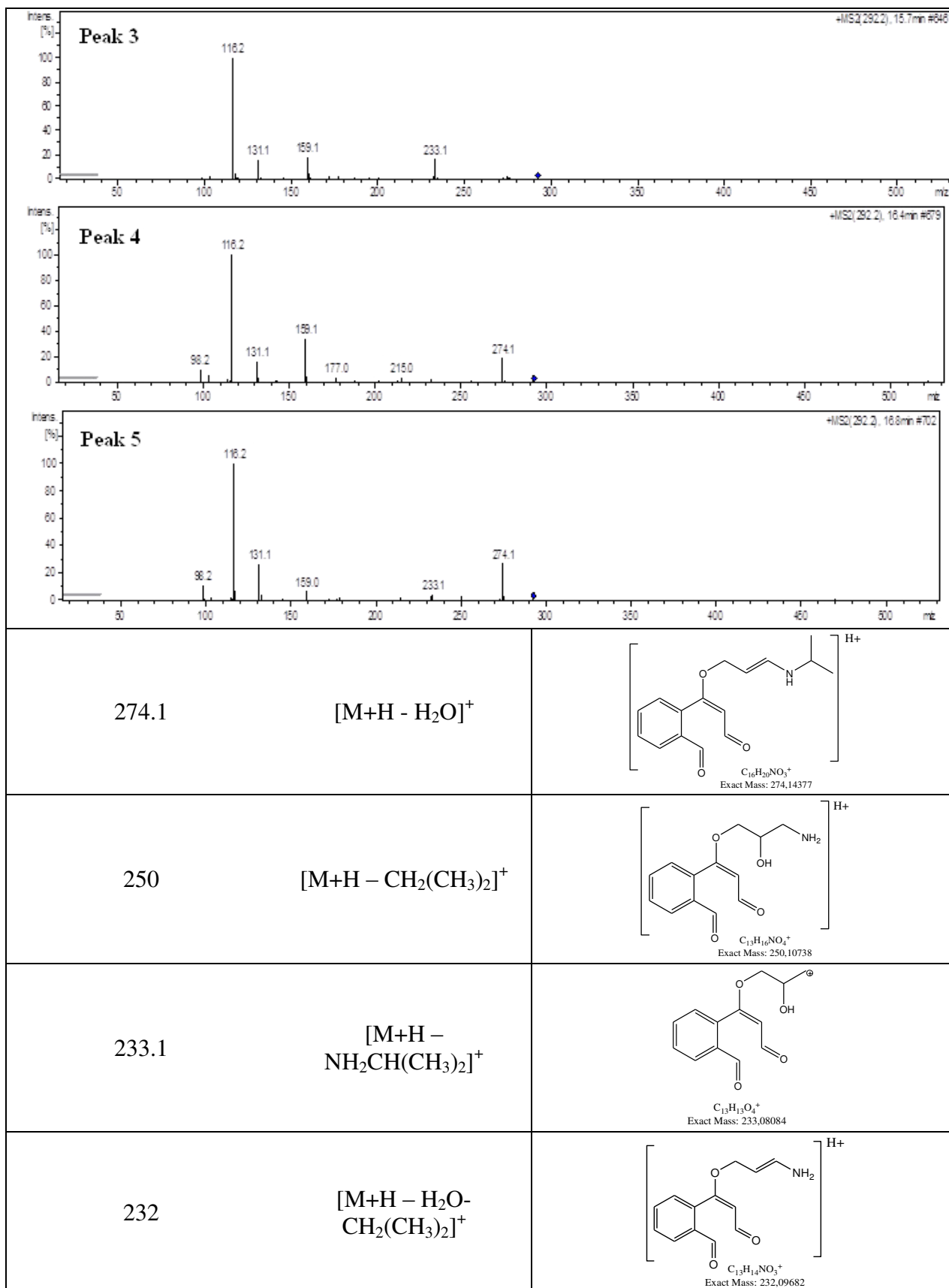
Peak5

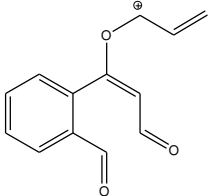
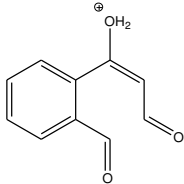
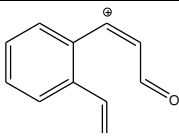
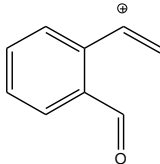
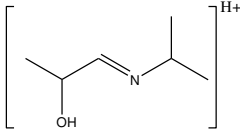
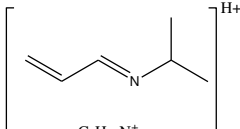
The MS2 for this peak cannot be extracted as the signal from m/z 260 interferes with this signal.

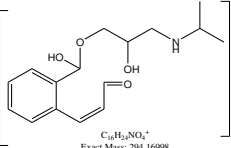
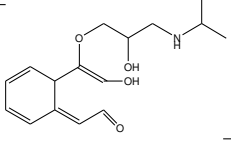
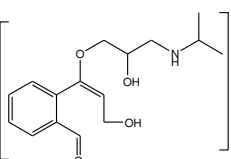
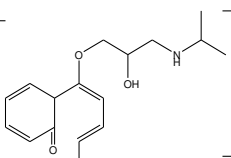
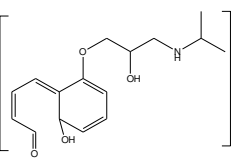
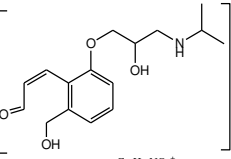
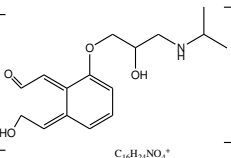
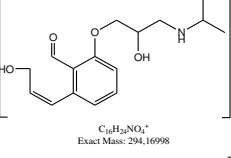
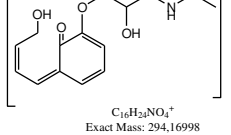
264.1	$[M+H-H_2O]^+$	<p><math>C_{14}H_{16}NO_2^+</math> Exact Mass: 264.12303</p>
246.0	$[M+H-H_2O-H_2O]^+$	<p><math>C_{14}H_{16}NO_3^+</math> Exact Mass: 246.11247</p>
240.0	$[M+H-CH_2(CH_3)_2]^+$	<p><math>C_{11}H_{14}NO_3^+</math> Exact Mass: 240.08665</p>
223.0	rearrangement of 222.1	<p><math>C_{11}H_{14}O_3^+</math> Exact Mass: 223.0601</p>

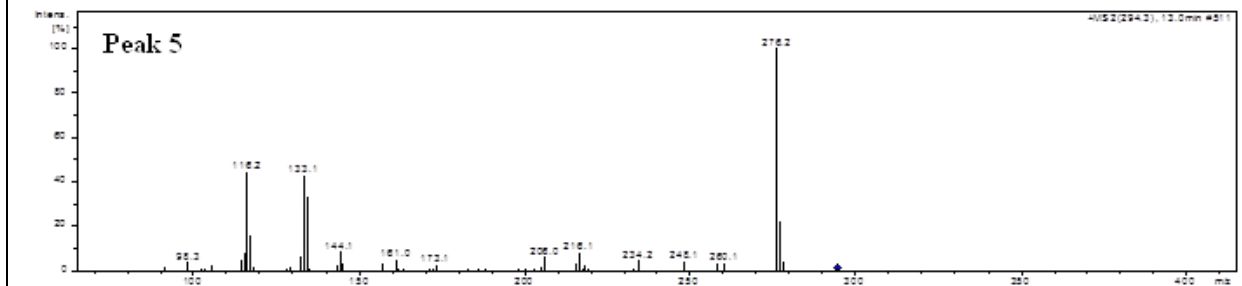
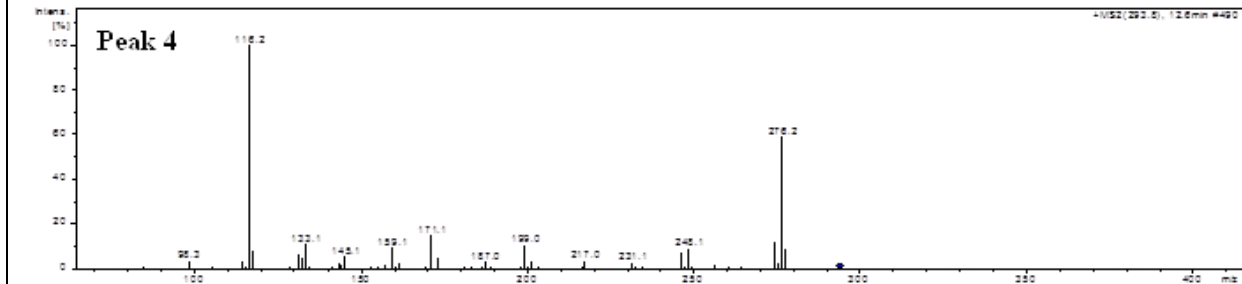
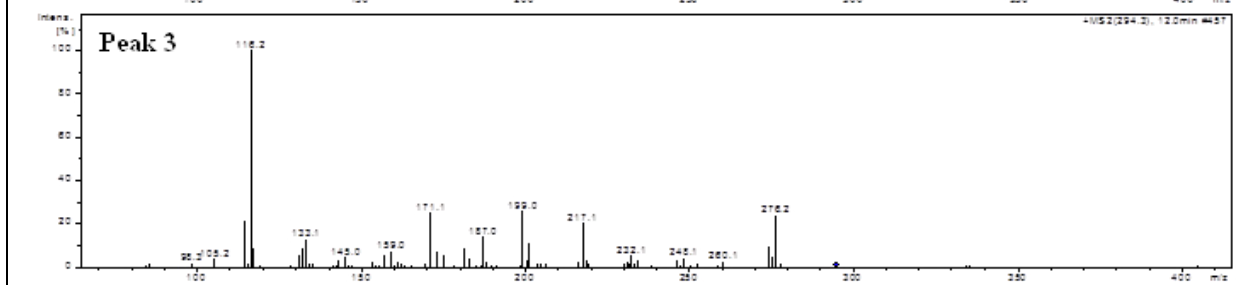
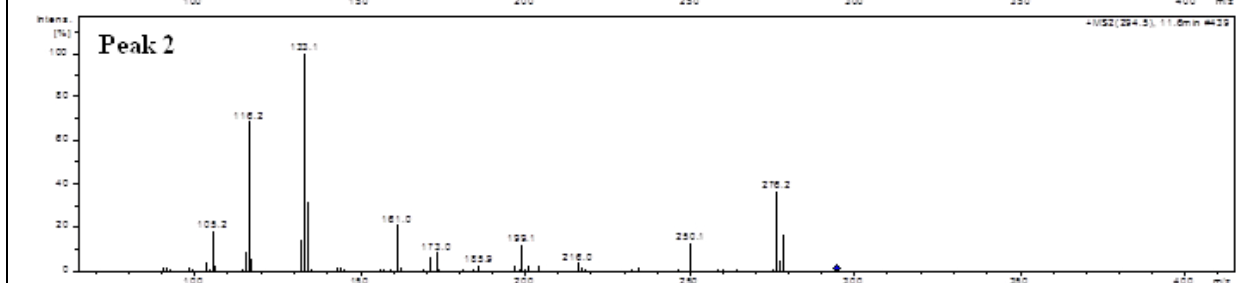
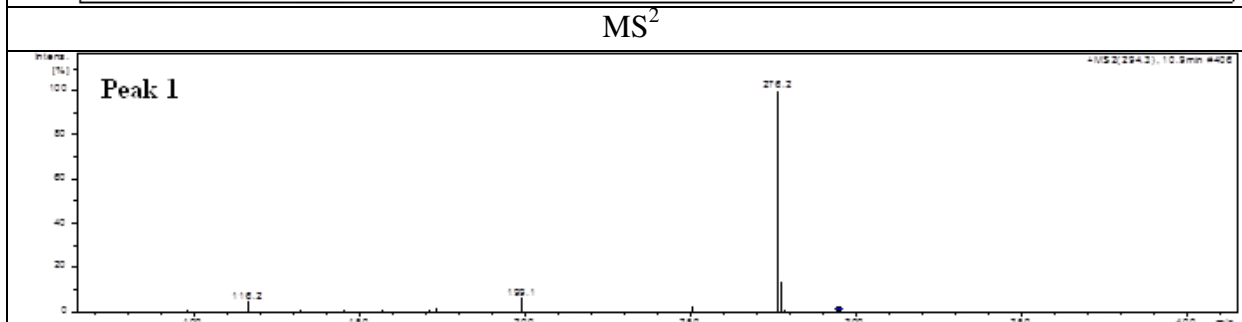
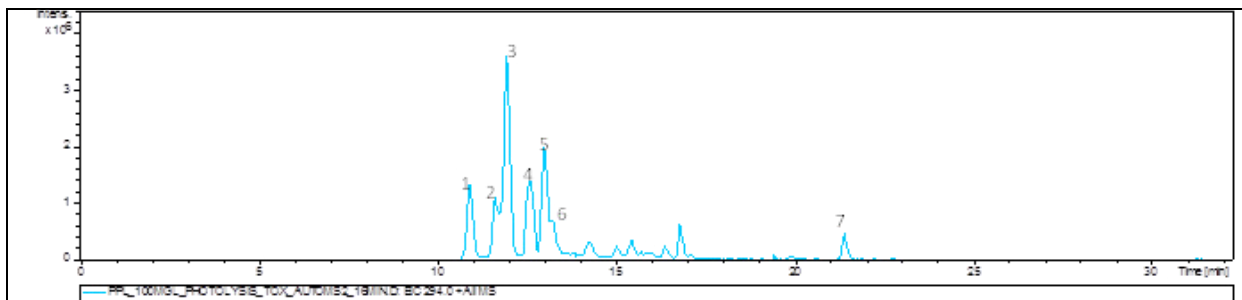
222.1	$[M+H-H_2O-CH_2(CH_3)_2]^+$	 <p><math>C_{11}H_{12}NO_4^+</math> Exact Mass: 222.07608</p>
204.0	$[M+H-H_2O-H_2O-CH_2(CH_3)_2]^+$	 <p><math>C_{11}H_{10}NO_3^+</math> Exact Mass: 204.06552</p>
208.1	rearrangement of 204	 <p><math>C_{11}H_{12}NO_4^+</math> Exact Mass: 208.09682</p>
149.1	$[M+H-C_6H_{15}NO_2]^+$	 <p><math>C_8H_9O_3^+</math> Exact Mass: 149.02332</p>
134.2	$[M+H-C_8H_6O_3]^+$	 <p><math>C_6H_{16}NO_2^+</math> Exact Mass: 134.11756</p>
116.2	$[M+H-C_8H_6O_3-H_2O]^+$	 <p><math>C_6H_{14}NO^+</math> Exact Mass: 116.10699</p>
98.2	$[M+H-C_8H_6O_3-H_2O-H_2O]^+$	 <p><math>C_6H_{12}N^+</math> Exact Mass: 98.09643</p>

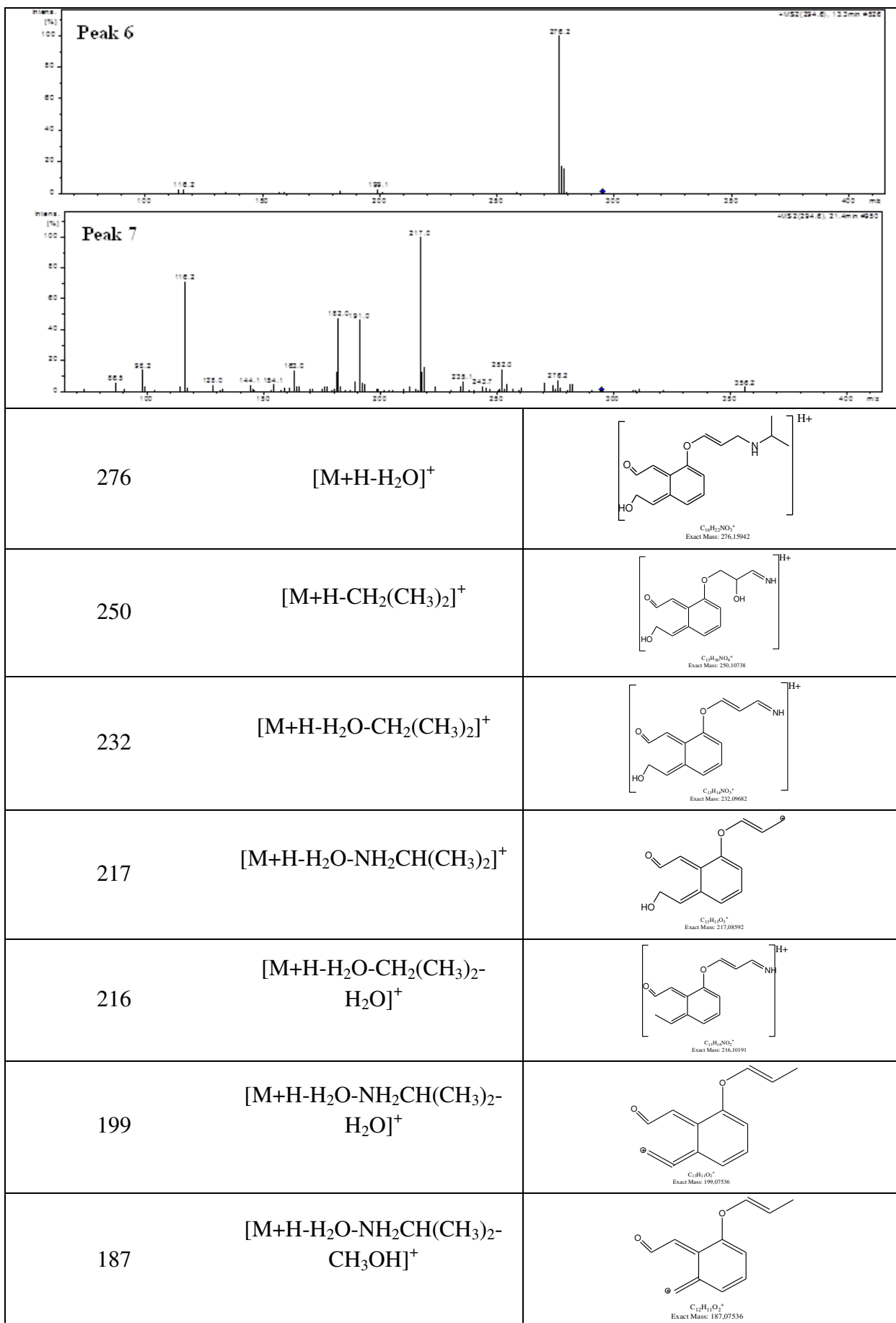
Fragments (m/z)	Retention time (min)	Precursor ion/Product ion	Structure	Reference
292.2	Multiple Peaks	[M+H] <sup>+</sup>	 <p> <chem>C16H22NO4+</chem>                      Exact Mass: 292.15433                 </p>	43, 38, 42, 44, 37
				
MS2				
 <p>Peak 1</p>				
 <p>Peak 2</p>				



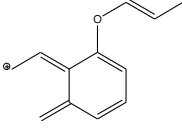
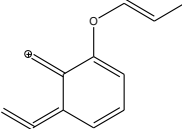
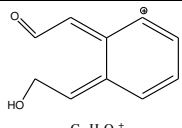
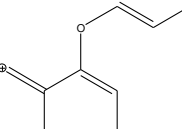
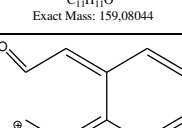
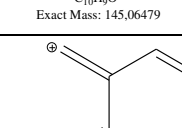
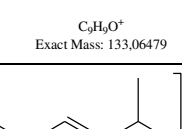
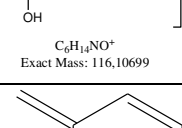
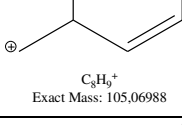
215.0	$[M+H - H_2O-NH_2CH(CH_3)_2]^+$	 <p><math>C_{13}H_{11}O_3^+</math> Exact Mass: 215.07027</p>
177.0	$[M+H - CH_3CH(OH)CH_2NHC(H)(CH_3)_2]^+$	 <p><math>C_{10}H_9O_3^+</math> Exact Mass: 177.05462</p>
159.0	$[M+H - CH_3CH(OH)CH_2NHC(H)(CH_3)_2 - H_2O]^+$	 <p><math>C_{10}H_7O_2^+</math> Exact Mass: 159.04406</p>
131.1	$[M+H - CH_3CH(OH)CH_2NHC(H)(CH_3)_2 - H_2O - HCHO]^+$	 <p><math>C_9H_7O^+</math> Exact Mass: 131.04914</p>
116.2	$[M+H-C_{10}H_{10}O_3]^+$	 <p><math>C_6H_{14}NO^+</math> Exact Mass: 116.10699</p>
98.2	$[M+H-C_{10}H_{10}O_3-H_2O]^+$	 <p><math>C_6H_{12}N^+</math> Exact Mass: 98.09643</p>

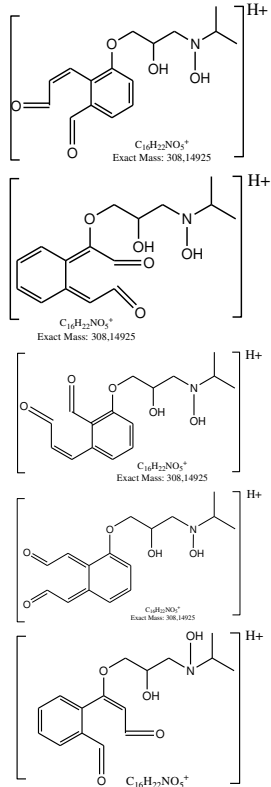
Fragments (m/z)	Retention time (min)	Precursor ion/Product ion	Structure	Reference
294	Multiple peaks	[M+H] <sup>+</sup>	 <p><math>C_{16}H_{22}NO_4^+</math> Exact Mass: 294,16998</p>	44
			 <p><math>C_{16}H_{22}NO_4^+</math> Exact Mass: 294,16998</p>	
			 <p><math>C_{16}H_{22}NO_4^+</math> Exact Mass: 294,16998</p>	
			 <p><math>C_{16}H_{22}NO_4^+</math> Exact Mass: 294,16998</p>	
			 <p><math>C_{16}H_{22}NO_4^+</math> Exact Mass: 294,16998</p>	
			 <p><math>C_{16}H_{22}NO_4^+</math> Exact Mass: 294,16998</p>	
			 <p><math>C_{16}H_{22}NO_4^+</math> Exact Mass: 294,16998</p>	
			 <p><math>C_{16}H_{22}NO_4^+</math> Exact Mass: 294,16998</p>	
			 <p><math>C_{16}H_{22}NO_4^+</math> Exact Mass: 294,16998</p>	

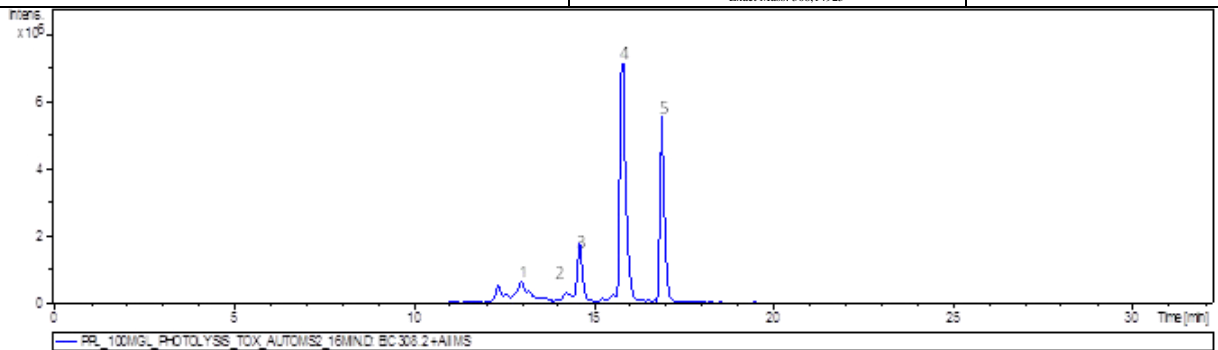






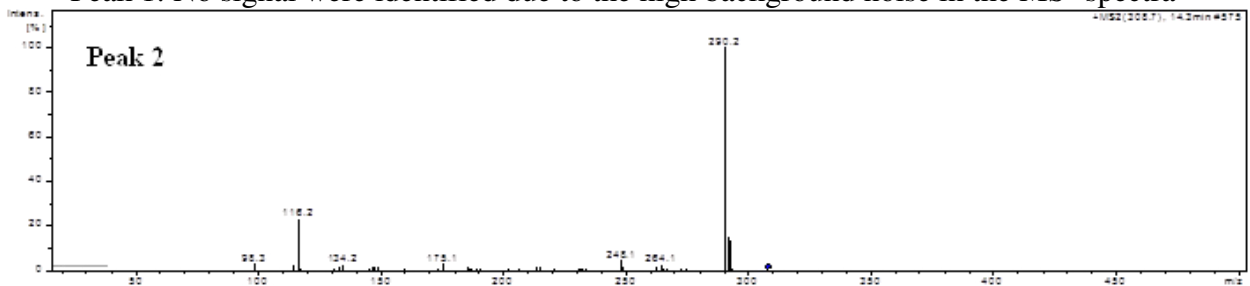
173	$[M+H-H_2O-NH_2CH(CH_3)_2-CH_3OH-H_2O]^+$	 <p><math>C_{12}H_{13}O^+</math> Exact Mass: 173.09609</p>
171	$[M+H-H_2O-NH_2CH(CH_3)_2-H_2O-HCHO]^+$	 <p><math>C_{12}H_{11}O^+</math> Exact Mass: 171.08044</p>
161	$[M+H-C_6H_{15}NO_2]^+$	 <p><math>C_{10}H_9O_2^+</math> Exact Mass: 161.05971</p>
159	$[M+H-H_2O-NH_2CH(CH_3)_2-CH_3OH-HCHO]^+$	 <p><math>C_{11}H_{11}O^+</math> Exact Mass: 159.08044</p>
145	$[M+H-C_6H_{15}NO_2-H_2O]^+$	 <p><math>C_{10}H_9O^+</math> Exact Mass: 145.06479</p>
133	$[M+H-C_6H_{15}NO_2-HCHO]^+$	 <p><math>C_9H_9O^+</math> Exact Mass: 133.06479</p>
116	$[M+H-C_{10}H_{10}O_3]^+$	 <p><math>C_6H_{14}NO^+</math> Exact Mass: 116.10699</p>
105	$[M+H-C_6H_{15}NO_2-HCHO-CH_3OH]^+$	 <p><math>C_8H_9^+</math> Exact Mass: 105.06988</p>
98	$[M+H-C_{10}H_{10}O_3-H_2O]^+$	 <p><math>C_6H_{12}N^+</math> Exact Mass: 98.09643</p>

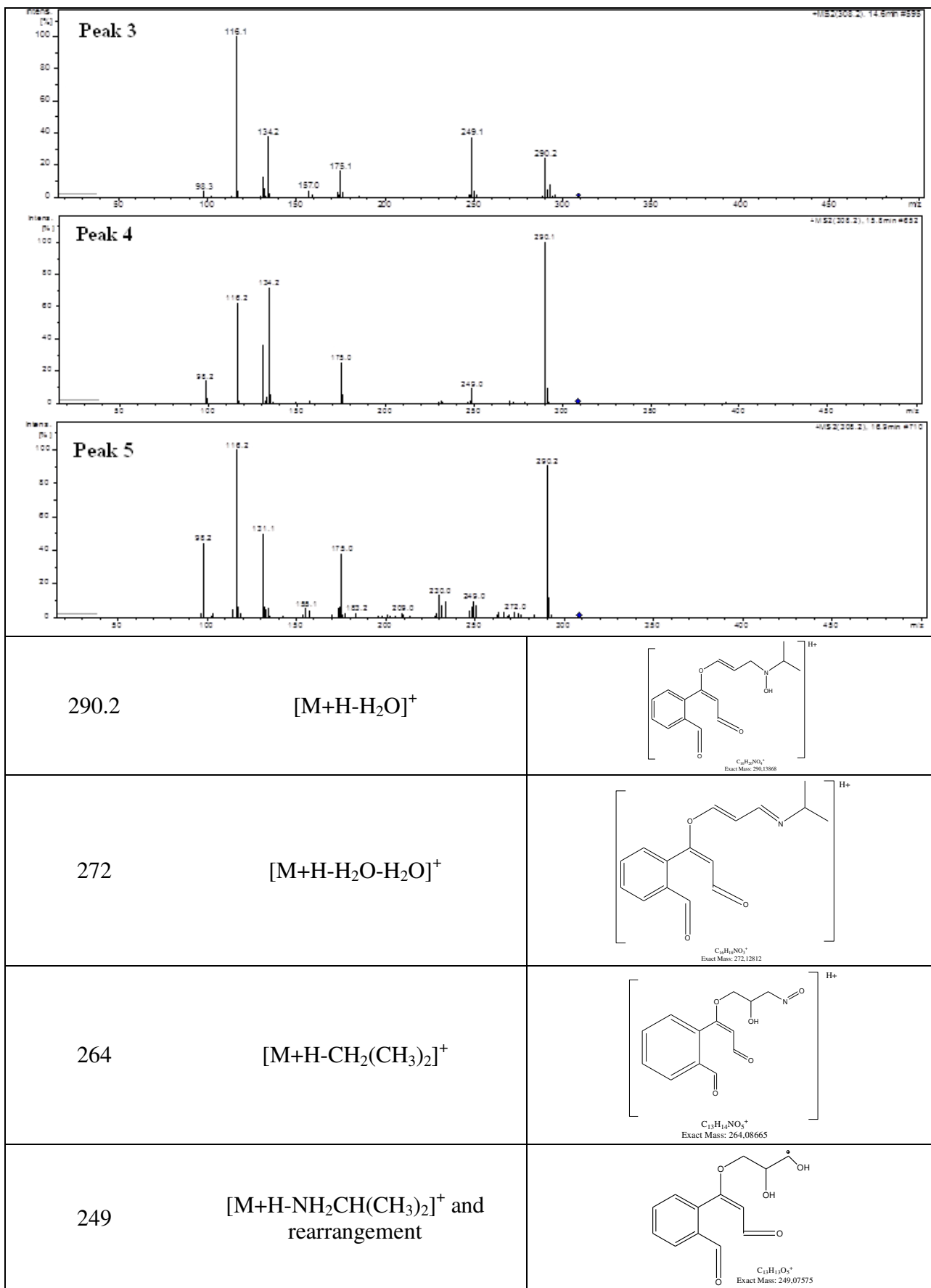
Fragments (m/z)	Retention time (min)	Precursor ion/Product ion	Structure	Reference
308.2	Multiple peaks	[M+H] <sup>+</sup>	 <p> <chem>C18H22NO3+</chem>                      Exact Mass: 308.14925                 </p>	38, 42, 44

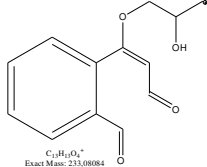
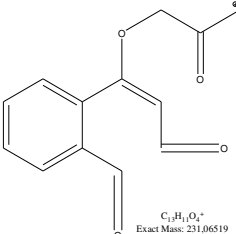
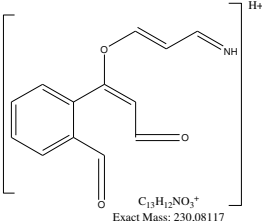
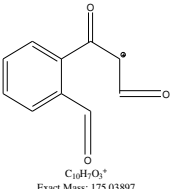
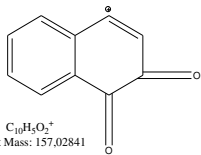
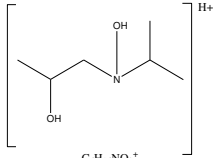
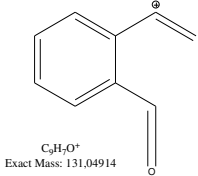
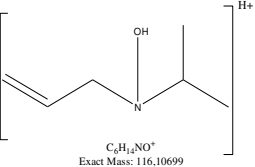
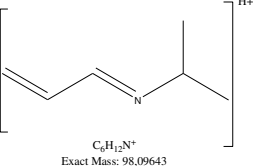


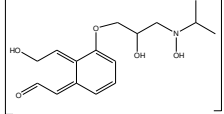
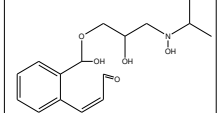
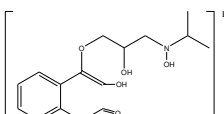
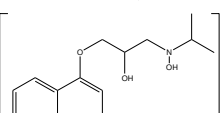
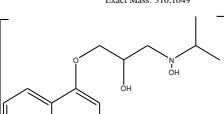
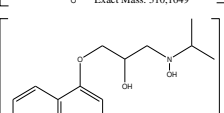
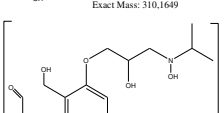
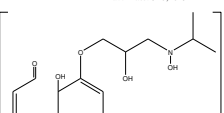
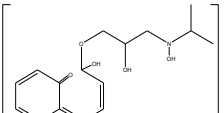
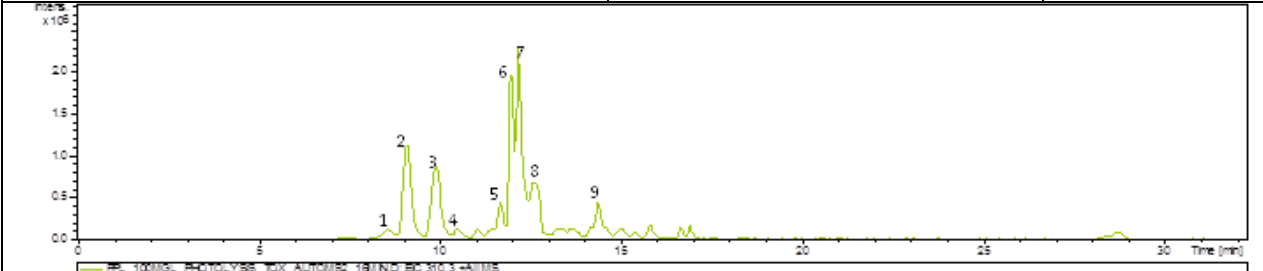
MS2

Peak 1: No signal were identified due to the high background noise in the MS<sup>2</sup> spectra

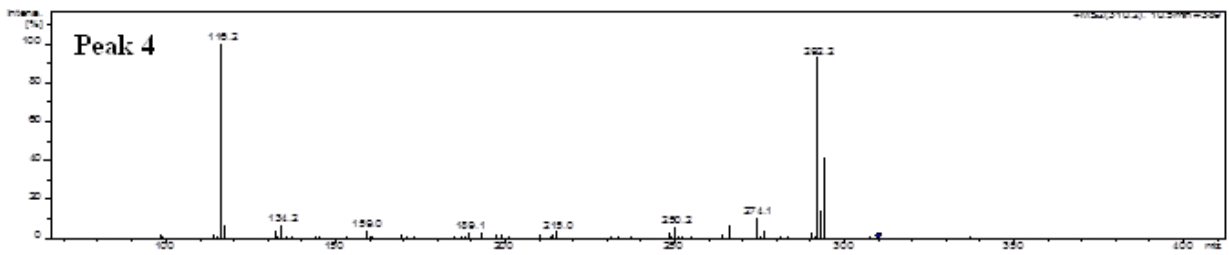
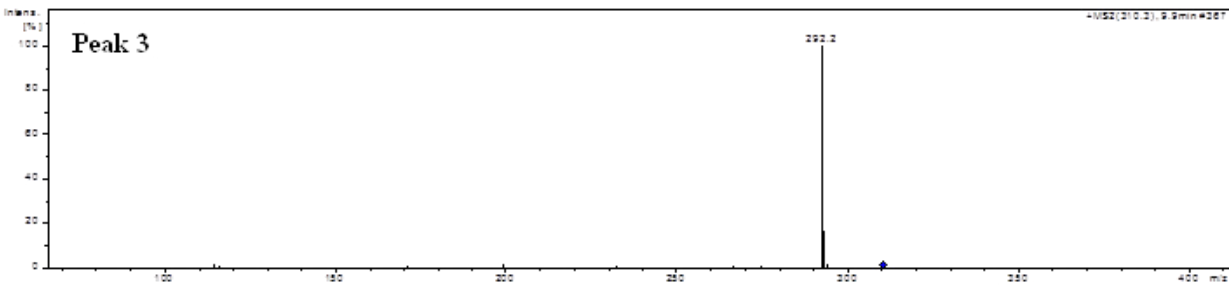
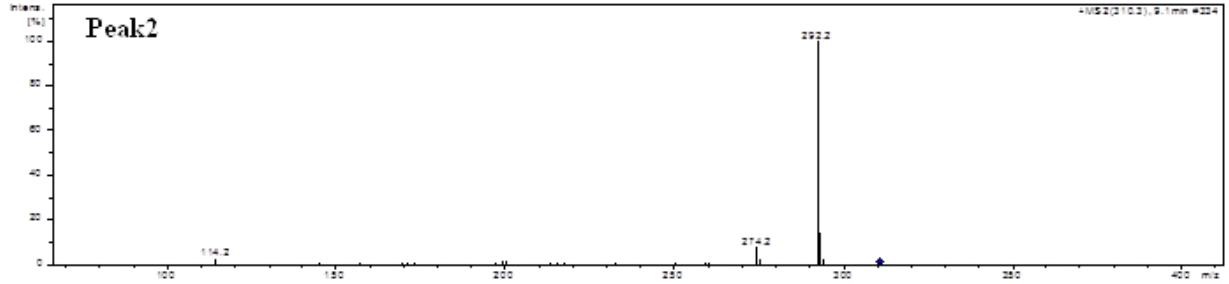
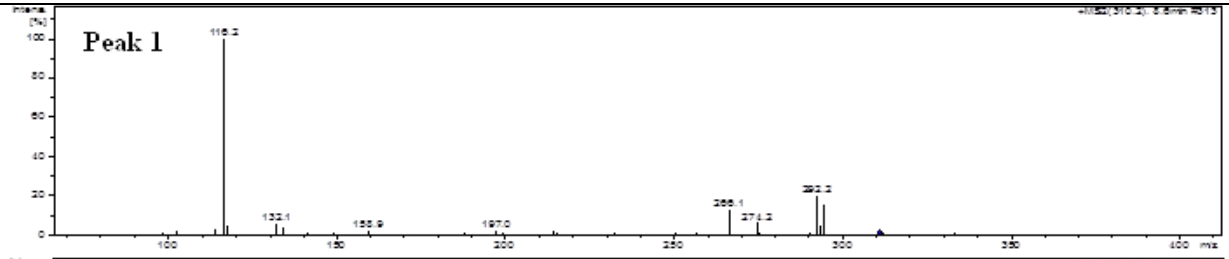




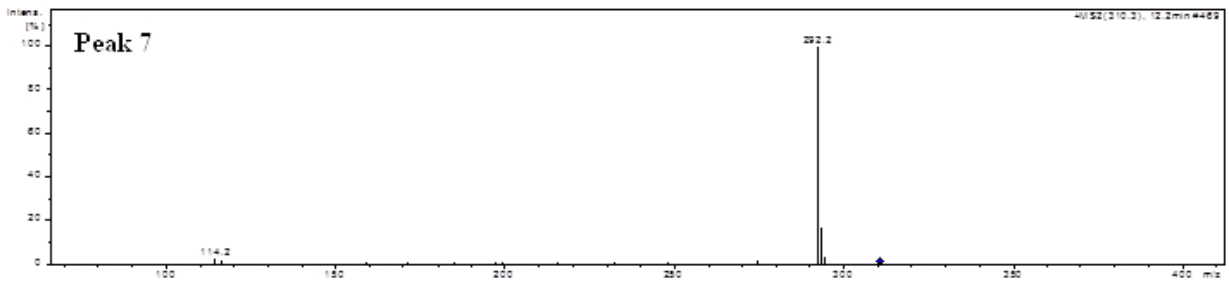
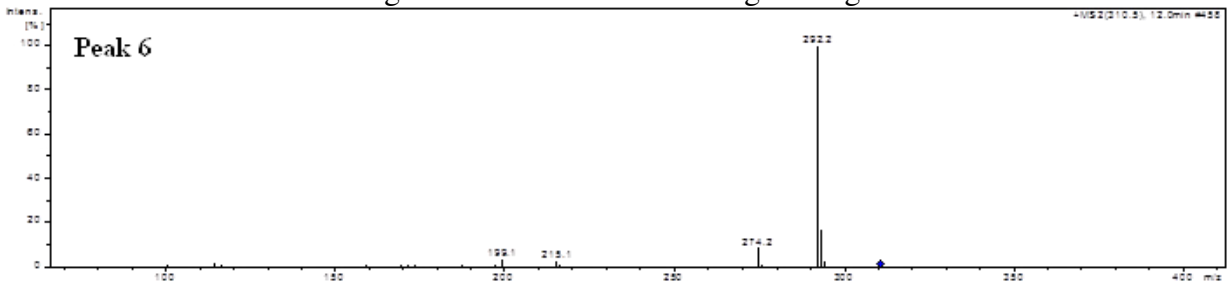
233	$[M+H-N(OH)CH(CH_3)_2]^+$	 <p><math>C_{13}H_{15}O_4^+</math> Exact Mass: 233.0884</p>
231	rearrangement of 233	 <p><math>C_{13}H_{15}O_3^+</math> Exact Mass: 231.06519</p>
230	$[M+H-H_2O-H_2O-CH_2(CH_3)_2]^+$	 <p><math>C_{13}H_{12}NO_3^+</math> Exact Mass: 230.08117</p>
175	$[M+H-C_6H_{15}NO_2]^+$	 <p><math>C_{10}H_9O_3^+</math> Exact Mass: 175.03897</p>
157	$[M+H-C_6H_{15}NO_2-H_2O]^+$	 <p><math>C_{10}H_9O_2^+</math> Exact Mass: 157.02841</p>
134	$[M+H-C_{10}H_8O_3]^+$	 <p><math>C_6H_{16}NO_2^+</math> Exact Mass: 134.11756</p>
131	$[M+H-C_6H_{15}NO_2-H_2O-HCHO]^+$	 <p><math>C_8H_9O^+</math> Exact Mass: 131.04914</p>
116.2	$[M+H-C_{10}H_8O_3-H_2O]^+$	 <p><math>C_6H_{14}NO^+</math> Exact Mass: 116.10699</p>
98.2	$[M+H-C_{10}H_8O_3-H_2O-H_2O]^+$	 <p><math>C_6H_{12}N^+</math> Exact Mass: 98.09643</p>

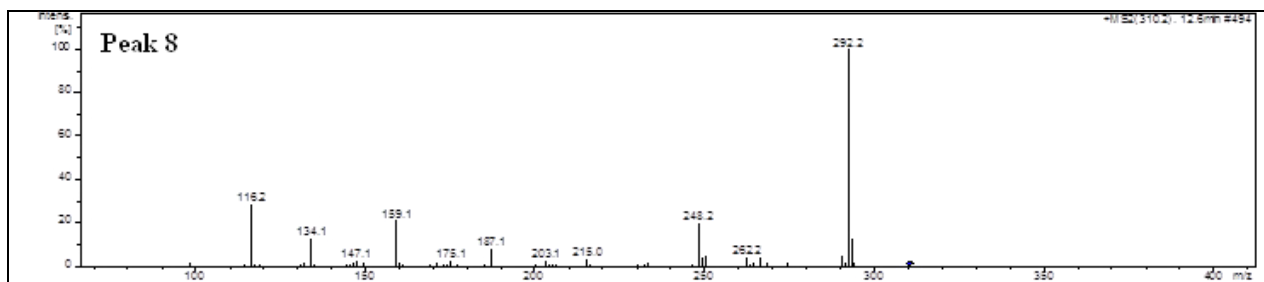
Fragments (m/z)	Retention time (min)	Precursor ion/Product ion	Structure	Reference
310.2	Multiple peaks	[M+H] <sup>+</sup>	<div style="display: flex; flex-direction: column; align-items: center;"> <div style="text-align: center;">  <p><math>C_{16}H_{22}NO_5^+</math> Exact Mass: 310,1649</p> </div> <div style="text-align: center;">  <p><math>C_{16}H_{22}NO_5^+</math> Exact Mass: 310,1649</p> </div> <div style="text-align: center;">  <p><math>C_{16}H_{22}NO_5^+</math> Exact Mass: 310,1649</p> </div> <div style="text-align: center;">  <p><math>C_{16}H_{22}NO_5^+</math> Exact Mass: 310,1649</p> </div> <div style="text-align: center;">  <p><math>C_{16}H_{22}NO_5^+</math> Exact Mass: 310,1649</p> </div> <div style="text-align: center;">  <p><math>C_{16}H_{22}NO_5^+</math> Exact Mass: 310,1649</p> </div> <div style="text-align: center;">  <p><math>C_{16}H_{22}NO_5^+</math> Exact Mass: 310,1649</p> </div> <div style="text-align: center;">  <p><math>C_{16}H_{22}NO_5^+</math> Exact Mass: 310,1649</p> </div> <div style="text-align: center;">  <p><math>C_{16}H_{22}NO_5^+</math> Exact Mass: 310,1649</p> </div> </div>	44
				

# MS<sup>2</sup>



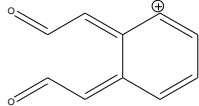
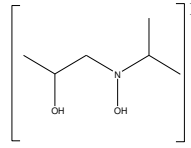
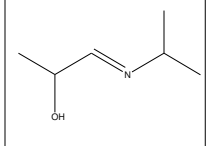
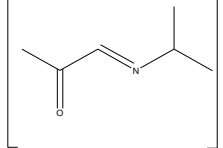
Peak 5: No signal were detected due to high background noise





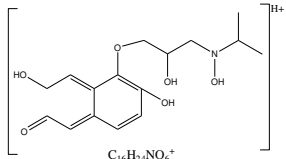
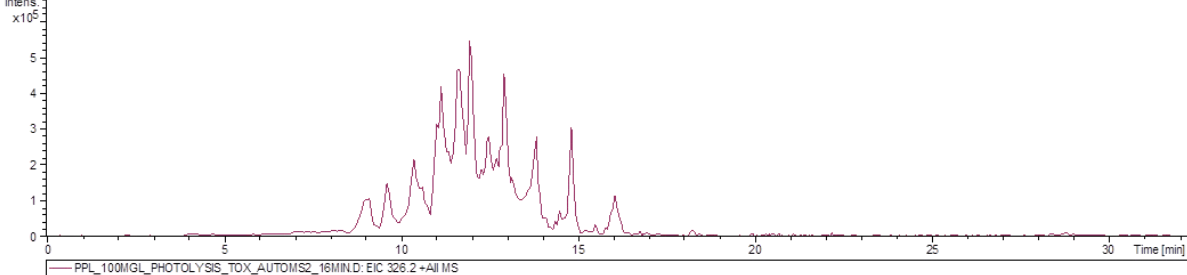
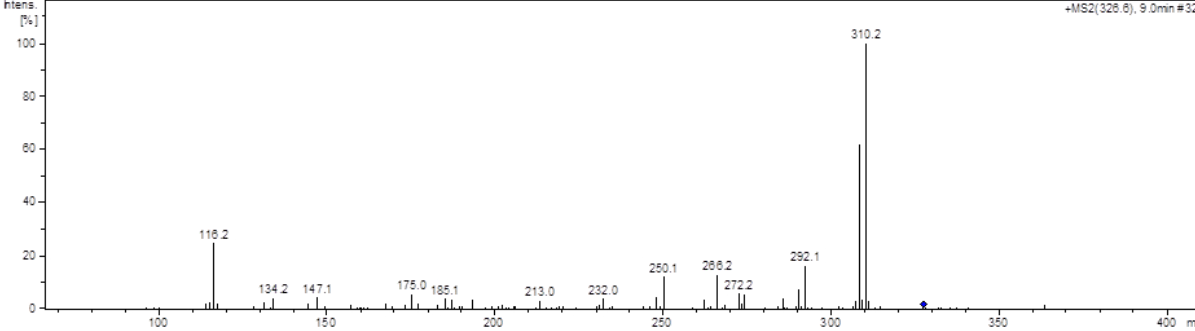
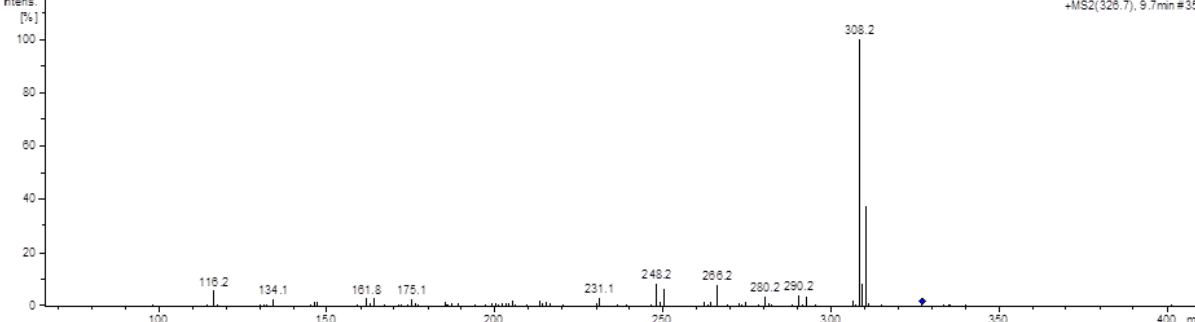
Peak 9: No signal were detected due to high background noise

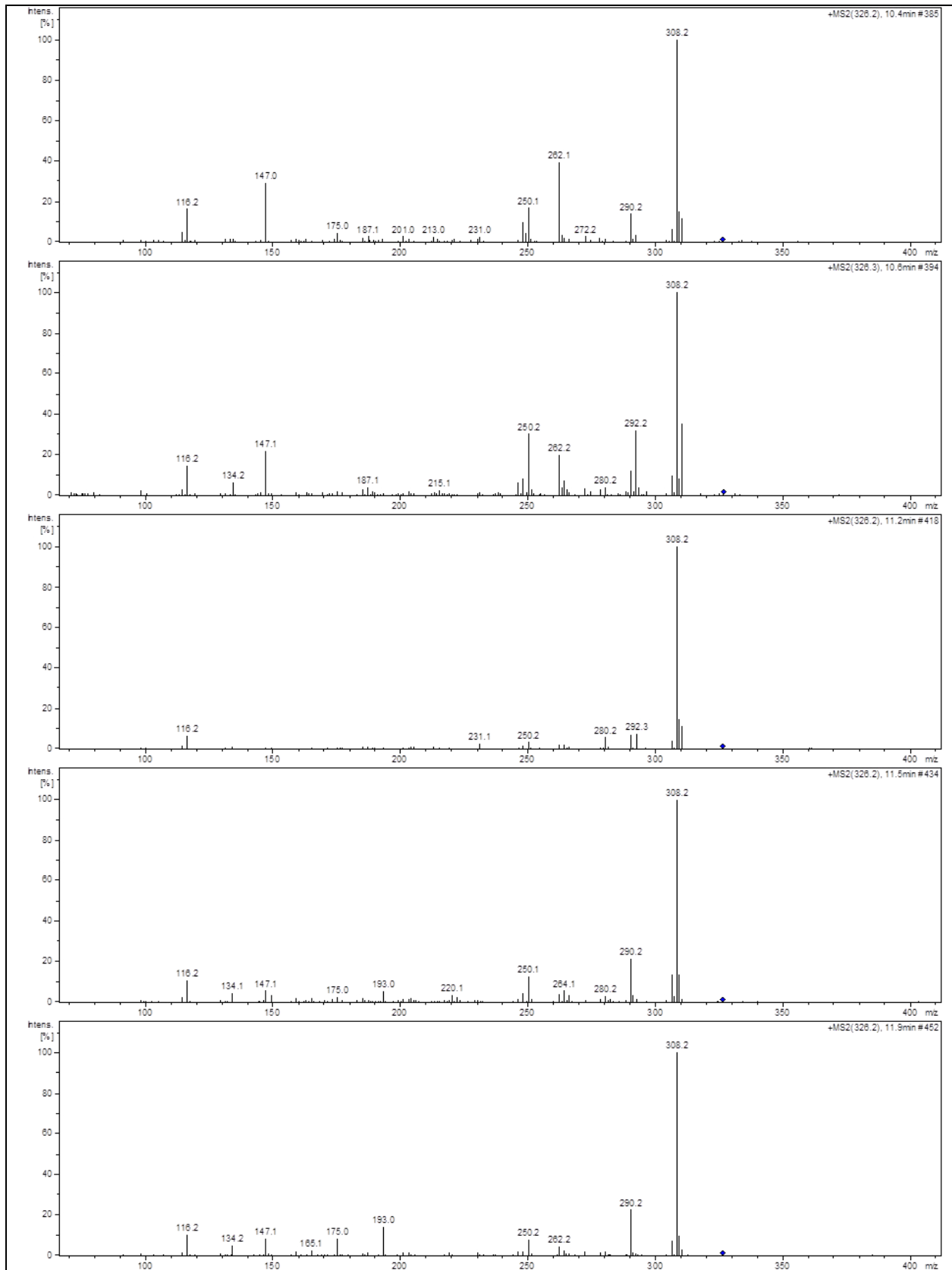
292	$[M+H-H_2O]^+$	<p><math>C_{16}H_{22}NO_3^+</math> Exact Mass: 292.15433</p>
274	$[M+H-H_2O-H_2O]^+$	<p><math>C_{16}H_{20}NO_3^+</math> Exact Mass: 274.14377</p>
266	$[M+H-CH_2(CH_3)_2]^+$	<p><math>C_{13}H_{16}NO_5^+</math> Exact Mass: 266.1023</p>
248	$[M+H-CH_2(CH_3)_2-H_2O]^+$	<p><math>C_{13}H_{14}NO_4^+</math> Exact Mass: 248.09173</p>
215	$[M+H-NH(OH)CH(CH_3)_2-H_2O]^+$	<p><math>C_{13}H_{11}O_3^+</math> Exact Mass: 215.07027</p>
199	$[M+H-NH(OH)CH(CH_3)_2-H_2O-H_2O]^+$	<p><math>C_{13}H_{11}O_2^+</math> Exact Mass: 199.07536</p>
187	$[M+H-CH_3N(OH)CH(CH_3)_2-H_2O-H_2O]^+$	<p><math>C_{12}H_9O_2^+</math> Exact Mass: 187.07536</p>

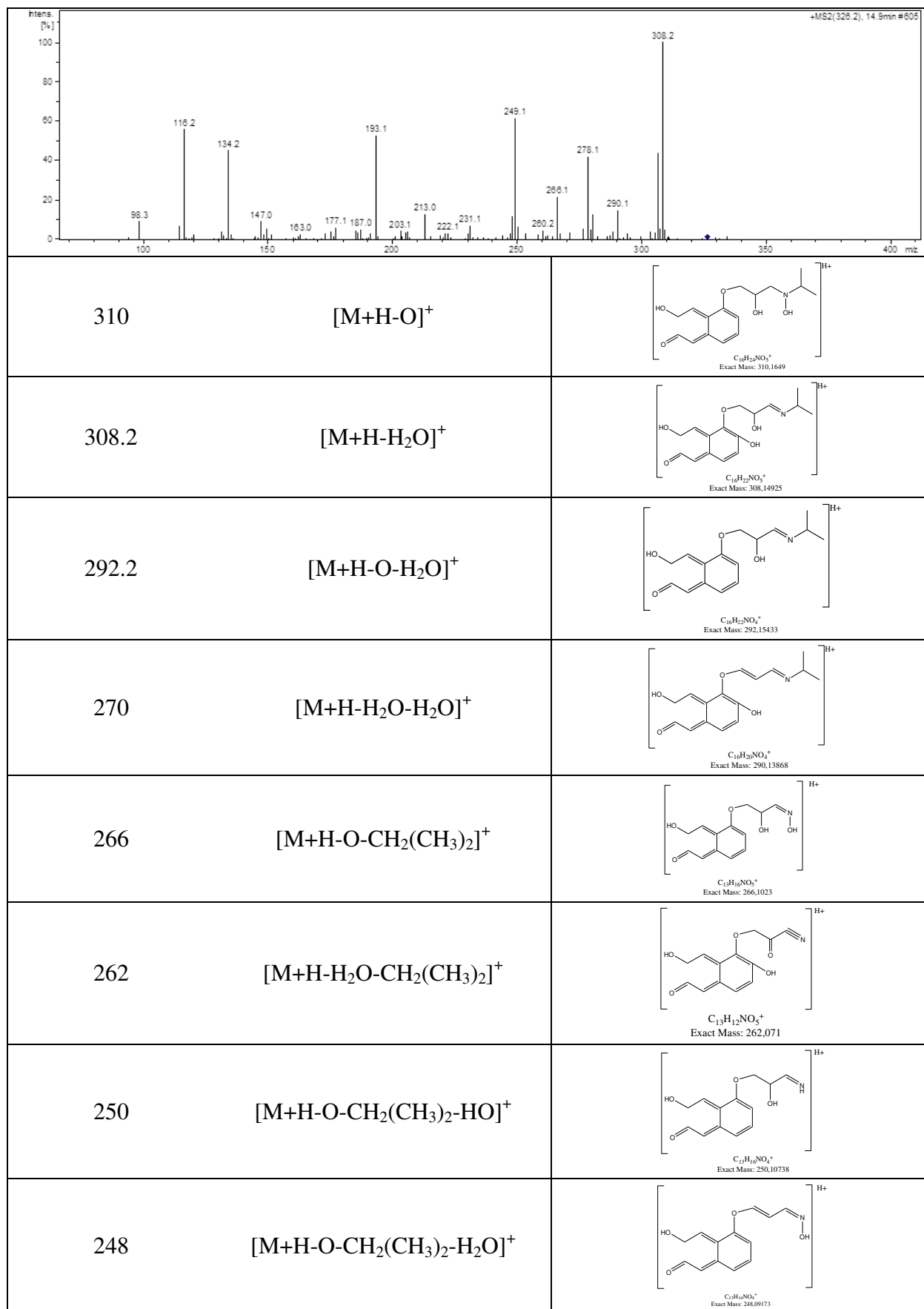
159	$[M+H-C_6H_{15}NO_3]^+$	 $C_{10}H_7O_2^+$ Exact Mass: 159.04406
134	$[M+H-C_{10}H_{10}O_3]^+$	 $C_6H_{16}NO_2^+$ Exact Mass: 134.11756
116	$[M+H-C_{10}H_{10}O_3-H_2O]^+$	 $C_6H_{14}NO^+$ Exact Mass: 116.10699
114	rearrangement of 116	 $C_6H_{12}NO^+$ Exact Mass: 114.09134

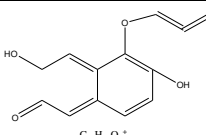
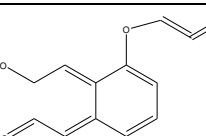
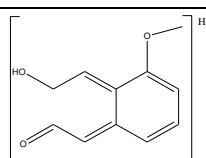
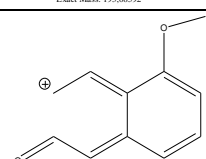
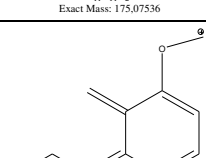
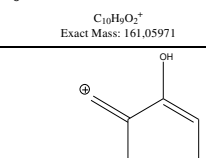
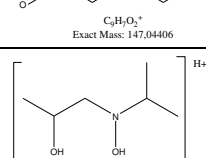
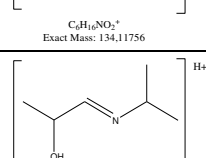
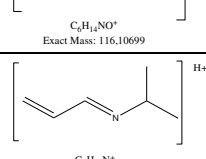
431

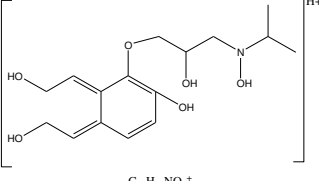


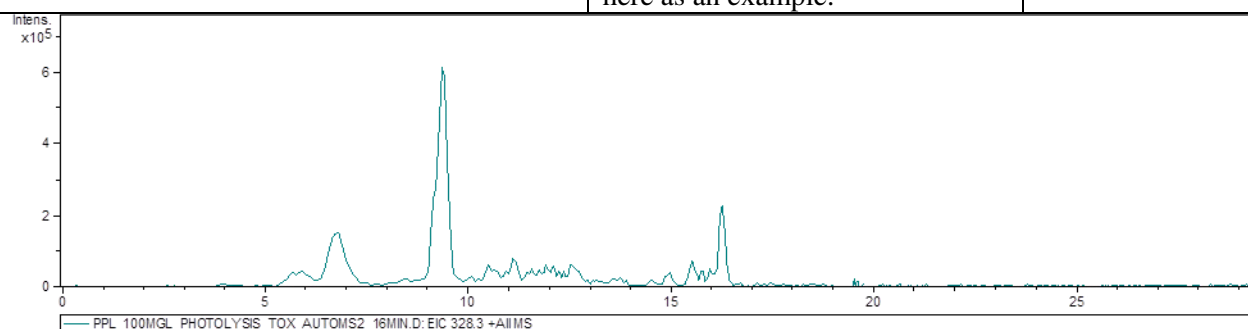
Fragments (m/z)	Retention time (min)	Precursor ion/Product ion	Structure	Reference
326.2	Multiple peaks	[M+H] <sup>+</sup>	 <p data-bbox="927 483 1050 517">C<sub>16</sub>H<sub>24</sub>NO<sub>6</sub><sup>+</sup> Exact Mass: 326.15981</p> <p data-bbox="794 528 1190 656">There were a lot of structural isomers for this PD. Therefore only 1 structure is represented here.</p>	44
 <p data-bbox="252 920 671 936">PPL_100MGL_PHOTOLYSIS_TOX_AUTOMS2_16MIN.D: EIC 326.2+All MS</p>				
<p data-bbox="185 943 1410 1122">There were a lot of peaks in the EIC were observed and they cannot be integrated into different peaks. The few peaks which were separated have same MS<sup>2</sup> fragmentation. Therefore, it could be assumed that all these peaks have the same MS<sup>2</sup> fragmentation pattern and therefore they were analyzed together without any MS<sup>2</sup> fragmentation for particular peak. This phenomenon indicates the formation of the constitutional isomers.</p>				
MS <sup>2</sup>				
				
				



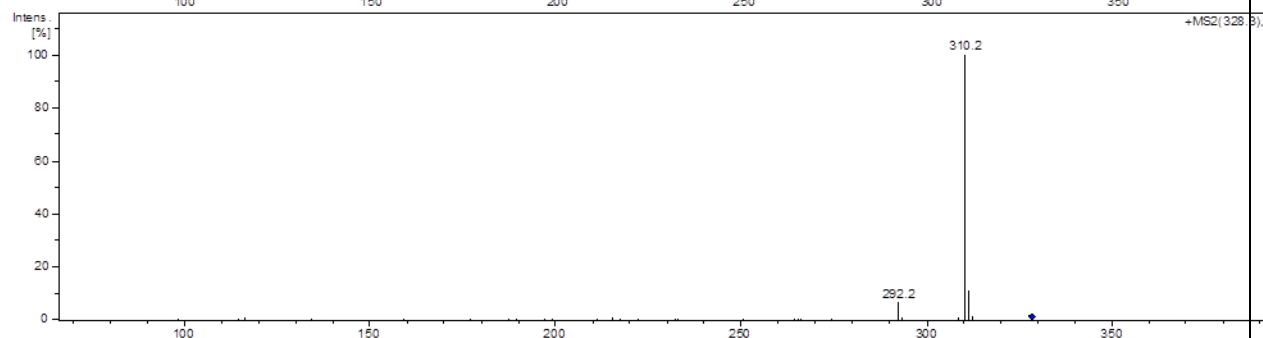
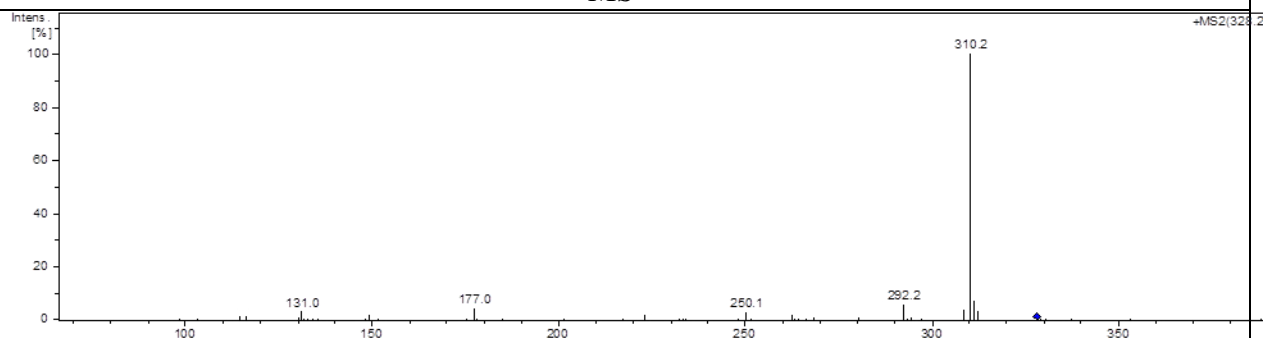


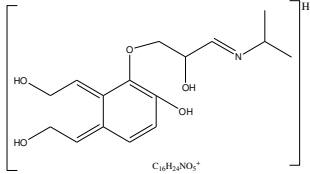
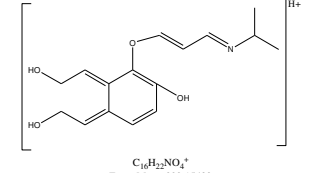
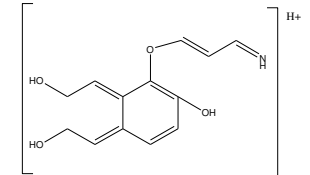
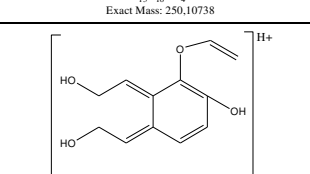
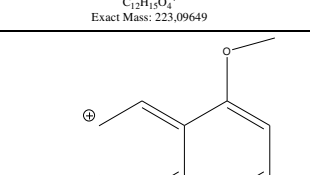
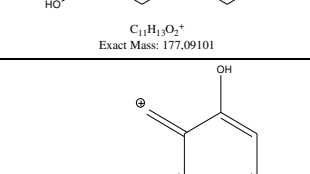
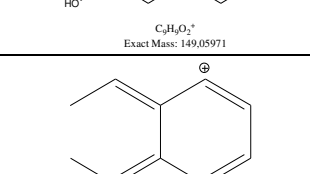
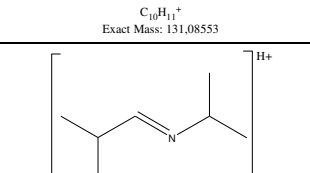
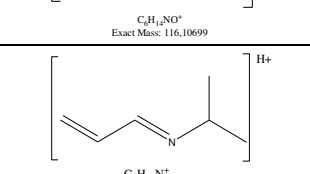
231	$[M+H-H_2O-C_3H_9O]^+$	 <p><math>C_{13}H_{11}O_4^+</math> Exact Mass: 231.06519</p>
215	$[M+H-O-H_2O-C_3H_9O]^+$	 <p><math>C_{13}H_{11}O_3^+</math> Exact Mass: 215.07027</p>
193	$[M+H-O-H_2O-C_5H_{13}O]^+$	 <p><math>C_{17}H_{19}O_4^+</math> Exact Mass: 193.08592</p>
175	$[M+H-O-H_2O-C_5H_{13}O-H_2O]^+$	 <p><math>C_{17}H_{17}O_4^+</math> Exact Mass: 175.07536</p>
161	$[M+H-O-H_2O-C_5H_{13}O-CH_3OH]^+$	 <p><math>C_{10}H_9O_2^+</math> Exact Mass: 161.05971</p>
147	$[M+H-O-H_2O-C_6H_{15}O-CH_3OH]^+$	 <p><math>C_8H_7O_3^+</math> Exact Mass: 147.04406</p>
134	$[M+H-C_{10}H_{10}O_4]^+$	 <p><math>C_6H_{10}NO_2^+</math> Exact Mass: 134.11756</p>
116	$[M+H-C_{10}H_{10}O_4-H_2O]^+$	 <p><math>C_9H_{12}NO^+</math> Exact Mass: 116.10699</p>
98	$[M+H-C_{10}H_{10}O_4-H_2O-H_2O]^+$	 <p><math>C_8H_{12}N^+</math> Exact Mass: 98.09643</p>

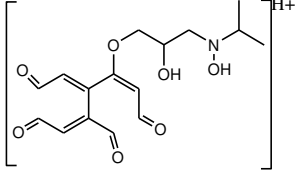
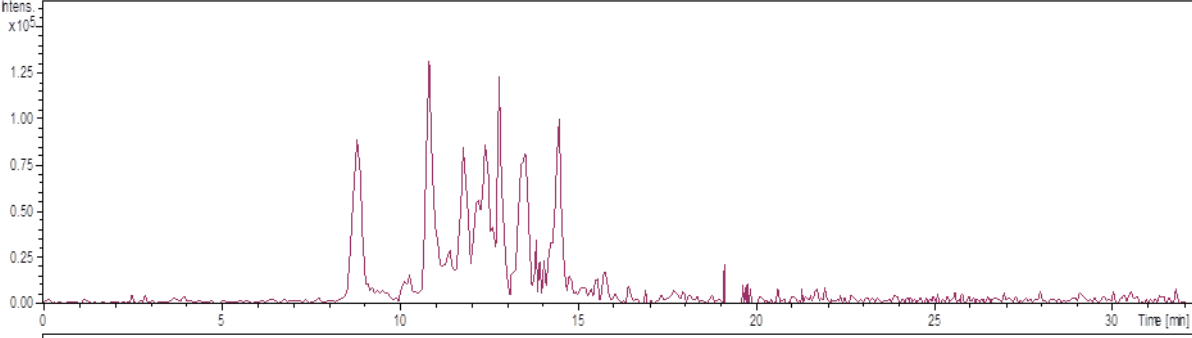
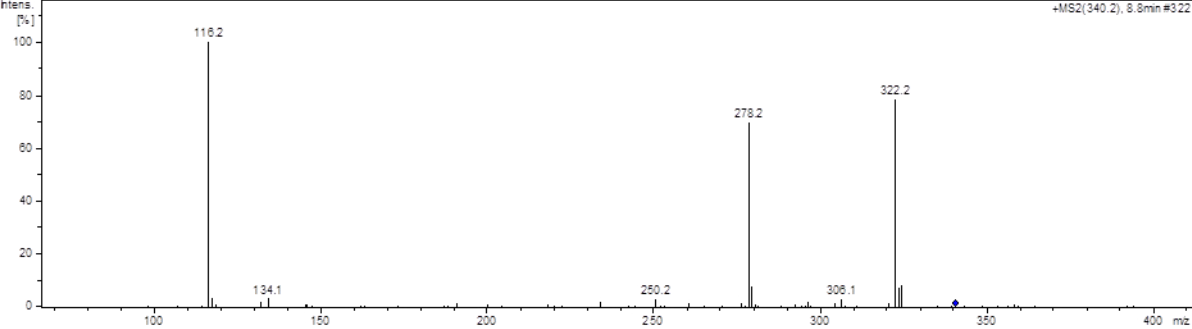
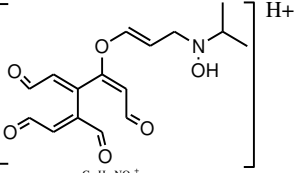
Fragments (m/z)	Retention time (min)	Precursor ion/Product ion	Structure	Reference
328.2	Multiple peaks	[M+H] <sup>+</sup>	 <p data-bbox="933 526 1061 548">C<sub>18</sub>H<sub>26</sub>NO<sub>6</sub><sup>+</sup> Exact Mass: 328.17546</p> <p data-bbox="790 560 1204 683">There were a lot of structural isomers for this PD. Therefore only 1 structure is represented here as an example.</p>	

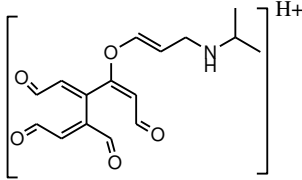
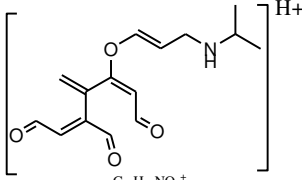
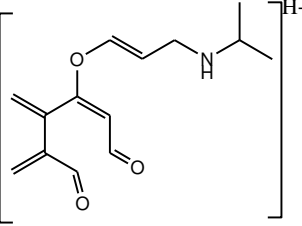
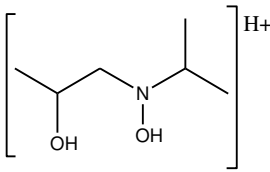
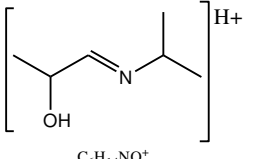


There were a lot of peaks in the EIC were observed and they cannot be integrated into different peaks. The few peaks which were separated have same MS<sup>2</sup> fragmentation. Therefore, it could be assumed that all these peaks have the same MS<sup>2</sup> fragmentation pattern and therefore they were analyzed together without any MS<sup>2</sup> fragmentation for particular peak. This phenomenon indicates the formation of the constitutional isomers.

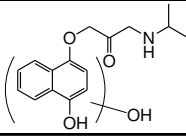
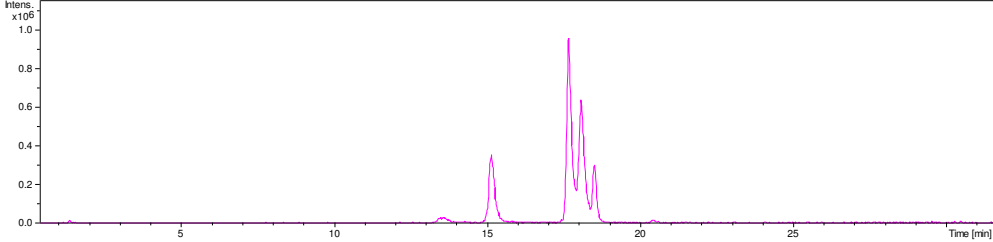
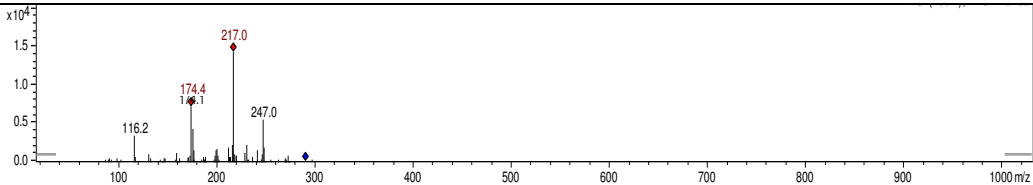
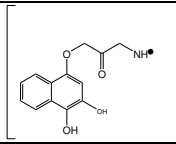
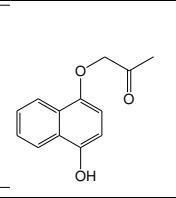
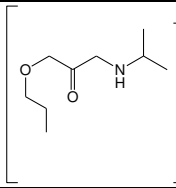
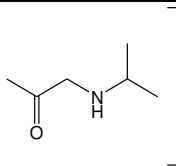
MS<sup>2</sup>

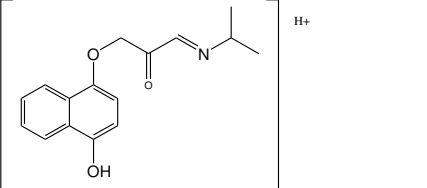
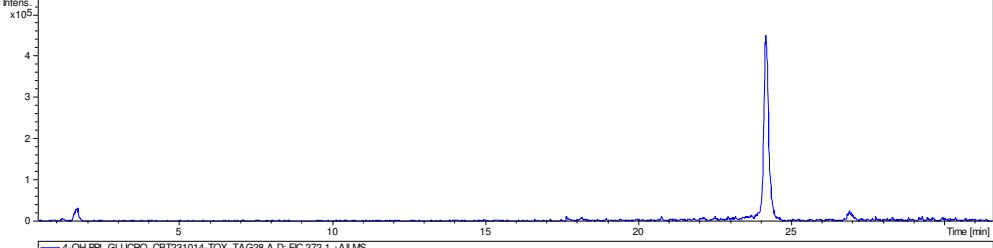
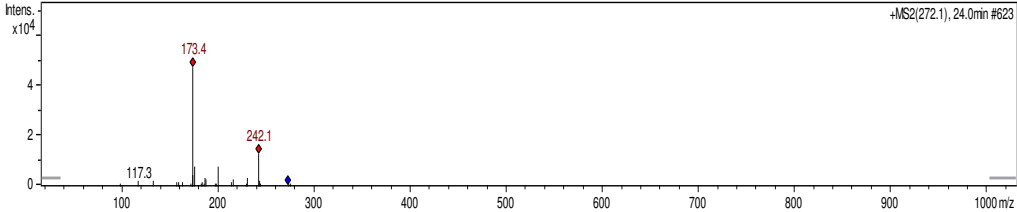
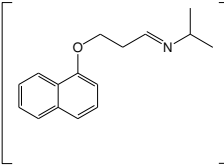
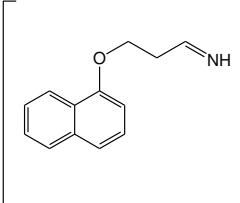
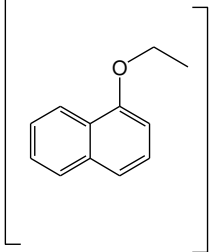
310	$[M+H-H_2O]^+$	 <p><math>C_{16}H_{22}NO_3^+</math> Exact Mass: 310.1649</p>
292	$[M+H-H_2O-H_2O]^+$	 <p><math>C_{16}H_{22}NO_3^+</math> Exact Mass: 292.15433</p>
250	$[M+H-H_2O-H_2O-CH(CH_3)_2]^+$	 <p><math>C_{13}H_{16}NO_4^+</math> Exact Mass: 250.10738</p>
223	$[M+H-H_2O-CH_3N(OH)CH(CH_3)_2]^+$	 <p><math>C_{12}H_{15}O_4^+</math> Exact Mass: 223.09649</p>
177	$[M+H-H_2O-C_2H_4N(OH)CH(CH_3)_2-H_2O-H_2O]^+$	 <p><math>C_{11}H_{11}O_5^+</math> Exact Mass: 177.09101</p>
149	$[M+H-H_2O-C_3H_8N(OH)CH(CH_3)_2-H_2O-CH_3OH]^+$	 <p><math>C_9H_9O_2^+</math> Exact Mass: 149.05971</p>
131	$[M+H-C_6H_{15}NO_3-H_2O-H_2O-H_2O]^+$	 <p><math>C_{10}H_{11}^+</math> Exact Mass: 131.08553</p>
116	$[M+H-C_{10}H_{12}O_4-H_2O]^+$	 <p><math>C_8H_{12}NO^+</math> Exact Mass: 116.10699</p>
98.2	$[M+H-C_{10}H_{12}O_4-H_2O-H_2O]^+$	 <p><math>C_8H_{12}N^+</math> Exact Mass: 98.09643</p>

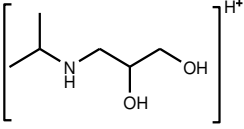
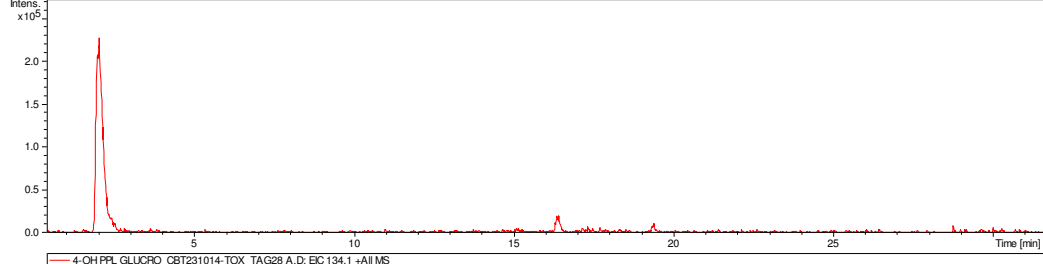
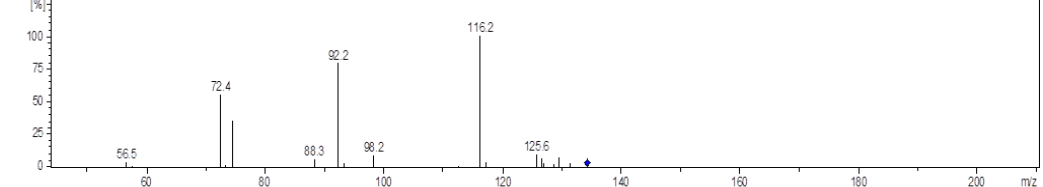
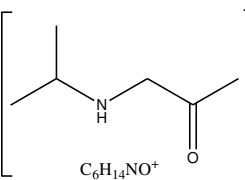
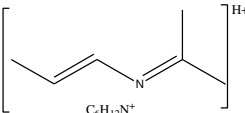
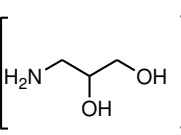
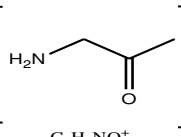
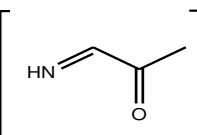
Fragments (m/z)	Retention time (min)	Precursor ion/Product ion	Structure	Reference
340.2	Multiple peaks	[M+H] <sup>+</sup>	 <p data-bbox="938 517 1059 551">C<sub>16</sub>H<sub>22</sub>NO<sub>7</sub><sup>+</sup> Exact Mass: 340.13908</p> <p data-bbox="788 555 1225 752">There were a lot of structural isomers for this PD is possible as the EIC indicated the co-elution of various peaks. Thus only 1 structure is represented here as an example</p>	44
 <p data-bbox="261 1093 778 1115">PPL_100MGL_PHOTOLYSIS_TOX_AUTOMS2_16MIN.D: EIC:340.0 +All MS, Masses excluded</p>				
<p data-bbox="181 1115 1442 1299">There were a lot of peaks in the EIC were observed and they cannot be integrated into different peaks. The few peaks which were separated have same MS<sup>2</sup> fragmentation. Therefore, it could be assumed that all these peaks have the same MS<sup>2</sup> fragmentation pattern and therefore they were analyzed together without any MS<sup>2</sup> fragmentation for particular peak. This phenomenon indicates the formation of the constitutional isomers.</p>				
MS <sup>2</sup>				
 <p data-bbox="1283 1339 1417 1361">+MS2(340.2), 8.8min #322</p>				
322.2		[M+H-H <sub>2</sub> O] <sup>+</sup>	 <p data-bbox="1091 1995 1171 2029">C<sub>16</sub>H<sub>20</sub>NO<sub>6</sub><sup>+</sup> Exact Mass: 322.12851</p>	

<p>306</p> <p>[M+H-H<sub>2</sub>O-O]<sup>+</sup> rearrangement</p>	 <p>C<sub>14</sub>H<sub>20</sub>NO<sub>3</sub><sup>+</sup> Exact Mass: 306.1336</p>
<p>278</p> <p>[M+H-H<sub>2</sub>O-O-HCHO]<sup>+</sup></p>	 <p>C<sub>15</sub>H<sub>20</sub>NO<sub>4</sub><sup>+</sup> Exact Mass: 278.13868</p>
<p>250</p> <p>[M+H-H<sub>2</sub>O-O-HCHO-HCHO]<sup>+</sup></p>	 <p>C<sub>14</sub>H<sub>20</sub>NO<sub>3</sub><sup>+</sup> Exact Mass: 250.14377</p>
<p>134.2</p> <p>[M+H-C<sub>10</sub>H<sub>8</sub>O<sub>5</sub>]<sup>+</sup></p>	 <p>C<sub>6</sub>H<sub>16</sub>NO<sub>2</sub><sup>+</sup> Exact Mass: 134.11756</p>
<p>116.2</p> <p>[M+H-C<sub>10</sub>H<sub>8</sub>O<sub>5</sub>-H<sub>2</sub>O]<sup>+</sup></p>	 <p>C<sub>6</sub>H<sub>14</sub>NO<sup>+</sup> Exact Mass: 116.10699</p>



Fragments (m/z)	Retention time (min)	Structure	Reference
290.1	Several Peaks		
 <p data-bbox="252 728 582 745">4-OH-FPL-GLUCO-CBT231014-TOX-TAG28 A.D. EC 290.1 -All MS</p>			
<b>MS<sup>2</sup></b>			
			
247.0			
217.0			
174.4			
116.2			

Fragments (m/z)	Retention time (min)	Structure	Reference
272.1	24.1		
			
<b>MS<sup>2</sup></b>			
			
242.1			
200.1			
173.1			

Fragments (m/z)	Retention time (min)	Structure	Reference
134.1	2.1	 $C_6H_{16}NO_2^+$ Exact Mass: 134,11756	
 4-OH PPL GLUCRO_CBT231014_TOX_TAG28 A.D. EC 134.1 -All MS			
<b>MS<sup>2</sup></b>			
			
116.2		 $C_6H_{14}NO^+$ Exact Mass: 116,10699	
98.2		 $C_6H_{12}N^+$ Exact Mass: 98,09643	
92.2		 $C_5H_{10}NO_2^+$ Exact Mass: 92,0706	
74.4		 $C_3H_8NO^+$ Exact Mass: 74,06004	
72.4		 $C_3H_6NO^+$ Exact Mass: 72,04439	

443 **Reference**

- 444 (1) Rastogi, T.; Leder, C.; Kümmerer, K. Qualitative environmental risk assessment of  
445 photolytic transformation products of iodinated X-ray contrast agent diatrizoic acid. *Sci.*  
446 *Total Environ.* **2014**, 482–483 (0), 378–388.
- 447 (2) Rastogi, T.; Leder, C.; Kümmerer, K. Designing green derivatives of  $\beta$ -blocker  
448 Metoprolol: A tiered approach for green and sustainable pharmacy and chemistry.  
449 *Chemosphere* **2014**, 111 (0), 493–499.
- 450 (3) ISO 8245. *Water quality -- Guidelines for the determination of total organic carbon*  
451 *(TOC) and dissolved organic carbon (DOC)*, 2nd ed., 1999.
- 452 (4) OECD. *OECD Guidelines for the Testing of Chemicals. Ready Biodegradability 301D:*  
453 *Closed Bottle Test*; OECD Pub., 1992.
- 454 (5) OECD. *OECD Guidelines for the Testing of Chemicals. Ready Biodegradability 301F:*  
455 *Manometric Respiratory Test*; OECD Pub., 1992.
- 456 (6) Friedrich, J.; Längin, A.; Kümmerer, K. Comparison of an electrochemical and  
457 luminescence-based oxygen measuring system for use in the biodegradability testing  
458 according to Closed Bottle Test (OECD 301D). *CLEAN – Soil, Air, Water* **2013**, 41 (3),  
459 251–257.
- 460 (7) Mahmoud, W. M. M.; Trautwein, C.; Leder, C.; Kümmerer, K. Aquatic photochemistry,  
461 abiotic and aerobic biodegradability of thalidomide: Identification of stable  
462 transformation products by LC–UV–MSn. *Sci. Total Environ.* **2013**, 463–464, 140–150.
- 463 (8) OECD. *Revised introduction of the OECD guidelines for testing of chemicals, Section*  
464 *3*; Organisation of Economic Cooperation and Development, 2006.
- 465 (9) Nyholm, N. The european system of standardized legal tests for assessing the  
466 biodegradability of chemicals. *Environ. Toxicol. Chem.* **1991**, 10 (10), 1237–1246.
- 467 (10) Innis, R. B.; Corrêa, F. M. A.; Snyder, S. H. Carazolol, an extremely potent  $\beta$ -  
468 adrenergic blocker: Binding to  $\beta$ -receptors in brain membranes. *Life Sci.* **1979**, 24 (24),  
469 2255–2264.
- 470 (11) Shelley, J. C.; Cholleti, A.; Frye, L. L.; Greenwood, J. R.; Timlin, M. R.; Uchimaya, M.  
471 Epik: a software program for pK a prediction and protonation state generation for drug-  
472 like molecules. *J. Comput. Aided Mol. Des.* **2007**, 21 (12), 681–691.
- 473 (12) Friesner, R. A.; Banks, J. L.; Murphy, R. B.; Halgren, T. A.; Klicic, J. J.; Mainz, D. T.;  
474 Repasky, M. P.; Knoll, E. H.; Shelley, M.; Perry, J. K.; Shaw, D. E.; Francis, P.;  
475 Shenkin, P. S. Glide: A new approach for rapid, accurate docking and scoring. 1.  
476 Method and assessment of docking accuracy. *J. Med. Chem.* **2004**, 47 (7), 1739–1749.
- 477 (13) Jorgensen, W. L. *Small-Molecule Drug Discovery Suite 2013-3: QikProp*; Schrödinger:  
478 New York, 2013.
- 479 (14) Jorgensen, William L. QikProp 3.8: User Manual. [http://helixweb.nih.gov/schrodinger-](http://helixweb.nih.gov/schrodinger-2013.3-docs/qikprop/qikprop_user_manual.pdf)  
480 [2013.3-docs/qikprop/qikprop\\_user\\_manual.pdf](http://helixweb.nih.gov/schrodinger-2013.3-docs/qikprop/qikprop_user_manual.pdf) (accessed April 2, 2014).

- 481 (15) Lipinski, C. A.; Lombardo, F.; Dominy, B. W.; Feeney, P. J. Experimental and  
482 computational approaches to estimate solubility and permeability in drug discovery and  
483 development settings. *Adv. Drug Delivery Rev.* **2001**, *46* (1–3), 3–26.
- 484 (16) Jorgensen, W. L.; Duffy, E. M. Prediction of drug solubility from structure. *Adv. Drug*  
485 *Delivery Rev.* **2002**, *54* (3), 355–366.
- 486 (17) Trudeau, M. C.; Warmke, J. W.; Ganetzky, B.; Robertson, G. A. HERG, a human  
487 inward rectifier in the voltage-gated potassium channel family. *Science* **1995**, *269*, 92–  
488 95.
- 489 (18) Sanguinetti, M. C.; Jiang, C.; Curran, M. E.; Keating, M. T. A mechanistic link between  
490 an inherited and an acquired cardiac arrhythmia: HERG encodes the IKr potassium  
491 channel. *Cell* **1995**, *81* (2), 299–307.
- 492 (19) Hedley, P. L.; Jørgensen, P.; Schlamowitz, S.; Wangari, R.; Moolman-Smook, J.; Brink,  
493 P. A.; Kanters, J. K.; Corfield, V. A.; Christiansen, M. The genetic basis of long QT and  
494 short QT syndromes: A mutation update. *Hum. Mutat.* **2009**, *30* (11), 1486–1511.
- 495 (20) Sanguinetti, M. C.; Tristani-Firouzi, M. hERG potassium channels and cardiac  
496 arrhythmia. *Nature* **2006**, *440* (7083), 463–469.
- 497 (21) Hidalgo, I. J.; Raub, T. J.; Borchardt, R. T. Characterization of the human colon  
498 carcinoma cell line (Caco-2) as a model system for intestinal epithelial permeability.  
499 *Gastroenterology* **1989**, *96* (3), 736–749.
- 500 (22) Artursson, P. Epithelial transport of drugs in cell culture. I: A model for studying the  
501 passive diffusion of drugs over intestinal absorbtive (Caco-2) cells. *J. Pharm. Sci.* **1990**,  
502 *79* (6), 476–482.
- 503 (23) Artursson, P.; Karlsson, J. Correlation between oral drug absorption in humans and  
504 apparent drug permeability coefficients in human intestinal epithelial (Caco-2) cells.  
505 *Biochem. Biophys. Res. Comm.* **1991**, *175* (3), 880–885.
- 506 (24) Irvine, J. D.; Takahashi, L.; Lockhart, K.; Cheong, J.; Tolan, J. W.; Selick, H. E.;  
507 Grove, J. R. MDCK (Madin-Darby canine kidney) cells: A tool for membrane  
508 permeability screening. *J. Pharm. Sci.* **1999**, *88* (1), 28–33.
- 509 (25) Mahmoud, W. M. M.; Toolaram, A. P.; Menz, J.; Leder, C.; Schneider, M.; Kümmerer,  
510 K. Identification of phototransformation products of thalidomide and mixture toxicity  
511 assessment: An experimental and quantitative structural activity relationships (QSAR)  
512 approach. *Water Res.* **2014**, *49* (0), 11–22.
- 513 (26) Chakravarti, S. K.; Saiakhov, R. D.; Klopman, G. Optimizing predictive performance of  
514 CASE Ultra expert system models using the applicability domains of individual toxicity  
515 alerts. *J. Chem. Inf. Model.* **2012**, *52* (10), 2609–2618.
- 516 (27) Saiakhov, R.; Chakravarti, S.; Klopman, G. Effectiveness of CASE Ultra expert system  
517 in evaluating adverse effects of drugs. *Mol. Inf.* **2013**, *32* (1), 87–97.

- 518 (28) Saiakhov, R.; Chakravarti, S.; Sedykh, A. An improved workflow to perform in silico  
519 mutagenicity assessment of impurities as per ICH M7 guideline. *Toxicol. Letters* **2014**,  
520 *229, Supplement (0)*, S164.
- 521 (29) Roberts, G.; Myatt, G.; Johnson, W.; Cross, K.; Blower, P. LeadScope: Software for  
522 exploring large sets of screening data. *J. Chem. Inf. Model.* **2000**, *40* (6), 1302–1314.
- 523 (30) Leadscope. A new ICH M7 compliant expert alert system to predict the mutagenic  
524 potential of impurities. [http://www.leadscope.com/white\\_papers/ICHM7-WhitePaper-](http://www.leadscope.com/white_papers/ICHM7-WhitePaper-0314.pdf)  
525 [0314.pdf](http://www.leadscope.com/white_papers/ICHM7-WhitePaper-0314.pdf) (accessed April 9, 2015).
- 526 (31) Laboratory of Mathematical Chemistry Bulgaria. *OASIS Catalogic software*  
527 *V.5.11.6TB*, 2012.
- 528 (32) DiscoverRx. PathHunter®  $\beta$ -Arrestin GPCR Assay Platform.  
529 [http://www.discoverx.com/technologies-platforms/enzyme-fragment-complementation-](http://www.discoverx.com/technologies-platforms/enzyme-fragment-complementation-technology/pathhunter-efc-cell-based-assay-platform/protein-protein-interactions/gpcrs-b-arrestin)  
530 [technology/pathhunter-efc-cell-based-assay-platform/protein-protein-interactions/gpcrs-](http://www.discoverx.com/technologies-platforms/enzyme-fragment-complementation-technology/pathhunter-efc-cell-based-assay-platform/protein-protein-interactions/gpcrs-b-arrestin)  
531 [b-arrestin](http://www.discoverx.com/technologies-platforms/enzyme-fragment-complementation-technology/pathhunter-efc-cell-based-assay-platform/protein-protein-interactions/gpcrs-b-arrestin) (accessed April 24, 2014).
- 532 (33) DiscoverRx. User Manual: PathHunter® eXpress  $\beta$ -Arrestin Human and Ortholog GPCR  
533 Assays. [http://www.discoverx.com/tools-resources/document-resource-](http://www.discoverx.com/tools-resources/document-resource-library/documents/pathhunter-express-%CE%B2-arrestin-human-and-ortholog-g)  
534 [library/documents/pathhunter-express-%CE%B2-arrestin-human-and-ortholog-g](http://www.discoverx.com/tools-resources/document-resource-library/documents/pathhunter-express-%CE%B2-arrestin-human-and-ortholog-g)  
535 (accessed April 24, 2014).
- 536 (34) Henry, P. J.; Goldie, R. G.  $\beta$ 1-Adrenoceptors mediate smooth muscle relaxation in  
537 mouse isolated trachea. *Br. J. Pharmacol.* **1990**, *99* (1), 131–135.
- 538 (35) Briley, M.; Cavero, I.; Langer, S. Z.; Roach, A. G. Evidence against beta-adrenoceptor  
539 blocking activity of diltiazem, a drug with calcium antagonist properties. *Br. J.*  
540 *Pharmacol.* **1980**, *69* (4), 669–673.
- 541 (36) Chen, Y.; Liu, Z.; Wang, Z.; Xue, M.; Zhu, X.; Tao, T. Photodegradation of propranolol  
542 by Fe(III)–citrate complexes: Kinetics, mechanism and effect of environmental media.  
543 *J. Hazard. Mat.* **2011**, *194* (0), 202–208.
- 544 (37) Liu, Q.-T.; Williams, H. E. Kinetics and Degradation Products for Direct Photolysis of  
545  $\beta$ -Blockers in Water. *Environ. Sci. Technol.* **2007**, *41* (3), 803–810.
- 546 (38) Romero, V.; La Cruz, N. de; Dantas, R. F.; Marco, P.; Giménez, J.; Esplugas, S.  
547 Photocatalytic treatment of metoprolol and propranolol. *Catal. Today* **2011**, *161* (1),  
548 115–120.
- 549 (39) Santiago-Morales, J.; Agüera, A.; Gómez, M. d. M.; Fernández-Alba, A. R.; Giménez,  
550 J.; Esplugas, S.; Rosal, R. Transformation products and reaction kinetics in simulated  
551 solar light photocatalytic degradation of propranolol using Ce-doped TiO<sub>2</sub>. *Appl. Catal.*  
552 *B: Environ.* **2013**, *129*, 13–29.
- 553 (40) Song, W.; Cooper, W. J.; Mezyk, S. P.; Greaves, J.; Peake, B. M. Free Radical  
554 Destruction of  $\beta$ -Blockers in Aqueous Solution. *Environ. Sci. Technol* **2008**, *42* (4),  
555 1256–1261.

- 556 (41) Anquandah, G. A. K.; Sharma, V. K.; Panditi, V. R.; Gardinali, P. R.; Kim, H.; Oturan,  
557 M. A. Ferrate(VI) oxidation of propranolol: Kinetics and products. *Chemosphere* **2013**,  
558 *91* (1), 105–109.
- 559 (42) Benner, J.; Ternes, T. A. Ozonation of Propranolol: Formation of Oxidation Products.  
560 *Environ. Sci. Technol.* **2009**, *43* (13), 5086–5093.
- 561 (43) Dantas, R. F.; Sans, C.; Esplugas, S. Ozonation of Propranolol: Transformation,  
562 Biodegradability, and Toxicity Assessment. *J. Environ. Eng.* **2011**, *137* (8), 754.
- 563 (44) Wilde, M. L.; Mahmoud, W. M. M.; Kümmerer, K.; Martins, A. F. Oxidation–  
564 coagulation of  $\beta$ -blockers by K<sub>2</sub>FeVIO<sub>4</sub> in hospital wastewater: Assessment of  
565 degradation products and biodegradability. *Sci. Total Environ.* **2013**, *452–453* (0), 137–  
566 147.
- 567 (45) Barrett, A. M.; Cullum, V. A. The biological properties of the optical isomers of  
568 propranolol and their effects on cardiac arrhythmias. *Br. J. Pharmacol.* **1968**, *34* (1),  
569 43–55.
- 570 (46) Fitzgerald, J. D.; O'Donnell, S. R. Pharmacology of 4-hydroxypropranolol, a metabolite  
571 of propranolol. *Br. J. Pharmacol.* **1971**, *43* (1), 222–235.
- 572 (47) Marco-Urrea, E.; Radjenović, J.; Caminal, G.; Petrović, M.; Vicent, T.; Barceló, D.  
573 Oxidation of atenolol, propranolol, carbamazepine and clofibric acid by a biological  
574 Fenton-like system mediated by the white-rot fungus *Trametes versicolor*. *Water Res.*  
575 **2010**, *44* (2), 521–532.  
576